

INTERNATIONAL COUNCIL FOR BUILDING RESEARCH STUDIES AND DOCUMENTATION

WORKING COMMISSION W18A - TIMBER STRUCTURES

CIB - W18 A

MEETING TWENTY - THREE

LISBON

PORTUGAL

SEPTEMBER 1990

CONTENTS

1	List of Participants
2	Chairman's Introduction
3	Cooperation with other Organisations
4	Trussed Rafter Subgroup
5	Subgroup on Derivation of Characteristic Values
6	Limit States Design
7	Timber Beams
8	Fracture Mechanics
9	Trussed Rafters
10	Laminated Members
11	Structural Stability
12	Stresses for Solid Timber
13	Timber Joints and Fasteners
14	Other Business
15	List of CIB-W18A Papers / Lisbon, Portugal 1990
16	Current List of CIB-W18A Papers

CIB-W18A Papers 23-1-1 up to 23-19-3

MINUTES OF 23rd MEETING OF CIB-W18A

LNEC Lisbon, Portugal, 10-14 September 1990

1. LIST OF PARTICIPANTS

BELGIUM

J Rathe Laboratory, Ghent

CANADA

J D Barrett University of British Columbia, Vancouver
H Griffin Council of Forest Industries of British Columbia
C K A Stieda Forintek Canada, Vancouver

DENMARK

A Egerup Self-employed
T Feldborg Danish Building Research Institute, Horsholm
H J Larsen Danish Building Research Institute, Horsholm
H Riberholt Technical University of Denmark, Lyngby

FINLAND

J Kangas Technical Research Centre of Finland, Espoo
A Ranta-Maunus Technical Research Centre of Finland, Espoo
K Riipola Forest Products Laboratory, Espoo

FRANCE

F Rouger CTBA Department, Paris
A Vergne Civil Engineering Laboratory, Aubiere

GERMANY

H J Blass University of Karlsruhe
H Bruninghoff University of Wuppertal
F Colling University of Karlsruhe
J Ehlbeck University of Karlsruhe
W Rug Self-employed

ISRAEL

U Korin National Building Research Institute, Haifa

ITALY

G Bignotti Holzbau SpA, Bressanone
A Ceccotti University of Florence
N de Robertis University of Florence

JAPAN

Y Hirashima University of Shizuoka
M Yasumura Building Research Institute, Tsukuba

NETHERLANDS

J Kuipers Self-employed
A J M Leijten University of Technology, Delft
T C van der Put University of Technology, Delft

NORWAY

E Aasheim Norwegian Institute of Wood Technology, Oslo
T Ramstad Norwegian Building Research Institute, Oslo

PORTUGAL

P P De Sousa National Laboratory of Civil Engineering, Lisbon

SWEDEN

B L O Edlund Chalmers University of Technology, Goteborg
U A Girhammar Royal Institute of Technology, Stockholm
B Kallsner Swedish Institute for Wood Technology Research,
Stockholm
J Konig Swedish Institute for Wood Technology Research,
Stockholm
S Mohager Swedish National Testing and Research Institute,
Stockholm
S Ohlsson Chalmers University of Technology, Goteborg
S Thelandersson University of Lund

SWITZERLAND

U A Meierhofer Federal Laboratory for Materials Testing and
Research, Duebendorf

UK

A R Abbott TRADA, High Wycombe
H J Burgess TRADA, High Wycombe
V Enjily Building Research Establishment, Watford
A Fewell Building Research Establishment, Watford
J P Marcroft TRADA, High Wycombe
R F Marsh Ove Arup & Partners, London
C J Mettem TRADA, High Wycombe
J G Sunley Self-employed
L R J Whale Gang-Nail Systems Ltd, Aldershot

USA

E G Elias American Plywood Association, Tacoma
D W Green USDA Forest Products Laboratory, Madison
R R Kincaid Southern Pine Marketing Council, London
M R O'Halloran American Plywood Association, Tacoma
E G Stern Virginia Polytechnic Institute and State University,
Blacksburg
M F Stone Weyerhaeuser Co, Washington

2. CHAIRMAN'S INTRODUCTION

DR STIEDA opened the meeting and welcomed the participants, and in particular those who were attending a CIB-W18A meeting for the first time. Special mention was made of some of the new developments that have taken place recently, in particular the growing interest in seismic design and the Eurocode proposals on truss design and glulam. In concluding his introduction, DR STIEDA reiterated the main objective of CIB-W18A, which is to prepare model codes for the design of timber structures.

3. COOPERATION WITH OTHER ORGANISATIONS

ISO/TC 165

MR LARSEN said that very little had happened within this Group over the past year, because of parallel activities with CEN. Mr LARSEN announced that he will be resigning as Chairman of TC 165 because of conflicts with CEN work and that a new Chairman will take over in 1991. Mr SUNLEY stressed the importance of the new Chairman's maintaining close liaison with W18A and enquired as to the procedure within ISO for the election of a new Chairman. Mr LARSEN replied that he was unclear as to the exact procedure, but stressed that if W18A had a proposal, then ISO might be persuaded to accept.

Three draft Standards had been prepared and sent to central Secretariat and these will be circulated by the end of the year.

RILEM

DR CECCOTTI briefly summarised the objectives of the four existing timber related Groups:-

- . "Behaviour of timber structures under seismic action" held a meeting on 10 September, with approximately 20 participants. Papers were prepared and presented on the following subjects:-
 - . Basic actions - earthquake design linked with probabilistic design
 - . Behaviour of joints
 - . Test methods for joints
 - . Calculation methods and computer simulation.

It was agreed that the main emphasis of this group in future should be on testing methods, with the objective of preparing an interim report for the next meeting, which will be held in conjunction with CIB-W18A, on 2 March 1991 in Copenhagen.

- . "Application of fracture mechanics to timber structures". PROFESSOR RANTA-MAUNUS said that this group had prepared a draft state-of-the-art report and that the final report will be ready in approximately six months. The report includes assessment of the application of fracture mechanics to the splitting of wood, the probabilistic nature of loads, materials and cracks, and duration of load as influenced by moisture variations.

This group recommended that further effort should be concentrated in the following areas:-

- . Standards for testing (fracture of clear wood/cracked beams)
 - . Design methods (shear design of notched/unnotched beams)
 - . Research into the development of fracture criteria.
- . PROFESSOR RANTA-MAUNUS also reported on the activities of the group concerned with "Creep in timber structures", under the chairmanship of Professor Morlier. The main task of this group is to prepare a state-of-the-art report and areas of work include basic knowledge about creep of wood, including temperature and moisture effect; experimental and numerical data concerning creep of timber; slip and time-dependent slip of connectors; codes of practice; structural analysis and numerical treatments of timber; variations of moisture content in wood structures.

The next meeting will be held in 1991, in Sweden.

- . DR CECCOTTI reported that the group concerned with "Behaviour of timber and concrete composite load-bearing structures" had met twice so far and would meet again after the current CIB-W18A meeting. This group has produced three reports and it is intended ultimately to produce a book for RILEM, covering the subject areas.

DR CECCOTTI said that in addition to the existing committees, three new timber committees had recently been formed, dealing with:

- . design by testing,
- . probabilistic methods in design
- . prediction techniques in service life.

EC5

MR LARSEN reported that as from 1 January 1990, work on EC5 had been transferred from the European Commission to CEN and that the Technical Committee responsible for Eurocodes (TC 250) would hold its first meeting during the week commencing 17 September 1990, in Berlin. A meeting of the sub-group dealing with EC5 is scheduled for 19-20 November. The aim of CEN is to review the draft EC5 in the light of comments received and representatives of all CEN countries will be involved in this activity. A revised draft of EC5 will be issued as a prEN in approximately one year and the final drafting is expected to take between three and four years. MR LARSEN added that there are a number of items still requiring major decisions, eg design of cracked beams, instability design, etc and that the Committee will rely heavily on CIB-W18A input to resolve these.

CEN

MR SUNLEY said that approximately 130 standards on timber related subjects are being written by CEN, with most of these being mandated by the CEC. These standards will mostly be completed in the next two years (by the end of 1992) and about 40 of them are already available as first drafts for comment. They are being prepared in five Committees:-

TC 38 "Wood Preservation" (AFNOR Secretariat) comprises ten working groups, with six concerned with test methods and one looking at hazard classification. The Committee have developed five hazard classes (these are not the same as the EC5 moisture classes) advocating the introduction of results-type rather than process-type specifications for wood preservation. This is giving rise to considerable problems in testing.

TC 103 "Wood Adhesives" (BSI Secretariat) has no working groups. MR VAN DER VELDEN is the Convenor. This group has produced five standards: four relating to test methods and one on adhesives for load-bearing structures, a draft of which is now available.

TC 112 "Wood-based Panel Products" (DIN Secretariat); PROFESSOR NOACK is the Chairman of this group, which has a programme of work for the production of over 70 standards. There are six working groups: WG1 "Particleboard", German Convenor; WG2 "Plywood", French convenor; WG3 "Fibreboard", Italian convenor; WG4 "Test methods", UK convenor; WG5 "Formaldehyde emissions", German convenor; WG6 "Cement bonded particleboard", combined French/UK convenor. Over 20 standards have already been prepared and have been circulated for comment.

TC 124 "Timber Structures" - MR LARSEN is the Chairman of this Committee, which has a programme of work of 25 standards, half of which are already completed as first drafts and are out for public comment. The Committee has four working groups: WG1 "Test methods", Irish convenor; WG2 "Solid timber joints", French/UK convenor; WG3 "Glulam", Danish convenor; WG4 "Timber connectors", German convenor.

TC 175 "Round and sawn timber for non-structural use" has four working groups: WG1 "Definition and methods of measurement", Italian convenor; WG2 "Sawmill output", French/German convenor; WG3 "User requirements", Swedish/UK convenor; WG4 "Round timber", Belgian/Swiss convenor.

There are other CEN Technical Committees which also have a timber part-involvement, including TC 127 "Fire" and TC 139 "Paints and varnishes". DR STIEDA asked what the current situation is within CEN with regard to fire. In reply, MR LARSEN said that the Commission had set up a working group and that this has drafted a proposal for a chapter in EC5 covering fire design. There is much discussion on this draft, which many consider is unacceptable, in that it complicates timber design unduly.

CEI-BOIS/FEMIB

In his report, PROFESSOR BRUNINGHOFF said that the European Glulam Association is very active with regard to promotion, but that no technical work is currently underway. PROFESSOR EHLBECK asked if any activities from this glulam group are appropriate to the work of CEN. PROFESSOR BRUNINGHOFF replied that discussions on thickness of laminations is one such area.

In view of the fact that no technical work is planned for this group for the foreseeable future, it was agreed that a report of CEI-BOIS/FEMIB should not be included on the agenda for future meetings.

IABSE

PROFESSOR EDLUND reported that IABSE is a world-wide association concentrating mainly on structural engineering. It is dominated by people with predominantly steel and concrete interests and despite strenuous efforts, very little interest has been shown in the group by those concerned with timber engineering. PROFESSOR EDLUND is Chairman of WG2, which held a symposium on mixed structures including new materials, in Brussels in early September 1990. This meeting attracted 600 participants, including 110 from Japan, and there were only five contributions on timber with other materials, none of which came from W18A members. A new IABSE periodical (A4 format) is to be published quarterly in 1991. The next meeting of IABSE is in Leningrad, 11-13 September 1991. The deadline for papers was June 1990, but PROFESSOR EDLUND said that abstracts can still be accepted on new applications for timber in bridges.

IUFRO S5.02

DR BLASS said that S5.02 had recently held a meeting at St John in New Brunswick, which included joint RILEM/IUFRO sessions. MR METTEM, who attended the St John meeting, said that concern was expressed that wood scientists, engineers and foresters do not talk sufficiently to each other and this was evident from some of the papers submitted. DR GREEN said that one of the sessions at the recent IUFRO world congress in Montreal was intended to have some more general papers included. The next meeting of IUFRO Division 5 will take place 23-29 August 1992 in Nancy. A meeting of S5.02 will be held the previous week, 17-21 August 1992, in Bordeaux.

1991 INTERNATIONAL TIMBER ENGINEERING CONFERENCE, LONDON

MR MARCROFT reported that 278 abstracts had so far been received, with slightly over 50% coming from outside Europe. A meeting of the Steering Group for the Conference is to be held immediately after this meeting of W18A, to review the abstracts and agree an outline programme. Registration forms will be sent out in February next year.

CIB-W18A 1991, UK

MR ABBOTT reported that provisional arrangements have been made to hold the 1991 meeting of CIB-W18A at Mansfield College, Oxford, UK, from 7-9 September. The meeting will commence on the morning of 7 September and will allow those attending the International Timber Engineering Conference to travel from London to Oxford on 6 September. The meeting will finish at 5.00 pm on 9 September and overnight accommodation will be available for those wishing to stay and depart on 10 September.

CIB-W85 Structural Serviceability

DR OHLSSON gave a brief report of the activities of this working group, which covers serviceability of structures in general. He invited those interested in the group to get in touch with him, either during or after this meeting.

CIB Task Group 6 - Assessment of punched metal plate timber fasteners

PROFESSOR STERN reported that the CIB board established TG 6 in May 1990, with the principal aim of updating the UEATc rule of assessment of punched metal plate timber fasteners (MOAT No 16 of 1979). PROFESSOR EHLBECK asked what is the specific aim of TG6 in particular, he enquired how CIB can establish this group without reference to the chairman of W18A and the RILEM group and was it the intention to parallel existing work? MR LARSEN, who is Chairman of the programme committee responsible for setting up task groups, said that they are defined as having very specific goals: for example, there is a task group on NDT methods for the building envelope. PROFESSOR STERN said that it would be logical if the task group could report to W18A. MR SUNLEY expressed surprise that TG6 had been formed and this view was generally acknowledged by the meeting. It was felt there should have been more detailed discussion within W18A, particularly in view of the work already done on the subject of punched metal plate timber fasteners and trussed rafters. PROFESSOR STERN concluded by saying that all of these issues could be discussed at the first meeting of TG6, which was scheduled to take place immediately after the CIB-W18A meeting.

UNIDO

DR STIEDA reported that a preparatory meeting on consultation on the wood and wood products industry had been held in April 1990 in Nairobi and that a report had been produced. The subject matter is likely to be of greater interest to W18B, although it was not felt that this group would be in a position to respond. MR METTEM asked if there are any plans for an overlap between W18A and W18B. DR STIEDA replied that so far there had not been; however, this could be discussed later in the meeting.

CIB-W18B

There were no members of W18B present at the meeting and no report was given of its activities. MR LARSEN said that CIB were concerned that very little activity was taking place in this group and suggested that perhaps the CIB Secretariat should be reminded that W18A does provide a forum for discussing world wide timber engineering issues. PROFESSOR EDLUND suggested that a joint session with W18B members should be held at the next W18A meeting at Oxford in 1991. This was accepted and it was agreed to make a special effort to invite W18B members to participate in the next meeting.

4. TRUSS RAFTER SUBGROUP

MR RIBERHOLT reported on the truss group set up since the last W18A meeting in Berlin to produce guidelines for the analysis of truss rafters for use in design. This group met in April 1990 and agreed on a working plan to investigate the analysis of trusses by (i) plain frame analysis and (ii) hand calculation methods. This was discussed at the June meeting of a small group in Sweden. MR RIBERHOLT added that he would welcome comments from the meeting on the papers on this subject, which were to be presented later in the meeting.

5. CHARACTERISTIC VALUES SUBGROUP

MR SUNLEY gave a brief report of the activities within this group, which is chaired by PROFESSOR GLOS. CEN TC 124 has drafted a standard on characteristic values for solid timber, which is now out for public comment. Following much discussion, it was agreed that a non-parametric method should be used for calculation of characteristic values.

MR SUNLEY also reported that drafting was in progress for a standard to derive characteristic values for wood-based panels and at the moment, this was based on the assumption of a normal distribution. MR FEWELL added that the paper at the 21st meeting of CIB-W18A at Parksville in 1988 formed the basis of the solid timber standard. It was agreed that the draft standards for panel products and solid timber should be included with the proceedings of this meeting.

6. LIMITS STATES DESIGN

PROFESSOR KUIPERS presented his paper 23-1-1, "Some remarks on the safety of timber structures". Referring to Figure 1 in the paper, MR RIBERHOLT commented that a straight line relationship had been used for the duration of load factor, with the result that a shorter life is given for higher loads. PROFESSOR KUIPERS replied that it is not possible to use the greater strength for short durations of load in design and that the difference is likely to be less for lower coefficients of variation. It was further added that computer calculation methods are needed to verify the hypotheses. MR THELANDERSSON asked if it was valid to assume that no damage occurs until late in the loading history, just before failure, and if not, how would this alter the conclusions. PROFESSOR KUIPERS replied that tests which have been conducted where structures are loaded to high levels of load for short periods do not show damage (as verified by short term failure tests), and that these observations substantiate the assumptions made in the paper.

PROFESSOR RANTA-MAUNUS pointed out that duration of load effects are not only related to damage accumulation. The stress distribution will change with time, resulting in stress peaks caused by creep effects and variations in moisture content. Results on this were presented at the recent IUFRO timber engineering meeting in New Brunswick. DR ENJILY asked what is the relationship between strength reduction factors and the creep factors in EC5. MR LARSEN replied none.

Paper 23-1-2 "Reliability of wood structural elements - a probabilistic method to Eurocode 5 calibration" by Rouger, Lheritier, Racher and Fogli was presented by MR ROUGER. DR BLASS commented that in the section dealing with reliability of bolted joints only three failure modes had been considered, all of which assume elastic behaviour until failure. He asked if consideration had been given to the wood splitting mode. MR ROUGER replied that this was not included in the study: however, it was intended to extend the work to other modes of failure, including elasto-plastic behaviour. DR BLASS went on to ask if the effects of group action had been studied where the influence of the number of fasteners could be greater than, for example, the influence of the failure mode type or moisture content. MR ROUGER accepted this point and agreed that further work is necessary.

DR LEIJTEN pointed out that no duration of load factor had been assumed in the first part of the paper and asked what is the influence on the reliability index when the duration of load factor is less than 1.0. MR ROUGER replied that some work had been done in North America on this and that it is necessary to use stochastic processes for live loads. DR STIEDA added that in North America, work is under way on reliability based design procedures and invited MR O'HALLORAN to give a summary of this. In his reply, MR O'HALLORAN said that the programme had just entered its third and final year and that there currently exists a draft specification with design equations and qualification procedures, including the derivation of characteristic values. Three drafts are soon to be released, covering panel products, solid sawn lumber products and glulam. The aim is to refine the documents by the end of the third year and it is anticipated that there will be a protracted review period, similar to that for Eurocode 5, before it is adopted.

7. TIMBER BEAMS

MR VAN DER PUT presented his paper, 23-10-1 "Tension perpendicular to the grain at notches and joints". MR LARSEN pointed out that for mode 1 splitting, there is little difference between the proposals presented in this paper and those of Gustafsson and asked if this observation is correct. Gustafsson has a reduced stiffness around the notch whereas this paper assumes full stiffness. MR VAN DER PUT replied that it is correct to assume a reduced stiffness adjacent to the notch.

Paper 23-10-2 "Dimensioning beams with cracks, notches and holes - an application of fracture mechanics" by MISS RIIPOLA, was presented by the author. Referring to Figure 2, MR LARSEN commented that the test results do not accord with the theory presented elsewhere in the paper. MISS RIIPOLA accepted this observation and pointed out that it is hoped that a better correlation can be derived when more data is available.

Paper 23-10-3 "Size factors for the bending and tension strength of structural timber" by Barrett and Fewell was presented by DR BARRETT. DR OHLSSON said that when testing deep beams, even in constant moment situations, other failure modes, eg shear, often occur, and asked how this is handled. DR BARRETT agreed and said that great care needs to be taken in any experimental programme and that adjustments should only be applied where appropriate. The percentage of shear failures in the data was very small and those that did occur were in the higher strength members. MR THELANDERSSON pointed out that the Weibull theory assumes that failure occurs at the weakest link and that you have a pure Weibull situation for length effects, but not for width and depth. DR BARRETT agreed and said that statistical theories provide a framework for data analysis and that the paper does not necessarily follow the weakest link theory.

MR RIBERHOLT asked how the narrow test specimens were restrained against lateral buckling. DR BARRETT said that the testing was carried out according to CEN and ASTM methods and that in his experience, lateral buckling had not been a problem. MR FEWELL added that it was necessary to take measures to resist buckling for deep beams, but it is not usually necessary for typical structural sizes. MR LARSEN said that the 0.4 value in the modification factor is influenced by the small depth specimens and asked how these were selected and prepared. MR Fewell replied that the 50mm material was bought from the UK timber trade as commercial material of a quality often used for beam flanges, etc. Mr Larsen further added

that different sized members are used for different applications and questioned whether it was correct to use the results from one size of material, ie for one type of structure as the basis for another. Mr FEWELL replied that this is not an issue, as similar results are obtained if the small size test specimens are ignored.

DR OHLSSON enquired if there is any information on the long-term loading of different sizes of timber. DR BARRETT replied that long-term testing is very expensive and time-consuming to undertake and that a lot of laboratories are having to stop work in this area. DR LEIJTEN asked if it would be possible to give an indication of the density range of the specimens tested. DR BARRETT said that for the North American species, the densities were typically spruce 300 kg/m³, Southern pine 500-550 kg/m³, Douglas fir 500 kg/m³. MR FEWELL said that the UK data includes low-density Sitka spruce and Scandinavian redwood.

8. FRACTURE MECHANICS

Paper 23-19-1 "Determination of the fracture energy of wood with tension perpendicular to the grain" by Rug, Badstube and Schone was presented by DR RUG. DR LEIJTEN said that the paper referred to red pine and whitewood and asked if the presenter could be more specific of the species used. DR RUG replied that they had used *Pinus sylvestris* and *Picea abies*.

Paper 23-19-3 "The fracture energy of wood in tension perpendicular to the grain" by Larsen and Gustaffson was presented by MR LARSEN. MR O'HALLORAN pointed out that there was a transition in the results at a density of 600 kg/m³ and asked the reason for this. MR LARSEN said that the results did not lead to any obvious conclusions. DR GREEN commented that the samples tested came from three mills and were commercially dried material tested as small clears. MR LARSEN said that the use of small clears was important, as even a small knot will significantly reinforce the piece. Also, juvenile wood should not be used, as this leads to unreliable results. DR MEIERHOFER said that moisture content also has a significant effect on fracture energy and asked if this had been investigated. MR LARSEN said that there is no effect if test results are brought to the same density. MR VERGNE asked if it is true that there is a size effect. MR LARSEN replied that it is, if matched specimens are considered, but not for general samples. DR GREEN said that the Forest Products Laboratory in Madison has a similar programme underway with specimens of different moisture content.

9. TRUSSED RAFTERS

Paper 23-14-1 "Analyses of timber trussed rafters of the W type" by Riberholt was presented by the author. MR STONE asked if many failures occur at the heel joint because of the eccentricity of the support, to which MR RIBERHOLT replied that this was not the case. DR EGERUP said that the analysis is based on one particular truss where assumptions have been made regarding geometry and loading. If the top to bottom chord load ratio is increased and there is a different stiffness, will similar results be obtained? MR RIBERHOLT replied that this will be taken account of by the frame analysis and that the theory is independent of such assumptions. DR EGERUP further asked if second order deflections had been taken into account. MR RIBERHOLT replied that they had not. PROFESSOR EDLUND enquired as to the reason for the proposed increase in bending strength. MR RIBERHOLT said there were two reasons:-

1. If there is a bending failure at the top of the T joint (approximately mid-span of the rafter), this is not the same as total failure of the truss
2. the probability of a grade determining defect coinciding with the peak stress is low and therefore it is possible to have an increased moment value at this point.

DR OHLSSON said that from his experience in Sweden, there is strong competition in the truss market, which is resulting in highly engineered products. Emphasis should therefore be placed on using correct loads and member properties in these models.

MR RIBERHOLT then presented his paper 23-14-2 "Proposal for Eurocode 5 test on timber trussed rafters" which was in the form of three annexes. These were discussed in turn:-

Annex 1 "Guidelines for the stress analysis of trussed rafters modelled as plain frames": DR EGERUP asked if anybody has compared the calculation models presented in the paper with full-scale testing. MR RIBERHOLT said that this would be extremely time-consuming to do. However, there are some results. MR KALLSNER said that a similar model has shown a good agreement with test results in Sweden. MR RIBERHOLT added that in Sweden it is also allowed to use a strength increase at the load peak. DR LEIJTEN said that previous codes have only given properties of joints which the engineer can use when designing a structure and asked why the author is proposing a complete calculation method. DR STIEDA added that it was his understanding that this is one of a number of alternative methods. MR RIBERHOLT responded that care is needed when using sophisticated models and that what is presented here are simple procedures. DR LEIJTEN said that structural safety should be determined at the design life and that it is therefore necessary to consider creep, which has a particularly large effect on the rotational stiffness of joints. MR THERLANDERSSON said that the paper presents a calculation method to determine load transfer and distribution, with the aim of arriving at a simple optimum method. DR EGERUP added that long-term safety is not a major problem, based on experience from trusses made in the 1960s.

Annex 2 "Guidelines for the stress analysis of statically determinate fully triangulated timber trussed rafters": there were no comments on this annex.

Annex 3 "Strength verification of the timber in trussed rafters. Special effects": PROFESSOR RANTA-MAUNUS asked if the author had compared the increase in bending strength with the length effects reported by Dr Barrett. MR RIBERHOLT replied that the two effects are not the same, as for trusses total collapse will not result if there is a bending failure in the chord at a moment peak. DR EGERUP commented that there is a combination of an axial force and a moment at such places, to which MR RIBERHOLT replied that this will only be applicable to chord members in compression. MR METTEM asked if the author had considered checking instability in the weakest direction, ie out of plane. MR BURGESS added that there is a completely different basis in the British code for bending out of plane and that the trussed rafter code is for bi-axial bending. MR METTEM urged the committee to look closely at the British Code and at what was done with regard to out of plane instability.

MR THELANDERSSON asked if the methods can be made more general to cover more than simply trussed rafters. Also, has it been considered extending the analysis to using computer programmes, which can take into account second order effects. MR RIBERHOLT replied that there is some disagreement as to what is exactly meant by second order effects and that the programs of which he is aware are not really practical for this application. He further suggested that any extensions should start with non-linearities and then geometric imperfections. PROFESSOR KUIPERS said that the paper refers to trussed rafters, however, the discussion had been about trusses and asked whether the analysis was appropriate to trusses in general. MR RIBERHOLT said that this would be clarified before the final version is produced. DR EGERUP said that second order effects are not important when the assumptions given for the simplified method are followed. Dr Ohlsson commented that it is important to be aware of the relationship between the accuracy of design analysis and what is actually built.

10. LAMINATED MEMBERS

Paper 23-12-1 "Bending strength of glulam beams - a design proposal" by Ehlbeck and Colling, was presented by DR COLLING. MR LARSEN pointed out that the length and depth effects described in the paper are as a result of the model developed at Karlsruhe and asked if they have been verified in practice. DR COLLING replied that this proposal is only valid for high-strength members and therefore is not appropriate if there are large knots. Size effects were determined following tests carried out on beams with a depth of 600 mm, which were modified by size factors. MR LARSEN added that if the theory was extrapolated to deep beams, then the predictions of strength would clearly be far below what was observed in practice. PROFESSOR EHLBECK replied that there will be a reduction of around 30% in strength for a 2.5 m deep beam. MR LARSEN commented that the model had assumed that the ratio of length to depth has no effect and this is not true. PROFESSOR RANTA-MAUNUS pointed out that size effects are already included in the Finnish code. MR LARSEN added that there are no allowances for size effects in the Danish code.

PROFESSOR EDLUND asked if the diagram in the paper was produced from tests results, or from computer simulations. DR COLLING replied that it was calculated on the assumption that size effects are only applicable to beams in excess of 300 mm deep. MR RIBERHOLT asked if the curves are based on statistical distributions or simulations using the Karlsruhe model. DR COLLING replied that they were based on the latter. MR RIBERHOLT went on to say that there will be volume effects using the Karlsruhe model and that it would be of considerable interest to see actual test results. DR COLLING replied that there were some test results published four years ago, but there were no finger joints in the failed region of the samples. MR THELANDERSSON pointed out that the paper states that the characteristic strength of glulam is determined by finger joint failure, whereas in Figure 4, the lowest value in each group is controlled by wood failure - how is this explained? DR COLLING replied that the characteristic value is controlled by finger joint failure. However, the finger joint might not be in a region of highest stress. DR BARRETT asked what distribution has been assumed for finger joint strength. DR COLLING said that regression equations were used from 240 tension tests on finger jointed specimens undertaken by Professor Glos. PROFESSOR EDLUND asked what was the laminate thickness. DR COLLING replied 33 mm.

MR SUNLEY said that if the work had been approached differently, with different models, it might have been possible to have proved that there were no size effects. MR RIBERHOLT added that even though researchers often observe size effects, this does not mean that there must be size effects in codes, for example, there are no size effects in concrete codes. MR LARSEN added that errors within loading codes should not be countermanded by inaccurate materials codes. DR STIEDA commented that this problem should not be approached from the loading side of the equation, but that it should be developed from observations of material effects. MR SUNLEY commented that the first draft of Eurocode 5 had no size effects or enhancements due to the laminating effect because it was considered that they cancel one another out. MR METTEM disagreed with this, pointing out that in his opinion, the enhancement factor for laminating gives more benefit in design than the depth reduction.

Paper 23-12-3 "Glulam beams bending strength in relation to the bending strength of finger joints" by Mr Riberholt, was presented by the author. DR COLLING said that there is little conflict with his previous paper and pointed out that the author had used tests conducted by Larsen and refers to mean values, whereas his work had used five-percentiles. Also, the tests had a mean depth of 200 mm, whereas his results were based on 300 mm, therefore the results should be higher. MR RIBERHOLT said that if the size effects presented by Dr Colling are used, then he would calculate a depth factor of 1.1. DR COLLING replied that if the bending strength of the finger joint equalled the bending strength of the beam, it is not possible to have a factor of 1.0 for other than a one lamination glulam beam.

Paper 23-12-4 "Draft EN TC 124.207 Glued laminated timber strength classes and determination of characteristic properties" by Riberholt, Ehlbeck and Fewell, was presented by MR RIBERHOLT. DR LEIJTEN said that he felt there were some deficiencies in the formulae proposed, in that the values for the strength class system had been used directly to get strength values for glulam, thereby ignoring the lamination thickness. Also, the tension strength values in the proposed system are obtained by factoring the bending values: have these been verified by test? In responding to DR LEIJTEN, MR RIBERHOLT said that the tension values have not been validated by testing glulam beams. DR LEIJTEN went on to add that it was not clear how the values for glulam had been derived. PROFESSOR EHLBECK said that the K_{Lam} factor may have a hidden size factor within it. Also the tension perpendicular to grain figures look incorrect, but there is no evidence as to what the true values should be.

DR WHALE asked if the E_{mean} for laminations is based on the grade determining area, such that the deflection calculations are conservative. PROFESSOR EHLBECK replied that the E values were measured in accordance with ISO 8375 and that he had measured an increase in E for glulam. Referring to Table 1, DR LEIJTEN pointed out that the E_{mean} for LH40 grade is 13,000 N/mm², whereas the calculations give 14000 N/mm² - how is this reconciled? MR RIBERHOLT said that the value in the table had been lowered, based on test evidence on Northern European glulam. MR FEWELL added that it is often not possible to tie up all of the loose ends when writing a draft standard and that these are invariably picked up at the prEN stage.

Paper 23-12-2 "Probability based design methods for glued laminated timber" by MR STONE was presented by the author. There was no technical discussion.

11. STRUCTURAL STABILITY

MR BURGESS presented his paper 23-15-1 "Calculation of a wind girder loaded also by discretely spaced braces or roof members". There was no discussion.

Paper 23-15-2 Stability design and code rules for straight timber beams" by MR VAN DER PUT was presented by the author. MR LARSEN said that many papers on instability are strong on the derivation of equations, but there are no acceptable failure criteria, for example, equation 15 in the paper is not appropriate for bending about two axes. More effort is required on defining the failure criteria. MR VAN DER PUT agreed and said that his work had only looked at bending about one axis. DR BRUNINGHOFF said that there is a great need for all researchers to adopt the same philosophy with regard to calculation procedures dealing with instability problems and how these should be included in codes. DR STIEDA agreed and said that in future meetings, there should be much more discussion about how to tackle this problem with regard to codes. PROFESSOR EHLBECK suggested that W18A should form a subgroup on stability - DR STIEDA agreed to discuss this later as an item under "Any other business".

Paper 23-15-3 "A brief description of formula of beam columns in China code" by Mr Huang was presented by MR LARSEN. In the absence of the author, no discussion was invited.

DR YASUMURA presented his paper 23-15-4 "Seismic behaviour of braced frames in timber construction". DR CECCOTTI pointed out that there are many differences between the European and the Japanese approach concerning seismic behaviour and design: in particular, in Europe it is accepted that the ductility factor cannot be less than 1.0. DR YASUMURA replied that his experimental results gave values less than those obtained by calculation and therefore the ductility factor was less than 1.0. However, he agreed that theoretically, it should not be less than 1.0. DR BLASS asked if it is possible to increase the ductility of connectors by increasing the spacing perpendicular to grain. DR YASUMURA said that this is possible, but up to a limit and he suggested that there would be no increase above approximately 7d.

Paper 23-15-5 "On a better evaluation of the seismic factor of low dissipative timber structures" by DR CECCOTTI was presented by the author. MR VERGNE asked what is the time period of the portals. DR CECCOTTI said that it was half a second.

Paper 23-15-6 "Disproportionate collapse of timber structures" by Mettem and Marcroft was presented by MR MARCROFT. MR LARSEN commented that the paper had set out two interpretations, of which only the second is applicable, and hence TRADA's project should concentrate on this interpretation only. MR MARCROFT commented that although the paper had concluded by advocating the use of the second interpretation, the project needs to continue to consider both interpretations, because of the viewpoint of the UK national body responsible for Building Regulations.

MR O'HALLORAN presented his paper 23-15-7 "Performance of timber frame structures during the Loma Prieta California earthquake". DR STIEDA asked if any attempts have been made to calculate the forces which were imposed on timber structures, both those which had failed and those which remained standing. MR O'HALLORAN said that he had not done this, but that he believed some of the research centres in America had. DR EGERUP asked if an investigation of glulam and other structures had been undertaken. MR O'HALLORAN replied that he had looked at structures other than plywood built after the code change in 1972 and that they had exhibited very little damage.

DR CECCOTTI said that at the seismic behaviour of timber structures workshop in Florence last year, there was a belief that timber structures do not have problems if designed and built correctly.

12. STRESSES FOR SOLID TIMBER

Paper 23-6-1 "Timber compression perpendicular to grain" by Dr Korin was presented by the author. MR METTEM said that it would be useful to look at the deformations in other parts of the structure when certain members had been subjected to high compression perpendicular to grain stresses. DR KORIN agreed. PROFESSOR EHLBECK said that an ISO standard was prepared some 10-15 years ago which gives a definition of the strength perpendicular to grain. DR LEIJTEN commented that the paper compares EC5 values with ASTM values and asked which values were taken from EC5. DR KORIN said that he had used strength vs density relationships. MR LARSEN said that what was really at issue is a serviceability, not an ultimate limit state, and that the design of the specimen cannot lead to failure. He suggested that compression perpendicular to strength values are only appropriate for serviceability concerns. PROFESSOR EHLBECK agreed with this. PROFESSOR RANTA-MAUNUS said that there are occasions when compression perpendicular to grain is not only a serviceability problem: for example, in quality control testing of trusses, where it is often the determining factor for failure. DR LEIJTEN added that you also need compression perpendicular to grain stresses for use in the design formulae for curved beams.

13. TIMBER JOINTS AND FASTENERS

Paper 23-7-1 "Proposal for a design code for nail plates" by Aasheim and Solli was presented by MR AASHEIM. PROFESSOR RANTA-MAUNUS commented that in his opinion the formulae presented are over-simplified. MR AASHEIM replied that the simplified method proposed is only for the steel capacity and that the anchorage formulae developed previously for timber should be used. MR KALLSNER said that the proposed rules for plate capacity seemed to work for normal plates and asked if there was any evidence that they could be applied to other types of plate. MR ASSHEIM replied that they have not tested any other plates in Norway other than those referred to by the paper. MR KALLSNER said that the paper gives rules for compression of the plate itself but not for the joint as a whole and in design it is possible to use the contact between timber members in bearing, but that this is not done in the test method.

Paper 23-7-2 "Load distribution in nailed joints" by Dr Blass was presented by the author. MR STONE asked if the nail spacing had any effect on the results presented. DR BLASS replied that if the load slip behaviour is as shown, with substantial yield, then load spacing has no effect. However, this is not the case if timber splitting results. MR SUNLEY asked why the work had concentrated on nails but not on bolts. DR BLASS replied that this was primarily due to the ease of testing with nailed joints. PROFESSOR STERN asked what nail diameter can be accounted for. DR BLASS replied that this will depend upon the nature of the load slip characteristics. MR METTEM said that with large fasteners, manufacturing tolerances are very important and that there will be a significant difference in joint behaviour with and without pre-drilled holes. MR LARSEN said that it is important to develop a theory which can model reality.

14. ANY OTHER BUSINESS

1. Trussed rafter subgroup - this subgroup has now completed its work and it was therefore recommended by the Chairman MR RIBERHOLT that the group be discontinued. This was accepted by the meeting. DR STIEDA thanked MR RIBERHOLT and the other members of the group for their work which was much appreciated.

2. Stability of structures - a proposal to create a new subgroup dealing with stability of structures was put to the meeting and agreed. PROFESSOR BRUNINGHOFF was elected as chairman. The objectives of the group were set as:-

- i. to prepare recommendations on analysis procedures which can be used by design engineers. This will include development of rules for standards for design of elements (columns, beams, bracing);
- ii. to determine guidelines for inclusion in design codes for stability problems.

PROFESSOR EDLUND said that it was important that the group should address stability problems in general and not just matters relating to bracing. This was accepted. DR STIEDA asked those who had an interest in structural stability and were willing to participate in the workings of this group to contact PROFESSOR BRUNINGHOFF.

3. Subgroup on board materials. There was a suggestion that there could be a need for the formation of a further subgroup dealing with panel products matters. PROFESSOR EHLBECK said that he felt this was not really necessary, as such matters could be discussed by CEN TC 112. MR LARSEN replied that there was still a need for more global requirements for panel products. MR SUNLEY agreed with this, and said it was important to redress the balance of timber versus panel products. DR STIEDA accepted that there is a valid need for a subgroup on panel products, which should have the primary aim of developing procedures for the derivation of characteristic values. MR ELIAS was asked to chair this subgroup, and he agreed. It was agreed that a report on the workings of this group would be presented at the meeting next year.

4. Venues for next meetings:-

- 1991 - to be held at Mansfield College Oxford, commencing in the morning of Saturday 7 September and finishing pm on Monday 9 September.
- 1992 - Sweden, tentative date week beginning 24 August.
- 1993 - France, proposed for either 2nd or 3rd week of September.
- 1994 or 1995 - Germany (Karlsruhe).
- 1995 or 1994 - Atlanta Georgia.

5. Overheads - the Chairman made a plea for more legible overheads to be prepared for future meetings.

6. Chairman - DR STIEDA announced his intention of resigning as chairman of W18A after the 24th meeting in Oxford in 1991. A small committee comprising MR LARSEN, MR SUNLEY and PROFESSOR EHLBECK was appointed to identify a successor.

7. Programme for next meeting - the following were suggested as priority themes for the next meeting:-

- 1. drafts of standards - need for more commentary on standards and codes to give a clear understanding of the background
- 2. seismic design
- 3. fire/hot design

8. Close - the Chairman expressed his thanks to MR DE SOUSA and his staff for their efficient organisation of this meeting. He also expressed his thanks to the various contributors, to MR ABBOTT and the staff at TRADA for their work as secretary and in preparing the papers for the meeting, and to DR BLASS and his colleagues at Karlsruhe for their preparation of the proceedings. DR STIEDA then closed the 23rd meeting of CIB-W18A and said he looked forward to seeing members in Oxford, England next year for the 24th meeting, to be held from 7-9 September.

15. List of CIB-W18A Papers
Lisbon, Portugal 1990

15. LIST OF CIB-W18A PAPERS
LISBON, PORTUGAL 1990

- 23-1-1 Some Remarks about the Safety of Timber Structures -
J Kuipers
- 23-1-2 Reliability of Wood Structural Elements: A Probabilistic
Method to Eurocode 5 Calibration - F Rouger, N Lheritier,
P Racher and M Fogli
- 23-6-1 Timber in Compression Perpendicular to Grain - U Korin
- 23-7-1 Proposal for a Design Code for Nail Plates - E Aasheim and
K H Solli
- 23-7-2 Load Distribution in Nailed Joints - H J Blass
- 23-10-1 Tension Perpendicular to the Grain at Notches and Joints -
T A C M van der Put
- 23-10-2 Dimensioning of Beams with Cracks, Notches and Holes.
An Application of Fracture Mechanics - K Riipola
- 23-10-3 Size Factors for the Bending and Tension Strength of
Structural Timber - J D Barret and A R Fewell
- 23-12-1 Bending Strength of Glulam Beams, a Design Proposal -
J Ehlbeck and F Colling
- 23-12-2 Probability Based Design Method for Glued Laminated Timber -
M F Stone
- 23-12-3 Glulam Beams, Bending Strength in Relation to the Bending
Strength of the Finger Joints - H Riberholt
- 23-12-4 Glued Laminated Timber - Strength Classes and Determination
of Characteristic Properties - H Riberholt, J Ehlbeck and
A Fewell
- 23-14-1 Analyses of Timber Trussed Rafters of the W-Type -
H Riberholt
- 23-14-2 Proposal for Eurocode 5 Text on Timber Trussed Rafters -
H Riberholt
- 23-15-1 Calculation of a Wind Girder Loaded also by Discretely
Spaced Braces for Roof Members - H J Burgess
- 23-15-2 Stability Design and Code Rules for Straight Timber Beams -
T A C M van der Put
- 23-15-3 A Brief Description of Formula of Beam-Columns in China Code
- S Y Huang
- 23-15-4 Seismic Behavior of Braced Frames in Timber Construction -
M Yasumara

- 23-15-5 On a Better Evaluation of the Seismic Behavior Factor of Low-Dissipative Timber Structures - A Ceccotti and A Vignoli
- 23-15-6 Disproportionate Collapse of Timber Structures - C J Mettem and J P Marcroft
- 23-15-7 Performance of Timber Frame Structures During the Loma Prieta California Earthquake - M R O'Halloran and E G Elias
- 23-19-1 Determination of the Fracture Energie of Wood for Tension Perpendicular to the Grain - W Rug, M Badstube and W Schöne
- 23-19-2 The Fracture Energy of Wood in Tension Perpendicular to the Grain. Results from a Joint Testing Project - H J Larsen and P J Gustafsson
- 23-19-3 Application of Fracture Mechanics to Timber Structures - A Ranta-Maunus

16. CURRENT LIST OF CIB-W18A PAPERS

Technical papers presented to CIB-W18A are identified by a code CIB-W18A/a-b-c, where:

a denotes the meeting at which the paper was presented. Meetings are classified in chronological order:

- 1 Princes Risborough, England; March 1973
- 2 Copenhagen, Denmark; October 1973
- 3 Delft, Netherlands; June 1974
- 4 Paris, France; February 1975
- 5 Karlsruhe, Federal Republic of Germany; October 1975
- 6 Aalborg, Denmark; June 1976
- 7 Stockholm, Sweden; February/March 1977
- 8 Brussels, Belgium; October 1977
- 9 Perth, Scotland; June 1978
- 10 Vancouver, Canada; August 1978
- 11 Vienna, Austria; March 1979
- 12 Bordeaux, France; October 1979
- 13 Otaniemi, Finland; June 1980
- 14 Warsaw, Poland; May 1981
- 15 Karlsruhe, Federal Republic of Germany; June 1982
- 16 Lillehammer, Norway; May/June 1983
- 17 Rapperswil, Switzerland; May 1984
- 18 Beit Oren, Israel; June 1985
- 19 Florence, Italy; September 1986
- 20 Dublin, Ireland; September 1987
- 21 Parksville, Canada; September 1988
- 22 Berlin, German Democratic Republic; September 1989
- 23 Lisbon, Portugal; September 1990
- 24 Oxford, United Kingdom; September 1991

b denotes the subject:

- | | |
|--|-------------------------------|
| 1 Limit State Design | 7 Timber Joints and Fasteners |
| 2 Timber Columns | 8 Load Sharing |
| 3 Symbols | 9 Duration of Load |
| 4 Plywood | 10 Timber Beams |
| 5 Stress Grading | 11 Environmental Conditions |
| 6 Stresses for Solid Timber | 12 Laminated Members |
| 13 Particle and Fibre Building Boards | |
| 14 Trussed Rafters | |
| 15 Structural Stability | |
| 16 Fire | |
| 17 Statistics and Data Analysis | |
| 18 Glued Joints | |
| 19 Fracture Mechanics | |
| 100 CIB Timber Code | |
| 101 Loading Codes | |
| 102 Structural Design Codes | |
| 103 International Standards Organisation | |
| 104 Joint Committee on Structural Safety | |
| 105 CIB Programme, Policy and Meetings | |
| 106 International Union of Forestry Research Organisations | |

c is simply a number given to the papers in the order in which they

16. Current List of CIB-W18A Papers

16. CURRENT LIST OF CIB-W18A PAPERS

Technical papers presented to CIB-W18A are identified by a code CIB-W18A/a-b-c, where:

a denotes the meeting at which the paper was presented. Meetings are classified in chronological order:

- 1 Princes Risborough, England; March 1973
- 2 Copenhagen, Denmark; October 1973
- 3 Delft, Netherlands; June 1974
- 4 Paris, France; February 1975
- 5 Karlsruhe, Federal Republic of Germany; October 1975
- 6 Aalborg, Denmark; June 1976
- 7 Stockholm, Sweden; February/March 1977
- 8 Brussels, Belgium; October 1977
- 9 Perth, Scotland; June 1978
- 10 Vancouver, Canada; August 1978
- 11 Vienna, Austria; March 1979
- 12 Bordeaux, France; October 1979
- 13 Otaniemi, Finland; June 1980
- 14 Warsaw, Poland; May 1981
- 15 Karlsruhe, Federal Republic of Germany; June 1982
- 16 Lillehammer, Norway; May/June 1983
- 17 Rapperswil, Switzerland; May 1984
- 18 Beit Oren, Israel; June 1985
- 19 Florence, Italy; September 1986
- 20 Dublin, Ireland; September 1987
- 21 Parksville, Canada; September 1988
- 22 Berlin, German Democratic Republic; September 1989
- 23 Lisbon, Portugal; September 1990
- 24 *Subject, World Programme, 1991-1992*

b denotes the subject:

- | | |
|--|-------------------------------|
| 1 Limit State Design | 7 Timber Joints and Fasteners |
| 2 Timber Columns | 8 Load Sharing |
| 3 Symbols | 9 Duration of Load |
| 4 Plywood | 10 Timber Beams |
| 5 Stress Grading | 11 Environmental Conditions |
| 6 Stresses for Solid Timber | 12 Laminated Members |
| 13 Particle and Fibre Building Boards | |
| 14 Trussed Rafters | |
| 15 Structural Stability | |
| 16 Fire | |
| 17 Statistics and Data Analysis | |
| 18 Glued Joints | |
| 19 Fracture Mechanics | |
| 100 CIB Timber Code | |
| 101 Loading Codes | |
| 102 Structural Design Codes | |
| 103 International Standards Organisation | |
| 104 Joint Committee on Structural Safety | |
| 105 CIB Programme, Policy and Meetings | |
| 106 International Union of Forestry Research Organisations | |

c is simply a number given to the papers in the order in which they appear:

Example: CIB-W18/4-102-5 refers to paper 5 on subject 102 presented at the fourth meeting of W18.

Listed below, by subjects, are all papers that have to date been presented to W18. When appropriate some papers are listed under more than one subject heading.

LIMIT STATE DESIGN

- 1-1-1 Limit State Design - H J Larsen
- 1-1-2 The Use of Partial Safety Factors in the New Norwegian Design Code for Timber Structures - O Brynildsen
- 1-1-3 Swedish Code Revision Concerning Timber Structures - B Norén
- 1-1-4 Working Stresses Report to British Standards Institution Committee BLC/17/2
- 6-1-1 On the Application of the Uncertainty Theoretical Methods for the Definition of the Fundamental Concepts of Structural Safety - K Skov and O Ditlevsen
- 11-1-1 Safety Design of Timber Structures - H J Larsen
- 18-1-1 Notes on the Development of a UK Limit States Design Code for Timber - A R Fewell and C B Pierce
- 18-1-2 Eurocode 5, Timber Structures - H J Larsen
- 19-1-1 Duration of Load Effects and Reliability Based Design (Single Member) - R O Foschi and Z C Yao
- 21-102-1 Research Activities Towards a New GDR Timber Design Code Based on Limit States Design - W Rug and M Badstube
- 22-1-1 Reliability-Theoretical Investigation into Timber Components A Proposal for a Supplement of the Design Concept - M Badstube, W Rug and R Plessow
- 23-1-1 Some Remarks about the Safety of Timber Structures - J Kuipers
- 23-1-2 Reliability of Wood Structural Elements: A Probabilistic Method to Eurocode 5 Calibration - F Rouger, N Lheritier, P Racher and M Fogli

TIMBER COLUMNS

- 2-2-1 The Design of Solid Timber Columns - H J Larsen
- 3-2-1 The Design of Built-Up Timber Columns - H J Larsen
- 4-2-1 Tests with Centrally Loaded Timber Columns - H J Larsen and S S Pedersen

- 4-2-2 Lateral-Torsional Buckling of Eccentrically Loaded Timber Columns - B Johansson
- 5-9-1 Strength of a Wood Column in Combined Compression and Bending with Respect to Creep - B Källsner and B Norén
- 5-100-1 Design of Solid Timber Columns (First Draft) - H J Larsen
- 6-100-1 Comments on Document 5-100-1, Design of Solid Timber Columns - H J Larsen and E Theilgaard
- 6-2-1 Lattice Columns - H J Larsen
- 6-2-2 A Mathematical Basis for Design Aids for Timber Columns - H J Burgess
- 6-2-3 Comparison of Larsen and Perry Formulas for Solid Timber Columns - H J Burgess
- 7-2-1 Lateral Bracing of Timber Struts - J A Simon
- 8-15-1 Laterally Loaded Timber Columns: Tests and Theory - H J Larsen
- 17-2-1 Model for Timber Strength under Axial Load and Moment - T Poutanen
- 18-2-1 Column Design Methods for Timber Engineering - A H Buchanan, K C Johns, B Madsen
- 19-2-1 Creep Buckling Strength of Timber Beams and Columns - R H Leicester
- 19-12-2 Strength Model for Glulam Columns - H J Blaß
- 20-2-1 Lateral Buckling Theory for Rectangular Section Deep Beam-Columns - H J Burgess
- 20-2-2 Design of Timber Columns - H J Blaß
- 21-2-1 Format for Buckling Strength - R H Leicester
- 21-2-2 Beam-Column Formulae for Design Codes - R H Leicester
- 21-15-1 Rectangular Section Deep Beam - Columns with Continuous Lateral Restraint - H J Burgess
- 21-15-2 Buckling Modes and Permissible Axial Loads for Continuously Braced Columns - H J Burgess
- 21-15-3 Simple Approaches for Column Bracing Calculations - H J Burgess
- 21-15-4 Calculations for Discrete Column Restraints - H J Burgess

- 22-2-1 Buckling and Reliability Checking of Timber Columns -
S Huang, P M Yu and J Y Hong
- 22-2-2 Proposal for the Design of Compressed Timber Members by
Adopting the Second-Order Stress Theory - P Kaiser

SYMBOLS

- 3-3-1 Symbols for Structural Timber Design - J Kuipers and B Norén
- 4-3-1 Symbols for Timber Structure Design - J Kuipers and B Norén
- 1 Symbols for Use in Structural Timber Design

PLYWOOD

- 2-4-1 The Presentation of Structural Design Data for Plywood
- L G Booth
- 3-4-1 Standard Methods of Testing for the Determination of
Mechanical Properties of Plywood - J Kuipers
- 3-4-2 Bending Strength and Stiffness of Multiple Species Plywood
- C K A Stieda
- 4-4-4 Standard Methods of Testing for the Determination of
Mechanical Properties of Plywood - Council of Forest
Industries, B.C.
- 5-4-1 The Determination of Design Stresses for Plywood in the
Revision of CP 112 - L G Booth
- 5-4-2 Veneer Plywood for Construction - Quality Specifications
- ISO/TC 139. Plywood, Working Group 6
- 6-4-1 The Determination of the Mechanical Properties of Plywood
Containing Defects - L G Booth
- 6-4-2 Comparison of the Size and Type of Specimen and Type of Test
on Plywood Bending Strength and Stiffness - C R Wilson and
P Eng
- 6-4-3 Buckling Strength of Plywood: Results of Tests and
Recommendations for Calculations - J Kuipers and
H Ploos van Amstel
- 7-4-1 Methods of Test for the Determination of Mechanical
Properties of Plywood - L G Booth, J Kuipers, B Norén,
C R Wilson
- 7-4-2 Comments Received on Paper 7-4-1
- 7-4-3 The Effect of Rate of Testing Speed on the Ultimate Tensile
Stress of Plywood - C R Wilson and A V Parasin

- 7-4-4 Comparison of the Effect of Specimen Size on the Flexural Properties of Plywood Using the Pure Moment Test - C R Wilson and A V Parasin
- 8-4-1 Sampling Plywood and the Evaluation of Test Results - B Norén
- 9-4-1 Shear and Torsional Rigidity of Plywood - H J Larsen
- 9-4-2 The Evaluation of Test Data on the Strength Properties of Plywood - L G Booth
- 9-4-3 The Sampling of Plywood and the Derivation of Strength Values (Second Draft) - B Norén
- 9-4-4 On the Use of the CIB/RILEM Plywood Plate Twisting Test: a progress report - L G Booth
- 10-4-1 Buckling Strength of Plywood - J Dekker, J Kuipers and H Ploos van Amstel
- 11-4-1 Analysis of Plywood Stressed Skin Panels with Rigid or Semi-Rigid Connections - I Smith
- 11-4-2 A Comparison of Plywood Modulus of Rigidity Determined by the ASTM and RILEM CIB/3-TT Test Methods - C R Wilson and A V Parasin
- 11-4-3 Sampling of Plywood for Testing Strength - B Norén
- 12-4-1 Procedures for Analysis of Plywood Test Data and Determination of Characteristic Values Suitable for Code Presentation - C R Wilson
- 14-4-1 An Introduction to Performance Standards for Wood-base Panel Products - D H Brown
- 14-4-2 Proposal for Presenting Data on the Properties of Structural Panels - T Schmidt
- 16-4-1 Planar Shear Capacity of Plywood in Bending - C K A Stieda
- 17-4-1 Determination of Panel Shear Strength and Panel Shear Modulus of Beech-Plywood in Structural Sizes - J Ehlbeck and F Colling
- 17-4-2 Ultimate Strength of Plywood Webs - R H Leicester and L Pham
- 20-4-1 Considerations of Reliability - Based Design for Structural Composite Products - M R O'Halloran, J A Johnson, E G Elias and T P Cunningham
- 21-4-1 Modelling for Prediction of Strength of Veneer Having Knots - Y Hirashima

- 22-4-1 Scientific Research into Plywood and Plywood Building Constructions the Results and Findings of which are Incorporated into Construction Standard Specifications of the USSR - I M Guskov
- 22-4-2 Evaluation of Characteristic values for Wood-Based Sheet Materials - E G Elias
- 2-5-1 Fundamental Vibration Frequency as a Parameter for Grading Sawn Timber - T Nakai, T Tanaka and H Nagao

STRESS GRADING

- 1-5-1 Quality Specifications for Sawn Timber and Precision Timber - Norwegian Standard NS 3080
- 1-5-2 Specification for Timber Grades for Structural Use - British Standard BS 4978
- 4-5-1 Draft Proposal for an International Standard for Stress Grading Coniferous Sawn Softwood - ECE Timber Committee
- 16-5-1 Grading Errors in Practice - B Thunell
- 16-5-2 On the Effect of Measurement Errors when Grading Structural Timber - L Nordberg and B Thunell
- 19-5-1 Stress-Grading by ECE Standards of Italian-Grown Douglas-Fir Dimension Lumber from Young Thinnings - L Uzielli
- 19-5-2 Structural Softwood from Afforestation Regions in Western Norway - R Lackner
- 21-5-1 Non-Destructive Test by Frequency of Full Size Timber for Grading - T Nakai

STRESSES FOR SOLID TIMBER

- 4-6-1 Derivation of Grade Stresses for Timber in the UK - W T Curry
- 5-6-1 Standard Methods of Test for Determining some Physical and Mechanical Properties of Timber in Structural Sizes - W T Curry
- 5-6-2 The Description of Timber Strength Data - J R Tory
- 5-6-3 Stresses for EC1 and EC2 Stress Grades - J R Tory
- 6-6-1 Standard Methods of Test for the Determination of some Physical and Mechanical Properties of Timber in Structural Sizes (third draft) - W T Curry
- 7-6-1 Strength and Long-term Behaviour of Lumber and Glued Laminated Timber under Torsion Loads - K Möhler
- 9-6-1 Classification of Structural Timber - H J Larsen

- 9-6-2 Code Rules for Tension Perpendicular to Grain - H J Larsen
- 9-6-3 Tension at an Angle to the Grain - K Möhler
- 9-6-4 Consideration of Combined Stresses for Lumber and Glued Laminated Timber - K Möhler
- 11-6-1 Evaluation of Lumber Properties in the United States - W L Galligan and J H Haskell
- 11-6-2 Stresses Perpendicular to Grain - K Möhler
- 11-6-3 Consideration of Combined Stresses for Lumber and Glued Laminated Timber (addition to Paper CIB-W18/9-6-4) - K Möhler
- 12-6-1 Strength Classifications for Timber Engineering Codes - R H Leicester and W G Keating
- 12-6-2 Strength Classes for British Standard BS 5268 - J R Tory
- 13-6-1 Strength Classes for the CIB Code - J R Tory
- 13-6-2 Consideration of Size Effects and Longitudinal Shear Strength for Uncracked Beams - R O Foschi and J D Barrett
- 13-6-3 Consideration of Shear Strength on End-Cracked Beams - J D Barrett and R O Foschi
- 15-6-1 Characteristic Strength Values for the ECE Standard for Timber - J G Sunley
- 16-6-1 Size Factors for Timber Bending and Tension Stresses - A R Fewell
- 16-6-2 Strength Classes for International Codes - A R Fewell and J G Sunley
- 17-6-1 The Determination of Grade Stresses from Characteristic Stresses for BS 5268: Part 2 - A R Fewell
- 17-6-2 The Determination of Softwood Strength Properties for Grades, Strength Classes and Laminated Timber for BS 5268: Part 2 - A R Fewell
- 18-6-1 Comment on Papers: 18-6-2 and 18-6-3 - R H Leicester
- 18-6-2 Configuration Factors for the Bending Strength of Timber - R H Leicester
- 18-6-3 Notes on Sampling Factors for Characteristic Values - R H Leicester
- 18-6-4 Size Effects in Timber Explained by a Modified Weakest Link Theory - B Madsen and A H Buchanan

- 18-6-5 Placement and Selection of Growth Defects in Test Specimens
- H Riberholt
- 18-6-6 Partial Safety-Coefficients for the Load-Carrying Capacity
of Timber Structures - B Norén and J-O Nylander
- 19-6-1 Effect of Age and/or Load on Timber Strength - J Kuipers
- 19-6-2 Confidence in Estimates of Characteristic Values
- R H Leicester
- 19-6-3 Fracture Toughness of Wood - Mode I - K Wright and
M Fonselius
- 19-6-4 Fracture Toughness of Pine - Mode II - K Wright
- 19-6-5 Drying Stresses in Round Timber - A Ranta-Maunus
- 19-6-6 A Dynamic Method for Determining Elastic Properties
of Wood - R Görlacher
- 20-6-1 A Comparative Investigation of the Engineering Properties of
"Whitewoods" Imported to Israel from Various Origins
- U Korin
- 20-6-2 Effects of Yield Class, Tree Section, Forest and Size on
Strength of Home Grown Sitka Spruce - V Picardo
- 20-6-3 Determination of Shear Strength and Strength Perpendicular
to Grain - H J Larsen
- 21-6-1 Draft Australian Standard: Methods for Evaluation of
Strength and Stiffness of Graded Timber - R H Leicester
- 21-6-2 The Determination of Characteristic Strength Values for
Stress Grades of Structural Timber. Part 1 - A R Fewell
and P Glos
- 21-6-3 Shear Strength in Bending of Timber -
U Korin
- 22-6-1 Size Effects and Property Relationships for Canadian 2-inch
Dimension Lumber - J D Barrett and H Griffin
- 22-6-2 Moisture Content Adjustements for In-Grade Data -
J D Barrett and W Lau
- 22-6-3 A Discussion of Lumber Property Relationships in
Eurocode 5 - D W Green and D E Kretschmann
- 22-6-4 Effect of Wood Preservatives on the Strength Properties of
Wood - F Ronai
- 23-6-1 Timber in Compression Perpendicular to Grain - U Korin

TIMBER JOINTS AND FASTENERS

- 1-7-1 Mechanical Fasteners and Fastenings in Timber Structures
- E G Stern
- 4-7-1 Proposal for a Basic Test Method for the Evaluation of
Structural Timber Joints with Mechanical Fasteners and
Connectors - RILEM 3TT Committee
- 4-7-2 Test Methods for Wood Fasteners - K Möhler
- 5-7-1 Influence of Loading Procedure on Strength and
Slip-Behaviour in Testing Timber Joints - K Möhler
- 5-7-2 Recommendations for Testing Methods for Joints with
Mechanical Fasteners and Connectors in Load-Bearing Timber
Structures - RILEM 3 TT Committee
- 5-7-3 CIB-Recommendations for the Evaluation of Results of Tests
on Joints with Mechanical Fasteners and Connectors used in
Load-Bearing Timber Structures - J Kuipers
- 6-7-1 Recommendations for Testing Methods for Joints with
Mechanical Fasteners and Connectors in Load-Bearing Timber
Structures (seventh draft) - RILEM 3 TT Committee
- 6-7-2 Proposal for Testing Integral Nail Plates as Timber Joints
- K Möhler
- 6-7-3 Rules for Evaluation of Values of Strength and Deformation
from Test Results - Mechanical Timber Joints - M Johansen,
J Kuipers, B Norén
- 6-7-4 Comments to Rules for Testing Timber Joints and Derivation
of Characteristic Values for Rigidity and Strength - B Norén
- 7-7-1 Testing of Integral Nail Plates as Timber Joints - K Möhler
- 7-7-2 Long Duration Tests on Timber Joints - J Kuipers
- 7-7-3 Tests with Mechanically Jointed Beams with a Varying Spacing
of Fasteners - K Möhler
- 7-100-1 CIB-Timber Code Chapter 5.3 Mechanical Fasteners;
CIB-Timber Standard 06 and 07 - H J Larsen
- 9-7-1 Design of Truss Plate Joints - F J Keenan
- 9-7-2 Staples - K Möhler
- 11-7-1 A Draft Proposal for International Standard: ISO Document
ISO/TC 165N 38E
- 12-7-1 Load-Carrying Capacity and Deformation Characteristics of
Nailed Joints - J Ehlbeck

- 12-7-2 Design of Bolted Joints - H J Larsen
- 12-7-3 Design of Joints with Nail Plates - B Norén
- 13-7-1 Polish Standard BN-80/7159-04: Parts 00-01-02-03-04-05.
"Structures from Wood and Wood-based Materials. Methods of
Test and Strength Criteria for Joints with Mechanical
Fasteners"
- 13-7-2 Investigation of the Effect of Number of Nails in a Joint on
its Load Carrying Ability - W Nozynski
- 13-7-3 International Acceptance of Manufacture, Marking and Control
of Finger-jointed Structural Timber - B Norén
- 13-7-4 Design of Joints with Nail Plates - Calculation of Slip
- B Norén
- 13-7-5 Design of Joints with Nail Plates - The Heel Joint
- B Källsner
- 13-7-6 Nail Deflection Data for Design - H J Burgess
- 13-7-7 Test on Bolted Joints - P Vermeyden
- 13-7-8 Comments to paper CIB-W18/12-7-3 "Design of Joints with Nail
Plates" - B Norén
- 13-7-9 Strength of Finger Joints - H J Larsen
- 13-100-4 CIB Structural Timber Design Code. Proposal for Section
6.1.5 Nail Plates - N I Bovim
- 14-7-1 Design of Joints with Nail Plates (second edition)
- B Norén
- 14-7-2 Method of Testing Nails in Wood (second draft,
August 1980) - B Norén
- 14-7-3 Load-Slip Relationship of Nailed Joints
- J Ehlbeck and H J Larsen
- 14-7-4 Wood Failure in Joints with Nail Plates - B Norén
- 14-7-5 The Effect of Support Eccentricity on the Design of W- and
WW-Trussed with Nail Plate Connectors - B Källsner
- 14-7-6 Derivation of the Allowable Load in Case of Nail Plate
Joints Perpendicular to Grain - K Möhler
- 14-7-7 Comments on CIB-W18/14-7-1 - T A C M van der Put
- 15-7-1 Final Recommendation TT-1A: Testing Methods for Joints with
Mechanical Fasteners in Load-Bearing Timber Structures.
Annex A Punched Metal Plate Fasteners - Joint Committee
RILEM/CIB-3TT

- 16-7-1 Load Carrying Capacity of Dowels - E Gehri
- 16-7-2 Bolted Timber Joints: a Literature Survey - N Harding
- 16-7-3 Bolted Timber Joints: Practical Aspects of Construction and Design; a Survey - N Harding
- 16-7-4 Bolted Timber Joints: Draft Experimental Work Plan - Building Research Association of New Zealand
- 17-7-1 Mechanical Properties of Nails and their Influence on Mechanical Properties of Nailed Timber Joints Subjected to Lateral Loads - I Smith, L R J Whale, C Anderson and L Held
- 17-7-2 Notes on the Effective Number of Dowels and Nails in Timber Joints - G Steck
- 18-7-1 Model Specification for Driven Fasteners for Assembly of Pallets and Related Structures - E G Stern and W B Wallin
- 18-7-2 The Influence of the Orientation of Mechanical Joints on their Mechanical Properties - I Smith and L R J Whale
- 18-7-3 Influence of Number of Rows of Fasteners or Connectors upon the Ultimate Capacity of Axially Loaded Timber Joints - I Smith and G Steck
- 18-7-4 A Detailed Testing Method for Nailplate Joints - J Kangas
- 18-7-5 Principles for Design Values of Nailplates in Finland - J Kangas
- 18-7-6 The Strength of Nailplates - N I Bovim and E Aasheim
- 19-7-1 Behaviour of Nailed and Bolted Joints under Short-Term Lateral Load - Conclusions from Some Recent Research - L R J Whale, I Smith B O Hilson
- 19-7-2 Glued Bolts in Glulam - H Riberholt
- 19-7-3 Effectiveness of Multiple Fastener Joints According to National Codes and Eurocode 5 (Draft) - G Steck
- 19-7-4 The Prediction of the Long-Term Load Carrying Capacity of Joints in Wood Structures - Y M Ivanov and Y Y Slavic
- 19-7-5 Slip in Joints under Long-Term Loading - T Feldborg and M Johansen
- 19-7-6 The Derivation of Design Clauses for Nailed and Bolted Joints in Eurocode 5 - L R J Whale and I Smith
- 19-7-7 Design of Joints with Nail Plates - Principles - B Norén
- 19-7-8 Shear Tests for Nail Plates - B Norén

- 19-7-9 Advances in Technology of Joints for Laminated Timber
- Analyses of the Structural Behaviour - M Piazza and
G Turrini
- 19-15-1 Connections Deformability in Timber Structures:
a Theoretical Evaluation of its Influence on Seismic Effects
- A Ceccotti and A Vignoli
- 20-7-1 Design of Nailed and Bolted Joints-Proposals for the
Revision of Existing Formulae in Draft Eurocode 5 and the
CIB Code - L R J Whale, I Smith and H J Larsen
- 20-7-2 Slip in Joints under Long Term Loading - T Feldborg and
M Johansen
- 20-7-3 Ultimate Properties of Bolted Joints in Glued-Laminated
Timber - M Yasumura, T Murota and H Sakai
- 20-7-4 Modelling the Load-Deformation Behaviour of Connections with
Pin-Type Fasteners under Combined Moment, Thrust and Shear
Forces - I Smith
- 21-7-1 Nails under Long-Term Withdrawal Loading - T Feldborg
and M Johansen
- 21-7-2 Glued Bolts in Glulam-Proposals for CIB Code -
H Riberholt
- 21-7-3 Nail Plate Joint Behaviour under Shear Loading -
T Poutanen
- 21-7-4 Design of Joints with Laterally Loaded Dowels. Proposals for
Improving the Design Rules in the CIB Code and the Draft
Eurocode 5 - J Ehlbeck and H Werner
- 21-7-5 Axially Loaded Nails: Proposals for a Supplement to the
CIB Code - J Ehlbeck and W Siebert
- 22-7-1 End Grain Connections with Laterally Loaded Steel Bolts
A draft proposal for design rules in the CIB Code -
J Ehlbeck and M Gerold
- 22-7-2 Determination of Perpendicular-to-Grain Tensile Stresses in
Joints with Dowel-Type Fasteners - A draft proposal for
design rules - J Ehlbeck, R Görlacher and H Werner
- 22-7-3 Design of Double-Shear Joints with Non-Metallic Dowels
A proposal for a supplement of the design concept -
J Ehlbeck and O Eberhart
- 22-7-4 The Effect of Load on Strength of Timber Joints at high
Working Load Level - A J M Leijten
- 22-7-5 Plasticity Requirements for Portal Frame Corners -
R Gunnewijk and A J M Leijten

- 22-7-6 Background Information on Design of Glulam Rivet Connections in CSA/CAN3-086.1-M89 - A proposal for a supplement of the design concept - E Karacabeyli and D P Janssens
- 22-7-7 Mechanical Properties of Joints in Glued-Laminated Beams under Reversed Cyclic Loading - M Yasumura
- 22-7-8 Strength of Glued Lap Timber Joints - P Glos and H Horstmann
- 22-7-9 Toothed Rings Type Bistyp 075 at the Joints of Fir Wood - J Kerste
- 22-7-10 Calculation of Joints and Fastenings as Compared with the International State - K Zimmer and K Lissner
- 22-7-11 Joints on Glued-in Steel Bars Present Relatively New and Progressive Solution in Terms of Timber Structure Design - G N Zubarev, F A Boitemirov and V M Golovina
- 22-7-12 The Development of Design Codes for Timber Structures made of Compositive Bars with Plate Joints based on Cyclindrical Nails - Y V Piskunov
- 22-7-13 Designing of Glued Wood Structures Joints on Glued-in Bars - S B Turkovsky
- 23-7-1 Proposal for a Design Code for Nail Plates - E Aasheim and K H Solli
- 23-7-2 Load Distribution in Nailed Joints - H J Blass

LOAD SHARING

- 3-8-1 Load Sharing - An Investigation on the State of Research and Development of Design Criteria - E Levin
- 4-8-1 A Review of Load-Sharing in Theory and Practice - E Levin
- 4-8-2 Load Sharing - B Norén
- 19-8-1 Predicting the Natural Frequencies of Light-Weight Wooden Floors - I Smith and Y H Chui
- 20-8-1 Proposed Code Requirements for Vibrational Serviceability of Timber Floors - Y H Chui and I Smith
- 21-8-1 An Addendum to Paper 20-8-1 - Proposed Code Requirements for Vibrational Serviceability of Timber Floors - Y H Chui and I Smith
- 21-8-2 Floor Vibrational Serviceability and the CIB Model Code - S Ohlsson
- 22-8-1 Reliability Analysis of Viscoelastic Floors - F Rouger, J D Barrett and R O Foschi

DURATION OF LOAD

- 3-9-1 Definitions of Long Term Loading for the Code of Practice
- B Norén
- 4-9-1 Long Term Loading of Trussed Rafters with Different
Connection Systems - T Feldborg and M Johansen
- 5-9-1 Strength of a Wood Column in Combined Compression and
Bending with Respect to Creep - B Källsner and B Norén
- 6-9-1 Long Term Loading for the Code of Practice (Part 2)
- B Norén
- 6-9-2 Long Term Loading - K Möhler
- 6-9-3 Deflection of Trussed Rafters under Alternating Loading
during a Year - T Feldborg and M Johansen
- 7-6-1 Strength and Long Term Behaviour of Lumnber and
Glued-Laminated Timber under Torsion Loads - K Möhler
- 7-9-1 Code Rules Concerning Strength and Loading Time
- H J Larsen and E Theilgaard
- 17-9-1 On the Long-Term Carrying Capacity of Wood Structures
- Y M Ivanov and Y Y Slavic
- 18-9-1 Prediction of Creep Deformations of Joints - J Kuipers
- 19-9-1 Another Look at Three Duration of Load Models - R O Foschi
and Z C Yao
- 19-9-2 Duration of Load Effects for Spruce Timber with Special
Reference to Moisture Influence - A Status Report
- P Hoffmeyer
- 19-9-3 A Model of Deformation and Damage Processes Based on the
Reaction Kinetics of Bond Exchange - T A C M van der Put
- 19-9-4 Non-Linear Creep Superposition - U Korin
- 19-9-5 Determination of Creep Data for the Component Parts of
Stressed-Skin Panels - R Kliger
- 19-9-6 Creep an Lifetime of Timber Loaded in Tension and
Compression - P Glos
- 19-1-1 Duration of Load Effects and Reliability Based Design
(Single Member) - R O Foschi and Z C Yao
- 19-6-1 Effect of Age and/or Load on Timber Strength - J Kuipers
- 19-7-4 The Prediction of the Long-Term Load Carrying Capacity of
Joints in Wood Structures - Y M Ivanov and Y Y Slavic

- 19-7-5 Slip in Joints under Long-Term Loading - T Feldborg and M Johansen
- 20-7-2 Slip in Joints under Long-Term Loading - T Feldborg and M Johansen
- 22-9-1 Long-Term Tests with Glued Laminated Timber Girders - M Badstube, W Rug and W Schone
- 22-9-2 Strength of One-Layer solid and Lengthways Glued Elements of Wood Structures and its Alteration from Sustained Load - L M Kovaltchuk, I N Boitemirova and G B Uspenskaya

TIMBER BEAMS

- 4-10-1 The Design of Simple Beams - H J Burgess
- 4-10-2 Calculation of Timber Beams Subjected to Bending and Normal Force - H J Larsen
- 5-10-1 The Design of Timber Beams - H J Larsen
- 9-10-1 The Distribution of Shear Stresses in Timber Beams - F J Keenan
- 9-10-2 Beams Notched at the Ends - K Möhler
- 11-10-1 Tapered Timber Beams - H Riberholt
- 13-6-2 Consideration of Size Effects in Longitudinal Shear Strength for Uncracked Beams - R O Foschi and J D Barrett
- 13-6-3 Consideration of Shear Strength on End-Cracked Beams - J D Barrett and R O Foschi
- 18-10-1 Submission to the CIB-W18 Committee on the Design of Ply Web Beams by Consideration of the Type of Stress in the Flanges - J A Baird
- 18-10-2 Longitudinal Shear Design of Glued Laminated Beams - R O Foschi
- 19-10-1 Possible Code Approaches to Lateral Buckling in Beams - H J Burgess
- 19-2-1 Creep Buckling Strength of Timber Beams and Columns - R H Leicester
- 20-2-1 Lateral Buckling Theory for Rectangular Section Deep Beam-Columns - H J Burgess
- 20-10-1 Draft Clause for CIB Code for Beams with Initial Imperfections - H J Burgess
- 20-10-2 Space Joists in Irish Timber - W J Robinson

- 20-10-3 Composite Structure of Timber Joists and Concrete Slab
- T Poutanen
- 21-10-1 A Study of Strength of Notched Beams -
P J Gustafsson
- 22-10-1 Design of Endnotched Beams - H J Larsen and P J Gustafsson
- 22-10-2 Dimensions of Wooden Flexural Members under Constant Loads -
A Pozgai
- 22-10-3 Thin-Walled Wood-Based Flanges in Composite Beams -
J König
- 22-10-4 The Calculation of Wooden Bars with flexible Joints in
Accordance with the Polish Standart Code and Strict
Theoretical Methods - Z Mielczarek
- 23-10-1 Tension Perpendicular to the Grain at Notches and Joints -
T A C M van der Put
- 23-10-2 Dimensioning of Beams with Cracks, Notches and Holes.
An Application of Fracture Mechanics - K Riipola
- 23-10-3 Size Factors for the Bending and Tension Strength of
Structural Timber - J D Barret and A R Fewell
- 23-12-1 Bending Strength of Glulam Beams, a Design Proposal -
J Ehlbeck and F Colling
- 23-12-3 Glulam Beams, Bending Strength in Relation to the Bending
Strength of the Finger Joints - H Riberholt

ENVIRONMENTAL CONDITIONS

- 5-11-1 Climate Grading for the Code of Practice - B Norén
- 6-11-1 Climate Grading (2) - B Norén
- 9-11-1 Climate Classes for Timber Design - F J Keenan
- 19-11-1 Experimental Analysis on Ancient Downgraded Timber
Structures - B Leggeri and L Paolini
- 19-6-5 Drying Stresses in Round Timber - A Ranta-Maunus
- 22-11-1 Corrosion and Adaptation Factors for Chemically Aggressive
Media with Timber Structures - K Erler

LAMINATED MEMBERS

- 6-12-1 Directives for the Fabrication of Load-Bearing Structures of
Glued Timber - A van der Velden and J Kuipers
- 8-12-1 Testing of Big Glulam Timber Beams - H Kolb and P Frech

- 8-12-2 Instruction for the Reinforcement of Apertures in Glulam Beams - H Kolb and P Frech
- 8-12-3 Glulam Standard Part 1: Glued Timber Structures; Requirements for Timber (Second Draft)
- 9-12-1 Experiments to Provide for Elevated Forces at the Supports of Wooden Beams with Particular Regard to Shearing Stresses and Long-Term Loadings - F Wassipaul and R Lackner
- 9-12-2 Two Laminated Timber Arch Railway Bridges Built in Perth in 1849 - L G Booth
- 9-6-4 Consideration of Combined Stresses for Lumber and Glued Laminated Timber - K Möhler
- 11-6-3 Consideration of Combined Stresses for Lumber and Glued Laminated Timber (addition to Paper CIB-W18/9-6-4) - K Möhler
- 12-12-1 Glulam Standard Part 2: Glued Timber Structures; Rating (3rd draft)
- 12-12-2 Glulam Standard Part 3: Glued Timber Structures; Performance (3 rd draft)
- 13-12-1 Glulam Standard Part 3: Glued Timber Structures; Performance (4th draft)
- 14-12-1 Proposals for CEI-Bois/CIB-W18 Glulam Standards - H J Larsen
- 14-12-2 Guidelines for the Manufacturing of Glued Load-Bearing Timber Structures - Stevin Laboratory
- 14-12-3 Double Tapered Curved Glulam Beams - H Riberholt
- 14-12-4 Comment on CIB-W18/14-12-3 - E Gehri
- 18-12-1 Report on European Glulam Control and Production Standard - H Riberholt
- 18-10-2 Longitudinal Shear Design of Glued Laminated Beams - R O Foschi
- 19-12-1 Strength of Glued Laminated Timber - J Ehlbeck and F Colling
- 19-12-2 Strength Model for Glulam Columns - H J Blaß
- 19-12-3 Influence of Volume and Stress Distribution on the Shear Strength and Tensile Strength Perpendicular to Grain - F Colling
- 19-12-4 Time-Dependent Behaviour of Glued-Laminated Beams - F Zaupa
- 21-12-1 Modulus of Rupture of Glulam Beam Composed of Arbitrary Laminae - K Komatsu and N Kawamoto

- 21-12-2 An Appraisal of the Young's Modulus Values Specified for Glulam in Eurocode 5 - L R J Whale, B O Hilson and P D Rodd
- 21-12-3 The Strength of Glued Laminated Timber (Glulam): Influence of Lamination Qualities and Strength of Finger Joints - J Ehlbeck and F Colling
- 21-12-4 Comparison of a Shear Strength Design Method in Eurocode 5 and a More Traditional One - H Riberholt
- 22-12-1 The Dependence of the Bending Strength on the Glued Laminated Timber Girder Depth - M Badstube, W Rug and W Schone
- 22-12-2 Acid Deterioration of Glulam Beams in Buildings from the Early Half of the 1960s - Preliminary summary of the research project; Overhead pictures - B A Hedlund
- 22-12-3 Experimental Investigation of normal Stress Distribution in Glue Laminated Wooden Arches - Z Mielczarek and W Chanaj
- 22-12-4 Ultimate Strength of Wooden Beams with Tension Reinforcement as a Function of Random Material Properties - R Candowicz and T Dziuba
- 23-12-1 Bending Strength of Glulam Beams, a Design Proposal - J Ehlbeck and F Colling
- 23-12-2 Probability Based Design Method for Glued Laminated Timber - M F Stone
- 23-12-3 Glulam Beams, Bending Strength in Relation to the Bending Strength of the Finger Joints - H Riberholt
- 23-12-4 Glued Laminated Timber - Strength Classes and Determination of Characteristic Properties - H Riberholt, J Ehlbeck and A Fewell

PARTICLE AND FIBRE BUILDING BOARDS

- 7-13-1 Fibre Building Boards for CIB Timber Code (First Draft) - O Brynildsen
- 9-13-1 Determination of the Bearing Strength and the Load-Deformation Characteristics of Particleboard - K Möhler, T Budianto and J Ehlbeck
- 9-13-2 The Structural Use of Tempered Hardboard - W W L Chan
- 11-13-1 Tests on Laminated Beams from Hardboard under Short- and Longterm Load - W Nozynski
- 11-13-2 Determination of Deformation of Special Densified Hardboard under Long-term Load and Varying Temperature and Humidity Conditions - W Halfar

- 11-13-3 Determination of Deformation of Hardboard under Long-term Load in Changing Climate - W Halfar
- 14-4-1 An Introduction to Performance Standards for Wood-Base Panel Products - D H Brown
- 14-4-2 Proposal for Presenting Data on the Properties of Structural Panels - T Schmidt
- 16-13-1 Effect of Test Piece Size on Panel Bending Properties - P W Post
- 20-4-1 Considerations of Reliability - Based Design for Structural Composite Products - M R O'Halloran, J A Johnson, E G Elias and T P Cunningham
- 20-13-1 Classification Systems for Structural Wood-Based Sheet Materials - V C Kearley and A R Abbott
- 21-13-1 Design Values for Nailed Chipboard - Timber Joints - A R Abbott

TRUSSED RAFTERS

- 4-9-1 Long-term Loading of Trussed Rafters with Different Connection Systems - T Feldborg and M Johansen
- 6-9-3 Deflection of Trussed Rafters under Alternating Loading During a Year - T Feldborg and M Johansen
- 7-2-1 Lateral Bracing of Timber Struts - J A Simon
- 9-14-1 Timber Trusses - Code Related Problems - T F Williams
- 9-7-1 Design of Truss Plate Joints - F J Keenan
- 10-14-1 Design of Roof Bracing - The State of the Art in South Africa - P A V Bryant and J A Simon
- 11-14-1 Design of Metal Plate Connected Wood Trusses - A R Egerup
- 12-14-1 A Simple Design Method for Standard Trusses - A R Egerup
- 13-14-1 Truss Design Method for CIB Timber Code- A R Egerup
- 13-14-2 Trussed Rafters, Static Models - H Riberholt
- 13-14-3 Comparison of 3 Truss Models Designed by Different Assumptions for Slip and E-Modulus - K Möhler
- 14-14-1 Wood Trussed Rafter Design - T Feldborg and M Johansen
- 14-14-2 Truss-Plate Modelling in the Analysis of Trusses - R O Foschi
- 14-14-3 Cantilevered Timber Trusses - A R Egerup

- 14-7-5 The Effect of Support Eccentricity on the Design of W- and WW-Trusses with Nail Plate Connectors - B Källsner
- 15-14-1 Guidelines for Static Models of Trussed Rafters - H Riberholt
- 15-14-2 The Influence of Various Factors on the Accuracy of the Structural Analysis of Timber Roof Trusses - F R P Pienaar
- 15-14-3 Bracing Calculations for Trussed Rafter Roofs - H J Burgess
- 15-14-4 The Design of Continuous Members in Timber Trussed Rafters with Punched Metal Connector Plates - P O Reece
- 15-14-5 A Rafter Design Method Matching U.K. Test Results for Trussed Rafters - H J Burgess
- 16-14-1 Full-Scale Tests on Timber Fink Trusses Made from Irish Grown Sitka Spruce - V Picardo
- 17-14-1 Data from Full Scale Tests on Prefabricated Trussed Rafters - V Picardo
- 17-14-2 Simplified Static Analysis and Dimensioning of Trussed Rafters - H Riberholt
- 17-14-3 Simplified Calculation Method for W-Trusses - B Källsner
- 18-14-1 Simplified Calculation Method for W-Trusses (Part 2) - B Källsner
- 18-14-2 Model for Trussed Rafter Design - T Poutanen
- 19-14-1 Annex on Simplified Design of W-Trusses - H J Larsen
- 19-14-2 Simplified Static Analysis and Dimensioning of Trussed Rafters - Part 2 - H Riberholt
- 19-14-3 Joint Eccentricity in Trussed Rafters - T Poutanen
- 20-14-1 Some Notes about Testing Nail Plates Subjected to Moment Load - T Poutanen
- 20-14-2 Moment Distribution in Trussed Rafters - T Poutanen
- 20-14-3 Practical Design Methods for Trussed Rafters - A R Egerup
- 22-14-1 Guidelines for Design of Timber Trussed Rafters - H Riberholt
- 23-14-1 Analyses of Timber Trussed Rafters of the W-Type - H Riberholt
- 23-14-2 Proposal for Eurocode 5 Text on Timber Trussed Rafters - H Riberholt

STRUCTURAL STABILITY

- 8-15-1 Laterally Loaded Timber Columns: Tests and Theory
- H J Larsen
- 13-15-1 Timber and Wood-Based Products Structures. Panels for Roof Coverings. Methods of Testing and Strength Assessment Criteria. Polish Standard BN-78/7159-03
- 16-15-1 Determination of Bracing Structures for Compression Members and Beams - H Brüninghoff
- 17-15-1 Proposal for Chapter 7.4 Bracing - H Brüninghoff
- 17-15-2 Seismic Design of Small Wood Framed Houses - K F Hansen
- 18-15-1 Full-Scale Structures in Glued Laminated Timber, Dynamic Tests: Theoretical and Experimental Studies - A Ceccotti and A Vignoli
- 18-15-2 Stabilizing Bracings - H Brüninghoff
- 19-15-1 Connections Deformability in Timber Structures: a Theoretical Evaluation of its Influence on Seismic Effects - A Ceccotti and A Vignoli
- 19-15-2 The Bracing of Trussed Beams - M H Kessel and J Natterer
- 19-15-3 Racking Resistance of Wooden Frame Walls with Various Openings - M Yasumura
- 19-15-4 Some Experiences of Restoration of Timber Structures for Country Buildings - G Cardinale and P Spinelli
- 19-15-5 Non-Destructive Vibration Tests on Existing Wooden Dwellings - Y Hirashima
- 20-15-1 Behaviour Factor of Timber Structures in Seismic Zones
A Ceccotti and A Vignoli
- 21-15-1 Rectangular Section Deep Beam - Columns with Continuous Lateral Restraint - H J Burgess
- 21-15-2 Buckling Modes and Permissible Axial Loads for Continuously Braced Columns - H J Burgess
- 21-15-3 Simple Approaches for Column Bracing Calculations - H J Burgess
- 21-15-4 Calculations for Discrete Column Restraints - H J Burgess
- 21-15-5 Behaviour Factor of Timber Structures in Seismic Zones (Part Two) - A Ceccotti and A Vignoli
- 22-15-1 Suggested Changes in Code Bracing Recommendations for Beams and Columns - H J Burgess

- 22-15-2 Research and Development of Timber Frame Structures for Agriculture in Poland - S Kus and J Kerste
- 22-15-3 Ensuring of Three-Dimensional Stiffness of Buildings with Wood Structures - A K Shenghelia
- 22-15-5 Seismic Behavior of Arched Frames in Timber Construction - M Yasumura
- 22-15-6 The Robustness of Timber Structures - C J Mettem and J P Marcroft
- 22-15-7 Influence of Geometrical and Structural Imperfections on the Limit Load of Wood Columns - P Dutko
- 23-15-1 Calculation of a Wind Girder Loaded also by Discretely Spaced Braces for Roof Members - H J Burgess
- 23-15-2 Stability Design and Code Rules for Straight Timber Beams - T A C M van der Put
- 23-15-3 A Brief Description of Formula of Beam-Columns in China Code - S Y Huang
- 23-15-4 Seismic Behavior of Braced Frames in Timber Construction - M Yasumara
- 23-15-5 On a Better Evaluation of the Seismic Behavior Factor of Low-Dissipative Timber Structures - A Ceccotti and A Vignoli
- 23-15-6 Disproportionate Collapse of Timber Structures - C J Mettem and J P Marcroft
- 23-15-7 Performance of Timber Frame Structures During the Loma Prieta California Earthquake - M R O'Halloran and E G Elias

FIRE

- 12-16-1 British Standard BS 5268 the Structural Use of Timber: Part 4 Fire Resistance of Timber Structures
- 13-100-2 CIB Structural Timber Design Code. Chapter 9. Performance in Fire
- 19-16-1 Simulation of Fire in Tests of Axially Loaded Wood Wall Studs - J König

STATISTICS AND DATA ANALYSIS

- 13-17-1 On Testing Whether a Prescribed Exclusion Limit is Attained - W G Warren
- 16-17-1 Notes on Sampling and Strength Prediction of Stress Graded Structural Timber - P Glos
- 16-17-2 Sampling to Predict by Testing the Capacity of Joints, Components and Structures - B Norén

- 16-17-3 Discussion of Sampling and Analysis Procedures - P W Post
- 17-17-1 Sampling of Wood for Joint Tests on the Basis of Density
- I Smith, L R J Whale
- 17-17-2 Sampling Strategy for Physical and Mechanical Properties of
Irish Grown Sitka Spruce - V Picardo
- 18-17-1 Sampling of Timber in Structural Sizes - P Glos
- 18-6-3 Notes on Sampling Factors for Characteristic Values -
R H Leicester
- 19-17-1 Load Factors for Proof and Prototype Testing - R H Leicester
- 19-6-2 Confidence in Estimates of Characteristic Values
- R H Leicester
- 21-6-1 Draft Australian Standard: Methods for Evaluation of
Strength and Stiffness of Graded Timber - R H Leicester
- 21-6-2 The Determination of Characteristic Strength Values for
Stress Grades of Structural Timber. Part 1 - A R Fewell
and P Glos
- 22-17-1 Comment on the Strength Classes in Eurocode 5 by an Analysis
of a Stochastic Model of Grading - A proposal for a
supplement of the design concept - M Kiesel

FRACTURE MECHANICS

- 21-10-1 A Study of Strength of Notched Beams -
P J Gustafsson
- 22-10-1 Design of Endnotched Beams - H J Larsen and P J Gustafsson
- 23-10-1 Tension Perpendicular to the Grain at Notches and Joints -
T A C M van der Put
- 23-10-2 Dimensioning of Beams with Cracks, Notches and Holes.
An Application of Fracture Mechanics - K Riipola
- 23-19-1 Determination of the Fracture Energie of Wood for Tension
Perpendicular to the Grain - W Rug, M Badstube and W Schöne
- 23-19-2 The Fracture Energy of Wood in Tension Perpendicular to the
Grain. Results from a Joint Testing Project - H J Larsen and
P J Gustafsson
- 23-19-3 Application of Fracture Mechanics to Timber Structures -
A Ranta-Maunus

GLUED JOINTS

- 20-18-1 Wood Materials under Combined Mechanical and Hygral Loading
- A Martensson and S Thelandersson

- 20-18-2 Analysis of Generalized Volkersen - Joints in Terms of Non-Linear Fracture Mechanics - P J Gustafsson
- 20-18-3 The Complete Stress-Slip Curve of Wood-Adhesives in Pure Shear - H Wernersson and P J Gustafsson
- 22-18-1 Perspective Adhesives and Protective Coatings for Wood Structures - A S Freidin

CIB TIMBER CODE

- 2-100-1 A Framework for the Production of an International Code of Practice for the Structural Use of Timber - W T Curry
- 5-100-1 Design of Solid Timber Columns (First Draft) - H J Larsen
- 5-100-2 A Draft Outline of a Code for Timber Structures - L G Booth
- 6-100-1 Comments on Document 5-100-1; Design of Solid Timber Columns - H J Larsen and E Theilgaard
- 6-100-2 CIB Timber Code: CIB Timber Standards - H J Larsen and E Theilgaard
- 7-100-1 CIB Timber Code Chapter 5.3 Mechanical Fasteners; CIB Timber Standard 06 and 07 - H J Larsen
- 8-100-1 CIB Timber Code - List of Contents (Second Draft) - H J Larsen
- 9-100-1 The CIB Timber Code (Second Draft)
- 11-100-1 CIB Structural Timber Design Code (Third Draft)
- 11-100-2 Comments Received on the CIB Code
 - a U Saarelainen
 - b Y M Ivanov
 - c R H Leicester
 - d W Nozynski
 - e W R A Meyer
 - f P Beckmann; R Marsh
 - g W R A Meyer
 - h W R A Meyer
- 11-100-3 CIB Structural Timber Design Code; Chapter 3 - H J Larsen
- 12-100-1 Comment on the CIB Code - Sous-Commission Glulam
- 12-100-2 Comment on the CIB Code - R H Leicester
- 12-100-3 CIB Structural Timber Design Code (Fourth Draft)
- 13-100-1 Agreed Changes to CIB Structural Timber Design Code
- 13-100-2 CIB Structural Timber Design Code. Chapter 9: Performance in Fire

- 13-100-3a Comments on CIB Structural Timber Design Code
- 13-100-3b Comments on CIB Structural Timber Design Code
- W R A Meyer
- 13-100-3c Comments on CIB Structural Timber Design Code
- British Standards Institution
- 13-100-4 CIB Structural Timber Design Code. Proposal for Section
6.1.5 Nail Plates - N I Bovim
- 14-103-2 Comments on the CIB Structural Timber Design Code
- R H Leicester
- 15-103-1 Resolutions of TC 165-meeting in Athens 1981-10-12/13
- 21-100-1 CIB Structural Timber Design Code. Proposed Changes of
Sections on Lateral Instability, Columns and Nails -
H J Larsen
- 22-100-1 Proposal for Including an Updated Design Method for Bearing
Stresses in CIB W18 - Structural Timber Design Code -
B Madsen
- 22-100-2 Proposal for Including Size Effects in CIB W18A Timber
Design Code - B Madsen
- 22-100-3 CIB Structural Timber Design Code - Proposed Changes of
Section on Thin-Flanged Beams - J König
- 22-100-4 Modification Factor for "Aggressive Media" - a Proposal for
a Supplement to the CIB Model Code - K Erler and W Rug
- 22-100-5 Timber Design Code in Czechoslovakia and Comparison with
CIB Model Code - P Dutko and B Kozelouh

LOADING CODES

- 4-101-1 Loading Regulations - Nordic Committee for Building
Regulations
- 4-101-2 Comments on the Loading Regulations - Nordic Committee for
Building Regulations

STRUCTURAL DESIGN CODES

- 1-102-1 Survey of Status of Building Codes, Specifications etc.,
in USA - E G Stern
- 1-102-2 Australian Codes for Use of Timber in Structures
- R H Leicester
- 1-102-3 Contemporary Concepts for Structural Timber Codes
- R H Leicester
- 1-102-4 Revision of CP 112 - First Draft, July 1972
- British Standards Institution

- 4-102-1 Comparison of Codes and Safety Requirements for Timber Structures in EEC Countries - Timber Research and Development Association
- 4-102-2 Nordic Proposals for Safety Code for Structures and Loading Code for Design of Structures - O A Brynildsen
- 4-102-3 Proposal for Safety Codes for Load-Carrying Structures - Nordic Committee for Building Regulations
- 4-102-4 Comments to Proposal for Safety Codes for Load-Carrying Structures - Nordic Committee for Building Regulations
- 4-102-5 Extract from Norwegian Standard NS 3470 "Timber Structures"
- 4-102-6 Draft for Revision of CP 112 "The Structural Use of Timber" - W T Curry
- 8-102-1 Polish Standard PN-73/B-03150: Timber Structures; Statistical Calculations and Designing
- 8-102-2 The Russian Timber Code: Summary of Contents
- 9-102-1 Svensk Byggnorm 1975 (2nd Edition); Chapter 27: Timber Construction
- 11-102-1 Eurocodes - H J Larsen
- 13-102-1 Program of Standardisation Work Involving Timber Structures and Wood-Based Products in Poland
- 17-102-1 Safety Principles - H J Larsen and H Riberholt
- 17-102-2 Partial Coefficients Limit States Design Codes for Structural Timberwork - I Smith
- 18-102-1 Antiseismic Rules for Timber Structures: an Italian Proposal - G Augusti and A Ceccotti
- 18-1-2 Eurocode 5, Timber Structures - H J Larsen
- 19-102-1 Eurocode 5 - Requirements to Timber - Drafting Panel Eurocode 5
- 19-102-2 Eurocode 5 and CIB Structural Timber Design Code - H J Larsen
- 19-102-3 Comments on the Format of Eurocode 5 - A R Fewell
- 19-102-4 New Developments of Limit States Design for the New GDR Timber Design Code - W Rug and M Badstube
- 19-7-3 Effectiveness of Multiple Fastener Joints According to National Codes and Eurocode 5 (Draft) - G Steck
- 19-7-6 The Derivation of Design Clauses for Nailed and Bolted Joints in Eurocode 5 - L R J Whale and I Smith

- 19-14-1 Annex on Simplified Design of W-Trusses - H J Larsen
- 20-102-1 Development of a GDR Limit States Design Code for Timber Structures - W Rug and M Badstube
- 21-102-1 Research Activities Towards a New GDR Timber Design Code Based on Limit States Design - W Rug and M Badstube
- 22-102-1 New GDR Timber Design Code, State and Development - W Rug, M Badstube and W Kofent
- 22-102-2 Timber Strength Parameters for the New USSR Design Code and its Comparison with International Code - Y Y Slavik, N D Denesh and E B Ryumina
- 22-102-3 Norwegian Timber Design Code - Extract from a New Version - E Aasheim and K H Solli
- 23-7-1 Proposal for a Design Code for Nail Plates - E Aasheim and K H Solli

INTERNATIONAL STANDARDS ORGANISATION

- 3-103-1 Method for the Preparation of Standards Concerning the Safety of Structures (ISO/DIS 3250) - International Standards Organisation ISO/TC98
- 4-103-1 A Proposal for Undertaking the Preparation of an International Standard on Timber Structures - International Standards Organisation
- 5-103-1 Comments on the Report of the Consultation with Member Bodies Concerning ISO/TC/P129 - Timber Structures - Dansk Ingeniorforening
- 7-103-1 ISO Technical Committees and Membership of ISO/TC 165
- 8-103-1 Draft Resolutions of ISO/TC 165
- 12-103-1 ISO/TC 165 Ottawa, September 1979
- 13-103-1 Report from ISO/TC 165 - A Sorensen
- 14-103-1 Comments on ISO/TC 165 N52 "Timber Structures; Solid Timber in Structural Sizes; Determination of Some Physical and Mechanical Properties"
- 14-103-2 Comments on the CIB Structural Timber Design Code - R H Leicester
- 21-103-1 Concept of a Complete Set of Standards - R H Leicester

JOINT COMMITTEE ON STRUCTURAL SAFETY

- 3-104-1 International System on Unified Standard Codes of Practice for Structures - Comité Européen du Béton (CEB)

7-104-1 Volume 1: Common Unified Rules for Different Types of
Construction and Material - CEB

CIB PROGRAMME, POLICY AND MEETINGS

1-105-1 A Note on International Organisations Active in the Field of
Utilisation of Timber - P Sonnemans

5-105-1 The Work and Objectives of CIB-W18-Timber Structures
- J G Sunley

10-105-1 The Work of CIB-W18 Timber Structures - J G Sunley

15-105-1 Terms of Reference for Timber - Framed Housing Sub-Group
of CIB-W18

19-105-1 Tropical and Hardwood Timbers Structures - R H Leicester

21-105-1 First Conference of CIB-W18B, Tropical and Hardwood Timber
Structures Singapore,
26 - 28 October 1987 - R H Leicester

INTERNATIONAL UNION OF FORESTRY RESEARCH ORGANISATIONS

7-106-1 Time and Moisture Effects - CIB W18/IUFRO 55.02-03
Working Party

INTERNATIONAL COUNCIL FOR BUILDING RESEARCH STUDIES AND DOCUMENTATION

WORKING COMMISSION W18A - TIMBER STRUCTURES

SOME REMARKS ABOUT THE SAFETY OF TIMBER STRUCTURES

by

J Kuipers
Delft University of Technology
The Netherlands

MEETING TWENTY - THREE

LISBON

PORTUGAL

SEPTEMBER 1990

PREFACE

The purpose of this paper is to contribute to the discussion on safety, in particular of timber structures. The author is aware of the fact that much more advanced theories were developed with respect to the statistical treatment of loads and strength properties and the probability of failure. The way in which we have to deal with damage due to long duration of load however is less clear. For the design of competitive timber structures a better view on this problem is necessary; may this paper help to the development of such a view.

1 INTRODUCTION

In [1] a rather simple method for the determination of structural safety was developed and used in particular to try to find out if structures, made of different materials and designed according to then existing standards would show comparable probability of failure.

For timber it was assumed that the effect of duration of load according to Wood, the Madison-curve, could be used in a slightly simplified way and furthermore that every load of a certain duration would cause a strength reduction or damage proportional to the ratio of that load to the one, causing failure after that particular lapse of time.

Although several attempts have been made to demonstrate that the Madison curve has not a universal validity, until now there is not an accepted way to deal with the problem and to combine the different results.

In the following firstly some attention is paid to the interpretation of duration-of-load-effects. Secondly it is tried to give - in the same simplified manner as before, i.e. using normal distributions for loads and for strength - a general reasoning for the determination of the probability of failure if certain values for γ_q , γ_m , and k_{mod} will be prescribed.

2 A SIMPLIFIED STATISTICAL SAFETY METHOD

2.1 The method in [1].

For the determination of the safety of structures one has to take into account the variability of loads and strength. The safety of the structure or of the structural element then is expressed in the probability of failure, which should be small enough. This probability is given by the so-called safety or reliability index β . In the following we use R for a material strength property, G for the effect - expressed in the same quantity as R - of permanent loads and Q for the effect of variable loads. Furthermore s and v , with indexes r , g , and q stand for the standard deviation and the coefficient of variation respectively. In combination with R , G and Q the index m means the mean value and the index k the characteristic 5th percentile value.

The effect of the load-duration is given by a linearised "Madison-curve" as in fig. 1, where a constant load with magnitude $0.55 R$ causes failure after 100 years, R being the short-duration strength determined in a static test, reaching failure in about 5 minutes.

For materials without time effects the basic formula for the safety index is¹⁾

$$\beta = \frac{(R - G - Q) m}{s (R - G - Q)} = \frac{R_m - G_m - Q_m}{\sqrt{s_r^2 + s_g^2 + s_q^2}} \quad (1)$$

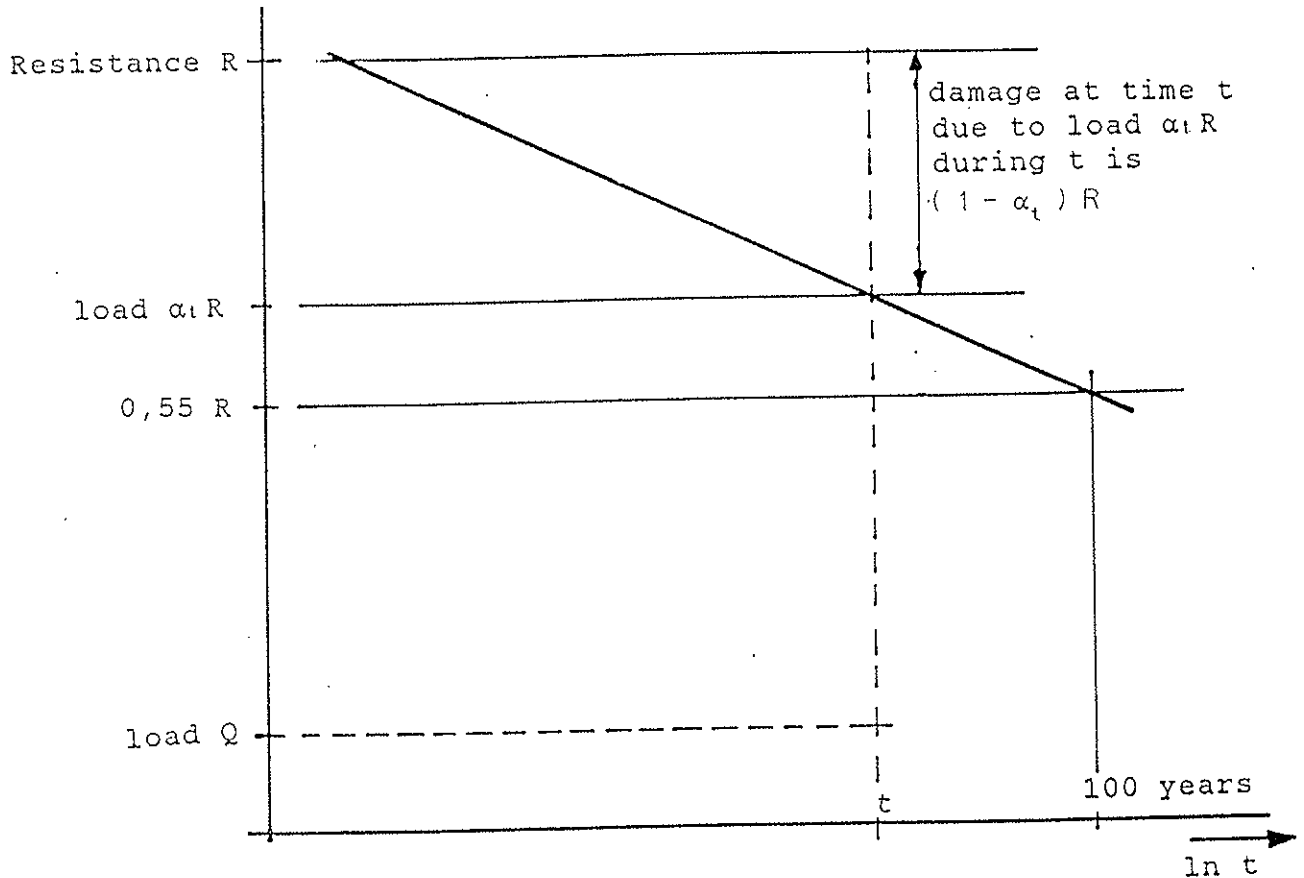


Fig.1.: Assumption in [1]: Q during t gives damage:

$$\frac{Q}{\alpha_t R} (1 - \alpha_t) R = \frac{1 - \alpha_t}{\alpha_t} Q$$

This expression is very general and independent of the probability-distribution of R, G and Q. The value of β determines the probability of failure p, and the relationship of β and p is distribution-dependent.

In [1] it was assumed, that a load of magnitude $\alpha_t R$ during a time t causes a strength reduction $[1 - \alpha_t] R$, so failure occurs at time t. Furthermore it was assumed that a smaller load Q, working during the same time t, causes a proportional damage, i.e.

¹⁾ It is assumed that R, G and Q are independent, not correlated quantities.

$$\frac{Q}{\alpha_t R} (1 - \alpha_t) R = \frac{1 - \alpha_t}{\alpha_t} Q$$

The safety-index with respect to the residual strength at time t of a material loaded to $\alpha_g G + \alpha_q Q$ becomes [see [1], formula 2a] :

$$\beta = \frac{R_m - (1/\alpha_g)G_m - (1/\alpha_q)Q_m}{\sqrt{s_r^2 + (1/\alpha_g)^2 s_g^2 + (1/\alpha_q)^2 s_q^2}} \quad (2)$$

Using this formula in [1] it was tried to determine values of β for different structural materials, based on the then used standards (1967).

So-called "stress-regions" were developed for combinations of G and Q, leading to constant values of β .

2.2 Criticism on 2.1

Objections to this method are the following:

- a) the variables will have other than normal distributions. This of course is true. The elaboration for other distributions has been done by others, e.g.[2], it is however much more complicated. Here the simple method is maintained to facilitate the discussion.
- b) the effect of load-duration is not right. This is also true:
 - b1) not all timber, timber products and joints will follow the same Madison-line. Especially for wood with defects the strength reduction is expected to be smaller than for clear wood. It seems very difficult to take into account such differences in a general standard, this even more if a system of strength classes will be adopted, because in one such a class different grades of different species will be put together. This means that even in one strength class the time effect can be different. The only solution will probably be the one of today: acceptance of the most dangerous expectation. Further extra punishment due to this effect should of course be avoided.
 - b2) the safety index is only judged at the end of the lifetime of the structure. According to people with more statistical insight than I have, the decrease of the total probability during the lifetime of the structure is only small.
 - b3) the forces and stresses in our timber structures are so low, that no damage will be caused by them. It is argued already for a long time that there is a threshold, below which no strength reduction will occur; Kuipers [3] tries to demonstrate this by referring to long-duration tests on trusses and on joints.

2.3 Does another question change the answer?

The idea of a threshold, and the fact that the stresses in our timber structures are so low, has given the impression that timber structures are much more safe than is recognised. At the moment however as far as I know there is not made any attempt to produce comparable values of the safety index, based on new results of tests.

If we accept the idea of a threshold, the assumption in the foregoing - i.e. that every load of a certain duration will decrease the strength - is not true any more. The allowable forces and stresses we accepted in the years behind us are of the order of 0,20 to 0,30 of the short duration strength, much below the generally accepted threshold of about 0,55 times this short-duration strength.

Nevertheless we could ask - like H.J.Larsen during discussions hereabout - what the probability would be that nowadays'accepted forces and stresses exceed the threshold values.

Using the Madison line we indeed assume, that every structure or every individual structural element, which is really loaded during the period t with the load $Q = \alpha_t R$ (fig.1) will fail at time t . Now both Q and R are variable quantities as was said before, but we take the load-duration-line as a deterministic quantity, i.e. that it has a fixed influence. We then can draw the load-duration-line for a low-strength-element, e.g. for an element with a strength of $0.8 R_m$, or in the same way for a high-strength individual, say with $1.2 R_m$ (fig.2).

All elements, having a strength lower than R_1 will fail after 100 year or earlier, if they are loaded by a permanent load of $0,55 R_1$. The probability of failure therefore can be found by the following expression:

$$\beta = \frac{\alpha_t R_m - Q_m}{\sqrt{s_{\alpha_t r}^2 + s_q^2}} = \frac{\alpha_t R_m - Q_m}{\sqrt{\alpha_t^2 s_r^2 + s_q^2}}$$

or for two loads G and Q :

$$\beta = \frac{\alpha_t R_m - G_m - Q_m}{\sqrt{\alpha_t^2 s_r^2 + s_g^2 + s_q^2}} \quad (3)$$

Bearing in mind that now $\alpha_g = \alpha_q = \alpha_t$ we see that the expression (3) is the same as (2), and so the results of both ideas about the effect of long duration of load are the same.

In the following we will try to answer the question about the safety index belonging to nowadays proposals for design rules.

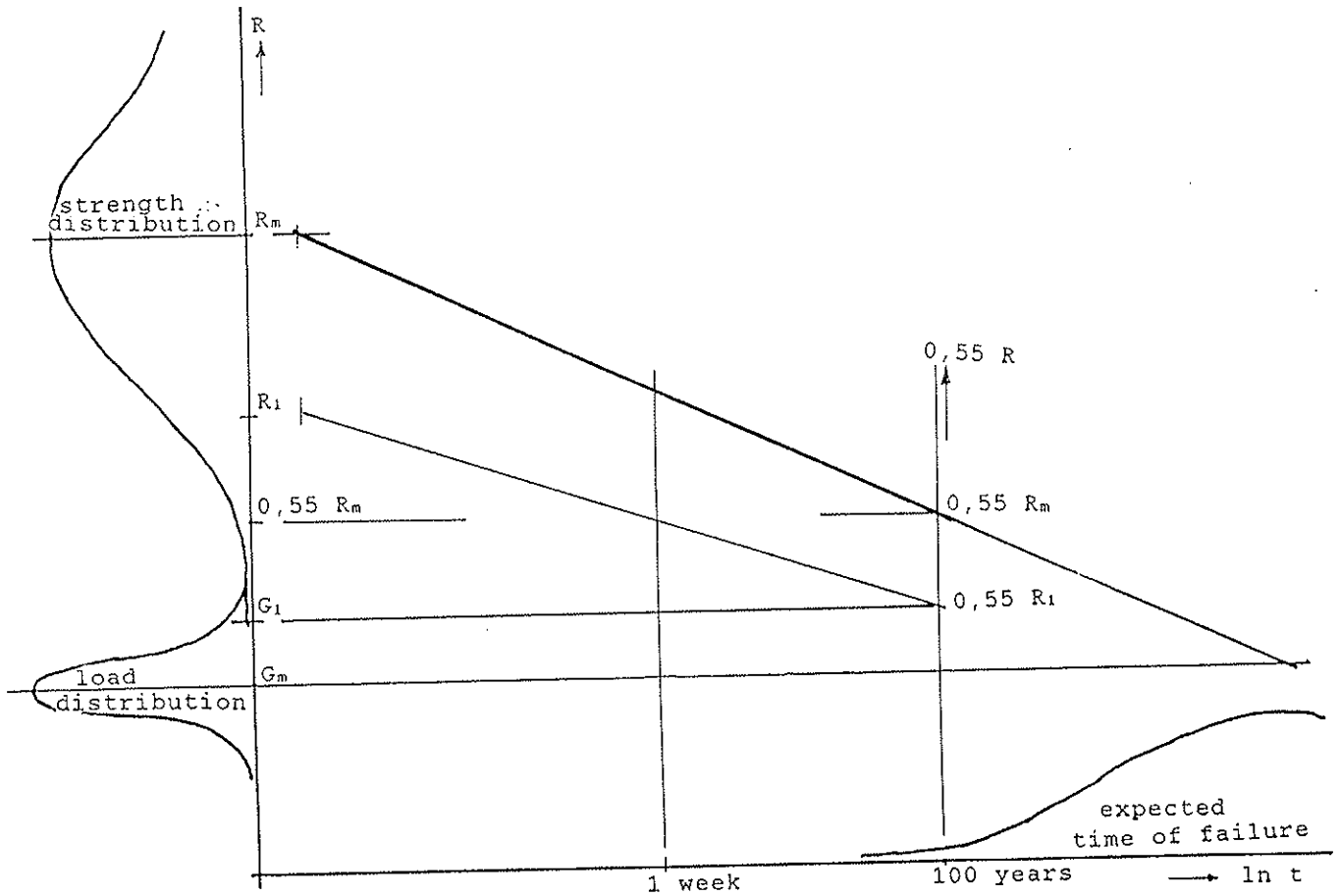


Fig.2: There always exists a probability that a weak structure with strength R_1 throughout its lifetime will be loaded by a high permanent load G_1 .

3 ESTIMATION OF SAFETY INDEX RESULTING FROM EUROCODE 5 AND OF EUROCODE-BASED DRAFT NATIONAL LOADING CODE.

3.1 Conditions for ultimate state.

Eurocode 5 states the following proposed values for the three variables determining the safety of timber structures:

- partial factor for actions:

$$\gamma_g = 1.35$$

$$\gamma_q = 1.5, \text{ for load-combinations of } G \text{ and } Q$$

- partial factor for materials:

$$\gamma_m = 1.4 \text{ "normal" case}$$

$$\gamma_m = 1.25 \text{ for glulam}$$

- modification factor k_{mod}

here limited to the usual strength properties and to moisture class 2 - :

long term 0.8 - order of duration 10 years

medium term 0.9 - " " " 6 months

short duration 1.0 - " " " 1 week

instantaneous 1.2

The design calculations have to proof that the forces and stresses resulting from a fictitious load combination

$$1.35 G_k + 1.5 Q_k,$$

will not be greater than a fictitious strength

$$\frac{k_{mod}}{\gamma_m} R_k$$

Using again G and Q directly as the notations for the results of the actions, e.g. stresses, we can write:

$$1.35 G_k + 1.5 Q_k \leq \frac{k_{mod}}{\gamma_m} R_k ; \text{ the index } k \text{ denotes the characteristic values.}$$

Normally the 5th percentile value is used as "the" characteristic value. With the assumed normal distributions it means that, for instance,

$$G_k = (1 + 1.64 v_g) G_m$$

We will use the following values for the coefficient of variation:

$$v_g = 0.05 \text{ for permanent load}$$

$v_q = 0.15$ for variable load, e.g. snow load; the characteristic values have to be given so, that they can be considered as extreme values with an exceptional character. The duration of such an extreme load is chosen here to be about one week during the lifetime of the structure.

Following the Dutch draft loading code, which is related to the EC loading code, the "momentane" value however must be considered as a permanent load; its value is 0.7 times the extreme value.

The value of β has been calculated for 18 examples.

Example 1: Permanent load only; sawn wood; coeff. of variation $v_r = 0.25$.

$$\text{Condition: } 1.35 G_k \leq (0.8/1.4) R_k$$

$$\text{From this: } G_k \leq 0.423 R_k , \text{ or}$$

$$G_m \leq 0.231 R_m , \text{ and}$$

$$\beta = \frac{0.55 R_m - 0.231 R_m}{R_m \sqrt{0.55^2 \cdot 0.25^2 + 0.231^2 \cdot 0.05^2}} = 2.31$$

Example 2 :Permanent load only; sawn wood; $v_r = 0.20$
 $G_m \leq 0.263 R_m ;$

$$\beta = \frac{0.55 - 0.263}{\sqrt{0.55^2 \cdot 0.20^2 + 0.263^2 \cdot 0.05^2}} = 2.59$$

Example 3: Permanent load only; glulam; $v_f = 0.15$.

$$\text{Condition : } 1.35 G_k \leq (0.8/1.25) R_k$$

From this: $G_k \leq 0.474 R_k$, or $G_m \leq 0.33 R_m$, and

$$\beta = \frac{0.55 - 0.33}{\sqrt{0.55^2 \cdot 0.15^2 + 0.33^2 \cdot 0.05^2}} = 2.62$$

Example 4: Load combination $G_k + Q_k$, for a construction where $G_k = Q_k$, so that the effects of the permanent load and the variable load are of the same magnitude; both loads are of long duration; the "momentane" value for the load Q, i.e. $0.7 Q_k$ has to be taken. Sawn wood, $v_f = 0.25$.

$$\text{Condition: } 1.35 G_k + 1.5 \cdot 0.7 Q_k \leq (0.8/1.4) R_k$$

$G_k \leq 0.238 R_k$ or $G_m = 0.130 R_m$, and $Q_m = 0.113 R_m$

$$\beta = \frac{0.55 - 0.130 - 0.113}{\sqrt{0.55^2 \cdot 0.25^2 + 0.130^2 \cdot 0.05^2 + 0.113^2 \cdot 0.15^2}} = 2.21$$

Example 5: Load combination $G + Q$, for a construction where $G_k = Q_k$, as above. Sawn wood; $v_f = 0.20$

Condition as above; $G_m = 0.148 R_m$, and $Q_m = 0.128 R_m$

$$\beta = \frac{0.55 - 0.148 - 0.128}{\sqrt{0.55^2 \cdot 0.20^2 + 0.148^2 \cdot 0.05^2 + 0.128^2 \cdot 0.15^2}} = 2.45$$

Example 6: Load combination as above; glulam; $v_f = 0.15$

$$\text{Condition: } 1.35 G_k + 1.5 \cdot 0.7 Q_k \leq (0.8/1.25) R_k$$

From this: $G_m = 0.186 R_m$ and $Q_m = 0.162 R_m$

$$\beta = \frac{0.55 - 0.186 - 0.162}{\sqrt{0.55^2 \cdot 0.15^2 + 0.186^2 \cdot 0.05^2 + 0.162^2 \cdot 0.15^2}} = 2.34$$

Example 7: Load combination $G+Q$, for a construction where again $G_k = Q_k$, but now the extreme case. This extreme load combination has aduration of 1 week. In the calculation of β the value from the Madison line for 1 week is 0.75. Sawn wood; $v_f = 0.25$.

Condition: $1.35 G_k + 1.5 Q_k \leq (1/1.4)R_k$

$G_m = 0.137 R_m$ and $Q_m = 0.119 R_m$

$$\beta = \frac{0.75 - 0.137 - 0.119}{\sqrt{0.75^2 \cdot 0.25^2 + 0.137^2 \cdot 0.05^2 + 0.119^2 \cdot 0.15^2}} = 2.62$$

Example 8: same case as in 7, but $v_r = 0.20$

Condition as above; $G_m = 0.156 R_m$ and $Q_m = 0.135 R_m$

$$\beta = \frac{0.75 - 0.156 - 0.135}{\sqrt{0.75^2 \cdot 0.20^2 + 0.156^2 \cdot 0.05^2 + 0.135^2 \cdot 0.15^2}} = 3.03$$

Example 9: same loading case as examples 7 and 8, but glulam, with $v_r = 0.15$.

Condition: $1.35 G_k + 1.5 Q_k \leq (1/1.25)R_k$

$G_m = 0.196 R_m$ and $Q_m = 0.170 R_m$

$$\beta = \frac{0.75 - 0.196 - 0.170}{\sqrt{0.75^2 \cdot 0.15^2 + 0.196^2 \cdot 0.05^2 + 0.170^2 \cdot 0.15^2}} = 3.31$$

Another 9 examples were calculated for the same materials and load cases as above, but the time-dependancy was assumed to be 0.65 for permanent load and 0.82 for 1 weeks loading.

All β -values were put together in table 1.

Table 1. Values of β for 18 examples

loading	$\frac{k_{mod}}{\alpha_t}$	sawn wood $\gamma_{rm} = 1.4$		glulam $\gamma_{rm} = 1.25$
		$v_r = 0.25$	$v_r = 0.20$	$v_r = 0.15$
permanent moment extreme	$\frac{0.80}{0.55}$	2.31	2.59	2.62
	$\frac{0.80}{0.55}$	2.21	2.45	2.34
	$\frac{1.00}{0.75}$	2.62	3.03	3.31
permanent moment extreme	$\frac{0.80}{0.65}$	2.57	2.95	3.24
	$\frac{0.80}{0.65}$	2.48	2.83	2.99
	$\frac{1.00}{0.82}$	2.74	3.21	3.60

3.2 Safety index during and at the end of the lifetime of a structure..

The values of β , calculated in the foregoing examples, show that there is a fair, although not excessive chance that the permanent load or a load combination exceeds the long-duration- strength belonging to that duration of load.

If it is true however, that the damage due to long-duration-of -load arises only in the short period before failure actually occurs, during say 70 or 80% of the lifetime of a structure we have a reliability-index β of a material without load-duration effects.

For the first example, of a permanently loaded structure, a value $\beta = 2.31$ was calculated at the end of the lifetime of 100 years. During the first 70 or 80 years of the existence of that structure however there is no damage to be expected, and during that period the value of β can also be calculated:

$$\beta = \frac{R_m - 0.231 R_m}{R_m \sqrt{0.25^2 + 0.231^2 \cdot 0.05^2}} = 3.07$$

For glulam the same figures are : $\beta = 2.62$ at the end of the lifetime, and $\beta = 4.44$ during the period before.

Although the differences are less dramatic than might be expected, they are nevertheless important enough, especially for glulam structures. This is the more so if it is true that the more sophisticated methods of reliability-calculations result in higher β -values.

It is not clear yet how this problem could be avoided, and therefore it is not yet possible to make use of the higher strength, available during the greatest part of the lifetime of timber structures.

4 CONCLUSIONS

- The probability of forces or stresses in a structure to exceed a certain long-duration strength can as a first approximation be calculated in the same way as has been done before in [1].
- The conditions of Eurocode 5 give β -values of about 2.5 to 3.5, which is of the same magnitude as what was calculated before in [1].
- It seems not true therefore that the safety in timber structures is significant higher than was estimated by earlier calculations.
- These β -values however were calculated at the end of the lifetime of the structure, say after 100 years. The damage due to the load will probably only occur at the end of this period. During far the greatest part of the lifetime of timber structures the reliability is much higher than the existant calculations show.
- The β -values increase - of course - if a lower variability in the strength properties may be assumed;
- For the extreme load combinations of short duration a higher β , so a higher safety is found than for the permanent loads.

- For glulam a higher safety is found than for sawn wood, even with the lower γ_m - value in Eurocode 5. Such a special rule for less variable material seems well justified.
- If the Madison-factor of 0.55 could be increased to e.g. 0.65 the β -values will be significant higher or, with the same β -values the values of the other variables could be chosen more competitive.

N.B. With other, more sophisticated methods, better estimations of the reliability of structures can be made. It may be expected that higher values of β - 3.5 to 4 - will be found, using the same Eurocode 5 proposals. It is highly recommended that such reliability studies for timber structures should be made. The way in which the influence of long and short duration of loading has to be taken into account should be given very careful attention.

References

- [1] Kuipers,J., Structural safety. Heron 5 [1968].
- [2] Vrouwenvelder, A.C.W.M., and A.J.M.Siemes., Probabilistic calibration procedure for the derivation of partial safety factors for the Netherlands building codes.
- [3] Kuipers,J., Effect of age and/or load on timber strength. Does time and/or load damage timber? Proceedings CIB-W18- meeting Firenze, September 1986; paper 19-6-1.

INTERNATIONAL COUNCIL FOR BUILDING RESEARCH STUDIES AND DOCUMENTATION
WORKING COMMISSION W18A - TIMBER STRUCTURES

RELIABILITY OF WOOD STRUCTURAL ELEMENTS:
A PROBABILISTIC METHOD TO EUROCODE 5 CALIBRATION

by

F Rouger
Centre Technique du Bois et de l'Ameublement, Paris
France
N Lheritier
P Racher
M Fogli
Centre Universitaire des Sciences Techniques
Laboratoire de Genie Civil
University of Clermont-Ferrand
France

MEETING TWENTY - THREE

LISBON

PORTUGAL

SEPTEMBER 1990

0.1 Introduction.

This communication reports some preliminary results of a research program which has been initiated in France on "Reliability of Wood Structures". The Centre Technique du Bois et de l'Ameublement and the University of Clermont-Ferrand have initiated this program for design codes calibrations and structural (systems) design purposes.

The Eurocode 5 "Limit State Design Code" requires probabilistic analysis further than simple conversions from working stress design codes. This approach has been already employed for other materials (steel and concrete) in the European Design Codes [1] but also for wood in North America [2], [3]. The safety levels are usually given for single components. The systems design has been recently more and more investigated.

Based on mechanical models, probabilistic design of wood systems might be of great interest at least for three reasons :

- get some benefit of material variability, at least for redundant structures in which the between members variability gives load sharing effects.
- effects of semi-rigid connections on structural behavior increase the global safety, compared with single components design.
- wood structures have a good behavior under seismic or wind actions. A probabilistic analysis based on stochastic processes should give practical consequences for design.

This paper describes only some results dealing with single components analysis. The systems analysis will be investigated in the next two years.

0.2 Abstract.

The first part of this paper describes the reliability theory and methods available to compute probabilities of failure. In order to formulate further design equations, we need to know the distributions for both material behavior and actions.

Random variables have been fitted to wood properties (MOE, MOR,...) using a French Database which covers different species. This database is the result of a large research program whose objective was to qualify French species through their physical and mechanical properties, in relation with the silviculture modes. Modelling has been done for different species, different grades and different cross-sections.

The actions have been modelled using information available in the existing Limit State Design Codes (CSA086, CEB,...). Extreme values distributions have been used to model wind, snow, occupancy loads. The permanent loads have been modelled by normal distributions.

The first reliability analysis has been done for the basic case of a solid wood beam in bending. This approach is similar to the other design codes, but changes in climate, materials or return periods might slightly change the partial coefficients. The target safety indexes might also be different with respect to different constructions.

The second reliability analysis reported in this paper focused on bolted joints. A simplified fracture model has been used together with design codes recommendations in order to formulate limit state functions. The influence of humidity was also investigated as a modification factor to partial coefficients.

1. Reliability theory: definitions and methods.

1.1 Definitions.

A reliability analysis is based on three ideas (see [4], [5] for ex.) :

(1) define random distributions (continuous or stochastic processes) for each of the variables which has "randomness" (material properties, dimensions, actions,...).

Random variables	X_i	
Probability Density Function		$f(X_i)$
Cumulative Distribution Function		$F(X_i)$

(2) define a limit state function $G(X_i)$ which expresses the state of the structure (or component) being studied :

$G(X_i) > 0$	safe state
$G(X_i) = 0$	limit state
$G(X_i) < 0$	fracture.

In the space of the random variables, the equation $G(X_i) = 0$ defines a boundary between the safe and the failure domains.

(3) the probability of failure occurrence is defined by a multidimensional integral :

$$\text{Prob}(G \leq 0) = P_f = \int_{G \leq 0} f(X_i) dX_i$$

1.2 Methods.

The above integral might be solved by three methods :

- Monte-Carlo simulation :

* generate (through a random number generator) a set of sample values for each of the basic variables and determine the safety margin $f(X_i)$.

* after a large number n of trials, k is the number of trials in which $f(X_i) \leq 0$. The probability of failure is given by :

$$P_f = \lim_{n \rightarrow \infty} \frac{k}{n}$$

- Cornell Safety Index :

In the case of linear safety margin G and normal basic variables, the reliability index β is defined by :

$$\beta = \frac{\mu_G}{\sigma_G}$$

where μ and σ are respectively the mean and standard deviation of G .

The probability of failure is given by :

$$P_f = \Phi(-\beta)$$

where Φ is the standard normal cumulative distribution function.

This definition of the safety index is not invariant with regard to the choice of the failure functions which would give the same probability of failure. Therefore, the following definition of β is preferred.

- Hasofer-Lind safety index :

The H-L safety index is formulated for the case of standard normal basic variables which are uncorrelated. It is defined as the shortest distance from the origin to the failure surface in the space of the basic variables :

$$\beta = \min_{x \in \partial G} \left(\sum_{i=1}^n x_i^2 \right)^{\frac{1}{2}}$$

This distance might be determined numerically (Racwitz-Fiesler algorithm for example). If the basic variables are correlated or not standard, we might use transformation methods as Rosenblatt. The probability of failure is given by a similar equation than before.

- In the case of systems (parallel, series or combined assemblies of failure functions), approximative equations give bounds for the safety indexes.

2. Random Variables.

2.1 Material.

Three distributions have been fitted to the data [6] , using a maximum likelihood method :

- Weibull 2 parameters.
- Log-Normal.
- Normal.

In order to test the best fit, we used a Kolmogorov-Smirnov test (maximum difference between the estimated and the experimental CDF). In tables 1 and 2 are reported results for the MOE and the MOR, this for different species, cross-sections and grades.

Species	Section	Grade	Distribution	Mean	STD	30%
Poplar	25x65	BS	LogNormal	11.6	2.0	10.4
Poplar	40x100	BS	LogNormal	10.9	2.0	9.8
Poplar	50x150	BS	LogNormal	12.8	1.5	12.0
Douglas	40x100	B	LogNormal	11.7	2.4	10.3
Douglas	40x100	S	LogNormal	14.3	3.0	12.6
Douglas	50x150	B	LogNormal	12.3	2.4	10.9
Douglas	50x150	S	LogNormal	13.8	2.9	12.1
Marit. Pine	50x150	BS	LogNormal	13.2	1.9	12.1
Marit. Pine	65x200	BS	LogNormal	13.6	1.9	12.6

Table 1 : MOE (GPa) distributions for French Species, results from Database.

Species	Section	Grade	Distribution	Mean	STD	5%
Poplar	25x65	BS	Weibull	63.0	11.0	44.0
Poplar	40x100	BS	Weibull	53.0	14.0	29.0
Poplar	50x150	BS	LogNormal	57.0	12.0	36.0
Douglas	40x100	B	LogNormal	53.0	19.0	28.0
Douglas	40x100	S	LogNormal	67.0	24.0	35.0
Douglas	50x150	B	LogNormal	48.0	18.0	25.0
Douglas	50x150	S	LogNormal	53.0	19.0	28.0
Marit. Pine	50x150	BS	Weibull	59.0	14.0	34.0
Marit. Pine	65x200	BS	Weibull	59.0	13.0	37.0

Table 2 : MOR (MPa) distributions for French Species, results from Database.

2.2 Actions.

2.2.1 Dead Load

Notation : G

These actions are modelled by Normal distributions. In this case, the characteristic value is equal to the mean. In further analysis, we consider three load cases :

Action	Mean	C.O.V.
Floor	37 daN/m ²	10%
Light roof cover	20 daN/m ²	10%
Heavy roof cover	90 daN/m ²	10%

2.2.2 Occupancy Loads.

Notation : Q

The instantaneous response of a such action is a stochastic process. The extreme values distribution (over the return period) follow a Gumbell model. The characteristic value (over 50 years) might be deducted from this distribution by :

$$Q_{50} = E_Q + \frac{S_Q \ln \frac{50}{T_Q} \sqrt{6}}{\pi}$$

where E_Q is the mean of Q

S_Q is the standard deviation of Q

T_Q is the return period of Q

For further floor calculations, we consider three load cases.

Action	E_Q	S_Q	T_Q	Q_{50}
Residential	40 daN/m ²	40 daN/m ²	7 years	100 daN/m ²
Offices (20 m ²)	50 daN/m ²	50 daN/m ²	5 years	145 daN/m ²
Commercials	70 daN/m ²	54 daN/m ²	5 years	170 daN/m ²

2.2.3 Snow Load

Notation : Q_H

Ground snow load might be evaluated by :

$$Q_{H0} = H v \quad \text{avec} \quad v = \begin{cases} 150 \text{ daN/m}^3 \\ 100 [3 - 2 \exp(-1.5 H)] \text{ daN/m}^3 \end{cases}$$

where H is the snow height and v its density, which might depend on height.

The roof snow load is deducted from the ground snow load by :

$$Q_H = \mu Q_{H0}$$

where μ is a factor which depends on the shape of the roof. For simple cases, $\mu = 0.8$.

In the French design codes (N84 for snow) are reported characteristic values (Return period = 50 years) Q_{Hk} . The characteristic heights H_k are deducted assuming $v = 150 \text{ daN/m}^3$. The instantaneous maxima distribution is a Gumbell model whose parameters are evaluated assuming a coefficient of variation of 20%. The mean is given by :

$$\left\{ \begin{array}{l} E_H = \frac{H_{50} \frac{\pi}{\text{COV} \sqrt{6}}}{\frac{\pi}{\text{COV} \sqrt{6}} - \gamma + 3.9} \Rightarrow E_H \approx 0.66 H_{50} \\ \text{COV} = 0.20 \end{array} \right.$$

For roof calculations, we chose four regions :

		Q_{50}	H_{50}	E_H	COV
Region A	< 100 m	36 daN/m ²	0.30 m	0.20 m	20%
Region B	< 100 m	44 daN/m ²	0.37 m	0.24 m	20%
Region B	1000 m	200 daN/m ²	1.67 m	1.10 m	20%
Region C	< 100 m	52 daN/m ²	0.43 m	0.29 m	20%

2.3.4 Wind loads

Notation : Q_w

Wind load is given by :

$$Q_w = \frac{W^2}{16.3}$$

where W is the wind velocity. In the French code (NV65 for wind), are reported characteristic values for both loads and velocities. The instantaneous maxima distribution is a Gumbell model whose parameters are :

$$\left\{ \begin{array}{l} E_w = \frac{W_{50} \frac{\pi}{\text{COV} \sqrt{6}}}{\frac{\pi}{\text{COV} \sqrt{6}} - \gamma + 3.9} \Rightarrow E_w \approx 0.66 W_{50} \\ \text{COV} = 0.20 \end{array} \right.$$

For roof calculations, we chose :

	Q_{50}	W_{50}	E_w	COV
Region I	50 daN/m ²	28.6 m/s	18.9 m/s	20%
Region II	70 daN/m ²	33.8 m/s	22.3 m/s	20%
Region III	90 daN/m ²	38.3 m/s	25.3 m/s	20%

2.3 Geometry.

In the first parts of the study, dimensions are considered as deterministic. The size effects are not taken into account and the material properties are given specifically for each cross-section.

In section 3.4, we reported a brief study of geometry variability, in which dimensions are modelled by normal variables.

3. The simple bending problem.

3.1 Load cases.

The following load cases have been investigated for ultimate limit states :

Floors : 3 load cases.

Dead load + Live Load (Residential, Office, Commercial)

Roofs : 20 Load Cases.

Dead Load (Light, Heavy) + Snow (Regions A₁₀₀, B₁₀₀, B₁₀₀₀, C₁₀₀)

Dead Load (Light, Heavy) + Wind (Regions I, II, III)

Dead Load (Light, Heavy) + Snow + Wind.

Floors have been studied with Maritime Pine 65x200 BS.

Roofs have been studied with Maritime Pine 65x200 BS, Maritime Pine 50x150 BS, Poplar 50x150 BS, Douglas 50x150 B&S.

3.2 Ultimate Limit States.

3.2.1 Limit state design equations.

For calibration purposes, a limit state design equation is the combination of a design formula given in the code and a corresponding failure function :

* Eurocode 5 design formula (example for dead load + 1 live load) :

$$\alpha(\gamma_G G_k + \gamma_Q Q_k) = \frac{X_k}{\gamma_m}$$

with

$$\gamma_G = 1.35 \quad \gamma_Q = 1.5 \quad \gamma_m = 1.4$$

X_k is the characteristic stress of the material.

α is a coefficient which gives the stress on the beam from the load. For example, in the case of uniform load, we have :

$$\alpha = \frac{s L^2}{8 (I_v)} \quad \text{with} \quad \begin{cases} s : \text{joists spacing} \\ L : \text{Span} \\ I_v : \text{Moment of Inertia} \end{cases}$$

* Corresponding failure function :

$$FF = R - \alpha(G + Q)$$

The combination of these equations requires the following notations :

$$\delta = \frac{G_k}{Q_k} \quad g = \frac{G}{G_k} \quad q = \frac{Q}{Q_k}$$

We obtain the following design equation :

$$LSDE = R - \frac{(g\delta + q)X_k}{\gamma_m(\gamma_G \delta + \gamma_Q)}$$

Similar design equations might be obtained for three load combinations. In the case of snow or wind load, the random variables are the snow heights and wind velocity respectively. These design formulae are therefore slightly different.

3.2.2 Results.

A parametric study has been done on partial coefficient γ_m . The objective is to evaluate the (γ_m, β) curves and to give values for target safeties. The following table is the result of these simulations. In Figure 1 are reported average curves for all species and grades.

Load Case	Partial coefficient γ_m					
	0.8	1.0	1.2	1.4	1.6	1.8
D + Q	2.5	2.9	3.1	3.4	3.5	3.7
	4.6%	3.7%	3.2%	2.8%	2.6%	2.4%
D + Q _H	2.6	3.1	3.5	3.8	4.1	4.3
	9.7%	8.6%	8.8%	9.4%	10.1%	10.8%
D + Q _W	2.7	3.2	3.5	3.8	4.0	4.3
	7%	6%	6%	7%	8%	8%
D + Q _H + Q _W	2.7	3.1	3.5	3.8	4.0	4.2
	9%	8%	9%	9%	10%	11%
Average	2.6	3.1	3.4	3.7	3.9	4.1

Table 3 : Mean β values (and COV in %), all species and load cases together.

ϕ	0.95	0.90	0.80	0.70	0.65
$1/\phi$	1.05	1.1	1.25	1.43	1.54
β	2.5	2.6	2.8	3.0	3.1

Table 4 : Results from Canadian Experience.

Etats Limites Ultimes en Flexion

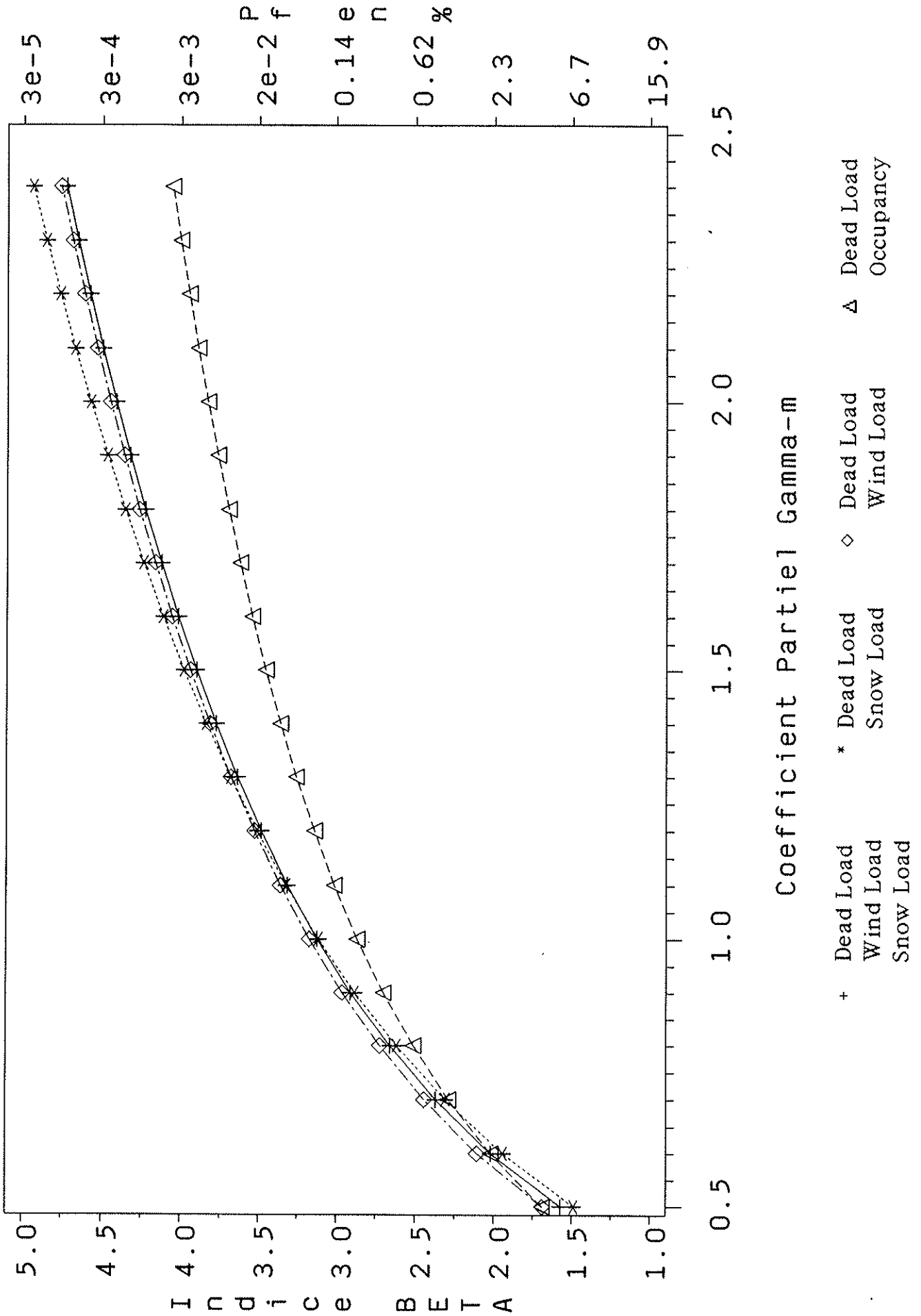


Figure 1 : Ultimate Limit States in Bending , all species.

The Canadian code [2] , [3] has adopted a target β of 2.8 ($\phi=0.8$), which is well adapted to light frame houses. In Eurocode 5, the current γ_m value is 1.4, which gives a safety index of 3.7. This should be compared to Steel or Concrete LSD codes which give β values of 3-4 for single components. This higher safety level corresponds to larger structures in which collapse might cause high damage.

If we compare β values (French/Canadian) for an equivalent partial coefficient, we see that safety level of French code is much higher than Canadian code. This is probably due to a return period which is only of 30 years in the Canadian Code.

3.3 Serviceability limit state.

Serviceability is checked for one live load (Snow/Wind/Occupancy). The deflection δ has to be lower than a ratio (L/K) of the span of the beam. As we did for ultimate limit states, the limit state design equation for calibration purposes is derived below :

* Eurocode 5 :

$$\delta = \frac{\alpha Q_k \gamma_m}{E_k} = \frac{L}{K}$$

* Failure Function :

$$FF = \frac{L}{K} - \frac{\alpha Q}{E}$$

* Limit State Design Equation :

$$LSDE = \frac{L}{K} \left[1.0 - \frac{q E_k}{E \gamma_m} \right]$$

Simulations have been done for each live load available, and for each species/grade/cross-section possible. Results are reported below.

Load Case	Partial coefficient γ_m							
	0.6	0.8	1.0	1.2	1.4	1.6	1.8	2.0
Q	0.7	1.2	1.5	1.8	2.1	2.4	2.6	2.8
	15%	11%	9%	8%	8%	7%	7%	7%
Q _H	0.2	1.1	1.8	2.3	2.7	3.0	3.4	3.6
	60%	10%	7%	6%	5.8%	5.8%	5.9%	6%
Q _W	0.9	1.5	1.9	2.3	2.5	2.8	3.0	3.2
	5%	4%	3%	3%	2.5%	2.5%	2.5%	2.4%
Average	0.6	1.3	1.7	2.1	2.4	2.7	3.0	3.2

Table 5 : Mean β values (and COV in %), all species and load cases together.

These results show that the safety level for deflections is much lower than for stresses. But the required target has to be lower with respect to low damage. The current Canadian value is $\phi = 0.5$ ($1/\phi = 2.0$) which gives a safety index of 2.0. This value is much lower than in Table 5. This is due to two reasons :

- Different return periods (30 years instead of 50 years).
- Different characteristic MOE (mean instead of 30% exclusion).

3.4 Geometrical Uncertainties.

In the current codes, dimensions are considered as deterministic. A random effect on geometry might occur due to tolerances during processing.

This variability has been investigated, modelling dimensions as normal distributions. The coefficient of variation of these distributions has been taken at COV = 5%.

The analysis has been done for (dead load+occupancy load) which is the worst case in terms of safety. Results are reported in Table 6 below :

Case	Partial coefficient γ_m					
	0.8	1.0	1.2	1.4	1.6	1.8
Deterministic	2.5	2.9	3.1	3.4	3.5	3.7
COV = 5%	2.5	2.85	3.1	3.3	3.5	3.7

Table 6 : Mean β values for different geometry variations.

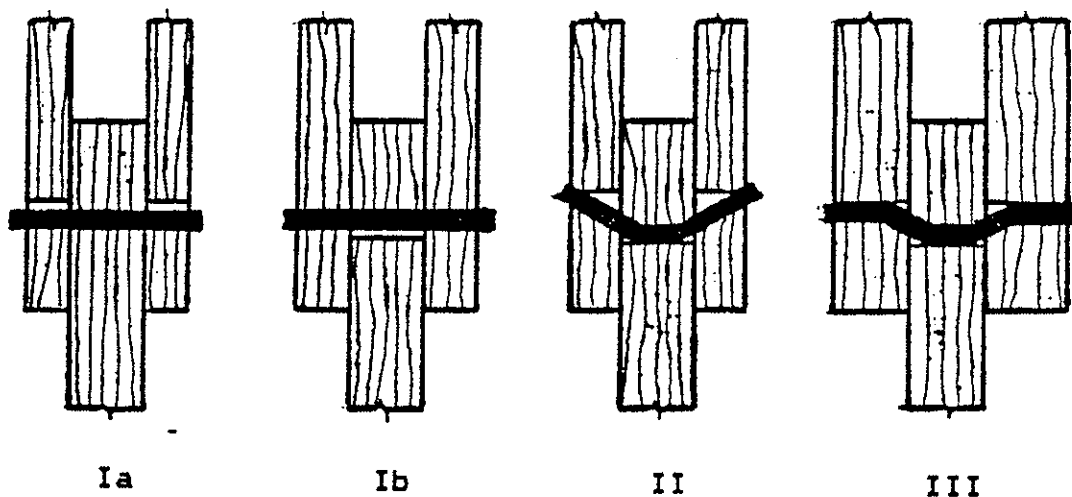
4. Reliability of bolted joints [7].

Joints behavior is another important aspect of single components analysis. Here is reported a study of double shear bolted joints, in which safety indexes are derived for different member thicknesses and bolt diameters.

4.1 Failure modes and load capacities of bolted joints.

The current rules used for design have been originally developed by Johansen and are based on theory of plasticity [8]. The load-deformation curves are assumed to be stiff-plastic for bending of the bolt as well as wood embedment.

Three different failure modes might occur in a 3 members joint :



In mode I, fracture is due to shear in wood.

In mode II, there is one plastic hinge.

In mode III, there is two plastic hinges.

The failure mode depends on members thickness, yield strength of bolt and wood, bolt diameter. For each mode, a ultimate load-carrying capacity might be evaluated. The joint ultimate load is the minimum of the three individual modes.

The embedment strength might be itself a function of wood density. In this study, we preferred to use a direct relation between the embedment strength f_b and the compression strength f_c .

$$f_b = 0.65 \cdot f_c$$

According to Johansen formulae, the ultimate load R is given by :

$$R = \min \{ \tilde{R}_i (f_{bj}, t_j, f_y, d, k_{\alpha,j}) \}$$

where

i describes the failure mode, which depends on t/d .

f_{bj} are the embedment strengths of wood members.

t_j are the members thicknesses.

f_y is the yield strength of the bolt.

d is the bolt diameter.

$k_{\alpha,j}$ are factors which depend on the angle between force and grain directions.

The current Eurocode 5 design equations give a characteristic load R_k which is derived from the original Johansen formulae.

4.2 Limit State Design Equation.

The limit state design equation for (dead load + 1 live load) combination is formulated as in 3.2.1 :

$$LSDE = R - \frac{(g\delta + q) R_k}{\gamma_m(\gamma_G\delta + \gamma_Q)}$$

The δ value has been taken at 1 and 4. The analysis has been done for 6 joints configurations.

The dimensions are deterministic :

Joint	d (mm)	t ₁ (mm)	t ₂ (mm)	t/d
1	20	50	100	5
2	20	100	200	10
3	12	12	24	2
4	12	36	72	6
5	20	20	40	2
6	12	60	120	10

The random variables for material properties are given below :

Variable	Distribution	Mean	COV
f_y (MPa)	LogNormal	400	0.1
f_b (MPa) (case A)	Lognormal	40	0.2
f_b (MPa) (case B)	Lognormal	40	0.35

4.3 Results and preconsisations.

As in previous analysis, (γ_m, β) curves have been derived for each joint configuration and load case. In figure 2 is reported an example (Joint n.2 , dead load only) in which (γ_m, β) curves are given for each individual failure mode (I, II, III). The safety β of the joint is given by the minimum of $(\beta_I, \beta_{II}, \beta_{III})$.

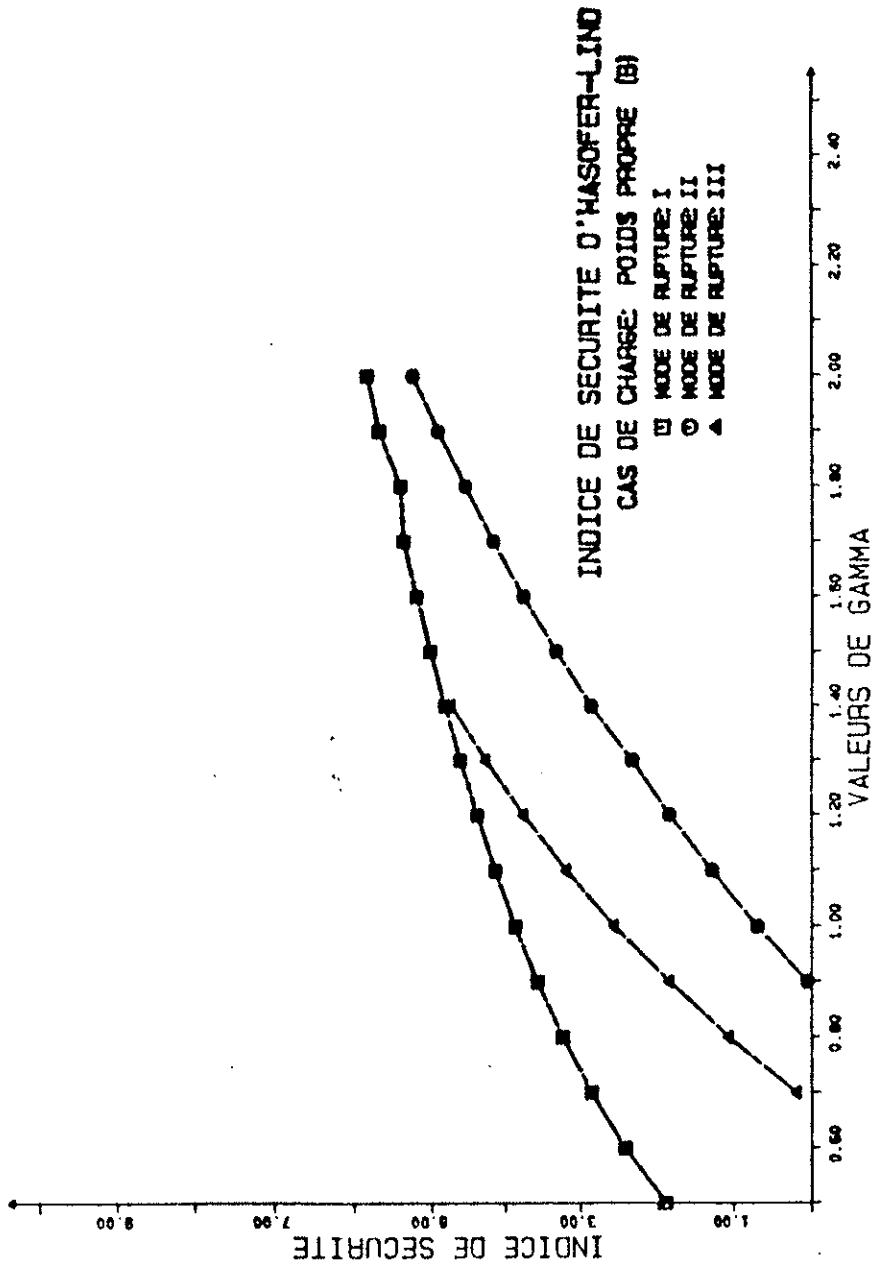
The joint curves are reported in figure 3. For a given γ_m value, the safety index β depends on t/d which influences the failure mode.

The average β values corresponding to a target γ_m of 1.4 are given in Table 6 for two joint configurations and for two material variabilities (Coefficient of variation of the embedment strength f_b). In brackets are reported the coefficients of variation of β within the load cases.

COV of f_b	$t/d = 2$	$t/d = 10$
20%	3.6 (8%)	4.1 (12%)
35%	2.2 (15%)	3.3 (11%)
Average	2.9	3.7

Table 6 : β values for different joint configurations.

~~The safety levels vary both with the material and with t/d . These levels are comparable to the previous bending study, except for the case ($t/d=2$ and $COV(f_b)=0.35$) in which the safety level is too low. The~~



ASSEMBLAGE II

Figure 2 : Individual Failure modes in a bolted connection.

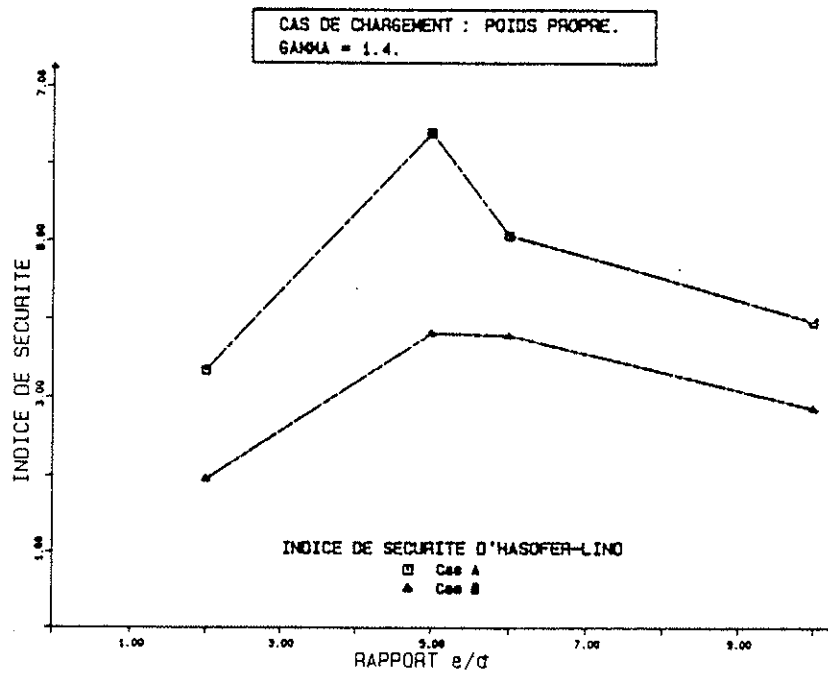
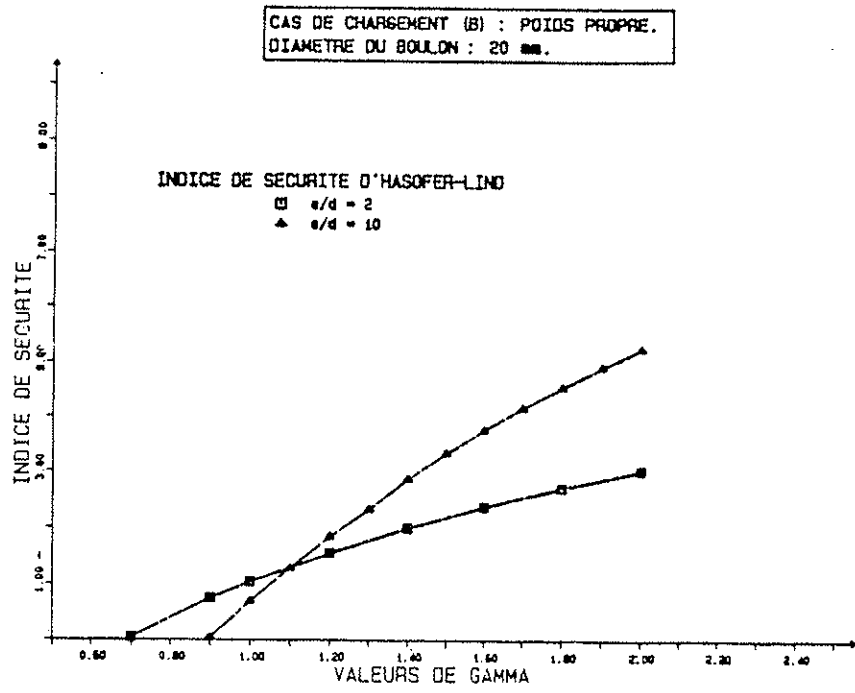


Figure 3 : Performance Curve of the connection , depending on t/d .

The safety levels vary both with the material and with t/d . These levels are comparable to the previous bending study, except for the case { $t/d=2$ and $COV(f_b)=0.35$ } in which the safety level is too low. The influence of (t/d) is much more important when the material is variable.

In Table 7 are given the intervals of γ_m which would give β values between 3 and 5.

COV of f_b	$t/d < 5$	$t/d \geq 5$
20%	[1.1 ; 2.0]	[1.1 ; 1.9]
35%	[1.6 ; 2.0]	[1.1 ; 2.0]

Table 7 : β values for different joint configurations.

4.4 Influence of humidity.

In order to calibrate modification factors which take into account the effect of humidity, an analysis has been done on the single shear joints. Humidity modifies the embedment strength (f_b) and the dimensions.

(1) The embedment strength f_b at humidity H , according to [9], is deduced from f_{b15} (at $H=15\%$) using a linear surface equation :

* if $0 < f_{b15} < 38.5$ MPa

$$f_b = f_{b15} + \alpha(H - 15)$$

with

$$\alpha = -2.367 \cdot 10^{-2} \cdot f_{b15} - 3.126 \cdot 10^{-4} \cdot f_{b15}^2$$

* if $f_{b15} > 38.5$ MPa

$$f_b = f_{b15} - 2.482 \cdot (H - 15)$$

(2) The dimensions are modified according to :

$$X_H = X_0 \cdot \left(1 + \alpha \frac{H - 15}{100}\right)$$

where

X_0 is the dimension at $H=0\%$

α is a retractibility coefficient ($\alpha=0.27$ for Douglas).

The design resistance R_d for $H \neq 15\%$ is given by :

$$R_d = k_{\text{mod}} \frac{R_k}{\gamma_m} \Leftrightarrow R_d = \frac{R_k}{\gamma_R} \quad \text{with} \quad \left(\gamma_R = \frac{\gamma_m}{k_{\text{mod}}} \right)$$

Using modification equations for f_b and X , (γ_m, β) curves are evaluated for different humidities (see figure 4 for example). The curves are horizontally shifted to the (15%) curve. The shift factors correspond to k_{mod} values, i.e. using γ_R partial coefficients, the safety levels are the same for different humidities.

In table 8 are reported average k_{mod} values for two joint geometries.

	H = 10%	H = 15%	H = 20%
t/d = 2	1.13	1.0	0.86
t/d = 10	1.10	1.0	0.90

Table 8 : k_{mod} values for different humidities and joint geometries.

These values are slightly different from the current Eurocode 5 values which are :

Class I and II ($H < 18\%$)	$k_{\text{mod}} = 1.0$
Class III ($H > 18\%$)	$k_{\text{mod}} = 0.8$

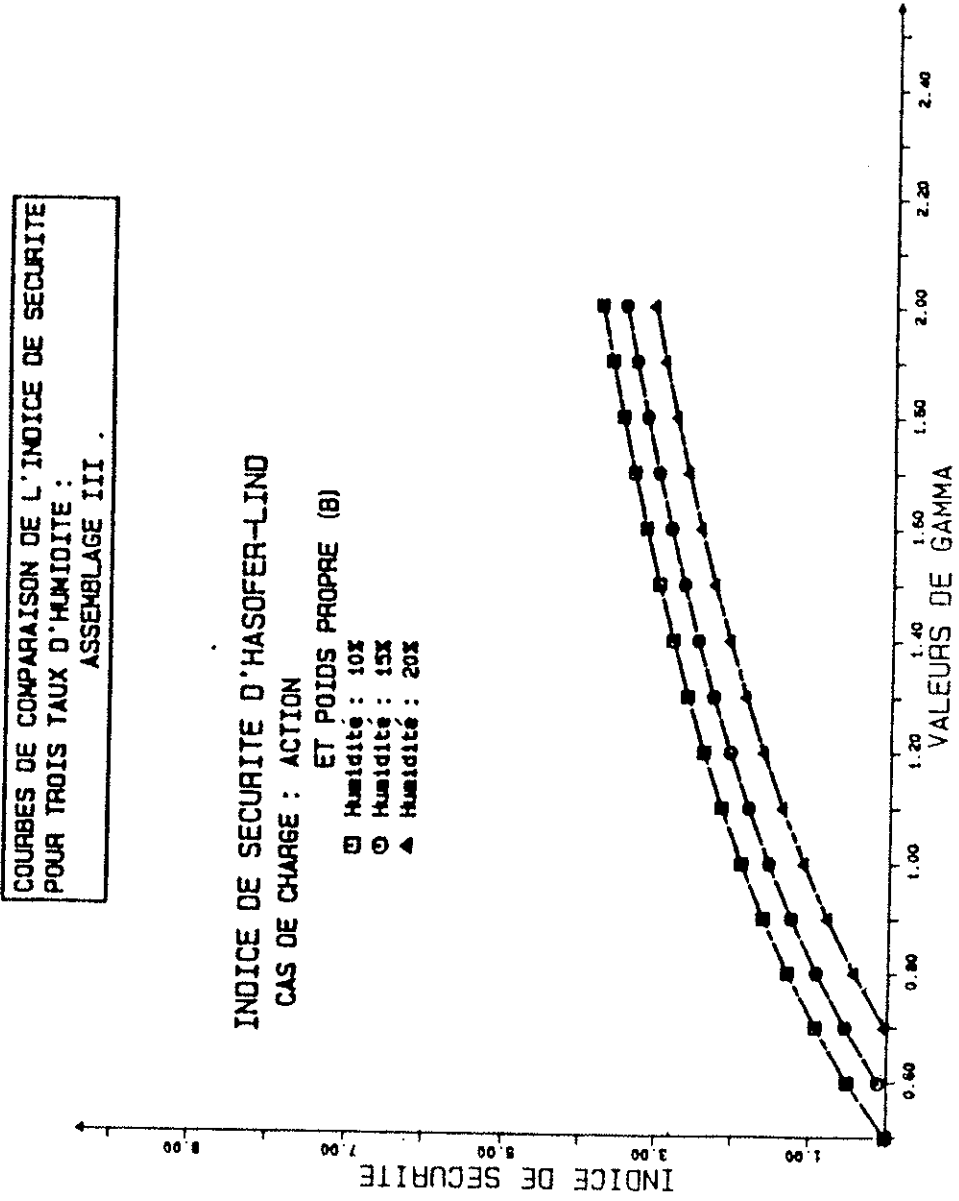


Figure 4 : Moisture content influence on safety.

5. Conclusion.

Single elements calibrations have shown that the current partial coefficients give safety levels comparable to other design codes.

The bending study has shown that the serviceability limit states give much lower safety levels than ultimate limit states. The geometrical uncertainties have a slight influence on the safety levels, which might be omitted in design codes, at least for a given humidity. The bending problem will have to be completed by other simple problems, as shear for example.

For bolted connections, it seems difficult to adopt only one value for γ_m because of a strong influence of joint geometries. The humidity effect is slightly higher than predicted by the Eurocode 5. The study has been done only for ultimate limit states, based on a theory of perfect plasticity. Further investigation should be done, taking into account elasto-plastic behaviors and looking at the deformations, which probably influence the safety of the connections.

In a near future, these simple investigations will give a basis for systems analysis in which interactions between elements influence the global safety of the structures.

6. References.

- [1] Manuel "Sécurité des Constructions" , bulletins d'information n. 127 et 128 du Comité Euro-International du Béton (CEB) , 1980.
- [2] CAN3-086.1-M90 "Engineering Design in Wood" (Limit States Design).
- [3] R.O. Foschi , B.R. Folz , F.Z. Yao, 1989
"Reliability Based Design of Wood Structures", Univ. of British Columbia, Vancouver, CANADA.
- [4] P. Thoft-Christensen, M.J. Baker, 1982
"Structural Reliability Theory and its applications", Springer-Verlag.
- [5] A.H.S Ang , W.H. Tang, 1975
"Probability Concepts in Engineering Planning and Design." ,
J. Wiley & Sons.
- [6] D. Guinard , J.L. Blachon , Ph. Crubilé, 1989
"La valorisation des Bois Français pour une utilisation en structure :
La démarche du CTBA", Rapport interne CTBA.
- [7] N. Lhéritier , 1989
"Approche probabiliste de la sécurité des assemblages bois",
Centre Universitaire des Sciences et Techniques, Université de
Clermont-Ferrand II .
- [8] H.J. Larsen , 1979
"Design of Bolted Joints" , CIBW 18 , 12th Meeting, Bordeaux, FRANCE.
- [9] J.D. Barrett , W. Lau , 1989
"Moisture Adjustments for in grade data" , CIBW 18 , 22nd Meeting,
Berlin , GDR.

INTERNATIONAL COUNCIL FOR BUILDING RESEARCH STUDIES AND DOCUMENTATION

WORKING COMMISSION W18A - TIMBER STRUCTURES

TIMBER IN COMPRESSION PERPENDICULAR TO GRAIN

by

U Korin
National Building Research Institute
The Technion, Haifa
Israel

MEETING TWENTY - THREE

LISBON

PORTUGAL

SEPTEMBER 1990

Timber in Compression Perpendicular to Grain

Dr. Uri Korin, National Building Research Institute,
The Technion Haifa, Israel

Summary

The compressive strength of timber perpendicular to grain was investigated. The study reports tests conducted on whitewood specimens 40 mm x 90 mm x 180 mm in size in central loading or end loading for varying lengths of loading sectors l/L . Upgrading experiment of bearing capacity of the timber by Nailplates reinforcement was found to be unsuccessful.

1. Introduction

Compression stresses perpendicular to grain are generally encountered in every timber beam element, and in some other structures such as trusses supporting points. This compression stresses are usually small, and special care is seldom taken for their check. However, in high and heavy timber beams and timber truss rafters, it is always necessary to study the bearing stresses perpendicular to grain in the supporting zones.

2. Compression stresses perpendicular to grain

Timber is an unisotropic material. Madsen et al⁽¹⁾ discuss the unisotropic arrangement of cells in the wood and the ways this arrangement is influencing the behaviour of the wood under compression stresses perpendicular to grain. The wood comprises tubular cellulose cells embedded in a lignin matrix (Fig. 1). Under the influence of stresses perpendicular to grain, a layered failure mode is obtained (Fig. 2).

The full model of the behaviour of the unisotropic tubular composite under transvers stresses exhibits first the elastic deformation of the tubular

cells walls (the straight line zone of the stress-strain curve). Collaps of walls of some cells may occure in very low stresses and thus, a substensial deviation from the straight line may be met in many cases. The stress-strain curve is moving on in a shallow slope until all the tubes are flatened and a strain hardening may appear (Fig. 3). This mode of layered failure of tubular cells is associated with relatively high strains of the wood when it is loaded perpendicular to grain.

As some of the cells are collapsed at very low stresses, we do not possess any elastic straight zone, and the stress-strain curve is a curved line in all it's length, expressing the combination of elastic behaviour of some of the cells and the same time collapse of the others. In compression tests up to strains of 10 percent, we usually end in the second zone of the stress-strain curve (Fig. 4).

The standard compression perpendicular to grain test method of ASTM D 143(2) (Fig. 5) expresses the practical approach of those who dealt with timber multivalent behaviour. The test specimens 6" long, 2" high and 2" thick are supported in all their length and are transversly loaded along a central sector of 2" ($l/L=0.333$). The test method does not include a clear definition of the strength. It is recommended to monitor the load for 0.2" (10 percent) deformation and the point of deviation of the stress-strain curve from the straight line. A plastic deformation of 10 percent as a strength cretiria for an engineering material is seldom accepted, and as it was said before, the exact point of deviation of the curve from the straight line is also very hard to define.

The loading of the central sector permits the tested specimen to take advantage of the unisotropic structure of the wood and to engage the longitudinal tubes to increase the monitored strength, in comparison with a specimen loaded in all its length.

Madsen suggests the intersection of a parallel line at distance of 0.2 percent strain as a strength cretiria. As it was said before, the straight line is very difficult to define, and thus, its slope, and the slope of the parallel line will not be a precise instrument for assessment of the transvers compression strength of timber.

Examination of the test results reported here as shown that the 0.2 percent parallel line intersects the stress-strain line at a strain of about 2.5 percent. Thus, it was decided to use a strain of 2.5 percent as the strength criteria for the specimens tested in this study (Fig. 6).

3. The loading pattern

Loading perpendicular to grain is usually applied to a small portion of the length of a loaded timber element. This is always correct for beams or truss rafters. There are only few cases where a timber element is transversely loaded and supported along all its length, (as we may find in some special types of pallets or in mining timber). However, loads are very often applied to timber elements at their ends, without any overhangs and this pattern of loading of timber perpendicular to grain should be taken in mind during the investigation.

4. The experimental stage

The experiments reported here are the first part of a comprehensive test programme of the behaviour of timber in compression perpendicular to grain.

The details of the experiments are briefly reported:

- 4.1 The timber used for this stage of the investigation was commercial whitewood marked: American White Wood, Maine, U.S.A., 45 mm x 95 mm x 3000 mm planks.
- 4.2 The following tests were conducted for characterization of the timber: modulus of rupture, modulus of elasticity in bending, compressive strength, and modulus of elasticity in compression in grain direction according to RILEM⁽³⁾ recommendations; compressive strength perpendicular to grain according to ASTM D-143. The density of each specimen used in this investigation was also measured.

4.3 The loading perpendicular to grain was conducted on test pieces with a cross section of 40 mm x 90 mm and a length L of 180 mm (Fig 7-10). The specimens were supported at the bottom along their complete length and loaded from the top along a length portion l, in the central sector (Fig. 7) or at the end of the length of the specimen (Fig. 8). The lengths of the loaded zone e were between 0.125 L and 1.0L.

4.4 Timber specimens were reinforced from two sides by nail plates.

(Fig. 9-10). These specimens were loaded as described in 4.3 above. The purpose of this part of the study was to investigate the possibility of upgrading methods for the compression perpendicular to grain.

5. Experimental results

5.1 Characterization of the timber - the data are presented in Table 1.

5.2 Compression perpendicular to grain. The relationship between the density of the timber and the compressive strength perpendicular to grain is given in Fig. 11.

It compares: (a) the strength calculated according to table A 2.3a of Eurocode No. 5⁽⁴⁾; (b) the compressive strength tested according to ASTM D143 (2.5 percent strain) and (c) the compressive resistance perpendicular to grain determined according to 4.3 for specimens loaded from two sides along their complete length (2.5 percent strain). The comparison shows that the bearing capacity of the timber obtained from the last method was lower from the calculated capacity or the ASTM D143 compressive strength.

5.3 The dependence of the bearing capacity of the centrally loaded specimens on the relative length of the central loaded sector l/L is shown in Fig. 12.

Table 1 - Structural properties of the timber

Specimen	1	2	3	4	5	Average
Density (Kg/m ³)	432	425	443	419	496	443
Modulus of rapture (MPa)	38.6	34.3	39.5	47.8	60.5	44.1
Modulus of elasticity in bending (MPa)	11,300	10,850	13,100	10,050	11,750	11,400
Compressive strength (MPa)	25.6	30.4	30.7	26.0	35.1	29.6
Modulus of elasticity in compression (MPa)	9,400	9,700	10,000	7,100	14,650	10,170

5.4 Fig. 13 shows the bearing capacities of the end sector loaded specimens against the ratio l/L .

5.5 The bearing capacities of the Nail Plates reinforced test specimens are shown in Fig. 14 and Fig. 15. Comparison of the bearing capacities of the reinforced and non-reinforced specimens, shows very little contribution of the reinforcement to the bearing capacity of the timber perpendicular to grain.

6. Discussion and Conclusions

6.1 It is necessary to agree about a clear strength-bearing capacity criteria for timber in compression perpendicular to grain.

6.2 Eurocode 5 brings a parameter $K_{c,90}$ for use in equation 5.1.5a:

$$\sigma_{c,90,d} \leq K_{c,90} f_{c,90,d}$$

K_c depends upon the length of the overhangs of the loaded member. Table 2 presents a comparison between the values of K_c calculated for the loading conditions in this investigation and the experimental results of this investigation. The differences between the compared values are very large and should be further studied.

6.3 The investigation covered sofar only one kind of timber and one cross section ($d/b=2$). There is a room for a much wider investigation on the subject.

Table 2 - Comparison between $K_{c,90}$ and experimental results.

l/L	Central Sector loaded		End sector loaded	
	K_c	Experimental results	K_c	Experimental results
1	1	1	1	1
0.875	1	1.063	1	1.063
0.75	1.006	1.188	1	1.156
0.625	1.025	1.375	1	1.281
0.50	1.061	1.625	1	1.438
0.375	1.124	1.969	1	1.625
0.25	1.237	2.344	1	1.875
0.125	1.478	2.781	1	2.156

References

1. Borg Madsen, R. F. Hooley and C.P. Hall, "A design method for bearing stresses in wood", CAN. J. CIV. ENG. VOL. 9, 1982, pp. 338-349.
2. Standard Methods of Testing Small Clear Specimens of Timber, ASTM D143-83, Compression perpendicular to grain, Par. 79-84.
3. Testing Methods for timber in structural sizes RILEM, 3TT-3.
4. Eurocode No. 5: Common unified rules for timber structures, EUR 9887 EN. 1988.

FIG. 1. Model of clear wood structure. (1)

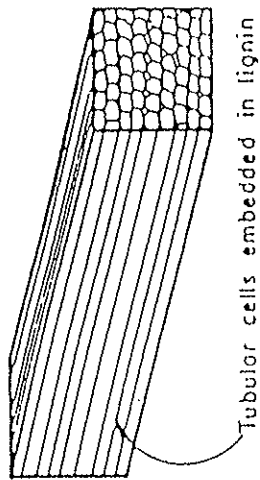


FIG. 2. Failure mode in compression perpendicular to grain. (2)

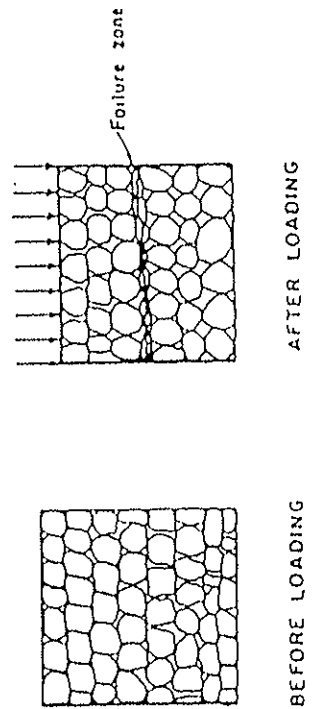


Fig. 3 - Stress strain relations of a tubular composite material

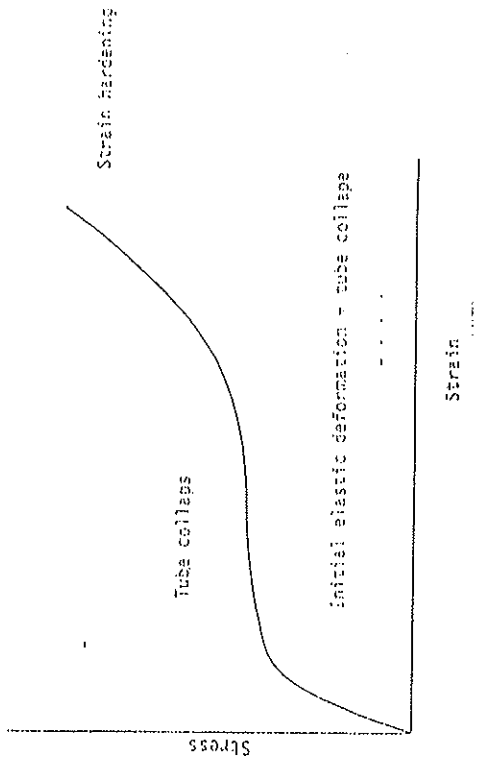


Fig. 4 . Typical load-deflection curves (spruce-pine-

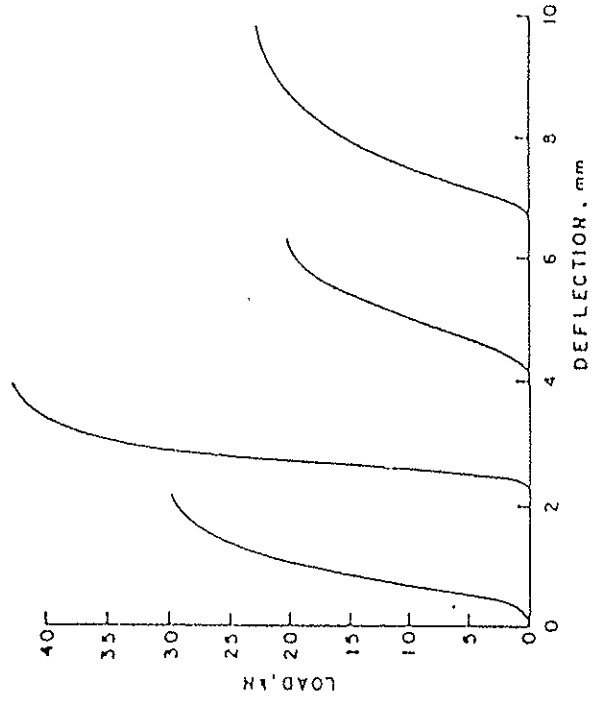


Fig. 5 - ASTM D 143 - Compression perpendicular to grain specimen

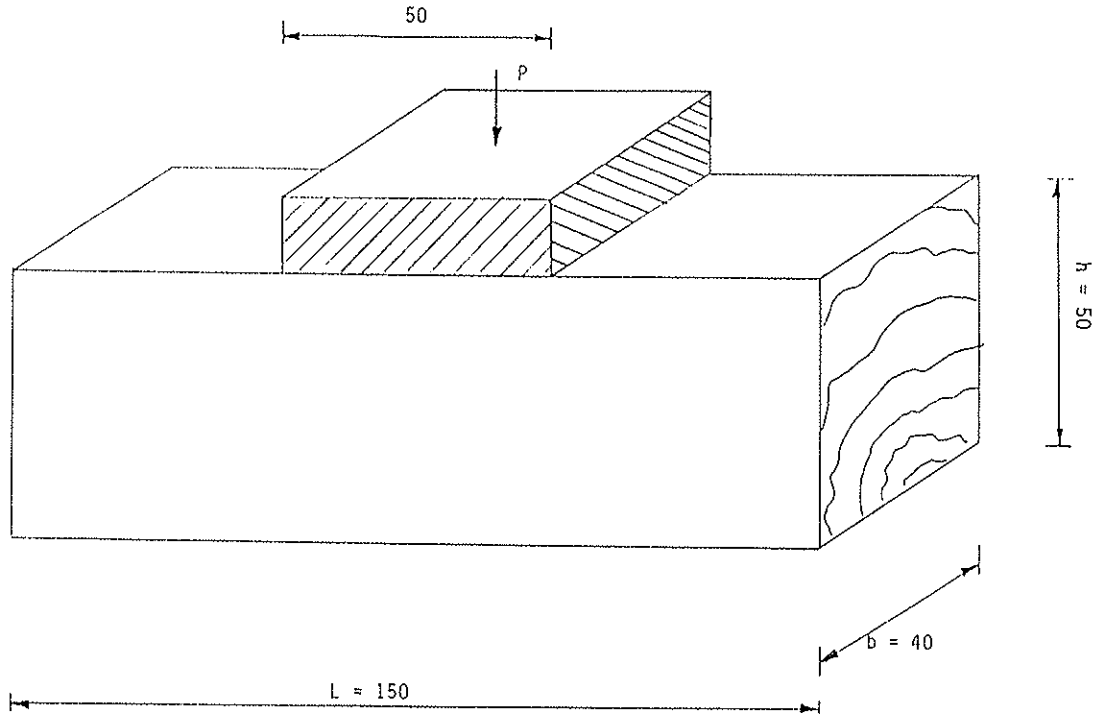


Fig. 6 - COMPRESSION STRESS-STRAIN RELATIONS

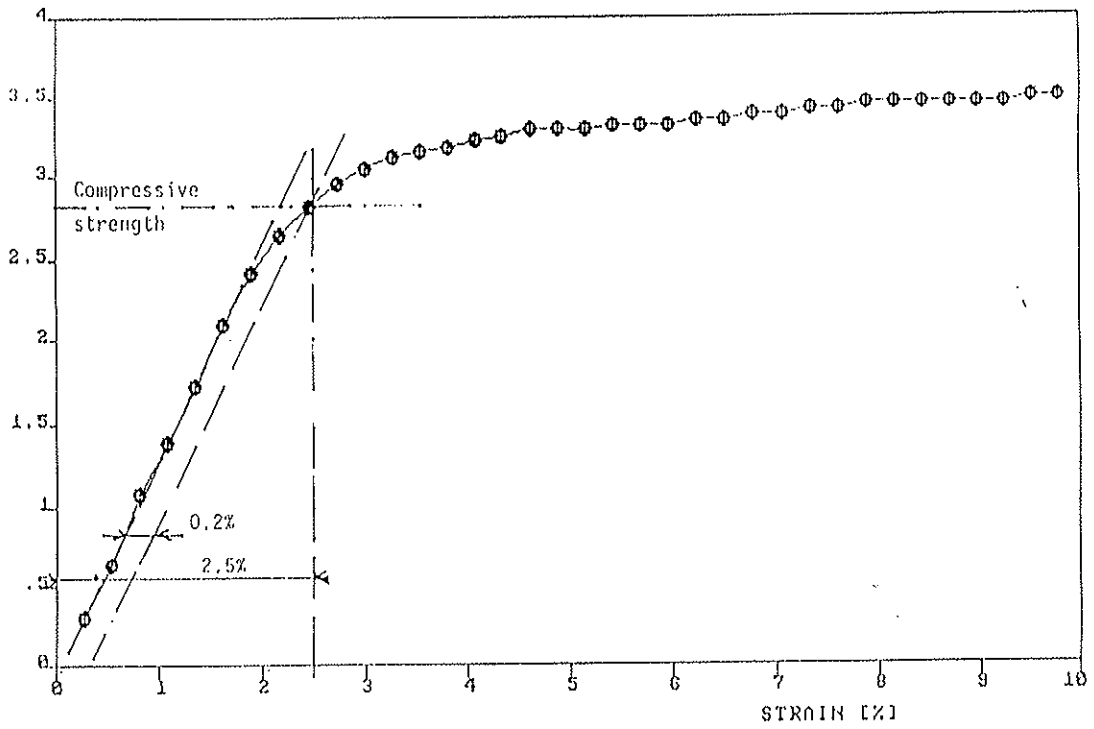


Fig. 7 - Central sector loaded - 10 -

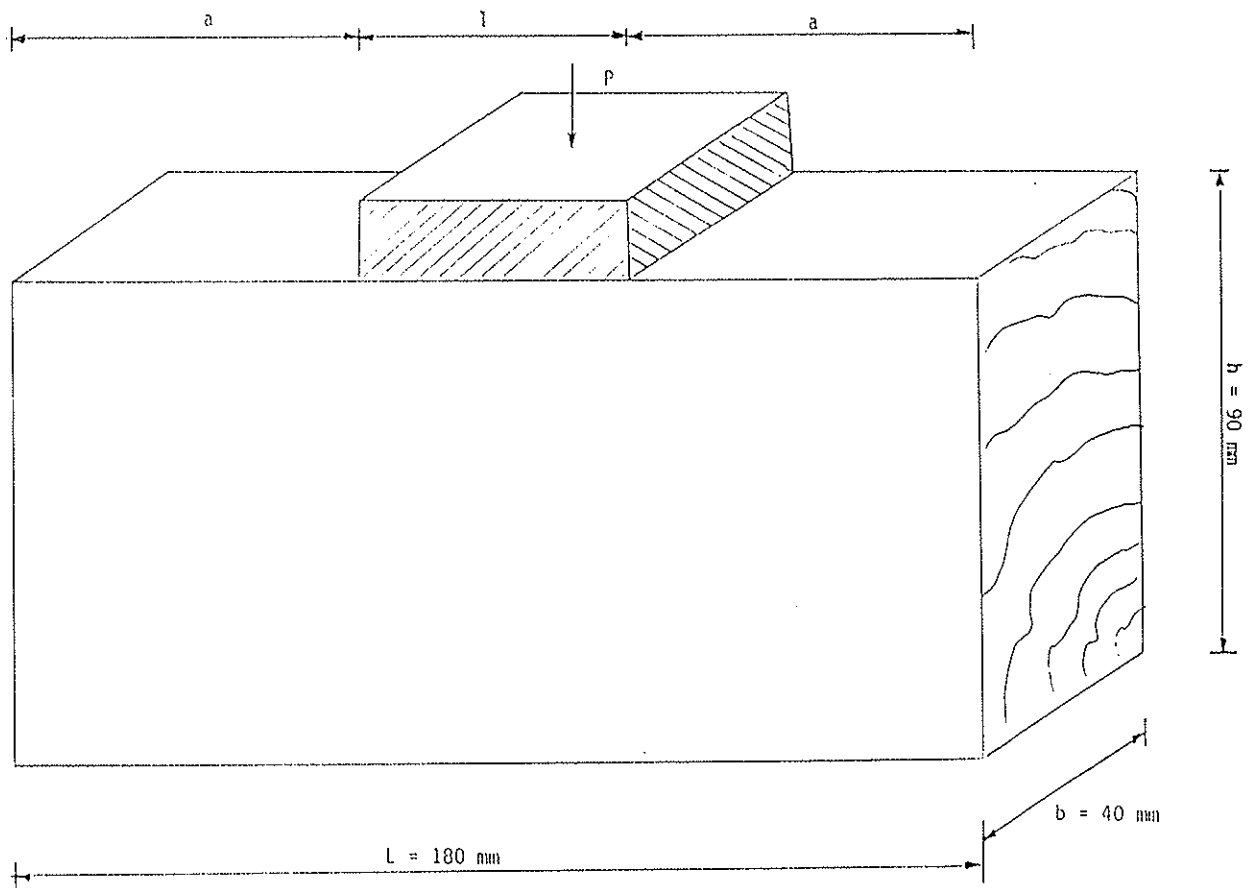


Fig. 8 - End sector loaded

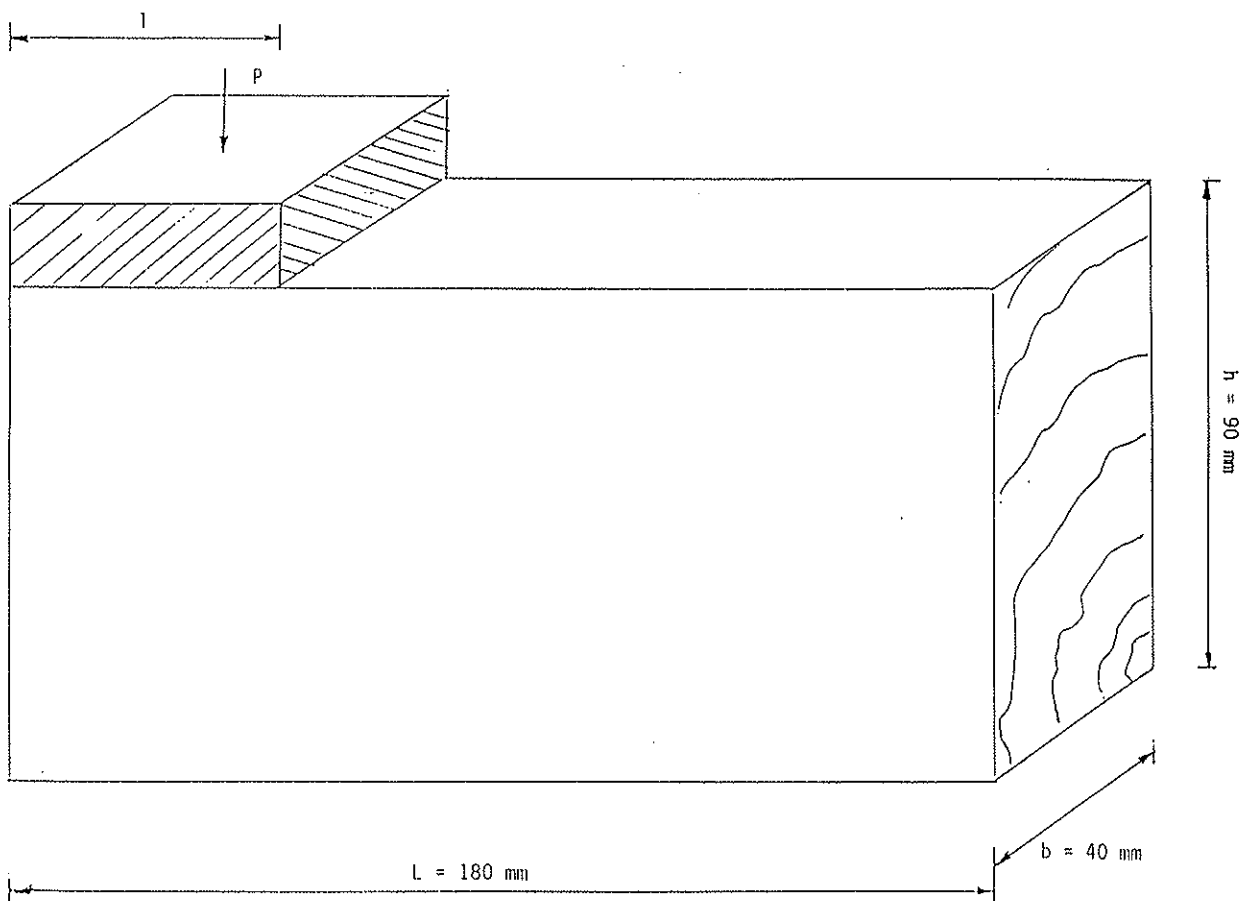


Fig. 9 - Central sector loaded(reinforced)

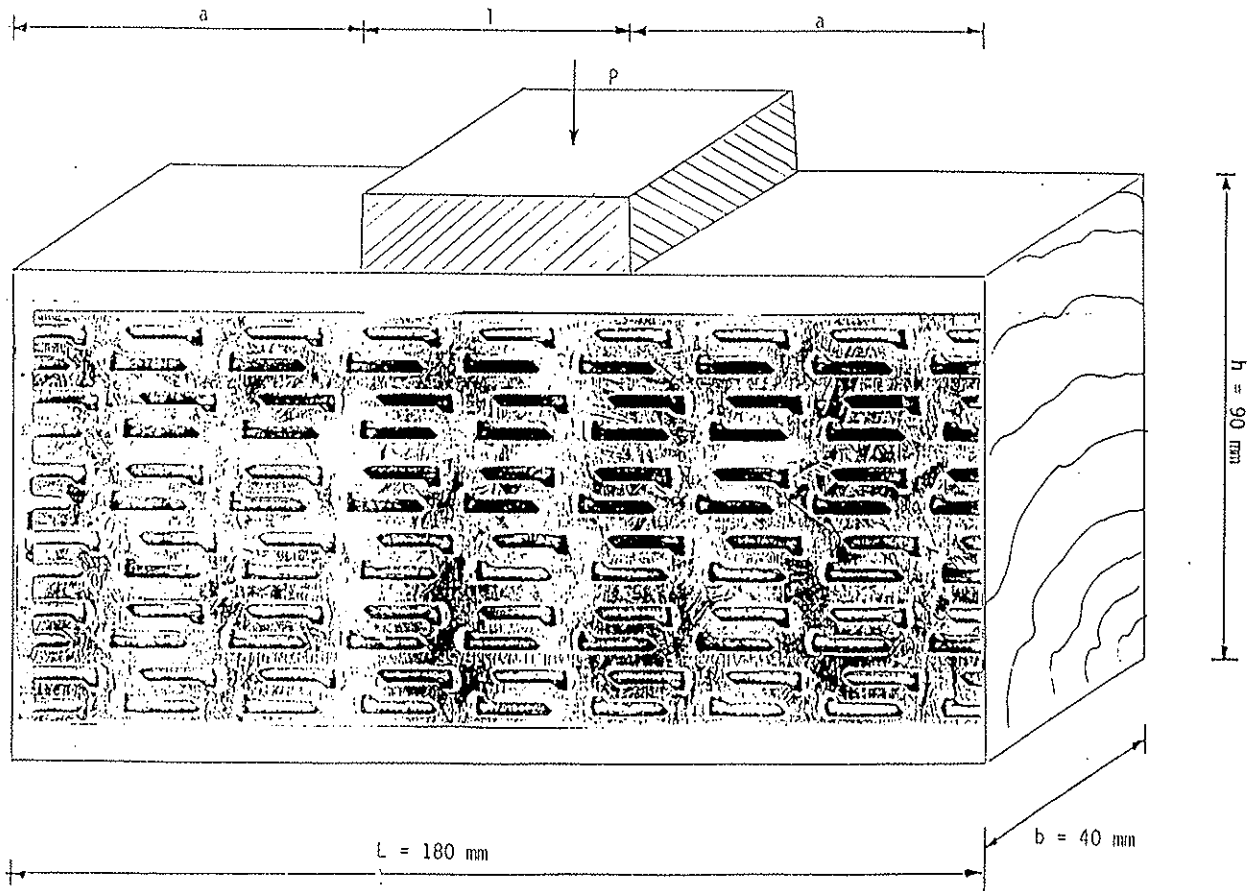


Fig. 10 - End sector loaded(reinforced)

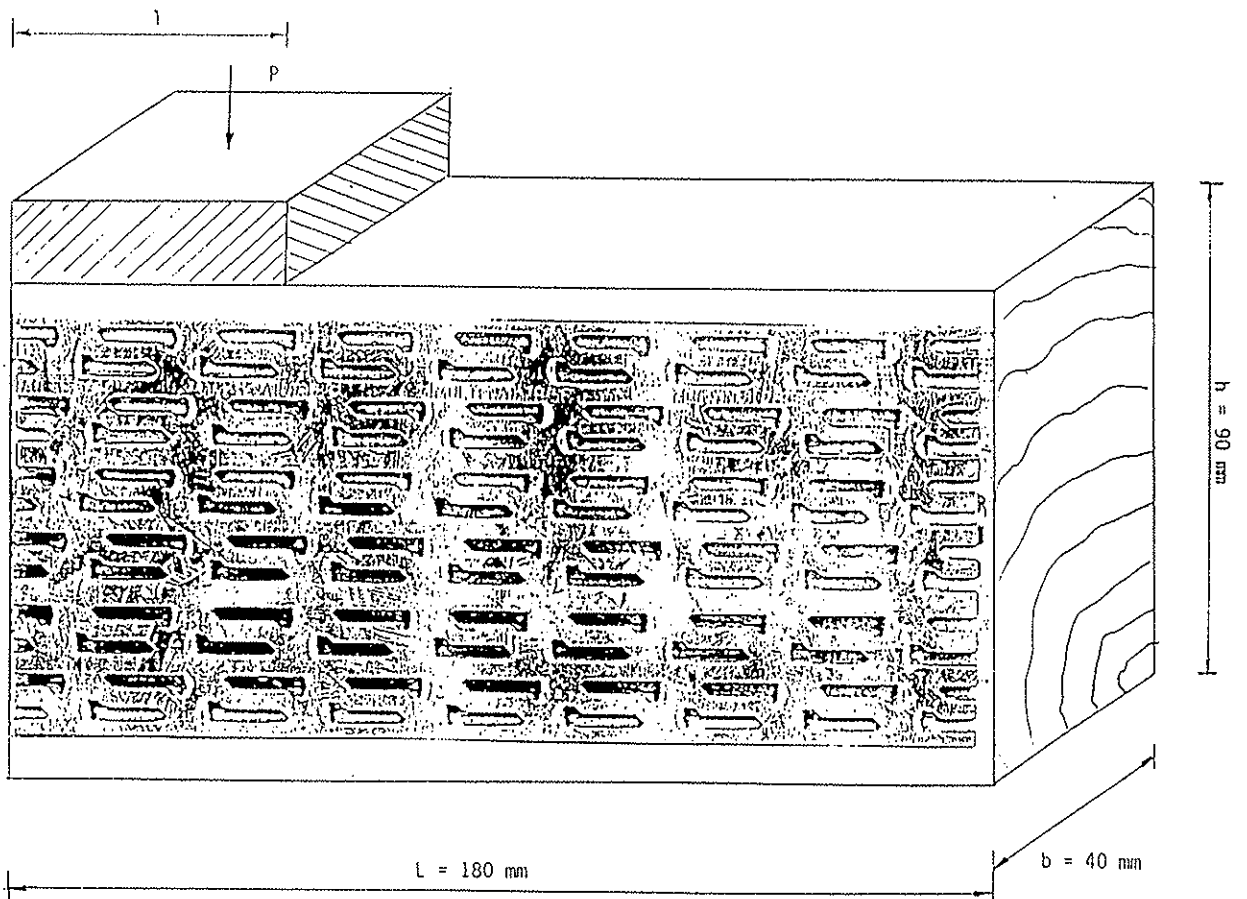
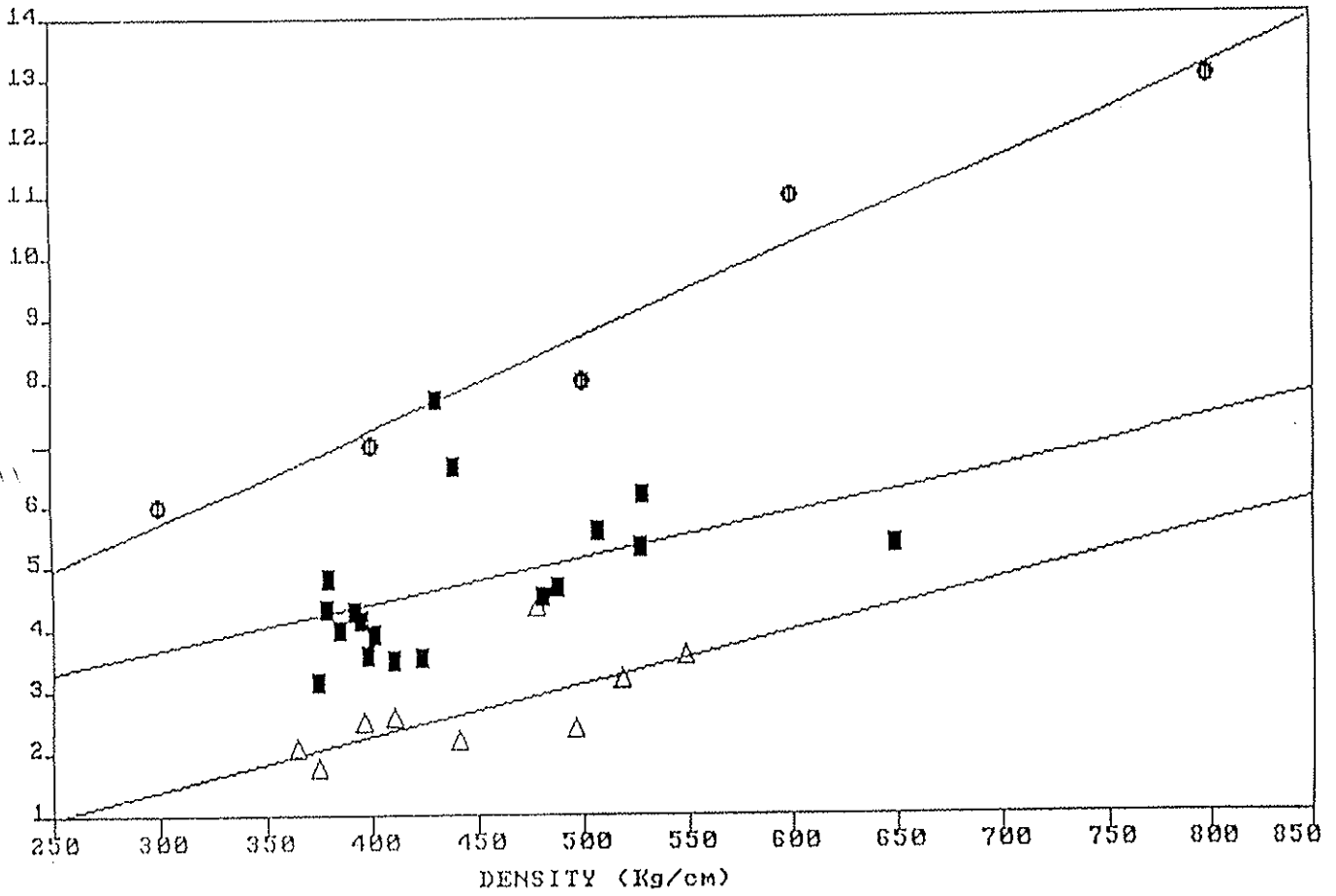


Fig. 11 - COMP STRENGTH PENPERDICULAR TO GRAIN US DENSITY



- - Eurocode 5
- - ASTM D 143
- △ - Experimental results

Fig. 12 - BEARING STRENGTH-CENTRAL SECTOR LOADED

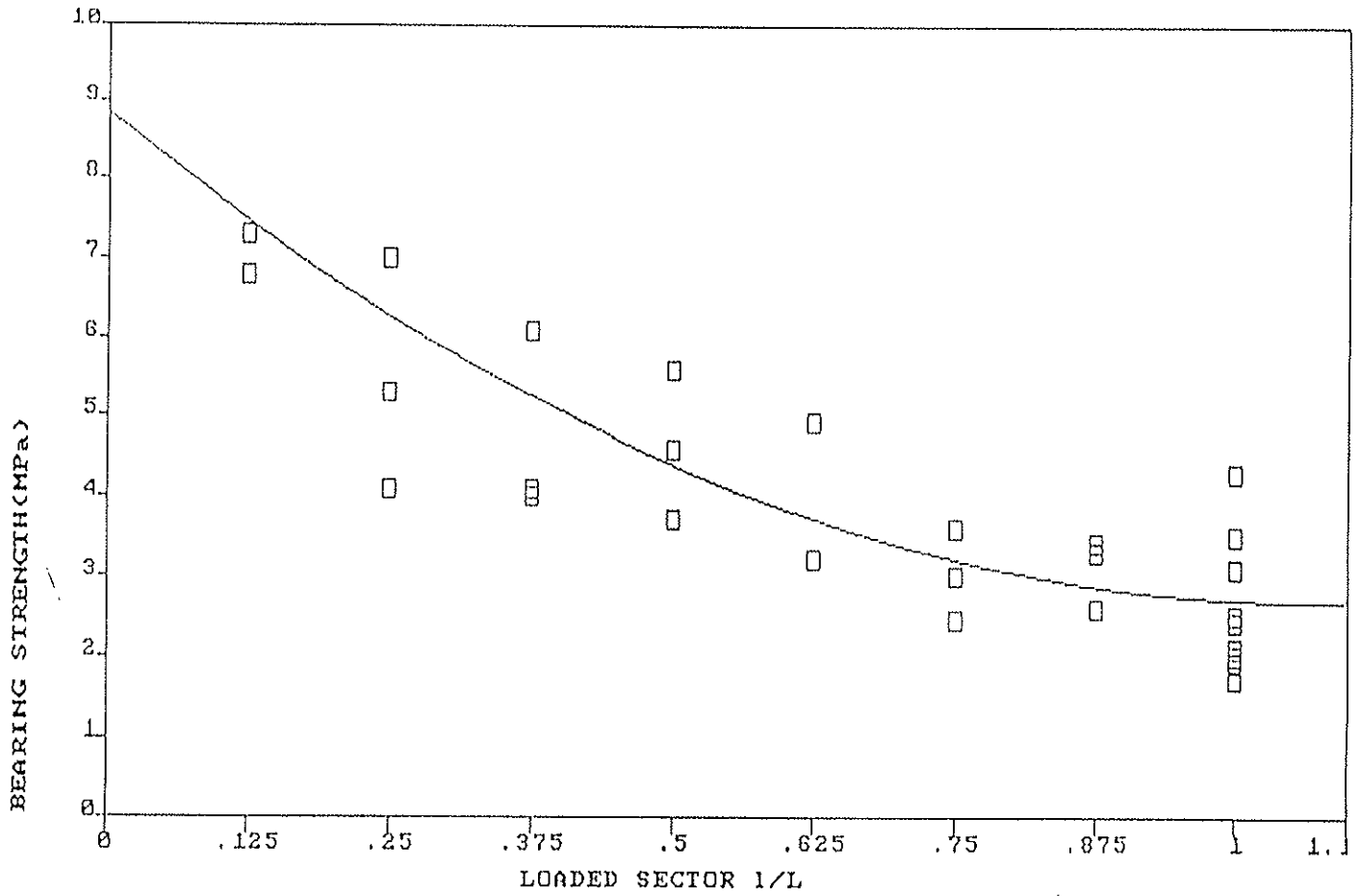


Fig. 13 - BEARING STRENGTH -END SECTOR LOADED

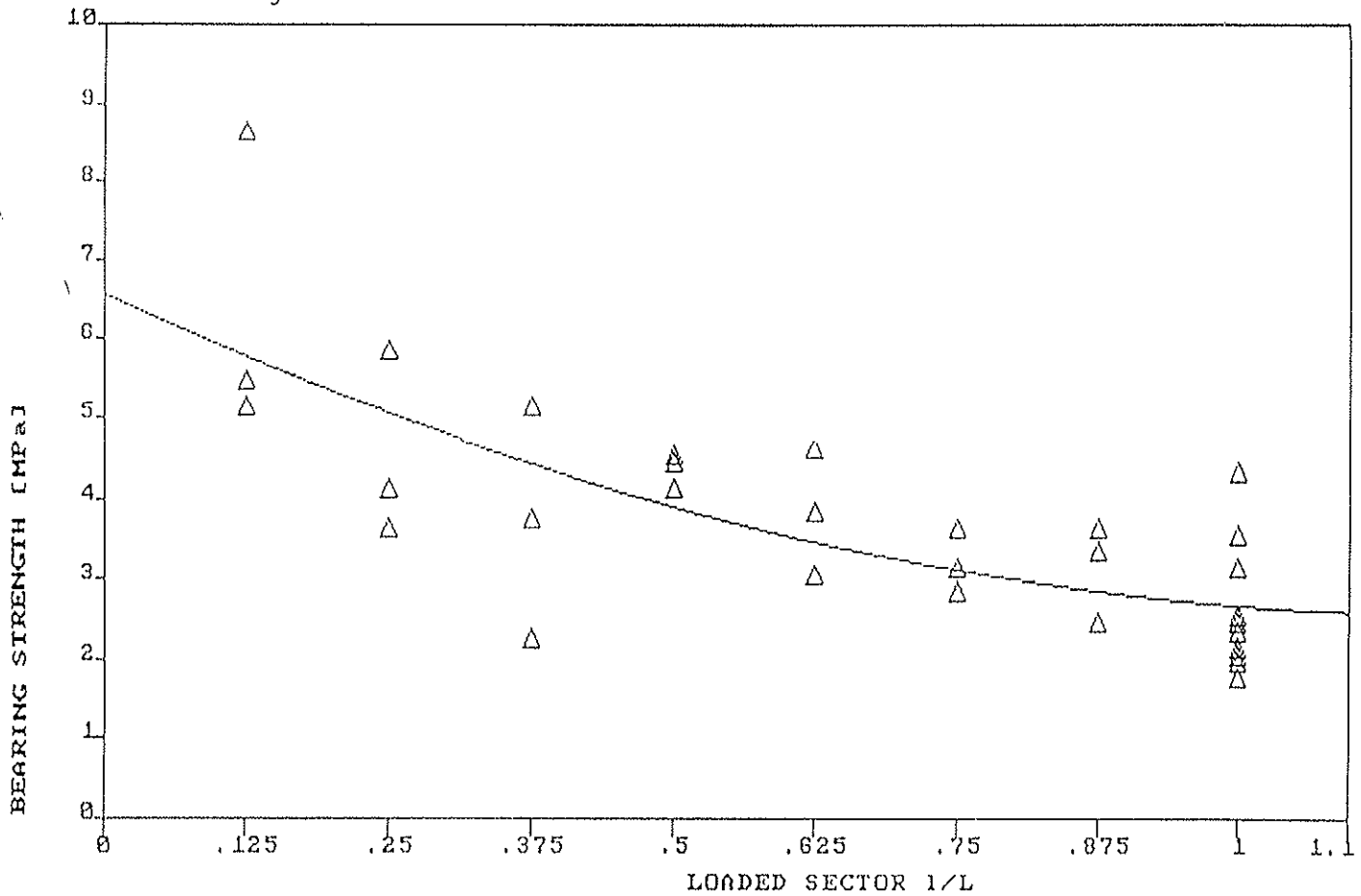


Fig. 14 - BEARING STRENGTH-CENTRAL SECTOR LOADED [REINFORCED]

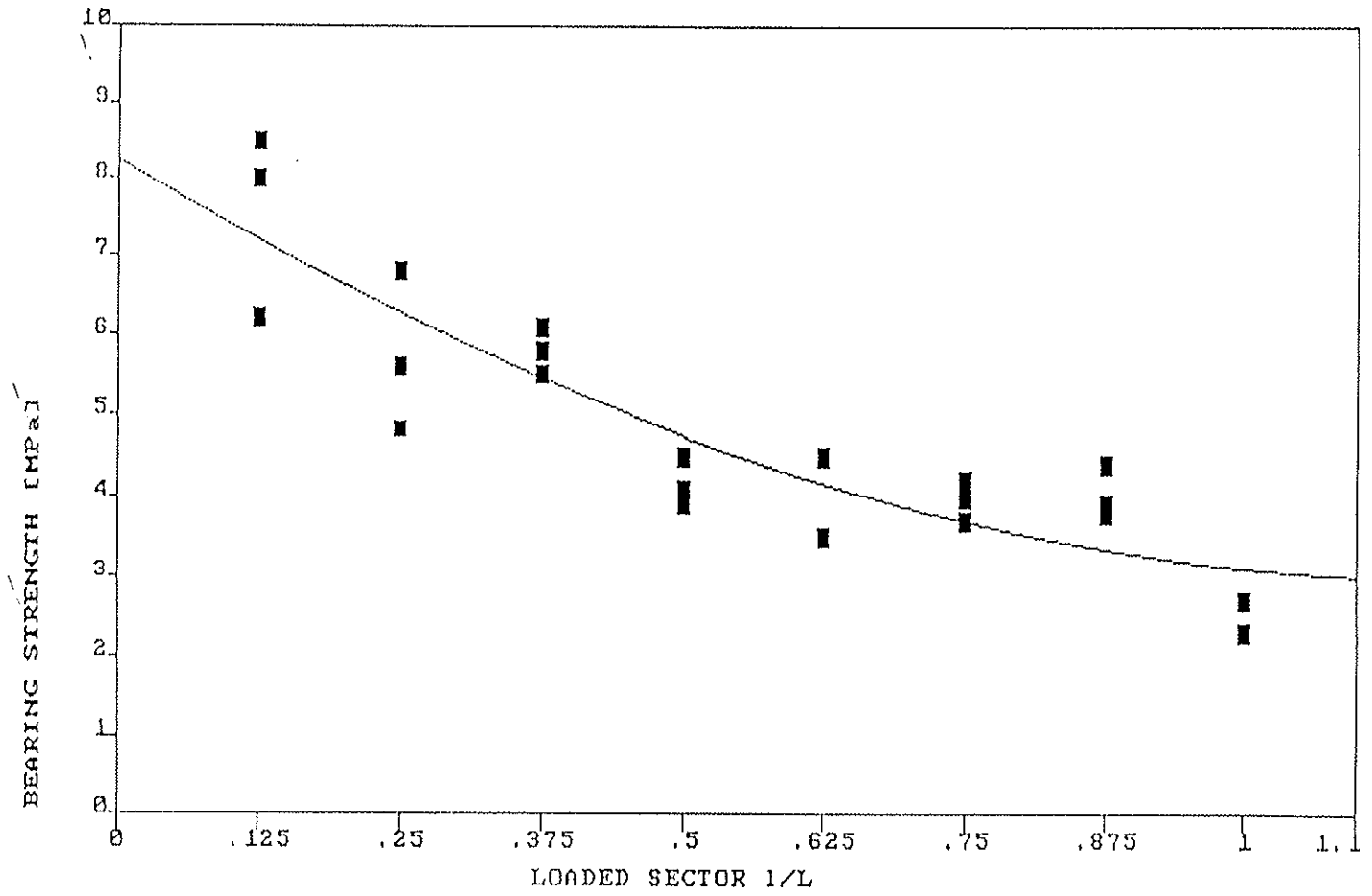
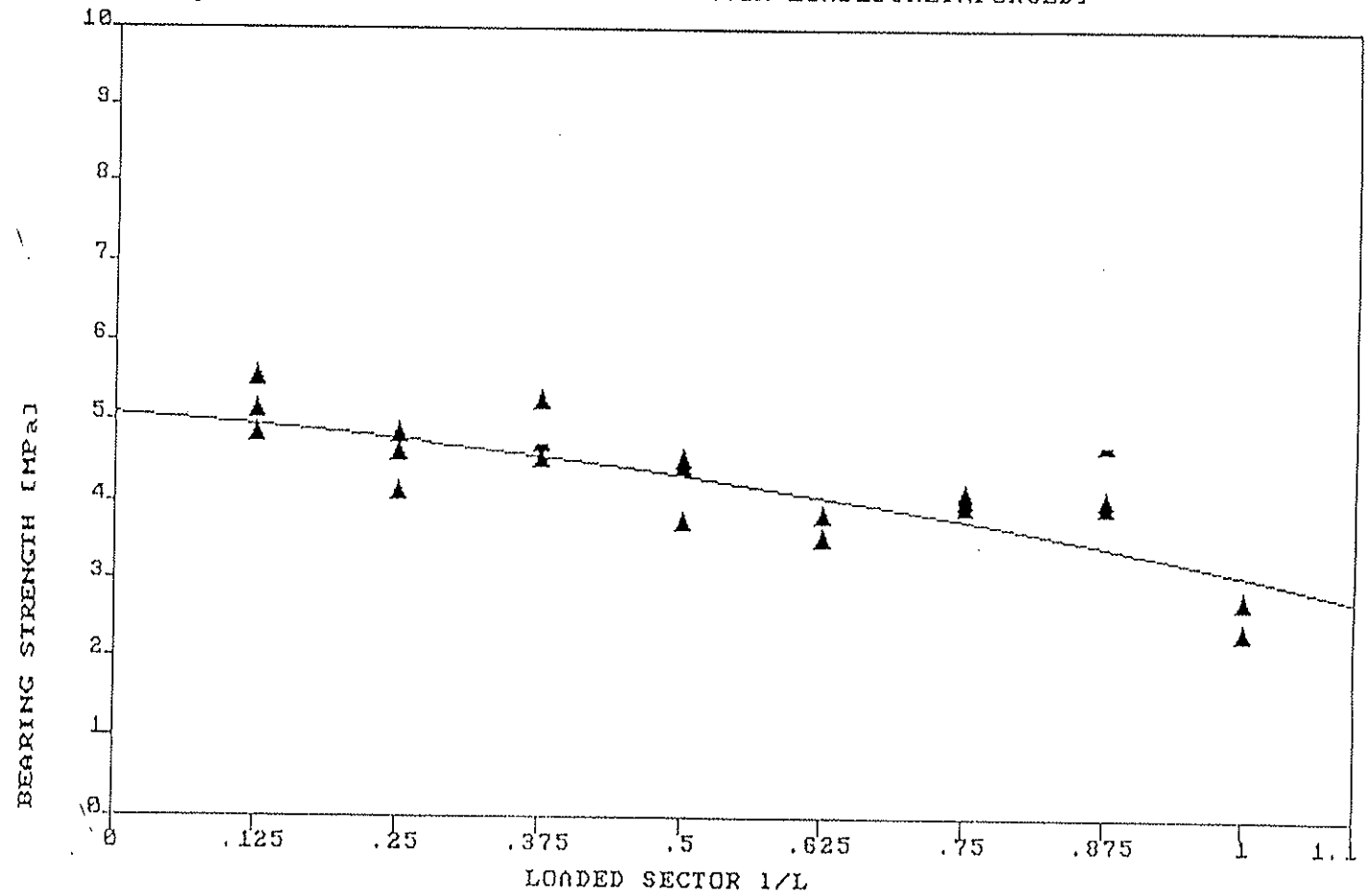


Fig. 15 - BEARING STRENGTH-END SECTOR LOADED [REINFORCED]



INTERNATIONAL COUNCIL FOR BUILDING RESEARCH STUDIES AND DOCUMENTATION
WORKING COMMISSION W18A - TIMBER STRUCTURES

PROPOSAL FOR A DESIGN CODE FOR NAIL PLATES

by

E Aasheim

K H Solli

The Norwegian Institute of Wood Technology
Norway

MEETING TWENTY - THREE

LISBON

PORTUGAL

SEPTEMBER 1990

PROPOSAL FOR A DESIGN CODE FOR NAIL PLATES

by Erik Aasheim and Kjell Helge Solli

The Norwegian Institute of Wood Technology

September 1990

INTRODUCTION

The Norwegian timber design code "NS 3470 Timber structures Design rules - 4th. edition" was published in november 1989. An extract from this design code has been presented by E. Aasheim and K. H. Solli in CIB/W18/paper 22-102-3.

The 4th. edition of NS 3470 includes a new subject compared with the earlier editions i.e. design rules for nail plates. Even though the rules are new in connection with NS 3470, they have been used for several years in Norway. The background of this rules has been presented in CIB/W18/paper 18-7-6 by N. I. Bovim and E. Aasheim.

It is expected that the Norwegian proposal for nail plates will be included in the proposal for the truss annexes in Eurocode no.5.

The present paper gives a translated version of the Norwegian rules:

PROPOSED DESIGN METHOD FOR NAIL PLATES.

This method applies to constructions in moisture class 1 and 2.

If there are no exact calculations of the stresses from handling, transport and installation, the nail plates and every elements anchoring to the nail plates shall be controlled for a design force of 4 kN. The force supposes to work in any direction in the plane of the construction.

The nail plate shall have approved values for the following characteristic properties:

f_{t0k}	the anchoring capacity for $\alpha = 0$
f_{txk}	the tension capacity of the plate in x-direction
f_{cxk}	the compression capacity of the plate in x-direction
f_{vxk}	the shear capacity of the plate in x-direction
f_{tyk}	the tension capacity of the plate in y-direction
f_{cyk}	the compression capacity of the plate in y-direction

f_{vyk} the shear capacity of the plate in y-direction
 C constant given for the actual type of nail plate

The x-direction is the main direction of the plate

The y-direction is perpendicular to the main direction of the plate

Controll of anchoring capacity.

The following conditions shall be satisfied:

$$\frac{\tau_{ax}}{(1 - C \cdot \sin \alpha) f_{t0d}} \leq 1.0$$

$$\frac{\tau_{my}}{2 \cdot (1 - C) f_{t0d}} \leq 1.0$$

$$\frac{\tau_{ax} + \tau_{my}}{1.5 \cdot f_{t0d}} \leq 1.0$$

where $\alpha \leq 90^\circ$

and α is the maximum angel between

- the directions of grain and force
- the directions of the x-direction and the force
- the directions of the x-direction and the grain

$$\tau_{ax} = \frac{F_{gx}}{A_{ef}}$$

Where F_{gx} is calculated as the force in the centre of gravity of A_{ef} .

The effective area A_{ef} is the total area of contact between the plate and the timber reduced with those parts of the area which are outside the given lengths from edges and ends. Normally the length from loaded edge or end is 10 mm and the length from unloaded edge or end is 5 mm.

$$\tau_{my} = \frac{M_{gx} \cdot r_{max}}{I_p}$$

M_{gx} is calculated as the moment acting in the centre of gravity of A_{ef} .

I_p is the polar moment of area for A_{ef} , and r_{max} is the distance from the centre of gravity of A_{ef} to the farrest point of A_{ef} .

Controll of steel capacity in the nail plate.

The following condition shall be satisfied:

$$\left(\frac{F_{x\gamma}}{R_{xd}} \right)^2 + \left(\frac{F_{y\gamma}}{R_{yd}} \right)^2 \leq 1.0$$

From the theory of plastisity:

$$F_{x\gamma} = F_{\gamma} \cdot \cos \alpha + 2 \cdot F_{M\gamma} \sin \beta$$

$$F_{y\gamma} = F_{\gamma} \cdot \sin \alpha + 2 \cdot F_{M\gamma} \cos \beta$$

$$F_{M\gamma} = \pm \frac{M_{\gamma}}{f/2}$$

where

f is the length of the joint covered by nailplate, measured along the gap between connected members.

α is the angle between the x-direction and the force (fig.22)

β is the angle between the x-direction and the gap.

R_{xd} and R_{yd} are the design values in x and y-direction.

R_{xd} is found as the maximum of the 2 following values:

$$1) f_{cxd} \cdot b_{net} \quad 1) \quad \text{respectively} \quad f_{txd} \cdot b_{net} \quad 2)$$

and

$$2) f_{vxd} \cdot a_{net} \quad 3)$$

R_{yd} is found as the maximum of the 2 following values:

$$1) f_{cyd} \cdot a_{net} \quad 1) \quad \text{respectively} \quad f_{tyd} \cdot a_{net} \quad 2)$$

and

$$2) f_{vyd} \cdot b_{net} \quad 3)$$

F_{γ} , M_{γ} , a_{net} and b_{net} are given in fig.1.

The modification factor k_r and the load sharing factor k_{lf} is 1.0.

- 1) Compression over the gap
- 2) Tension over the gap
- 3) Shear

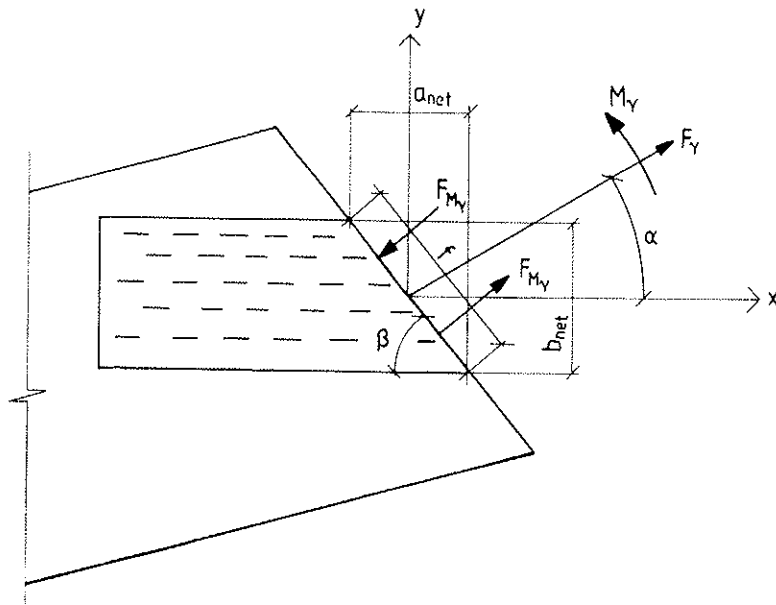


Fig. 1

REFERENCES

1. NS 3470 TIMBER STRUCTURES DESIGN RULES, 4th. edition. Norwegian Standards Association, November 1989.
2. CIB-W18/18-7-6: THE STRENGTH OF NAIL PLATES by N. I. Bovim and E. Aasheim.
3. CIB-W18/22-102-3: NORWEGIAN TIMBER DESIGN CODE - EXTRACT FROM A NEW VERSION by E. Aasheim and K. H. Solli.

INTERNATIONAL COUNCIL FOR BUILDING RESEARCH STUDIES AND DOCUMENTATION

WORKING COMMISSION W18A - TIMBER STRUCTURES

LOAD DISTRIBUTION IN NAILED JOINTS

by

H J Blass
University of Karlsruhe
Federal Republic of Germany

MEETING TWENTY - THREE

LISBON

PORTUGAL

SEPTEMBER 1990

Load distribution in nailed joints

H.J. Blass

Lehrstuhl für Ingenieurholzbau und
Baukonstruktionen, Universität Karlsruhe,
Kaiserstr. 12, D-7500 Karlsruhe

Abstract

An existing model has been extended to study the influence of plastic deformations on load distribution in multiple-pin timber joints. The model was verified experimentally with tension tests on double-shear specimens made from spruce and connected with nine nails aligned parallel to the direction of loading. The test results agree well with the model predictions. There is no significant influence of number of nails on ultimate load.

1 Introduction

During the last few years, the strength of mechanical timber connections and its different influencing parameters like embedment strength of wood or moment capacity of nails have been investigated extensively (Ehlbeck and Werner, 1988; Hilson et al., 1987; Massé et al., 1989; Rodd et al., 1987; Smith and Whale, 1984; Smith and Whale, 1985a; Smith and Whale, 1985b; Smith and Whale, 1987; Whale and Smith, 1986a; Whale and Smith, 1986b; Whale et al., 1989). This work did not consider load distribution in mechanical timber joints, though Steck (1986) showed great differences between the modification factors for number of fasteners in several international and national timber design standards and emphasized the need for further research in this area.

Even assuming ideal conditions - identical load-slip curves of single fasteners - the distribution of the load in multiple-fastener joints is nonuniform when the fasteners are aligned parallel to the direction of

loading. Therefore, in design standards, the load capacity per fastener decreases with increasing number of fasteners parallel to load. One reason for the nonuniform load distribution is the different elongation of connected members. For example, consider Fig. 1 between the first and second nail. Member 1 is loaded by force F minus fastener load 1 while member 2 resists only fastener load 1. Assuming the same extensional stiffnesses for both members, the elongation of member 1 between the first and second nail will be greater than the corresponding elongation of member 2. These different elongations must be compensated for by different displacements of the first and second nail. Different displacements mean - at least as long as the yield load is not yet reached - different fastener loads.

Assuming linear-elastic load-slip curves, theoretical solutions of this problem were presented by Lantos (1969) and Cramer (1968). The assumption of a linear-elastic behaviour of load-slip curves may be approximately valid in the proportional range, but its extension to ultimate loads is not realistic. If the load is increased over a proportional limit, the most highly stressed fasteners at the ends of the joint begin to deform plastically. Moreover, the embedment strength in the contact areas between these connectors and the wood is reached, and redistribution of load from the fasteners at the ends to those in the centre of the joint will result. After each fastener has reached its yield load, the differences in fastener loads become minimal and the joint reaches its yield load.

It follows that ideally, every fastener might reach its yield load at joint failure. Therefore load distribution in joints should not affect load capacity. Test results of several researchers (Potter, 1969; Nozynski, 1980; Massé et al., 1989) indicate, however, that the ultimate load per fastener decreases sometimes considerably with increasing number of fasteners arranged parallel to load. This suggests that the failure mode in many connections may not be attaining the joint's yield load. Instead, joint load capacity may be constrained by preliminary wood splitting. Consequently, the potential load capacity of the connection is not realized because load-slip curves of single

fasteners break off and ideal redistribution of load is prevented. Oversized and misaligned bolt holes or split ring grooves tend to make the situation even worse: by causing differences in initial slip of single fasteners which makes the load distribution very uneven. This may lead to some single fasteners reaching their maximum load while other fasteners just begin to carry load because of their greater initial slip. In case of long-term or repeated loading, creep deformations and residual plastic deformations after previous higher loading also affect load distribution.

A realistic model to describe load distribution in multiple fastener joints must therefore - apart from different elongations of the joint members - take into account influences from fabrication tolerances and variable load-slip curves within the joint. Wilkinson (1986) presented a model to calculate load distribution in bolted joints. Knowing the different shape of load-slip curves of different fasteners in the connection allows the calculation of load distribution up to ultimate load. Using Wilkinson's model, the following steps are proposed in developing modification factors for multiple-fastener joints:

- Determine variation of load-slip behaviour in connections.
- Determine variation of initial slip due to fabrication tolerances within joints.
- Extend Wilkinson's model to calculate load distribution taking into account all important parameters.
- Simulate joints with different number of fasteners taking into account correlation of load-slip behaviour within joints.
- Calculate maximum loads of simulated connections and determine characteristic values of ultimate load for different number of fasteners.
- Derive modification factors by comparing characteristic values

depending on number of fasteners.

The objective of the present investigation was to develop a model taking into account all important parameters influencing short term load distribution in mechanical timber joints. To verify the model, tests were carried out with specimens, which had been used in previous tests to determine variation in load-slip behaviour within joints. Therefore, single-nail load-slip curves of these specimens were already known.

2 Model

The model used in this investigation is based on Wilkinsons work and was extended to take into account the influence of remaining plastic deformations on load distribution in mechanical timber joints. Fig. 1 shows the principal outline of a connection.

With the symbols

F	joint load,
ΔF	unloading after previous joint load F ,
F_{1i}, F_{2i}	load between fastener i and $i+1$ carried by member 1 or 2, respectively,
P_i	load carried by fastener i ,
ΔP_i	unloading of fastener i after previous load P_i ,
r_i	spacing between fastener i and $i+1$ before loading,
E_1A_1, E_2A_2	extensional stiffness of member 1 or 2, respectively,
n	number of fasteners parallel to load,

- U_{1i}, U_{2i} elongation of member 1 or 2, respectively, between fastener i and $i+1$,
- P^*_{ji} j th load value of piecewise linear load-slip curve for fastener i ,
- δ^*_{ji} j th displacement value of piecewise linear load-slip curve for fastener i ,
- δ_i displacement of fastener i with first short term loading,
- $\delta_{i,res}$ displacement of fastener i after unloading with ΔP_i
- C_{ji} j th slope of piecewise linear load-slip curve for fastener i , and
- C_{ei} elastic slip modulus during loading and unloading of fastener i below fastener load P_i

the following relations apply (see Fig. 1):

2.1 First loading

Loading the joint with F yields (see Wilkinson, 1986):

$$r_i + U_{1i} + \delta_{(i+1)} = r_i + U_{2i} + \delta_i \quad (1)$$

$$\delta_{(i+1)} = \delta_i + U_{2i} - U_{1i} \quad (2)$$

The load in member 1 between fastener i and $i+1$ equals the joint load F minus fastener loads 1 to i :

$$F_{1i} = F - \sum_{k=1}^i P_k \quad (3)$$

correspondingly for member 2:

$$F_{2i} = \sum_{k=1}^i P_k \quad (4)$$

Assuming uniformly distributed longitudinal stresses over the cross sections results in an elastic elongation of a member section:

$$U_{1i} = \frac{F_{1i} \cdot r_i}{E_1 A_1} = \frac{\left(F - \sum_{k=1}^i P_k \right) \cdot r_i}{E_1 A_1} \quad \text{bzw.} \quad (5)$$

$$U_{2i} = \frac{F_{2i} \cdot r_i}{E_2 A_2} = \frac{\left(\sum_{k=1}^i P_k \right) \cdot r_i}{E_2 A_2} \quad (6)$$

The slope of a linear piece of the load slip curve is:

$$C_{ji} = \frac{P_{(j+1)i}^* - P_{ji}^*}{\delta_{(j+1)i}^* - \delta_{ji}^*} \quad (7)$$

Fastener load P_i induces a displacement of fastener i :

$$\delta_i = \delta_{ji}^* + \frac{P_i - P_{ji}^*}{C_{ji}} \quad (8)$$

and correspondingly for fastener $i+1$:

$$\delta_{(i+1)} = \delta_{j(i+1)}^* + \frac{P_{(i+1)} - P_{j(i+1)}^*}{C_{j(i+1)}} \quad (9)$$

Rearrangement of load and displacement terms yields:

$$\left(\frac{1}{C_{j1}} + \frac{r_1}{E_1 A_1} + \frac{r_1}{E_2 A_2} \right) \cdot P_1 - C_{j2} \cdot P_2 = \frac{r_1}{E_1 A_1} \cdot F - \delta_{j1}^* + \delta_{j2}^* + \frac{P_{j1}^*}{C_{j1}} - \frac{P_{j2}^*}{C_{j2}} \quad (10)$$

$$\begin{aligned} \frac{1}{C_{j(n-1)}} \cdot P_{(n-1)} - \left(\frac{1}{C_{jn}} + \frac{r_{(n-1)}}{E_1 A_1} + \frac{r_{(n-1)}}{E_2 A_2} \right) \cdot P_n = \\ - \frac{r_{(n-1)}}{E_2 A_2} \cdot F - \delta_{j(n-1)}^* + \delta_{jn}^* + \frac{P_{j(n-1)}^*}{C_{j(n-1)}} - \frac{P_{jn}^*}{C_{jn}} \end{aligned} \quad (11)$$

$$\begin{aligned} \frac{1}{C_{j(i-1)}} \cdot P_{(i-1)} - \left[\frac{1}{C_{ji}} \cdot \left(1 + \frac{r_{(i-1)}}{r_i} \right) + \frac{r_{(i-1)}}{E_1 A_1} + \frac{r_{(i-1)}}{E_2 A_2} \right] \cdot P_i + \frac{r_{(i-1)}}{r_i \cdot C_{j(i+1)}} \cdot P_{(i+1)} = \\ - \delta_{j(i-1)}^* + \left(1 + \frac{r_{(i-1)}}{r_i} \right) \cdot \delta_{ji}^* - \frac{r_{(i-1)}}{r_i} \cdot \delta_{j(i+1)}^* + \frac{1}{C_{j(i-1)}} \cdot P_{j(i-1)}^* - \\ \frac{1}{C_{ji}} \cdot \left(1 + \frac{r_{(i-1)}}{r_i} \right) \cdot P_{ji}^* + \frac{r_{(i-1)}}{r_i \cdot C_{j(i+1)}} \cdot P_{j(i+1)}^* \end{aligned} \quad (12)$$

The solution of the linear equations system formed by equations (10) to (12) yields the unknown fastener loads and their displacements.

2.2 Unloading and reloading

If the joint is unloaded, the displacement values of the single fasteners recover only partially, and some plastic displacement remains (see Fig. 2). The residual displacement of fastener i after unloading the joint by the load ΔF is:

$$\delta_{i, res} = \delta_i - \frac{\Delta P_i}{C_{e, i}} \quad (13)$$

Replacing δ_i by $\delta_{i, res}$ in equation (1) yields:

$$r_i + U_{1i} + \delta_{(i+1)} - \frac{\Delta P_{(i+1)}}{C_{e, i}} = r_i + U_{2i} + \delta_i - \frac{\Delta P_i}{C_{e, i}} \quad (14)$$

$$\frac{\Delta P_{(i+1)}}{C_{e, (i+1)}} = \delta_{(i+1)} - \delta_i + U_{1i} - U_{2i} + \frac{\Delta P_i}{C_{e, i}} \quad (15)$$

The load in member 1 or 2, respectively, between fastener i and $i+1$ becomes:

$$F_{1i} = (F - \Delta F) - \sum_{k=1}^i (P_k - \Delta P_k) \quad (16)$$

$$F_{2i} = \sum_{k=1}^i (P_k - \Delta P_k) \quad (17)$$

With that the elastic elongations of the member sections i are:

$$U_{1i} = \left[(F - \Delta F) - \sum_{k=1}^i (P_k - \Delta P_k) \right] \cdot \frac{r_i}{E_1 A_1} \quad (18)$$

$$U_{2i} = \left[\sum_{k=1}^i (P_k - \Delta P_k) \right] \cdot \frac{r_i}{E_2 A_2} \quad (19)$$

Substituting equations (18) and (19) into equation (15) yields:

$$\begin{aligned} \frac{\Delta P_{(i+1)}}{C_{e,(i+1)}} &= \delta_{(i+1)} - \delta_i + \frac{(F - \Delta F) \cdot r_i}{E_1 A_1} - \frac{r_i}{E_1 A_1} \cdot \sum_{k=1}^i (P_k - \Delta P_k) \\ &- \frac{r_i}{E_2 A_2} \cdot \sum_{k=1}^i (P_k - \Delta P_k) + \frac{\Delta P_i}{C_{e,i}} \end{aligned} \quad (20)$$

A corresponding equation for i gives:

$$\begin{aligned} \frac{\Delta P_i}{C_{e,i}} &= \delta_i - \delta_{(i-1)} + \frac{(F - \Delta F) \cdot r_{(i-1)}}{E_1 A_1} - \frac{r_{(i-1)}}{E_1 A_1} \cdot \sum_{k=1}^{i-1} (P_k - \Delta P_k) \\ &- \frac{r_{(i-1)}}{E_2 A_2} \cdot \sum_{k=1}^{i-1} (P_k - \Delta P_k) + \frac{\Delta P_{(i-1)}}{C_{e,(i-1)}} \end{aligned} \quad (21)$$

Solving equation (20) by $\sum_{k=1}^i (P_k - \Delta P_k)$ and substituting in equation (21) yields:

$$\begin{aligned} \frac{1}{C_{e,(i-1)}} \cdot \Delta P_{(i-1)} - \left[\frac{1}{C_{e,i}} \left(1 + \frac{r_{(i-1)}}{r_i} \right) + \frac{r_{(i-1)}}{E_1 A_1} + \frac{r_{(i-1)}}{E_2 A_2} \right] \\ \cdot \Delta P_i + \frac{r_{(i-1)}}{r_i \cdot C_{e,(i+1)}} \cdot \Delta P_{(i+1)} = \end{aligned} \quad (22)$$

$$\delta_{i-1} - \delta_i \cdot \left(1 + \frac{r_{(i-1)}}{r_i} \right) + \delta_{(i+1)} - P_i \cdot \left(\frac{r_{(i-1)}}{E_1 A_1} + \frac{r_{(i-1)}}{E_2 A_2} \right)$$

Equation (20) with $i = 1$ gives:

$$\left(\frac{1}{C_{e,1}} + \frac{r_1}{E_1 A_1} + \frac{r_1}{E_2 A_2} \right) \cdot \Delta P_1 - \frac{1}{C_{e,2}} \cdot \Delta P_2 =$$

$$- \frac{r_1}{E_1 A_1} \cdot (F - \Delta F) + \delta_1 - \delta_2 + \left(\frac{r_1}{E_1 A_1} + \frac{r_1}{E_2 A_2} \right) \cdot P_1 \quad (23)$$

Equation (21) with $i = n$ provides:

$$\frac{1}{C_{e,(n-1)}} \cdot \Delta P_{(n-1)} - \left(\frac{1}{C_{e,n}} + \frac{r_{(n-1)}}{E_1 A_1} + \frac{r_{(n-1)}}{E_2 A_2} \right) \cdot \Delta P_n =$$

$$\frac{r_{(n-1)}}{E_2 A_2} \cdot (F - \Delta F) - \delta_{(n-1)} + \delta_n - \left(\frac{r_{(n-1)}}{E_1 A_1} + \frac{r_{(n-1)}}{E_2 A_2} \right) \cdot P_n \quad (24)$$

The solution of the linear equations system formed by equation (22) to (24) yields the unknown ΔP_i . These, together with the previously determined fastener loads P_i , provide the load distribution within the joint, after unloading the joint by ΔF .

3 Tests

To verify the model tension tests with nailed double-shear connections were carried out. Test specimens were made from planed spruce (Western White Spruce) timber and nine nails aligned parallel to load. Each specimen had been used ten times as single-nail test specimen in a previous investigation (Blass, 1990) on the variation of load-slip behaviour in nailed joints. From the single-nail tests the load-slip curves of 10 nails per specimen were known (see Fig. 3). Since, during the single-nail tests, the wood had been damaged in areas where the nails had been placed (see shaded areas in Fig. 4), a staggered arrangement was chosen for the nine-nail tests, to avoid wood splitting. Preliminary tests with nails not staggered perpendicular to the grain induced partial wood splitting along the nail row before the expected maximum load was reached. The arrangement in Fig. 4 was chosen to have the force loading the joint centrally.

Test specimens were conditioned prior to testing to an equilibrium

moisture content corresponding to 20°C and 80% relative humidity resulting in an average moisture content of 18.0%. Testing was carried out immediately after manufacturing. The oven-dry density of the side and main members of all test specimens yielded a mean value of 407 kg/m³, and standard deviation of 44.6 kg/m³. The bending moment capacity of the bright box nails, 102 mm long and nominally 3.66 mm in diameter, was determined using a test method proposed by Johansen (1988) and yielded an average value of 7.62 Nm.

The nails were driven by hand hammer, without predrilling, with the nail heads protruding 2-3 mm above the surface of the timber. First, five nails were driven from one side of the test specimen, then the remaining four nails from the opposite side. During manufacturing, shims were placed between side members and the main member to provide a gap of about 0.5 mm in order to avoid any friction between the members during the tests. There were 109 test specimens with known single-nail load-slip curves from previous tests. The main test series contained 93 joint specimens because four specimens were used for preliminary tests and another twelve specimens were tested with galvanized nails. The tension tests were carried out according to ISO 6891 (1983). The displacements between the side members and the main member were measured with two transducers, one at each side of the specimen at the level of the nail closest to the free end of the main member. The displacement rate during both loading and unloading was 2.5 mm/min, which resulted in total testing times between 10 and 15 minutes.

4 Test results

The load-slip diagram of each of the 93 nailed-joint tests was recorded. Figures 5 and 6 present as solid lines examples for load-slip diagrams. As indicated in the bottom diagram in Fig. 5, during seven out of 93 tests the gripping device failed before a displacement of 15 mm was reached. The results of these seven tests were nevertheless included in the evaluation. In Figures 5 and 6 the expected load-slip behaviour is shown by dashed lines. It was determined by the

theoretical model as follows:

The load-slip behaviour of 10 individual nails per specimen was known from the previous single-nail tests. The expected load-slip curve of each nail of the nine-nail tests was calculated as average of the load values of two adjacent nails of the single-nail tests. A linear-elastic behaviour was assumed for the unloading and reloading range between 10% and 40% of the estimated maximum load. The slope in this range is referred to as elastic slip modulus and was computed using the elastic slip according to ISO 6891 (1983). The mean load-slip curves as well as the mean values of the elastic slip modulus were then used to iteratively calculate the expected load-slip behaviour of the connection. The moduli of elasticity of the main and the side wood members were estimated using their density (Forest Products Laboratory, 1987):

$$E = 25650 \cdot \alpha^{0.91} \quad (25)$$

where

E expected value of modulus of elasticity for main or side member at 12% moisture content [MPa],

α relative density of main or side member based on volume at 12% moisture content.

Trial calculations with uniform values of modulus of elasticity between 5000 MPa and 15000 MPa showed a negligible influence of modulus of elasticity on the expected load-slip behaviour. Therefore, the effect of changing moisture content between 12% and 18% upon wood modulus of elasticity may be ignored.

Fig. 5 and 6 show a good agreement between expected and actual load-slip behaviour. The ratio between actual maximum load according to ISO 6891 (1983) and expected load at the same displacement yields an average value of 0.99 for the 93 tests. Maximum and minimum values of

that ratio are 1.09 and 0.90, respectively. One reason for the discrepancy between the expected and actual load-slip diagrams is the variation of load-slip behaviour within the specimen caused by knots. A knot penetrated by a nail during the single-nail test caused a greater maximum load compared to the remaining knot-free single-nail tests within the same specimen. Therefore, during the nine-nail test with the same specimen, when knots are not penetrated by nails, the expected maximum load will be greater than the actual. Vice versa, the actual maximum load will be greater than the expected, if a knot is penetrated by a nail in the nine-nail test and not in the single-nail tests with the same specimen.

Table 1 shows mean and standard deviation as well as the nonparametric values of the 50th- and 5th-percentiles for the maximum load per nail from the single-nail tests or nine-nail tests, respectively. The first two lines in Table 1 only show the results of 86 or 859 tests, respectively. The true maximum load of those seven connections, where the gripping device had failed before a displacement of 15 mm was reached, could not be determined. Therefore, instead of the actual maximum load, the expected maximum load is indicated for all 93 specimens in line 3 and 4 of Table 1. Comparing the mean values by means of a Student's t test at a significance level of 0.05, the hypothesis of the true mean values being the same for the groups with 859 and 86 or 929 and 93 tests, respectively, could not be rejected. Consequently, a significant influence attributable to the number of nails on the maximum load per nail cannot be ascertained.

An influence of number of nails may only be expected, if the number of nails affects the failure mode of the joint. Even if the load acts parallel to grain nails cause tension perpendicular and shear parallel to grain. That is why tension strength perpendicular to grain and shear strength parallel to grain are essential parameters affecting the capacity of mechanical timber connections. This is especially true for large nonpredrilled nails or for small spacing and end distances parallel to grain. The distance between fasteners should be large enough to guarantee a yield failure mode, instead of a splitting

failure. In the present investigation all 93 nine-nail specimens failed due to yielding of nail steel and crushing of wood under the nail shanks.

5 Summary

An existing model to determine load distribution in mechanical timber joints was extended to take into account the influence of plastic displacements after previous higher load levels. To verify the model, tension tests were carried out with nailed double-shear specimens made from spruce and nine nails arranged parallel to load. The load-slip behaviour of ten single nails was known for each specimen from a previous investigation. The expected maximum load of the nine-nail tests was determined with the model using the known load-slip data of the single-nail tests. Comparing the expected with the actual maximum loads yielded very good agreement on the average. A visual comparison of load-slip curves from the tests with those from the model also showed good agreement in most cases.

The maximum load per nail for the single-nail tests did not differ significantly from the corresponding values from the nine-nail tests. Therefore, the maximum load of a multiple-nailed joint can be estimated as the sum of those for individual nails, provided joint failure is by nail yielding.

6 References

- Blass, H.J. 1990: Variation of load-slip behaviour in nailed joints. Variation parallel to the grain. Paper prepared for IUFRO/S5.02 Timber Engineering Meeting, St. John, New Brunswick.
- Cramer, C.O. 1968: Load distribution in multiple-bolt tension joints. Journal of the Structural Division, ASCE 94(ST5):1101-1117.
- Ehlbeck, J.; Werner, H. 1988: Untersuchungen über die Tragfähigkeit von Stabdübelverbindungen. Holz als Roh- und Werkstoff 46(8):281-288.
- Forest Products Laboratory. 1987: Wood Handbook: Wood as an Engineering Material. Agriculture Handbook 72, US Department of Agriculture, Washington D.C.
- Hilson, B.O.; Whale, L.R.J.; Pope, D.J.; Smith, I. 1987: Characteristic properties of nailed and bolted joints under short term lateral load. Part 3 - Analysis and interpretation of embedment test data in terms of density related trends. Journal of the Institute of Wood Science 11(2):65-71.
- International Organization for Standardization. 1983: Timber structures - Joints made with mechanical fasteners - General principles for the determination of strength and deformation characteristics. International Standard ISO 6891.
- Johansen, M. 1988: Bending strength of nails. Testing of proposal for Nordtest-method. Danish Building Research Institute, Documentation for SBI-project R13-78: "Nails in wood: Bending strength", Nordtest-project 710-87.
- Lantos, G. 1969: Load Distribution in a Row of Fasteners Subjected to Lateral Load. Wood Science 1(3):129-136.
- Massé, D.I.; Salinas, J.J.; Turnbull, J.J. 1989: Lateral strength and stiffness of single and multiple bolts in glued- laminated timber loaded parallel to grain. Contribution No. C-029, Engineering and Statistical Research Centre, Research Branch, Agriculture Canada, Ottawa, Ontario.
- Neville, A.M.; Kennedy, J.B. 1968: Basic Statistical Methods for Engineers and Scientists. Scranton, Pennsylvania: International Textbook Company
- Nozynski, W. 1980: Investigation on the effect of nails number in a joint on its load carrying ability. Paper 13-7-2, Proceedings, CIB-W18 Meeting, Otaniemi, Finland.

- Potter, F.H. 1969: The strength and stiffness of multiple-nailed joints. Proceedings, International Union of Forestry Research Organizations, Working Group on Structural Utilization, London, United Kingdom, Volume 1:107-122.
- Rodd, P.D.; Anderson, C.; Whale, L.R.J.; Smith, I. 1987: Characteristic properties of nailed and bolted joints under short term lateral load. Part 2 - Embedment test apparatus for wood and wood-based sheet material. Journal of the Institute of Wood Science 11(2):60-64.
- Smith, I.; Whale, L.J.R. 1984: Mechanical properties of nails and their influence on mechanical properties of nailed timber joints subjected to lateral loads. Paper 17-7-1, Proceedings, CIB-W18 Meeting, Rapperswil, Switzerland.
- Smith, I.; Whale, L.J.R. 1985: Mechanical properties of nails and their influence on mechanical properties of nailed timber joints subjected to lateral load. Part 1. Background and tests on nails of UK origin. Research Report 4/85, Timber Research and Development Association, High Wycombe, Buckinghamshire, United Kingdom.
- Smith, I.; Whale, L.J.R. 1985: Mechanical properties of nails and their influence on mechanical properties of nailed timber joints subjected to lateral load. Part 2. Tests on nails of mainland-European origin, comparison of results with those for nails of UK origin and conclusions. Research Report 9/85, Timber Research and Development Association, High Wycombe, Buckinghamshire, United Kingdom.
- Smith, I.; Whale, L.J.R. 1987: Characteristic properties of nailed and bolted joints under short term lateral load. Part 1 - Research philosophy and test programme. Journal of the Institute of Wood Science 11(2):53-59.
- Steck, G. 1986: Effectiveness of multiple fastener joints according to national codes and Eurocode 5 (draft). Paper 19-7-3, Proceedings, CIB-W18 Meeting, Florence, Italy.
- Whale, L.R.J.; Smith, I. 1986: Mechanical joints in structural timber - information for probabilistic design. Research Report 17/86, Timber Research and Development Association, High Wycombe, Buckinghamshire, United Kingdom.
- Whale, L.R.J.; Smith, I. 1986: The derivation of design clauses for nailed and bolted joints in Eurocode 5. Paper 19-7-6, Proceedings, CIB-W18 Meeting, Florence, Italy.
- Whale, L.R.J.; Smith, I.; Hilson, B.O. 1989: Characteristic properties of nailed and bolted joints under short term lateral load. Part 4. The influence of testing mode and fastener diameter upon embedment test data. Journal of the Institute of Wood Science 11(5):156-161.
- Wilkinson, T.L. 1986: Load Distribution among Bolts Parallel to Load. Journal of Structural Engineering 112(4):835-852.

Table 1.

50th-percentile und 5th-percentile of maximum load F_{\max} (ISO 6891, 1983) per nail for single-nail or nine-nail tests, respectively.
 $F_{\max,1}$: Maximum load per nail for single-nail tests; $F_{\max,9}$: Maximum load per nail for nine-nail tests; $F_{\max,9e}$: Expected maximum load per nail for nine-nail tetsts

	Mean	Standard-deviation	50th-percentile	5th-percentile	Sample size
$F_{\max,1}$ (N)	1846	281.1	1780	1463	859
$F_{\max,9}$ (N)	1806	234.3	1760	1489	86
$F_{\max,1}$ (N)	1838	277.3	1793	1463	929
$F_{\max,9e}$ (N)	1823	241.9	1803	1472	93

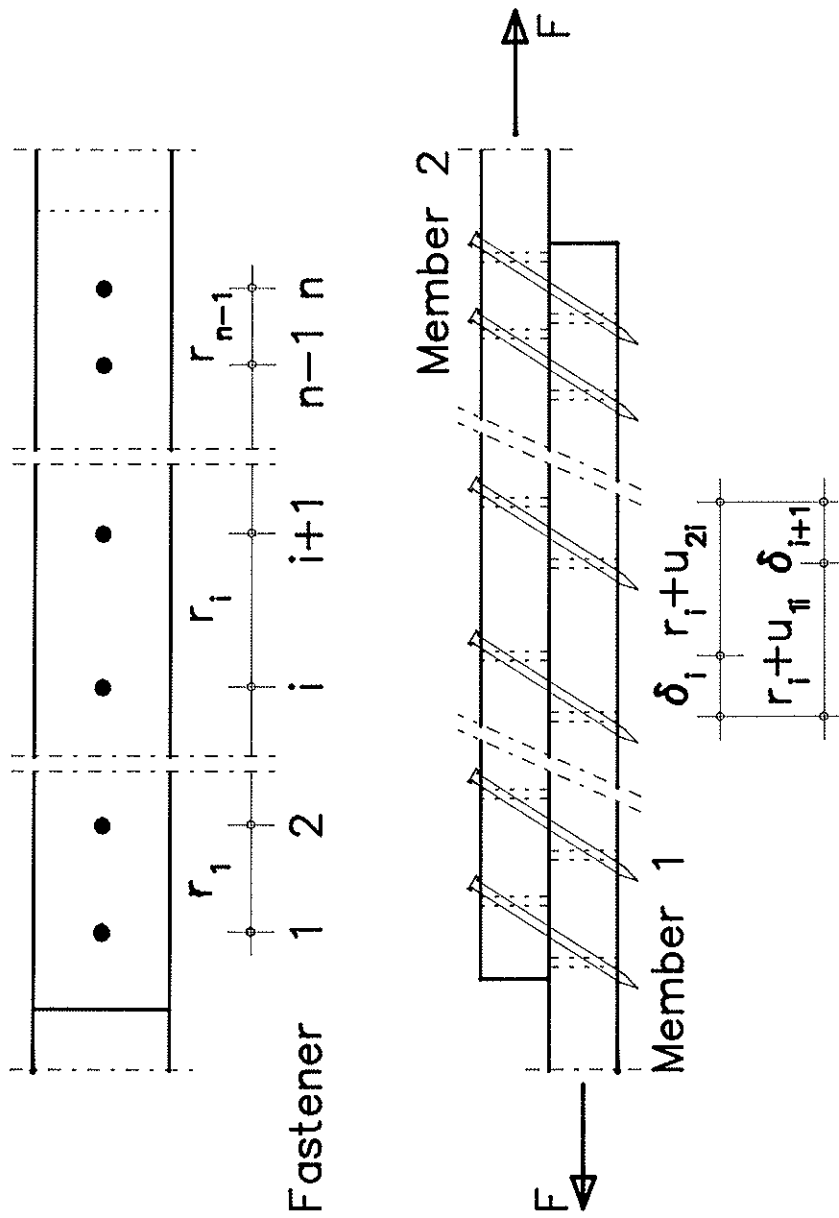


Fig. 1. View of undeformed connection (top) and section showing deformed position (bottom).

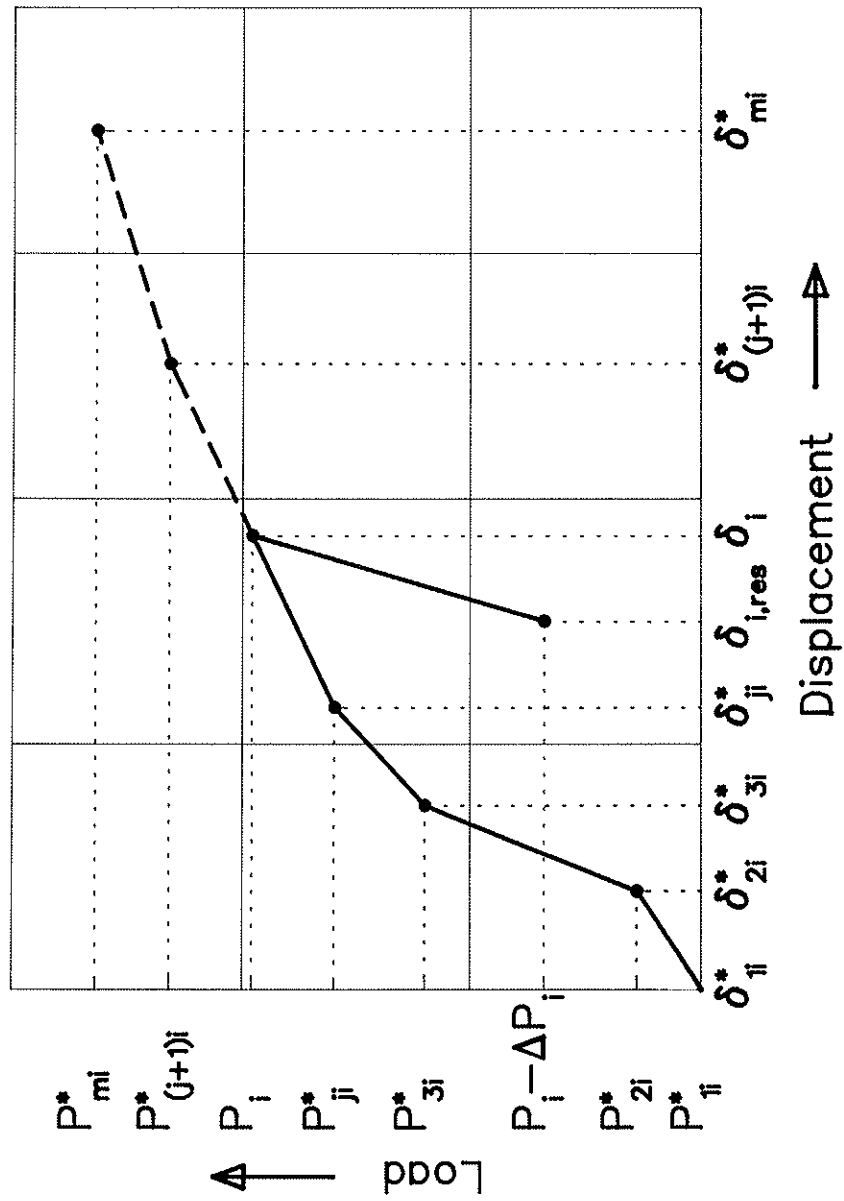


Fig. 2. Piecewise linear load-slip curve for fastener i .

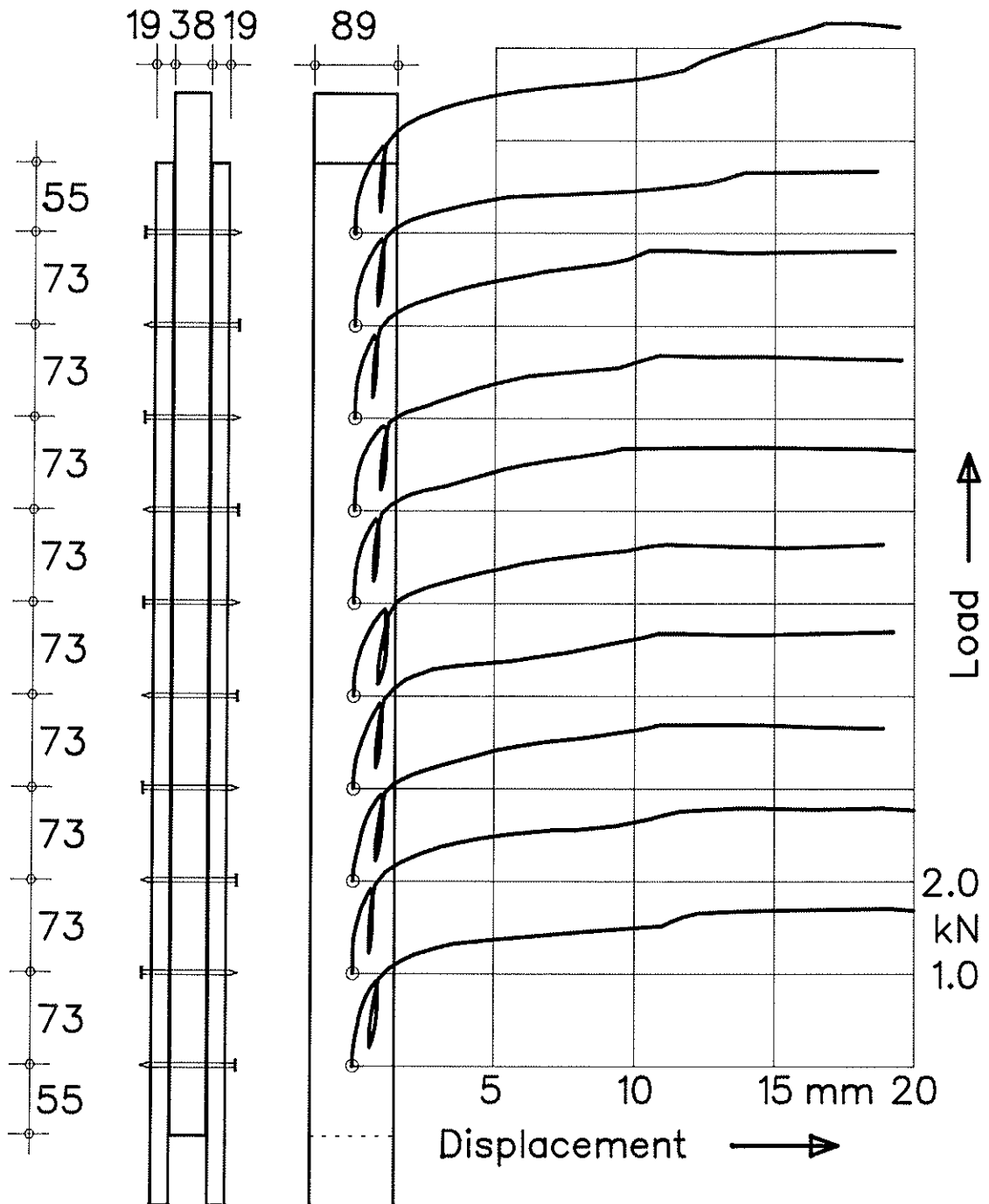


Fig. 3. Load-slip curves from 10 single-nail tests for specimen 32D20A.

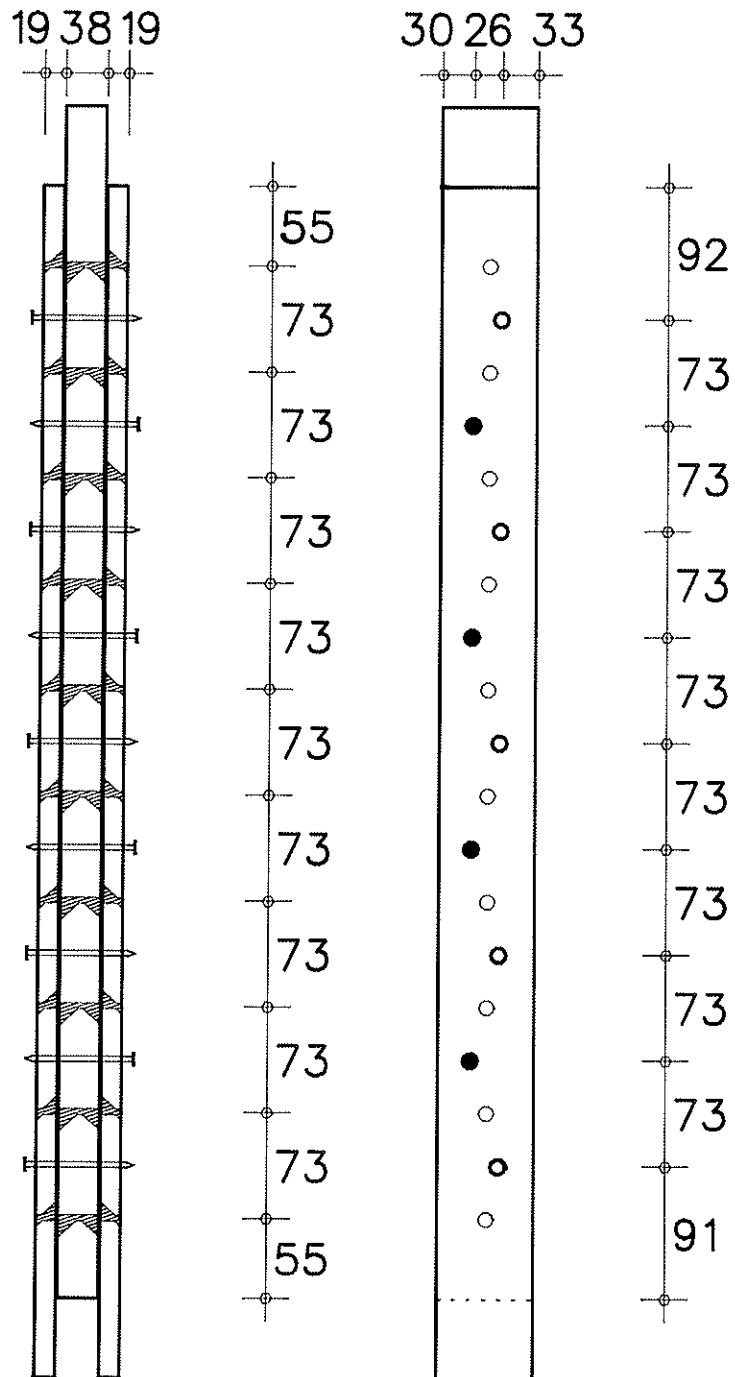


Fig. 4. Nail location in nine-nail tests, showing areas of damage due to previous single-nail tests.

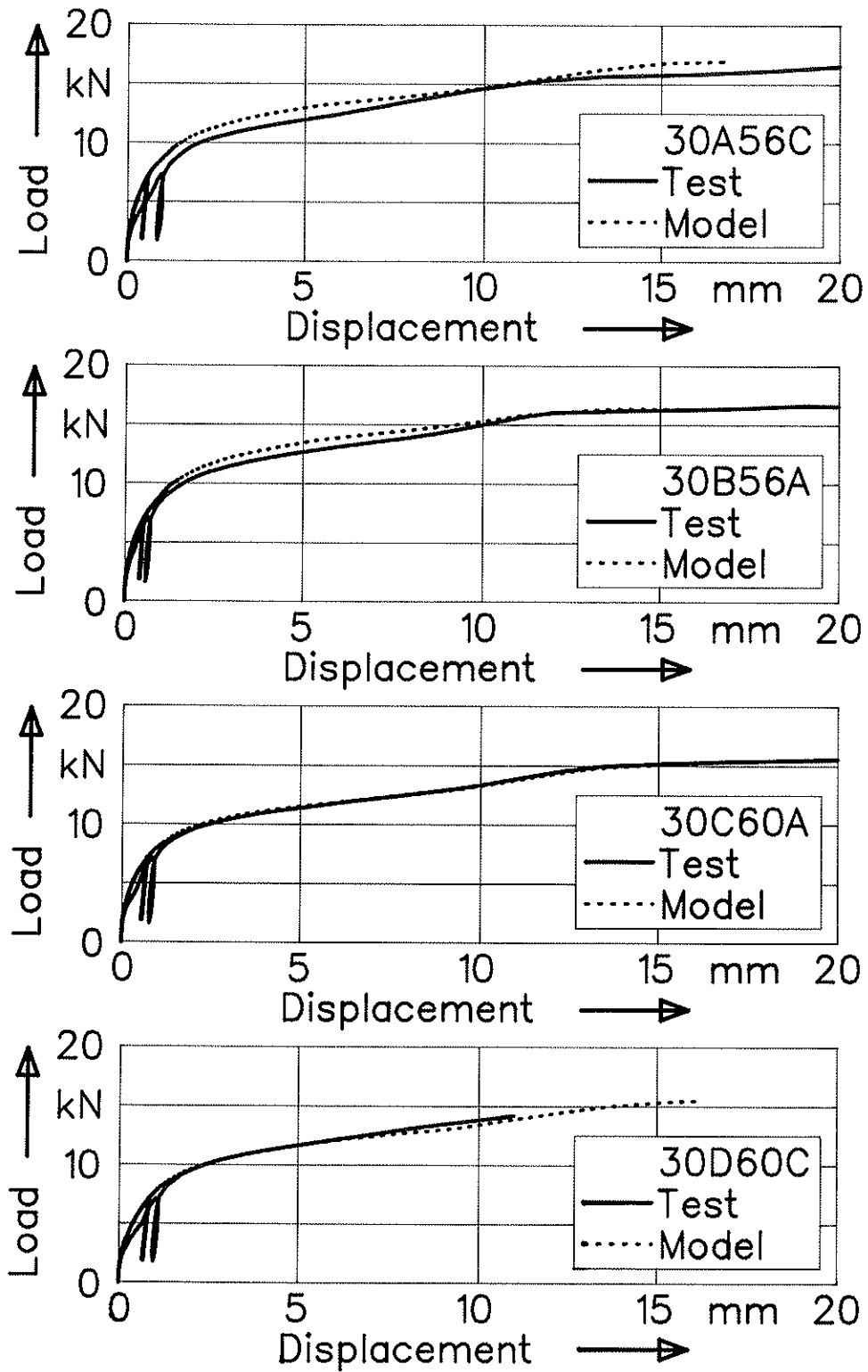


Fig. 5. Load-slip diagrams for specimens 30A56C to 30D60C showing test and model results.

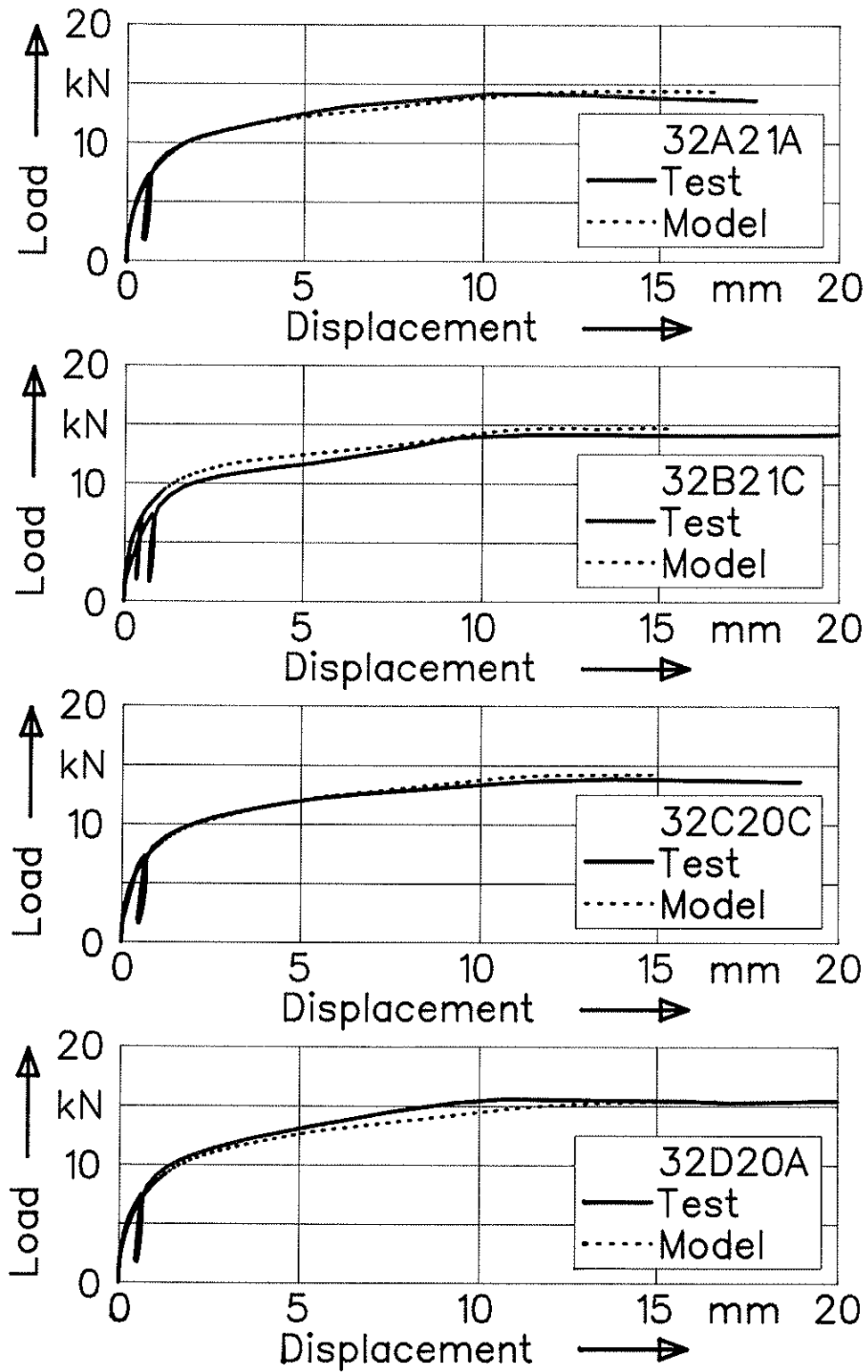


Fig. 6. Load-slip diagrams for specimens 32A21A to 32D20A showing test and model results.

INTERNATIONAL COUNCIL FOR BUILDING RESEARCH STUDIES AND DOCUMENTATION

WORKING COMMISSION W18A - TIMBER STRUCTURES

TENSION PERPENDICULAR TO THE GRAIN AT NOTCHES AND JOINTS

by

T A C M van der Put
Delft University of Technology
The Netherlands

MEETING TWENTY - THREE

LISBON

PORTUGAL

SEPTEMBER 1990

Summary

Constructive details as notches may cause high tension perpendicular to the grain and should not be applied. However rules are necessary if alternative solutions are not possible and design rules are proposed for the Dutch Code TGB-1990 as a better alternative than the Eurocode rules 5.1.7.1 and 5.3.1.

Although the background of the design rules of the American Code for notched beams is not known it is possible to derive these rules and it is shown that they are only applicable for narrow span, high beams.

Design rules are derived using the simple fracture mechanics approach of [1]. Except for splitting along the grain the method is also used for crack propagation perpendicular to the grain. The same is applied for joints at the lower edge of a beam leading to an equivalent instable crack length. Simple design rules appear to be possible based on a lowest upper bound of the strength leading to the equations of 5.1 for notched beams and of 5.2 for excentric joints.

1. Introduction

Structural details like notches, causing high tensile peak stresses perpendicular to the grain, should be regarded as building faults and beside the design rules for exceptional cases the codes should provide solutions (as given in [3]) eliminating the influence of these peak-stresses.

The stress situation for connections at the tensional side of a beam may be similar to that of notched beams and often the same design rules are given for these joints. In [1] a method is given to explain the behaviour of notches and probably this can be extended, as proposed here, to explain the behaviour of splitting joints as well. The results of [1] show a good agreement between theory and tests except for short beams showing that an other mechanism is determining in this case. Probably this is the result of crack propagation perpendicular to the grain at weak spots and a first lower bound estimation is given here.

2. Explanation of the U.S. design rules for notched beams and for connections at the tensional side of a beam

Although the background of the design rules for beams with notches at the ends in the different codes cannot be found in literature and is not known any more a derivation of these rules is possible and will be given below. For connections at the lower part of the beam eq.(5) or (6) are used and it will be shown that this only ap-

plies for short beams.

A crack may propagate from the corner of a notch at the support along the grain until the loading point in the field is reached in a three- or four- point bending test. The lower bound of the strength is thus determined by the strength of the remaining beam, after the crack propagation, with a height h_e .

If a beam according to fig. 1 may fail, at the same time, by bending or by shear the shear force V_d will be:

$$V_d = M_d/L = \frac{f_{0,d} \cdot b h^2}{6L} \quad (1)$$

and in the same time:

$$V_d = \frac{2}{3} f_{v,d} \cdot b h \quad (2)$$

Thus from (1) and (2):

$$\frac{h}{L} = \frac{4f_{v,d}}{f_{0,d}} \quad (3)$$

When this beam is notched at the ends (fig. 2) the strength of the remaining beam after crack propagation is:

$$V_d = M_d/L = \frac{f_{0,d} \cdot b h_e^2}{6L} \quad (4)$$

or with eq.(3):

$$V_d = \frac{2}{3} f_{v,d} \cdot b h_e \cdot \frac{h_e}{h} \quad (5)$$

This equation for the strength reduction by a notch is the Code equation of the U.S.A and was proposed for the first draft of the Eurocode.

When bending failure is not determining for the unnotched beam is: $h/L > 4f_{v,d}/f_{0,d}$ and is V_d higher than the value according to eq.(5) with a maximum of:

$$V_d = \frac{2}{3} f_{v,d} \cdot b h_e \quad (6)$$

This occurs when: $h_e/L \geq 4f_{v,d}/f_{0,d}$ and thus also shear failure of the remaining beam is determining for the strength.

When only bending failure is determining ($h/L < 4f_{v,d}/f_{0,d}$), V_d is lower than according to eq.(5) and is for the remaining beam:

$$V_d = \frac{f_{0,d} \cdot b h_e^2}{6L} = \frac{2}{3} f_{v,d} \cdot b h_e \cdot \frac{f_{0,d}}{4f_{v,d}} \cdot \frac{h_e}{L} \quad (7)$$

This, also measured, lower value with respect to eq.(5) should be used for longer beams if there is not accounted for a strength perpendicular to the grain. The measurements show that eq.(7) applies for the failure mode of splitting along the grain and is safe for small specimens (when the splitting strength is high).

It can be concluded that the design of notched beams can be based on the strength of the remaining beam (that would remain after crack propagation) when cracking of the beam need not to be regarded as a limit state of the utility of the beam.

If the splitting is regarded as a limit state of the beam the higher strength of the small beams and lower "strength" of the large beams have to be estimated by fracture mechanics as given in 3.

3. Explanation of the strength of notched beams and derivation of design rules

In the following the simple fracture mechanics approach of [1] is followed, with a slightly different starting point, to estimate the bound for splitting and the simple beam theory is used for the determination of the deformation δ by crack propagation. In the neighbourhood of the cracktip the stresses deviate from the beam theory according to an internal equilibrium system and it can be assumed that the dissipation by this system will not cause an increase of δ and is the same for all beams (Every flat crack has the same stress gradient). So an apparent value of the fracture energy is determined. This is not a disadvantage here because accounting for these effects would also provide an apparent value in this model because of the mixed mode crack propagation.

The potential energy of the symmetrical half of the beam according to fig. 2 is:

$W = V\delta/2$. When V is constant the increase of the crack length with Δx will increase the deflection with $\Delta\delta$. When the lost of the potential energy ΔW becomes equal to the energy of crack formation, crack propagation occurs. The energy of crack formation is: $G_c b \Delta x = G_c b h \Delta\beta$, where G_c is the crack formation energy per unit crack area. Thus crack propagation occurs at $V = V_f$ when:

$$\Delta W = V \Delta\delta/2 = V^2 \Delta(\delta/V)/2 = G_c b h \Delta\beta, \quad \text{or when:}$$

$$V_f = \sqrt{\frac{2G_c b h}{\frac{\partial \delta/V}{\partial \beta}}} \quad (8)$$

The change of δ by the increase of shear deformation is with $h_e = \alpha h$:

$$\delta_v = \frac{2}{G} \left(\frac{\beta h}{b \alpha h} - \frac{\beta h}{b h} \right) \cdot V \quad (9)$$

The change of δ by the increase of the deflection is:

$$\delta_m = \frac{V(\beta h)^3}{3Eb(\alpha h)^3/12} - \frac{V(\beta h)^3}{3Eb h^3/12} = \frac{4V\beta^3}{Eb} \cdot \left(\frac{1}{\alpha^3} - 1 \right) \quad (10)$$

Thus:

$$\frac{\partial \delta/V}{\partial \beta} = \frac{2}{Gb} \cdot \left(\frac{1}{\alpha} - 1 \right) + \frac{12\beta^2}{Eb} \cdot \left(\frac{1}{\alpha^3} - 1 \right) \quad (11)$$

The critical value of V thus is according to eq.(8):

$$V_f = \sqrt{\frac{G_c h b^2}{\frac{1}{G}(\frac{1}{\alpha} - 1) + (\frac{1}{\alpha^3} - 1) \cdot \frac{6\beta^2}{E}}} \quad (12)$$

or:

$$\frac{V_f}{b\alpha h} = \frac{\alpha \sqrt{GG_c/h}}{\sqrt{\alpha^3 - \alpha^4 + 6\beta^2(\alpha - \alpha^4)G/E}} \quad (13)$$

For small values of β eq.(13) becomes:

$$\frac{V_f}{b\alpha h} = \frac{\alpha \sqrt{GG_c/h}}{\sqrt{\alpha^3 - \alpha^4}} \quad (14)$$

For high values of β , $\beta = c\eta$ with $\eta = L/h$, eq.(13) becomes with $E/G = 30$:

$$\frac{V_f}{b\alpha h} = \frac{\alpha \sqrt{GG_c/h}}{\beta \sqrt{0.2 \cdot (\alpha - \alpha^4)}} = \frac{\alpha \sqrt{GG_c/h}}{c\eta \sqrt{0.2 \cdot (\alpha - \alpha^4)}} \left(= \frac{\alpha K_1}{c\eta \sqrt{6h(\alpha - \alpha^4)}} \right) \quad (15)$$

where K_1 is the stress intensity factor.

Because $\sqrt{\alpha - \alpha^4}$ doesn't change much with the usual values of α this equation is comparable with eq.(7) for the lower bound of the strength and depending on the value of c , V_f will be higher or lower than V according to eq.(7) and crack propagation will be instable respectively stable.

An example of measured high values of β can be found in the investigation of Murphy, mentioned in [1], done on a notch starting at $\beta = 2.5$ and proceeding to $\beta = 5.5$ ($\eta = 10$, or $c = 0.55$). Further also beams are tested with a cut at a distance $\beta = 2.5$ ($\eta = 10$, or $c = 0.25$). Because of the high value of β eq.(15) approximately applies and the measurements show a mean value of $\sqrt{GG_c} = 8.9 \text{ N/mm}^{1,5}$. For all specimens was: $\alpha = 0.7$; $\eta = 10$; $b = 79 \text{ mm}$. The other data are given in table 1.

Table 1. Strength of clear laminated Douglas fir with notches in the tensile zone in MPa (Murphy)

h mm	β	num- ber	V/ $\alpha b h$ tests	eq.(15)
305	2.5	2	0.46	0.47
305	5.5	2	0.24	0.22
457	2.5	2	0.38	0.38
457	5.5	1	0.16	0.17

From the table it follows that for high values of η , the strength, also at high values

of β , is only determined by eq.(15) or only by horizontal crack propagation. An estimation of the conditions for the bend off of the crack can be made by determining the crack propagation in vertical direction.

The energy of crack formation in y-direction is:

$$G_m b \Delta y = G_m b h \Delta \alpha = V \Delta \delta / 2 = V^2 \Delta (\delta / V) / 2.$$

Thus crack propagation occurs when:

$$V_m = \sqrt{\frac{2G_m b h}{\frac{\partial \delta / V}{\partial \alpha}}} \quad (16)$$

If it is assumed that vertical crack propagation is accompanied with horizontal crack propagation over a long distance than equations (9) and (10) apply for δ and is, with $\beta h = L$ (as lower bound):

$$-\frac{\partial \delta / V}{\partial \alpha} = \frac{2\eta}{Gb} \cdot \left(-\frac{1}{\alpha^2}\right) - \frac{12\eta^3}{Eb} \cdot \frac{1}{\alpha^4} \quad (17)$$

or, according to eq.(16):

$$\frac{V_m}{b\alpha h} = \frac{\alpha \sqrt{GG_m/h}}{\sqrt{\alpha^2 \eta + 6\eta^3 G/E}} = \frac{\alpha \sqrt{GG_m/h}}{\eta \sqrt{\alpha^2/\eta + 6\eta G/E}} \quad (18)$$

Application of this equation on the data of table 1 for $\beta = 5.5$ and $E/G = 30$ shows that $\sqrt{GG_m}$ has to be smaller than 70 to 85 N/mm^{1.5} (if this mechanism was determining at the same time with horizontal splitting).

In order to get simplifications for the Code it can be seen that the variation of the denominator of eq.(13) is not much at smaller values of β and the usual values of α so that as a first estimate:

$$\frac{V_f}{\alpha b h} = \alpha f_v \sqrt{\frac{h_v}{h}} \quad (19)$$

Eq.(18) also doesn't vary much with the denominator under the square root sign for the values of η wherefore this equation is determining so that as a first estimate:

$$\frac{V_m}{\alpha b h} = \frac{\alpha}{\eta} f_{m0} \sqrt{\frac{h_m}{h}} = \alpha f_v \sqrt{\frac{h_v}{h}} \cdot \frac{\eta_0}{\eta} \quad (20)$$

where h_v , h_m and η_0 are constants. The last equation is determining when $\eta \leq \eta_0$ because crack propagation occurs at V_f according to eq.(19) as if $\eta = \eta_0$ in eq.(20) and hardening can occur after crack formation when $\eta \leq \eta_0$.

An example whereby the shear strength is determining for the un-notched beam, $V = (2/3) b h f_v$ is measured by Kollmann and given in [1]. Because only the ratio of the strength of the notched beam with respect to the strength of the un-notched

beam is published the test results are calculated by assuming $f_v = 10 \text{ N/mm}^2$ for "Red tulip oak". For this case of small η the strength of the remaining beam is high and there will be no instant failure after the occurrence of the horizontal crack. In table 2 the crack formation energies are calculated according to the different equations.

Table 2. Strength of notched beams, Red tulip oak, Kollmann.

h	α	β	η/α	b	n	$\frac{V}{b\alpha h}$	var. coef.	$\sqrt{GG_f}$ tests	$\sqrt{GG_m}$ tests	$f_v\sqrt{h_v}$ approximations	$f_m\sqrt{h_m}$ approximations
mm				mm		N/mm ²	%		N/mm ^{1.5}		
100	.875	~ 0.3	2.0	50	1	5.56	-	18.4	101	63.5	111
	.75		2.4		2	3.47	-	15.0	<u>68.3</u>	46.3	<u>83.3</u>
	.625		2.9		1	2.77	-	13.4	<u>60.6</u>	44.3	<u>80.3</u>
	.5		3.6		2	2.53	-	12.7	<u>64.3</u>	50.6	<u>91.1</u>
	.25		7.2		1	~1.9	-	<u>8.2</u>	85.9	76	137

Splitting is possibly determining for $\alpha = 0.25$ met $\sqrt{GG_f} = 8.2$, comparable with Douglas Fir. For higher values of α vertical crack propagation, or bending failure of the remaining beam, is determining with:

$$\sqrt{GG_m} = 64,4 \text{ N/mm}^{1.5}$$

Possibly there is a more favourable mechanism at $\alpha = 0.875$ (lower splitting stresses).

For this case (and for $\alpha = 0.25$) eq.(5) is satisfied or: $V_d/b\alpha h = 2/3 \cdot \alpha f_{v,d}$.

In the following tables the crack formation energy is determined for the other cases of [1].

Table 3. Strength of notched beams depending on the height of the beam

h	α	β	η/α	b	n	$\frac{V}{b\alpha h}$	var. coef.	$\sqrt{GG_f}$ tests	$\sqrt{GG_m}$ tests	$f_v\sqrt{h_v}$ approximations	$f_m\sqrt{h_m}$ approximations
mm				mm		N/mm ²	%		N/mm ^{1.5}		
5 min. test, m.c. 14.9 %, $\rho = 467 \text{ kg/m}^3$, Gustafsson, Pinus sylvestris L.											
12	.75	.5	3.6	44	7	3.32	16	5.5	35.8	15.3	41.4
48						2.75	10	<u>9.1</u>	59.3	<u>25.4</u>	68.6
196						1.3	25	<u>8.7</u>	56.7	<u>24.3</u>	65.5

Table 4. Strength of notched beams depending on the height of the beam
(continuation of table 3)

h	α	β	η/α	b	n	$\frac{V}{b\alpha h}$	var. coef.	$\sqrt{GG_f}$	$\sqrt{GG_m}$	$f_v\sqrt{h_v}$	$f_m\sqrt{h_m}$
mm				mm		N/mm ²	%	tests	N/mm ^{1.5}	approximations	
m.c. 12 %, Carlson, Shahabi, Sunding, Pinus sylvestris											
50	.5	.5	10	45	2	2.0	-	<u>8.2</u>	145	<u>28.3</u>	141
100			5			1.46	-	<u>8.5</u>	56.5	<u>29.2</u>	73
200			2.5			1.18	-	<u>9.7</u>	28.0	<u>33.4</u>	42
m.c. 18 %, Gustafsson, Pinus sylvestris											
45	.5	.5	6.7	45	6	1.72	9	<u>6.7</u>	66.7	<u>23.1</u>	77.3
195			6.2			0.93	17	<u>7.5</u>	67.4	<u>26.0</u>	80.5
m.c. 18 %, Gustafsson, Pinus sylvestris											
45	.5	.5	6.7	45	4	1.92	9	<u>7.5</u>	74.5	<u>25.7</u>	86.3
195			6.2			0.96	4	<u>7.8</u>	69.6	<u>26.8</u>	83.1
Eucalyptus, Leicester											
9.5	.5	1.92	9.3	38	4	3.9	-	<u>14.9</u>	110.9	<u>24.0</u>	111.8
19					4	3.08	-	<u>16.7</u>	123.8	<u>26.8</u>	124.9
37					≥ 2	1.9	-	<u>14.3</u>	106.6	<u>23.1</u>	107.5
58					4	1.77	-	<u>16.7</u>	124.3	<u>27.0</u>	125.4
154					4	1.07	-	<u>16.5</u>	122.5	<u>26.6</u>	123.5

For very small specimens (h = 12 mm) the crack length has to be adjusted (see [1]). It follows from table 3 that for Pinus sylvestris: $\sqrt{GG_f} = 8.1$ and: $f_v\sqrt{h_v} = 25.6$ N/mm^{1.5}. For Eucalyptus this is resp. 15.8 en 25.9 N/mm^{1.5}. The two times higher crack formation energy of Eucalyptus is not shown in the approximation value. Thus the approximation only can be used for the usual applied small values of β .

In the next table the measurements are given for Spruce wherefore also vertical crack propagation is determining. Because for all softwoods the same crack formation energy is measured the values of table 5 can be used in all cases.

Table 5. Strength of notched beams, Spruce, Moher en Mistler.

h	α	β	η/α	b	n	$\frac{V}{b\alpha h}$	var. coef.	$\sqrt{GG_f}$ tests	$\sqrt{GG_m}$	$f_v\sqrt{h_v}$ approximations	$f_m\sqrt{h_m}$
mm				mm		N/mm ²	%		N/mm ^{1.5}		
testing time ore than 1 min., clear, m.c. 11 %, $\rho = 510 \text{ kg/m}^3$											
120	.917	.25	3.4	32	6	2.36	11	<u>7.3</u>	84.1	<u>28.2</u>	87.9
	.833		3.8		27	1.93	15	<u>8.1</u>	73.7	<u>25.4</u>	80.3
	.75		4.2		43	1.68	19	<u>8.2</u>	69.5	<u>24.5</u>	77.3
	.667		4.7		14	1.52	18	<u>8.1</u>	69.1	<u>25.0</u>	78.3
	.583		5.4		10	1.5	18	<u>8.4</u>	76.3	<u>28.2</u>	88.7
	.5		6.3		49	1.59	18	<u>9.1</u>	92.4	<u>34.8</u>	109.7
	.333		9.5		10	1.48	16	<u>8.2</u>	125.1	<u>48.7</u>	154.0
gluelam. Spruce. $\rho = 470 \text{ kg/m}^3$.											
600	.917	.417	2.2	100	5	2.00	13	14.3	96.8	53.4	107.8
	.833		2.4		4	1.61	28	15.6	81.8	47.3	94.6
	.75		2.7		4	0.88	12	10.0	<u>47.4</u>	28.7	<u>58.2</u>
	.667		3.0		4	0.86	16	10.7	<u>49.8</u>	31.6	<u>63.2</u>
	.5		4.0		4	0.75	7	10.2	<u>53.2</u>	36.7	<u>73.5</u>

It follows from the table for Spruce: $\sqrt{GG_f} = 8.4$ and: $f_v\sqrt{h_v} = 28.5 \text{ N/mm}^{1.5}$ ($\alpha \geq 0.5$). The representative value is about: $(1 - 1,64 \cdot 0.2) = 0.67$ times as high.

For gluelam there is possibly a more favourable crack mechanism at $\alpha \leq 0.833$ (as also follows from the two times higher coefficient of variation at this boundary value of 0,83). A safe value for: $\sqrt{GG_m} = 50$ and $f_m\sqrt{h_m} = 65 \text{ N/mm}^{1.5}$ so that: $\eta_0 = 65/28.5 = 2,3$.

The Australian code also shows for timber an increase in strength at $\alpha \geq 0,9$.

4. Explanation of the strength of connections at the lower boundary of a beam and derivation of design rules

For a connection at the middle of a beam the following applies after splitting (see fig. 3). The part above the crack (stiffness I_2) only carries a moment (M_2) and the part below the crack (stiffness I_1) carries a moment (M_1) and the shearforce (V).

The rotation φ at the end of half the crack length $\lambda = \beta h$ then is:

$$\varphi = \frac{M_2 \lambda}{EI_2} = \frac{M_1 \lambda}{EI_1} + \frac{V \lambda^2}{2EI_1} = \frac{(M - M_1) \lambda}{EI_2} \quad (21)$$

with: $M = M_1 + M_2$ being the moment at the end of the crack or:

$$M_1 \left(1 + \frac{I_2}{I_1}\right) = M - \frac{V \lambda I_2}{2I_1} \quad \text{and} \quad \varphi = \frac{\bar{M} \lambda}{E(I_1 + I_2)} \quad (22)$$

\bar{M} is the mean moment over the length λ ($\bar{M} = M + V\lambda/2$).

According to fig. 3 this is the mean moment over the length βh : $\bar{M} = VL(1 - \beta h/2L)$ and the relative deflection of the support follows from: $\delta = \delta_v + \varphi(L - \beta h/2)$ so that the increase of the deflection by splitting is:

$$\begin{aligned} \delta &= \frac{2}{G} \left(\frac{\beta h}{b\alpha h} - \frac{\beta h}{bh} \right) \cdot V + VL \left(1 - \frac{\beta h}{2L} \right) \frac{\beta h}{E} \left(L - \frac{\beta h}{2} \right) \cdot \left(\frac{12}{(\alpha h)^3 + (1 - \alpha)^3 h^3} - \frac{12}{h^3} \right) = \\ &= \frac{2}{G} \left(\frac{\beta h}{b\alpha h} - \frac{\beta h}{bh} \right) \cdot V + \frac{12VL^2}{Eh^2} \cdot \left(1 - \frac{\beta h}{2L} \right)^2 \cdot \beta \cdot \frac{3\alpha(1 - \alpha)}{1 - 3\alpha(1 - \alpha)} \end{aligned} \quad (23)$$

so that:

$$\frac{\partial \delta / V}{\partial \beta} = \frac{2}{Gb} \cdot \left(\frac{1}{\alpha} - 1 \right) + \frac{12V^2}{Eb} \cdot \frac{3\alpha(1 - \alpha)}{1 - 3\alpha(1 - \alpha)} \cdot \left(1 - \frac{\beta h}{2L} \right) \cdot \left(1 - \frac{3\beta h}{2L} \right) \quad (24)$$

and eq.(8) becomes for small values of β of the initial crack with $E/G = 30$:

$$\frac{V_f}{b\alpha h} = \frac{\sqrt{GG_c/h}}{\sqrt{\alpha - \alpha^2 + 0.6\eta^2(\alpha^3 - \alpha^4) \cdot (1 - 2\beta/\eta)/(1 - 3\alpha + 3\alpha^2)}} \quad (25)$$

The second term in the denominator has a small influence for small values of α and for increasing (stable) crack increase (= increase of β) the equation is, for $\beta h \approx L/2$, equal to eq.(14) giving the same equation as for notched beams with short notches at the ends. Eq.(14) is here an upper limit because there is no exchange of energies of shear- and split- deformation. So it is to be expected that the measured failure data will not be far below the values according eq.(14) and $\beta \approx \eta/2$ can be used as approximation.

In the measuring range of [2] eq.(25) can be written for $\alpha \approx 0.15$ to 0.55 :

$$\frac{V_f}{b\alpha h} \approx \frac{\sqrt{GG_c/h}}{\sqrt{(\alpha - \alpha^2) \cdot (1 + 5.4\eta(\eta - 2\beta)\alpha^3)}} \quad (26)$$

With this equation a first estimate of β can be made for sufficient small values of α and sufficient high values of η . For higher values of α ($\alpha \geq 0.7$) splitting will not occur, at least not in the measuring range of [2] where is measured on relatively short beams. For small values of η the strength of the remaining beam may be deter-

mining so that the horizontal crack propagation remains stable until failure of this beam (the start of cracking in vertical direction). If, by the higher loading, only I_1 changes by crack formation perpendicular to the grain it follows from eq.(23):

$$-\frac{\partial \delta/V}{\partial \alpha} = -\frac{2}{Gb} \cdot \left(\frac{\beta}{\alpha^2}\right) - \frac{12\beta\eta^2}{Eb} \cdot \left(1 - \frac{\beta}{2\eta}\right)^2 \cdot \frac{3 \cdot \alpha^2}{(\alpha^3 + (1 - \alpha_0)^3)^2} \quad (27)$$

or according to eq.(16) is for $\alpha = \alpha_0$:

$$\frac{V_m}{b\alpha h} = \frac{\sqrt{GG_m}/h}{\sqrt{\beta + 18\beta\alpha^4(\eta - \beta/2)^2 G/(E \cdot (\alpha^3 + (1 - \alpha)^3)^2)}} \quad (28)$$

For $\beta = \eta$, as lower bound, this becomes:

$$\frac{V_m}{b\alpha h} = \frac{\sqrt{GG_m}/h}{\sqrt{\eta + 4,5\alpha^4\eta^3 G/(E \cdot (\alpha^3 + (1 - \alpha)^3)^2)}} \quad (29)$$

In the measuring range of [2], eq.(29) can be written for $\alpha \approx 0,15$ to $0,55$:

$$\frac{V_m}{b\alpha h} \approx \frac{\sqrt{GG_m}/h}{\sqrt{\eta + 7,9 \cdot \eta^3 \alpha^6}} \quad \left(\geq \frac{\sqrt{GG_m}/h}{\sqrt{\beta_m + 31 \cdot \beta_m \alpha^6 (\eta - \beta_m/2)^2}} \right) \quad (30)$$

The second term in the denominator has a small influence for small values of α and eq.(30) is therefore about comparable with eq.(18) for notches (for small η).

For higher values of η (not measured in [2]) for instance at $\eta \geq 5$ the strength is high according to the American Code and independent of η . Then the lower bound $\beta = \eta$ according to eq.(29) doesn't occur but $\beta = \beta_{\max} = \text{constant}$ en $V_m/b\alpha h \approx \sqrt{GG_m}/h\beta_m \approx \text{constant} \geq f_v$ in the measuring range of the American Code as given in eq.(30).

Eq.(31) (or (14)), (29) and (25) are tested in the following tables. In the measuring range of small values of η both equations (32) and (29) may be determining. According to eq.(14) is:

$$\sqrt{GG_c} = \frac{V_f}{\alpha h} \cdot \frac{\sqrt{h}}{b} \cdot \sqrt{\alpha \cdot (1 - \alpha)} \quad (31)$$

By multiplication with: $\sqrt{1 + 5,4\alpha^3\eta(\eta - 2\beta)}$ according to eq.(26) a first estimate is possible of β , in the un-cracked stage, for higher values of η .

For simplicity mean values of β are regarded in the table. By this $\sqrt{GG_c}$ is too high for higher values of α and too small for small α in series b where β has influence. However the differences are not much and will have no influence on the mean value of $\sqrt{GG_c}$.

Table 6. Strength of the connection, Möhler en Lautenschläger

h	b	type	d	numb. per row	numb. of rows	numb. of tests	αh mm	$\frac{V}{b\alpha h}$ N/mm ²	$\sqrt{GG_c}$ eq.(14) N/mm ^{1.5}	$2\bar{\beta}$	$\sqrt{GG_c}$ eq.(25)	η	$\sqrt{GG_m}$ eq.(29)
Assumption L/h = 2.5 (L is not given in [2] and sometimes different from 2.5h)													
pindowels													
180	40	a	8,0	1	1	1	28	2,32	11,3	0	12,1	2,5	49,2
120						3		2,70	12,5		15,0		47,1
nails													
180	40	b/c	3,8	5	1	5	28	3,54	17,2	1,2	17,8	2,37	73,2
						<u>3</u>		<u>3,92</u>	<u>19,1</u>		<u>19,7</u>		<u>81,0</u>
					mean	8		3,68	17,9		18,5		76,1
		b	"	5	1	1	47	2,85	16,8		18,9		59,5
						<u>3</u>		<u>2,54</u>	<u>15,0</u>		<u>16,9</u>		<u>53,0</u>
					mean	4		2,62	15,5		17,4		54,7
				5	1	3	66	2,26	14,6		19,2		50,4
							85	1,97	13,2		20,7		52,4
							104	2,27	15,1		26,5		71,2
180	40	c	"	5	2	1	47	3,59	21,2	> 2,4	21,2		75,0
						<u>3</u>		<u>3,32</u>	<u>19,5</u>		19,5		<u>69,3</u>
					mean	4		3,38	19,9		19,9		70,6
				5	3	3	66	3,57	23,1		23,1		79,6
				5	4	3	85	3,11	20,8		20,8		82,7
				5	5	3	104	3,34	22,2		22,2		104,7
120	40	d		2	1	3	28	4,25	19,7	0	22,8	2,18	69,1
								3,60	16,7		19,5	2,26	59,6
								3,04	14,1		16,6	2,34	51,2
								2,87	13,3		15,8	2,42	49,2
		e		1	1	3		3,10	14,4		17,3	2,5	54,0

For types a, d and e in the table where V is carried by 1 or 2 nails (or half a dowel) failure of the connection is probably determining for the strength and splitting is due to a secondary stress concentration after proceeded "plastic" deformation and hardening by failure of the dowel mechanism. So splitting of the wood is not the primary failure mechanism.

In table 7 measurements are given for small values of η . It can be expected that failure of the remaining beam is determining. If the highest value ($\alpha = 0.75$) is not regarded (because splitting will not occur) the mean value or $\sqrt{GG_m} = 53,9 \text{ N/mm}^{1.5}$. For each parameter only one test is done except in one case where 2 specimens show values of $\sqrt{GG_m}$ of 46 and 61 $\text{N/mm}^{1.5}$. This shows a high variation of this parameter because there is no well defined initial crack length.

The value of $\sqrt{GG_c}$ of $21,8 \text{ N/mm}^{1.5}$ according to eq.(14) in table 7, has to be higher than the real value of $\sqrt{GG_c}$ (by hardening after splitting). This means that for the connection type c of table 6 eq.(14) applies or that the critical crack-length $2\beta \approx \eta = 2.37$ because then the smallest value of $\sqrt{GG_c} \approx 20 \text{ N/mm}^{1.5}$ is reached (being smaller). The calculated value of $\sqrt{GG_m}$ is high indicating immediate failure (of the remaining beam) after splitting.

Table 7. Strength of the connection, Möhler en Siebert

h	b	type	d	numb. per row	numb. of rows	numb. of tests	αh	$\frac{V}{b\alpha h}$	$\sqrt{GG_c}$ eq.(14)	η	$\sqrt{GG_m}$ eq.(29)
mm	mm		mm	row	rows	tests	mm	N/mm^2	$\text{N/mm}^{1.5}$		
nails (type n)											
1200	100	n	4,2	10	4	1	300	1,24	18,6	1,42	51,3
							600	0,99	17,1		46,6
pinsowels (type s)											
1200	100	s	16,0	3	2	1	300	1,5	22,5	1,43	62,3
							900	1,06	15,8		53,9
					3	4	300	1,87	28,0		77,7
					3	6	600	1,49	25,9		70,6
					2	2	300	1,08	16,3	1,37	44,0
600	100			3	4	1	300	1,83	22,4	0,94	46,4
						<u>1</u>		<u>2,40</u>	<u>29,4</u>		<u>60,8</u>
					gem.	2		2,12	25,9		53,7
				3	2	1	450	2,0	21,2		52,6
						1		2,22	23,6		58,3
						1		3,44	25,9	1,4	(121,5)
						1	150	2,32	24,6		67,4
						1		2,08	22,1	0,44	34,0
						1	300	1,25	15,3	1,4	41,2
				2	2	1	150	1,87	19,8	0,83	41,8

Table 8. Strength of the connection, Ehlbeck en Görlacher

h	b	type	d	numb. per row	numb. of rows	numb. of tests	αh	$\frac{V}{b\alpha h}$	$\sqrt{GG_C}$ eq.(14)	$2\bar{\beta}$	$\sqrt{GG'_C}$ eq.(25)	η	$\sqrt{GG_m}$ eq.(29)
mm	mm		mm				mm	N/mm ²	N/mm ^{1.5}				
250	100	a	4.0	2	4	3	100	1,87	14,5	1,8	19,0	2,6	55,0
								2,08	16,2		20,7	2,53	60,0
								2,14	16,6		20,3	2,4	59,4
		2,40				18,6		20,7	2,12	61,0			
		b				150	1,77	13,7	1,9	20,5	2,53	71,6	
							1,92	14,9		20,7	2,4	73,3	
	2,37		18,4		21,4		2,12	79,3					
	c	100	1,79	13,8	~ 0	21,3	2,0	43,8					
			1,95	15,1		20,0	1,5	39,8					
	250	80	a					2,18	16,9	1,8	21,6	2,53	62,8
	250	120					3		1,93	14,9		19,0	2,53
<u>1,94</u>									<u>15,1</u>		<u>19,3</u>		<u>55,9</u>
mean											15,0	19,2	55,8
250	100		6.0			3	100	1,85	14,3		18,3	53,3	
400	100	d	4.0			3	100	1,98	17,1	~ 0	19,7	1,95	55,6
								160	1,61	15,8		24,0	49,0
150		e					90	2,63	15,8	2,2	20,2	2,53	82,4
250		f		2	2		100	1,78	13,8	1,5	18,9	2,52	51,2
								1,68	13,0		17,8		48,3
								2,11	16,3		22,4		60,6
											eq.(16)		eq.(21)
		g			4			1,89	14,6	1,0	17,9	2,48	< 139
								2,35	18,2		22,2	2,16	< 143

In series f of table 8 the nail again was probably determining.

Series g of table 8 is an end-support and fracture will occur according to the equations of the notched beams (the split off part of the beam is unloaded). However $\sqrt{GG_C}$ is a factor $20/8.1 = 2.5$ higher with respect to the notched beam because there is no clear initial crack.

The equivalent critical relative crack length $\bar{\beta}$ in the middle of the beam of a connection pattern at the lower part of a beam height is about 0.9 (exclusif the length of the pattern in beam direction) for an uniform spread pattern over the height αh .

For a concentrated pattern (in one row in beam direction) this is about the half.

The higher value in the middle of the beam with respect to an end-support (where $\beta = 0.5$) is due to the moment carrying capacity of the split off part of the beam in the middle of the beam.

Series c and d in table 8 show an early failure (β is small) and also $\sqrt{GG_m}$ is small. Comparable tests of other series show much higher values.

The boundary η_g between horizontal splitting and vertical splitting lies theoretically lower for small values of α than for higher values of α . The high values of $\sqrt{GG_m}$ in table 6 (except for the series where the joints are determining) show that η_g is below 2.37. Table 8 shows that η_g may be below 2. If it is assumed that η_g lies below 1.4 in table 7 than is:

$\sqrt{GG'_c} \approx 21$ and $\sqrt{GG_m} \approx 49 \text{ N/mm}^{1.5}$ if both mechanisms are determining at the same time. It can be concluded that:

$\sqrt{GG_m}$ is about 49 to 53.9 and as for notches can be estimated at $50 \text{ N/mm}^{1.5}$ and: $\sqrt{GG'_c}$ is about 20 to 21 $\text{N/mm}^{1.5}$.

A design rule could be based on an equivalent critical crack length of about $0.9 \cdot h$ (where h is the height of the beam) for connections in the middle of the span and about $0.4 \cdot h$ for connections at the end of a beam and for concentrated patterns of connections. Easier however is to base the method on an equivalent work term according to eq.(14) (because the shear-mode of cracking is strongly dominating) and to give a lower bound for all cases.

Series b of table 6 gives a mean: $\sqrt{GG_c} = 15.9$ (21 tests) and series a to e of table 8 shows a mean of 15.7 (48 tests). The coefficient of variation is about 8 %. For vertical cracking V is mainly dependent on $\sqrt{\eta}$ in eq.(30). In table 9 the values are calculated according to these design formulas:

$$\frac{V_f}{\alpha b h} = f_v \sqrt{\frac{h_v}{h}} \quad (32)$$

and for $\eta \leq \eta_0$:

$$\frac{V_m}{\alpha b h} = f_v \sqrt{\frac{h_v}{h} \cdot \frac{\eta_0}{\eta}} \quad (33)$$

It follows from table 9:

$$f_v \sqrt{h_v} = 34,1 \quad \text{and}$$

$$f_v \sqrt{h_v \eta_0} = 49,3 \text{ N/mm}^{1.5}$$

so that: $\eta_0 = (49,3/34,1)^2 = 2,1$.

Table 9. Strength of the connections according to the proposed design rules

h	b	type	d	num. per row	num. of rows	num. of tests	αh mm	$\frac{V}{b\alpha h}$ N/mm ²	$f_v\sqrt{h_v}$ N/mm ^{1.5}	η	$\eta_0 f_v\sqrt{h_v}$ $\eta \leq \sim 2$ N/mm ^{1.5}
Strength connection according to table 6 series b											
180	40	b/c	3,8	5	1	5	28	3,54	47,5	2,37	
						<u>3</u>		<u>3,92</u>	<u>52,6</u>		
					mean	8		3,68	49,4		
		b	"	5	1	1	47	2,85	38,2		
						<u>3</u>		<u>2,54</u>	<u>34,1</u>		
					mean	4		2,62	35,2		
				5	1	3	66	2,26	30,3		
							85	1,97	26,4		
							104	2,27	30,5		
Strength of the connection according to table 8 series a to e											
250	100	a	4,0	2	4	3	100	1,87	29,6	2,6	
								2,08	32,9	2,53	
								2,14	33,8	2,4	
								2,40	37,9	2,12	55,2
		b					150	1,77	28,0	2,53	
								1,92	30,4	2,4	
								2,37	37,5	2,12	54,6
		c					100	1,79	28,3	2,0	40,0
								1,95	30,8	1,5	37,8
250	80	a						2,18	34,5	2,53	
250	120					3		1,93	30,5	2,53	
						3		1,94	30,7		
250	100		6,0			3	100	1,85	29,3		
400	100	d	4,0			3	100	1,98	39,6	1,95	55,3
							160	1,61	32,2		45,0
150		e					90	2,63	<u>32,2</u>	2,53	
						mean			34,1		48,0

5. Proposal for design rules for the Dutch code and Eurocode

5.1 Beams with notches at the ends.

For notches at the ends of a beam applies:

$$\frac{V_{\text{rep}}}{\alpha b h} = \alpha f_v \sqrt{\frac{h_v}{h}} = \alpha \cdot 19,1 / \sqrt{h} = \frac{2}{3} \cdot f_{v,\text{rep}} \cdot 1,5 \cdot 19,1 \cdot \alpha / (f_{v,\text{rep}} \cdot \sqrt{h}) = \frac{2}{3} \cdot f_{v,\text{rep}} \cdot \alpha \cdot 9,55 / \sqrt{h}$$

with: $f_v \sqrt{h_v} = 28,5 \text{ N/mm}^{1,5}$ at failure. The representative or characteristic value is about: $(1 - 1,64 \cdot 0,2) = 0,67$ times higher or: $0,67 \cdot 28,5 = 19,1 \text{ N/mm}^{1,5}$. $f_{v,\text{rep}} = 3 \text{ N/mm}^2$

For small values of η is for notched beams:

$$\frac{V_{\text{rep}}}{\alpha b h} = \frac{\alpha}{\eta} f_m \cdot \sqrt{\frac{h_m}{h}} = \frac{2}{3} \cdot f_{v,\text{rep}} \cdot 1,5 \cdot 43,6 \cdot \alpha / (3 \cdot \eta \cdot \sqrt{h}) = \frac{2}{3} \cdot f_{v,\text{rep}} \cdot \alpha \cdot 9,55 \cdot 2,3 / (\eta \cdot \sqrt{h})$$

with: $f_m \sqrt{h_m} = 65 \text{ N/mm}^{1,5}$ at failure or with $0,67 \cdot 65 = 43,6 \text{ N/mm}^{1,5}$ as representative (characteristic) value.

Thus the design rules can be based on:

$$V_d \leq \frac{2}{3} f_{v,d} b h_e \cdot \frac{h_e}{h} \cdot \sqrt{\frac{90}{h}} \quad \text{when } \eta \geq 2,3$$

and:

$$V_d \leq \frac{2}{3} f_{v,d} b h_e \cdot \frac{h_e}{h} \cdot \sqrt{\frac{90}{h} \cdot \frac{2,3}{\eta}} \quad \text{when } \eta < 2,3$$

where $\eta = M_d / (V_d h)$ and h is in mm.

Alternatively the last proposal of the Dutch TGB-1990 art. 11.10 or Eurocode 5 art. 5.1.7.2 can be changed to:

$$k_{\text{jon}} = 1 + (k_{\text{kee}} - 1) \cdot \left(1 - \frac{a}{3 \cdot (h - h_e)}\right)$$

where $k_{\text{jon}} = 1$ when $h_e = h$ and $a \geq 3 \cdot (h - h_e)$

$$k_{\text{kee}} = \frac{h_e}{h} \cdot \sqrt{\frac{90}{h}} \quad \text{when } \eta \geq 2,3,$$

and:

$$k_{\text{kee}} = \frac{2,3}{\eta} \cdot \frac{h_e}{h} \cdot \sqrt{\frac{90}{h}} \quad \text{when } \eta < 2,3$$

with: $\eta = M_d / (V_d h)$. In the Eurocode k_{jon} is denoted by k_v .

When $h > h_e \geq 0.9 \cdot h$ linear interpolation is allowed between $k_{jon} = 1$ at $h = h_e$ and the value of k_{jon} at $h_e = 0.9 \cdot h$.

5.2 Connections at the lower part of a beam

For connections at the lower part of the height of a beam applies:

$$\frac{V_{rep}}{\alpha b h} = f_v \sqrt{\frac{h_v}{h}} = \frac{2}{3} \cdot f_{v,rep} \cdot 1.5 \cdot 22,85 / (3 \cdot \sqrt{h}) = \frac{2}{3} \cdot f_{v,rep} \cdot 11,4 / \sqrt{h} = \frac{2}{3} \cdot f_{v,rep} \sqrt{\frac{130}{h}}$$

with a representative value of: $f_v \sqrt{h_v} = 0,67 \cdot 34,1 = 22,85 \text{ N/mm}^{1,5}$.

For $\eta \leq \eta_0$ is:

$$\frac{V_m}{\alpha b h} = f_v \sqrt{\frac{h_v}{h} \cdot \frac{\eta_0}{\eta}} = \frac{2}{3} \cdot f_{v,rep} \cdot 1,5 \cdot 33,0 / (3 \cdot \sqrt{h \eta}) = \frac{2}{3} \cdot f_{v,rep} \cdot \sqrt{\frac{130}{h} \cdot \frac{2,1}{\eta}}$$

with the representative value of: $f_v \sqrt{h_v \eta_0} = 0,67 \cdot 49,3 = 33,03 \text{ N/mm}^{1,5}$.

For the TGB-1990 art. 13.1.4 or Eurocode art. 5.3.1 can be proposed:

$$V_d \leq \frac{2}{3} f_{v,d} b h_e \cdot \sqrt{\frac{130}{h}} \quad \text{when } \eta \geq 2.1$$

and:

$$V_d \leq \frac{2}{3} f_{v,d} b h_e \cdot \sqrt{\frac{130}{h} \cdot \frac{2,1}{\eta}} \quad \text{when } \eta < 2.1$$

$$V_d \leq \frac{2}{3} f_{v,d} b h_e \quad \text{when } h_e \geq 0.7 \cdot h$$

where $\eta = M_d / (V_d h)$ and h is in mm.

In the Eurocode is h_e denoted by b_e and b by t .

Literature

- [1] P.J. Gustafsson, CIB-W18A/21-10-1, meeting 21, Parksville, Vancouver Island, Canada, Sept. 1988.
- [2] J. Ehlbeck, R. Gortlacher, H. Werner, CIB-W18A/22-7-2, meeting 22, Berlin, Germany, Sept. 1989.
- [3] T.A.C.M. van der Put, Stevinrapport 25.4-90-02/A/HA-45 Trek loodrecht op de vezelrichting bij staafophangingen en uitkepingen, april 1990.

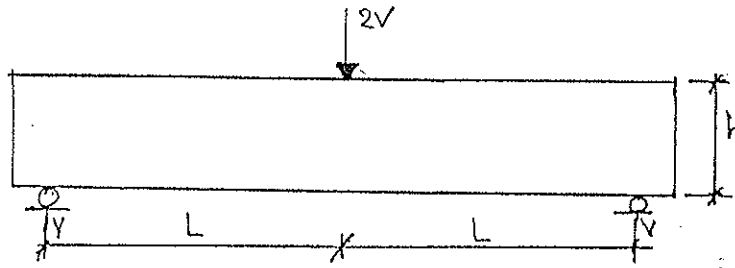


fig. 1.

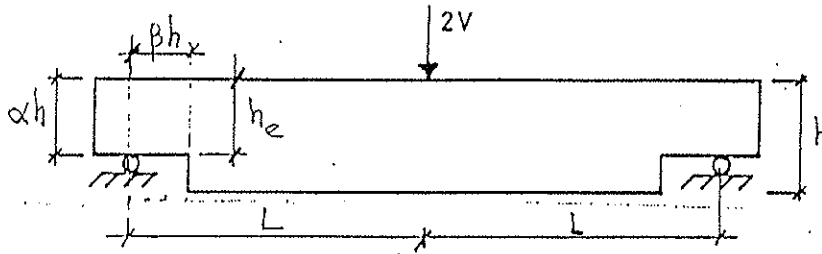


fig. 2.

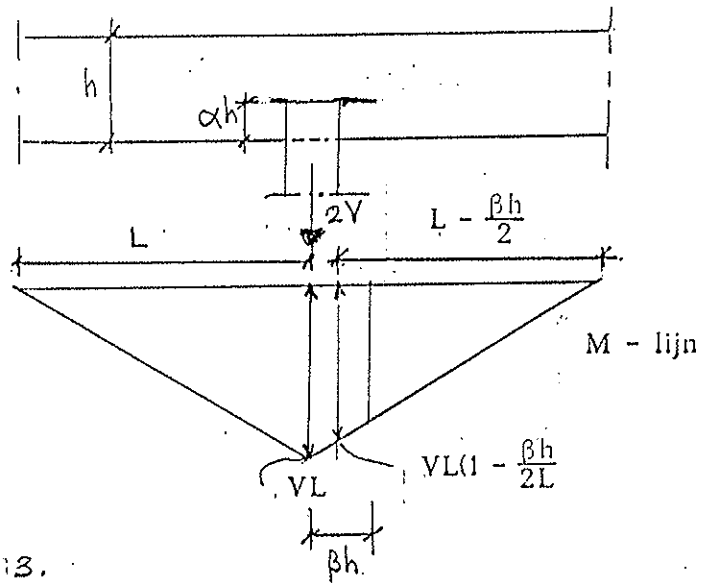
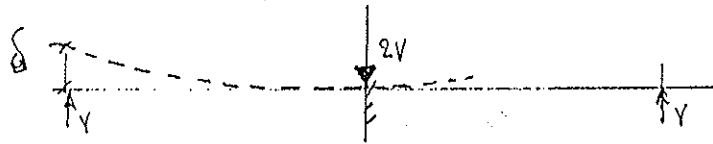


fig. 3.

INTERNATIONAL COUNCIL FOR BUILDING RESEARCH STUDIES AND DOCUMENTATION
WORKING COMMISSION W18A - TIMBER STRUCTURES

DIMENSIONING OF BEAMS WITH CRACKS, NOTCHES AND HOLES.

AN APPLICATION OF FRACTURE MECHANICS.

by

K Riipola
Forest Products Laboratory
Finland

MEETING TWENTY - THREE

LISBON

PORTUGAL

SEPTEMBER 1990

DIMENSIONING OF BEAMS WITH CRACKS, NOTCHES, AND HOLES AN APPLICATION OF FRACTURE MECHANICS

Kirsti Riipola

Abstract

A dimensioning method based on fracture mechanics is presented. Fracture energy for a beam with an infinite crack is calculated with the beam theory and the energy principle. Mode separation is done by the definition of mode II and the superposition principle. The material is assumed to be orthotropic in the stress intensity calculations. A parabolic fracture criterion is used to predict failure. To evaluate the method, some experiments in the literature are re-analyzed.

Introduction

Many experiments regarding beams with cracks, notches, and holes are reported in the literature. For the dimensioning, several methods are proposed. General for these methods is, that they are based on the experiments. In most cases, shear force has been chosen to be the dimensioning factor. Unfortunately, the material parameter (modified shear strength) used in dimensioning is not well-known.

A fracture energy based method for beams with notches has previously been proposed by Gustafsson (1988). The method is, however, restricted in the case of almost pure mode I fracture and the material parameter needed is difficult to find out experimentally. In this paper, a general method based on the fracture mechanics is proposed. The method has much in common with the ideas described by Pook (1979) and Williams (1988). The dimensioning principle is independent of the art of the fracture source, but the different support conditions reflected by the different fracture modes must be considered.

Fracture mechanics concerns structures with cracks. Therefore, it is a natural approach when dimensioning of cracked beams is concerned. The concept of a crack can, however, be extended. The drying of the wood causes small cracks parallel to the fibre in the orthotropic material. Thus, it is not unreasonable to make an assumption of an infinite crack also in such cases, where no immediate crack is found. Such constructive details are notches and quadratic holes. Also, circular holes can be dimensioned by the same way, if the results of Penttala (1980) are considered. For holes between the support and about one third of the span length, he found by finite element calculations, that, in the failure, the initial point of the crack growth was in the angle of 50° calculated from the beam axis. In the experiments, the mean value of the measured angle was found to be 34° . Thus, the assumption is reasonable, that the crack growth associated with the circular hole corresponds to the one of an inscribed quadratic hole.

Material parameters needed in fracture mechanics calculations have been studied since sixties. For North European species (*Pinus silvestris* and *Picea abies*) as well as Kerto LVL, a large base material has been collected in VTT fracture mechanics projects.

Definition of fracture modes

For a beam, the fracture modes are defined consistently with the common definitions. Mode I, also called opening mode, is present, when the upper and lower part of the beam will be separated transverse to the crack plane by the growing crack. Mode II, also called shearing mode, is present, when the crack is growing so that the upper and lower part of the beam will keep together and have the same curvature and deflection. Mode III (not considered here), also called tearing mode, would be present when the upper and lower part of the beam would be separated in the direction of the crack front.

Deformation of a cracked beam

In the following, stress intensities for a beam with a crack are calculated by the means of an energy balance consideration. A simply supported symmetric beam loaded by point loads is considered. The deflection of the beam is calculated as a sum of bending deformation and shear deformation. An infinite increase of the crack length is assumed. This increase is reflected by an increased deflection. The external work done by the loading is equal to the fracture energy consumed by the crack growth.

The notation is shown in figure 1. For the simply supported beam with point loads in figure 1, the bending deformation is calculated with the common differential equations. For the parts 1 to 4, the slope of the beam is given by the equation 1, and the deflection of the beam is given by the equation 2.

$$- E_X I_j v'_j = \int M_j dx + C_j \quad (1)$$

$$- E_X I_j v_j = \iint M_j dx dx + C_j x + D_j \quad (2)$$

Additional deformation is caused by the shear deformation. For the parts 1 to 3, the slope of the beam is proportional to the shear force, equation 3. For the part 4, the slope is zero. The additional deflection is given by the equation 4.

$$\frac{5}{6} G_{XY} A_j v' = M'_j \quad (3)$$

$$\frac{5}{6} G_{XY} A_j v = \int M'_j dx + F_j \quad (4)$$

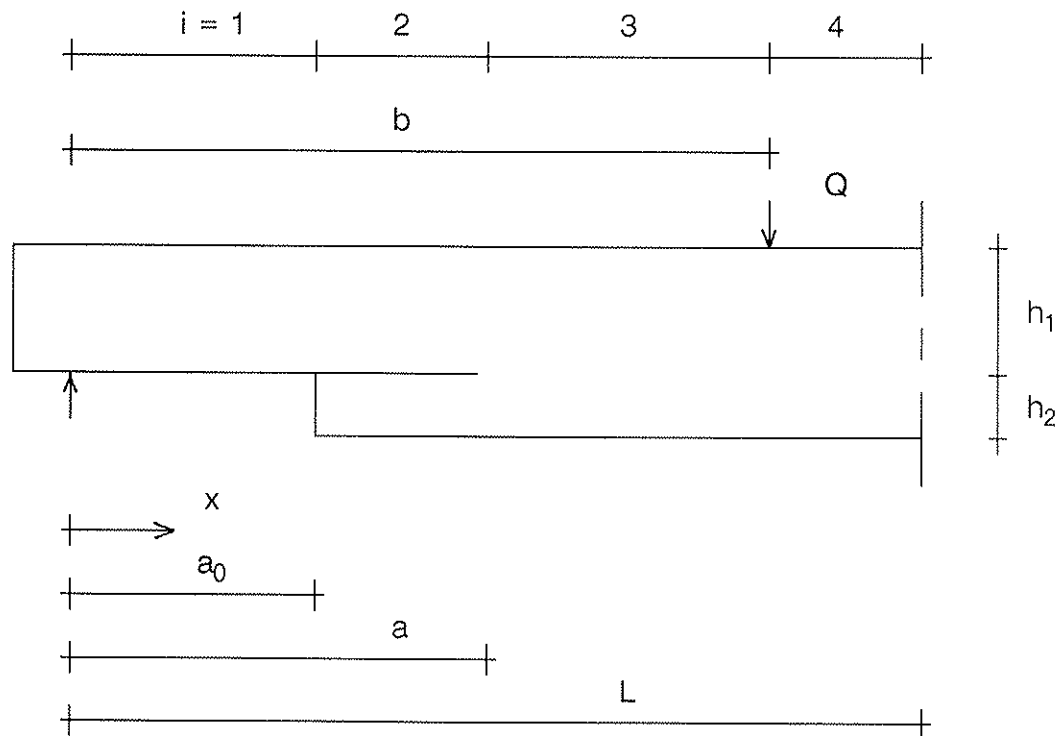


Figure 1. A beam with total depth h and thickness t is loaded by a couple of point loads Q with the distance b from the support. Span width is $2L$. For every part of the beam, the area of the beam is noted A_i and the moment of inertia is noted I_i . For the uncracked beam cross section, $A_i = A_0$ and $I_i = I_0$. The ratio I_0/I_i is noted k_{ij} and the ratio $6E_x I_0 / 5G_{xy} A_i L^2$ is noted k_{Ai} .

For the bending deformation, boundary conditions $v'(L) = 0$ and $v(0) = 0$ as well as the six continuity conditions $v'_l = v'_r$ and $v_l = v_r$ give the following solution of the integrating constants.

$$k_{i4} C_4 = -k_{i4} \frac{1}{2} q b L \quad (5)$$

$$k_{i3} C_3 = k_{i4} C_4 + (k_{i4} - k_{i3}) \frac{1}{2} q b^2 + k_{i4} \frac{1}{2} q b^2 \quad (6)$$

$$k_{i2} C_2 = k_{i3} C_3 + (k_{i3} - k_{i2}) \frac{1}{2} q a^2 \quad (7)$$

$$k_{i1} C_1 = k_{i2} C_2 + (k_{i2} - k_{i1}) \frac{1}{2} q a_0^2 \quad (8)$$

$$k_{I1} D_1 = 0 \quad (9)$$

$$k_{I2} D_2 = k_{I1} D_1 + (k_{I2} - k_{I1}) \frac{1}{3} Q a^3 \quad (10)$$

$$k_{I3} D_3 = k_{I2} D_2 + (k_{I3} - k_{I2}) \frac{1}{3} Q a^3 \quad (11)$$

$$k_{I4} D_4 = k_{I3} D_3 + (k_{I4} - k_{I3}) \frac{1}{3} Q b^3 + k_{I4} \frac{1}{6} Q b^3 \quad (12)$$

For the shear deformation, boundary condition $v(0) = 0$ as well as the three continuity conditions $v_l = v_r$ give the following solution of integrating constants.

$$k_{A1} F_1 = 0 \quad (13)$$

$$k_{A2} F_2 = k_{A1} F_1 - (k_{A2} - k_{A1}) Q a_0 \quad (14)$$

$$k_{A3} F_3 = k_{A2} F_2 - (k_{A3} - k_{A2}) Q a \quad (15)$$

$$k_{A4} F_4 = k_{A3} F_3 - (k_{A4} - k_{A3}) Q b + k_{A4} Q b \quad (16)$$

Related to the deflection stiffness of the uncracked beam, $E_X I_0$, the expression for the total deflection of the beam at the point load reads as equation 17.

$$- E_X I_0 v_Q = k_{I3} \frac{1}{6} Q b^3 - k_{A3} Q b L^2 + k_{I3} C_3 b + k_{I3} D_3 - k_{A3} F_3 L^2 \quad (17)$$

Energy balance

For half the beam, if the crack growth is da , an energy balance equation can be written. Fracture energy J consumed by the creation of the new surface is equal to the work done by external loading.

$$2 J t da = Q dv_Q \quad (18)$$

$$2 J t = Q \frac{dv_Q}{da} \quad (19)$$

When the deflection according to equation 17 is inserted, the energy balance equation 19 can be developed as follows.

$$2 J_{E_x} I_0 t = - Q b k_{I3} \frac{dC_3}{da} - Q k_{I3} \frac{dD_3}{da} + Q L^2 k_{A3} \frac{dF_3}{da} \quad (20)$$

$$2 J_{E_x} I_0 t = Q^2 a^2 (k_{I2} - k_{I3}) + Q^2 L^2 (k_{A2} - k_{A3}) = M_a^2 (k_{I2} - k_{I3}) + M_a^2 L^2 (k_{A2} - k_{A3}) \quad (21)$$

Extending the solution

For arbitrary beam with arbitrary point loads, the dimension L can be chosen so that the boundary conditions above are true. In the final expression (equation 21) the length L will disappear. The superposition principle will be valid, and the influence of every separate load can be taken into account as the total moment M and total shear force M' .

Similarly, continuous load can be interpreted as point loads infinitely close each other. Thus, the solution can be extended to every kind of loading and boundary conditions.

Separation of modes

The expression in equation 21 is quite general as far as the fracture modes are concerned. If the case is considered that the lower part of the beam in figure 1 is working as a part of the beam having the same deflection and curvature as the upper part, we have by definition the mode II component of the fracture energy. In this case, the constants are expressed by equations 22 to 24.

$$k_{A2} = k_{A3} = \frac{6 E_x I_0}{5 G_{xy} A_0 L^2} \quad (22)$$

$$k_{I2} = \frac{th^3}{t(h_1^3 + h_2^3)} \quad (23)$$

$$k_{I3} = \frac{I_0}{I_0} = 1 \quad (24)$$

Thus, the mode II component of the energy will read as equation 25.

$$(J_{E_x})_{II} = \frac{6}{t^2 h^3} M_a^2 \frac{3 h h_1 h_2}{(h_1^3 + h_2^3)} \quad (25)$$

For cracked beams or beams with holes supported below the cracked part, the beam theory gives only this mode II component. If, instead, a beam with a notch is considered, it is obvious that the lower part is not compelled to have the same deflection and curvature as the upper part. Thus, we have also the mode I component present. The

total energy expressed by equation 30 will be found, when the constants in equations 26 to 29 are inserted in equation 21.

$$k_{A2} = \frac{6 E_x I_0}{5 G_{xy} t h_1 L^2} \quad (26)$$

$$k_{A3} = \frac{6 E_x I_0}{5 G_{xy} t h L^2} \quad (27)$$

$$k_{I2} = \frac{t h^3}{t h_1^3} \quad (28)$$

$$k_{I3} = \frac{I_0}{I_0} = 1 \quad (29)$$

$$J_{E_x} = \frac{6}{t^2 h^3} M_a^2 \frac{h^3 - h_1^3}{h_1^3} + \frac{6}{t^2 h^3} M_a^2 L^2 \frac{E_x h^2}{10 G_{xy} L^2} \frac{h_2}{h_1} \quad (30)$$

Mode I component of the energy expressed by equation 31 will be found, when the mode II component of energy is subtracted from the total energy.

$$(J_{E_x})_I = \frac{6}{t^2 h^3} M_a^2 \frac{h^3 h_2^3}{h_1^3 (h_1^3 + h_2^3)} + \frac{6}{t^2 h^3} M_a^2 L^2 \frac{E_x h^2}{10 G_{xy} L^2} \frac{h_2}{h_1} \quad (31)$$

Calculation of stress intensities

Stress intensities are found from the corresponding fracture energy expressions, when the relationships given by Leicester (1971) are used.

$$K_I^2 = (J_{E_x})_I c_I^2 \quad (32)$$

$$K_{II}^2 = (J_{E_x})_{II} c_{II}^2 \quad (33)$$

$$c_I^4 = c_{II}^4 E_y / E_x \quad (34)$$

$$c_{II}^4 = \frac{4}{\frac{E_x}{G_{xy}} - 2 \nu_{xy} + 2 \left[\frac{E_x}{E_y} \right]^{1/2}} \quad (35)$$

The elasticity values for spruce for the common crack plane of Finnish softwoods are $E_x = 11\,000 \text{ kNm}^{-2}$, $E_y = 390 \dots 650 \text{ kNm}^{-2}$, $G_{xy} = 650 \dots 710 \text{ kNm}^{-2}$, and $\nu_{xy} = 0.26 \dots 0.20$. This gives the values of the orthotropicity constants $c_I = 0.305 \dots 0.317$ and

$c_{II} = 0.620 \dots 0.645$. The coefficients c_I and c_{II} are constant for a given material and crack plane and do not depend on the load configuration. Suitable approximations are $c_I = 1/3$ and $c_{II} = 2/3$.

Thus, the expressions for stress intensities will read as equations 36 and 37.

$$K_I = \frac{M_a}{3th} \left[\frac{6 h^2 h_2^3}{h_1^3(h_1^3+h_2^3)} + \frac{M_a^2}{M_a^2} \frac{3 E_x}{5 G_{xy}} \frac{h h_2}{h_1} \right]^{1/2} \quad (36)$$

$$K_{II} = \frac{2 M_a}{th} \left[\frac{2 h_1 h_2}{(h_1^3+h_2^3)} \right]^{1/2} \quad (37)$$

Fracture criterion and critical values

In the literature, several proposals for the fracture criterion have been made. Mall et al. (1983) found the criterion proposed by Wu (1967, equation 38) to be the best one.

$$\frac{K_I}{K_{IC}} + \left[\frac{K_{II}}{K_{IIC}} \right]^2 = 1 \quad (38)$$

The critical stress intensity values are usually called fracture toughness values. The mean values of the fracture toughness values for Finnish softwoods are given in table I. These values are based on the previous reports (Fonselius 1986, Fonselius and Riipola 1989, Wright 1986), and they are short term mean values in constant moisture conditions. Long term loading in constant moisture conditions has less effect than predicted by the Madison curve, but cyclic moisture variations combined with the long term loading will weaken the specimens.

For other species, values are frequently found in the literature. For Douglas fir, the mean values for mode I are collected by Wright and Leppävuori (1984). For mode II, values 1400...1600 $\text{kNm}^{-3/2}$ are given by Murphy (1988).

Table I. The fracture toughness values for pine, spruce, and Douglas fir. The values are given in $\text{kNm}^{-3/2}$. For mode I, the effect of orientation is given as fracture system RL and TL values. A fracture system is defined so, that the first letter gives the normal of the fracture plane and the second letter gives the direction of the crack growth.

Mode and system	Pine	Spruce	Douglas fir
Mode I TL	240	200	300
Mode I RL	280	250	400
Mode II RL-TL	1900	1500	1500

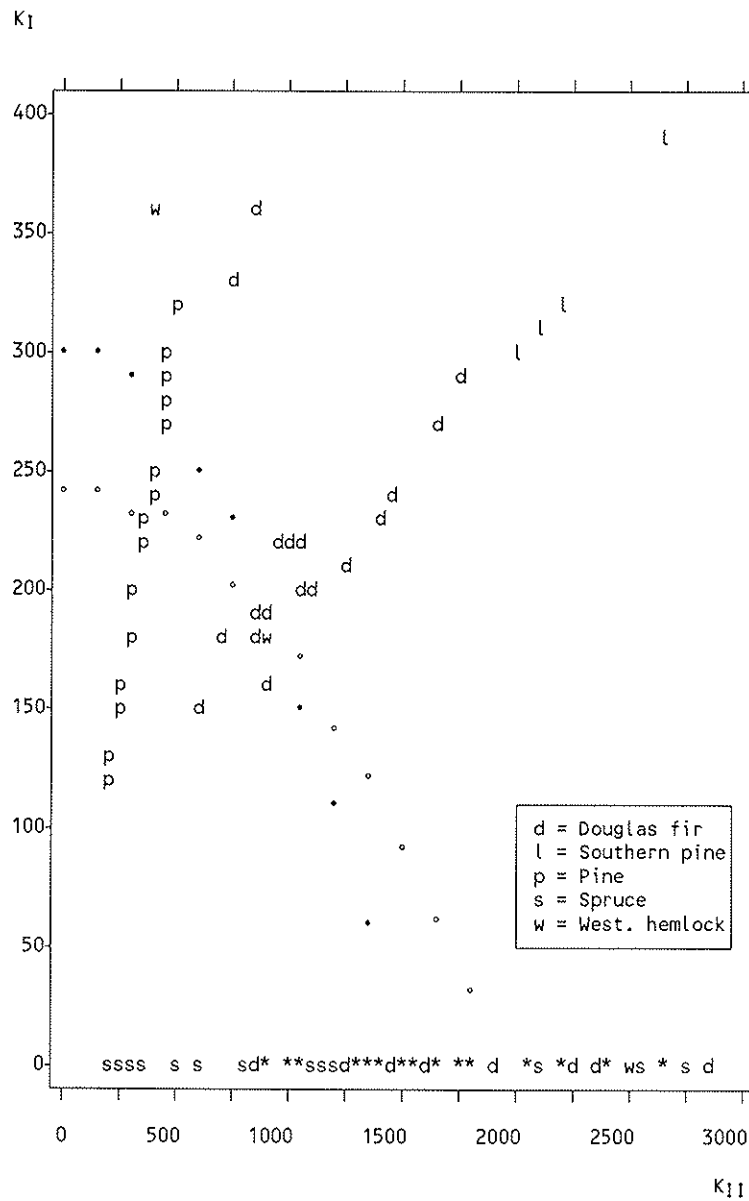


Figure 2. Fracture toughness values in $\text{kNm}^{-3/2}$ of several experiments found in the literature. Wu's fracture criterion for pine is marked with \circ and for Douglas fir with \bullet (fracture system TL). Several species are marked with $*$.

Evaluation of the method

In order to evaluate the outlined method, it was applied to experiments reported in the literature. Beams with holes are studied by Penttala (1980) and by Johannesson (1983). Notched beams have been studied by Gustafsson and Enquist (1988), Lum and Foschi (1988), and Murphy (1979b, 1986). Beams with cracks across the grain at the beam edge have been studied by Schniewind and Centeno (1973). Beams with a crack along the grain at the support have been studied by Murphy (1979a, 1988), Barrett and Foschi (1977), and Smith and Penney (1980). From the given data the support reaction

corresponding to the beginning of crack growth has been found out needed in stress intensity calculations. It is supposed, that E_x/G_{xy} is equal to 15.

In figure 2, the calculated stress intensity components, mode I and mode II, are shown together with the fracture criteria for pine and Douglas fir. The scatter of the results is large, and the material is not equally distributed along the fracture criteria. The values of the large and medium size notched pine specimens by Gustafsson and Enquist (1988) and the major part of Douglas fir experiments fit with the critical values. Especially Douglas fir and southern pine specimens by Smith and Penney (1980) show clearly larger values than the proposed method. Their load value is, however, not the one corresponding to the beginning of the crack growth but the ultimate load.

The most important reason for scatter is the orientation of the specimens. In figure 2, the fracture criteria are given for fracture system TL. For the system RL, higher mode I values are found, because of the reinforcing effect of the rays. For mode II, the orientation has a minor effect. Actually, the values by Smith and Penney are RL-values. Also, density has a pronounced effect on the measured fracture toughness values.

For the pure mode II experiments the scatter is large. Results for Johannesson's specimens marked with s and having fracture toughness values below 1 000 kNm^{-3/2} are partly explained by the reported weakness of the material. Another reason for apparently low fracture toughness values is, that for very large holes, the beam is no longer acting like a beam but a frame, and an opening mode I component is present in the crack corner. This component is, however, not found by the simple beam theory. On the opposite, the exceptionally large apparent values are found, because a closing mode I component is hampering the crack growth. This phenomenon is also observed by Johannesson. He reports that for some specimens, crack growth was arrested for a longer time before the final fracture. In figure 2, 20 cases of total 148 cases had stress intensity values larger than 3000 kNm^{-3/2} and are thus not included.

Conclusions

A fracture mechanics based method for dimensioning of beams with cracks, notches, and holes is proposed to be included in the CIB code. According to the proposal, capacity of a beam with a true or a supposed crack can be estimated as follows:

- Consider the support conditions of the beam. If the lower part can freely be separated from the upper part, a mixed mode case is present. Else, if the parts cannot be separated, (almost) pure mode II is present.
- Calculate the stress intensities according to the following equations:

$$K_I = \frac{M_a}{3th} \left[\frac{6 h^2 h_2^3}{h_1^3(h_1^3+h_2^3)} + \frac{M_a^2}{M_a^2} \frac{3 E_x}{5 G_{xy}} \frac{h h_2}{h_1} \right]^{1/2} \quad (36)$$

$$K_{II} = \frac{2 M_a}{th} \left[\frac{2 h_1 h_2}{(h_1^3+h_2^3)} \right]^{1/2} \quad (37)$$

- Find out the fracture toughness values for the present modes and fracture systems. In the case of dimensioning, mode I system TL should be assumed, because it is weaker than mode I system RL.
- Use a suitable fracture criterion, as Wu's:

$$\frac{K_I}{K_{IC}} + \left[\frac{K_{II}}{K_{IIC}} \right]^2 = 1 \quad (38)$$

- Solve the equation to get the critical load.

Literature

- Barrett, J.D., Foschi, R.O., 1977.
Mode II stress-intensity factors for cracked wood beams. Eng. Fract. Mech. 9:371-378.
- Barrett, J.D., Foschi, R.O., 1978 b.
Duration of load and probability of failure in wood. Part II. Constant, ramp, and cyclic loadings. Can. J. Civ. Eng. 5:515-532.
- Fonselius, M., 1986.
Brottmekanisk studie på gran och skikträ. [Fracture mechanics of spruce and PLV.] Teknillinen korkeakoulu, Rakennusinsinööriosasto, Rakennetekniikan laitos, Julkaisu 80. 55 p. + app. 13 p.
- Fonselius, M., Riipola, K., 1989
Fastställandet av modus II brottseghet K_{IIC} för trämaterial. [Determination of mode II fracture toughness K_{IIC} for wood.] VTT forskningsrapporter 597. Espoo. 87 p. + app. 23 p.
- Gustafsson, P.J., 1988
A study of strength of notched beams. CIB-W18A/21-10-1, Meeting twenty-one, Parksville, Vancouver Island, Canada, September 1988.
- Gustafsson, P.J., Enquist, B., 1988.
Träbalks hållfasthet vid rätvinklig urtagning. Tekniska högskolan i Lund, avdelningen för byggnadsmekanik. Report TVSM-7042, Lund 111 p. + app. 19 p.
- Johannesson, B., 1983.
Design problems for glulam beams with holes. Chalmers University of Technology, Division of Steel and Timber Structures. Doktorsavhandlingar vid Chalmers Tekniska Högskola, Ny serie Nr 458. Göteborg. 73 p.
- Leicester, R.H., 1971.
Some aspects of stress fields at sharp notches in orthotropic materials. I. Plane stress. CSIRO Aust. Div. For. Prod. Technol. Pap. No. 57, Melbourne, 16 p.
- Lum, C., Foschi, R.O., 1988.
Arbitrary V-notches in orthotropic plates. ASCE J. Eng. Mech. 114(4):638-655.
- Mall, S., Murphy, J.F., Schottafer, J.E., 1983.
Criterion for the mixed mode fracture in wood. ASCE J. Eng. Mech. Div. 109(3):680-690.

- Murphy, J.F., 1979 a.
Strength of wood beams with end splits. U.S. For. Serv. Res. Pap. FPL347 U.S. For. Prod. Lab., Madison.
- Murphy, J.F., 1979 b.
Using fracture mechanics to predict failure in notched wood beams. Proc. 1st Int. Conf. Wood Fract. Banff, Alberta, Canada. Aug. 1978, pp. 159-173.
- Murphy, J.F., 1986.
Strength and stiffness reduction of large notched beams. J. Struct. Eng. 112(9):1989-2000.
- Murphy, J.F., 1988.
Mode II wood test specimen: beam with central slit. Journal of Testing and Evaluation, 16(4):364-368.
- Penttala, V., 1980.
Reiällinen liimapuupalkki. [Glulam beam with hole.] Helsinki University of Technology, Division of Structural Engineering, publication 33. Espoo. 101 p.
- Pook, L.P., 1979.
Approximate stress intensity factors obtained from simple plate bending theory. Eng. Fract. Mech. 12:505-522.
- Schniewind, A.P., Centeno, J.C., 1973.
Fracture toughness and duration of load factor I. Six principal systems of crack propagation and the duration factor for cracks propagating parallel to grain. Wood & Fiber 5(2):152-159.
- Smith, F.W., Penney, D.T., 1980.
Fracture mechanics analysis of butt joints in laminated wood beams. Wood Sci. 12(4):227-235.
- Williams, J.G., 1988.
On the calculation of energy release rates for cracked laminates. Int. J. Fract. 36:101-119.
- Wright, K., 1986.
Männyn ja kuusen murtumissitkeyden määrittäminen CT-koekappaleilla. [Fracture toughness of pine and spruce determined with the CT-specimens.] VTT tutkimuksia 387. Espoo. 78 s. + liitt. 19 s.
- Wright, K., Leppävuori, E.K.M., 1984.
Murtumismekaniikan soveltaminen puuhun. [Application of fracture mechanics to timber.] VTT tiedotteita 373. Espoo. 101 p.
- Wu, E.M., 1967.
Application of fracture mechanics to anisotropic plates. J. Appl. Mech. Trans. ASME E 34(4):967-974.

Notations

A_i	Area of the beam cross section
C_i	Integrating constant
D_i	Integrating constant
E_x	Modulus of elasticity in the longitudinal direction of the grain
E_y	Modulus of elasticity across the grain
F_i	Integrating constant
G_{xy}	Shear modulus
I_i	Moment of inertia of the beam cross section
J	Fracture energy
K_I, K_{II}	Stress intensity, mode I and mode II
L	Characteristic length of the beam
M	Bending moment of the beam
M'	Shear force of the beam
Q	Point load
a	Crack length
a_0	Location of the crack indentation
b	Location of the point load
c_I, c_{II}	Orthotropicity coefficient for stress intensity, mode I and mode II
h	Beam depth
h_1, h_2	Depth of the upper and lower part of the cracked beam
k_{Ai}	Proportionality coefficient between the moment of inertia of the uncracked beam cross section and the area of the i :th cross section modified with the elasticity constants
k_{Ii}	Proportionality coefficient between the moment of inertia of the uncracked beam cross section and the i :th cross section
t	Thickness of beam
v	Deflection of the beam
v'	Slope of the beam
ν	Poisson's constant

**INTERNATIONAL COUNCIL FOR BUILDING RESEARCH STUDIES AND DOCUMENTATION
WORKING COMMISSION W18A - TIMBER STRUCTURES**

**SIZE FACTORS FOR THE BENDING AND TENSION STRENGTH
OF STRUCTURAL TIMBER**

by

J D Barret
University of British Columbia
Canada
A R Fewell
Building Research Establishment
United Kingdom

MEETING TWENTY - THREE

LISBON

PORTUGAL

SEPTEMBER 1990

SIZE FACTORS FOR THE BENDING AND TENSION STRENGTH OF STRUCTURAL TIMBER

By J.D. Barrett and A.R. Fewell

INTRODUCTION

For many years it has been recognized that the bending strength, and more recently tension strength, of timber are affected by the size of the specimen. While this effect may in reality be associated with the stressed volume, grade, and the size and age of the tree from which it was cut, it is generally described as a depth effect (for bending) or a width effect (for tension).

This paper examines the available test data to determine the effect of length and depth or width on bending and tension strength and provides depth and width factors applicable to Eurocode 5¹ and the supporting CEN standards.

RELEVANT HISTORY

Depth effect was first investigated by Newlin and Trayer in 1924². In 1954 Freas and Selbo³ published the results of tests on beams with depths up to 406mm (16in) and derived an equation that defined a depth effect ratio indexed to 1.0 at 50mm depth. This equation was included in North American design methods and was subsequently adopted in the UK Code of Practice for the structural use of timber, CP112:1967⁴. For design purposes the equation was indexed to 1.0 at 300mm depth. Indexing this equation to 1.0 at the European standard depth of 200mm gives;-

$$k_d = 0.73 (h^2 + 92300)/(h^2 + 56800).....(1)$$

where k_d is the factor by which a bending stress specified for a depth of 200mm should be multiplied to obtain the stress value for a depth of h mm.

A theoretical study by Bohannan⁵ in 1966 using the Weibull 'weakest link' theory produced an equation applicable to clear wood bending strength which became commonly used in North America of;-

$$k_d = (200/h)^{0.11}(2)$$

The results of an extensive investigation made in Canada in 1977/8 were analyzed by Bury⁶, who produced a set of equations for the effect of depth on the characteristic, i.e., lower fifth percentile, values of bending stress for timber in standard joist sizes and visually stress graded to the NLGA rules⁷. When the equations for all stress grades are combined and indexed to 1.0 at 200mm depth, the resulting equation becomes;-

$$k_d = (200/h)^{0.403}(3)$$

A study by Fewell and Curry⁸ in 1983 considered the Canadian data and UK data and derived an equation;-

$$k_d = (200/h)^{0.39} \text{ which was rounded to;} \\ k_d = (200/h)^{0.4}(4)$$

A similar factor for the effect of width on tension strength was also reported by Fewell⁹ in a committee paper, from very limited data, to be;-

$$k_w = (200/h)^{0.192} \dots\dots\dots(5)$$

For the UK Code of Practice, BS5268:Part 2¹⁰ published in 1984, design stresses indexed to 300mm were derived from test data of various sizes by adjusting with equations 4 and 5 (but indexed to 300mm) for bending strength and tension strength respectively. BS5268 permits the design stresses to be adjusted for member size using the factors $k_d = k_w = (300/h)^{0.11}$ for members with depth or width between 72mm and 300mm. Below 72mm $k_d = k_w = 1.17$ and above 300mm $k_w = (300/h)^{0.11}$ and k_d is found from equation (1) indexed to 300mm. The fact that the lower fifth percentile value for test data for say 100mm timber would be adjusted using $k_d = (300/h)^{0.4}$ to obtain a tabulated design stress at 300mm which, if a design stress for 100mm was then required in practice, would be only adjusted by $k_d = (300/h)^{0.11}$, introduces an extra degree of safety. At the time this was justified on the basis that a) there was a lot of scatter in the data, b) the equation $k = (300/h)^{0.11}$ agreed with Bohannan's theoretical exercise, and c) having the same equation for bending and tension simplified the design procedure.

In Annex A of the Eurocode 5 draft, bending and tension stresses are listed for 200mm depth or width and are adjusted for other sizes using the factor;-

$$k_d = k_w = (200/h)^{0.2} \dots\dots\dots(6)$$

This equation was used because of the uncertainties due to insufficient data and the desire to achieve simplicity by having $k_d = k_w$. The subsequent CEN or prEN standards on strength classes¹¹ and the determination of characteristic values¹² have followed the lead given by Eurocode 5, i.e., test data of various sizes are adjusted to 200mm using equation (6) to determine characteristic values, and this same equation is used to adjust the characteristic values to the size required in design.

Size effects apparent in a more recent Canadian full-size lumber data set were reported by Barrett and Griffin¹³. The study yielded size adjustment factors for bending, tension and compression parallel to grain properties. The size factor (k_d) for bending for three species was found to be

$$k_d = (200/h)^{0.46} \dots\dots\dots(7)$$

which agrees closely with earlier results^{6,8} and recent results published in the U.S.¹⁴.

Barrett and Griffin¹³ examined the relationships between the length and depth factors and size factors appropriate for applications where the test procedures require constant ratios of member width to length. The depth effect for bending members of constant length was found to be represented by the expression

$$k_d = (200/h)^{0.24} \dots\dots\dots(8)$$

The significant differences in the depth or width adjustments for members of constant length (Eqn. 8) and members with a constant depth to length ratio (Eqn. 7) demonstrates the importance of developing size adjustment expressions which are capable of accommodating differences in member width and length. Clearly the size adjustment procedures to be provided in codes and standards must be chosen to be consistent with standard test procedures and the procedures specified for development of characteristic values.

DISCUSSION

The equations for size adjustments in bending given above, with the exception of Eqn. 8, all assume a constant relation between timber size and test gauge length because firstly the standard test procedures require test lengths to be a constant factor times the member width or depth (ISO 8375^{15,20}) and secondly there is a tendency in use for wider members to be used on longer spans. This allows structural codes to adopt a simplified approach wherein size adjustments for characteristic values can be represented as width or depth effects.

To determine a characteristic bending or tension stress to meet the prEN¹², lower fifth percentile values for a number of samples of different size specimens, are adjusted to 200mm using Eqn. 6. The mean of these values then becomes the characteristic value. If the factors given by Eqn. 6 are incorrect then the sample lower fifth percentile values, after adjustment for size, will have a far greater range and the characteristic value will be incorrect. This can cause problems with the procedures for the verification of strength properties given in the prEN¹². It can also result in unsafe design values even though the same factors would be used to carry out the design.

Consider Figure 1a which shows the lower fifth percentiles for three samples, indicated thus 'x'. If we assume that the correct depth factor is say $k_d = (200/h)^{0.4}$ and the three sample values fit this equation exactly, then when they are adjusted to 200mm all would have the same value 'o'. Their mean, and therefore the characteristic stress would also have that same value. If the above equation was also used for design then the characteristic value would be adjusted back to the correct design stress for any of the sizes. In Figure 1b it is assumed that the correct equation is $k_d = (200/h)^{0.4}$ but that $k_d = (200/h)^{0.2}$ is used to determine the characteristic value and for design. After adjustment to 200mm the same three lower fifth percentiles, indicated 'x', take up the value shown thus '•', and the mean and therefore characteristic value is then adjusted in design for the four sizes shown, the design values are those indicated by 'o'. For this example, as indicated in Figure 1b, it can be calculated that at 200mm the design value is 8% too high, at 175mm it is 5% too high, at 150mm it is 2% too high and at 100mm it is 6% too low. The high values reduce safety.

Some work in Canada and recent unpublished work in the United States has indicated that a thickness change from 38mm to 89mm causes an increase in strength of approximately 10 percent. It was decided to leave thickness effects out of this analysis because the database was considered insufficient to analyze thickness effects and because the adjustment is small compared to the degree of complication that would be added in structural design procedures.

ANALYSIS

The equations governing size effects are assumed to be of the form $k = (A/B)^S$, where k is a factor applied to adjust a characteristic value at the standard size A, and B is the size of the member for which k is required. S is the index coefficient determining the magnitude of the size effect adjustment. In general, S has two subscripts, the first R, W, or L and the second m or t.

R denotes that the equation applies to the situation where there is a common ratio between member width or depth and test length. W denotes that the size effect is entirely due to member width changes and L denotes the size effect corresponds to length changes only. The bending and tension properties are denoted by the second subscripts m and t respectively.

For example, $k = (200/h)^{S_{Rm}}$ is an equation for adjusting bending properties when a constant ratio of member depth to length is assumed.

The expression $k = (A/B)^{S_{Lt}}$ is used for adjusting tension strength data for length when member width is constant,

and $k = (200/h)^{S_{Wt}}$ is the equation for adjusting tension data for member width when length remains constant.

When a sample strength value is adjusted to the standard size it is divided by k , and when the strength value for a non-standard size is required the value for the standard size is multiplied by k .

Length Effects

Bending

Test data are available from Madsen¹⁶ who tested 38x89 and 38x184mm S-P-F in both Standard and better and No. 2 and better grade combinations, and Madsen and Neilson¹⁷ who reported results for 38x89, 38x140, 38x184 and 38x235mm Hem-Fir No.2 and better grade combinations. All tests were conducted using one-third point loading. Data for the 5th and 50th percentiles was included in the analysis and are shown in Table 1.

Treating each data set separately an analysis of covariance was used to determine values of S_{Lm} for each data set and all data combined. There were no significant differences in the size parameters at the 95 percent level of significance between data sets, and the common size parameter was $S_{Lm} = 0.17$.

Tension

Test data are available from Lam and Varoglu¹⁸ who tested 38x89mm S-P-F in both Select structural and No. 2 NLGA grades; Showalter, Woeste and Bendtsen¹⁹ who tested 38x89 and 38x235mm in the 2250f MSR grade and the No. 2 visual grades of Southern Pine, and from Madsen¹⁶ who tested 38x89 and 38x184mm S-P-F in the Standard and better and No. 2 and better grade combinations.

As for bending strength the 5th and 50th percentile data were analyzed in combination with the mean strengths available from reference 18, and the data are shown in Table 2.

Treating each data set separately, an analysis of covariance was conducted as for bending to determine the value of the length size effect parameter S_{Lt} . Although the statistical analysis leads to a rejection of the hypothesis of a common slope (significance level 95 %) for the tension data alone, when all bending and tension length effect data are combined the statistical test showed no significant differences in the size parameters at the 95% level of significance. The length effect for both tension and bending can therefore be concluded to be the same value, i.e., $S_{Lt} = S_{Lm} = 0.17$ and the relevant size adjustment equations become;-

$$k_{Lt} = (1800/L)^{0.17} \dots\dots\dots(9)$$

$$k_{Lm} = (3600/L)^{0.17} \dots\dots\dots(10)$$

for adjusting tension and bending strength respectively for length when cross section size remains constant.

The reference lengths of 1800mm and 3600mm were chosen to be consistent with the CEN standard width of 200mm, and the 9 to 1 length to width ratio for tension tests and the 18 to 1 span to depth ratio for the bending tests given in ISO 8375 and the CEN test standard.

Figure 2 shows the tension data with Eqn. 9 and Figure 3 shows the bending data with Eqn. 10.

The data points in Figures 2 and 3 are plotted using the following procedure. Having determined Eqns. 9 and 10 from the analysis of covariance, the equations are used to adjust the strength values for each data set to the standard length. A sample size weighted mean of these values for each data set is then divided into each unadjusted strength value in the data set to obtain values of k which are plotted against the length (or width or depth for other equations) associated with each strength value. The use of sample size weighting and means of the lower fifth percentile values in this procedure follows that used by the CEN prEN¹² for determining characteristic values.

Depth Effects

A considerable amount of data on bending strength from tests carried out at the Building Research Establishment in the UK is available and is listed in Table 3. In addition to this is some new data from a UK/Canadian project sponsored by COFI which is listed in Table 4. All of the data in Tables 3 and 4 was obtained from tests conducted according to the ISO and CEN test standards except for the 35x35, 35x47, 35x60 and 45x45mm samples in data sets 1 and 2 in Table 3 which used different spans. However these results were corrected to the standard spans using the configuration factor in the CEN standard for determining characteristic values. It should be noted that the tables contain results for a mixture of species and grades.

Data from the Canadian Wood Council full-size lumber test program are given in Table 5. The test method used a higher rate of loading and a span to depth ratio of 17:1.

The analytical procedure was the same used to determine the length effect. An analysis of covariance was carried out on the data in Tables 3 and 4 which concluded that there was no significant difference at the 95% level and the value of S_{Rm} is equal to 0.4.

Figure 4 shows the data plotted using the procedure described for Figures 2 and 3 with the equation

$$k_{Rm} = (200/h)^{0.4} \dots\dots\dots(11)$$

Exactly the same procedure was used for the data in Table 5 and again the data sets were shown to have no significant differences in the size parameters. For this data the value of S_{Rm} is equal to 0.45 giving

$$k_{Rm} = (200/h)^{0.45}$$

This equation is plotted with the k_{Rm} results in Figure 5.

When the data in Tables 3, 4 and 5 were combined the statistical test again showed no significant difference and the best overall common value $k_{Rm} = 0.4$ was obtained and so the equation for k_{Rm} is as given in Eqn. 11. Figure 6 shows this equation with the plotted data.

The size index for depth effects in bending members of constant length S_{Wm} is related to S_{Rm} and S_{Lm} according to $S_{Wm} = S_{Rm} - S_{Lm}^{13}$. Thus the effect of width for bending members when length is constant is

$$k_{Wm} = (200/h)^{0.23} \dots\dots\dots(12)$$

Width Effects

The UK data on tension strength is shown in Table 6 and comprises lower fifth percentile values for various combinations of species and grades. Table 7 lists data from the Canadian Wood Council. Each data set in both tables has one test length so that the value of $S = S_{Wt}$ can be derived independent of member length.

The 38x89mm data in Table 7 was tested at 2640mm and adjusted to 3680mm to conform with the other data, by using the factor $k = (2640/3680)^{0.17}$.

The data in Tables 6 and 7 were analyzed as before and results in values for S_{Wt} of 0.12 and 0.23, respectively. The hypothesis that the width effect is the same for each data set was rejected for the data in Table 6 and a plot of the data in Figure 7 indicates that the data for the smallest size is inconsistent with the trends for the remainder of the data. With very small sizes, tension strength becomes very variable and has the effect of reducing the sample lower fifth percentile value. The analysis was repeated with the 35x35mm samples omitted and this time it showed no significant difference and gave a value for S_{Wt} equal to 0.24. This data is shown in Figure 8. When the analysis was repeated using both Table 6 data (with the 35x35mm omitted) and Table 7 data, no significant difference was found and the value of S_{Wt} was equal to 0.23 as shown in Figure 9. Therefore

$$k_{Wt} = (200/h)^{0.23} \dots\dots\dots(13)$$

This analysis indicates that a minimum size should be included in the Eurocode 5 and the CEN standards.

The width factor for tension strength required for the standards is k_{Rt} . The value of $S_{Rt} = S_{Wt} + S_{Lt}$. Therefore $S_{Rt} = 0.23 + 0.17 = 0.40$ and the adjustment equation for tension strength is given by

$$k_{Wt} = (200/h)^{0.40} \dots\dots\dots(14)$$

It should be noted that by comparing S_{Rt} with S_{Rm} , S_{Lt} with S_{Lm} and S_{Wt} with S_{Wm} that:-

- The width effect on tension strength is the same as the depth effect on bending strength when member length is a constant factor times the member width or depth. i.e., $k = (200/h)^{0.4}$.
- The width effect on tension strength is the same as the depth effect on bending strength when the member length is constant. i.e., $k = (200/h)^{0.23}$.

- The length effect on tension strength is the same as for bending strength when the width or depth are constant. i.e., $k_W = (1800/L)^{0.17}$ and $k_d = (3600/L)^{0.17}$.

The fact that the results show the same values of S for the length effect in bending and tension and the same value of S for the width effect in bending and tension is consistent with the weakest link concept for brittle materials.

CONCLUSIONS AND RECOMMENDATIONS

From an analysis of test data comprising many different grades and species, the following conclusions were reached;-

1. The factor (k) for adjusting characteristic values in codes and standards for both the depth effect on bending strength and the width effect on tension strength, when each property is based on a constant span to depth ratio, is given by

$$k = (200/h)^{0.4}$$

where h is the depth or width of the member for which the strength value is required.

2. In using the factor given above a minimum size of around 35mm x 47mm needs to be specified for tension members.
3. The factor (k_W) for adjusting tension or bending stresses to other depths or widths, when the length remains constant, is given by;-

$$k_W = (A / B)^{0.23}$$

where A is the width or depth relevant to the stress value to be adjusted and B is the width or depth relevant to the required stress value.

4. The factor (k_L) for adjusting bending and tension stresses to other member lengths when the width remains constant, is given by;-

$$k_L = (A / B)^{0.17}$$

where A is the length relevant to the stress value to be adjusted and B is the length relevant to the required stress value.

REFERENCES

1. EUR 9887. 1988. EN Eurocode No. 5. Common unified rules for timber structures. EEC.
2. Newlin, J.A. and G.W. Trayer. 1924. Form factor of beams subjected to transverse loading only. NACA Report No. 181.
3. Freas, A.D. and M.L. Selbo. 1954. Fabrication and design of glued laminated wood structural members. U. S. Dept. of Agriculture. Technical Bulletin No. 1069.

4. CP 112:Part 2:1967. The structural use of timber. BSI.
5. Bohannon, W. 1966. Effect of size on bending strength of wood beams. US Forest Products Laboratory. Bulletin No. 56.
6. Bury, K.V. 1981. Statistical analysis of NLGA bending tests, University of British Columbia.
7. NLGA Standard Grading Rules for Canadian Lumber. 1987. National Lumber Grades Authority, Vancouver, Canada.
8. Fewell, A.R. and W.J. Curry. 1983. Depth factor adjustments in the determination of characteristic bending stresses for visually graded timber. Structural Engineer, Vol. 61B, No. 2.
9. Fewell, A.R. 1982. Size factors for bending and tension stresses. BSI Committee paper CSB32/2 - 82/27. Princess Risborough Laboratory.
10. BS 5268:Part 2:1988. Structural use of timber. Part 2. Code of practise for permissible stress design, materials and workmanship. BSI.
11. prEN XXXX 1990. Structural timber. Strength Classes CEN.TC124.203.
12. prEN XXXX 1990. Structural timber. Determination of characteristic values for mechanical properties and density. CEN.EN.TC.124.202.
13. Barrett, J.D. and H. Griffin. 1989. Size effects for Canadian 2-inch (38mm) dimension lumber. Proceedings CIB-W18A / 22-6-1, Berlin.
14. Johnson, L.A., J.W. Evans and D.W. Green. 1989. Volume effect adjustments for the in-grade data. In-grade Testing of Structural Lumber. Forest Products Research Society. Madison. Wisc.
15. ISO 8375. 1985. Timber structures. Solid timber in structural sizes. Determination of some physical and mechanical properties. ISO.
16. Madsen, B. 1990. Length effects in 38mm spruce-pine-fir dimension lumber. Can. Journal of Civil Engineering. Vol. 17 No. 2 pp 226-237.
17. Madsen, B. and P.C. Neilson. 1976. In-grade testing - size investigation on lumber subjected to bending. Structural Research Series Report No. 15. Dept of Civil Engineering. Vancouver.
18. Lam, F. and E. Varoglu. 1990. Effect of length on the tensile strength of lumber. Forest Products Journal Vol. 40, No. 5. pp 37-42.
19. Showalter, K.L., F.E. Woeste and B.A. Bendtsen. 1987. Effect of length on the tensile strength of lumber. Research Paper FPL-RP-482 USDA Forest Service., Forest Products Laboratory, Madison. 9pp.
20. prEN XXXX. 1990. Structural timber. Test methods for determination of certain physical and mechanical properties . CEN.EN.TC124/WG1.

Table 1. Length Effect on Bending Strength

	Data Set	b (mm)	h (mm)	L (mm)	N	MOR 0.05 (MPa)	MOR 0.5 (MPa)
Madsen 90	1	38	89	1113	100	24.48	52.21
S-P-F	1	38	89	2250	80	28.09	48.39
Std + btr							
Madsen 90	2	38	89	780	135	31.80	58.21
S-P-F	2	38	89	1113	134	23.32	49.94
Std + btr	2	38	89	2250	134	24.09	44.02
Madsen 90	3	38	184	1371	150	22.96	37.42
S-P-F	3	38	184	2250	150	23.75	35.37
No. 2 + btr	3	38	184	4776	150	18.62	30.81
Madsen 76	4	38	89	1067	100	22.06	51.02
H-F	4	38	89	1626	100	17.24	39.99
No. 2 + btr	4	38	89	2286	97	16.89	38.95
	4	38	89	3429	100	15.86	41.02
Madsen 76	5	38	140	1626	100	19.99	45.50
H-F	5	38	140	2642	100	22.06	51.02
No. 2 + btr	5	38	140	3505	101	18.27	40.68
	5	38	140	5385	100	16.55	38.61
Madsen 76	6	38	184	2210	99	18.27	45.85
H-F	6	38	184	3480	100	19.65	46.54
No. 2 + btr	6	38	184	4724	100	13.79	36.54
	6	38	184	5944	99	16.55	38.26
Madsen 76	7	38	235	2819	100	14.13	38.95
H-F	7	38	235	4420	103	17.58	39.30
No. 2 + btr	7	38	235	5944	100	14.82	35.16

H-F: Canadian hem fir

S-P-F: Canadian spruce pine fir

Std + btr: Standard and better grades

No. 2 + btr: NLGA No. 2 + better grades

Table 2. Length Effect on Tensile Strength

	Data Set	b (mm)	h (mm)	L (mm)	N	MORt 0.05 (MPa)	MORt 0.5 (MPa)
Lam 90	1	38	89	2642	132	22.53	34.73
S-P-F	1	38	89	3683	133	21.35	32.86
SEL	1	38	89	4877	134	20.09	32.75
Lam 90	2	38	89	2642	122	10.03	22.87
S-P-F	2	38	89	3683	122	9.328	22.45
No. 2	2	38	89	4877	124	9.383	21.55
Madsen 90	3	38	89	670	120	19.76	33.87
S-P-F	3	38	89	1530	119	16.05	31.96
Std + btr	3	38	89	3970	116	12.82	27.49
Madsen 90	4	38	89	457	134	19.33	38.62
S-P-F	4	38	89	670	134	19.24	35.49
No. 2 + btr	4	38	89	1530	134	12.86	29.89
Madsen 90	5	38	184	747	150	17.01	28.66
S-P-F	5	38	184	1530	150	16.16	27.44
No. 2 + btr	5	38	184	3970	150	12.36	25.44
Showalter 87	6	38	89	762	100	-	65.05
S.Pine	6	38	89	2286	98	-	55.89
2250f-1.9E	6	38	89	3048	100	-	55.84
Showalter 87	7	38	235	762	100	-	63.91
S.Pine	7	38	235	2286	98	-	56.11
2250f-1.9E	7	38	235	3048	99	-	54.98
Showalter 87	8	38	89	762	98	-	39.63
S.Pine	8	38	89	2286	98	-	33.56
No. 2	8	38	89	3048	98	-	33.19
Showalter 87	9	38	235	762	104	-	35.78
S.Pine	9	38	235	2286	104	-	27.89
No. 2	9	38	235	3048	101	-	25.44

S-P-F: Canadian spruce pine fir
 S. Pine: U.S.A. southern pine

SEL: NLGA Select Structural grade
 No. 2: NLGA No. 2 Grade
 No. 2 + btr: NLGA No. 2 and better grades
 Std + btr: NLGA Standard and better grades
 2250f-1.9E: NLGA Machine Stress Rated grade

Table 3. Depth Effect on Bending Strength: U.K. Data

	Data Set	b (mm)	h (mm)	N	MOR 0.05 (MPa)
R/W S8	1	38	150	450	24.00
	1	50	150	425	27.70
	1	50	200	459	24.40
	1	58	170	85	22.80
	1	70	195	91	22.80
	1	38	100	214	26.50
	1	38	150	202	22.50
	1	50	200	202	22.70
	1	35	35	124	38.50
	1	35	47	153	39.90
	1	35	60	156	38.60
R/W S6	1	45	45	102	39.20
	2	35	35	115	34.40
	2	35	47	103	30.40
	2	35	60	105	23.90
H-F S8	2	45	45	34	31.80
	3	74	150	83	20.70
	3	74	248	85	23.00
	3	44	100	150	25.20
	3	44	150	112	27.40
H-F SEL	3	44	200	110	21.60
	4	44	100	59	33.50
	4	44	150	57	29.10
H-F No. 2	4	44	200	44	25.20
	5	44	100	79	23.50
	5	44	150	45	23.50
S-P-F S8	5	44	200	39	16.40
	6	38	89	215	30.40
	6	38	184	264	21.10
S-P-F SEL	7	38	89	273	24.60
	7	38	184	225	19.80
S-P-F No. 2	8	38	89	74	24.50
	8	38	184	41	22.70
B.G D-F S8	9	38	100	95	20.60
	9	47	200	140	18.20
B.G Sitka S8	10	47	228	43	16.50
	10	72	250	68	15.70
	10	73	154	57	16.00

R/W: European redwood/whitewood
 B.G. D-F: British Douglas fir
 B.G. Sitka: British Sitka spruce
 H-F: Canadian hem fir
 S-P-F: Canadian spruce pine fir

S8: ECE S8 grade (same as SS grade in BS4978)
 S6: ECE S6 grade (same as GS grade in BS4978)
 SEL: NLGA Select Structural grade
 No. 2: NLGA No. 2 grade

Table 4. Depth Effect on Bending Strength: COFI Data

Data Set	b (mm)	h (mm)	N	MOR 0.05 (MPa)	
S-P-F	1	38	89	119	30.06
S8	1	38	235	122	21.33
S-P-F	2	38	89	132	29.32
SEL	2	38	235	190	21.14
S-P-F	3	38	89	73	19.50
No. 2	3	38	235	89	13.04
S-P-F	4	38	89	101	20.44
S6	4	38	235	102	13.25

S-P-F: Canadian spruce pine fir

S8: ECE S8 grade (same as SS grade in BS4978)

S6: ECE S6 grade (same as GS grade in BS4978)

SEL: NLGA Select Structural grade

No. 2: NLGA No. 2 grade

Table 5. Depth Effect on Bending Strength: Canadian Data

	Data Set	b (mm)	h (mm)	N	MOR 0.05 (MPa)
D-F	1	38	89	370	35.71
SEL	1	38	184	373	25.15
	1	38	235	372	21.08
D-F	2	38	89	370	20.50
No. 2	2	38	184	370	15.64
	2	38	235	374	14.20
H-F	3	38	89	381	37.20
SEL	3	38	184	382	25.35
	3	38	235	379	20.83
H-F	4	38	89	380	25.99
No. 2	4	38	184	402	18.76
	4	38	235	385	16.24
S-P-F	5	38	89	441	32.88
SEL	5	38	184	444	23.15
	5	38	235	440	20.80
S-P-F	6	38	89	440	21.18
No. 2	6	38	184	986	16.91
	6	38	235	441	14.89

D-F: Canadian Douglas fir

H-F: Canadian hem fir

S-P-F: Canadian spruce pine fir

SEL: NLGA Select Structural grade

No. 2: NLGA No. 2 grade

Table 6. Width Effect on Tensile Strength: U.K. Data

	Data Set	b (mm)	w (mm)	L (mm)	N	MOR _t 0.05 (MPa)
R/W	1	35	35	880	88	15.20
S8	1	35	47	880	87	20.80
	1	35	60	880	141	19.40
R/W	2	38	100	3000	103	17.30
S8	2	38	150	3000	105	15.20
	2	38	200	3000	91	14.20
R/W	3	35	35	880	103	13.90
S6	3	35	47	880	51	18.80
	3	35	60	880	108	14.30
R/W	4	38	100	3000	43	15.70
S6	4	38	150	3000	48	13.40
	4	38	200	3000	60	10.20
S-P-F	5	38	89	1900	218	17.20
S8	5	38	184	1900	259	14.50
S-P-F	6	38	89	1900	61	11.70
S6	6	38	184	1900	38	11.70
S-P-F	7	38	89	1900	285	14.20
SEL	7	38	184	1900	247	14.40

R/W: European redwood/whitewood

S-P-F: Canadian spruce pine fir

S8: ECE S8 grade (same as SS grade in BS4978)

S6: ECE S6 grade (same as GS grade in BS4978)

SEL: NLGA Select Structural grade

Table 7. Width Effect on Tensile Strength: Canadian Data

	Data Set	b (mm)	w (mm)	L (mm)	N	MORt 0.05 (MPa)
D-F	1	38	89	3680	372	17.46
SEL	1	38	184	3680	373	14.94
	1	38	235	3680	373	14.04
D-F	2	38	89	3680	373	10.96
No. 2	2	38	184	3680	371	9.29
	2	38	235	3680	370	8.40
H-F	3	38	89	3680	360	17.27
SEL	3	38	184	3680	381	14.72
	3	38	235	3680	383	13.37
H-F	4	38	89	3680	362	12.34
No. 2	4	38	184	3680	381	10.42
	4	38	235	3680	378	8.98
S-P-F	5	38	89	3680	440	15.71
SEL	5	38	184	3680	441	12.27
	5	38	235	3680	446	12.07
S-P-F	6	38	89	3680	440	9.31
No. 2	6	38	184	3680	440	8.32
	6	38	235	3680	463	8.50

D-F: Canadian Douglas fir
H-F: Canadian hem fir
S-P-F: Canadian spruce pine fir

SEL: NLGA Select Structural grade
No. 2: NLGA No. 2 grade

Fig. 1 An Effect of the Use of Incorrect Depth Factors in Codes and Standards

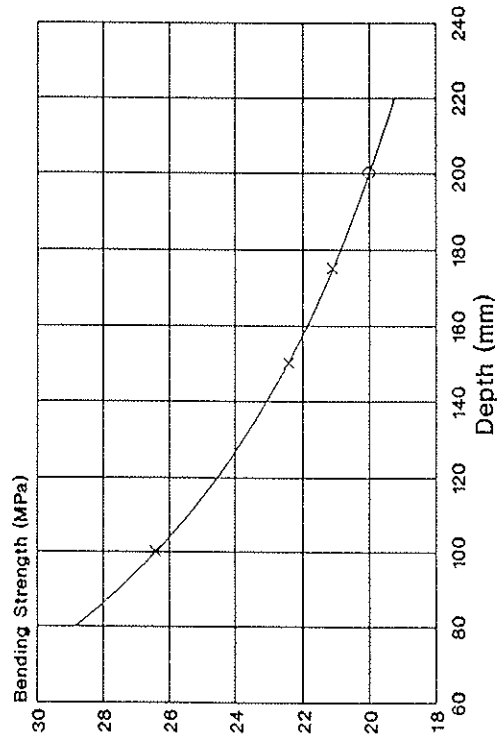


Fig. 1a

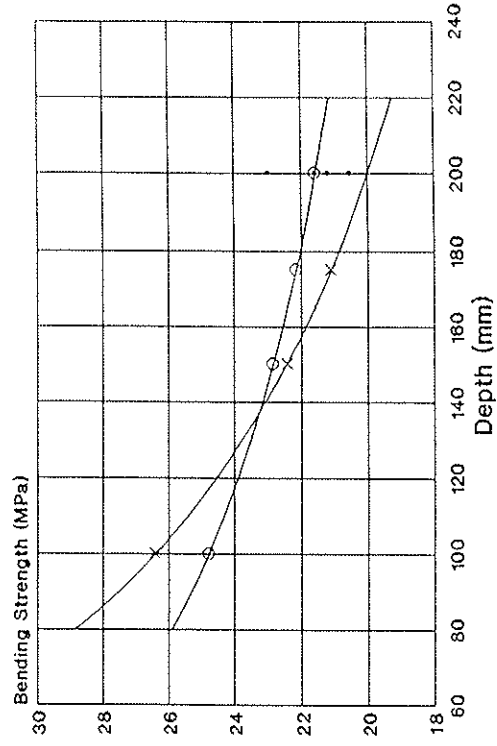


Fig 1b

Fig. 3 Length Effect on MOR
 $S_{Lm} = 0.17$

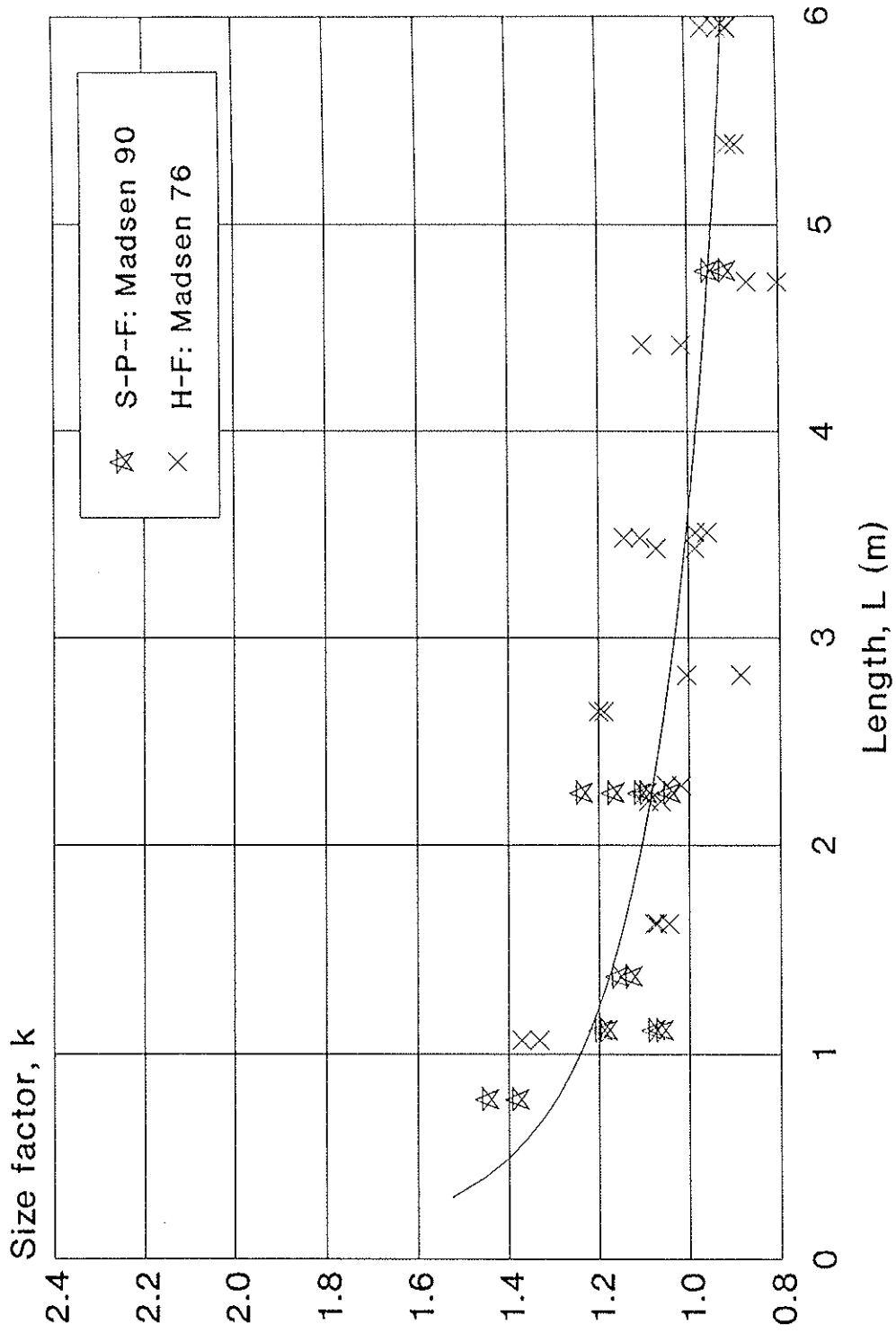


Fig. 4 Depth Effect on Fifth Percentile MOR

U.K. and COFI data: $S_{Rm} = 0.4$

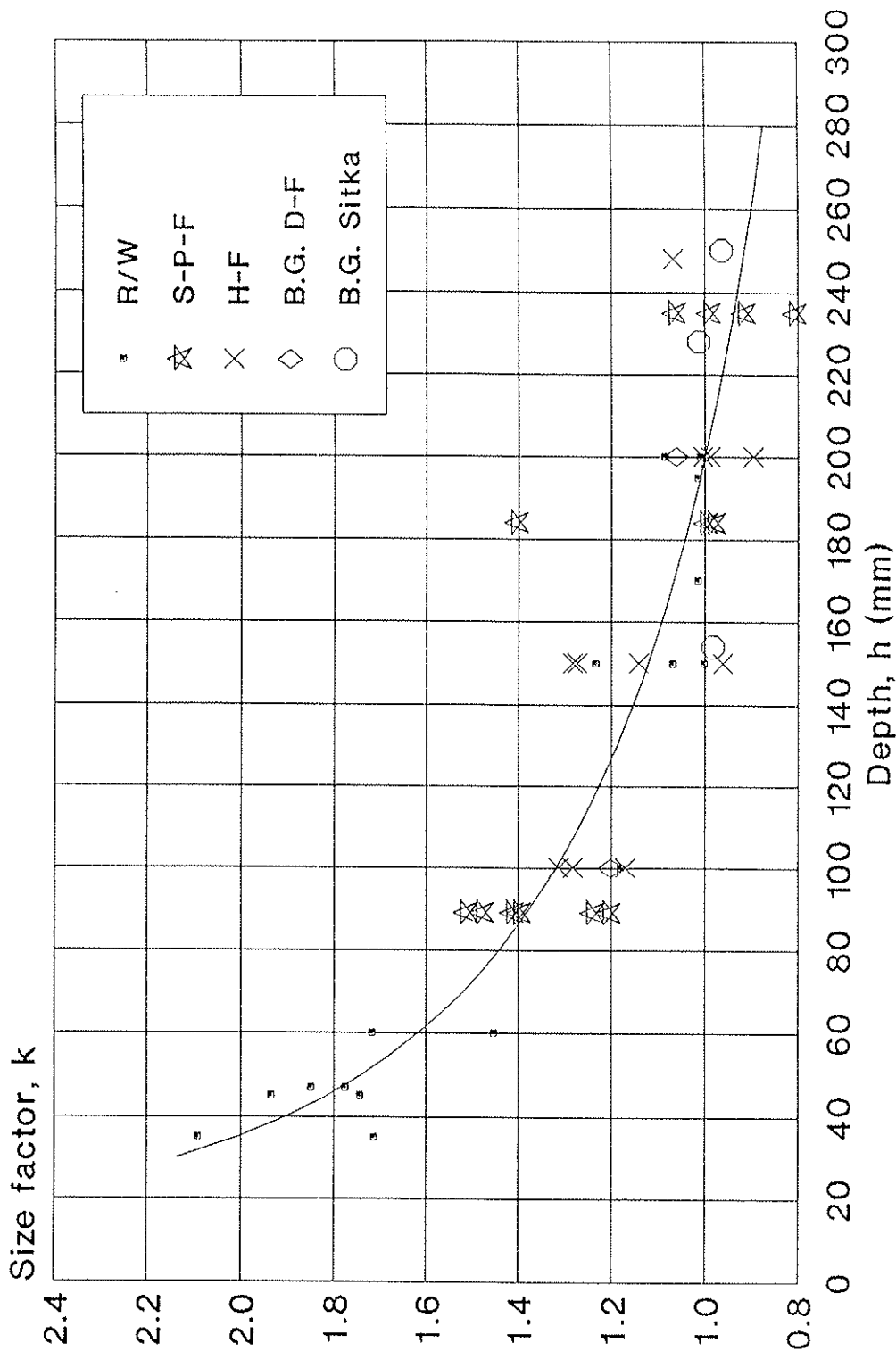


Fig. 5 Depth Effect on Fifth Percentile MOR
Canadian Data: $S_{Rm} = 0.45$

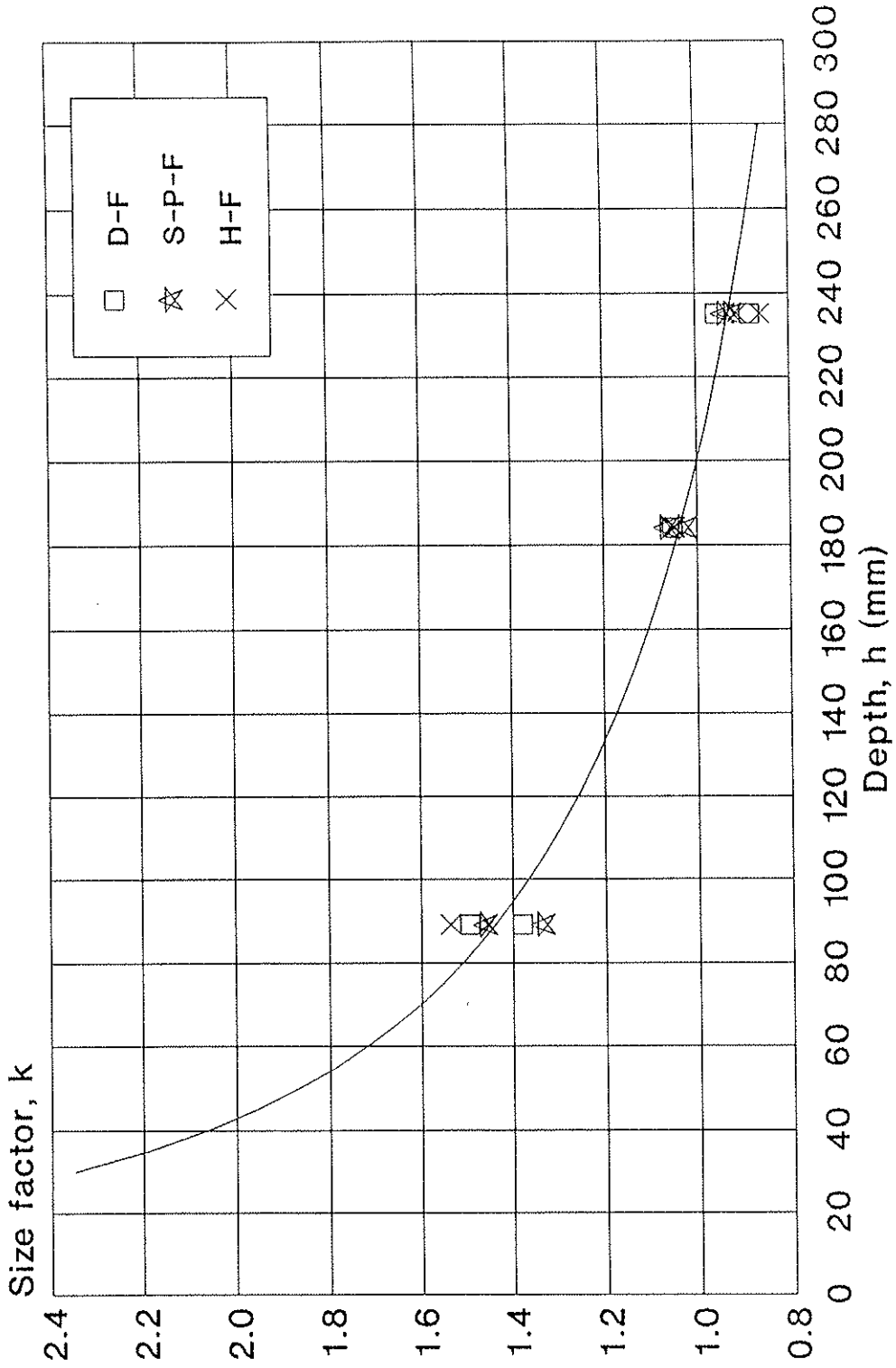


Fig. 6 Depth Effect on Fifth Percentile MOR

U.K. and Canadian Data: $S_{Rm} = 0.4$

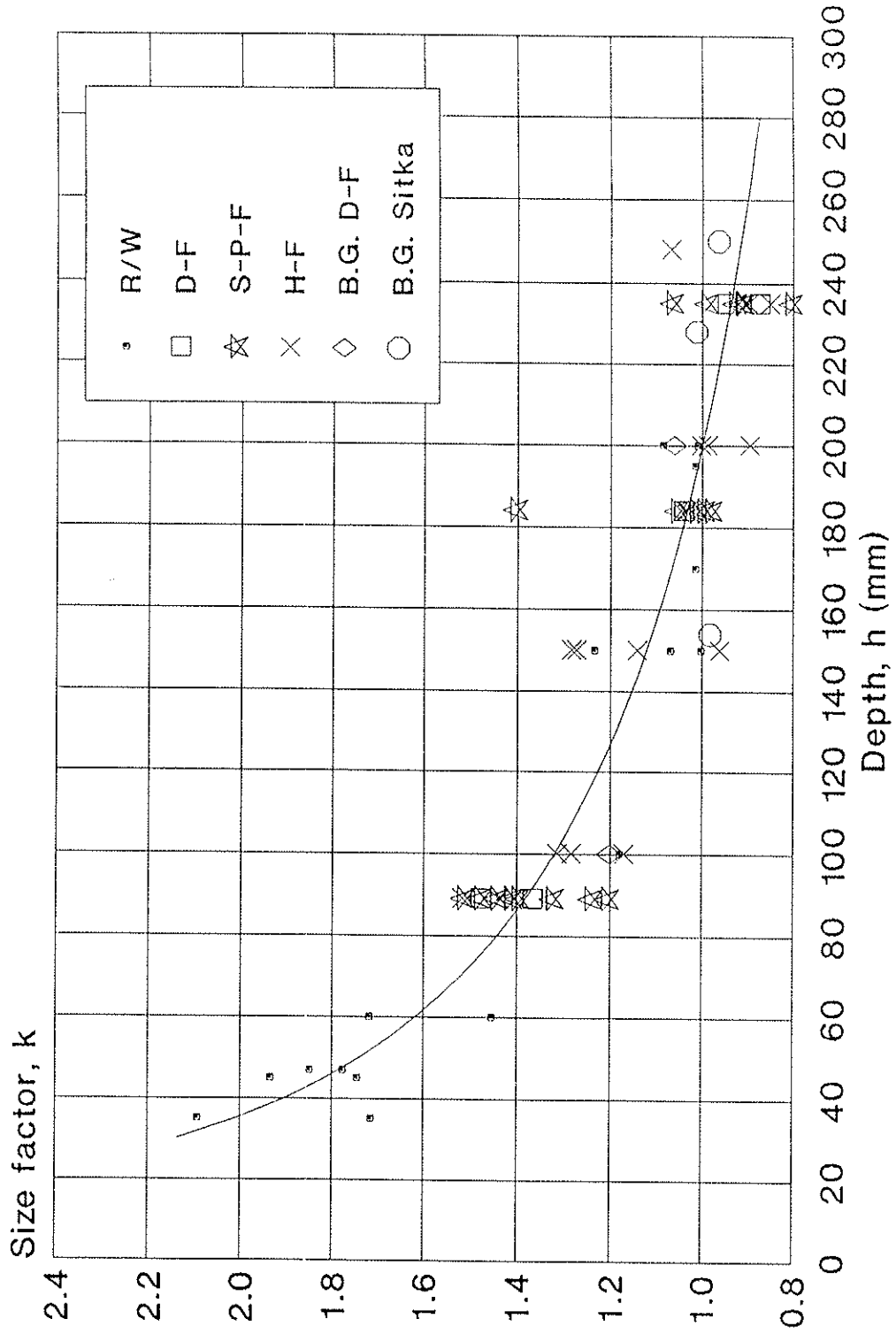


Fig. 7 Width Effect on Tensile Strength
U.K. Data: $S_{wt} = 0.12$

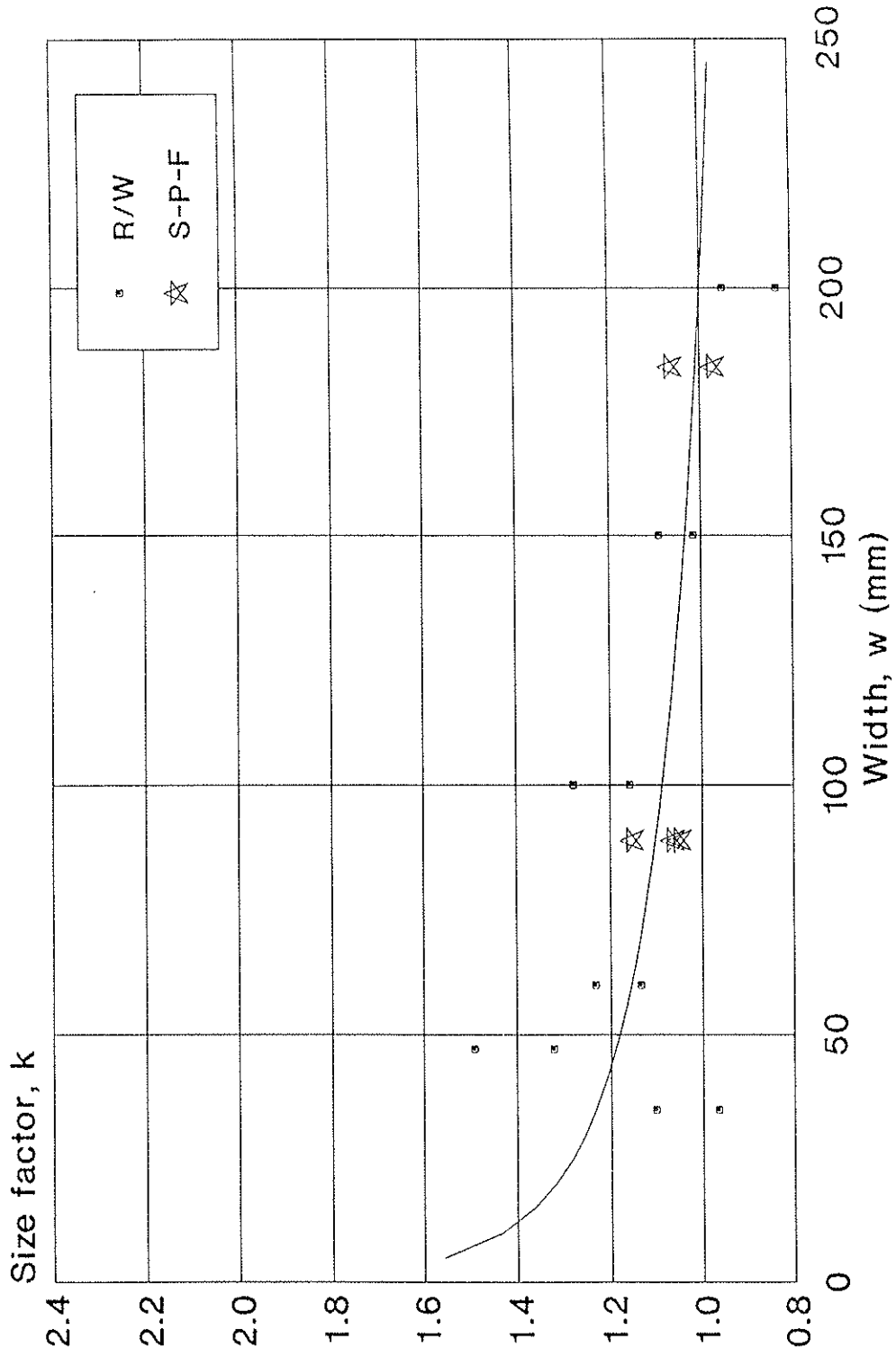


Fig. 8 Width Effect on Tensile Strength
Censored U.K. Data: $S_{wt} = 0.24$

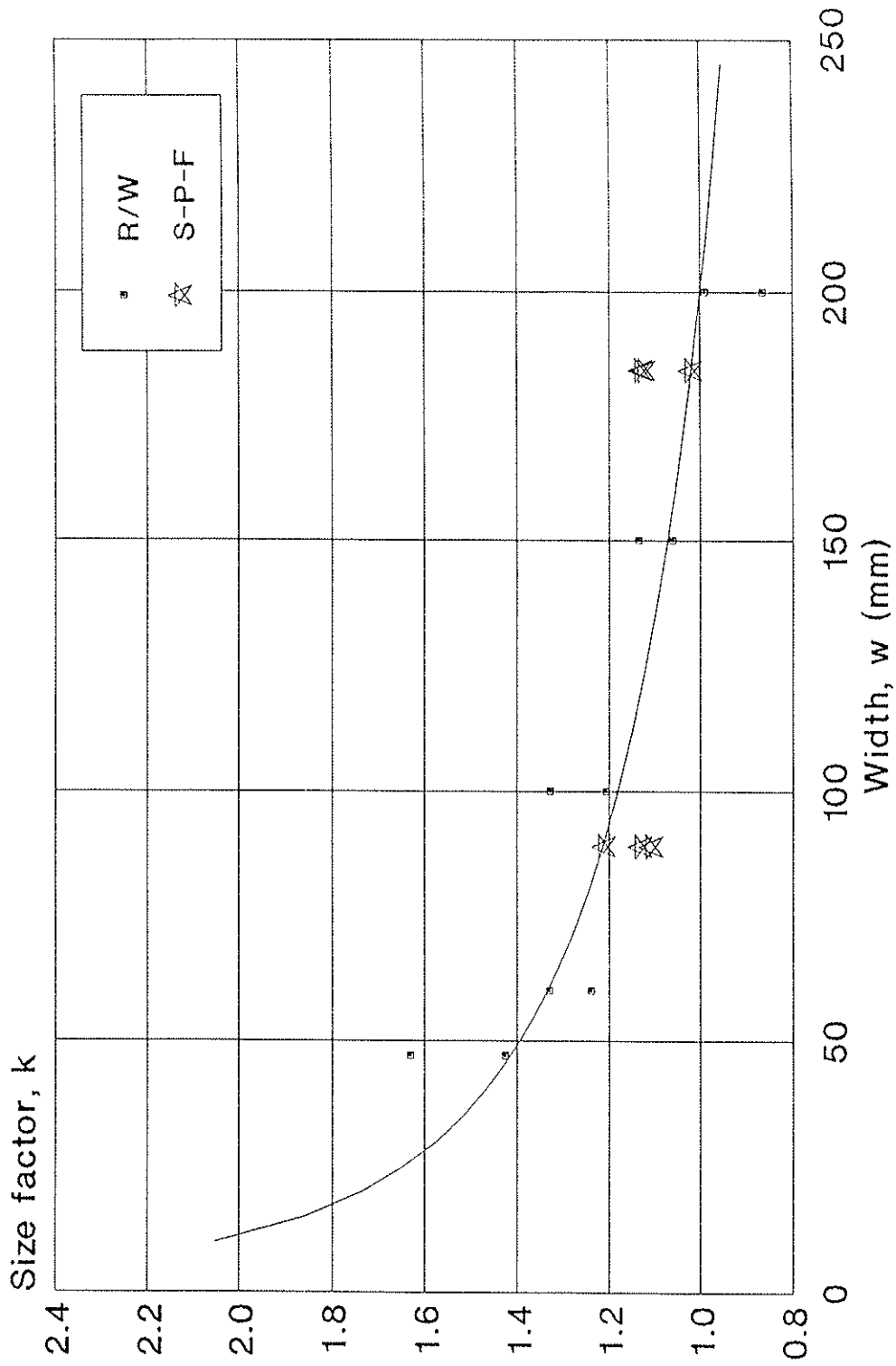
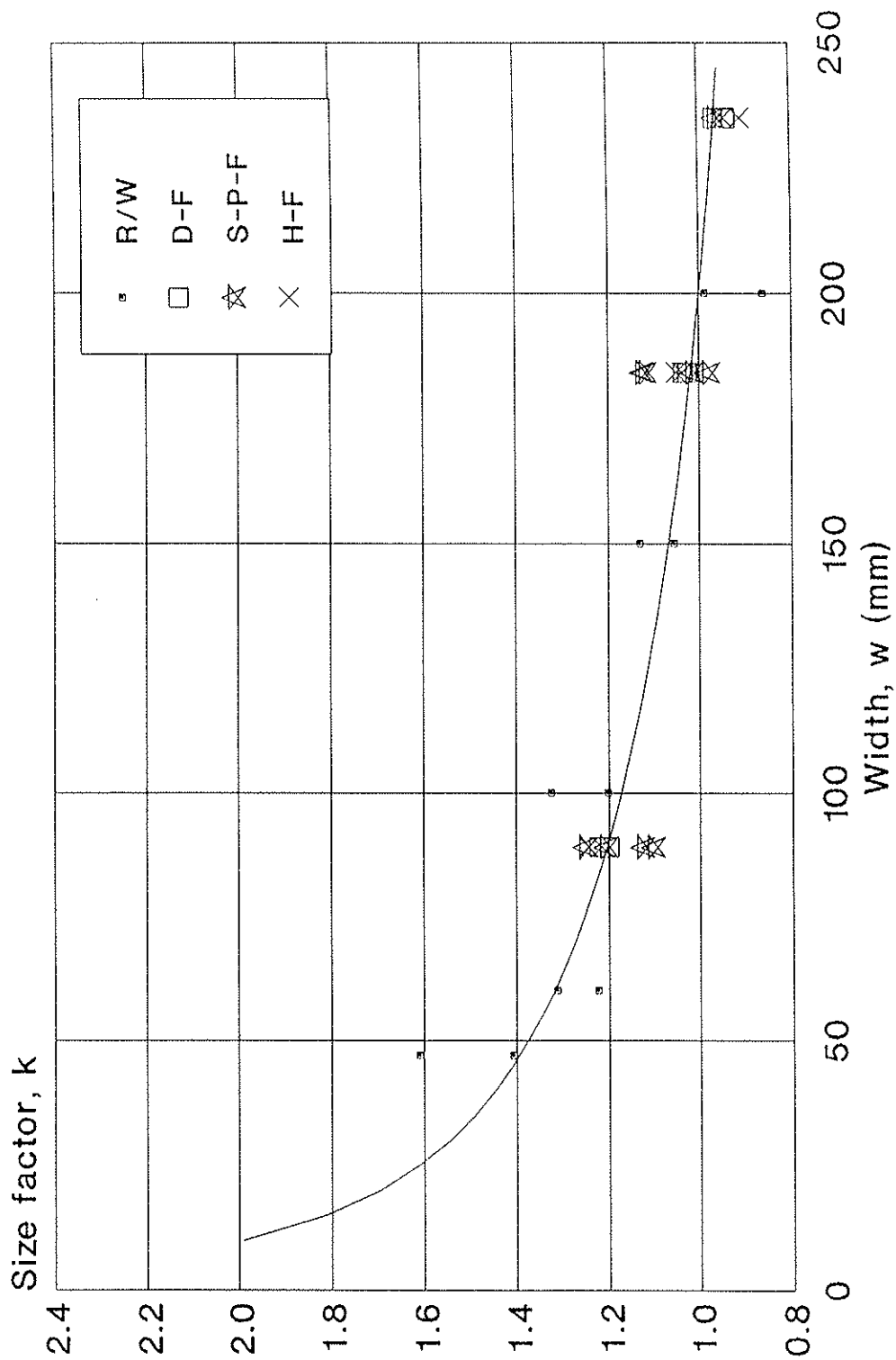


Fig. 9 Width Effect on Tensile Strength
Censored U.K. & Canadian Data: $S_{wt} = 0.23$



**INTERNATIONAL COUNCIL FOR BUILDING RESEARCH STUDIES AND DOCUMENTATION
WORKING COMMISSION W18A - TIMBER STRUCTURES**

BENDING STRENGTH OF GLULAM BEAMS

A DESIGN PROPOSAL

by

J Ehlbeck
F Colling
University of Karlsruhe
Federal Republic of Germany

MEETING TWENTY - THREE

LISBON

PORTUGAL

SEPTEMBER 1990

Bending strength of glulam beams

- A design proposal -

by

Jürgen Ehlbeck and François Colling

The scope of a current research project¹ is the investigation of the bending strength of glulam beams aiming at the development of design proposals. The "Karlsruhe calculation model" (Ehlbeck et al 1985a, Colling 1988) - a finite element model calculating the strength of glulam beams by means of Monte Carlo simulations - was thought to achieve this purpose.

The simulations showed, however, that the strength of glulam beams is a very complex field and that it is very difficult to describe the influence of one single parameter. The "Karlsruhe calculation model" takes into account every possible tendency, but the problem was to describe these tendencies mathematically.

Therefore, a statistical model (Colling 1990) was developed, which divides the totality of glulam beams into two groups: beams with wood failure (knots) and beams failing due to finger joints. On the basis of the "true" strength distributions of these two groups, it is possible to calculate the strength characteristics of the resultant glulam beams.

According to this model, the strength distribution of the final product glulam orientates itself very strongly by the lower of these two strength distributions and the characteristic bending strength of glulam beams is governed by the lower 5th-percentile of this group ("weaker material").

In *fig. 1* the characteristic bending strength (5th-percentile) depending on KAR, oven-dry density and MOE of the laminations is shown for beams with finger joint failure ($x_{5,fj}^0$) and wood failure ($x_{5,wood}^0$). The index "0" indicates, that the strength values are valid for a standard beam with a depth of 300 mm (see *fig. 2*). Based on these calculation results, beams with finger joint failure were found to be the "weaker material" having the lower 5th-percentile. This tendency even increases with increasing beam dimensions, because size

¹ Ehlbeck, J.; Colling, F.: Biegefestigkeit von Brettschichtholzträgern in Abhängigkeit von den Eigenschaften der Brett lamellen im Hinblick auf Normungsvorschläge

effects are more pronounced in case of beams with finger joint failure than in case of beams with wood failure. This may be explained by the higher variability of strength data in case of beams with failure due to finger joints .

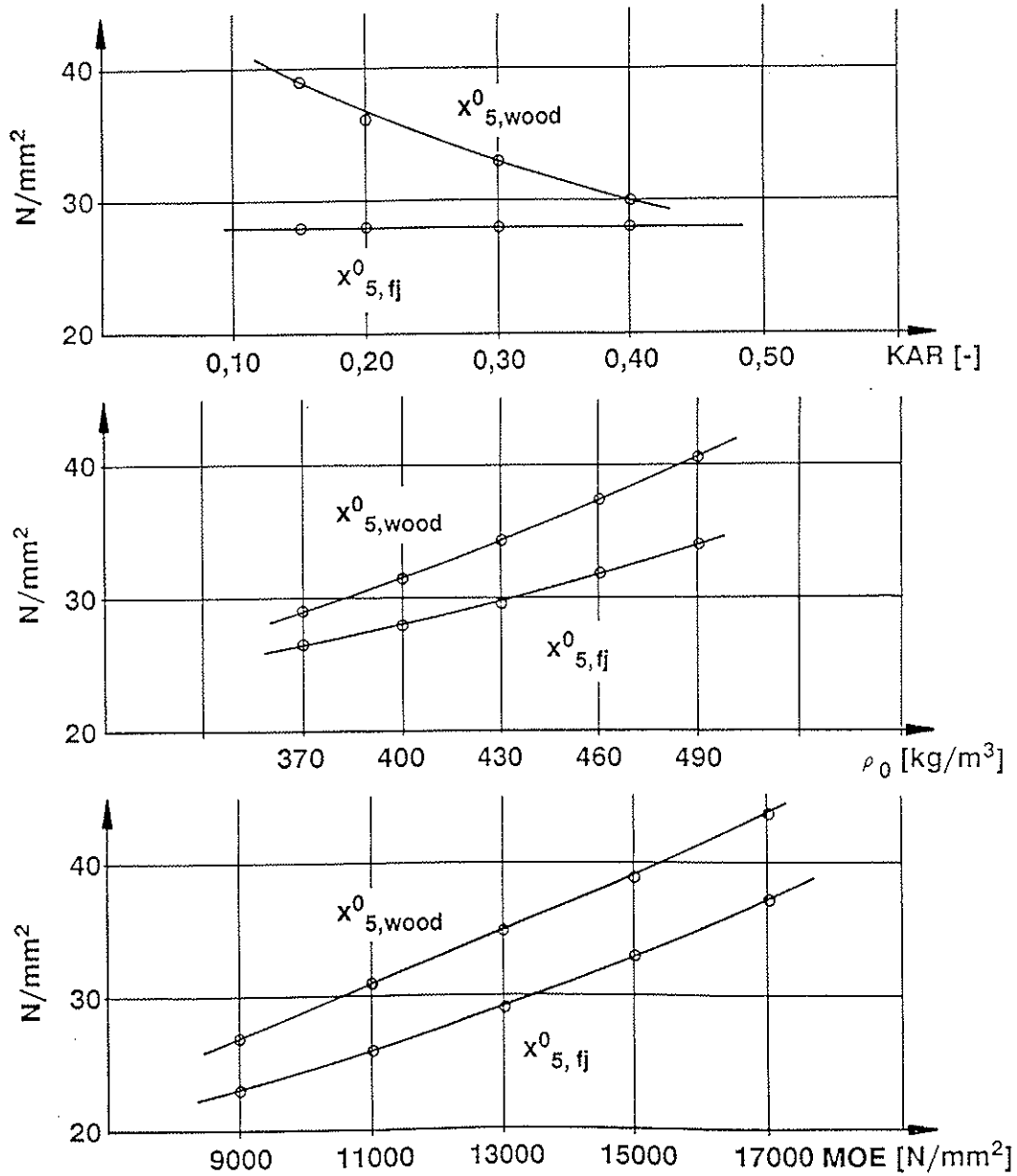


fig. 1: Characteristic bending strength of glulam beams with finger joint failure ($x^0_{5,fj}$) and wood failure ($x^0_{5,wood}$)

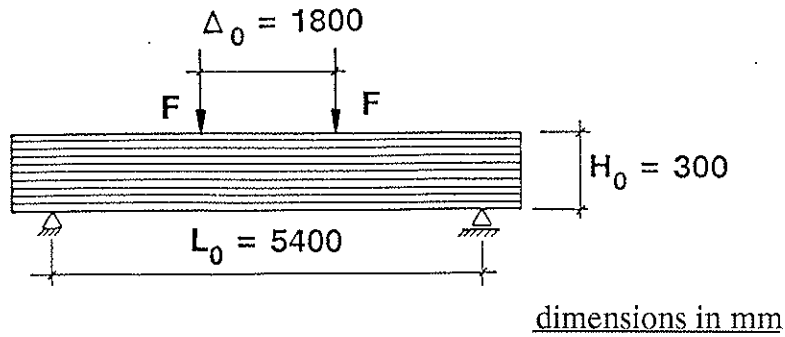


fig. 2: Standard beam

The reliability of the statistical model and of calculation results was verified by beam tests. A total of 42 bending tests were performed. Test set-up and beam dimensions are given in fig. 3.

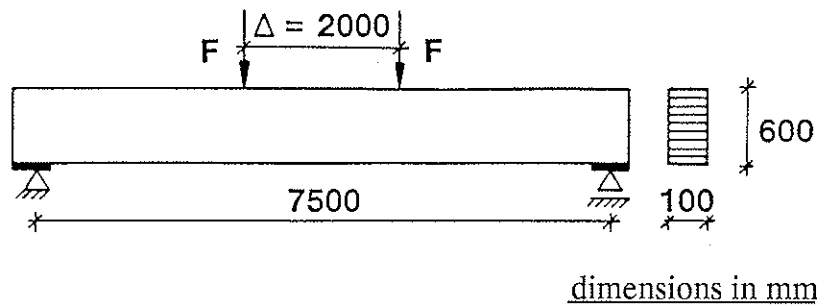


fig. 3: Test set-up and beam dimensions

Six test series with seven replications were performed. The three outer laminations of the beams had to meet the requirements given in table 1.

A comparison between test results and calculation results proved very good agreement (see fig. 4).

table 1: Requirements raised to the wood properties of the three outer laminations on both sides

test series	requirements
I	$0,35 \leq KAR$
II	$0,20 \leq KAR \leq 0,35$
III	$KAR \leq 0,20$
IV	$500 \text{ kg/m}^3 \leq \rho^1$
V	$15000 \text{ N/mm}^2 \leq E$
VI	$15000 \text{ N/mm}^2 \leq E$ und $KAR \leq 0,20$

¹ density at a moisture content of 12 - 14%

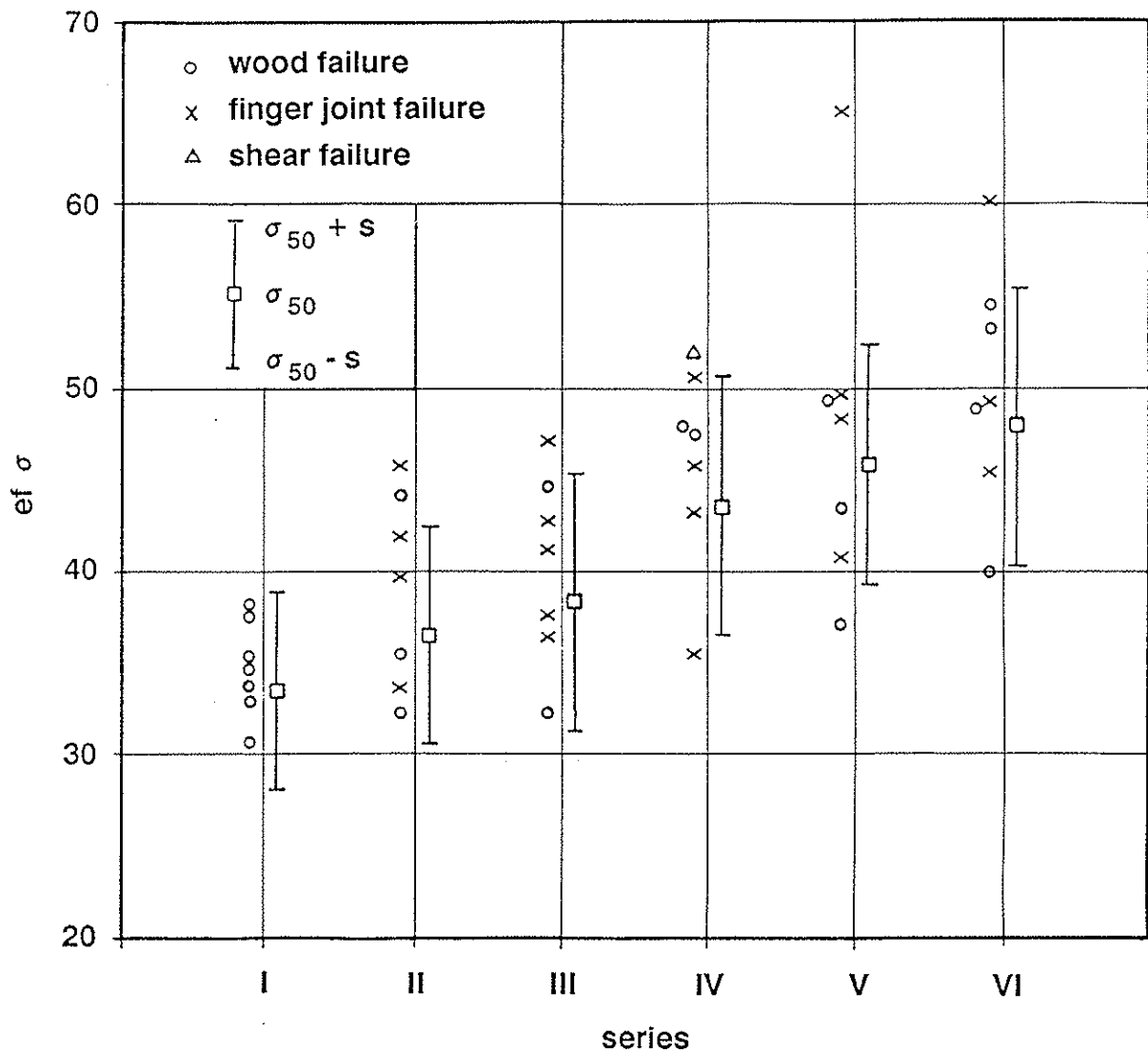


fig. 4: Comparison between test results and calculation results;
 σ_{50} = median value and s = standard deviation

Contrary to the test results, calculation results allowed some statements concerning the expected characteristic strength values and it was shown that the 5th-percentile of the bending strength of $f_{m,k}$ glulam beams is almost equal to the 5th-percentile of those beams with failure due to finger joints.

In case of the standard beam of *fig. 2*, this strength value $f_{m,k}^0$ was found to be 20% higher than the characteristic tensile strength $f_{t,0,k,fj}$ of the occurring finger joints. Hence it may be written:

$$f_{m,k}^0 = 1.20 \cdot f_{t,0,k,fj} \quad (1)$$

where

$$\begin{aligned} f_{m,k}^0 &= \text{characteristic bending strength of the standard beam,} \\ f_{t,0,k,fj} &= \text{characteristic tensile strength of the finger joints.} \end{aligned}$$

But as tensile strength can hardly be controlled by glulam factories during current quality control, the desired strength value $f_{t,0,k,fj}$ should be estimated by the corresponding bending strength value $f_{m,k,fj}$: knowing the ratio of tensile/bending strength of finger joints, it is possible to estimate the tensile strength by means of bending tests.

On the basis of numerous tests with finger joints (Ehlbeck et al. 1985b, Ehlbeck et al 1989) a ratio of

$$f_{t,0,k,fj}/f_{m,k,fj} = 23,4/36,3 = 0,64$$

may be expected. The ratio of the corresponding mean values was found to be

$$f_{t,0,fj}/f_{m,fj} = 35,0/50,6 = 0,69.$$

Tests of Radovic/Rohlfing 1986 with finger jointed laminated veneer lumber (LVL) however showed ratios of

$$f_{t,0,fj}/f_{m,fj} = 0,72 - 0,79.$$

These values correspond well to those found by Johansson (1983 and 1986):

$$f_{t,0,fj}/f_{m,fj} = 0,70 - 0,79.$$

The ratio of tensile/bending strength of finger joints is systematically investigated in a current research project in Karlsruhe, so that definitive values will be available within one year.

The following assumptions seem to be reasonable:

$$f_{t,0,k,fj}/f_{m,k,fj} \approx 0,70 \quad (2)$$

and

$$f_{t,0,fj}/f_{m,fj} \approx 0,75.$$

With *eq(2)*, *eq(1)* may be written as:

$$f_{m,k}^0 = 0,84 \cdot f_{m,k,fj} \quad (3)$$

This relationship is valid for the standard beam, shown in *fig. 2*. The characteristic bending strength $f_{m,k}$ of any given beam may then be calculated as follows:

$$f_{m,k} = k_L \cdot k_H \cdot k_F \cdot f_{m,k}^0 \quad (4)$$

where

k_L, k_H, k_F = factors taking into account the effects of length L , depth H and load configuration F

According to Colling 1990, these factors may be calculated according to Weibull's theory of brittle fracture as:

$$k_L = \left(\frac{L}{L_0} \cdot \frac{BL_0}{BL} \right)^{-0,15} \quad (5)$$

and

$$k_H = \left(\frac{H}{H_0} \right)^{-0,15} \quad (6)$$

L and H are the actual dimensions of the beam, whereas L_0 (=5400 mm) and H_0 (=300 mm) are the dimensions of the standard beam. BL and BL_0 (=4 m) are the average lengths of the boards used.

Assuming a mean value of board length of about 4 m, *eq(5)* may be reduced to:

$$k_L = \left(\frac{L}{L_0} \right)^{-0,15} \quad (7)$$

The load configuration factor k_F may be determined according to Colling (1986). In case of a beam with uniformly distributed load, a value of

$$k_F = 1,04 \quad (8)$$

may be assumed.

Based on *eq(3)*, the characteristic bending strength of the standard beam with constant loading may then be calculated as:

$$\begin{aligned} f_{m,k}^0 &= 1,04 \cdot 0,84 \cdot f_{m,k,fj} \\ &= 0,874 \cdot f_{m,k,fj} \end{aligned} \quad (9)$$

From this equation can be derived that the characteristic bending strength of finger joints must be 15% ($1/0,874 = 1,144$) higher than the characteristic bending strength to be achieved for the final glulam beam.

Thus, the following proposal for the design of glulam beams may be established:

Based on the characteristic bending strength $f_{m,k}^0$ of a standard beam under constant loading, the characteristic bending strength $f_{m,k}$ of any glulam beam may be calculated as

$$f_{m,k} = \left(\frac{L}{5400} \cdot \frac{H}{300} \right)^{-0,15} \cdot k_F \cdot f_{m,k}^0 \quad (10)$$

with

L and H = length and depth of the beam in mm,

k_F = load configuration factor (=1 in case of a single span beam with uniformly distributed load).

The finger joints in the beam have to meet the following requirement:

$$f_{m,k,fj} \geq 1,15 \cdot f_{m,k}^0 \quad (11)$$

It is essential to point out that in case of beams, systematically built up with laminations having significantly different MOE-values, the ultimate bending stress (in the outermost lamination) must be calculated according to the theory of transformed sections.

References

Colling, F. 1986: Influence of volume and stress distribution on the shear strength and tensile strength perpendicular to grain. CIB-W18/19-12-3, Florence, Italy

Colling, F. 1988: Estimation of the effect of different grading criterions on the bending strength of glulam beams using the "Karlsruhe calculation model". IUFRO, Turku, Finland

Colling, F. 1990: Bending strength of glulam beams - a statistical model. IUFRO, Saint John/New Brunswick, Canada

Ehlbeck, J.; Colling, F.; Görlacher, R. 1985a: Einfluß keilgezinkter Lamellen auf die Biegefestigkeit von Brettschichtholzträgern. Teil 1: Entwicklung eines Rechenmodells. Holz als Roh- und Werkstoff 43: 333 - 337

Ehlbeck, J.; Colling, F.; Görlacher, R. 1985a: Einfluß keilgezinkter Lamellen auf die Biegefestigkeit von Brettschichtholzträgern. Teil 2: Eingangsdaten für das Rechenmodell. Holz als Roh- und Werkstoff 43: 369 - 373

Ehlbeck, J.; Colling, F. 1990: Bending strength of finger joints. IUFRO, Saint John/New Brunswick, Canada

Johansson, C.-J. 1983: Hallfasthet hos fingerskarvat virke till limträ: Bestämning av böj- och draghallfasthet hos fingerskarvade limträlamellar. Teknisk Rapport, Sp.-rapp 10, Borås, Statens Provningsanstalt

Johansson, C.-J. 1986: Hallfasthet hos fingerskarvat virke till limträ: Fingerskarvade höghallfasta limträlamellar. Teknisk Rapport, Sp.-rapp 09, Borås, Statens Provningsanstalt

Radovic, B.; Rohlfig, H. 1986: Untersuchungen über die Festigkeit von Keilzinkenverbindungen mit unterschiedlichem Verschwächungsgrad. Forschungsvorhaben I.4-34701, FMPA Stuttgart

INTERNATIONAL COUNCIL FOR BUILDING RESEARCH STUDIES AND DOCUMENTATION
WORKING COMMISSION W18A - TIMBER STRUCTURES

PROBABILITY BASED DESIGN METHOD FOR GLUED LAMINATED TIMBER

by

M F Stone
Weyerhaeuser Co.
United States of America

MEETING TWENTY - THREE

LISBON

PORTUGAL

SEPTEMBER 1990

A copy of paper 23-12-2, Probability Based Design Methods for Glued Laminated Timber, can be obtained from the author, Mr. M. Stone, Weyerhaeuser Co., 32901 Weyerhaeuser Way, South Federal Way, WA 98003, U.S.A.

INTERNATIONAL COUNCIL FOR BUILDING RESEARCH STUDIES AND DOCUMENTATION
WORKING COMMISSION W18A - TIMBER STRUCTURES

GLULAM BEAMS. BENDING STRENGTH IN RELATION TO
THE BENDING STRENGTH OF THE FINGER JOINTS

by

H Riberholt
Technical University of Denmark
Denmark

MEETING TWENTY - THREE

LISBON

PORTUGAL

SEPTEMBER 1990

Glulam beams. Bending strength in relation to the bending strength of the finger joints

1. Scope

The scope of this paper is to illustrate the relation between the bending strength of glulam beams and that of the finger joints. It is written as a contribution similar to that in *Ehlbeck & Colling* which also deals with this subject. But this paper employs another experimental source.

2. The relation between the bending strengths

The tests, which form the basis for this paper, have all been conducted at AUC and they are reported in *Larsen, 1979* and *Larsen, 1982*.

When the failure in glulam takes place at a finger joint then the tensile strength of the finger joint has been decisive. So in research the investigations have been aimed at the tensile strength of the finger joints. But in practice the strength check is carried out as a bending test of the finger joints. Therefore one has determined the relation between the tensile and bending strength of the finger joints.

Finger joints: f_t/f_m

In table 3.1 of *Larsen, 1979* there is given in brackets the mean values of the relation between the tensile strength $f_{t,fj}$ and bending strength $f_{m,fj}$ of the tested finger joints from 10 different manufacturers, 15 replicants were tested. This relation varies from 0.56 to 0.76 and the mean value of all is

$$f_{t,fj}/f_{m,fj} = 0.64 \quad (2.1)$$

The relation between the bending strengths

In table 5.3a of *Larsen, 1982* there is given the bending stress σ_0 at failure in the outer fibre of the tensioned part of the cross section. The different moduli of elasticity in the laminations have been considered by means of a transformed moment of inertia. In the following σ_0 will be substituted by $f_{m,gl}$.

From this table the relation between the bending strength of glulam $f_{m,gl}$ and that of finger joints $f_{m,fj}$ can be calculated for some different cases by means of

$$f_{m,gl}/f_{m,fj} = (f_{m,gl}/f_{t,fj}) \cdot (f_{t,fj}/f_{m,fj}) \quad (2.2)$$

where $(f_{m,gl}/f_{t,fj})$ is equal to σ_0/f_t in table 5.3a of *Larsen, 1982*.

$(f_{t,fj}/f_{m,fj})$ is given in formula (2.1)

In table 2.1 the values of formula (2.2) are given for some tests with glulam beams typical for practice.

Table 2.1 The relation between the bending strength of glulam and that of finger joints.

Ident.	Description of laminations in the tensile side	$(f_{m,gl}/f_{t,fj})$	$(f_{m,gl}/f_{m,fj})$
1.31	2 high quality laminations	1.73	1.11
1.32	1 high quality lamination	1.60	1.02
4.1		1.57	1.00
1.33	Coinciding fingers in adja-	1.40	0.90
4.2	cent laminations	1.43	0.92
1.34	Coinciding fingers and the inner one is a weak finger joint.	1.41	0.90

It appears from table 2.1 that the relation between the bending strengths are close to unity. The relation is a little above 1.0 if a sound lay-up is employed and 10 per cent below in the case of coincidence between finger joints in the two outer laminations.

The decrease in the strength relation for coinciding finger joints suggests that the actual size of the joint (the weak part of the cross section) influences the relation. So apparently the strength relation decreases when the size of the finger joint increases. This is supported by the high bending strength of Laminated-Veneer-Lumber (Micro-Lam) despite the butt joints in the veneer.

Further, from series 1 and 2 in table 5.3c of *Larsen, 1982*, which is reproduced in table 2.2, it can be seen that the weaker the finger joints are compared with the rest of the lamination/glulam the smaller becomes the lamination factor expressed as $f_{m,gl}/f_{t,fj}$ (σ_0/f_t).

Table 2.2 Lamination factors for glulam with different lay-ups in the two outer laminations in the tensile side.

Lamination No.:		$f_{m,gl}/f_{t,fj}$
1	2	
Unjointed	Unjointed	1.39
Finger joint	Unjointed	1.61
Finger joint	F_j^* or weak F_j^*	1.42
Weak finger joint	Weak finger joint	1.06
Weak finger joint	Unjointed or weak F_j^* spaced more than 5·lam.thickness	1.26

* F_j = Finger joint.

This fact can maybe explain why *Ehlbeck & Colling, 1990* suggest a lower value of $f_{m,gl}/f_{m,fj}$. Because from the values in this report the range of the mean bending strength of the finger joints can be estimated from

$$\bar{f}_{m,fj} = \begin{array}{l} \text{I: } 33 \cdot \frac{1}{1.20 \cdot 0.75} = 37 \text{ MPa} \\ \text{VI: } 48 \cdot \frac{1}{1.20 \cdot 0.75} = 53 \text{ MPa} \end{array}$$

The high value corresponds to the bending strength of the finger joints used in the tests reported in *Larsen, 1982* and the low value corresponds to that of the weak finger joints.

3. Conclusion

The relation between the bending strength of glulam and that of the finger joints seems to depend on several factors. Among these are partly the size of the finger joints represented for example by the thickness of the lamination, partly the relation between the strength of the finger joint and that of the rest of the lamination. This could be explained by the fact that the weak finger joint is brittle and the surrounding wood is in the linear state, so stress redistribution will not take place.

In general it can be stated that the bending strength of the glulam is equal to that of the finger joints if these control the strength.

Literature

- Larsen, H.J. 1979. Limtræbjælkens styrke, delrapport 3. Inst. for Bygningsteknik, AUC, rapport 7902.
- Larsen, H.J. 1982. Strength of glued laminated beams, Part 5. Inst. for Bygningsteknik, AUC, Rapport 8201.
- Ehlbeck, j. & Francois Colling, 1990. Bending strength of glulam beams – A design proposal. CIB–W18A paper 23–12–1.

INTERNATIONAL COUNCIL FOR BUILDING RESEARCH STUDIES AND DOCUMENTATION

WORKING COMMISSION W18A - TIMBER STRUCTURES

GLUED LAMINATED TIMBER - STRENGTH CLASSES AND

DETERMINATION OF CHARACTERISTIC PROPERTIES

by

H Riberholt

Technical University of Denmark

Denmark

J Ehlbeck

University of Karlsruhe

Federal Republic of Germany

A Fewell

Building Research Establishment

United Kingdom

MEETING TWENTY - THREE

LISBON

PORTUGAL

SEPTEMBER 1990

0. PREFACE AND EXPLANATION

In the draft it has been necessary to introduce 2 tables of strength classes, one for glulam with a homogeneous cross-section and one for glulam where different lamination grades have been combined in the cross-section. The last mentioned is frequently employed in practise and it could be preferable to standardise this set of strength classes.

Another possibility would be to have more classes so that homogeneous and combined grades could be included in the same table of classes. But this solution would give some problem with the setting of the strength values for axial tension and compression. These would have to be set at a rather low level in order to cater for the combined grade glulam with the low quality inner laminations. This would penalise homogeneous glulam.

1. INTRODUCTION

A strength class system enables combinations of grade and species having similar strength properties to be classified together with a common set of strength properties. Such a system simplifies the process of marketing structural timber by reducing the number of options at the specification/supply interface.

2. SCOPE AND FIELD OF APPLICATION

This standard lays down a system of strength classes for structural glued laminated timber which caters for the strength range in common use throughout Europe. A number of strength classes are defined and characteristic strength and stiffness properties are given.

Further, this standard contains rules for the determination of the characteristic properties

by Specified strength classes for the laminations
by Calculation or
by proof testing.

3. DEFINITIONS

Glued laminated timber - A single structural member, not necessarily straight, formed by gluing together laminations of timber with the grain running essentially parallel.

Abbreviated: Glulam.

Homogeneous glulam - Glulam with a homogeneous cross-section where all laminations are of the same grade (strength class).

Combined glulam - Glulam with a cross-section comprising inner and outer

laminations of different grades (lamination strength classes, see Table 3). The outer laminations must cover the extreme one sixth of the depth on both sides and be at least two laminations.

4. REFERENCES

- EN.TC124.202 - 1989-06-19 Structural timber - Determination of characteristic values of mechanical properties and density.
- EN.TC124.203 - 1989-06-19 Structural timber - Strength classes
- EN.TC124.303 - 1989-07-19 Glued laminated timber - production requirements.
- ENXXX3 Determination of physical and mechanical properties (ISO 8375)
- ENXXX4 Proof testing (to be drafted)

5. STRENGTH CLASSES

- 5.1 Table 1 gives the characteristic strength properties for five strength classes for homogeneous glulam.
- 5.2 Table 2 gives the characteristic strength properties for five strength classes for combined glulam.
- 5.3 For both tables the values of bending strength, tension strength parallel to grain and compression strength parallel to grain are related to members with a greatest cross-section dimension equal to 300mm.

6. COMPLIANCE

- 6.1 Glued laminated members comply with the strength classes of Table 1 and 2 if they are manufactured in accordance with the production standard EN.TC124.303 and they meet the requirements of either 6.1.1, 6.1.2 or 6.1.3.

- 6.1.1 The grade and species shall meet the requirements of the relevant strength class for structural timber from EN.TC124.203 as given in table 3 and the characteristic bending strength of the laminate end joints ($f_{m,k,\bullet j}$) shall be greater or equal to the characteristic bending strength $f_{m,k,g}$ calculated in accordance with A.3.1 assuming homogeneous glulam lay-up. That is

$$f_{m,k,\bullet j} > f_{m,k,g}$$

where $f_{m,k,\bullet j}$ shall be determined in flatwise bending.

- 6.1.2 The grade and species shall have mechanical properties derived in accordance with ENXXX3 and EN.TC124.202, which when used as lamination properties in the formulae given in Annex A, produce mechanical

properties for glued laminated timber equal to or greater than the properties in one of the tables for the strength class to which it is assigned.

Further the requirement to the laminate end joints given in 6.1.1. shall be met.

6.1.3 The glued laminated members shall be proof tested in accordance with ENXXX4.

Table 1. CHARACTERISTIC STRENGTH PROPERTIES FOR HOMOGENEOUS GLULAM (N/mm²)

Strength class		LH25	LH28	LH30	LH35	LH40
Bending	$f_{m,k,g}$	25	28	30	35	40
Tension						
- par.	$f_{t,0,k,g}$	20	23	25	28	32
- perp.	$f_{t,90,k,g}$	0.3	0.4	0.4	0.4	0.4
Compression						
- par.	$f_{c,0,k,g}$	25	26	27	29	33
- perp.	$f_{c,90,k,g}$	5.7	5.9	6.3	6.9	7.4
Shear	$f_{v,k,g}$	2.7	2.9	3.1	3.5	4.0
Modulus of Elasticity par.						
+ bending	$E_{mean,m,g}$	10000	11000	11500	12500	13000
+ axial	$E_{mean,a,g}$	10000	11000	11500	12500	13000
Density	kg/m ³	320	350	380	410	450

The lower fifth percentile MOE ($E_{k,g}$) = 0.8 E_{mean}

Table 2. CHARACTERISTIC STRENGTH PROPERTIES FOR COMBINED GLULAM (N/mm²)

When calculating design values for strength and stiffness from the glulam properties given in this Table, it can be assumed that the section is homogeneous.

Strength class		LC24	LC26	LC28	LC33	LC38
Bending	$f_{m,k,g}$	24	26	28	33	38
Tension						
- par.	$f_{t,0,k,g}$	17	19	21	24	26
- perp.	$f_{t,90,k,g}$	0.3	0.3	0.3	0.4	0.4
Compression						
- par.	$f_{c,0,k,g}$	22	23	25	27	30
- perp.	$f_{c,90,k,g}$	5.7	5.9	6.3	6.9	7.4
Shear	$f_{v,k,g}$	2.5	2.6	2.7	2.9	3.1
Modulus of Elasticity par.						
+ bending	$E_{mean,m,g}$	9500	10500	11000	12000	13000
+ axial	$E_{mean,a,g}$	8500	9500	10500	11500	12000
Density	kg/m ³	250	300	320	350	380

The lower fifth percentile MOE ($E_{k,g}$) = 0.8 E_{mean}

Table 3. CLASSIFICATION OF GLULAM PRODUCED FROM LAMINATIONS MEETING THE REQUIREMENTS OF EN.TC124.203

Strength classes for homogeneous glulam	LH25	LH28	LH30	LH35	LH40
Required lamination strength class	C18-9E	C21-10E	C24-11E	C30-12E	C37-14E
Strength classes for combined glulam	LC24	LC26	LC28	LC33	LC38
Required strength class of:					
Outer laminations	C18-9E	C21-10E	C24-11E	C30-12E	C37-14E
Inner laminations	C13-7E	C15-8E	C18-9E	C21-10E	C24-11E

ANNEX A CALCULATION OF CHARACTERISTIC PROPERTIES

- A.1 The following formulae may be used to calculate mechanical properties for homogeneous glulam.

For combined glulam the formulae apply to the properties of the individual parts of the cross-section. The design calculation and the stress analysis can be carried out by linear elastic beam theory and transformed cross-sections. The strength verification shall be executed in all relevant points of the cross-section.

For design calculations for combined glulam which use a simplified analysis assuming the cross-section to be homogeneous, the mechanical properties given in Table 2 should be used.

All strength and stiffness values are given in MPa(N/mm²).

- A.2 The mechanical properties of glued laminated timber are derived by multiplying the laminate properties by a k_{lam} factor which makes allowance for:-
- the test methods used for single laminations, which may be less constrained than when laminations are bonded together in a single member.
 - differences due to the dispersion of laminate low strength and low stiffness areas throughout the volume of a glued laminated member.
 - differences between the coefficients of variation of single laminates and laminated members.

A.3 Mechanical properties.

A.3.1 Bending strength.

$$\begin{aligned} f_{m,k,g} &= k_{lam,m} f_{t,o,k} \\ &= (2.7 - 0.04f_{t,o,k})f_{t,o,k} \end{aligned}$$

where

- $f_{m,k,g}$ is the characteristic bending strength of the glulam
- $f_{t,o,k}$ is the characteristic tension parallel to grain strength of the laminations.

A.3.2 Modulus of elasticity

$$\begin{aligned} E_{\text{mean},g} &= k_{\text{lam},E} E_{\text{mean}} \\ &= (1.25 - E_{\text{mean}}/60000)E_{\text{mean}} \end{aligned}$$

where

$E_{\text{mean},g}$ is the mean modulus of elasticity for the glulam either in bending or tension/compression.

E_{mean} is the mean modulus of elasticity for the laminations in bending

A.3.3 Tension strength parallel to grain

$$\begin{aligned} f_{t,0,k,g} &= k_{\text{lam},t} f_{t,0,k} \\ &= (2.3 - 0.04f_{t,0,k})f_{t,0,k} \end{aligned}$$

where

$f_{t,0,k,g}$ is the characteristic parallel to grain tension strength of a glulam member.

$f_{t,0,k}$ is the characteristic parallel to grain tension strength of the laminations.

A.3.4 Compression strength parallel to grain

$$\begin{aligned} f_{c,0,k,g} &= k_{\text{lam},c} f_{c,0,k} \\ &= (1.5 - 0.01f_{c,0,k})f_{c,0,k} \end{aligned}$$

where

$f_{c,0,k,g}$ is the characteristic parallel to grain compression strength of a glulam member.

$f_{c,0,k}$ is the characteristic parallel to grain compression strength of the laminations.

A.3.5 Shear strength

$$f_{v,k,g} = 0.7f_{v,k,i} + 1.4 \text{ MPa}$$

where

$f_{v,k,g}$ is the characteristic shear strength of a glulam beam.

$f_{v,k,i}$ is the characteristic shear strength of the inner laminations.

A.3.6 Tension strength perpendicular to grain.

$$f_{t,90,k,g} = f_{t,90,k,i}$$

where

$f_{t,90,k,g}$ is the characteristic perpendicular to grain tension strength of a glulam member.

$f_{t,90,k,i}$ is the characteristic perpendicular to grain tension strength of the inner laminations.

A.3.7 Compression strength perpendicular to grain.

$$f_{c,90,k,g} = 1.1f_{c,90,k,o}$$

where

$f_{c,90,k,g}$ is the characteristic perpendicular to grain compression strength of a glulam beam.

$f_{c,90,k,o}$ is the characteristic perpendicular to grain compression strength of the outer laminations.

A.3.8 Density

The characteristic density of a glulam member shall be assumed to be equal to the characteristic density of the inner laminations. This statement assumes that the value will be used to determine the load capacity of mechanical fasteners. However, where any fasteners are secured to the outer laminations only then the characteristic density for the outer laminations may be used.

INTERNATIONAL COUNCIL FOR BUILDING RESEARCH STUDIES AND DOCUMENTATION

WORKING COMMISSION W18A - TIMBER STRUCTURES

ANALYSES OF TIMBER TRUSSED RAFTERS OF THE W-TYPE

by

H Riberholt
Technical University of Denmark
Denmark

MEETING TWENTY - THREE

LISBON

PORTUGAL

SEPTEMBER 1990

Contents:

1. Preface and scope
2. Description of the method of analysis
 - 2.1 Overview of varied assumptions
 - 2.2 Compared results
3. Sensitivity analyses
 - 3.1 The rotational stiffness of the joints
 - 3.2 Variation of the joint stiffnesses
4. Simplified frame models
5. Comparison with the present Danish hand calculation method
6. Conclusions

References

1. Preface and scope

The intention of this report is to throw light on the guidelines for design of timber trussed rafters given in /Riberholt, 1989/. This has been done by intensive analyses of a W-truss for which some different approximations have been investigated. This gives further a numerical background for the simplifications presented in that paper and a justification for the rules for these.

Further, there is given a consequence analysis, by comparing the results of strength verifications based on, partly a simple accepted method, partly the method described in /Riberholt, 1989/.

2. Description of the method of analysis

All the analyses have been carried out for a W-truss with a geometry, loading and timber quality and sizes as shown in figure 2.1. The analyses of the internal forces have been carried out by a plane frame program in order to investigate the effect of different stiffnesses or relative displacements (slip) of the connections. The calculations have been performed on a PC with a 80286 processor. The analyses have been based on timber cross-sections with a width of 50 mm, a top chord height of 150 mm, a bottom chord height of 125 mm and a height of the cross-sections of the diagonals of 75 mm. But the strength verification has been carried out for timber with a cross-sectional width of 47 mm and heights of 147, 122 and 72 mm. This little discrepancy has been chosen in order to have strength utilizations close to unity, and it does not influence the relative comparisons.

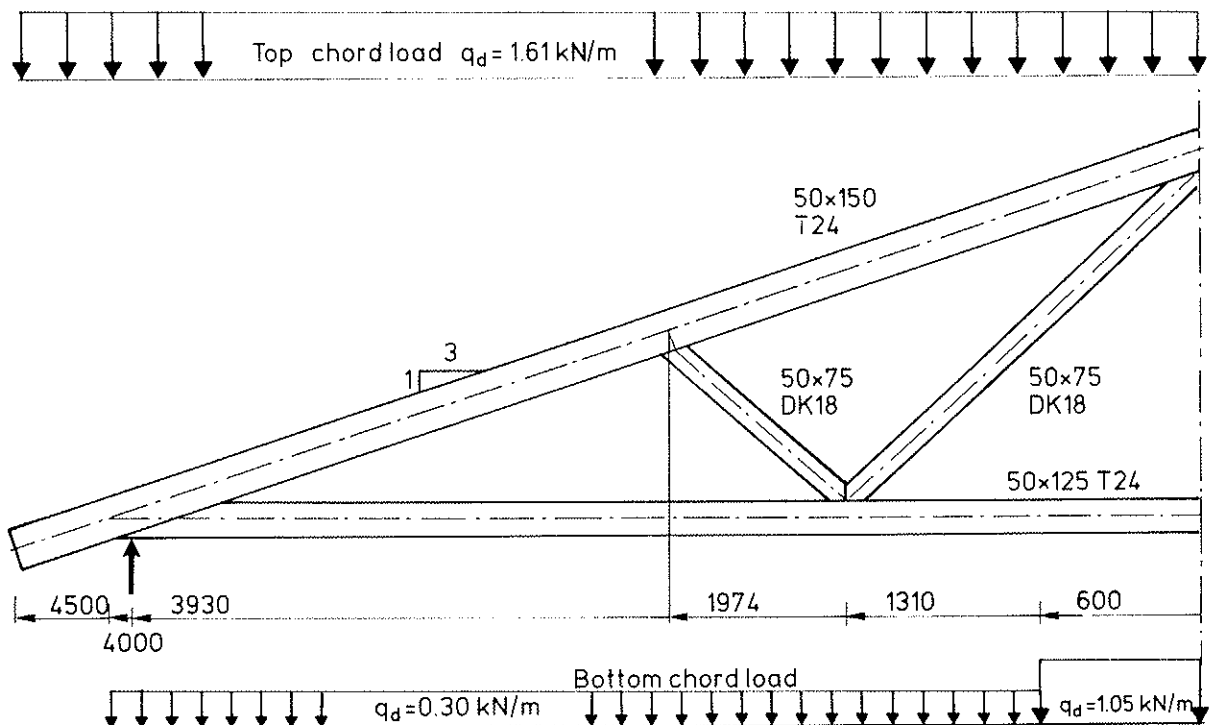


Figure 2.1 W-truss. Geometry, loading and timber grades and sizes. The truss and the loading has been assumed to be symmetrical.

Design basis

All calculations have been based on the Danish set of design codes relevant for timber structures. The loading is in accordance with /DS 409/ and /DS 410/ and the strength verification has been carried out in accordance with /DS 413/, which in principle is very similar to /CIB 1983/.

The stress analyses and strength verifications have been carried out in accordance with /Riberholt, 1989/.

Timber grades

The selected timber grades have for this case (Long term loading, Moisture class 1, Normal safety) the strength and stiffness values given in table 2.1.

Table 2.1 Design values of strength and stiffness for the selected timber grades, MPa

Grade	f_m	f_c	f_t	E_0
T24	11.2	10.7	7.5	8.400
DK18	9.0	8.5	4.3	7.200

Bracing

The top chord has been assumed braced laterally for every 1.00 m. For the compressed diagonal the column length has been assumed to be equal to the distance between the nodal points in the middle of the chords, i.e. 1.00 m.

Connection models

The models of the connections have been created from the guidelines in /Riberholt, 1989/. The connections have been modelled as pinned joints, completely stiff joints and as elastic joints. For some cases the slip in the connections have been modelled by a prescribed slip.

For the W-truss it is typical that the eccentricities in the joints between the chords and the diagonals have almost no effect in the top chord, but a significant one in the

bottom chord. The reason why is that in the connection between the top chord and the diagonal the force in the diagonal is almost perpendicular to the top chord. But in the K-connection between the diagonals and the bottom chord the resulting force transferred to the bottom is parallel to the chord so an eccentricity equal to half the cross-sectional height will result in an essential increase in the bending stress in the bottom chord.

Type of connections

The analyses have all focused on a timber truss with connections made of nail plates, which are the connectors most frequently used. The analyses have comprised both centric and eccentric connections in the truss.

2.1 Overview of varied assumptions

The modelling of the connections in a timber trussed rafter is of importance for the resulting strength utilization of the timber. It has been discussed whether the connections should be modelled as the extreme possibilities: Pinned or completely stiff joints or as the more realistic flexible joints. The last mentioned can be modelled as linear elastic joints or by the introduction of prescribed slip between the timber members.

The following sensitivity analyses have been carried out:

- 1: Variation of the rotational stiffness of the joints from zero to infinity (from pinned joints to completely moment stiff joints). No translations between the members in a connection. The truss was modelled with either eccentric or central connections.
- 2: Variation of all the joint stiffnesses from below "normal" to infinite stiffness.
- 3: The consequences of the proposed increase in the bending strength f_m .
- 4: How simple can a realistic model be?

2.2 Compared results

Concerning the strength of the timber it is obvious to focus on largest value of the Combined Stress Index in a timber member.

$$\text{CSI} = \begin{cases} \frac{\sigma_t}{F_t} + \frac{\sigma_m}{F_m} & \text{for members in tension} \\ \frac{\sigma_c}{k_s F_t} + \frac{\sigma_m}{F_m} & \text{for members in compression} \end{cases} \quad (2.1)$$

Basicly this has been done because this is what controls the dimensions of the timber parts.

It is typical for timber trussed rafters that changes in the model assumptions results in a change of the critical cross-sections, which are those with the largest CSI-values. In some cases, where a change in the model results in a reduction of the largest CSI-value, but too an increase in the second largest CSI-value, the second largest CSI-value has been given so that one gets an impression of how much the dimensions depend on the assumptions.

Since CSI depends on both the axial stress and the bending stress these have been compared too. It can be revealed here that the axial stress in a W-truss is very robust for changes in the model assumptions.

In a few cases the deflections of some selected points have been compared partly in order to investigate the effect on the deflections of flexible connections, partly to evaluate how simple the model can be in order to obtain the same results as from more detailed models.

3. Sensitivity analyses

3.1 The rotational stiffness of the joints

In this investigation the slip (the relative translation) in the connections have been disregarded by using very large translation stiffnesses for the spring elements shown in figure 3.1.

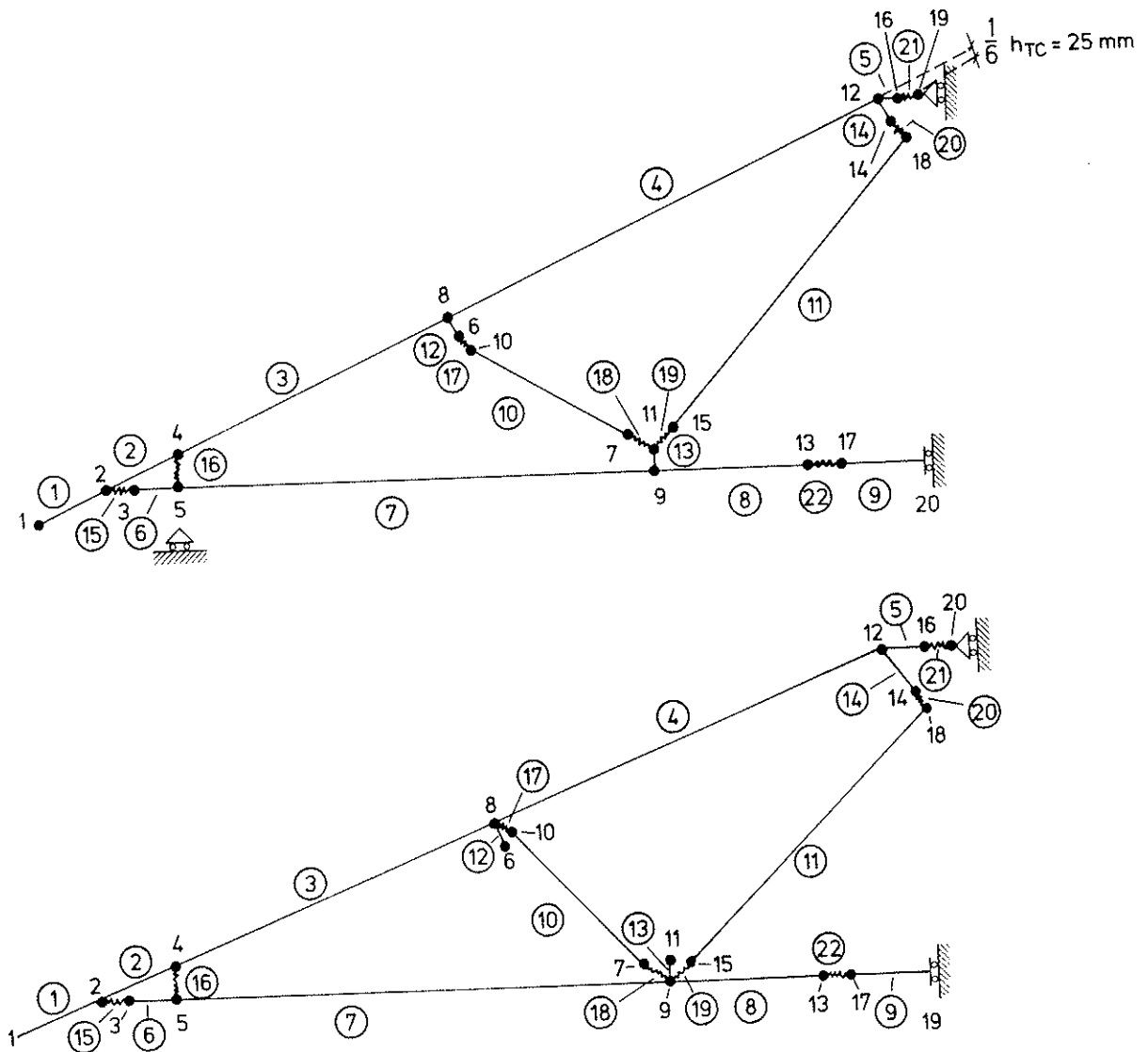


Figure 3.1 Static models in principle. The geometry is distorted in order to show the nodes and elements. Above is shown a W-truss with eccentric connections, below one with central connections.

The rotational stiffness S_θ of the joints have been varied from zero to infinity. The values of S_θ have been determined in relation to the rotational stiffness of the timber members connected to the node (joint). The stiffness has been fixed in relation to the timber member in the connection with the smallest bending stiffness.

$$S_\theta = k \cdot \text{minimum} \left(\frac{EI}{\ell} \right)$$

where k integer factor. Stiffness factor
 E Modulus of elasticity
 I Moment of inertia
 ℓ Bay length of the timber member

It must be realized, that the S_θ represents the rotational stiffness of gusset plates and splices, in which there in reality are two mechanical connections involved in the force transfer from one timber member to another. This influences the stiffness.

In figure 3.2 there is shown CSI values for the W-truss with eccentric and centric joints respectively. In this case the bending strength of cross-sections at peak moments has not been increased.

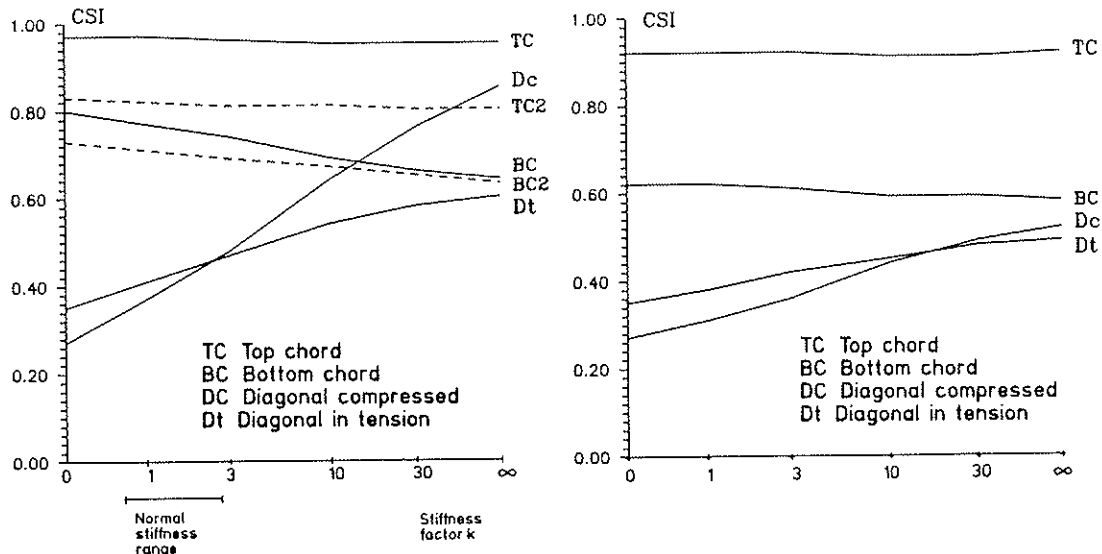


Figure 3.2 Combined Stress Index for varying rotational stiffness of the joints. Left the W-truss with eccentric connections, right with centric connections. The integer number after the chord legends give the rank of the critical cross section, see page 10.

Centric joints

The cross section in the chords with the largest CSI value has for all stiffness values been:

Chord	Bay	Position in bay at
Top chord	Lower	Heel joint
Bottom chord	Middle	Middle

For the top chord a reduction in the support eccentricity will reduce CSI at the heel joint and increase it in the middle of the lower bay. But the employed support eccentricity $4.000 - 3.930 = 70$ mm is very small and can hardly be reduced. Further $CSI = 0.81$ in the middle of the lower bay for $k = 1$, so a reduction in the support eccentricity will result in a decrease in CSI at the heel joint but the dimension of the top chord will be the same because of the increase in CSI at the middle of the lower bay so that this cross section becomes critical.

It can be seen that for the chords of a W-truss with centric connections CSI is influenced only marginally by the rotational stiffness of the joints. For the diagonals there is a certain effect. Meanwhile if one wants to simplify the static model it seems reasonable to assume:

$$\begin{array}{ll} \text{Pinned joints} & \text{if } S_{\theta} < 3 \frac{EI}{l} \\ \text{Completely stiff joints} & \text{if } S_{\theta} > 3 \frac{EI}{l} \end{array}$$

From figure 3.3 it can be seen that the stresses from the axial forces are almost independent of the rotational stiffness of the joints. The same is the case for the bending stresses in the chords, while there is an effect for the bending stresses in the diagonals, because they have such a little cross section that even small moments result in large stresses.

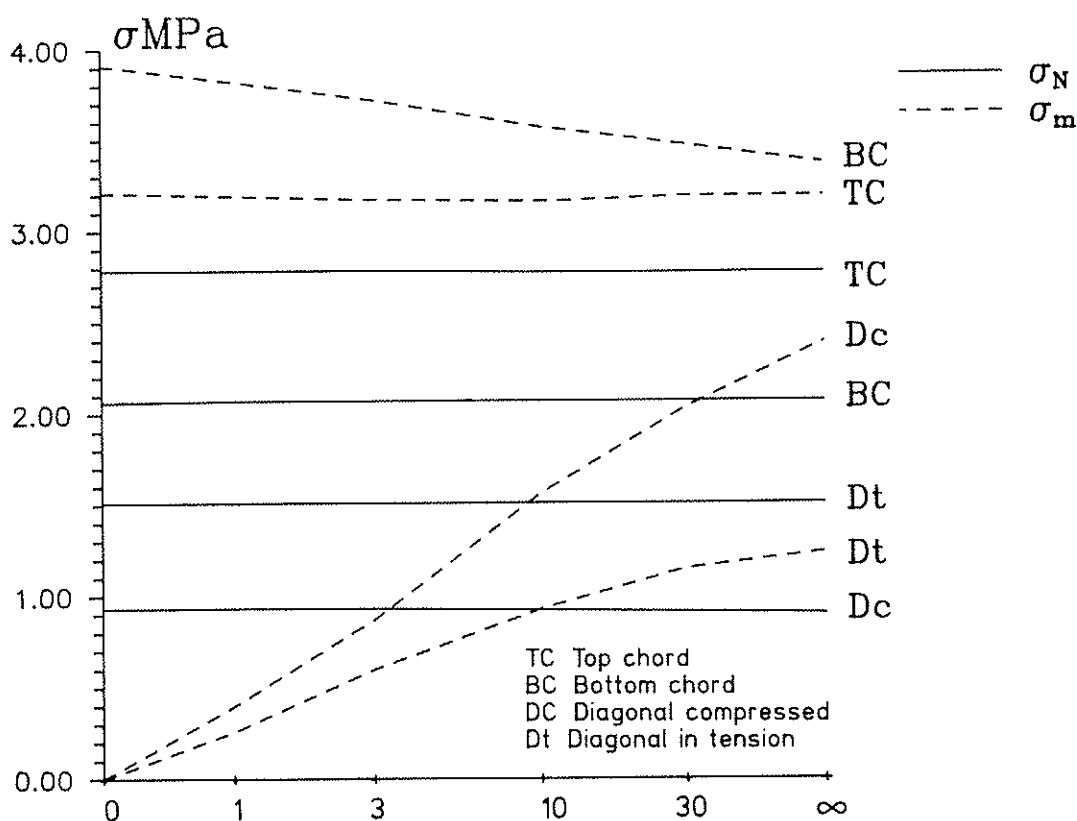


Figure 3.3 Stresses from axial force and moment for varying rotational stiffness of the joint connections. Centric joints.

Eccentric joints

In this case cross sections in the chords with the largest CSI value has for all stiffness values been:

Chord	Rank	Bay	Position in bay at
Top chord	1	Lower	Heel joint
	2	Upper	Middle
Bottom chord	1	Left	K-node
	2	Middle	Middle

The rank signifies the cross-sections with the largest and second largest CSI-values. In figure 3.2 the rank is shown with an integer after the chord abbreviation.

It can be seen from figures 3.2 and 3.4 that the influence of the rotational stiffness of

the joints is marginal for the top chord, while it has a certain effect for the bottom chord. The reason why is that the diagonals together with the bottom chord carry the eccentricity moments in the joints so that the bending stress in the bottom chord is reduced when the rotational stiffness of the joint is increased. As a consequence the CSI of the diagonals increases when the rotational stiffness is increased.

If one wants to simplify the static model it seems reasonable to employ pinned joints or completely stiff joints in accordance with the assumptions for centric connections.

In the figures 3.4 and 3.5 more details are given. From these it can be seen that the stresses from the axial forces are almost independent of the rotational stiffness of the joints, while there is an influence for the bending stresses in the bottom chord and the diagonals.

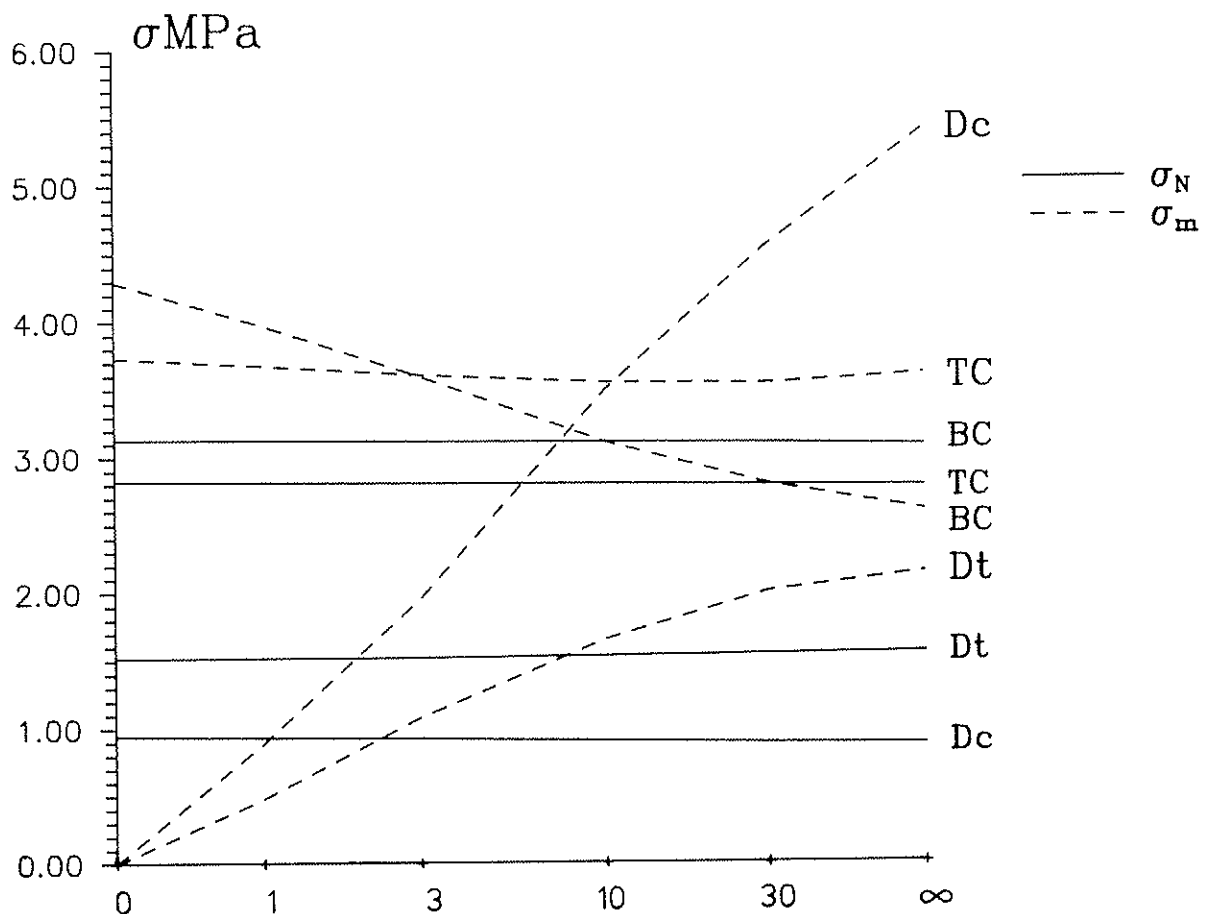


Figure 3.4 Stresses from axial force and moment for varying rotational stiffness of the joint connections. Eccentric joints.

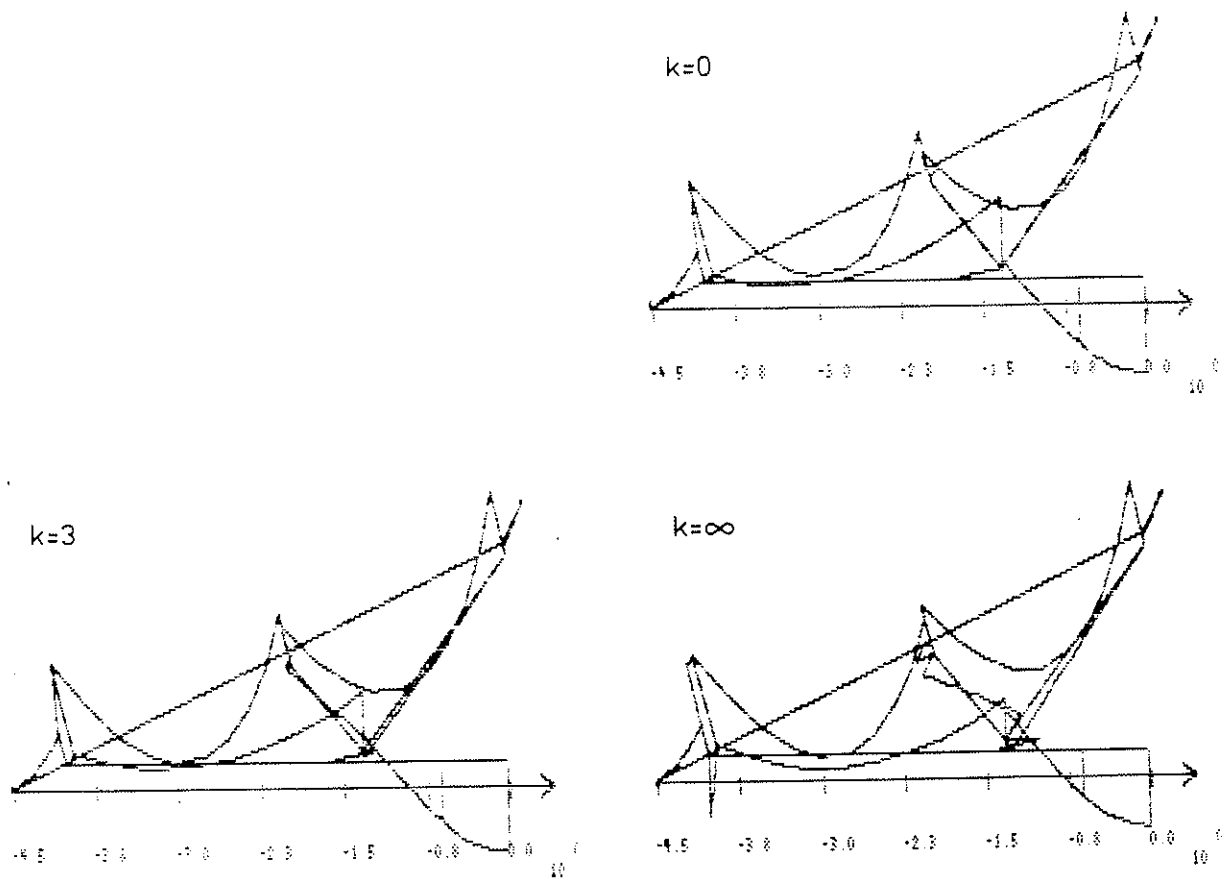


Figure 3.5 Moment distribution in the truss for $k = 0$ (pinned joints), 3 and ∞ .

3.2 Variation of the joint stiffnesses.

In this case the joint stiffnesses, both the translational and the rotational, have been varied from below normal to infinite stiffness (completely stiff joints).

Based on the guidelines in /Noren, 1981/ a "normal set of joint stiffnesses" have been determined. Since the nail plate connections have a non-linear stress-deformation relation and that the program only can analyse linear elastic members, it has been necessary to employ a secant modulus for the joint stiffnesses. It has been estimated that

for the case where failure occurs in the timber parts the stresses in the connections are only 60–80% of the short term strength. This is the background for the stiffness values given in table 3.1. This table also gives the calculated slips (relative displacements) of the joints. Further, analyses have been carried out with joint stiffnesses, which all approximately are proportional to the "normal set of stiffnesses", they were

Low	Normal / 3
High	Normal · 3
Extra high	Normal · 10

Table 3.1 Normal set of joint stiffnesses and calculated slips, that is relative displacements in the joints.

Connection	Spring no.	Stiffnesses:		Slip mm
		Rel. disp kN/mm	Rotation kNm/rad	
Heel joint	15	20	20	0.9
Diagonals–chords	17 and 18	4	4	0.6
	19 and 20	4	4	1.2
Ridge, horizontal	21	15	10	1.1
Splice in bottom chord	22	15	15	0.8

Since the W–truss with centric connection is less influenced by the joint stiffnesses than the truss with eccentric joints, only the latter has been investigated. Further this type is used commonly in praxis.

In figure 3.6 there is shown the Combined Stress Index for varying joint stiffnesses. For the chords there is shown two curves of CSI–values, partly one where the bending strength increase at moment peaks has not been considered, and partly one where it has been taken into account by an increase of 20%. The differences in these curves are in the range of 0 to 10%.

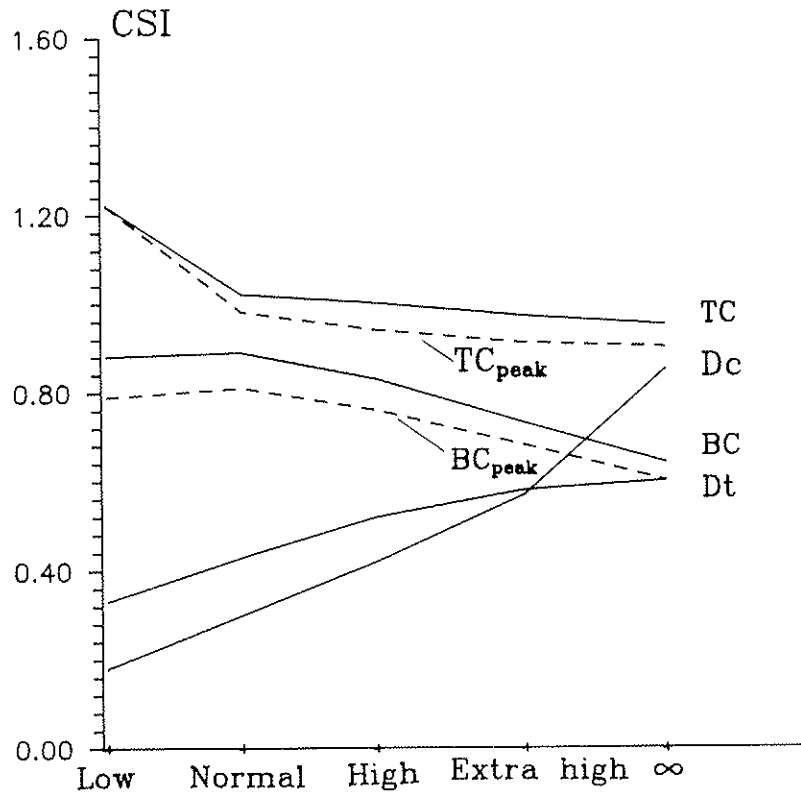


Figure 3.6 Combined Stress Index for varying joint stiffnesses. For the chords two curves have been drawn for each, one without and one with an increase in the bending strength of 20% at moment peaks. The latter has an extension "peak".

The critical cross-section in the top chord is for low and normal joint stiffness situated in the middle of the upper bay, but for larger stiffnesses this changes to the cross-section at the heel joint. For the bottom chord the critical cross-section is always at the K-joint. Figure 3.7, right, gives an overview for a truss with a normal joint stiffness.

In this figure there is shown the axial and bending stresses for varying stiffness of the joints. Further there is shown the moment distribution and the values of CSI are written at critical cross sections of the chords. Here CSI is calculated partly without and with increase in the bending strength at moment peaks. The smallest CSI-values are those with increased bending strength.

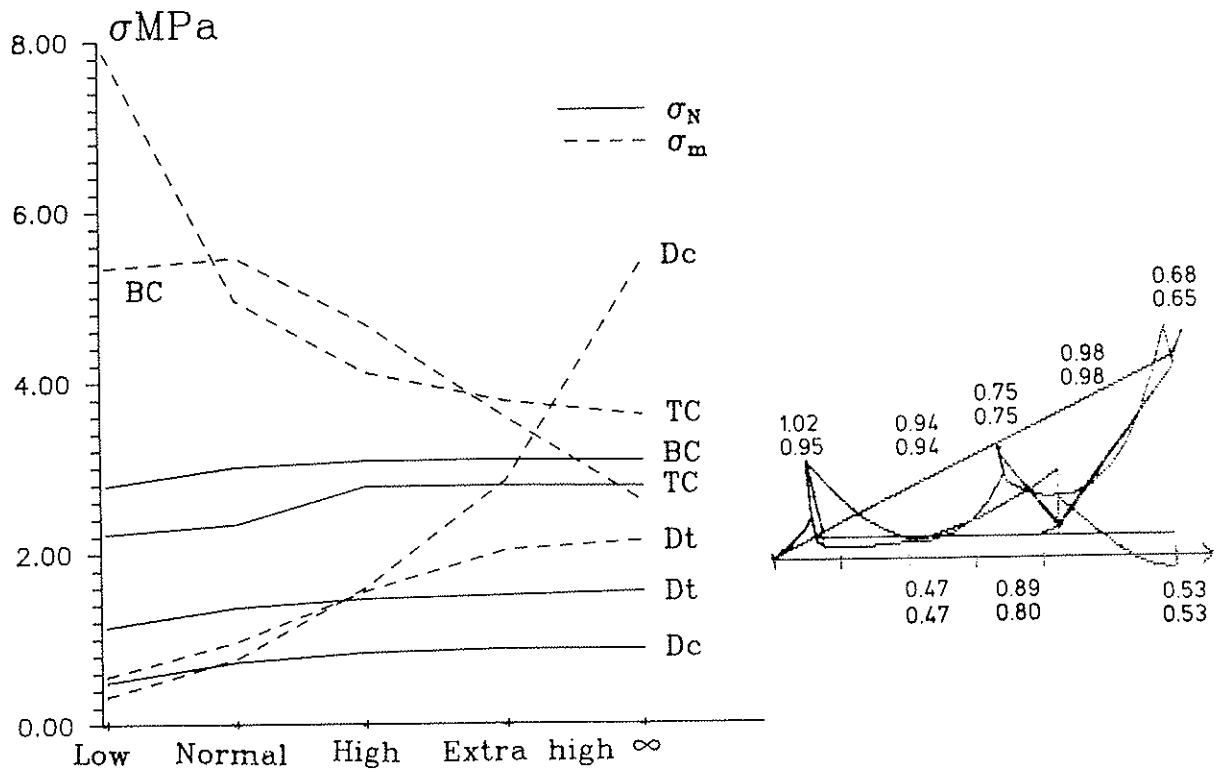


Figure 3.7 Left: Sensitivity curves for axial and bending stresses. Right: Moment distribution in a W-truss with normal joint stiffness plus CSI-values with and without increase in the bending strength at moment peaks.

The deflections are of course influenced directly by the joint stiffnesses, as can be seen from figure 3.8. For normal joint stiffness the influence is essential, deformations in the joints contribute more to the deflection than the deformations of the timber.

For a W-truss with a larger support eccentricity the increase in the bending strength has a more pronounced effect on the strength utilization of the cross-section at the heel joint. Figure 3.9 shows the CSI-values for a W-truss with a support eccentricity of 0.15 m. The values are given with and without increase in f_m at moment peaks.

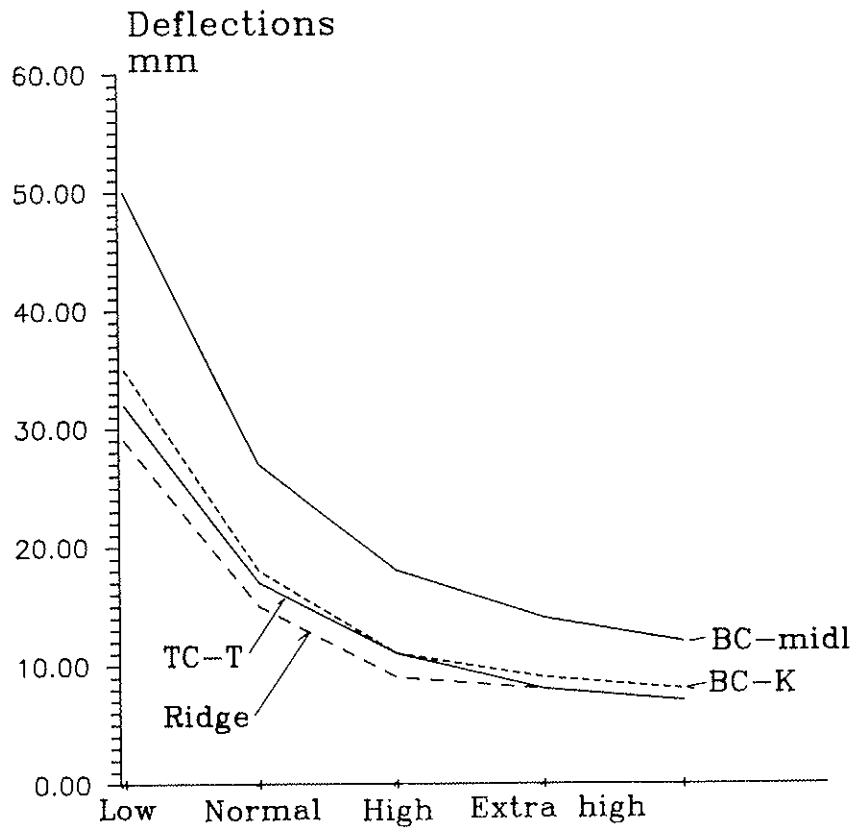


Figure 3.8

The influence of joint stiffnesses on deflections at the ridge, the T-joint in the top chord, the K-joint and the middle of the bottom chord.

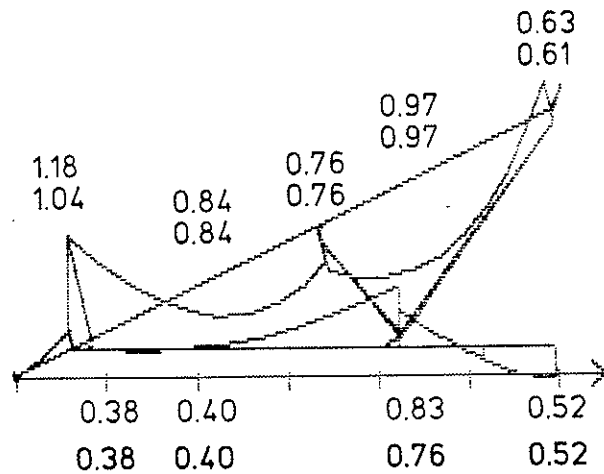


Figure 3.9

Combined Stress Index for the W-truss with a support eccentricity of 0.15 m, with normal joint stiffnesses, with and without increase in the bending strength, 30% at the heel joint cross-section in the top chord, 20% at other moment peaks.

4. Simplified frame models.

In this section two simplified frame models have been investigated. The simplification has resulted in that the number of nodes and thereby the number of degrees of freedom has been reduced to approximately the half.

Only a truss with eccentric joints has been investigated, because with centric joints it is very easy to set up a similar simple model, which is in agreement with the more detailed model shown in figure 3.1. The slip in the joints can be modelled by a prescribed slip.

In the simple model the force transfer by the nail plate at the heel joint has been modelled by a pinned joint positioned at the joint between the timber parts, and the contact stresses between the chords has been modelled by a spring. The eccentric connections have been modelled detailed, and at the ridge, there is introduced an eccentricity resulting in a negative moment at the ridge. The slip in the joints have been considered by a prescribed slip in the heel joint, the ridge and the splice plate with the values given in table 3.1, which are those found for a truss with normal stiffness. So the results should be compared with those in section 3.2 for a W-truss with normal joint stiffnesses.

In the extra simplified model the transfer of the internal forces at the heel joint has been modelled more crude. In the T-joint of the top chord the eccentricity has been disregarded and so the beneficial effect of the eccentricity in the ridge connection.

For both models analyses have been carried out for pinned joints as shown and for completely stiff joints. Further the slip in the joints have either been disregarded or taken into account by prescribed slips in the selected joints mentioned previously.

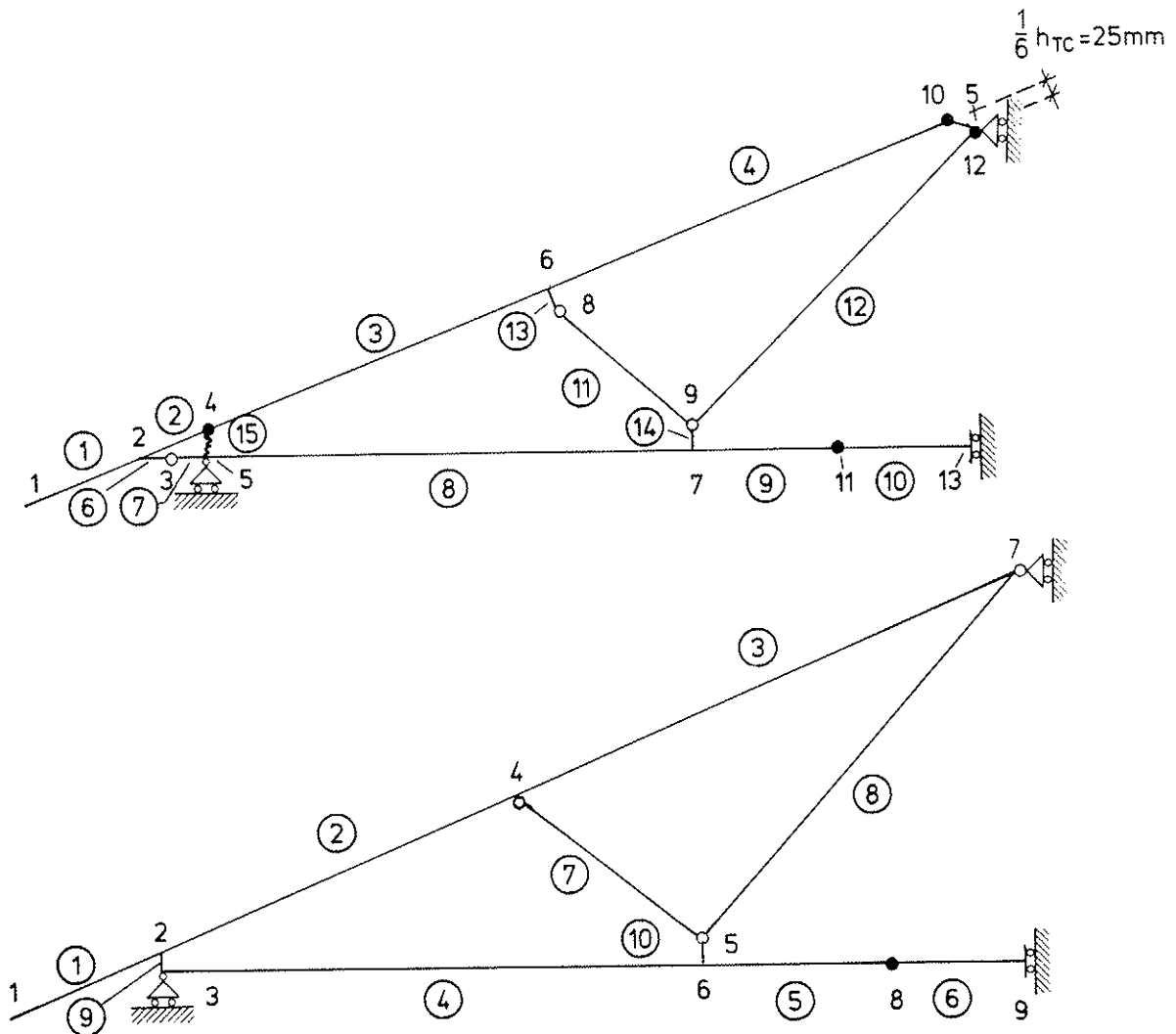


Figure 4.1 Frame models. Top: A simplified model, Below: An extra simplified model.

The bending strength of the chords has been increased by 20% in cross sections at moment peaks.

For the sake of simplicity it is an advantage to consider slip in the joints by a prescribed slip between the timber member and the global node. In this way slip can be incorporated in the analysis without the introduction of extra nodes or degrees of freedom.

Table 4.1 Simple model results. Axial and bending stresses in MPa, CSI and deflections in mm in the W-truss with either pinned joints or stiff joints and with or without prescribed slip in the joints.

		Pinned joints		Stiff joints	
		No slip	Slip	No slip	Slip
Centric connections					
Top chord	σ_N	-2.77	-2.72	-2.76	-2.71
	σ_m	3.82	3.79	3.52	3.50
	CSI	0.92	0.90	0.89	0.88
Bottom chord	σ_N	2.11	2.09	2.11	2.10
	σ_m	3.54	4.21	3.28	3.97
	CSI	0.60	0.66	0.57	0.63
Diagonal left	σ_N	-0.89	-0.84	-0.88	-0.83
	σ_m	0	0	2.76	2.64
	CSI	0.26	0.24	0.56	0.53
Diagonal middle	σ_N	1.44	2.38	1.46	1.39
	σ_m	0	0	1.01	1.59
	CSI	0.34	0.32	0.45	0.50
Deflec- tions	TC top	7	15	7	15
	TC middle	7	13	7	13
mm	BC middle	11	19	10	19
	BC node	7	15	7	15

Table 4.1 continued

		Pinned joints		Stiff joints	
		No slip	Slip	No slip	Slip
Eccentric connections					
Top chord	σ_N	-2.81	-2.76	-2.77	-2.72
	σ_m	4.33	4.30	3.80	3.76
	CSI	0.96	0.95	0.91	0.90
Bottom chord	σ_N	2.12	2.07	2.10	2.09
	σ_m	4.37	5.58	3.92	4.58
	CSI	0.74	0.77	0.63	0.69
Diagonal	σ_N	-0.90	-0.84	-0.85	-0.80
	σ_m	0	0	5.24	4.79
	CSI	0.26	0.24	0.82	0.76
Diagonal	σ_N	1.46	1.40	1.50	1.43
	σ_m	0	0	2.12	2.71
	CSI	0.34	0.33	0.59	0.63
Deflection	TC top	7	15	7	15
	TC middle	8	14	7	13
mm	BC middle	13	22	12	20
	BC node	8	15	8	15

Table 4.2 Extra simple model results. Axial and bending stresses in MPa, CSI and deflections in mm in the W-truss with either pinned joints or stiff joints and with or without prescribed slip in the joints

		Pinned joints		Stiff joints	
		No slip	Slip	No slip	Slip
Centric connections					
Top chord	σ_N	-2.64	-2.59	-2.59	-2.59
	σ_m	3.69	3.70	3.64	3.61
	CSI	0.88	0.87	0.86	0.85
Bot. chord	σ_N	1.95	1.94	2.05	2.03
	σ_m	3.84	4.58	3.32	4.02
	CSI	0.60	0.67	0.57	0.63
Diag.	σ_N	-0.89	-0.84	-0.72	-0.69
	σ_m	0	0	2.23	2.12
	CSI	0.26	0.24	0.45	0.43
Diag.	σ_N	1.42	1.36	1.27	1.23
	σ_m	0	0	1.48	1.93
	CSI	0.33	0.32	0.46	0.50
Deflec. mm	TC top	6	14	6	14
	TC middle	6	12	6	11
	BC middle	10	18	9	17
	BC node	6	13	6	13

Table 4.2 continued

		Pinned joints		Stiff joints	
		No slip	Slip	No slip	Slip
Eccentric connections					
Top chord	σ_N	-2.66	-2.61	-2.59	-2.54
	σ_m	4.27	4.25	3.94	3.90
	CSI	0.92	0.91	0.88	0.87
Bot chord	σ_N	2.93	1.93	2.05	2.03
	σ_m	4.24	5.61	3.84	4.52
	CSI	0.71	0.76	0.62	0.67
Diag. left	σ_N	-0.87	-0.82	-0.68	-0.65
	σ_m	0	0	4.07	3.81
	CSI	0.25	0.23	0.65	0.61
Diag. mid.	σ_N	1.45	1.38	1.29	1.24
	σ_m	0	0	2.48	2.95
	CSI	0.34	0.32	0.58	0.62
Deflec. mm	TC top	6	14	6	12
	TC middle	6	12	6	14
	BC middle	12	20	10	14
	BC node	7	14	6	18

In all the cases the cross-sections with the largest CSI-values are situated in:

Top chord: Lower bay at the heel joint.
 Bottom chord: Middle bay at the middle except for pinned joints and no slip, where it was at the K-node.

This result is rather similar to that obtained in the more detailed model. But some differences exist.

From a comparison with the results for the detailed model in chapter 3.2 with normal joint stiffnesses it can be seen that the agreement in CSI-values is:

Best	Poorer
Pinned joints	Completely stiff joints
Simple model	Extra simple model
Slip in the joints	No slip

Table 4.3 Relative deviations in CSI-values obtained by the simple models with pinned eccentric joints as compared with the detailed model with normal joint stiffnesses.

	Simple model		Extra simple model	
	No slip	Slip	No slip	Slip
Top chord	- 2%	- 3%	- 8%	- 9%
Bottom chord	- 9%	- 5%	-19%	- 9%
Diagonals: Compressed	-13%	-20%	-13%	-20%
Tensile	-21%	-23%	-23%	-26%

The deviations given in table 4.3 should be acceptable for the simple model when slip in the joints is considered.

5. Comparison with the present Danish hand calculation method

The present Danish hand calculation method is described in /Larsen & Riberholt, 1988/. It is similar to the method proposed in /Riberholt, 1984/, which transform the distributed load to concentrated nodal forces so that the axial forces can be determined from a lattice model, while the moments in the chords can be determined by moment coefficients, here 0.1 in the top chord, 0.1 in the outer bay of the bottom chord and 0.08 in the middle bay of the bottom chord.

The results of this hand calculation method are in table 5.1 compared with those of the models dealt with in this paper. The comparison is carried out only for a W-truss with

centric connections, since the hand calculations have this as an assumption. The frame models have been analyzed either by normal joint stiffnesses or by prescribed normal slips in the connections.

Table 5.1 Combined Stress Index in some cross-sections calculated by 4 different models/methods. W-truss with centric connections.

		Hand cal.	Detailed model	Simple model	Extra
simple					
Top chord	Low bay	0.99	0.92	0.83	0.74
	Up. bay		0.92	0.82	0.87
	Low node	0.99	0.91	0.90	0.87
Bottom chord:	K-node		0.63	0.49	0.49
	Mid. bay	0.71	0.51	0.66	0.67
Diagonal:	compres.	0.27	0.26	0.24	0.24
	tensile	0.35	0.39	0.32	0.32

It appears from table 5.1 that there is a reasonable agreement between the maximum CSI-values for the different timber parts. Further the frame model results are a little conservative compared with the present Danish hand calculation method. They should thus be applicable for praxis, and can be employed for an optimal geometric design of the W-truss, which the hand calculation method can't be used to, because it is limited by the geometric assumptions of equal bay length.

6. Conclusions

For a W-truss it appears that the following conclusions are valid:

- A: If the rotational stiffness S_{θ} of a joint fulfill the requirement below, then it is a reasonable simplification to assume that the connection is completely stiff for rotations if

$$S_{\theta} > \text{minimum} \left\{ 3 \frac{EI}{l} \right\}$$

where EI/ℓ is a stiffness measure for the adjacent timber members with bay length ℓ

- B: The relative displacements (slip) between the timber parts in the joints can be considered by spring elements or by prescribed slip. The max Combined Stress Index in the timber parts is relatively robust for practical variations in the stiffness of the joints.
- C: Even crude frame models of the truss give Combined Stress Indices similar to those obtained by more detailed models.
- D: The proposal to increase the bending strength of the chords at moment peaks result in a decrease in the CSI-values of typical 5–10%, and it results in truss designs, which have been used succesfully over a long period.
- E: The proposed frame models give Combined Stress Indices similar to those obtained by a Danish hand calculation method used for many years. The hand calculation method is a little more conservative.

The guidelines given in /Riberholt, 1989/ seems thus to be applicable for practical calculations.

References

DS 409 Safety requirements for structures. DIF Code of practice. 1. edition 1982.

DS 410 Loads on structures. DIF Code of practice. 3. edition 1982.

DS 413 Structural use of timber. DIF Code of practice. 4. edition 1982.

CIB 1983 Structural timber design code. Publication 66, Working group W18A.

Riberholt, Hilmer. 1989. Guidelines for design of timber trussed rafters. September and November 1989. CIB W18A/22-14-

Noren, Bengt. 1981. Design of joints with nail plates. CIB W18/14-7-1.

Larsen, H.J. & Riberholt, H. 1988. SBI-anvisning 135, 2. edition. Timber structures, calculations, in Danish.

Riberholt, H. 1984. Simplified static analysis and dimensioning of trussed rafters. CIB W18/17-14-2.

INTERNATIONAL COUNCIL FOR BUILDING RESEARCH STUDIES AND DOCUMENTATION
WORKING COMMISSION W18A - TIMBER STRUCTURES

PROPOSAL FOR EUROCODE 5 TEXT ON TIMBER TRUSSED RAFTERS

by

H Riberholt
Technical University of Denmark
Denmark

MEETING TWENTY - THREE

LISBON

PORTUGAL

SEPTEMBER 1990

Rider to section 4.1 Deflections. Or a separate section of 5.25.

For fully triangulated trusses the local deflection between the nodes should not exceed 1/300 of the bay length for either dead load or variable actions.

5.2.5 Trusses

Trusses may be analysed as frame structures where the influence of eccentricities, deformations of timber elements, stiffness of the joints, and stress redistribution are taken into consideration in the determination of the resultant stresses.

/* Horizontal load/deflection. Peter Ross will write a section how it should be considered by means of springs. May be guidelines for $\max u_{\text{horizontal}}$ */

Frame analysis

The analysis may be carried out assuming that the timber elements are linear elastic with a stiffness based on $E_{0,\text{mean}}$ divided by k_{creep} given in section 4.1. The load-slip relation of the joints are given in section 5.2.4 or they shall be assessed from standardized short term test data (ISO 6891, ISO/DIS 8969 or similar) published by approval systems (e.g. UEAtc or European Technical Approvals). If the static analysis is used for strength verification then the load-slip relation may be taken as a secant with the top point fixed to a load level of 60 per cent of the maximum load, and the stiffness and the slip shall be modified by the creep factor in table 5.2.4.6.

$$\begin{aligned}\text{Stiffness} &= (\text{Stiffness from test})/k_{\text{creep}} \\ \text{Slip} &= (\text{Slip from test}) k_{\text{creep}}\end{aligned}$$

The modelling of the joints may be simplified to pinned joints if the essential slip of the joints is considered by prescribed values. Annex X.1 gives guidelines for the modelling.

Simplified analysis

If the truss is a fully triangulated truss and external statical determinate then the axial forces may be determined from a lattice model with pinned joints. The bending moments should be determined considering continuity of the members and eccentricities e.g. in the connections or at supports. Annex X.2 gives guidelines.

Strength verification

The strength verification of the timber shall be carried out as described in section 5.1. Annex X.3 gives guidelines for the effective column length of the members. Further the bending strength of a member may be increased for cross sections at moment peaks if the internal forces and moments can be redistributed if such a cross section fails and if the eccentricities in the connections and at supports are taken into account.

Annex X.3 gives more details.

The strength verification of the joints shall be carried out as described in section 5.3. For nail plates the strength verification is described in Annex X.4.

Rider to section 6.6 Transportation and erection

For timber trussed rafters guidelines are given in Annex X.5.

Truss annexes:

- | | |
|------------|--|
| Annex X.1. | Guidelines for the stress analysis of timber trussed rafters modelled as plane frames. |
| Annex X.2. | Guidelines for the stress analysis of statical determinate fully triangulated trussed rafters of timber. |
| Annex X.3. | Strength verification of the timber in trussed rafters. Special effects. |
| Annex X.4. | Strength verification of nail plate connections in timber trussed rafters. |
| Annex X.5. | Production and practice of timber trussed rafters. (This is either a supplement to or should be incorporated in EN TC124.208, Production of timber trusses). The Truss Committee has considered this and finds that the necessary precautions are expected to be incorporated in EN TC124.208. |

Euro Code 5, Timber Structures

Annex X.1

Guidelines for the stress analysis of timber trussed rafters modelled as plane frames.

Truss Committee / Hilmer Riberholt

June 1990

Table of contents.

	Page	
1.	GENERAL	3
1.1	Object	3
1.2	Definitions	3
1.3	Symbols	4
2.	THE FRAME MODEL	4
2.1	General description of the elements and the methods of the model	4
2.2	Description of the elements	4
2.2.1	Beam elements	4
2.2.2	Fictitious beam elements	7
2.2.3	Spring elements	8
2.3	Description of the analysis methods	9
2.3.1	Loadings	9
2.3.2	Supports	9
2.3.3	Modelling the slip in the connections	10
	Enclosure 1. Connection models	11
E1.1	Connections between 2 timber parts	11
E1.2	Connections between 3 timber parts	13
E1.3	Connections between several timber parts	14
	Enclosure 2. Connections where slip shall be considered	15
E2.1	Truss configurations not sensitive to slip	15
E2.2	Truss configurations sensitive to slip	16

1. GENERAL

1.1 Object

Static analysis of a truss.

The object of the guidelines is to constitute a basis for the static analysis of timber trussed rafters in the serviceability state or the ultimate state.

If it is desired to use an alternative analysis different from the methods in the guidelines, this may be done, provided that the necessary justification is produced to show that the alternative gives a description of the static behaviour which is just as good as that achieved by the methods in the guidelines.

The guidelines concentrate on the analysis of plane timber trusses with nail plate connections by means of practical available plane frame programs. But the methods can too be applied to trusses with other types of connectors if the method is adapted to their static behaviour. Further they can be employed in more general models, which for example take into account spatial behaviour, trusses made of built up beams, non-linearities in the material or in the geometry.

1.2 Definitions

Bay:

Structure (timber beam) between two neighbouring nodes.

Beam element:

An element, which models a timber part.

Connections:

Domain where timber parts and/or nail plates are in contact in such a way that forces may be transferred between the parts.

Fictitious beam element:

Beam element, employed in connections in order to model their static behaviour.

Node:

Intersection point of system lines of beam elements.

Spring element:

An element, which can be used to model the mutual translation and rotation between timber parts in a connection.

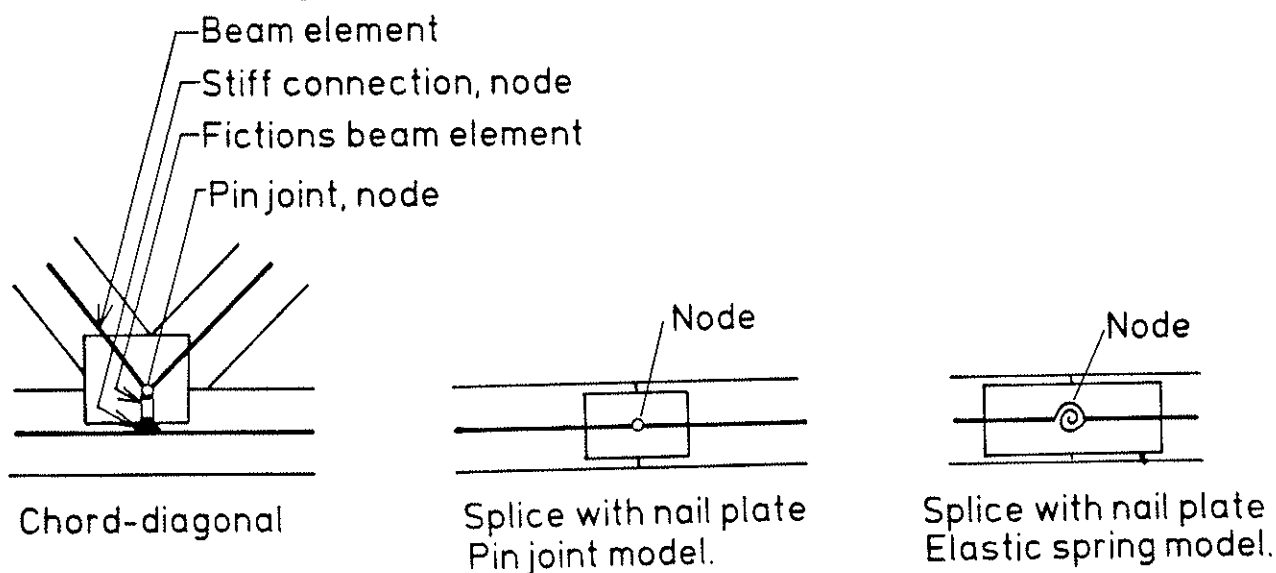


Figure 1.2 Examples of connection models.

1.3 Symbols

The definitions of the symbols are the same as given in /Euro Code 5, Timber Structures/ or they are defined locally in the text.

2. THE FRAME MODEL

2.1 General description of the elements and the methods of the model

The frame model is built up by means of some elements. Straight beam elements model the timber parts, fictitious beam elements model some constraints (ties) in or static behaviour of the connections and also spring elements model the elastic behaviour of the connections. In these guidelines the static models of the connection do not directly consider rotational stiffness and moment transfer in the connections, the connections are modelled as pinned joints. Meanwhile if the necessary data exist then moment transfer can be taken into account. Further splices in the chords may in some cases be modelled as completely rotational (moment) stiff.

The static properties of all elements shall be those, which are expected to be valid for the real structure. This means that the stiffness values or prescribed deformations shall be mean values. For nail plates these can be determined from calculations calibrated from tests.

All the elements can be linear elastic, but elements based on material non-linearity will with realistic material properties reflect reality better.

The deformation in the connections can be considered by means of a prescribed slip, elastic spring elements or by means of a combination of prescribed slip and elastic spring elements.

Geometric non-linearity (column effect) can be disregarded by the frame analysis if it is taken into account in the strength verification of the members.

If a geometric non-linear frame program is used for the analysis then the stiffness parameters shall be given the design values for the actual conditions and imperfections shall be considered.

2.2 Description of the elements

Beam elements are intended used for the modelling of the timber, fictitious beam elements are for the static behaviour of the connections and spring elements are for the slip in the connections. Further, spring elements can be used for the modelling of the mutual translation and rotation in chord splices.

2.2.1 Beam elements

The beam elements are intended used for the modelling of solid timber, but glued built up beams can be modelled similar. For built up beams where a slip can occur between the timber members, this shall be taken into account.

The timber parts are modelled as straight beam elements. These shall allow for the deformations originating in axial strain plus curvature of the timber parts.

Geometry

As a principal rule the system lines of the beam elements shall coincide with the centre of gravity of the timber parts. For the chords this shall always be the case.

In the diagonals the system lines of the beam elements do not need to coincide with the centre of gravity of the timber parts. However, the system lines shall lie within the cross section of the timber. In the case that there is not coinciding this must be taken into account at the strength verification, for example by adding an eccentricity moment.

Stiffness constants

The stiffness constants EA and EI are calculated based on the actual timber dimensions and qualities. For built up beams, of which the different parts have different moduli of elasticity, transformed cross-sectional constants may be employed.

For a bay member with a changing or variable cross section this can be modelled by several beam elements each with a constant cross section and with a stiffness adapted to the real member.

Degrees of freedom in the coupling to other elements

Connections between beam elements are modelled in the following ways depending on the static behaviour of the real connection if such one exists.

Pinned connections

Pinned connections and prescribed slip(s)

Completely stiff

Pinned connections

A pinned connection shall be used in general. The position of the pinned connection shall reflect the load transfer in the connection. Enclosure 1 gives some examples of the position for different types of nail plate connections.

Further the deformations of a connection can be modelled by a prescribed slip between the beam elements connected to the node in the connection.

Completely stiff connections

If two connected beam elements model the very same timber part they shall be connected completely stiff.

Nail plate splice connections in the chords can be modelled as completely rotational stiff if their real rotational deformation has no essential effect on the distribution of the internal stresses. This is the case in the following two cases.

- A: Splice connections positioned so that the chords would be stable even if all the splices acted as pinned joints. Further the splice connections shall only be subjected to a moment which is less than one third of the maximum chord moment for all loading cases and provided it is verified that the nail plate connection has sufficient load carrying capacity for the combined load of force and moment.
- B: Splice connections, which are designed for the actual internal forces and moments increased by 50 per cent.

2.2.2 Fictitious beam elements

A fictitious beam element can be employed to reflect the static behaviour of a connection. It can thus be used to model eccentricities or some constraints in the connections, for example originating in contact between timber parts or ties from nail plates. The use of fictitious beam elements is illustrated in Enclosure 1.

Note 1: If the increased bending strength – according to Annex X.3– is to be utilized then fictitious beam elements or similar shall be used to model any eccentricity.

Geometry

The system line of a fictitious beam element shall as well as possible coincide with the force transfer path.

Stiffness Constants

The result of the analysis is normally not sensitive to the values of the axial and bending stiffness constants EA and EI . The reason why is typical that the fictitious elements are short. So frequently they can be assigned stiffnesses of approximately the same order as that of the adjacent beam elements. Further, if the two nodes connected by the fictitious beam elements lie within the cross section of a timber piece, then the stiffness constants can be infinite large or a so-called eccentric beam element can be employed.

The axial stiffness constant EA can be calculated from the stiffness of a may be block of wood subjected to compression or a may be nail plate subjected to tension.

The bending stiffness constant EI can be determined in a similar way. If the fictitious beam element is connected to both nodes by pinned joints the value of EI may be chosen arbitrarily.

Degrees of freedom in the coupling to other elements

Generally the coupling should be modelled by a pinned connection. But completely stiff

connections can be used for the modelling of internal eccentricities, see for example enclosure 1.

2.2.3 Spring elements

A spring element can be employed to model slip in a connection or a moment transferring splice connection in a chord.

A simple spring element, which connect two coincident nodes, fulfil the static and kinematic principles if it is assigned translation stiffnesses in two ortogonal directions. But joints can also can be modelled by connection elements with multiple non-coincident nodes provided the static and kinematic principles are fulfilled.

Geometry

The spring element should be placed in the middle of the connection. It shall in no case be placed outside the connection area.

Stiffness Constants

The values of the stiffness constants shall be based on measurements. They shall be determined on secant moduli reflecting the actual stress level in the connection, and they shall consider creep of the connection.

The two points determining the secant shall be partly origo of the load-slip curve partly the slip at the actual stress level.

In a fully stressed connection the secant modulus shall be based on the stress level defined in section 2.3.3. If the stress level is lower then this can be taken into account by an increase in the secant modulus.

It is acceptable to assume, that the stiffness for the relative deformations are independent of each other. This means for example that the stiffness for a relative displacement in one direction can be assumed independent of the force in the other ortogonal direction.

For a moment transferring splice connection in a chord the influence of a may be gap between the timber members shall be considered by the determination of the stiffness constants for the mutual translation and rotation.

Degrees of freedom in the coupling to other elements

The spring elements should be coupled completely stiff to the nodes.

2.3 Description of the analysis methods.

A static model consists of the elements described in section 2.2, and they are connected in accordance with the given guidelines. In this section guidelines are given for the loading, the support and the consideration of the slip in the connections.

Since the purpose of the static analysis is different for the serviceability state and for the ultimate state there can be differences in the approximations and therefore different static models for the two states.

2.3.1 Loadings

In principle, the truss shall be subjected to the loads as they act in reality. For example, in a roof with purlins, the truss must in principle be loaded by concentrated forces.

A row of concentrated forces may be equated to a distributed line load if the difference between the moments from the two loading cases is less than 10%, or if it is on the safe side.

Note: For lattice trusses the concentrated loads from purlins with equidistant distances can be equated with a distributed load if the distance between the purlins is less than 40% of the bay length.

Larger concentrated forces, including reactions, shall be applied where they act in reality.

2.3.2 Supports

Unless the supports are designed specially they can be assumed to behave as pin joints positioned in the middle of the support areas.

The model shall consider the stiffness of the supporting structure when the deflection of the support nodes have an influence on the internal forces. This can be done by assigning stiffness values to the supporting nodes.

In some cases a simpler model can be used. For example for trusses on two supports and with both top and bottom chords, it can be assumed that vertical loads are taken by one firm simple support and the other supports being joints on rollers. For horizontal load all the supports can be assumed to behave as pinned joints on rollers but kept in position by springs, which are assigned stiffnesses, corresponding to that of the supporting structures.

2.3.3 Modelling the slip in the connections

The slip in the connections shall at least be considered in those connections, of which the slip is essential for the distribution of the internal forces and moments. Enclosure 2 contains examples, where it for some truss types is estimated necessary to consider the slip in some of the connections.

The slip in a connection can be considered by a prescribed slip, a spring element or a combination of these two methods.

The prescribed slip or the secant modulus of the spring element shall for each loading case be determined from the stress level which actually occurs in the connection.

But if the static analysis is used for the strength verification it is acceptable to use values valid at a stress level equal to 60 per cent of the characteristic short term strength of the connection. For serviceability analysis it is similar acceptable to use a stress level of 40 per cent.

Creep shall be considered by the determination of the prescribed slip or the secant modulus.

Guideline:

For stress levels deviating from 60 per cent the relation between stress and slip can be determined from

$$\text{Stress level} = \frac{\tau}{f_k} = 0.37 \frac{u}{u_{60}} \left(2 - 0.37 \frac{u}{u_{60}} \right)$$

where τ Shear stress between nail plate and timber

f_k Characteristic strength of τ

u Slip at the stress level

u_{60} Slip at a stress level of 60 per cent

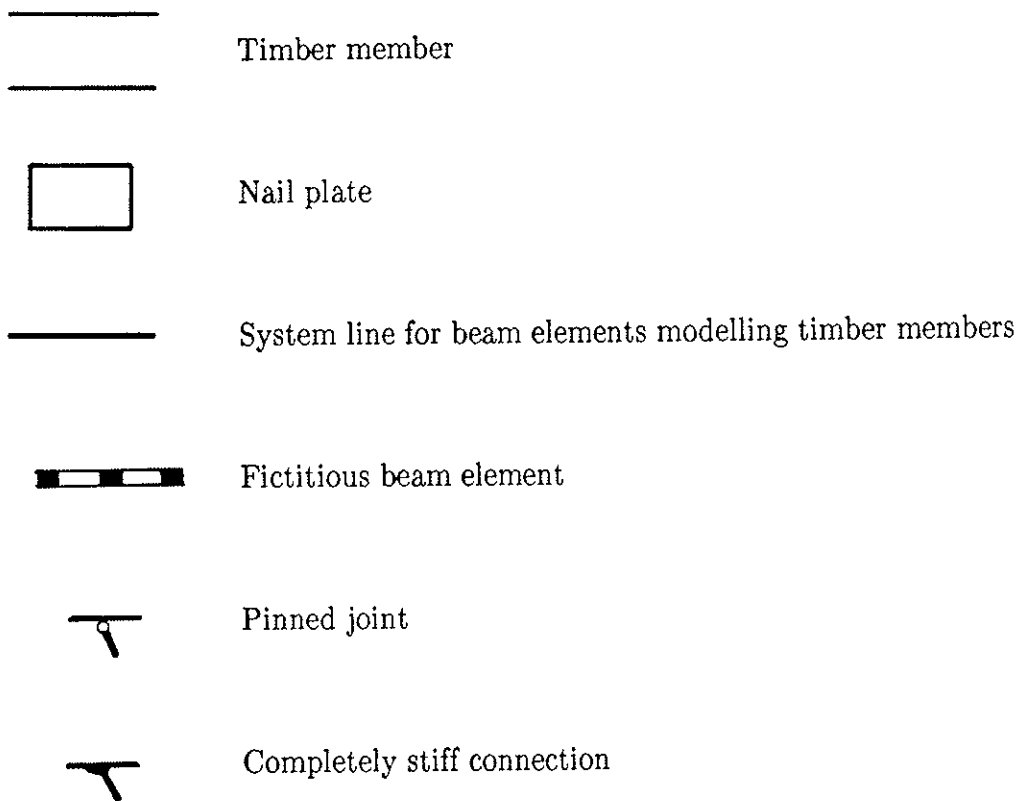
If there is used a combination of the two methods the employed prescribed slip and spring stiffness shall be determined so that the total slip in the model is equal to the real slip.

Enclosure 1. Connection models.

There is given some examples of the modelling of connections. The intention of the models is to reflect the static behavior as well as possible. The position of the resultant force in the connection and the load–deformation characteristics have been considered by the positioning of the pinned joint.

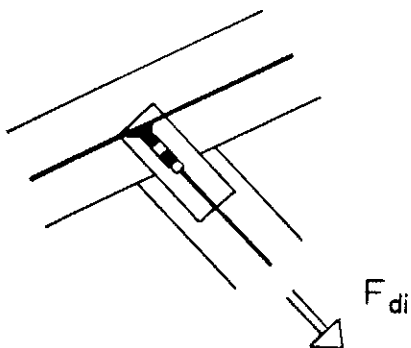
/* More examples will be elaborated by the Truss Committee */

Symbols



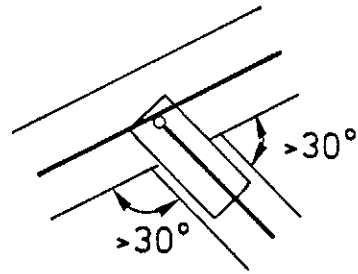
E1.1. Connections between 2 timber parts

Chord–diagonal

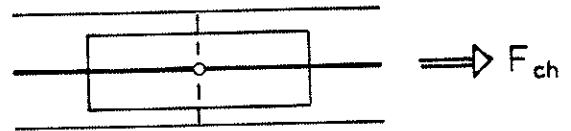


Chord-diagonal

No essential shear force in the diagonal

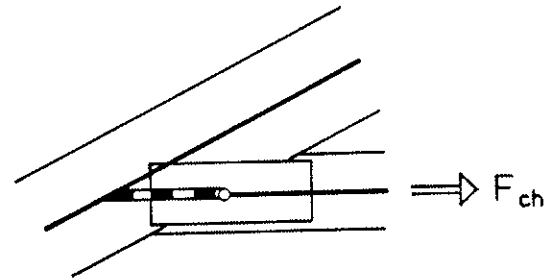


Splice



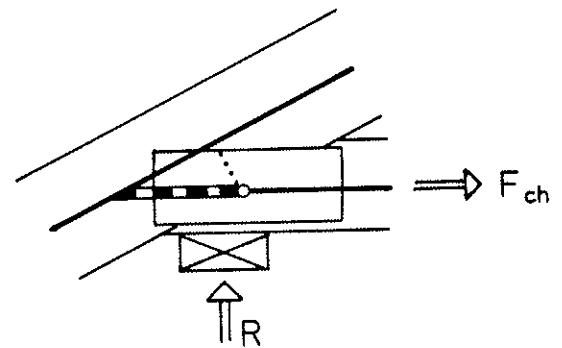
For a pinned joint in compression, $F_{ch} < 0$,
the plate connection shall be capable to transfer
at least 1/2 of the total force if the contact
eccentricity is disregarded.

2 Chords



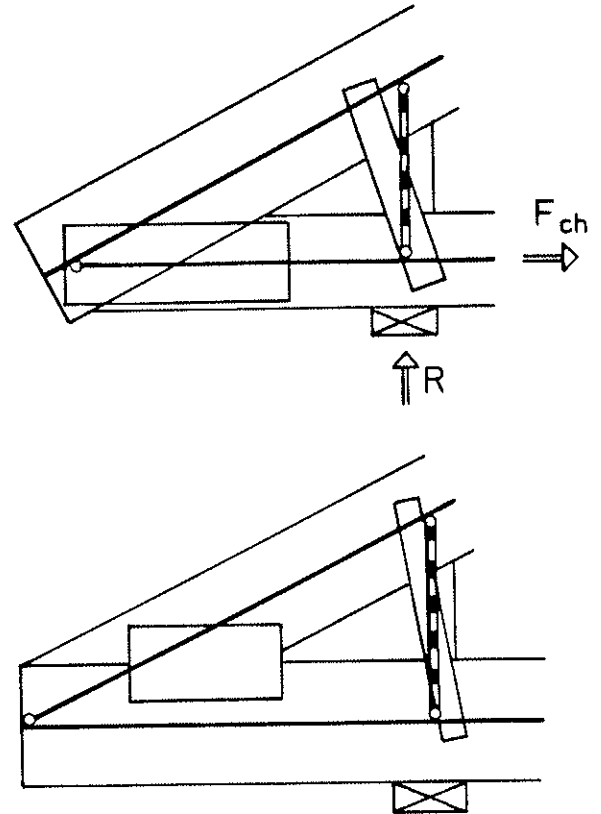
Heel joint, centric support

Further the fictitious beam member can be placed
as the dotted line.



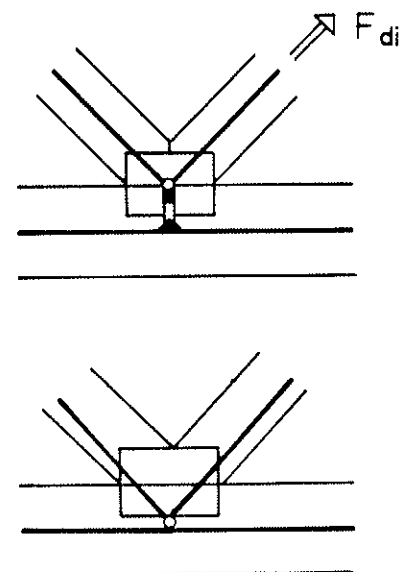
Heel joints, cantilevered

Above the support area there must always be contact between the top and bottom chord, for example by a wedge. If the height of the wedge h_w is larger than 200 mm, the grain direction in wedge should be perpendicular to the chord. The wedge must be kept in position by nail plating.



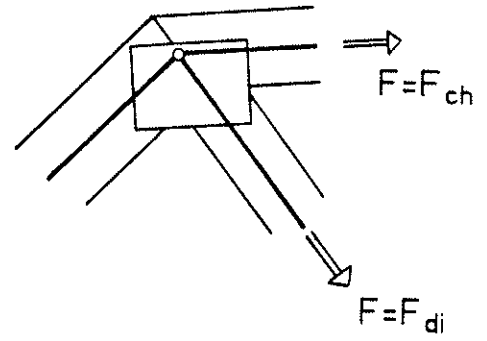
E1.2. Connections between 3 timber parts

Chord–diagonals



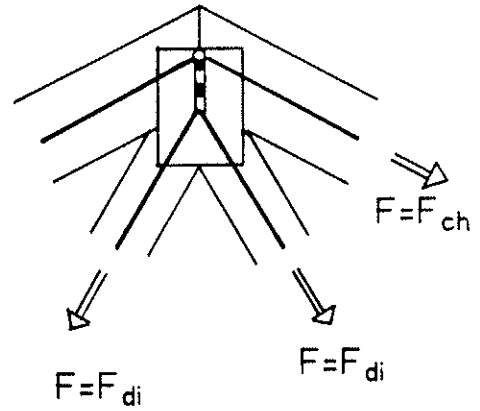
The nail plates must be capable to transfer the eccentric forces.

Inclined chords—diagonal

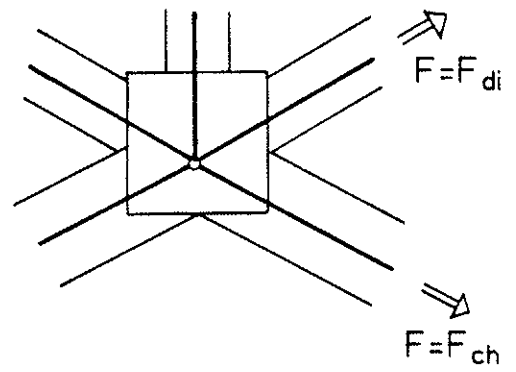


E1.3. Connections between several timber parts.

Ridge connection



Connection in a scissor truss



Enclosure 2. Connections where slip shall be considered.

The slip in the connections shall be considered when it is essential for the distribution of the internal forces and moments.

Some truss configurations are sensitive to slip in certain connections, so typical it is sufficient to model the slip in those connections. The connections in question are typical those in which a slip will cause large curvatures in timber parts.

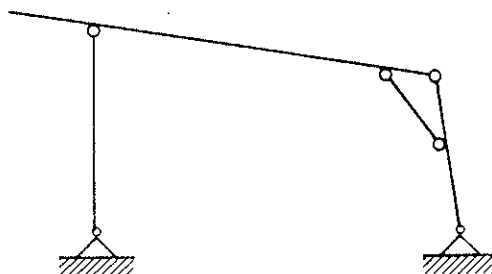
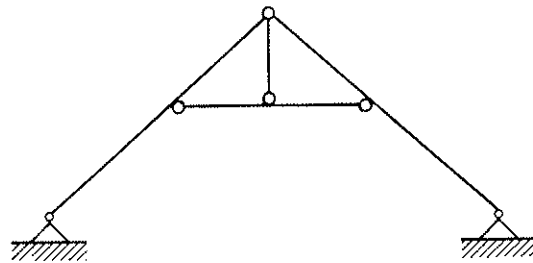
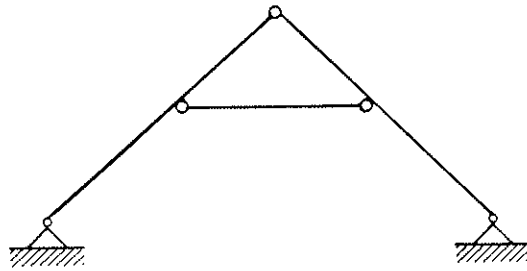
The following sections give examples of truss configurations and connections in which the slip shall be considered if nail plates are employed as connectors. It is typical that the connections in question are:

Heel joints: Slip in the chord directions.

Splices: Slip in the chord direction.

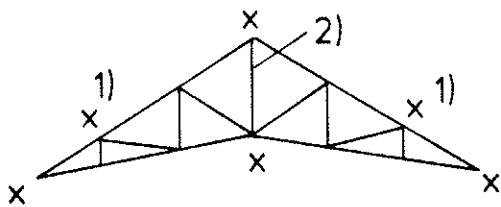
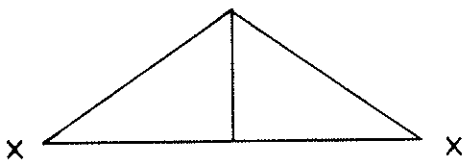
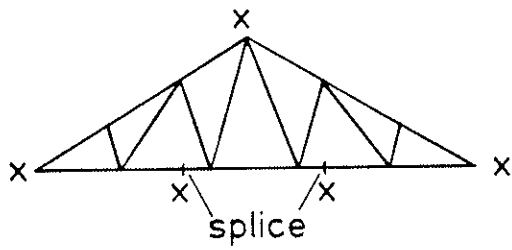
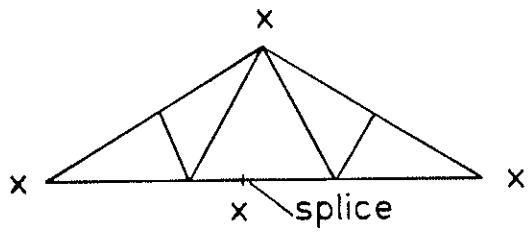
Ridge connections: Slip in the chord directions.

E.2.1. Truss configurations not sensitive to slip.

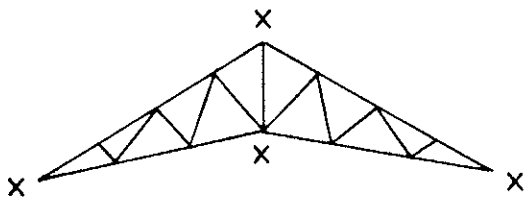


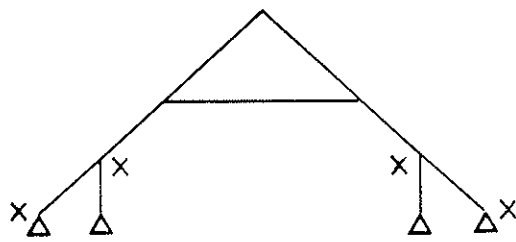
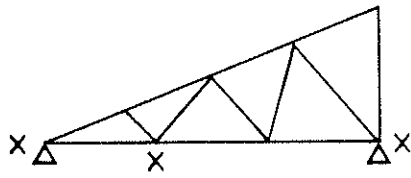
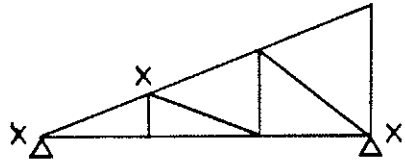
E.2.2. Truss configurations sensitive to slip.

The slip shall at least be considered in the connections marked with x.



Slip shall be considered:
1) Between chord and diagonal.
2) Vertical slip.





Euro Code 5, Timber Structures

Annex X.2

Guidelines for the stress analysis of external statically determinate fully triangulated timber trussed rafter using a simplified method of analysis.

Truss Committee / Luke Whale and Hilmer Riberholt

July 1990

Table of contents.

	Page
1. GENERAL	3
1.1 Object	3
2. DESCRIPTION OF THE SIMPLIFIED METHOD	3

1. GENERAL

1.1 Object

This annex describes a simplified method of analysis for trussed rafters. By the method the normal forces and internal moments in the timber members can be determined under some conditions. If these are not fulfilled then the more general method described in Annex 1 shall be used.

2. DESCRIPTION OF THE SIMPLIFIED METHOD

This method shall only be used for fully triangulated timber trussed rafters where the deflection of the nodes are small. This is the case for simple supported trusses with connection stiffnesses similar to that of nail plate connections and where:—

- i) The angle between the top and bottom chord exceeds 17 degrees or the truss height exceeds $0.15 \cdot \text{span}$ and
- ii) The truss height exceeds $7 \cdot \text{cross sectional height}$ of any of the chords.

The method shall only be applied where the system lines coincide inside the timber members i.e the maximum joint eccentricity should be half the chord depth from the centreline.

The method shall not be used on trusses with re—entrant areas.

For the chords in girder trusses, the maximum combined stress index shall be limited to 0.9 using this method of analysis. In this way there is taken account of that in reality some internal bending moments occur in the chords even when the girder truss is loaded only in the nodes.

Axial forces can be determined assuming a pin—jointed framework.

For chords continuous over several bays the internal bending moments should be determined assuming that members are continuous beams throughout their length and with simple pin supports at the nodes. Deflection at the nodes and partial fixity at the joints should be allowed for by a reduction of 10 percent in the bending moments which would occur at the nodes with no node deflection and no joint fixity. These reduced node moments shall be used to calculate bending moments between the nodes.

Where the trussed rafter supports are not in accordance with Figure 1, allowance should be made for bending moments induced by eccentricity of the forces.

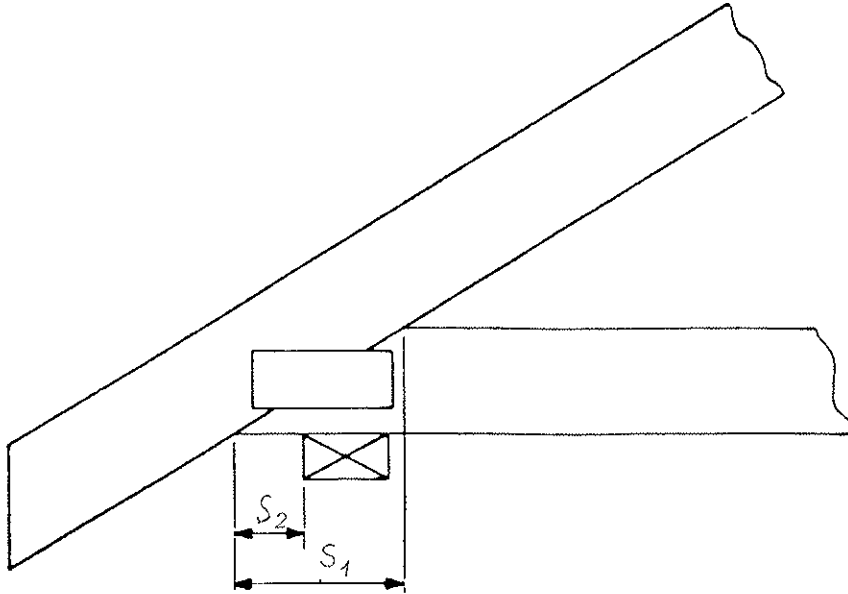


Figure 1. Location of wall plate when the eccentricity may be disregarded. Support shall be located so that not less than half the width of each bearing is vertically below the eaves joint fastener and the distance S_2 is less than $S_1/2$ or 100 mm whichever is the greater.

The rules for positioning and design of splice joints should follow those given in Annex X.1 and X.4.

HRi/Annex X.3

Euro Code 5, Timber Structures

Annex X.3

Strength verification of the timber in trussed rafters. Special effects.

Truss Committee / Hilmer Riberholt

June 1990

Table of contents.

	Page
1. GENERAL	3
1.1 Object	3
1.2 Definitions	3
1.3 Symbols	3
2. STRENGTH VERIFICATION OF THE TIMBER PARTS	4
2.1 Effective column lengths	4
2.2 Strength verification of cross sections at a moment peak	5
2.3 Strength verification for small concentrated forces	6

1. GENERAL

1.1 Object

This annex describes how there can be dealt with some effects, which are special for timber trussed rafters and which are not dealt with in /Euro Code 5, Timber Structures/.

1.2 Definitions

Bay:

Structure (timber beam) between two neighbouring nodes.

Beam element:

An element, which models a timber part.

Connections:

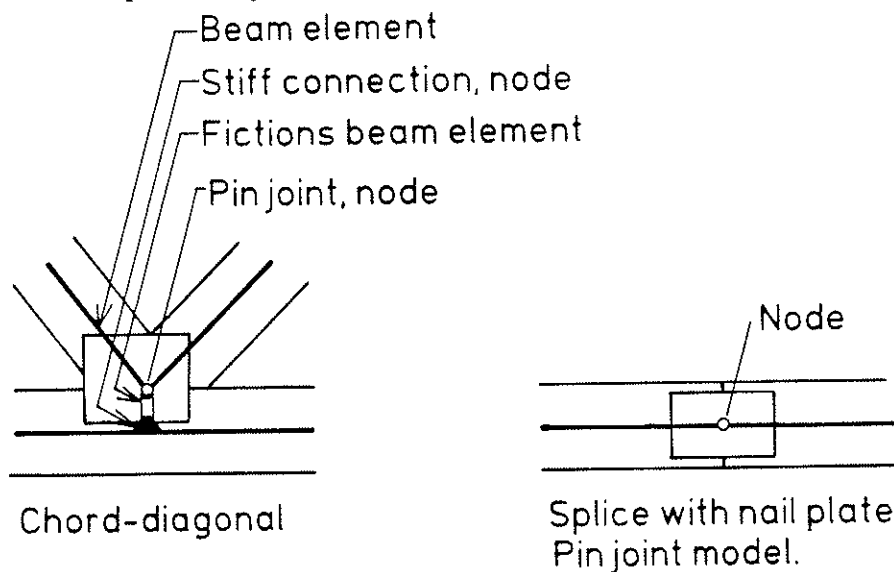
Domain where timber parts and/or nail plates are in contact in such a way that forces may be transferred between the parts.

Fictitious beam element:

Beam element, employed in connections in order to model their static behaviour.

Node:

Intersection point of system lines of beam elements.



1.3 Symbols

The definition of the symbols are the same as given in /Euro Code 5, Timber Structures/ or they are defined locally in the text.

2. STRENGTH VERIFICATION OF THE TIMBER PARTS

The strength verification of the timber parts shall be carried out as described in /Euro Code 5, Timber Structures/.

If the frame analysis is geometric non-linear (internal forces and moments are determined in the deflected state) then the column effects in the rupture criteria given in /Euro Code 5, Timber Structures/ can be disregarded. But the effects of initial imperfections shall be considered.

In the following sections there are given guidelines for how to deal with some effects, which are special for timber trusses, and which are not considered by /Euro Code 5, Timber Structures/.

2.1 Effective column lengths

The effective column lengths shall be determined based on the principles in /Euro Code 5, Timber Structures/ and by considering the design of connections and splices.

The length may be judged to be the distance between two adjacent points between which the deflected member is in a single curvature. For fully triangulated trusses the effective column length is equal to the distance between points of contraflexure.

For bars or members over one bay and without special stiff connections to the nodes the reduced column length is equal to the length between the nodes.

Fully triangulated trusses

For continuous members, i.e. chords, with a distributed lateral load of constant intensity along the total length, the following reduced column lengths are valid. A continuous member is a member over several bays either without splices or with splices positioned so that the compressed beam would be stable even if all the splices behaved as pinned joints. It is further assumed that the splices are designed for combined internal force and moment.

For continuous members with lateral load but without essential end moments the following reduced column lengths are valid. Further, they are illustrated in figure 2.1a.

In an outer bay	: $0.8 \cdot \text{bay length}$
In an inner bay	: $0.6 \cdot \text{bay length}$
At a node	: $0.6 \cdot \text{largest adjacent bay length}$

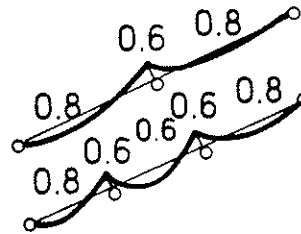


Figure 2.1a Reduced column lengths related to the bay lengths or the largest adjacent bay length. Valid for moment distributions approximately as shown.

For continuous beams with lateral load and an essential end moment the following reduced column lengths are valid. Further, they are illustrated in figure 2.1b.

Beam end with moment	: 0.0, i.e. no column effect
In the bay second from the end	: 1.0 bay length
Remaining bays and nodes	: As described previously

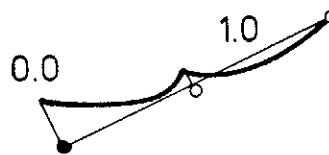


Figure 2.1b Reduced column lengths related to the bay lengths. Valid for moment distributions approximately as shown.

For continuous beams without lateral load (centrally loaded columns) the reduced column lengths may be assumed equal to the bay length.

2.2 Strength verification of cross sections at a moment peak.

This section does only apply if internal eccentricities and support eccentricities have been considered in the static analysis.

For the strength verification of normal stresses in a cross section at a distinct moment peak the bending strength can be increased by a factor k_m . It is further a condition that the

cross section is a part of a static indeterminate part of a truss, e.g. a continuous chord, or that it together with other timber parts carries the moment, e.g. when the top chord and the bottom chord together carry the eccentricity moment at an eccentric support.

Further it is an assumption, that the internal moment in the timber member changes sign within $0.3 \cdot$ bay length from the moment peak. See figure 2.2.

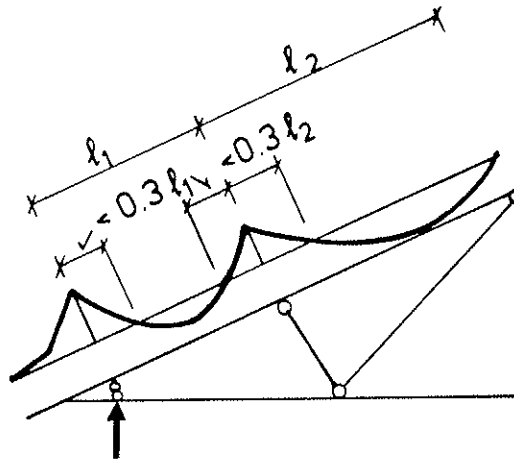


Figure 2.2 Requirements to be fulfilled by the moment distribution in a chord, here as an example in the top chord of a truss, in order that the bending strength may be increased.

The moment increase factor k_m is calculated from

$$k_m = \begin{cases} 1 + 0.4 \frac{C.V.}{25\%} & \text{for } C.V. \leq 25\% \\ 1.4 & \text{for } C.V. > 25\% \end{cases}$$

where C.V. is the coefficient of variation of the bending strength of the timber. C.V. shall be inserted in per cent. Unless other values can be justified C.V. can for conifers be determined from

$$C.V. = 43 - f_{m,k}$$

where C.V. is given in per cent

$f_{m,k}$ is the characteristic bending strength of the timber in MPa.

2.3 Strength verification for small concentrated forces.

For loading cases with only dead load and a concentrated force, for example man load, it is acceptable for lattice trusses, for which the stress in the timber ~~part~~ from the axial force is *Handwritten*

less than 40 per cent of the tensile or compression design strength, to undertake the strength verification by

$$\sigma_m = \frac{\frac{1}{4} F \ell \sin v}{W} \leq 0,75 \cdot f_m$$

where F is the concentrated force

ℓ is the bay length between the nodes

v is the angle between the timber member and the force

W is the section modulus.

HRI/Annex X.4

Euro Code 5, Timber Structures

Annex X.4

Strength verification of nail plate connections in timber trussed rafters.

Hilmer Riberholt

June 1990.

Table of contents

	Page
1. GENERAL	3
1.1 Object	3
1.2 Definitions	3
2. STRENGTH CAPACITIES	4
3. STRENGTH VERIFICATION	5
3.1 Anchorage capacity of nail plate	5
3.2 The capacity of the steel cross section in the nail plate	6
4. ROBUSTNES REQUIREMENTS	9
4.1 Minimum anchorage requirements	
4.2 Minimum requirements from horizontal transportation	9

1. GENERAL

1.1 Object

This annex describes how the strength verification of the very nail plate connections can be carried out for structures in moisture class 1 and 2. If contact occurs between the timber members this shall be considered by the determination of the forces and moment acting on the very nail plate connection.

1.2 Definitions

The geometry of the nail plate connection is given in figure 1.2.

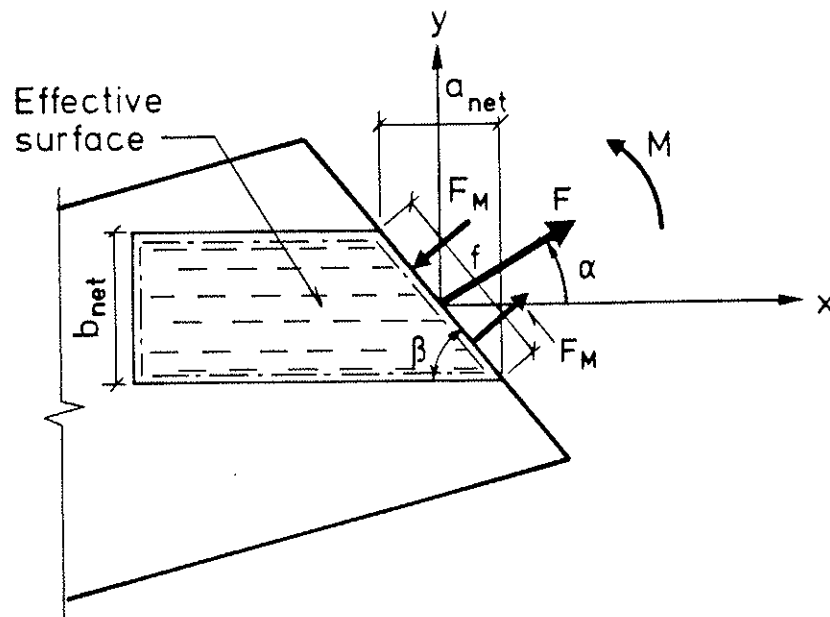


Figure 1.2 Geometry of the nail plate connection subjected to a force and a moment.

The x-direction is the main direction of the plate.

The y-direction is perpendicular to the main direction of the plate.

The net dimensions a_{net} and b_{net} are the actual dimensions. Meanwhile, in the approval a reduction may be prescribed to be applied at both ends.

The effective surface is the total surface of contact between the plate and the timber reduced with those parts of the surface which are outside some specified lengths from edges and ends. These reduction lengths take into account that the nails at the edges have a reduced anchorage capacity and that the plate may be misplaced.

α is the angle between the x-direction and the force

β is the angle between the x-direction and the gap.

2. STRENGTH CAPACITIES

The nail plate shall have approved values for the following characteristic properties. The test methods are described in / ISO/DIS 8969 /:

$f_{a,0,k}$	the anchorage capacity pr. area for $\alpha = 0$
$f_{t,x,k}$	the tension capacity pr. width of the plate in x-direction
$f_{c,x,k}$	the compression capacity pr. width of the plate in x-direction
$f_{v,x,k}$	the shear capacity pr. width of the plate in x-direction
$f_{t,y,k}$	the tension capacity pr. width of the plate in y-direction
$f_{c,y,k}$	the compression capacity pr. width of the plate in y-direction
$f_{v,y,k}$	the shear capacity pr. width of the plate in y-direction
c	constant given for the actual type of nail plate.

For the anchorage capacity the modification factor k_{mod} depends on moisture class and load duration class in the same way as described for joints in section 5.3. The partial coefficient for the material is given in section 2.3.3.2 of /Euro Code 5/.

For the tension, compression and shear capacities of the very plate the modification factor k_{mod} is 1.0. The partial coefficient for the material is given in /Euro Code 5, Steel Structures/.

3. STRENGTH VERIFICATION

Contact pressure between the timber parts can be taken into account if the gap between the timber parts in the joint fulfil:

$$\begin{aligned}\text{Max gap} &< 2 \text{ mm} \\ \text{Mean gap} &< 1 \text{ mm}\end{aligned}$$

Friction between the timber parts should normally be disregarded.

In a compressed connection the nail plate connection shall at least be designed for half the compression force.

3.1 Anchorage capacity of nail plate

The anchorage stresses are determined from the force F_A and moment M_A acting at the centre of gravity of the effective area.

The anchorage stresses from the force τ_F and the moment τ_M are calculated from

$$\tau_F = \frac{F_A}{A_{\text{ef}}} \quad (3.1 \text{ a})$$

$$\tau_M = \frac{M_A r_{\text{max}}}{I_P} \quad (3.1 \text{ b})$$

Where A_{ef} is the area and I_P is the polar moment of the effective area, r_{max} is the distance from the centre of gravity to the farthest point of the effective area.

The following conditions shall be satisfied

$$\tau_F \leq (1 - c \sin \gamma) f_{a0d} \quad (3.1 \text{ c})$$

$$\tau_M \leq 2(1 - c) f_{a0d} \quad (3.1 \text{ d})$$

$$\tau_F + \tau_M \leq 1.5 f_{a0d} \quad (3.1 \text{ e})$$

where the angle γ is less than or equal to 90° and its value is

$$\gamma = \max \begin{cases} \text{the angle between grain and force} \\ \alpha \\ \text{the angle between grain and x-direction} \end{cases}$$

3.2 The capacity of the steel cross section in the nail plate.

3.2.1 One straight joint

For a connection with one straight joint the formal forces in the two main directions are determined from the following formul. A positive value signifies that it is a tension force, a negative value that it is a compression force. See figure 1.2.

$$F_x = F \cos \alpha \pm 2 F_M \sin \beta \quad (3.2.1 \text{ b})$$

$$F_y = F \sin \alpha \pm 2 F_M \cos \beta \quad (3.2.1 \text{ b})$$

where

F is the force in thr joint

F_M is the force from the moment M in the joint. $F_M = 2M/f$ (3.2.1 c)

f is the length of the joint covered by nailplate, measured along the gap between connected members.

The formal forces shall satisfy the following criteria

$$\left(\frac{F_x}{R_{x,d}}\right)^2 + \left(\frac{F_y}{R_{y,d}}\right)^2 \leq 1 \quad (3.2.1 d)$$

where $R_{x,d}$ and $R_{y,d}$ are the design values in the x- and y-directions. They are determined as the maximum of the capacities in formal sections parallel with or perpendicular to the main axes.

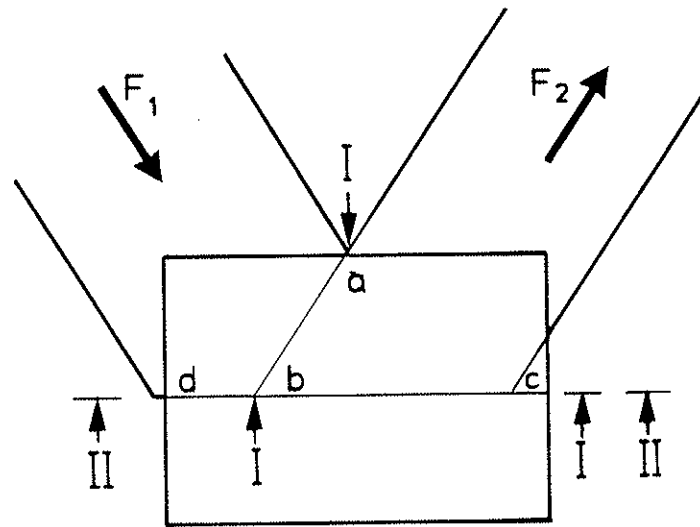
$$R_{x,d} = \max \begin{cases} f_{ax,x} b_{net} \\ f_{v,x,d} a_{net} \end{cases} \quad f_{ax,x} = \begin{cases} f_{t,x,d} & \text{if tension} \\ f_{c,x,d} & \text{if compression} \end{cases}$$

$$R_{y,d} = \max \begin{cases} f_{ax,y} a_{net} \\ f_{v,y,d} b_{net} \end{cases} \quad f_{ax,y} = \begin{cases} f_{t,y,d} & \text{if tension} \\ f_{c,y,d} & \text{if compression} \end{cases}$$

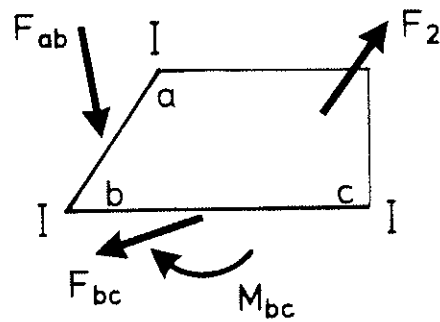
3.2.2 Several straight joints

If there are several straight joints then the forces in each straight joint can be chosen so that equilibrium is fulfilled and that criteria (3.2.1d) is satisfied in each straight joint.

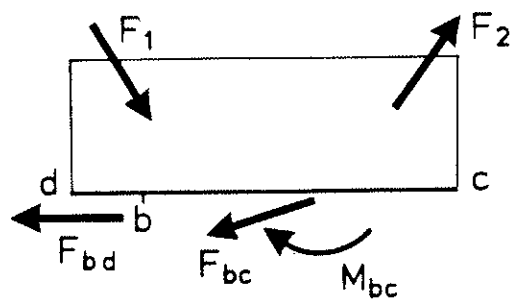
All critical sections shall be considered. If several sections have common parts then the forces in these shall be assumed to be the same when the different sections are considered. Figure 3.2.2 illustrates an example.



Joint between a chord and 2 diagonals



Section I - I



Section II - II

Figure 3.2.2 Joint between a chord and 2 diagonals.

4. ROBUSTNES REQUIREMENTS

4.1 Minimum anchorage requirements

Any timber member shall at all connections be connected so that a force F_r acting in the truss plane in any direction can be transferred. The value of F_r depends on the size of the truss, it is a short term load, and the timber is assumed to have a moisture content corresponding to moisture class 2.

$$F_r = 1.0 + 0,1\ell \quad (4.1 a)$$

where

F_r Minimum design force in kN
 ℓ The largest dimension of the truss in m.

The bite of nail plates connecting a timber member to the side of another shall fulfil.

$$\text{Bite} \geq \min \begin{cases} h/2 \\ 50 \text{ mm} \end{cases} \quad (4.1 b)$$

where h is the cross sectional height of the timber member being connected sideways.

Nail plates in chord splices shall cover at least two thirds of the cross sectional height.

4.2 Minimum requirements from horizontal transportation

All connections between chord members shall be designed so that their characteristic capacity is larger than the actions during the transportation.

If there are no exact calculations of the actions then the connections shall be designed for one of the following moments acting about an axis in the truss plane.

Calculated from the total dead load G and largest dimension ℓ (span) of the truss:

$$M = 1/8 G\ell \quad (4.2 a)$$

Calculated from the characteristic bending strength about the weak axis of the timber

$$M = 1/6 hb^2 f_{m,k} \quad (4.2 b)$$

where h cross sectional height
 b cross sectional width, $b < h$, (timber thickness)
 $f_{m,k}$ characteristic bending strength of the timber.

The force in one of the nail plates from the moment M can be calculated from

$$F = M/b \quad (4.2 c)$$

It is only necessary to verify the strength of the nail plate in tension.

INTERNATIONAL COUNCIL FOR BUILDING RESEARCH STUDIES AND DOCUMENTATION

WORKING COMMISSION W18A - TIMBER STRUCTURES

CALCULATION OF A WIND GIRDER LOADED ALSO

BY DISCRETELY SPACED BRACES FOR ROOF MEMBERS

by

H J Burgess

Timber Research and Development Association

United Kingdom

MEETING TWENTY - THREE

LISBON

PORTUGAL

SEPTEMBER 1990

1.

CONTENTS

	Page no.
Introduction	3
JUSTIFICATION FOR 2.5% RESTRAINT	3
BRACING FORMULAE FOR IDEAL COLUMNS	3
End force less than interbrace Euler load	4
Full bracing values from Tu's formula	4
STIFFNESS TO LIMIT ADDITIONAL DEFLECTION	4
COMBINATION OF END FORCES AND MOMENTS FOR RESTRAINT OF A BEAM-COLUMN	5

CALCULATION OF FLEXURAL RIGIDITY FOR A BEAM RESTRAINING A NUMBER OF COLUMNS	6
RESTRAINT GIRDER LOAD TREATED AS A DISTRIBUTED LOAD	6
Sinusoidal loading	6
RESTRAINT BEAM DEFLECTION FROM FINITE DIFFERENCE EQUATIONS	7
Loading of restraint beam	7
Bending moment	7
Slope and deflection	9
Solution for slope	9
Solution for deflection	11
Mode 1	12
GRAPHS FOR DISCRETE RESTRAINTS	12
RESTRAINT BEAM FLEXURAL RIGIDITY	13
Mode r	13
Mode 1	13
INTERCONNECTION OF COLUMNS AND BEAMS	14
Restraint beam loading	14
Bending moment in restraint beam	14
Initial and loaded curvature in columns	14
Deflection of restraint beam	15
Interconnection for mode 1	15

	Page no.
DISCRETE RESTRAINT WITH WIND LOADING	15
DEFLECTIONS DUE TO COMBINATION OF BRACING AND WIND LOAD	15
Mode 1	15
Mode r	16
Ratio	16
MODE r AS DESIGN BASIS	17
FLEXURAL RIGIDITY REQUIRED FOR RESTRAINT BEAM	19
Without wind load	19
With wind load	20
Graphs for $E_x I_x$ required	21
DESIGN FORMULAE	22
REFERENCES	23

**CALCULATION OF A WIND GIRDER LOADED ALSO BY
DISCRETELY SPACED BRACES FOR ROOF MEMBERS**

A previous paper, CIB-W18/22-15-1 (Burgess, 1989b) made a proposal for a bracing feature not included in the current draft of EC5 (2.5% or 2% restraint) and also for the combination of end forces and moments when calculating the restraint required for a beam-column. The following work gives a sounder basis for the first proposal and revises the second one following further study. The main part of the paper follows, developing a calculation for the necessary flexural rigidity of a wind girder restraining a number of top chords against buckling by means of a series of discretely spaced braces.

JUSTIFICATION FOR 2.5% RESTRAINT

The previous paper found an expression for the deflection at each of r discrete restraints for a column of length L with restraint spacing $l = \frac{L}{m}$. Taking an initial curvature in r sinusoidal half-waves, the expression found was

$$\frac{\delta_1}{c} = \frac{\frac{P}{r^2 P_e}}{\left(1 - \frac{P}{r^2 P_e}\right) \left(1 - \frac{S}{S_{r, id}}\right)} \quad (1)$$

where c is the initial deviation from straightness, S is the restraint stiffness and $S_{r, id}$ is the stiffness required for bracing an ideal column under the same end load P . With the additional deflection δ_1 limited to c , an approximate method was applied to show that a restraint force of $0.025P$ would be needed at each restraint to correspond with an amplitude of $0.003l$ in the initial curvature.

For initial curvature in a number of half-waves different from r , including the case with a single half-wave, similar formulae were found but with r replaced by the number of half-waves.

BRACING FORMULAE FOR IDEAL COLUMNS

The previous report used the approach by Klemperer and Gibbons (1932, 1933) for ideal columns. This was fortunate because the approach brought out the simple manner of expressing the results for initially curved columns shown by (1). However the expression for $S_{r, id}$ becomes complicated even for three restraints, and more convenient expressions may be found using finite difference equations as shown by Tu Shou Ngo (1944).

With some changes of symbols, the result he gives is

$$\cos \frac{2n\pi}{m} - \left\{ 2 + 2 \cos t - \frac{K_2}{t^3} (t - \sin t) \right\} \cos \frac{n\pi}{m} + \left\{ 1 + 2 \cos t + \frac{K_2}{t^3} (\sin t - t \cos t) \right\} = 0 \quad (2)$$

where

$$K = \frac{S_{id} l^3}{EI} = \frac{S_{id} l^3}{EI m^3}$$

$$t = l \sqrt{\frac{P}{EI}} = \frac{L}{m} \sqrt{\frac{P}{EI}}$$

Although not stated by Tu, n represents the number of half-waves in which buckling occurs.

End force less than interbrace Euler load

For buckling in r half-waves, the ideal restraint stiffness $s_{r, id} = \frac{S_{r, id} L}{P_e}$ for an end load less than $m^2 P_e$ is found by putting $n = r$ in (2) and transposing to give

$$\Delta_{r, id} = \frac{P}{P_e} t m \frac{(2 + 2 \cos t) \cos \frac{r}{m} \pi - \cos^2 \frac{r}{m} \pi - (1 + 2 \cos t)}{(t - \sin t) \cos \frac{r}{m} \pi + (\sin t - t \cos t)} \quad (3)$$

In the previous report $\frac{P}{P_e}$ was taken as 0.5 m^2 to limit interbrace deflection. The figure 0.5 was derived for a single-piece solid column, and higher values are encountered in design. To cater for a wider range, $\frac{P}{P_e}$ in (3) may be taken as $f m^2$ with $f = 0.5, 0.6 \dots 0.9$.

Full bracing values from Tu's formula

When $\frac{P}{P_e} = m^2$, (3) reduces to

$$\begin{aligned} \Delta_{f, id} &= \frac{S_{f, id} L}{P_e} = \frac{m^3 (1 - \cos \frac{2r\pi}{m})}{1 + \cos \frac{r\pi}{m}} \\ &= 2m^3 (1 + \cos \frac{\pi}{m}) \end{aligned} \quad (4)$$

Formula (4) is used by Möhler and Schelling (1968) who quote a 1924 book by F. Bleich as the source. Strangely, the formula is not given in Bleich's 1952 book 'Buckling Strength of Metal Structures.'

For a single half-wave the corresponding formula is found by putting $n = 1$ instead of r in (2), and when $\frac{P}{P_e} = m^2$ the result found is

$$\Delta_{f, id} = 2m^3 (1 - \cos \frac{\pi}{m}) \quad (5)$$

STIFFNESS TO LIMIT ADDITIONAL DEFLECTION

Putting $\delta_1 = c$ in (1) and solving for S gives

$$S = \Delta_{r, id} \left(1 - \frac{\frac{P}{r^2 P_e}}{1 - \frac{P}{r^2 P_e}} \right) \quad (6)$$

- using the values $\delta = \frac{S_1 L}{P_e}$ and $\delta_{r, id} = \frac{S_{r, id} L}{P_e}$ instead of S and $S_{r, id}$. With $s_{r, id}$ inserted from (3), equation (6) gives the restraint stiffness limiting the additional deflection to the original deviation from straightness. If the original deviation is taken as $0.003 \frac{L}{m}$, the force applied by the restraint will be $\delta \frac{P_e}{L} \times 0.003 \frac{L}{m}$ giving

$$\begin{aligned} \frac{\text{restraint force}}{\text{end force}} &= \frac{\delta P_e \times 0.003}{m \times f m^2 P_e} \\ &= \frac{0.003 \delta}{f m^3} \end{aligned} \quad (7)$$

This ratio expressed as a percentage is plotted in Figure 1 for $m = 2$ to 9. The figures on the graphs show the number of restraints, $r = m - 1$. The previous report with $\frac{P}{P_e} = 0.5 m^2$ assumed a straight line relationship between $\frac{P}{P_e}$ and $s_{r, id}$. The restraint stiffness for the halved end load with deflection limited by $\frac{\delta_1}{C} = 1$ was then the same as $s_{r, id}$ for full bracing, $s_{f, id}$. A dashed line with this basis is added in Figure 1, plotted from (7) with s replaced by $s_{f, id}$. It was used as confirmation of the 2.5% recommendation in the British steel code, and Figure 1 shows that this figure makes provision for end loads up to $\frac{P}{P_e} = 0.8 m^2$ with the formal calculation method applied here.

COMBINATION OF END FORCES AND MOMENTS FOR RESTRAINT OF A BEAM-COLUMN

A proposal in paper 22-15-1 for combining end forces and moments to calculate the discrete restraints needed for a beam-column may now be revised following further work (Burgess 1990a, 1990b).

With equal end moments it is always conservative to express the combination as

$$\frac{N}{P_e} = \frac{M^2}{M_c^2} + \frac{P}{P_e}$$

or

$$N = \frac{M^2}{M_c^2} P_e + P \quad (8)$$

This applies when there is only lateral restraint at the centroid, and no torsional restraint. To allow for the effect of torsional restraint, brief formulae are derived in (Burgess 1990b) by incorporating $s_{r, id}$ values from (3) above.

**CALCULATION OF FLEXURAL RIGIDITY
FOR A BEAM RESTRAINING A NUMBER OF COLUMNS**

The calculations refer to the type of roof system studied by Möhler and Schelling (1968), shown in plan in Figure 2. The latticed girder resists wind loading as well as supporting compression members which form the top flanges of a number of latticed girders placed vertically to span the width of the roof. Figure 2 is drawn to show the wind load as a distributed load on the restraint girder, although in practice it may be applied at least partially by discrete forces.

RESTRAINT GIRDER LOAD TREATED AS A DISTRIBUTED LOAD

Möhler and Schelling treated both the wind load and the column restraint load as uniformly distributed in work leading to the simple formula in DIN 1052. The formula has the effect of limiting deflection in a single half-wave (first mode deflection) to a desired value for a given initial curvature in a single half-wave. Buckling in r half-waves (mode r) is also considered, recommending the use of equation (4) above to estimate the brace forces, and this is catered for in DIN 1052 by a 2% rule corresponding to the 2.5% rule in the British steel code.

Sinusoidal loading

CIB-W18 paper 21-15-3 (Burgess 1988) has shown that an easier approach may be made for the mode 1 calculation by using sinusoidal loading, and this leads to essentially the same result as adopted for the German code. An extension to mode r buckling is developed in a separate paper (Burgess 1990c), leading to the following results for the required flexural rigidity of a restraint beam which is regarded as a solid beam to eliminate joint slip. The subscripts of EI represent the mode number. When EI is written without subscripts or the symbol P_e appears without modification, these values refer to the column and not the restraint beam.

$$E_1 I_1 = N E I (2t m^2 - 1) + \frac{L^2}{\pi^2} \frac{M}{a} \quad (9)$$

$$E_r I_r = \frac{N}{m} \times 2t E I \left(2t \frac{m^2}{r^2} - 1 \right) + \frac{L^2}{\pi^2} \frac{M}{a} \quad (10)$$

$$\frac{E_r I_r}{E_1 I_1} = \frac{\frac{2t}{m} \left(2t \frac{m^2}{r^2} - 1 \right) + \frac{M}{N a P_e}}{(2t m^2 - 1) + \frac{M}{N a P_e}} \quad (11)$$

The initial curvature is a for mode 1 and $\frac{a}{m}$ for mode r . The end force ratio is $\frac{P}{P_e} = t m^2$ with $t = 0.5, 0.6 \dots 0.9$ and N is the number of columns braced.

Writing $\frac{M}{a P_e} = v \frac{P}{P_e} = v t m^2$, (11) is plotted in Figure 3 showing that a restraint beam designed for mode 1 will always be stiff enough for mode r , and amply stiff if there is more than one restraint.

**RESTRAINT BEAM DEFLECTION
FROM FINITE DIFFERENCE EQUATIONS**

Figure 3 is shown only as an approximation to simplify the results of the following calculation for discrete loading. Since values are required only at discrete, equally-spaced intervals, the method using finite difference equations is appropriate (von Kármán and Biot, 1940).

Loading of restraint beam

Initially the restraint beam is examined as an isolated member carrying loads the same as those restraining the column but with no connection between the two members.

Figure 4 is drawn for 7 restraints. For the general case with m intervals and r restraints ($m = r + 1$), the initial curvature for mode r is $y = a \sin \frac{r\pi}{m} x$. Making the additional column deflection at each restraint equal to the initial deviation from straightness at the same point, the additional deflection at restraint n is

$$y_n = a \sin \frac{nr}{m} \pi \quad (12)$$

with $n = 1, 2 \dots r$. The restraint force required by the set of N columns at restraint n is

$$p_n = NSa \sin \frac{nr}{m} \pi \quad (13)$$

giving the load values shown in Figure 4 for the restraint beam. S is obtained from (6) as $S = s \frac{P_c}{L}$ and has the same value for all restraints.

Bending moment

Figure 5 is adapted from a diagram given by Tu (1944) in relation to the restraint of ideal columns. The symbol x in the diagram means the same as n . It is used only to express values at the discrete points $x = 0, 1 \dots m$. For intermediate positions a different variable will be used to express the distance along the length of the beam between the points x and $x + 1$. In the diagram,

$$p_- = \frac{1}{l} (M_x - M_{x-1})$$

$$p_+ = \frac{1}{l} (M_x - M_{x+1})$$

Adding these and equating their sum to the load at point x or n shown in Figure 4,

$$N\delta a \sin \frac{r}{m} \pi x = \frac{1}{l} (-M_{x-1} + 2M_x - M_{x+1})$$

$$M_{x-1} - 2M_x + M_{x+1} = -N\delta a \sin \frac{r}{m} \pi x \quad (14)$$

Replacing the right-hand side by zero to form the homogeneous equation and putting $M_x = \beta^x$ gives

$$\beta^{x-1} - 2\beta^x + \beta^{x+1} = 0$$

$$\beta^2 - 2\beta + 1 = 0$$

with the double root $\beta_1 = 1$ corresponding to the solution $M_x = C_1 + C_2 x$

For a particular solution, writing $M_x = c \sin \frac{r}{m} \pi x$ in (14)

$$c \sin \frac{r}{m} \pi (x-1) - 2c \sin \frac{r}{m} \pi x + c \sin \frac{r}{m} \pi (x+1) = -N\delta a \sin \frac{r}{m} \pi x$$

$$2c \left(\cos \frac{r}{m} \pi - 1 \right) \sin \frac{r}{m} \pi x = -N\delta a \sin \frac{r}{m} \pi x$$

Equating the coefficients of $\sin \frac{r}{m} \pi x$

$$c = \frac{-N\delta a}{2 \left(\cos \frac{r}{m} \pi - 1 \right)}$$

so the complete solution of (14) is

$$M_x = C_1 + C_2 x - \frac{N\delta a}{2 \left(\cos \frac{r}{m} \pi - 1 \right)} \sin \frac{r}{m} \pi x \quad (15)$$

When $x = 0$, $M_x = 0$ so $C_1 = 0$

When $x = m$, $M_x = 0$:

$$0 = m C_2 - \frac{N\delta a}{2 \left(\cos \frac{r}{m} \pi - 1 \right)} \sin r \pi$$

$$C_2 = \frac{N\delta a}{2m \left(\cos \frac{r}{m} \pi - 1 \right)} \sin r \pi = 0 \quad \text{since } r \text{ is an integer,}$$

so $C_2 = 0$ and the complete solution (15) becomes

$$M_x = \frac{NLSa}{2m(1 - \cos \frac{r}{m}\pi)} \sin \frac{r}{m}\pi x \quad (16)$$

which is valid only at the ends and at the restraints, where $x = 1, 2 \dots r$.

Slope and deflection

In Figure 5, the variable z is used for intermediate distances in the interval x to $x + 1$. Temporarily using EI without subscripts to refer to the restraint beam, the change of deflection u over this interval may be found from

$$EI \frac{d^2 u}{dz^2} = -p_z z + M_x \quad (17)$$

where

$$\begin{aligned} p_z &= \frac{1}{\ell} (M_x - M_{x+1}) \\ &= -\frac{1}{\ell} \frac{NLSa}{2m(1 - \cos \frac{r}{m}\pi)} \left\{ \sin \frac{r}{m}\pi (x+1) - \sin \frac{r}{m}\pi x \right\} \end{aligned}$$

--using (16). Writing $F = \frac{NLSa}{2m(1 - \cos \frac{r}{m}\pi)}$ (18)

and inserting in (17)

$$\begin{aligned} EI \frac{d^2 u}{dz^2} &= \frac{F}{\ell} \left\{ \sin \frac{r}{m}\pi (x+1) - \sin \frac{r}{m}\pi x \right\} z + F \sin \frac{r}{m}\pi x \\ EI \frac{du}{dz} &= \frac{F}{\ell} \left\{ \sin \frac{r}{m}\pi (x+1) - \sin \frac{r}{m}\pi x \right\} \frac{z^2}{2} + Fz \sin \frac{r}{m}\pi x + A \end{aligned} \quad (19)$$

Solution for slope

Expressing the slope as $\frac{du}{dz} = v$, when $z = 0$, $EI v_x = A$ and when $z = \ell$

$$EI v_{x+1} = \frac{F\ell}{2} \left\{ \sin \frac{r}{m}\pi (x+1) - \sin \frac{r}{m}\pi x \right\} + F\ell \sin \frac{r}{m}\pi x + EI v_x$$

Expanding the term in the chain bracket leads to the difference equation for slope:

$$v_{x+1} - v_x = \frac{F\ell}{2EI} \left\{ (1 + \cos \frac{r}{m}\pi) \sin \frac{r}{m}\pi x + \sin \frac{r}{m}\pi \cos \frac{r}{m}\pi x \right\} \quad (20)$$

To find a particular solution, put

$$v_x = D \sin \frac{r}{m}\pi x + B \cos \frac{r}{m}\pi x$$

The left-hand side of (20) then becomes after expansion

$$D \left\{ \left(\cos \frac{r}{m} \pi - 1 \right) \sin \frac{r}{m} \pi x + \sin \frac{r}{m} \pi \cos \frac{r}{m} \pi x \right\} + B \left\{ \left(\cos \frac{r}{m} \pi - 1 \right) \cos \frac{r}{m} \pi x - \sin \frac{r}{m} \pi \sin \frac{r}{m} \pi x \right\}$$

and equating coefficients gives the two simultaneous equations

$$D \left(\cos \frac{r}{m} \pi - 1 \right) - B \sin \frac{r}{m} \pi = \frac{Fl}{2EI} \left(1 + \cos \frac{r}{m} \pi \right) \quad (21)$$

$$D \sin \frac{r}{m} \pi + B \left(\cos \frac{r}{m} \pi - 1 \right) = \frac{Fl}{2EI} \sin \frac{r}{m} \pi \quad (22)$$

which are solved to yield $D = 0$ and

$$B = - \frac{Fl}{2EI} \frac{\sin \frac{r}{m} \pi}{1 - \cos \frac{r}{m} \pi}$$

or with F inserted from (18)

$$B = - \frac{NL^2 S a \sin \frac{r}{m} \pi}{4EI m^2 \left(1 - \cos \frac{r}{m} \pi \right)^2} \quad (23)$$

The particular solution of (20) is therefore

$$v_x = B \cos \frac{r}{m} \pi x = - \frac{NL^2 S a \sin \frac{r}{m} \pi}{4EI m^2 \left(1 - \cos \frac{r}{m} \pi \right)^2} \cos \frac{r}{m} \pi x \quad (24)$$

For the homogeneous equation $v_{x+1} - v_x = 0$, trying $v_x = C_1 \beta^x$ gives

$$C_1 \beta^{x+1} - C_1 \beta^x = 0 \quad (25)$$

$$C_1 \beta^x (\beta - 1) = 0 \quad (26)$$

with the single root $\beta_1 = 1$ so the solution is $v_x = C_1 (\beta_1)^x = C_1$, and the complete solution of (20) is given by adding C_1 to (24). However C_1 is easily seen to be zero. For symmetrical loading (r odd) $\cos \frac{r}{m} \pi x = \cos \frac{r}{2}$ at the centre and $r = 1, 3, 5, \dots$ gives $\cos \frac{\pi}{2}, \cos \frac{3\pi}{2}, \cos \frac{5\pi}{2}, \dots$ which is zero in all cases so C_1 must be zero to make the slope zero at the centre. For antisymmetrical loading, $\cos \frac{r}{m} \pi x = 1$ when $x = 0$ and when $x = m, \cos r\pi = \cos 2\pi, \cos 4\pi, \cos 6\pi, \dots$ all with the value $+1$. To make the slope numerically the same at both ends of the beam, C_1 must again be zero and the complete solution for slope is as given by (24).

Solution for deflection

Integrating (19) with $A = EIv_x$,

$$EIu = \frac{F}{l} \left\{ \sin \frac{l}{m} \pi (x+1) - \sin \frac{l}{m} \pi x \right\} \frac{x^3}{6} + F \frac{x^2}{2} \sin \frac{l}{m} \pi x + EIv_x \} + B$$

When $z = 0$, $EIu = EIY_x = B$

When $z = l$,

$$EIY_{x+1} = \frac{Fl^2}{6} \left\{ \sin \frac{l}{m} \pi (x+1) - \sin \frac{l}{m} \pi x \right\} + \frac{Fl^2}{2} \sin \frac{l}{m} \pi x - \frac{Fl^2}{2} \frac{\sin \frac{l}{m} \pi}{(1 - \cos \frac{l}{m} \pi)} \cos \frac{l}{m} \pi x + EIY_x$$

Expanding the term in the chain bracket and simplifying gives the difference equation for deflection

$$Y_{x+1} - Y_x = \frac{Fl^2}{6EI} (2 + \cos \frac{l}{m} \pi) \left(\sin \frac{l}{m} \pi x - \frac{\sin \frac{l}{m} \pi}{1 - \cos \frac{l}{m} \pi} \cos \frac{l}{m} \pi x \right) \quad (27)$$

For a particular solution, putting

$$Y_x = G \sin \frac{l}{m} \pi x + H \cos \frac{l}{m} \pi x \quad (28)$$

the left-hand side of (27) becomes after expansion

$$G \left\{ (\cos \frac{l}{m} \pi - 1) \sin \frac{l}{m} \pi x + \sin \frac{l}{m} \pi \cos \frac{l}{m} \pi x \right\} + H \left\{ (\cos \frac{l}{m} \pi - 1) \cos \frac{l}{m} \pi x - \sin \frac{l}{m} \pi \sin \frac{l}{m} \pi x \right\}$$

Equating coefficients,

$$G (\cos \frac{l}{m} \pi - 1) - H \sin \frac{l}{m} \pi = \frac{Fl^2}{6EI} (2 + \cos \frac{l}{m} \pi)$$

$$G \sin \frac{l}{m} \pi + H (\cos \frac{l}{m} \pi - 1) = - \frac{Fl^2}{6EI} \frac{(2 + \cos \frac{l}{m} \pi)}{1 - \cos \frac{l}{m} \pi} \sin \frac{l}{m} \pi$$

which yield $H = 0$ and

$$G = - \frac{Fl^2 (2 + \cos \frac{l}{m} \pi)}{6EI (1 - \cos \frac{l}{m} \pi)}$$

Inserting F from (18), the particular solution of (27) is

$$Y_x = - \frac{NL^3 Sa (2 + \cos \frac{l}{m} \pi)}{12 m^3 EI (1 - \cos \frac{l}{m} \pi)^2} \sin \frac{l}{m} \pi x \quad (29)$$

The solution of the homogeneous equation $Y_{x+1} - Y_x = 0$ may be found as indicated by equations (25) and (26) for the slope, v . The result $Y_x = C_2$ is to be added to (29) to give the complete solution but either of the boundary conditions $Y_x = 0$ when $x = 0$ or $Y_x = 0$ when $x = m$ will eliminate C_2 and (29) therefore gives the required complete solution for deflection.

Mode 1

For initial column curvature in a single half-wave the restraint beam loading in (13) changes to

$$p_n = NS\alpha \sin \frac{n}{m} \pi \quad (30)$$

and the whole solution for moment, slope and deflection at the restraints remains as above except that r is replaced by 1 in (16), (24) and (29).

GRAPHS FOR DISCRETE RESTRAINTS

The equations derived for moment, slope and deflection are plotted for three restraints in Figure 6 for mode r and Figure 7 for mode 1, with all scales divided by 10 for the latter. In each case the top diagram plots $\frac{M_x}{NS\alpha L}$ from (16), the centre one is a plot of $\frac{v_x}{NL^2 S\alpha}$ from (24) and the straight line segments in the bottom diagram show a graph for $\frac{y_x EI}{NL^3 S\alpha}$ plotted from (29).

All three equations are valid only at the points $x = 0, 1, \dots, 5$ and the values plotted for these points are joined by straight lines. This gives a correct diagram at the top for bending moment, but for slope and deflection the intermediate values are not correctly given by straight lines.

The curved line in the bottom diagram of Figures 6 and 7 does give correct intermediate values for deflection, plotted from the following equation derived by the method of Macaulay (1919):

$$\frac{EI y_x}{NS\alpha L^3} = \frac{R}{6} \left(\frac{x}{L}\right)^3 - \frac{1}{6} \left(\frac{x}{L} - \frac{1}{m}\right)^3 \sin \frac{\pi}{m} - \frac{1}{6} \left(\frac{x}{L} - \frac{2}{m}\right)^3 \sin \frac{2\pi}{m} - \dots - \frac{1}{6} \left(\frac{x}{L} - \frac{r}{m}\right)^3 \sin \frac{r\pi}{m} + A \frac{x}{L} \quad (31)$$

$$\text{where } R = \sum_{n=1}^r \left(1 - \frac{n}{m}\right) \sin \frac{n\pi}{m} \quad (32)$$

$$A = -\frac{L^2}{6} \sum_{n=1}^r \left(1 - \frac{n}{m}\right) \sin \frac{n\pi}{m} + \frac{L^2}{6} \sum_{n=1}^r \left(1 - \frac{n}{m}\right)^3 \sin \frac{n\pi}{m} \quad (33)$$

and in (31) the terms $\left(\frac{x}{L} - \frac{n}{m}\right)$ for $n = 1, 2, \dots, r$ are to be omitted if zero or negative.

The sign is reversed compared with equation (29) to separate the diagrams and the three crosses are plotted from (29) to demonstrate agreement. They could alternatively be plotted using

$$\frac{EIY_n}{NScl^3} = \frac{1}{6} \left(\frac{n}{m} \right)^3 \sum_{n=1}^r \left(1 - \frac{n}{m} \right) \sin \frac{n\pi}{m} \pi - \frac{1}{6} \left(\frac{1}{m} \right)^3 \sum_{t=1}^{3r} (n-t)^3 \sin \frac{t\pi}{m} \pi - \frac{1}{6} \frac{a}{m} \sum_{n=1}^r \left(1 - \frac{n}{m} \right) \sin \frac{n\pi}{m} \pi + \frac{1}{6} \frac{a}{m} \sum_{n=1}^r \left(1 - \frac{n}{m} \right)^3 \sin \frac{n\pi}{m} \pi \quad (34)$$

which gives the Macaulay solution for the restraint points where $x = n = 0, 1, \dots, m$. Equations (34) and (29) are of course mathematically identical and the object of applying finite difference equations is to express (34) in the much neater form given by (29).

RESTRAINT BEAM FLEXURAL RIGIDITY

The solution (29) for the restraint beam deflection at restraint n (or x) takes the same form as (12) for the additional deflection in the column at restraint n . The calculation for the restraint beam has been made without assuming it is connected to the column. However equation (29) may be used to find the flexural rigidity of the restraint beam which makes its deflections at the restraints the same as those in the column, and then rigid braces may be inserted to transmit the bracing forces from column to beam. This will make no difference to the calculation, and the restraint beam will supply exactly the restraint force required to limit the additional deflection to its initial value at each column restraint.

Mode r

Writing
$$\alpha_r = \frac{2 + \cos \frac{r\pi}{m}}{12m^3 (1 - \cos \frac{r\pi}{m})^2} \quad (35)$$

in (29) and reversing the sign so that the beam deflects in the same sense as the column, then with x replaced by n ,

$$y_n = \frac{NL^3 S_r a}{E_r I_r} \alpha_r \sin \frac{n\pi}{m} \pi \quad (36)$$

If y_n is to be the same in (36) and (12), dividing (36) by (12) gives

$$E_r I_r = \alpha_r N L^3 S_r \quad (37)$$

Mode 1

Again using (29) and (12) but with r replaced by 1,

$$\alpha_1 = \frac{2 + \cos \frac{\pi}{m}}{12m^3 (1 - \cos \frac{\pi}{m})^2} \quad (38)$$

$$y_n = \frac{NL^3 S_1 a}{E_1 I_1} \alpha_1 \sin \frac{n\pi}{m} \pi \quad (39)$$

$$E_1 I_1 = \alpha_1 N L^3 S_1 \quad (40)$$

α_r and α_1 have the same meaning as the right-hand side of (34). When using (34) for mode 1, the summation is still taken for r restraints but r is put equal to 1 in the arguments of all the sine terms.

To provide in a better way for a varying number of half-waves in the initial column curvature, (12) would be expressed $y_n = a \sin \frac{\rho n}{m} \pi$ where ρ is the number of half-waves, and r would continue to mean the number of restraints.

INTERCONNECTION OF COLUMNS AND BEAMS

For columns buckling in mode r , if $E_r I_r$ for the restraint beam has the value given by (37) then the restraint points in the beam and column deflect to the same extent. This may be confirmed by inserting $E_r I_r$ from (37) into (36) to give (12). The restraint points in the beam and column may therefore be joined by rigid braces as shown in Figure 8. The graphs are shown for the particular case of six restraints, plotted as described by the following notes.

Restraint beam loading

This is symbolized in the top diagram by arrows with a length proportional to

$$\frac{p_n}{NS_r a} = \sin \frac{n r}{m} \pi \quad (41)$$

from (13), where p_n is the load in brace n . Including S_r in such plots for increasing values of r would of course produce arrows of increasing length.

Bending moment in restraint beam

The second graph represents bending moments at the restraints as

$$\frac{M}{NS_r a L} = \frac{\sin \frac{n r}{m} \pi}{2m \left(1 - \cos \frac{r}{m} \pi\right)} \quad (42)$$

derived from (16), and these points are correctly joined by straight lines to produce the complete bending moment diagram for the restraint beam.

Initial and loaded curvature in columns

The third diagram, which is joined by 'braces' to the bottom one, represents a number of columns with initial curvature $\frac{y}{a} = \sin \frac{n r}{m} \pi$ and a loaded curvature which is correct only at the restraints. Intermediate values for one to three restraints could be plotted from formulae in Burgess

(1989a) but are not needed here and the loaded curvature is shown simply as $\frac{y}{a} = 2 \sin \frac{N\pi x}{mL}$, again assuming the additional deflection at a restraint is equal to the initial deviation.

Deflection of restraint beam

On the other hand the deflection of the restraint beam in the bottom diagram is represented exactly at all points by using (31). Writing the right-hand side as $\sum k_M$ to signify the Macaulay summation, if $E_r I_r = \alpha_r NS_r L^3$ from (37) then $\frac{y}{a} = \frac{k_M}{\alpha_r}$ and all the k_M values plotted against $\frac{x}{L}$ are scaled by dividing by α_r to agree with the scale used in plotting column deflection.

Interconnection for mode 1

Similar results are found for initial column curvature in a single half-wave and the computer plotting program used for Figure 8 needs little modification to produce the graphs for mode 1 with six restraints shown in Figure 9.

DISCRETE RESTRAINT WITH WIND LOADING

In a background paper of greater length (Burgess 1990c) some trouble is taken to express a sinusoidal wind load as a series of discrete loads so that the above theory may be applied. A later stage of the work reverts to sinusoidal wind loading to gain simplicity in the final results with no significant change compared with entirely discrete loading. The work below retains sinusoidal wind load for combination with the discrete mode r or mode 1 bracing loads applied to the restraint beam.

DEFLECTIONS DUE TO COMBINATION OF BRACING AND WIND LOAD

For a sinusoidal wind load producing bending moments with central value M , the central deflection of a restraint beam with flexural rigidity $E'I'$ is

$$\frac{M}{P_e'} = \frac{L^2}{\pi^2} \frac{M}{E'I'}$$

where $P_e' = \pi^2 E'I'/L^2$.

Mode 1

With discrete mode 1 brace loads also applied, using (39) the total central deflection u_1 for an odd number of restraints is

$$u_1 = \frac{NS_1 L^3}{E_1 I_1} \alpha_1 a + \frac{L^2}{\pi^2} \frac{M}{E_1 I_1}$$

If u_1 is limited to $\alpha = 0.003L$ for example,

$$E_1 I_1 = NS_1 L^3 \alpha_1 + \frac{L^2}{\pi^2} \frac{M}{a}$$

or expressing S_1 as $\delta_1 \frac{P_e}{L}$,

$$E_1 I_1 = EI \left(\pi^2 N \delta_1 \alpha_1 + \frac{M}{a P_e} \right) \quad (43)$$

Mode r

From (36), the total central deflection for an odd number of restraints is

$$u_1 = \frac{NS_r L^3}{E_r I_r} \alpha_r a' + \frac{L^2}{\pi^2} \frac{M}{E_r I_r}$$

where $a' = \frac{a}{m}$ represents the amplitude of the mode r initial column curvature.

Again limiting u_1 to a gives

$$E_r I_r = \frac{NS_r L^3}{m} \alpha_r + \frac{L^2}{\pi^2} \frac{M}{a}$$

$$E_r I_r = EI \left(\pi^2 \frac{N \delta_r \alpha_r}{m} + \frac{M}{a P_e} \right) \quad (44)$$

Ratio

Dividing (44) by (43) gives

$$\frac{E_r I_r}{E_1 I_1} = \frac{\pi^2 \frac{\delta_r \alpha_r}{m} + \frac{M}{N a P_e}}{\pi^2 \alpha_1 \delta_1 + \frac{M}{N a P_e}} \quad (45)$$

Putting $\frac{M}{a P_e} = v \frac{P_e}{L^2} = v t m^2$ as when plotting (11) the ratio (45) is plotted in Figure 10 for comparison with Figure 3 from the purely sinusoidal approach developed in the background paper (Burgess 1990c). The agreement is good for $r = 3$ or more; the two sets of graphs are indistinguishable for $r = 4$ or more. Much better agreement may be obtained by replacing the term $\frac{\delta_r \alpha_r}{m}$ in (45) by $\frac{\delta_r \alpha_r}{\gamma}$, implying that the amplitude of initial column curvature $a' = 0.003 \frac{L}{\gamma}$ instead of $0.003 \frac{L}{m}$. The result is plotted in Figure 11, showing that (11) is a really good approximation for (45) modified in this way. Although (45) looks as simple as (11), it contains α_r from (35) and s_r from (6), so (45) is really a complicated expression.

MODE r AS DESIGN BASIS

Figures 10 and 11 validate the sinusoidal approximation applied for Figure 3 but an important element is omitted in the numerator of (45). In Figure 12 for three restraints, the total central deflection may be found by superposition of the results for r half-waves and one half-wave given in (Burgess, 1989a) and its Appendix, giving at the centre

$$\varepsilon_1 = \frac{\frac{P}{P_e} a'}{\left(1 - \frac{P}{P_e}\right) \left(1 - \frac{\delta}{\delta_{1,ud}}\right)} + \frac{\frac{M}{N P_e}}{\left(1 - \frac{P}{P_e}\right) \left(1 - \frac{\delta}{\delta_{1,ud}}\right)} \quad (46)$$

where $a' = \frac{a}{m}$ is the amplitude of the mode r initial curvature. Considering the first mode component separately and assuming this is to be limited to 'a' gives

$$1 = \frac{\frac{M}{N a P_e}}{\left(1 - \frac{P}{P_e}\right) \left(1 - \frac{\delta_1}{\delta_{1,ud}}\right)} \quad (47)$$

The first-mode initial curvature is here zero. If such curvature exists in addition to the mode r curvature, (47) takes the form

$$1 = \frac{\frac{P}{P_e} + \frac{M}{N a P_e}}{\left(1 - \frac{P}{P_e}\right) \left(1 - \frac{\delta_1}{\delta_{1,ud}}\right)} \quad (48)$$

- and the required brace stiffness is

$$\delta_1 = \delta_{1,ud} \left(1 - \frac{\frac{P}{P_e} + \frac{M}{N a P_e}}{1 - \frac{P}{P_e}}\right) \quad (49)$$

For example with $\frac{M}{N a P_e} = \frac{\sigma P}{N P_e} = \frac{2}{5} \times 0.9 \text{ m}^2 = \frac{2}{5} \times 14.4$, the value of $\delta_{1,ud}$ from (3) for $\frac{P}{P_e} = 14.4$ is 33.43 and (49) gives

$$\begin{aligned} \delta_1 &= 33.43 \left(1 + \frac{14.4}{13.4}\right) + 33.43 \times \frac{\frac{2}{5} \times 14.4}{13.4} \\ &= 69.355 + 14.37 \\ &= 83.73 \end{aligned}$$

In deriving (40), which leads to (43), the additional deflection is again a $\sin \frac{\pi}{m}$ and y_n in (39) has the same formula but with a modified value for S , so the required flexural rigidity of the restraint beam is

$$\frac{E_1 I_1}{N E I} = \pi^2 \alpha_1 \delta_1 = \pi^2 \times 0.0410891 \times 83.73 = 33.96 \quad (50)$$

Using the combined value $\frac{P}{P_2} + \frac{M}{NaP_2}$ is equivalent to taking the amplitude of initial curvature as $(\alpha + \frac{M}{P})$. Alternatively the two terms may be separated as in deriving (43) and the result obtained is

$$\begin{aligned} \frac{E_1 I_1}{NEI} &= \pi^2 \alpha_1 \delta_1 + \frac{M}{NaP_2} & (51) \\ &= \pi^2 \times 0.0410891 \times 69.355 + \frac{2}{5} \times 14.4 \\ &= 28.13 + 5.76 \\ &= 33.89 \end{aligned}$$

In this calculation, with a result differing only slightly from the exact value 33.96, s_1 is not increased to allow for wind curvature but has its ordinary value 69.355 from (6) with $r = 1$ as seen in the working below (49).

Reverting now to (47) for zero first-mode curvature in the mode r case which is being considered, the equation corresponding to (49) is

$$\begin{aligned} s_1 &= s_{1, id} \left(1 - \frac{\frac{M}{NaP_2}}{1 - \frac{P}{P_2}} \right) & (52) \\ &= 33.43 \left(1 + \frac{2}{5} \times \frac{14.4}{13.4} \right) = 33.43 + 14.37 \\ &= 47.802 \end{aligned}$$

The calculation corresponding to (50) is

$$\begin{aligned} \frac{E_1 I_1}{NEI} &= \pi^2 \times 0.0410891 \times 47.802 \\ &= 19.385 \end{aligned}$$

and the one corresponding to (51) is

$$\begin{aligned} \frac{E_1 I_1}{NEI} &= \pi^2 \alpha_1 s_{1, id} + \frac{M}{NaP_2} & (53) \\ &= \pi^2 \times 0.0410891 \times 33.43 + 5.76 \\ &= 13.56 + 5.76 \\ &= 19.32 \text{ compared with } 19.385 \text{ above} \end{aligned}$$

Thus in (53) the figure '1' of (52) has led to the term $\pi^2 \alpha_1 s_{1, id}$ when the first-mode curvature is zero in the mode r case, and this is just what should be expected compared with (51) for the case with initial first-mode curvature. When $M = 0$ the term $\pi^2 \alpha_1 s_{1, id}$ still remains, and this again seems correct.

The additional term $\pi^2 \alpha_1 s_{1, id}$ is to be inserted in the numerator of (45), with the denominator unchanged as confirmed by (51), giving

$$\frac{E_r I_r}{E_1 I_1} = \frac{\frac{\pi^2}{m} \alpha_r \delta_r + \pi^2 \alpha_1 \delta_{1, id} + \frac{M}{NaP_2}}{\pi^2 \alpha_1 \delta_1 + \frac{M}{NaP_2}} & (54)$$

This is plotted in Figure 13, which still shows that a restraint beam designed for mode 1 will always be stiff enough for mode r , and amply stiff if there is more than 1 restraint. The relation between mode r and mode 1 requirements is emphasised because the German code and EC5 basically require design for mode 1 column restraint accompanied by wind loading, and the calculations above have shown that this is a conservative procedure for multiple braces.

A question that arises is whether the procedure is over-conservative. As explained by Möhler et al (1971) in a commentary on the 1969 version of DIN 1052, the code recommendations arising from the work by Möhler and Schelling (1968) were not fully implemented. It was decided to add only half the wind load to the first-mode restraint load because (1) established methods of wind-girder design had proved satisfactory in practice and (2) it seemed unlikely that first-mode initial curvature would occur in the same direction in all the braced members.

The object of bracing is to hold the columns essentially straight over their full length. The calculations for mode r assume this is mainly achieved for the overall length of the column but that there remains a more localised 'curvature' which is intended to allow also for initial imperfections. Taking this curvature in $r = m - 1$ half-waves maximizes the required brace stiffness and the practice has seemed reasonable after many years of consideration since the report of work by Winter (1958). However the work above shows that a mode 1 effect must be included when considering mode r behaviour, even when there is no initial mode 1 curvature.

FLEXURAL RIGIDITY REQUIRED FOR RESTRAINT BEAM

The necessary $E_r I_r$ values without wind load and with wind load may be investigated as follows. For the first mode component of mode r behaviour, instead of $s_{1,1a}$ the value s_1 will be applied to limit the additional column deflection at a restraint to the initial value there. This allows for a degree of imperfection even though the columns are initially as straight as possible.

Without wind load

The mode 1 component then requires $\frac{E_r I_r}{NEI} = \pi^2 \alpha_1 s_1$. For the mode r component the flexural rigidity of the restraint beam needs to be $\frac{E_r I_r}{NEI} = \pi^2 \alpha_r s_r$ to limit the mode r deflection at each column restraint in the same way. Thus $\frac{E_r I_r}{NEI}$ must be the greater of $\pi^2 \alpha_1 s_1$ and $\pi^2 \alpha_r s_r$.

r	s_r	α_r	s_1	α_1
1	32.5616	0.0208334	32.5616	0.0208334
2	186.0585	0.0020576	51.0971	0.0308643
3	542.7968	0.0005777	69.3547	0.0410891
4	1173.6249	0.0002426	87.4401	0.0513423
5	2131.6453	0.0001256	105.4269	0.0616030
6	3454.2693	0.0000739	123.3536	0.0718664
7	5168.3765	0.0000473	141.2415	0.0821311
8	7295.0317	0.0000322	159.1028	0.0923962

From the above table of values, when r increases from 1 to 8 $\alpha_1 s_1$ increases from 0.6784 to 14.7005 while $\alpha_r s_r$ reduces from 0.6784 to 0.2349. The two values are equal when $r = 1$ and for a larger number of restraints $\alpha_1 s_1$ becomes much greater than $\alpha_r s_r$. A restraint beam with $\frac{E_r I_r}{NEI} = \pi^2 \alpha_1 s_1$ will be more than adequate for the restraint of mode r when r exceeds 1, and just adequate when r is equal to 1. The required flexural rigidity for the case without wind load is therefore given by

$$\frac{E_r I_r}{NEI} = \pi^2 \alpha_1 s_1 \quad (55)$$

This will ensure that the mode r stiffness is great enough to limit the mode r deflection of each column restraint to its initial value, and generally to a value much smaller than the initial deviation.

With wind load

The case of zero initial first-mode curvature has been discussed, but it is preferable to allow for a small mode 1 curvature in addition to the mode r initial curvature. As an example, the required restraint beam rigidity will be calculated for an initial first-mode curvature of 0.001L with the additional deflection limited to 0.003L. Equation (48) then becomes

$$1 = \frac{\frac{P}{3P_e} + \frac{M}{NaP_e}}{\left(1 - \frac{P}{P_e}\right)\left(1 - \frac{\delta_1}{\delta_{1d}}\right)} \quad (56)$$

and the example for 3 restraints continues as

$$\begin{aligned} s_1 &= s_{1d} \left(1 - \frac{\frac{P}{3P_e} + \frac{M}{NaP_e}}{1 - \frac{P}{P_e}} \right) \quad (57) \\ &= 33.43 \left\{ 1 - \frac{14.4 \left(\frac{1}{3} + \frac{2}{9} \right)}{1 - 14.4} \right\} = 33.43 \left(1 + \frac{14.4 \times 0.7333}{13.4} \right) \\ &= 33.43 (1 + 0.7880) \\ &= 59.77 \end{aligned}$$

giving $\frac{E_r I_r}{NEI} = \pi^2 \alpha_1 s_1 = \pi^2 \times 0.04109 \times 59.77$
 $= 24.24$

The alternative calculation corresponding to (51) uses a value of s_1 excluding the wind effect, calculated as

$$\begin{aligned} s'_1 &= s_{1d} \left(1 - \frac{\frac{P}{3P_e}}{1 - \frac{P}{P_e}} \right) \quad (58) \\ &= 33.43 \left(1 + \frac{14.4}{3 \times 13.4} \right) \\ &= 45.4 \end{aligned}$$

$$\begin{aligned}
 \text{Then } \frac{E_r I_r}{NEI} &= \pi^2 \alpha_1 s_1' + \frac{M}{NaP_e} & (59) \\
 &= \pi^2 \times 0.04109 \times 45.4 + 5.76 \\
 &= 18.41 + 5.76 \\
 &= 24.17 \text{ compared with } 24.24 \text{ above.}
 \end{aligned}$$

This simplified method may be applied in a different way by combining the terms $\frac{P}{3P_e}$ and $\frac{M}{NaP_e}$ to represent an equivalent initial curvature, giving

$$\begin{aligned}
 \frac{E_r I_r}{NEI} &= \pi^2 \alpha_1 s_{1d} + \frac{P}{P_e} \left(\frac{0.001}{0.003} + \frac{V}{N} \right) & (60) \\
 &= \pi^2 \times 0.04109 \times 33.43 + 14.4 \times 0.7333 = 13.56 + 10.56 \\
 &= 24.12
 \end{aligned}$$

Equation (44) allowed for mode r deflection by incorporating a term $\frac{\pi^2}{m} \alpha_r s_r$, and the total central deflection was limited to a for an odd number of restraints. The corresponding expression incorporating (59) is

$$\frac{E_r I_r}{NEI} = \frac{\pi^2}{m} \alpha_r s_r + \pi^2 \alpha_1 s_1' + \frac{M}{NaP_e} \quad (61)$$

Graphs for $E_r I_r$ required

Equation (61) is plotted in Figure 14 with $v = 1, 2, \dots, 5$ to represent the last term $\frac{M}{NaP_e} = \frac{V P}{N P_e} = \frac{V}{N} t m^2$ with $t = 0.9$ and $N = 5$ for the number of columns braced. A single dashed line is added using (55), which represents the minimum bracing to be applied, irrespective of wind loading. With two or more braces, the graphs show that the minimum bracing caters also for the lower wind loads and need only be increased for the higher values.

The first term of (61) assumes that the mode r component of restraint deflection is equal to the initial deviation from straightness in mode r, which is taken as $a' = 0.003l = 0.003L/m$. This is not correct because the flexural rigidity necessary for mode 1 restraint is often much greater than that for mode r, as noted below equation (55). Even as it stands, (61) gives quite a low value for the first term, from

$$\begin{aligned}
 \frac{E_r I_r}{NEI} &= \frac{\pi^2}{4} \times 0.0005777 \times 542.8 + \pi^2 \times 0.04109 \times 45.4 + \frac{2}{5} \times 14.4 \\
 &= 0.7737 + 18.412 + 5.760 \\
 &= 24.95
 \end{aligned}$$

- so for design it would be satisfactory to omit the first term on the right of (61), which would then have the effect of limiting the additional mode 1 deflection to the desired value such as 0.003L used for illustration above.

DESIGN FORMULAE

The chief formula to be developed for cases with wind loading would then be

$$\frac{E_r I_r}{NEI} = \pi^2 \alpha_1 \delta_1' + \frac{M}{N \alpha P_e} \quad (62)$$

which could be expressed in the form $q = Nq_s + q_w$ in the symbols adopted by Brüninghoff (1983) and is only needed for cases where the value from (61) exceeds that from (55). An alternative form for (62) is shown by (60) and a simpler form for (55) may be obtained from (9).

REFERENCES

- Brüninghoff, H (1983) - Determination of bracing structures for compression members and beams. CIB-W18 paper no. 16-15-1, Lillehammer, 1983.
- Burgess, H J (1988) - Simple approaches for column bracing calculations. CIB-W18 paper no. 21-15-3, Vancouver, 1988.
- Burgess, H J (1989a) - Calculation of discrete restraints for columns with initial imperfections. Eleventh report of lateral stability and bracing projects (TRADA internal report), July 1989.
- Burgess, H J (1989b) - Suggested changes in Code bracing recommendations for beams and columns. CIB-W18 paper no. 22-15-1, East Berlin, Sept. 1989.
- Burgess, H J (1990a) - Calculation of discrete restraints for beam-columns without torsional restraint and for ideal beam-columns with torsional restraint. Twelfth report of lateral stability and bracing projects (TRADA internal report), January 1990.
- Burgess, H J (1990b) - Discrete bracing of beams and beam-columns with initial imperfections. Thirteenth report of lateral stability and bracing projects (TRADA internal report), March 1990.
- Burgess, H J (1990c) - Calculation of flexural rigidity for a beam restraining a number of columns. Fourteenth report of lateral stability and bracing projects (TRADA internal report), July 1990.
- v. Kármán, T and M A Biot (1940) - Mathematical Methods in Engineering. McGraw-Hill, 1940.
- Klemperer, W B and H B Gibbons (1932) - On the buckling strength of beams under axial compression, bridging elastic intermediate supports. Paper no. 35, unpublished papers presented at ASME meetings in 1932, June 1932.
- Klemperer, W B and H B Gibbons (1933) - Über die Knickfestigkeit eines auf elastischen Zwischenstützen gelagerten Balkens. Z. angew. Math u. Mech., Vol 13, p. 251, 1933.
- Macaulay, R (1919) - Note on the deflection of beams. Messenger of Mathematics, vol. 48, 1919.
- Möhler, K, J Ehlbeck, G Hempel and P Köster (1971) - Erläuterungen zu DIN 1052, Blatt 1 und 2 - Holzbauwerke - Ausgabe Oktober 1969, Bruderverlag, Karlsruhe, 1971.
- Möhler, K and W Schelling (1968) - Zur Bemessung von Knickverbänden und Knickaussteifungen im Holzbau. Der Bauningenieur, Vol 43, Part 2, S, pp. 43-48, 1968.

Tu Shou Ngo (1944) - Column with equal-spaced elastic supports. Jour. Aeronaut. Sci., Vol 11, pp. 67-72, 75, 1944.

Winter, G (1958) - Lateral bracing of columns and beams. J1 Struct Div, ASCE, paper 1561, March 1958.

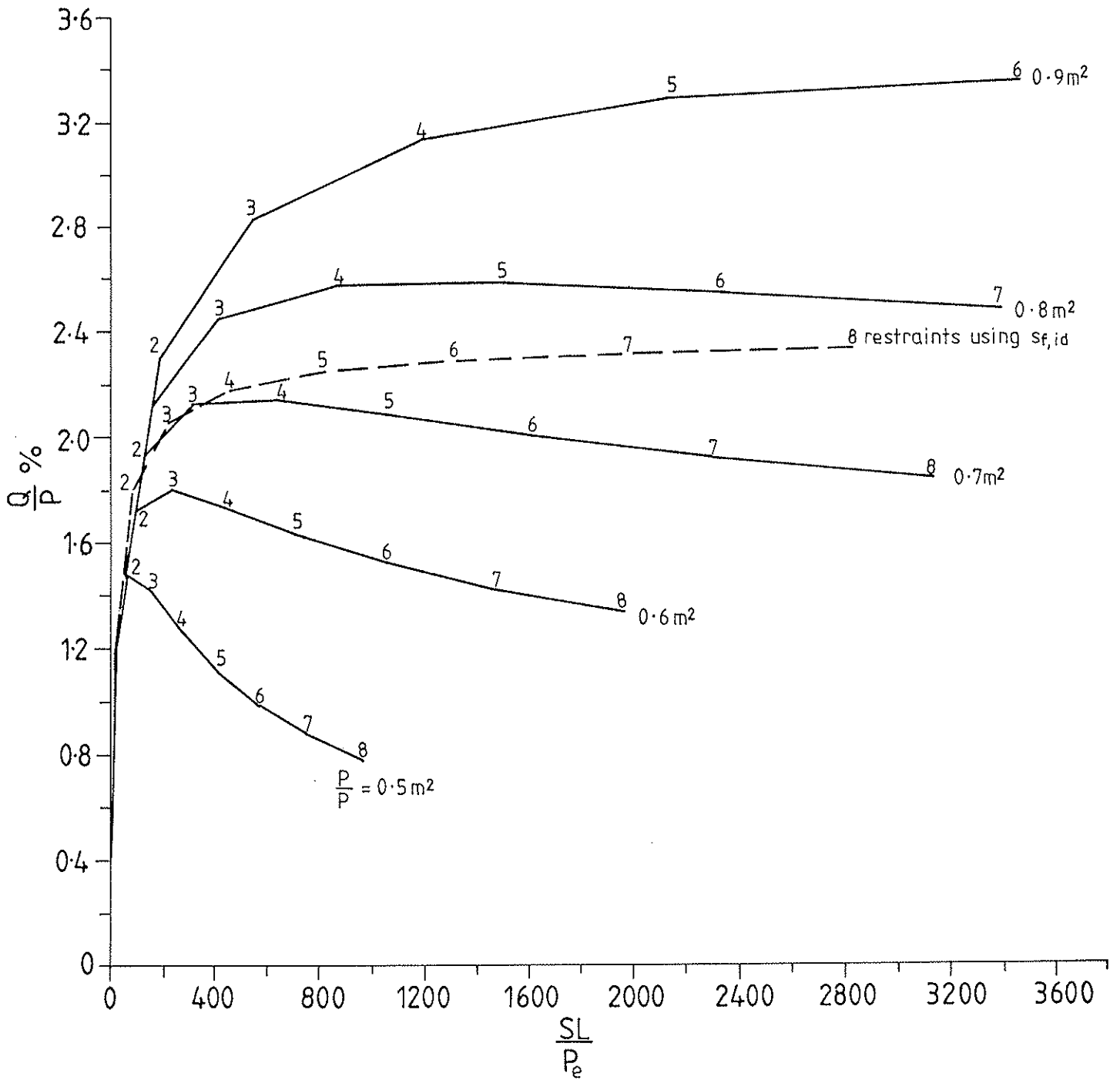


Fig.1

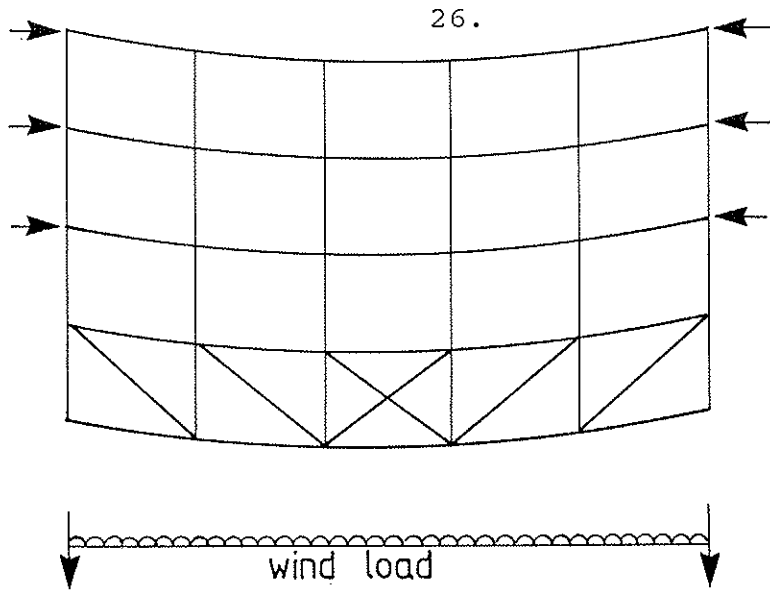


Fig. 2

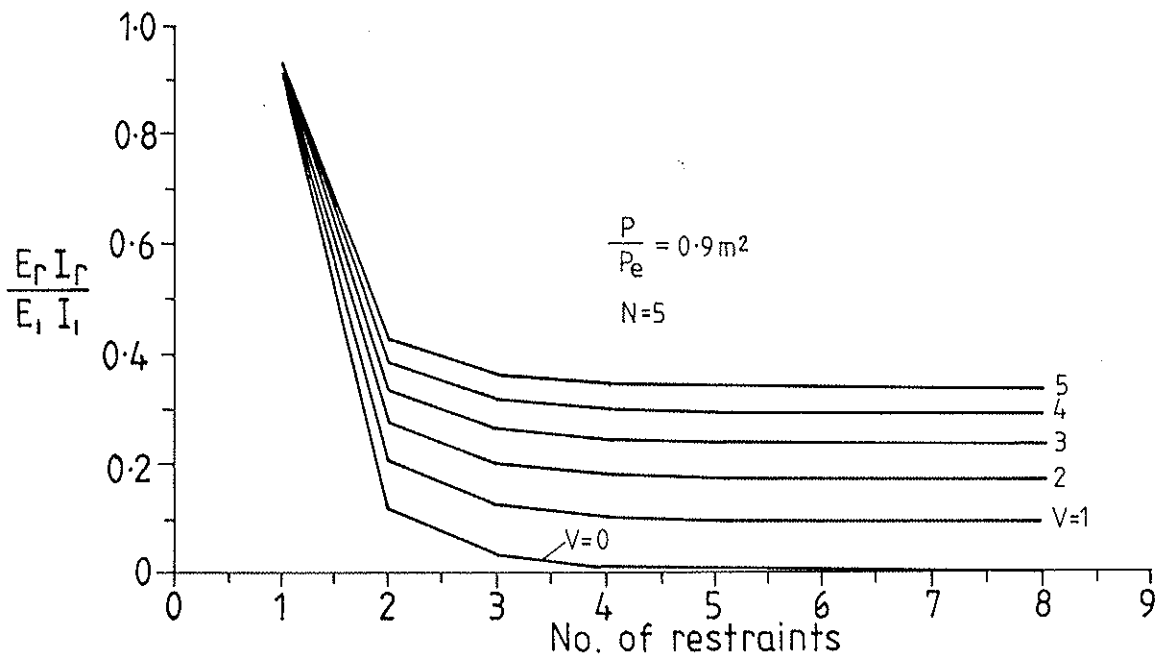


Fig. 3

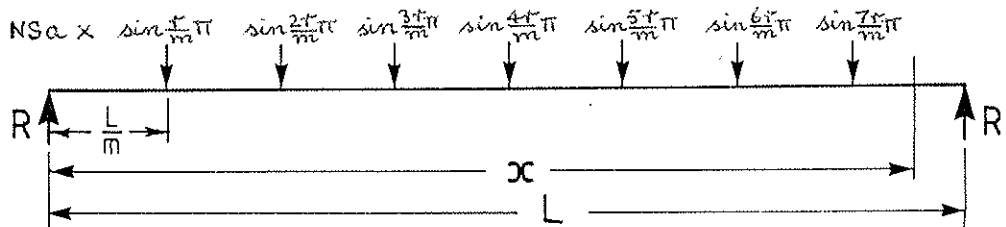


Fig. 4

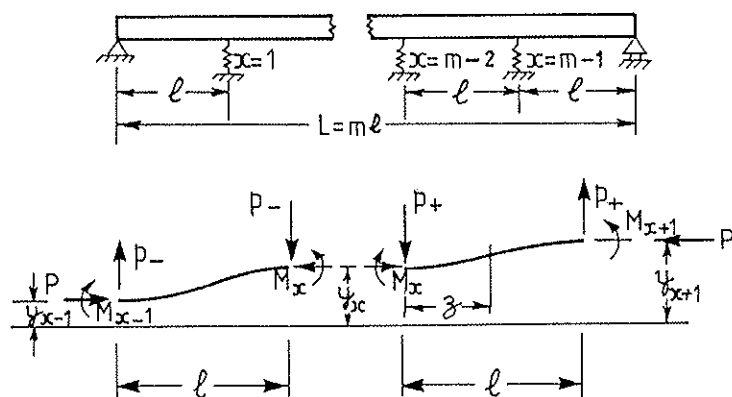


Fig. 5

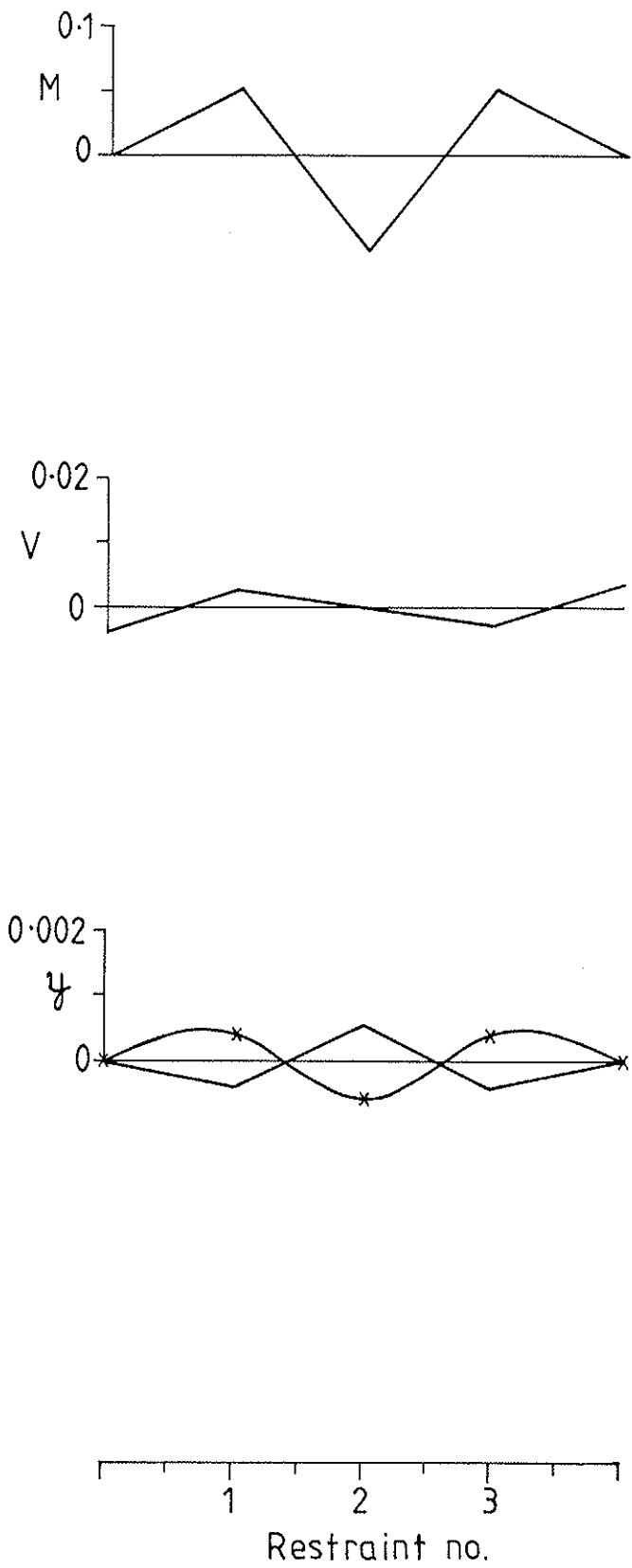


Fig. 6

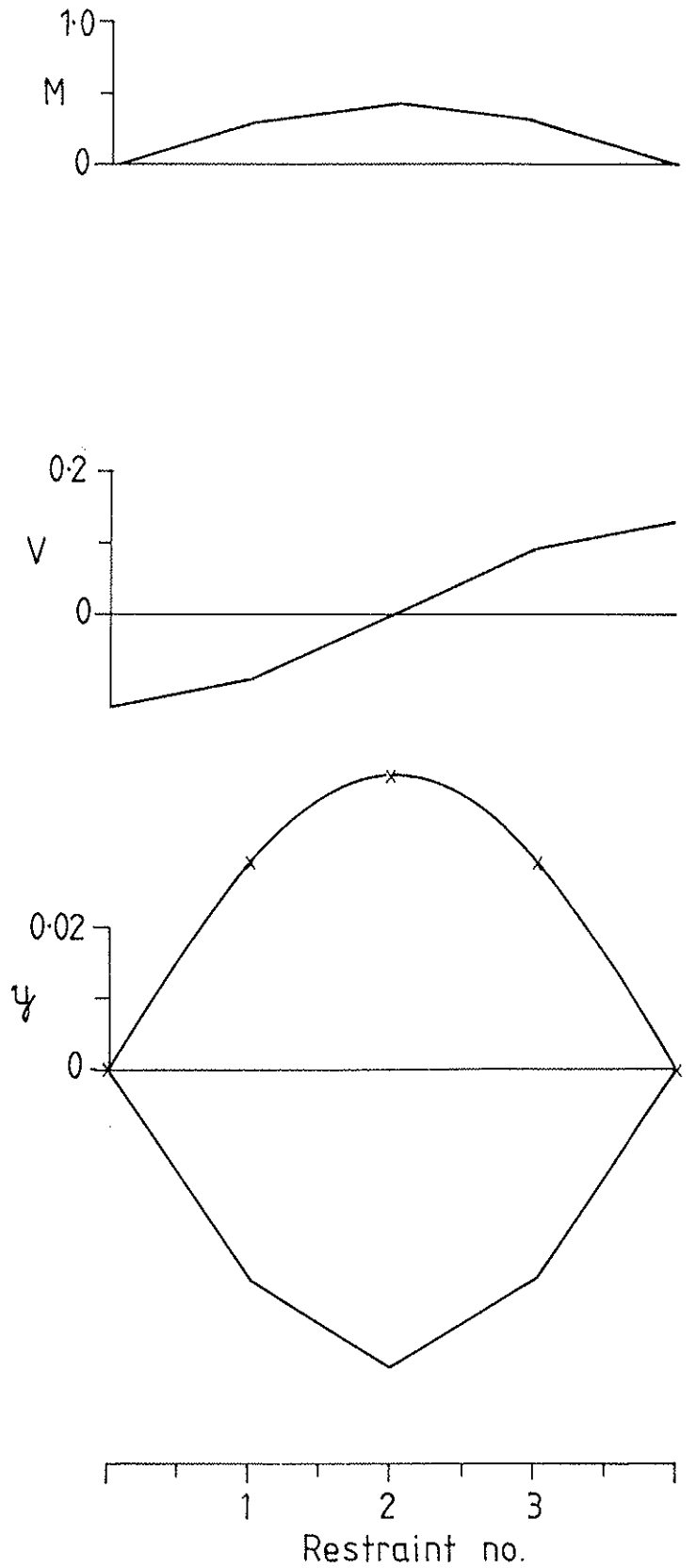


Fig. 7

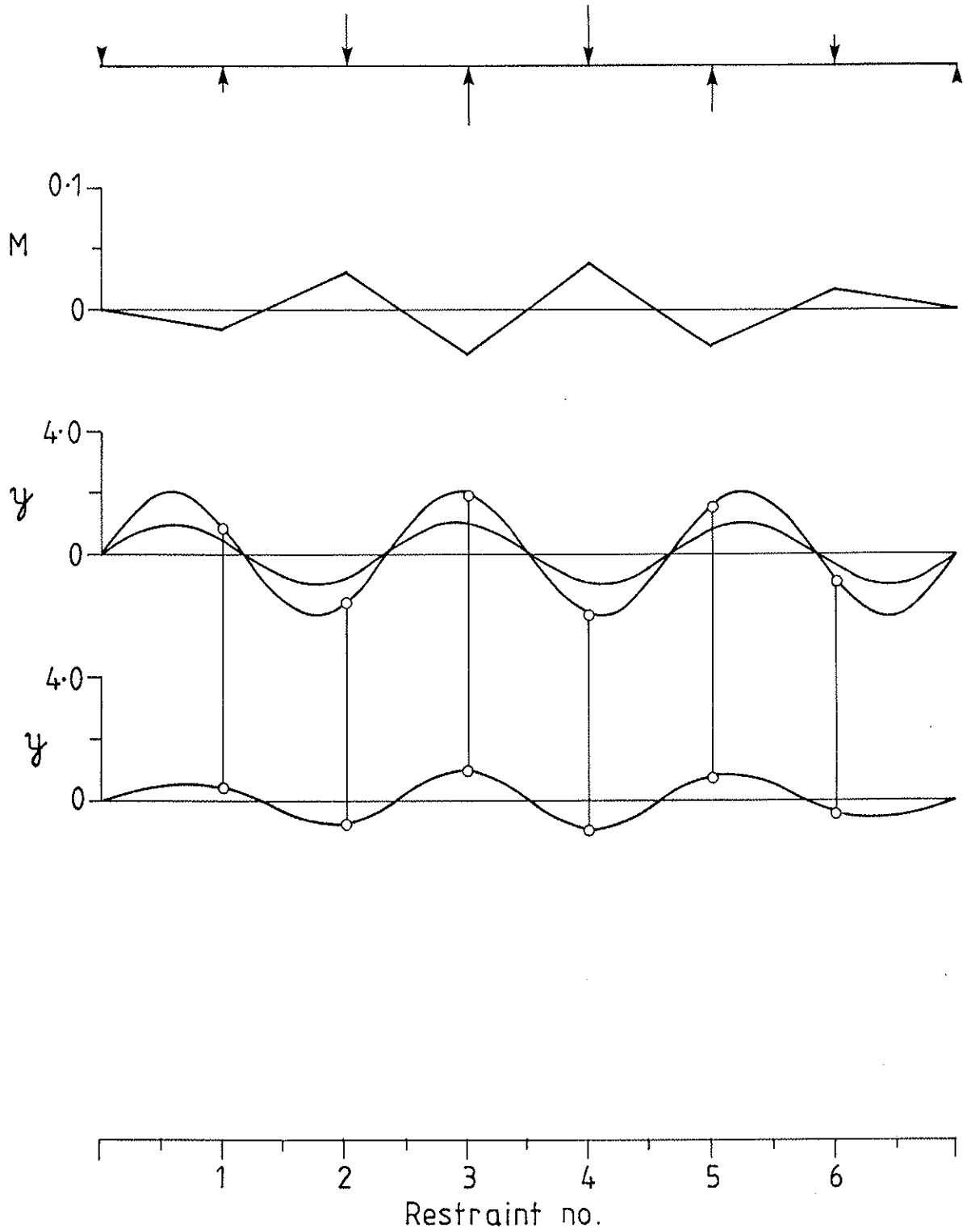


Fig. 8

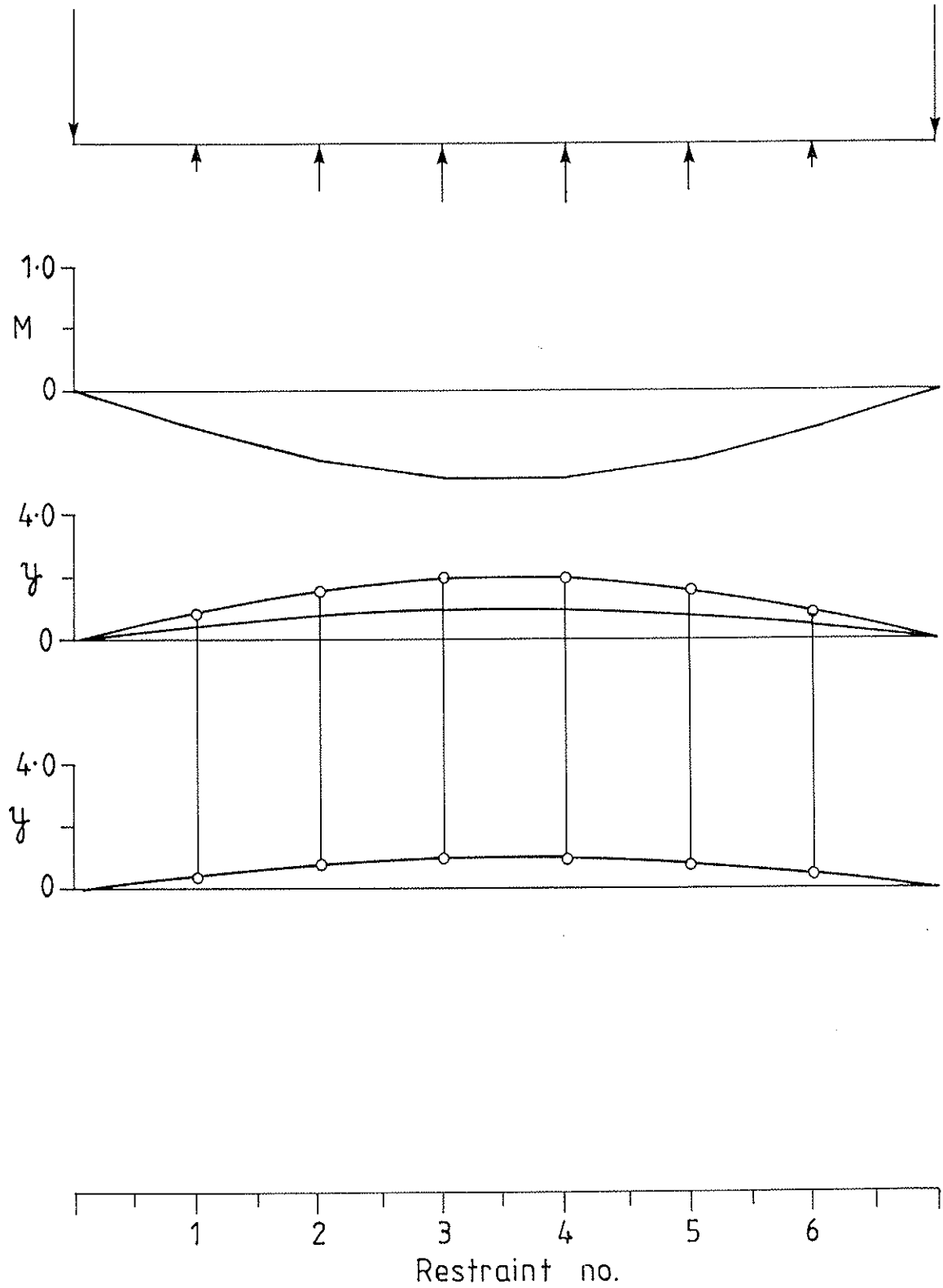


Fig. 9

Fig 10

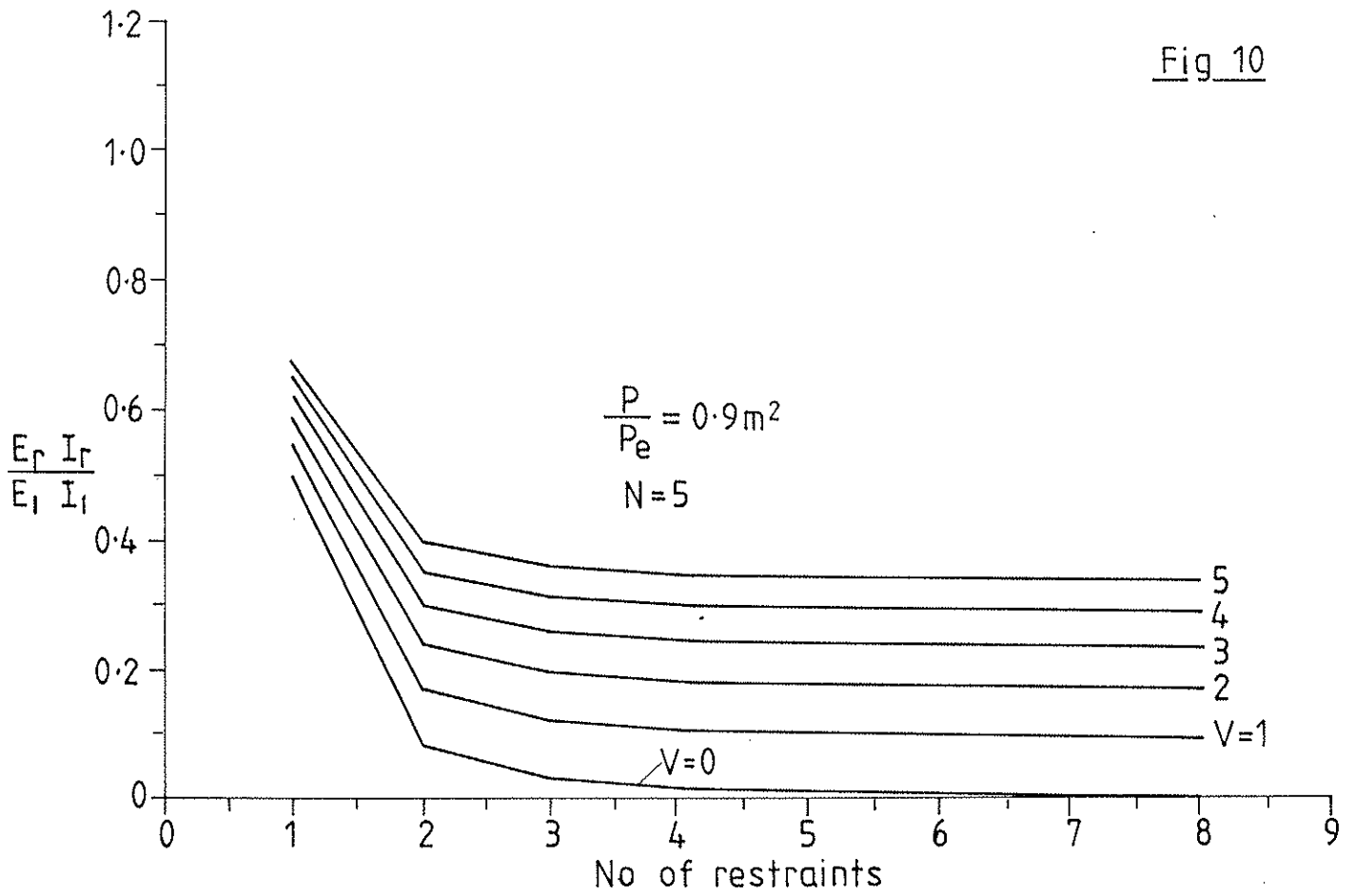
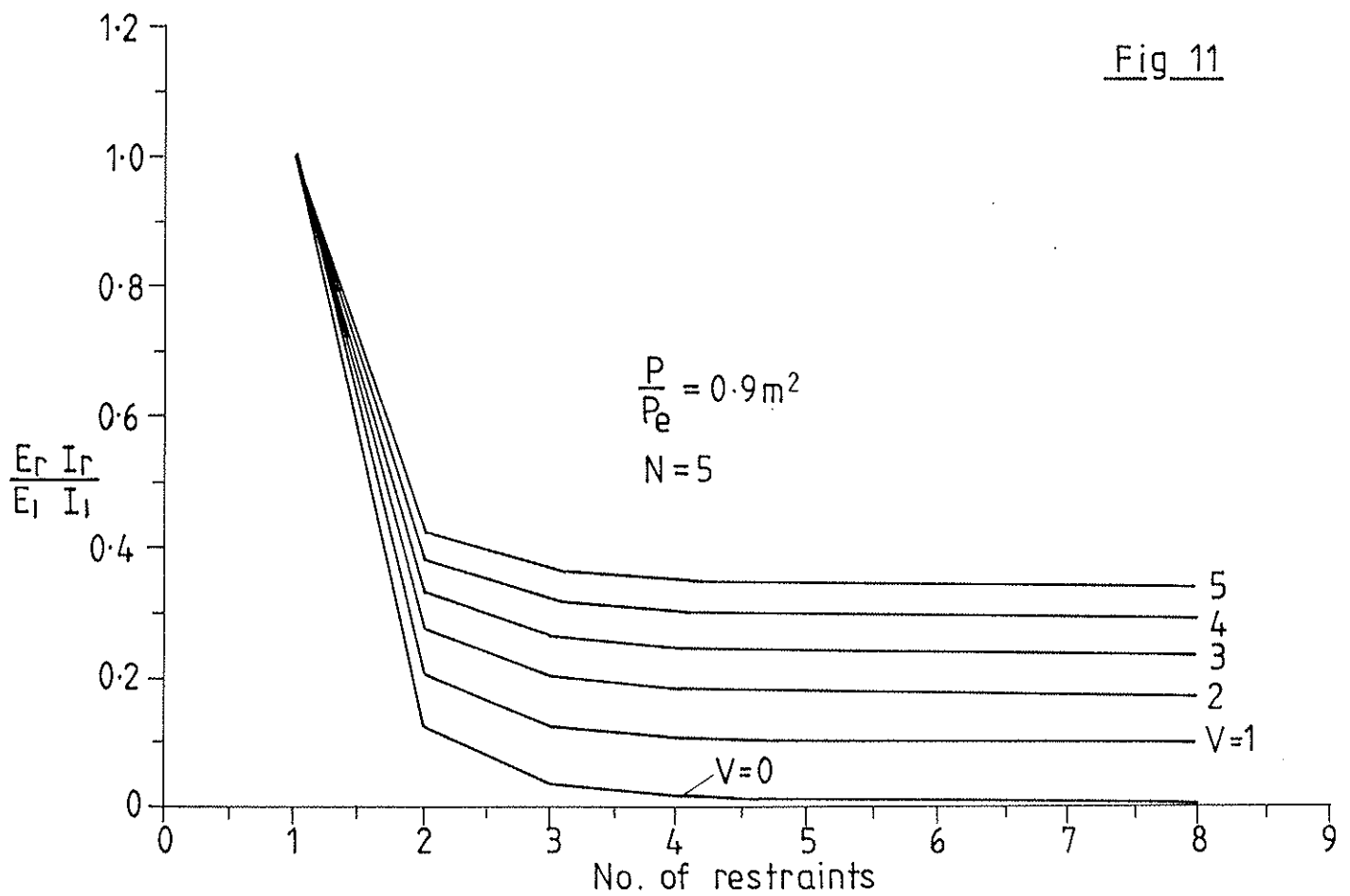


Fig 11



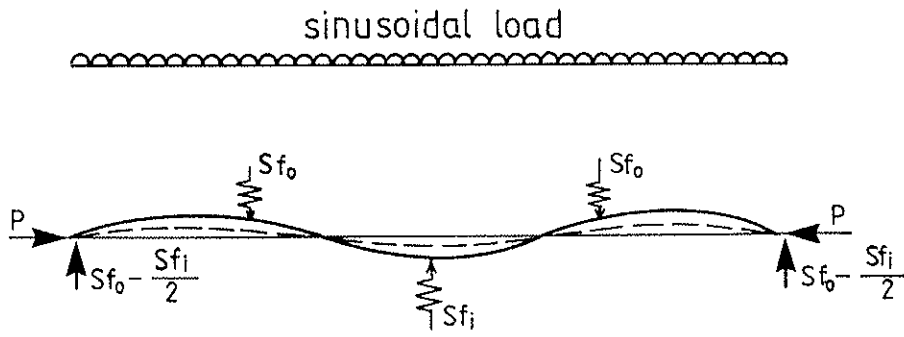


Fig. 12

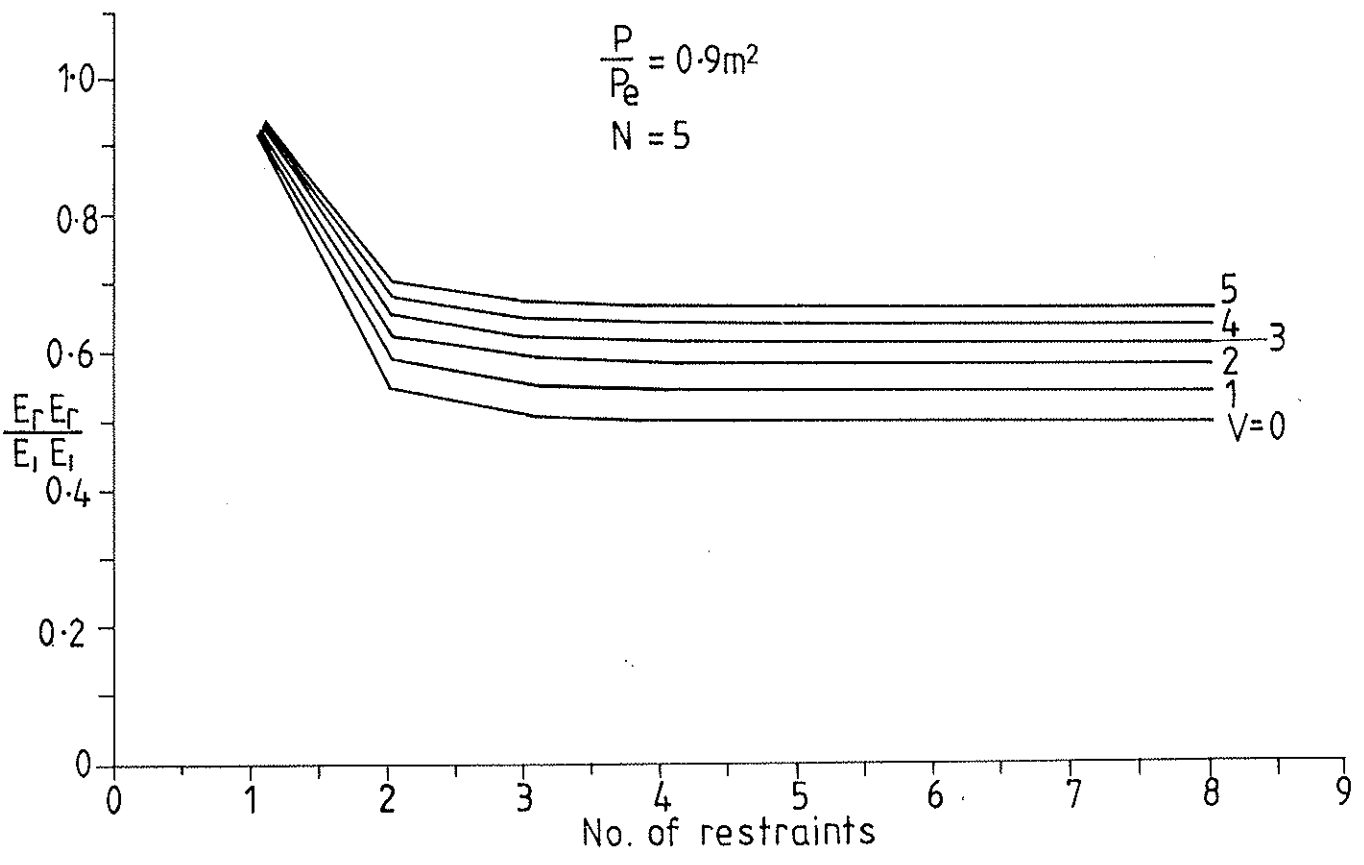


Fig. 13

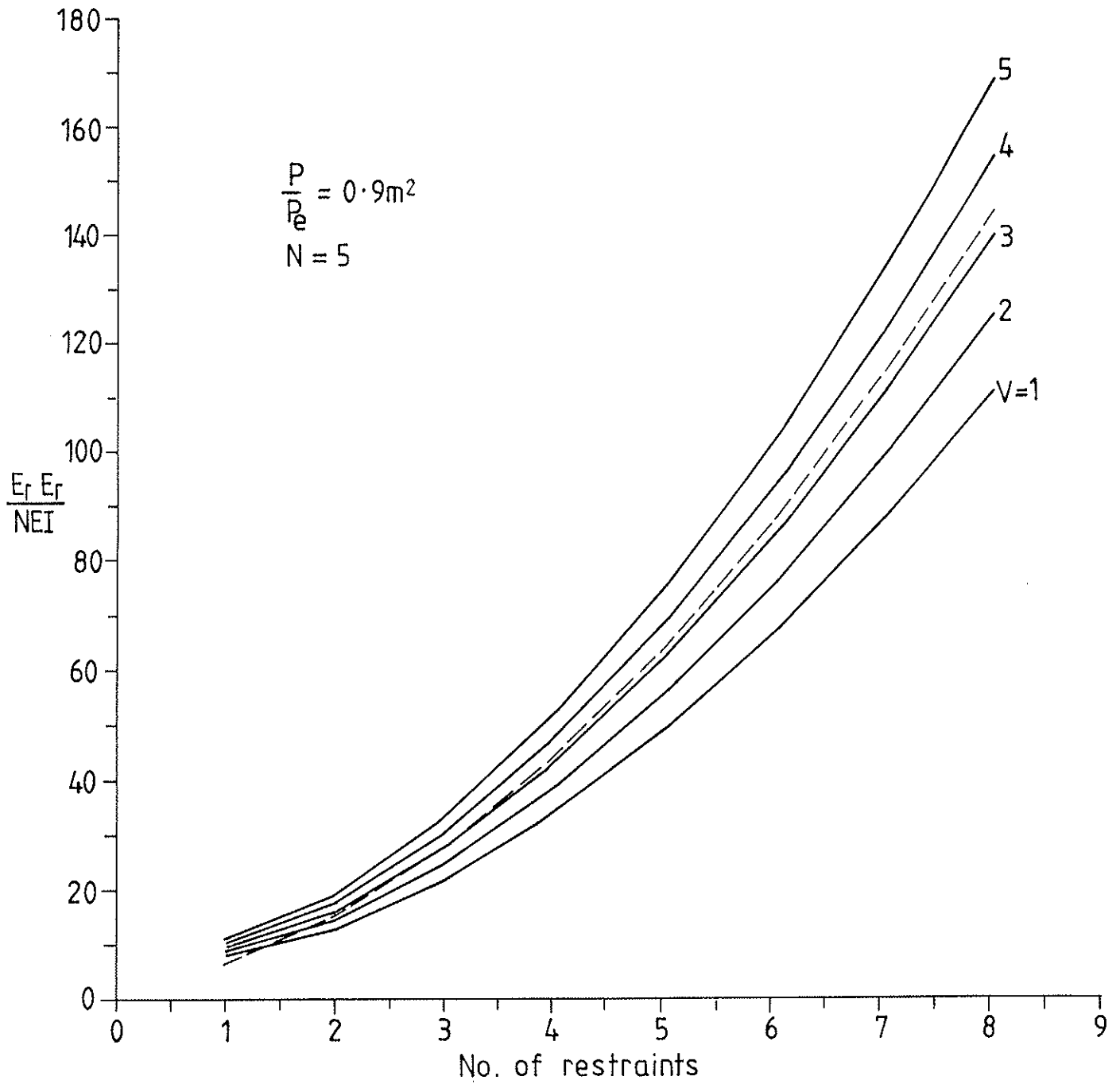


Fig. 14

INTERNATIONAL COUNCIL FOR BUILDING RESEARCH STUDIES AND DOCUMENTATION

WORKING COMMISSION W18A - TIMBER STRUCTURES

STABILITY DESIGN AND CODE RULES FOR STRAIGHT TIMBER BEAMS

by

T A C M van der Put
Delft University of Technology
The Netherlands

MEETING TWENTY - THREE

LISBON

PORTUGAL

SEPTEMBER 1990

Contents

Summary	2
Conclusion	2
Notation	3
1 Introduction	4
2 Stability of a symmetrical beam loaded in compression and double bending	
2.1 General differential equations	4
2.2 Solution of the differential equations	7
2.3 Simplification and asymptotical values of twist-bend buckling.	9
2.4 Stress criterion	10
3 Simplified design equations	
3.1 In plane buckling	12
3.2 Flexural-torsional buckling	14
3.3 Interaction equation for flexural-torsional buckling with compression.	17
4 Loading of the stability bracing	
4.1 General equations	19
4.2 Bracing and loading on the upper boundary of the lateral supported beams	20
4.3 Bracing at the center or in the tension zone of lateral supported beams	21
Literature	22
Appendix 1	
Galerkin resolution of the differential equations	23
Appendix 2	
Approximations of M_C	25
Appendix 3	
Proposal desing rules for the Eurocode	28

Summary

The design rules of the Eurocode for lateral buckling are not general enough and not consistent and need to be revised. A general approach is therefore given of the buckling and twist-bend buckling problem of symmetrical profiles loaded in bending in the two main directions and at the same time in torsion and compression.

The model, according to the second order stress theory, gives an extension of the existing models by accounting for eccentric lateral loading, for instance by purlin hangers, in combination with bending in the horizontal direction (wind loading etc.), with the influence of the initial eccentricities, the warping rigidity and the failure criterion.

The failure criterion is related to a linear behaviour until fracture, because the experimental strength of the beam is based on this approach.

Local buckling of thin webs and flanges is assumed to be prevented by stiffeners. For the stability calculation of this case, the Eurocode or [1] can be followed.

The derivation is based on an extension of the general differential equations of Chen and Atsuta [2], to eccentrically applied lateral loading. These equations can be modified to the form of those of Brüninghoff [6], with an equivalent torsional rigidity to account for the influence of warping and the Wagner effect. (The Wagner effect is the torsional moment appearing by the components of the normal stresses in a warped cross section).

The solution of the differential equations is done by the Galerkin method and results in a generalisation of the solution of [6].

Application of the failure criterion gives comparable expressions as given by Larsen [4], [5], extended for eccentrically applied lateral loading.

The equations of Brüninghoff and Larsen are thus special cases of the general expression, and are verified by tests for these and other cases [3], [5], [6] (and thesis work Stevin-laboratory).

Conclusion

The theory gives an extension of the existing methods to the general loading case of eccentrically loading in all directions (double bending with torsion and compression) and predicts low instability values for a short beam with a low warping stiffness, loaded laterally on the compression side. The existing design methods are unsafe for this case and it can be shown that the warping stiffness of rectangular beams is not neglectable in this situation.

The method provides more general and better rules for the Eurocode and will be proposed to replace art. 5.1.6, 5.1.10, 5.2.6 (see appendix 2).

Notation

M_x, M_y	bending moment about the x-axis and y-axis
M'_x	first derivative of M_x to z , along the axis of the beam
M_t	torsional moment about the beam-axis
M_u	ultimate moment for failure = $f_b \cdot W$ (ultimate stress times moment of rigidity)
M_k	theoretical twist-bend moment for pure bending and compression = $\sqrt{F_{ey} \cdot GI_m}$
M_c	theoretical twist-bend moment for lateral loading = $M_k \cdot \alpha$
M_{c0}	is M_c for $F = 0$, so for bending without compression
M_{lat}	real twist-bend moment with initial eccentricities (lateral buckling)
F	normal force
F_e	Eulerian buckling load = $\pi^2 EI / L^2$
F_c	buckling load (with initial eccentricities)
F_u	Ultimate compressive force = $f_c \cdot A$ (ultimate normal stress times section-area)
F_t	twist buckling force = $GI_t \cdot (1 + (\pi^2 \cdot EI_w / (GI_t \cdot L^2))) / (I_x + I_y)$
u, v	deformations in resp. x- and y- axis
u', v'	differentiation of u and v with respect to z
φ	rotation about the z- axis
α	factor due to the eccentricity of the lateral load
λ	is: $L/i = L \cdot \sqrt{A/I}$ slenderness
σ_d	compressive stress; f_c is the compressive strength
σ_b	bending stress; f_b is the bending strength
EI_x, EI_y	bending rigidity about resp. the x- axis and y- axis
EI_w	warping rigidity
K	Wagner effect = $-F \cdot (I_x + I_y) / A$
GI_v	equivalent torsional rigidity for high beams = $GI_t \cdot (1 - \frac{F}{F_t}) \cdot (1 + \frac{\pi^2 \cdot EI_w}{GI_t \cdot L^2})$
GI_t	Torsional rigidity (St. Venant)
GI_m	equivalent torsional rigidity = $GI_v \cdot (1 - \frac{F}{F_{ex}}) \cdot \frac{1}{1 - EI_y / EI_x}$
W_x, W_y	moment of rigidity
e, s	eccentricity of the lateral loading
p, q	lateral loading
r	is: W/A , radius of rigidity
L	span, or effective buckling length
A	Area of the cross-section of the beam

1. Introduction

The stability design of the Eurocode is not general and consistent enough. For instance, in the Eurocode the warping rigidity is neglected for free beams without a horizontal bracing. For braced beams however the torsional rigidity is neglected. Further the initial eccentricities are regarded for braced beams and neglected for free beams although the reversed would have been better. The given influence of the point of application of the lateral loading on I_{ef} applies only for long beams. So a more general approach is necessary. However the known calculation methods for twist-bend buckling are incomplete and often mutually contradictory and need to be extended.

By Chen and Atsuta [2], general equations are given for thin walled beams. However solutions are only given for pure bending with compression (thus without lateral loading).

The influence of lateral loading is given by Halasz and Cziesselski [3], however without initial eccentricities and without normal loading. The influence of warping is also not regarded there and thus there is no distinction between I-beams and box-beams. This is well done in [4] for I-beams, while the warping rigidity of rectangular- and box-beams is neglected. By Larsen [5], general equations are given for the case of pure bending and compression, including the influence of initial eccentricities and the failure criterion. The warping rigidity is however neglected (as also is done by all authors for rectangular beams) although there is accounted for warping deformation by the reduction of the torsional rigidity by the negative Wagner effect. This means that it is assumed that there is an unrestrained warping. However restraint warping and warping rigidity is always assumed to exist for thin-webbed beams and trusses (beams with low torsional rigidity), for instance in most regulations, because the twist-bend buckling of these profiles is calculated from the column buckling of the compressed flange, what is equivalent to a dominating warping rigidity.

By Brüninghoff [6], the influence of the eccentricity of the lateral loading and the initial eccentricities are regarded for high rectangular beams. However the failure criterion is not regarded and also the warping rigidity neglected, as is only right for long rectangular beams. Because comparable general equations, including the influence of warping and the failure criterion, for the general loading case are lacking for beams and for thin-webbed beams, the derivation is given here.

2 Stability of a symmetrical beam loaded in compression and double bending

2.1 General differential equations

From equilibrium of a deformed element, the general differential equations are given by Chen and Atsuta ([2], eq.(2.179a)). For symmetrically beams these simplify to (see notations):

$$EI_x \cdot v'''' + F \cdot v'' + (\varphi \cdot M_y)'' - u'''' \cdot M_t - 2 \cdot u'' \cdot M_t' + M_x'' = 0 \quad (1)$$

$$EI_y \cdot u'''' + F \cdot u'' + (\varphi \cdot M_x)'' - v'''' \cdot M_t - 2 \cdot v'' \cdot M_t' + M_y'' = 0 \quad (2)$$

$$EI_w \cdot \varphi'''' - (GI_t + K) \cdot \varphi'' + u'' \cdot M_x + v'' \cdot M_y - u \cdot M_x'' - v \cdot M_y'' + M_t' = 0 \quad (3)$$

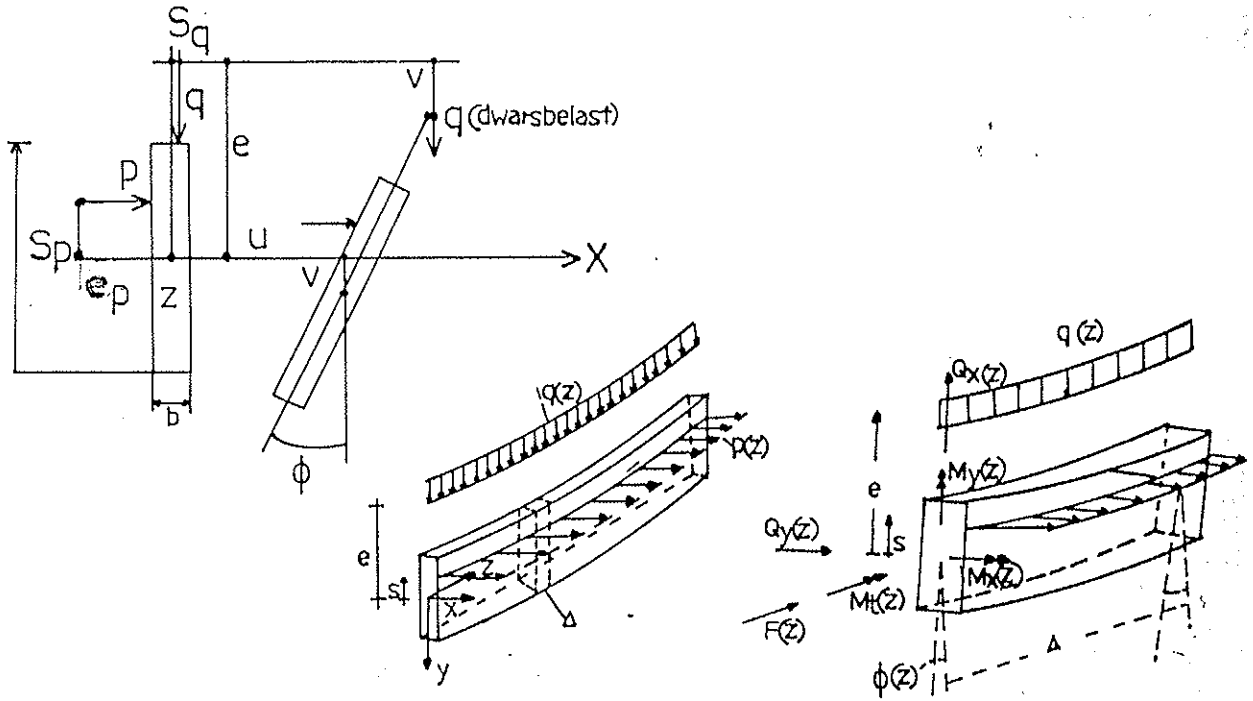


fig. 1

Further simplification is possible by omitting small terms. This can be seen by using the first term of the Fourier expansion of the variables.

For simply supported beams is for instance: $u = \bar{u} \cdot \sin(\pi \cdot z/L)$ and $M_t = \bar{M}_t \cdot \cos(\pi \cdot z/L)$ and the term: $u'''' \cdot M_t'$ of eq.(1) has a maximum value of order: $\bar{u} \cdot \bar{M}_t \cdot \pi^3/L^3$. Also the maximum value of $u'''' \cdot M_t$ is of this order. As shown later, eq.(5), the top-value of $2 \cdot u'' \cdot M_t'$ is: $(\pi^2/L^2) \cdot \bar{u} \cdot (\bar{p} \cdot h + \bar{q} \cdot b)$, what is neglectable with respect to: $- \bar{M}_x'' = \bar{q}$ in eq.(1).

In the same way, it can be shown that if $q = 0$, the term: $2 \cdot u'' \cdot M_t'$ is small with respect to the terms $(\varphi \cdot M_y)''$ and $EI_x \cdot v''''$ and the terms with M_t and M_t' can be omitted in eq.(1) and for the same reason also in eq.(2).

The values $v'' \cdot M_y$ and $v \cdot M_y''$ are also comparable and equal to: $\frac{\pi^2}{L^2} \cdot \bar{v} \cdot \bar{M}_y \cdot \sin(\frac{2\pi}{L} \cdot z)$ and in the same way is: $u'' \cdot M_x = u \cdot M_x'' = -q \cdot u$ in eq.(3).

From fig. 1, it follows that the increase of the torsional moment per unit length is:

$$- M_t' = p \cdot s_p + q \cdot s_q - p \cdot v + q \cdot u + p \cdot \varphi \cdot e_p + q \cdot \varphi \cdot e_q \quad (4)$$

So $2 \cdot u'' \cdot M_t' \hat{=} 2 \cdot u \cdot (\pi^2/L^2) \cdot (p \cdot s_p + q \cdot s_q - p \cdot v + q \cdot u + p \cdot \varphi \cdot e_p + q \cdot \varphi \cdot e_q)$, and for high eccen-

tricities, for instance: $s_p = h/2$ and $s_q = b/2$, the terms: $p \cdot h/2 + q \cdot b/2$ dominate (because $v \ll h/2$; $u \ll b/2$; $\varphi \cdot e_p \ll h/2$; $\varphi \cdot e_q \ll b/2$) and $2 \cdot u'' \cdot M_t'$ becomes:

$$2 \cdot u'' \cdot M_t' \approx u \cdot (\pi^2/L^2) \cdot (p \cdot h + q \cdot b) \quad (5)$$

For small eccentricities, for instance $s_p = s_q = 0$, this term is much smaller and it is seen that this term is always neglectable.

In eq.(3), φ'''' can be replaced by: $\varphi'''' = -(\pi^2/L^2) \cdot \varphi''$, and eq.(3) can be written in the same form as given in [6]:

$$(EI_W \cdot (\pi^2/L^2) + GI_t + K) \cdot \varphi'' - u'' \cdot M_x - M_t' - q \cdot u = 0 \quad (6)$$

According to eq.(4) is:

$$- M_t' - q \cdot u = p \cdot s_p + q \cdot s_q - p \cdot v + p \cdot \varphi \cdot e_p + q \cdot \varphi \cdot e_q = p \cdot s_v + q \cdot \varphi \cdot e_v - p \cdot v, \text{ with:}$$

$$s_v = s_p \cdot \left(1 + \frac{q \cdot s_q}{p \cdot s_p}\right) \text{ and } e_v = e_q \cdot \left(1 + \frac{p \cdot e_p}{q \cdot e_q}\right)$$

$$\text{With: } GI_v = \frac{\pi^2}{L^2} \cdot EI_W + GI_t + K = GI_t \cdot \left(1 + \frac{\pi^2 EI_W}{L^2 \cdot GI_t} - \frac{F(l_x + l_y)}{GI_t \cdot A}\right) = GI_t \cdot \left(1 + \frac{\pi^2 EI_W}{L^2 \cdot GI_t}\right) \cdot \left(1 - \frac{F}{F_t}\right),$$

where: $F_t = \frac{GI_t \cdot A}{l_x + l_y} \cdot \left(1 + \frac{\pi^2 EI_W}{L^2 \cdot GI_t}\right)$ is the twist buckling force, eq.(6) can be written:

$$GI_v \cdot \varphi'' - u'' \cdot M_x + p \cdot s_v + q \cdot \varphi \cdot e_v - p \cdot v = 0 \quad (7)$$

For high beams the term: $p \cdot v$ is small and can be neglected in eq.(7).

For high beams, $l_x \gg l_y$ and thus $p \ll q$, is in eq.(1) also the term: $(\varphi \cdot M_y)''$ neglectable because:

$$(\varphi \cdot M_y)'' \approx 4 \cdot p \cdot \varphi \ll M_x'' = -q.$$

However in eq.(2) is, for high beams, $(\varphi \cdot M_x)'' \approx 4 \cdot q \cdot \varphi$ not always of lower order than: $-p$ or $EI_y \cdot u''''$ and can only be neglected for low beams. So for high beams, eq.(1) to eq.(3) are:

$$EI_x \cdot v'''' + F \cdot v'' - q = 0 \quad (1')$$

$$EI_y \cdot u'''' + F \cdot u'' + (\varphi \cdot M_x)'' - p = 0 \quad (2')$$

$$GI_v \cdot \varphi'' - u'' \cdot M_x + p \cdot s_v + q \cdot \varphi \cdot e_v = 0 \quad (3')$$

For low beams, where l_x and l_y are not far apart, eq.(1) to eq.(3) become:

$$EI_x \cdot v'''' + F \cdot v'' - q = 0 \quad (1'')$$

$$EI_y \cdot u'''' + F \cdot u'' - p = 0 \quad (2'')$$

$$GI_v \cdot \varphi'' + q \cdot u - p \cdot v + p \cdot s_p + q \cdot s_q + p \cdot e_p \cdot \varphi + q \cdot e_q \cdot \varphi = 0 \quad (3'')$$

Now is: $q \cdot u - p \cdot v = q \cdot u \cdot \left(1 - \frac{p \cdot v}{q \cdot u}\right) = q \cdot u \cdot \frac{1 - EI_y/EI_x}{1 - F/F_{ex}}$, because according to eq.(1'') and (2''):

$$\frac{p \cdot v}{q \cdot u} = \frac{(EI_y \cdot \pi^4 / L^4 - F \cdot \pi^2 / L^2) \cdot u \cdot v}{(EI_x \cdot \pi^4 / L^4 - F \cdot \pi^2 / L^2) \cdot u \cdot v} = \frac{EI_y}{EI_x} \cdot \frac{1 - F/F_{ey}}{1 - F/F_{ex}} = \frac{EI_y / EI_x - F/F_{ex}}{1 - F/F_{ex}}$$

where: $F_{ex} = (\pi^2 / L^2) \cdot EI_x$ and: $F_{ey} = (\pi^2 / L^2) \cdot EI_y$ are the Eulerian buckling loads.

Eq.(3'') can now be written with $q \cdot u = -M_x'' \cdot u = -M_x \cdot u''$:

$$\frac{GI_y \cdot (1 - F/F_{ex})}{1 - EI_y / EI_x} \cdot \varphi'' - M_x \cdot u'' + \frac{1 - F/F_{ex}}{1 - EI_y / EI_x} \cdot (p \cdot s_v + q \cdot e_v \cdot \varphi) = 0 \quad (8)$$

or:

$$GI_m \cdot \varphi'' - M_x \cdot u'' + p \cdot s_m + q \cdot e_m \cdot \varphi = 0 \quad (8')$$

where: GI_v , s_v and e_v are multiplied by: $\frac{1 - F/F_{ex}}{1 - EI_y / EI_x}$, to get resp. GI_m , s_m , e_m .

Equation (8') has the same form as eq.(3') and can safely also be applied for high beams, where $l_y \ll l_x$, because then also: $F \ll F_{ex}$ and eq.(8') approaches eq.(3').

Equations (8'), (1') and (2') can now be used as well as for high beams ($l_x \gg l_y$) as for low beams ($l_y \rightarrow l_x$) because this system turns to eq.(1'), (2'), (3') for high beams and to eq.(1''), (2''), (3'') for low beams.

If now the initial eccentricities u_0 , v_0 and φ_0 are introduced, then the general applicable differential equations for $l_x > l_y$ are:

$$EI_x \cdot (v'''' - v_0'''') + F \cdot v'' + M_x'' = 0 \quad (1''')$$

$$EI_y \cdot (u'''' - u_0'''') + F \cdot u'' + (\varphi \cdot M_x)'' + M_y'' = 0 \quad (2''')$$

$$GI_m \cdot (\varphi'' - \varphi_0'') - M_x \cdot u'' + p \cdot s_m + q \cdot e_m \cdot \varphi = 0 \quad (3''')$$

where eq.(3''') is at the safe side if φ_0 is important.

Equations (2''') and (3''') have the same form as those of [6]. The differences are the equivalent eccentricities and rigidity GI_m (in stead of GI_y) due to warping effects.

2.2 Solution of the differential equations

Equation (1''') is directly solvable. For instance with: $v = \bar{v} \cdot \sin(\pi \cdot x / L)$; $v_0 = \bar{v}_0 \cdot \sin(\pi x / L)$ and $q = \bar{q} \cdot \sin(\pi x / L)$ is eq.(1'''):

$$\bar{v} = \frac{F_{ex} \bar{v}_0 + \bar{M}_x}{F_{ex} - F} \quad \text{with: } \bar{M}_x = \bar{q} \cdot L^2 / \pi^2 \quad \text{and } F_{ex} = \pi^2 \cdot EI_x / L^2.$$

Because $M_{x,F} = -EI_x \cdot (v - v_0)''$, is: $\bar{M}_{x,F} = \frac{\pi^2}{L^2} \cdot EI_x \cdot (\bar{v} - \bar{v}_0)$ and:

$$M_{x,F} = \frac{M_x + F \cdot v_0}{1 - F/F_{ex}} \quad (9)$$

The solution of eq.(2''') and eq.(3''') can be found by the Galerkin method:

For a given differential equation: $L(u) = 0$, in which L is a differential operator, a solution is assumed in a series form as: $u(z) = \sum_1^n a_i \cdot f_i(z)$, where $f_i(z)$ are known functions which satisfy all boundary conditions (both geometric and static), then the coefficients a_i 's can be obtained from the n conditions:

$$\int_0^L \overline{L}(u) \cdot f_j(z) \cdot d(z) = \int_0^L \overline{L}(\sum_1^n a_i \cdot f_i(z)) \cdot f_j(z) \cdot d(z) = 0 \quad (10)$$

This gives n algebraic simultaneous equations for determination of a_1 to a_n .

The application of this method for eq.(2''') and eq.(3'''), is given in the appendix. For the f_i 's, the first expanded term of the Fourier sine series are taken:

$$u = \bar{u} \cdot \sin(\pi z/L); \quad \varphi = \bar{\varphi} \cdot \sin(\pi z/L); \quad u_0 = \bar{u}_0 \cdot \sin(\pi z/L); \quad \varphi_0 = \bar{\varphi}_0 \cdot \sin(\pi z/L);$$

$$p = \bar{p} \cdot \sin(\pi z/L); \quad q = \bar{q} \cdot \sin(\pi z/L); \quad M = \bar{M} \cdot \sin(\pi z/L).$$

Multiplication by $f_j = \sin(\pi z/L)$ in eq.(10) and integration over the length L of the beam, gives two solvable equations in \bar{u} and $\bar{\varphi}$ (see appendix).

Substitution of: $u = \bar{u} \cdot \sin(\pi z/L)$ in: $M_y = -EI_y \cdot (u - u_0)''$, or: $\bar{M}_y = \frac{\pi^2}{L^2} \cdot EI_y \cdot (\bar{u} - \bar{u}_0)$ gives:

$$\bar{M}_{y,F} = \frac{F \cdot \bar{u}_0 \cdot \left(1 - \frac{q \cdot L^2}{\pi^2} \cdot \frac{e_m}{Gl_m}\right) + \bar{u}_0 \cdot F \cdot e_y \cdot \frac{M_x^2}{M_k^2} + \bar{\varphi}_0 \cdot M_x + \bar{M}_y \cdot \left(1 + \frac{M_x \cdot s_m \cdot p \cdot L^2}{\pi^2 \cdot Gl_m \cdot \bar{M}_y} - \frac{e_m \cdot q \cdot L^2}{\pi^2 \cdot Gl_m}\right)}{\left(1 - \frac{q \cdot L^2}{\pi^2} \cdot \frac{e_m}{Gl_m}\right) \cdot \left(1 - \frac{F}{F_{ey}}\right) - \frac{M_x^2}{M_k^2}} \quad (11)$$

in which: $q = \frac{8}{3 \cdot \pi} \cdot \bar{q}$; $M_x = \frac{8}{3 \cdot \pi} \cdot \bar{M}_x$ and $M_k = \sqrt{F_{ey} \cdot Gl_m}$, with: $F_{ey} = \frac{\pi^2}{L^2} \cdot EI_y$.

If M_x and M_y are only due to lateral loading resp. q and p , then: $M_x = \frac{q \cdot L^2}{\pi^2}$ and $\bar{M}_y = \frac{\bar{p} \cdot L^2}{\pi^2}$

and eq.(11) becomes (with omission of the top-bar-sign):

$$M_{y,F} = \frac{F \cdot u_0 \cdot \left(1 - \frac{e_m \cdot M_x}{Gl_m}\right) + F_{ey} \cdot u_0 \cdot \frac{M_x^2}{M_k^2} + \varphi_0 \cdot M_x + M_y \cdot \left(1 + \frac{M_x}{Gl_m} \cdot (s_m - e_m)\right)}{\left(1 - \frac{F}{F_{ey}}\right) \cdot \left(1 - \frac{e_m \cdot M_x}{Gl_m}\right) - \left(\frac{M_x}{M_k}\right)^2} \quad (11')$$

If the beam is only loaded by boundary moments, for instance: $M_x = M_0$ at $z = 0$, and for $z = L$: $M_x = M_L$, then $M_x'' = 0$ and $q = 0$ has to be taken in eq.(11).

For a combination of an eccentrical lateral loading: q with boundary moments: $M_{x,m}$ is, for a proportional loading increase, the ratio: $M_{x,m}/q$ constant and eq.(11') is generally applicable if e_m is corrected to e'_m according to:

$$e'_m = e_m \cdot \frac{q \cdot L^2 / \pi^2}{M_x} = e_m \cdot \frac{q \cdot L^2 / \pi^2}{M_{x,m} + q \cdot L^2 / \pi^2} = \frac{e_m}{1 + M_{x,m} \cdot \pi^2 / (q \cdot L^2)} = \frac{e_m}{1 + \bar{M}_{x,m} \cdot \pi^2 / (\bar{q} \cdot L^2)}$$

and s'_m according to:

$$s'_m = \frac{s_m}{1 + M_{y,m} \cdot \pi^2 / (p \cdot L^2)}$$

$\bar{M}_{x,m}$ is the top-value of the first expanded term of the Fourier expansion of the moment surface due to the boundary moments.

The same applies for the moments about the y-axis: $M_{y,m}$.

The equations (9) and (11') are thus the wanted solutions of the system eq.(1'''), (2''') and (3''').

2.3 Simplification and asymptotical values of twist-bend buckling.

In eq.(11') is: $M_k = \sqrt{F_{ey} \cdot GI_m}$, the theoretical twist-bend moment for pure bending.

This means that for: $e = s = u_0 = \varphi_0 = F = 0$, is:

$$M_{y,F} = \frac{M_y}{1 - \left(\frac{M_x}{M_k}\right)^2} \text{ and this becomes very large if } M_x \text{ approaches } M_k.$$

According to measurements of Larsen [5], $\varphi_0 \cdot M_x$ in eq.(11') is neglectable and then in eq.(11'), the nominator and denominator can be divided by: $1 - (M_x \cdot e_m) / GI_m$ and eq.(11') becomes:

$$M_{y,F} = \frac{u_0 \cdot \left(F + F_{ey} \cdot \frac{M_x^2}{(M'_c)^2}\right) + M_y \cdot \left(1 + \frac{M_x \cdot F_{ey} \cdot s_m}{(M'_c)^2}\right)}{1 - \frac{F}{F_{ey}} - \frac{M_x^2}{(M'_c)^2}} \quad (11'')$$

with: $(M'_c)^2 = M_k^2 \cdot \left(1 - \frac{e_m \cdot M_x}{GI_m}\right)$. This term $(M'_c)^2$ can be written as:

$$(M'_c)^2 = M_c^2 \cdot \frac{1 - \frac{e_m \cdot M_x}{GI_m}}{1 - \frac{e_m \cdot M_c}{GI_m}} \approx M_c^2 \cdot \left(1 - \frac{e_m \cdot M_x}{GI_m} + \frac{e_m \cdot M_c}{GI_m}\right) \geq M_c^2$$

where M_c follows from the zero value of the denominator of eq.(11'). So M_c is the reduced theoretical twist-bend buckling moment by lateral loading and normal force because for $M_x \rightarrow M_c \cdot \sqrt{1 - F/F_{ey}}$, $M_{y,F}$ becomes very large.

For high values of M_x , M_x approaches M_c , so $M'_c \rightarrow M_c$ and for high values of F is M_x small and so $(M_x/M'_c)^2$ is very small and the deviation between M'_c and M_c has a little influence. So with a small neglection on the safe side, M'_c can be replaced by M_c and is eq.(11'')

$$M_{y,F} = \frac{u_0 \cdot \left(F + F_{ey} \cdot \frac{M_x^2}{(M_c)^2}\right) + M_y \cdot \left(1 + \frac{M_x \cdot F_{ey} \cdot s_m}{(M_c)^2}\right)}{1 - \frac{F}{F_{ey}} - \frac{M_x^2}{(M_c)^2}} \quad (11''')$$

As defined above, M_c follows from the equation:

$$M_c^2 + \frac{e_m \cdot M_k^2}{G I_m} \cdot M_c - M_k^2 = 0 \quad (12)$$

The resolution of eq.(12) is:

$$M_c = \sqrt{F_{ey} \cdot G I_m} \cdot \left(\sqrt{\left(\frac{e_m}{2}\right)^2 \cdot \frac{F_{ey}}{G I_m} + 1} - \sqrt{\left(\frac{e_m}{2}\right)^2 \cdot \frac{F_{ey}}{G I_m}} \right) = M_k \cdot \alpha \quad (13)$$

So the influence of the lateral loading can be accounted for by a constant α .

The real theoretical twist-bend buckling moment that makes the denominator of (11') zero

$$M_{c,F} = M_c \cdot \sqrt{1 - F/F_{ey}} \text{ is:}$$

$$M_{c,F} = \frac{\pi}{L} \cdot \sqrt{\frac{E I_y \cdot G I_t \cdot \left(1 + \frac{\pi^2}{L^2} \cdot \frac{E I_w}{G I_t}\right) \cdot \left(1 - \frac{F}{F_t}\right) \cdot \left(1 - \frac{F}{F_{ey}}\right) \cdot \left(1 - \frac{F}{F_{ex}}\right)}{1 - \frac{E I_y}{E I_x}} \cdot \left[\sqrt{\left(\frac{e_{m0}}{2}\right)^2 \cdot \frac{F_{ey}}{G I_t} \cdot \frac{\left(1 - F/F_{ex}\right) \cdot \left(1 - F/F_{ey}\right)}{1 - F/F_t} + 1} - \sqrt{\left(\frac{e_{m0}}{2}\right)^2 \cdot \frac{F_{ey}}{G I_t} \cdot \frac{\left(1 - F/F_{ex}\right) \cdot \left(1 - F/F_{ey}\right)}{1 - F/F_t}} \right] \quad (14)$$

For pure bending, $e_{m0} = 0$, this is a well known equation from theory (see for instance [2]).

The index 0 of e_{m0} means that F in the expression for e_m is zero.

2.4 Stress criterion

The maximal stresses in the beam due to the moments $M_{x,F}$ and $M_{y,F}$, wich contain the second order effects, have to satisfy the stress criterium for failure. A reasonable approximation of this criterion, (see [4]) is:

$$\frac{\sigma_c}{f_c} + \frac{\sigma_b}{f_b} \leq 1 \quad (15)$$

with: $\sigma_b = (M_x/W_x) + (M_y/W_y)$, and $\sigma_c = F/A$ and f_c and f_b are resp. the compression and bending strengths.

This criterion is especially right for wet, high grade wood of smaller dimensions and is safe for dry lower grade timber (for combinations of bending and compression).

Substitution of eq.(9) and eq.(11''') in eq.(15) gives:

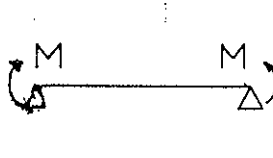
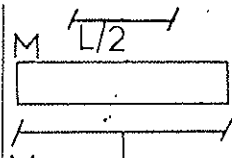
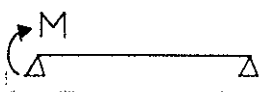
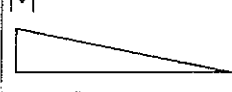
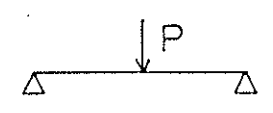
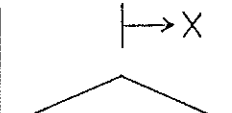
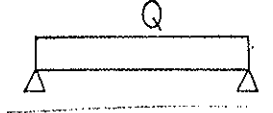
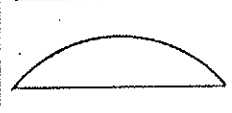
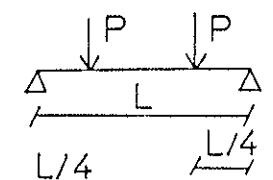
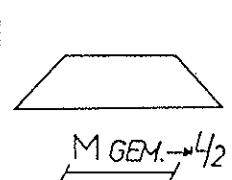
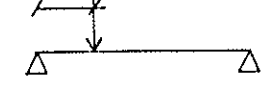
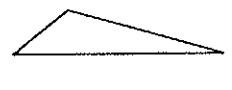
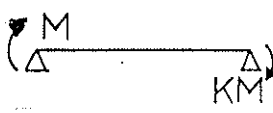
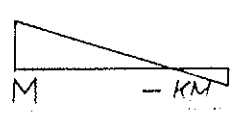
$$\frac{F}{f_c \cdot A} + \frac{M_x + F \cdot v_0}{f_b \cdot W_x \cdot \left(1 - \frac{F}{F_{ex}}\right)} + \frac{u_0 \cdot \left(F + F_{ey} \cdot \frac{M_x^2}{M_c^2}\right) + M_y \cdot \left(1 + \frac{M_x \cdot s_m \cdot F_{ey}}{M_c^2}\right)}{f_b \cdot W_y \cdot \left(1 - \frac{F}{F_{ey}} - \frac{M_x^2}{M_c^2}\right)} \leq 1 \quad (15')$$

This equation has the form of the equation of Larsen [5]. However it contains now the influence of warping, normal force and eccentrical lateral loading.

M_x in this equation stands for $\frac{8}{3 \cdot \pi} \bar{M}_x$, where \bar{M}_x is the top-value of the first term of the Fourier series expansion of the moment area. M_y is equal to \bar{M}_y .

In stead of a Fourier expansion the following approximation is possible. The value: $\frac{8}{3 \cdot \pi} \bar{M}_x$

Table 1

loading	bending moment	$\frac{8}{3 \cdot \pi} \bar{M} =$ $= M_{max}/\rho$	exact value	M/ρ
		$\frac{M}{0.93}$	$\frac{M}{1}$	$\frac{M}{1}$
		$\frac{M}{1.85}$	$\frac{M}{1.75}$	$\frac{M}{1.67}$
		$\frac{PL/4}{1.45}$	$\frac{PL/4}{1.35}$	$\frac{PL/4}{1.33}$
		$\frac{q \cdot L^2/8}{1.14}$	$\frac{q \cdot L^2/8}{1.13}$	$\frac{q \cdot L^2/8}{1.09}$
		$\frac{PL/4}{1.03}$	$\frac{PL/4}{1.04}$	$\frac{PL/4}{1}$
		$\frac{3PL/16}{1.54}$	$\frac{3PL/16}{1.44}$	$\frac{3PL/16}{1.33}$
		i^{st} expanded insufficient	$M \cdot (0.6 + 0.4 \cdot x)$ $\geq 0.4 \cdot M$	

can be replaced by the mean moment of the middle half (at the largest buckling deformation) of the beam (with a minimum of $0.4 \cdot M_{\max}$ if the moment changes sign along the beamlength and the beam buckles with double curvature).

$$\text{So: } \frac{M}{\rho} \approx \int_{-L/4}^{+L/4} \frac{M \cdot dx}{L/2} \quad (= M_{m,L/2}) \text{ given in the last column of the table.}$$

With this, a simple rule is given for the values of ρ .

Eq.(15') can be written in the well known form:

$$\frac{F}{F_u} + \frac{n_x}{n_x - 1} \cdot \frac{F \cdot v_0 + M_x}{M_{ux}} + \frac{n'_y}{n'_y - 1} \cdot \frac{F' \cdot u_0 + M'_y}{M_{uy}} \leq 1 \quad (15'')$$

$$\text{with: } n_x = \frac{F_{ex}}{F}; \quad n'_y = \frac{F_{ey}}{F'} \quad \text{with } F' = F + \frac{M_x^2}{M_c^2} \cdot F_{ey} \quad \text{and: } M'_y = M_y \cdot \left(1 + \frac{M_x \cdot s_m \cdot F_{ey}}{M_c^2}\right)$$

3 Simplified design equations

Equation (15') is general applicable and simply programmable. For practice, possibly still more simply equations are desired.

Simplification is possible by expressing the combined loading cases in the instability equation in expressions for in plane buckling by compression and lateral buckling by bending alone. Then the instability equation turns into the so called interaction equation. This interaction equation and also the equations for in plane buckling and lateral buckling can then be simplified. For comparison, the usual cases of the codes will first be regarded.

3.1 In plane buckling

Usually the case of a lateral supported beam is in the regulations. For this case is:

$$u_0 = \varphi_0 = 0; \quad M_y = 0; \quad F_{ey} \rightarrow \infty \quad \text{and} \quad M_c \rightarrow \infty.$$

Eq.(15') becomes:

$$\frac{F}{F_u} + \frac{M_x + F \cdot v_0}{M_{ux} \cdot (1 - F/F_{ex})} = 1 \quad (16)$$

For $M_x = 0$, is: $F = F_c$ (centrically loaded beam) and the equation is:

$$\frac{F_c}{F_u} + \frac{F_c \cdot v_0}{M_u \cdot (1 - F_c/F_{ex})} = 1 \quad (17)$$

F_c can be resolved of this equation and is:

$$\frac{F_c}{F_u} = \frac{1}{2} \cdot \left\{ \left(1 + \frac{F_{ex}}{F_u} + \frac{F_{ex} \cdot v_0}{M_{ux}} \right) - \sqrt{\left(1 + \frac{F_{ex}}{F_u} + \frac{F_{ex} \cdot v_0}{M_{ux}} \right)^2 - \frac{4 \cdot F_{ex}}{F_u}} \right\} \quad (18)$$

The same equation applies for an unsupported high beam or column, buckling in the weak direction. Then the index: x has to be replaced by: y.

Eq.(18) is the same as eq.(5.1.10 g) of the Eurocode.

Introducing: $k_E = F_{ex}/F_u$, and: $v_0/r = \eta \cdot L/i = \eta \cdot \lambda$, or $F_{ex} \cdot v_0/M_{ux} = k_E \cdot \eta \cdot \lambda \cdot f_c/f_b$ and $k_{col} = F_c/F_u$ then eq.(18) is:

$$k_{col} = 0.5 \cdot \left\{ \left(1 + \left(1 + \eta \cdot \lambda \cdot \frac{f_c}{f_b} \right) \cdot k_E \right) - \sqrt{\left(1 + \left(1 + \eta \cdot \lambda \cdot \frac{f_c}{f_b} \right) \cdot k_E \right)^2 - 4 \cdot k_E} \right\} \quad (18')$$

This was an earlier proposal for the Eurocode.

From eq.(17), it can be seen that for a short test-specimen, when $F_{ex} \rightarrow \infty$, the strength is:

$$F_{c0} \cdot (1 + v_0 \cdot F_u/M_{ux}) = F_u = F_{c0} (1 + \eta \cdot \lambda_0 \cdot f_c/f_b) = F_{c0} \cdot (1 + c \cdot \eta) \quad (17')$$

If there is accounted for the slenderness and initial eccentricity of the test-specimen for compression, by: $f_c = f_{c0} \cdot (1 + 20 \cdot \eta)$, then, with: $k'_{col} = \sigma_c/f_{c0}$, and $k_{eu} = k_E \cdot (1 + 20 \cdot \eta) = F_{ex}/F_{c0}$, eq.(18') becomes, according to the new Eurocode:

$$k'_{col} = 0.5 \cdot \left\{ 1 + \left(1 + \eta \cdot \lambda \cdot \frac{f_{c0}}{f_b} \cdot (1 + 20 \cdot \eta) \right) \cdot \frac{k_{eu}}{1 + 20 \cdot \eta} + \sqrt{\left(1 + \left(1 + \eta \cdot \lambda \cdot \frac{f_c}{f_b} \cdot (1 + 20 \cdot \eta) \right) \cdot \frac{k_{eu}}{1 + 20 \cdot \eta} \right)^2 - \frac{4 \cdot k_{eu}}{1 + 20 \cdot \eta}} \right\} \cdot (1 + 20 \cdot \eta) \quad (18'')$$

Because $\lambda \approx 20$ for the test-specimen in compression the term $20 \cdot \eta$ in the expressions above can better be replaced by $(20 \cdot \eta \cdot f_c/f_b)/(1 - 1/k_E)$.

In the Dutch code T.G.B. 1972 is $v_0 = (0,1 + \lambda/200) \cdot r$ and eq.(17') is with $\lambda = 0$:

$$\frac{F_{c0}}{F_u} = 1 - \frac{v_0 \cdot F_{c0}}{M_{ux}} = 1 - 0,1 \cdot r \cdot \frac{f_c}{f_b} \cdot \frac{A}{W} = 1 - 0,1 \cdot 0,75 = 1 - 0,075 = 0,925$$

where $f_c/f_b = 0,75$. So: $F_u = F_{c0}/0,925$ is used and $k_E = \pi^2 \cdot E/(f_c \cdot \lambda \cdot 3,6)$. This gives comparable results as in the Eurocode. The condition of limited deformation is not used in the Eurocode because the strength condition is the only measure for safety.

For buckling and lateral buckling further simplifications are possible by re-arranging the terms of the equations for short beams as well as for slender beams in the form:

$$a = 1 - \frac{b}{1 - c} \quad \text{with } b \ll 1 \text{ and } c \ll 1$$

making the conservative approximation possible:

$$a = \left(1 - \frac{b}{1-c}\right) \cdot \frac{1 + \frac{b}{1-c}}{1 + \frac{b}{1-c}} = \frac{1 - \left(\frac{b}{1-c}\right)^2}{1 + \frac{b}{1-c}} \approx \frac{1}{1 + \frac{b}{1-c}}$$

This too conservative value of "a" can partly be corrected by:

$$a \approx \frac{1}{1 + \frac{b}{1-c} \cdot \frac{1+c}{1+c}} = \frac{1}{1 + \frac{b+bc}{1-c^2}} \approx \frac{1}{1 + b + bc_{\max}}$$

If this is done for eq.(17) than eq.(18') may be replaced by:

$$k_{\text{col}} = \frac{1}{1 + (f_c/f_m)\eta\lambda(1 + 1/k_E)} \quad \text{if } k_E \geq 1 \text{ and:}$$

$$k_{\text{col}} = \frac{1}{1/k_E + (f_c/f_m)\eta\lambda(1 + k_E)} \quad \text{if } k_E \leq 1$$

making a simple design possible. The equations are slightly unsafe in the neighbourhood of $k_E = 1$ and can be corrected in the same way as done in 3.2 for lateral buckling.

Elimination of: v_0 from eq.(16) and eq.(17) gives the interaction equation:

$$\frac{M_x}{M_{ux}} = \left(1 - \frac{F}{F_c}\right) \cdot \left(1 - \frac{F \cdot F_c}{F_{\text{ex}} \cdot F_u}\right) \quad (19)$$

what is identically to eq.(5.1.10 d) of the Eurocode.

With the unsafe neglect of: $F \cdot F_c / (F_{\text{ex}} \cdot F_u)$ with respect to 1 in eq.(19), this equation is:

$$\frac{M_x}{M_{ux}} + \frac{F}{F_c} = 1 \quad (20)$$

being art. 4.5.4 of the Dutch timber code T.G.B. 1972.

Although the neglect is unsafe, the failure condition is in the same way too safe, and eq.(20) will give a good approximation (especially for dry, low grade, large sized timber).

3.2 Flexural-torsional buckling

For bending in the main direction without compression ($M_y = 0$; $F = 0$), eq.(15') gives the expression for lateral buckling, M_{lat} :

$$\frac{M_{\text{lat}}}{f_b \cdot W_x} + \frac{u_0 \cdot \left(F_{ey} \cdot \frac{M_{\text{lat}}^2}{M_{c0}^2}\right)}{f_b \cdot W_y \cdot \left(1 - \frac{M_{\text{lat}}^2}{M_{c0}^2}\right)} = 1 \quad (21)$$

where the index 0 in M_{c0} means that $F = 0$ in the expression for M_c .

For short beams, $M_{\text{lat}} \rightarrow M_{ux} = f_b \cdot W_x$ and $M_{\text{lat}} \ll M_{c0}$. So eq.(21) is approximately:

$$\frac{M_{lat}}{M_{ux}} = 1 - \frac{u_0 \cdot F_{ey}}{M_{uy}} \cdot \frac{M_{lat}^2 / M_{c0}^2}{1 - M_{lat}^2 / M_{c0}^2} \approx 1 - \frac{u_0 \cdot F_{ey}}{M_{uy}} \cdot \frac{M_{lat}^2}{M_{c0}^2} \cdot (1 + M_{lat}^2 / M_{c0}^2)$$

Because the second term of the last expression is small and $M_{lat} \rightarrow M_{ux}$, this can safely be approximated to:

$$M_{lat} \approx \frac{M_{ux}}{1 + \frac{u_0 \cdot F_{ey}}{M_{uy}} \cdot \frac{M_{ux}^2}{M_{c0}^2} \cdot \left(1 + \frac{M_{ux}^2}{M_{c0}^2}\right)} \quad (22)$$

or neglecting the smallest term and using a correction factor β , eq.(22) becomes:

$$M_{lat} \approx \frac{M_{ux}}{1 + \frac{u_0 \cdot F_{ey}}{M_{uy}} \cdot \frac{M_{ux}^2}{M_{c0}^2} \cdot \beta} \quad (22')$$

For slender beams, $M_{lat} \rightarrow M_{c0} \ll M_{ux}$. So eq.(21) is approximately:

$$\left(\frac{M_{lat}}{M_{c0}}\right)^2 = \frac{1}{1 + \frac{u_0 \cdot F_{ey}}{M_{uy}} \cdot \frac{1}{1 - M_{lat} / M_{ux}}} \approx \frac{1}{1 + \frac{u_0 \cdot F_{ey}}{M_{uy}} \cdot \left(1 + \frac{M_{c0}}{M_{ux}}\right)} \quad (23)$$

or:

$$\frac{M_{lat}}{M_{c0}} \approx \frac{1}{1 + \frac{u_0 \cdot F_{ey}}{2 \cdot M_{uy}} \cdot \left(1 + \frac{M_{c0}}{M_{ux}}\right)} \quad (24)$$

Eq.(24) is safe for slender beams but needs a correction factor β when applied outside the slender region and can be given like:

$$\frac{M_{lat}}{M_{c0}} \approx \frac{1}{1 + \frac{u_0 \cdot F_{ey}}{2 \cdot M_{uy}} \cdot \left(1 + \frac{M_{c0}}{M_{ux}}\right) \beta} \quad (24')$$

Eq.(22) and eq.(24) are close together in the neighbourhood where $M_{c0} = M_{ux}$ and there eq.(22') is equal to eq.(24'). The factor β can be determined from eq.(21) for that case.

Calling: $M_{lat} / M_{c0} = M_{lat} / M_{ux} = X$ and $u_0 \cdot F_{ey} / M_{uy} = c$, then eq.(21) is, using eq.(24'):

$$\frac{1}{1 + \beta c} + \frac{c}{(1 + \beta c)^2 - 1} \approx 1 \quad \text{or: } 2\beta^2 c = \frac{1 + \beta c}{1 + \beta c / 2} \approx 1 + \beta c / 2 \quad \text{giving:}$$

$$\beta \approx \frac{1}{\sqrt{2c}} + \frac{1}{8} \approx \frac{1}{\sqrt{2c}} \quad \text{and in the whole range is:}$$

$$\beta c = \sqrt{\frac{u_0 \cdot F_{ey}}{2 M_{uy}}} \cdot \sqrt{\frac{F_{ey}}{F'_{ey}}} = \sqrt{\frac{u_0 \cdot F_{ey}}{2 M_{uy}}} \cdot \frac{M_{c0}}{M_{ux}} \quad (25)$$

The equations above may also be related to the bending strength of the standard specimen. According to the Eurocode is then: $M_{u,lat} / M_{c0} = (0,75)^2 = 0,5625$ and eq.(22') becomes:

$$M_{u,lat} \approx \frac{M_{ux}}{1 + \sqrt{\frac{u_0 \cdot F'_{ey}}{2 M_{uy}} \cdot \frac{M_{u,lat}}{M_{c0}}}} = \frac{M_{ux}}{1 + \sqrt{\frac{u_0 \cdot F'_{ey}}{2 M_{uy}} \cdot (0,75)^2}} \quad (22'')$$

with the specific values of F'_{ey} and M_{c0} (F'_{ey} and M'_{c0}) for the specimen.

$u_0 F'_{ey} / 2 M_{uy} = 0,5 \cdot k'_{ey} \eta \lambda_y f_c / f_m = \eta E / (8 f_m)$ (being for instance 30η) for the test-specimen with a distance of the bracing of $L = 40 \cdot i_y$ ($\lambda_y = 40$).

With the notations:

$$k_m = M_{c0} / (M_{u,lat} (1 + 0,56 \cdot \sqrt{\eta E / (8 f_m)}))$$

$$k_{ins} = M_{lat} / M_{u,lat}$$

eq.(22') and (24') are corrected to the real bending strength $M_{u,lat}$:

$$k_{ins} = \frac{1 + 0,56 \sqrt{\eta E / (8 f_m)}}{1 + \frac{1}{k_m} \cdot \sqrt{0,5 \cdot k_{ey} \eta \lambda_y f_c / f_m}} \leq 1 \quad \text{for } k_m \geq 1 \quad (26)$$

$$k_{ins} = \frac{1 + 0,56 \sqrt{\eta E / (8 f_m)}}{\frac{1}{k_m} + \frac{1}{2} (1 + k_m) \sqrt{0,5 \cdot k_{ey} \eta \lambda_y f_c / f_m}} \quad \text{for } k_m \leq 1 \quad (27)$$

u_0 or η in this last equation is unsafely taken to be zero for the Eurocode eq.(5.1.6 e).

Thus for: $M_{lat} < M_{u,lat} / (1,4)^2$ is stated: $k_{inst} = M_{lat} / M_{u,lat} = M_{c0} / M_{u,lat} = k'_m$.

$M_{c0} = M_{k0} \cdot \alpha_0$, according to eq.(13) and: $M_{k0} = \sqrt{F'_{ey} \cdot Gl_{m0}}$. For high beams is: $EI_y \ll EI_x$, and neglecting the warping rigidity, as is possible for long beams with a rectangular cross section, $Gl_{m0} = Gl_t$. So:

$$M_{c0} = \sqrt{\frac{\pi^2 \cdot h \cdot b^3}{L^2 \cdot 12} \cdot E \cdot G \cdot \frac{h \cdot b^3}{3} \cdot \alpha_0} = \frac{\pi \cdot b^3 \cdot h}{6 \cdot L} \cdot E \cdot \sqrt{G_{mean} / E_{mean}} \cdot \alpha_0$$

Because G is related to E , the mean values of the division can be taken. From this the expression of the Eurocode follows:

$$\sigma_{c0} = M_{c0} / W_x = \frac{\pi \cdot b^2}{L \cdot h} \cdot E \cdot \alpha_0 \cdot \sqrt{G_{mean} / E_{mean}} \quad (28)$$

If the real first order bending-stress is compared with σ_{c0} , then σ_{c0} has to be replaced by $\rho \cdot \sigma_{c0}$, according to table 1. Then with $l_{ef} = L / (\rho \cdot \alpha_0)$, eq.(28) is identically to eq. (5.1.6 e) of the Eurocode. The factor: α_0 gives the influence of the eccentricities of the lateral loading (see eq.(13)) and ρ , the influence of the moment distribution. It can be seen from eq.(13) that the values of l_{ef} of the code are for slender beams and are not on the safe side for short beams. A more simple approach is to regard the mean moment over the middle half of the beam as mentioned before and to use directly the expressions for the eccentricity. It can be concluded that the Eurocode description of k_m and k_{ins} are not general enough and a better description is necessary.

3.3 Interaction equation for flexural-torsional buckling with compression.

If the rigidities EI_x and EI_y are mutually comparable, or when a beam is only loaded in the weak direction, the stability calculation of in plane buckling (without lateral buckling) is sufficient. For the general case of lateral buckling eq.(15') applies.

For only compression ($F = F_c$; $M_x = M_y = 0$), is eq.(15'):

$$\frac{F_c}{F_u} + \frac{F_c \cdot v_0}{M_{ux} \cdot \left(1 - \frac{F_c}{F_{ex}}\right)} + \frac{F_c \cdot u_0}{M_{uy} \cdot \left(1 - \frac{F_c}{F_{ey}}\right)} = 1 \quad (29)$$

For only bending ($F = 0$; $M_x = M_{lat}$; $M_y = 0$), is eq.(15') equal to eq.(21).

Elimination of u_0 and v_0 from: eq.(15'), eq.(21) and eq.(29) gives, with safe neglect of of:

$$\left(\frac{F \cdot F_c}{F_{ex} \cdot F_u} - \frac{F^2}{F_{ex} \cdot F_u}\right); \left(\frac{M_x^2 \cdot M_{lat}}{M_c^2 \cdot M_{ux}} - \frac{M_x^3}{M_c^2 \cdot M_{ux}}\right) \text{ and } \left(\frac{F \cdot M_x}{F_{ey} \cdot M_{ux}} - \frac{F \cdot M_x^2}{F_c \cdot M_c^2}\right), \text{ the equation:}$$

$$-\frac{F \cdot M_x}{F_{ey} \cdot M_{ux}} + \frac{F}{F_c} + \frac{M_x}{M_{ux}} + \left(\frac{M_x^2}{M_{lat}^2} - \frac{M_x^2}{M_{lat} \cdot M_{ux}}\right) \cdot \frac{1}{\left(1 - \frac{F}{F_t}\right) \cdot \left(1 - \frac{F}{F_{ey}}\right)} \approx 1 \quad (30)$$

For very slender beams, is: $M \leq M_{lat} \ll M_{ux}$ and is eq.(30) approximately:

$$M_x^2 \approx M_{lat}^2 \cdot \left(1 - \frac{F}{F_c}\right) \cdot \left(1 - \frac{F}{F_t}\right) \cdot \left(1 - \frac{F}{F_{ey}}\right) \quad (31)$$

Because for such beams useally: $F \leq F_c \rightarrow F_{ey} \ll F_t$ is eq.(31):

$$\frac{M_x}{M_{lat}} \approx \sqrt{\left(1 - \frac{F}{F_c}\right) \cdot \left(1 - \frac{F}{F_{ey}}\right)} \approx 1 - \frac{F}{F_c} \quad (32)$$

For short beams is: $F_{ey} \gg F_c$ and $M_{lat} \rightarrow M_{ux}$ and in eq.(30), the dominating terms are:

$$\frac{F}{F_c} + \frac{M_x}{M_{ux}} \approx 1 \quad (33)$$

Equations (32) and (33) are approximately linear and a linear interaction equation is better than a parabolic one as often is chosen in regulations, for instance in the form of eq.(31), without the terms with F_t and F_{ey} . Also the choice of such a parabolic equation in combination with eq.(33), as is proposed in [5], can be unsafe. Better, but conservative, is to use eq.(32), that approaches eq.(33) for short beams because $M_{lat} \rightarrow M_{ux}$.

In fig. 2 some possible interaction curves are given for rectangular beams ($\lambda_y = 25$ to 150) It can be seen that this curve can be approximated by two straight lines: $y = 1 - c \cdot x$ and: $y = (1 - x)/c$. The intersection of the lines is in the point $\left(\frac{1}{1+c}, \frac{1}{1+c}\right)$, or the point of intersection of the line: $y = x$, with the interaction curve, eq.(30). This point of intersection is dependent on the parameters: $K_m = M_{lat}/M_{ux}$ and: $K_c = F_c/F_{ey} = k_{col}/k_{eu}$ and if the expression for intersection is approached by the first terms of a row expansion in these pa-

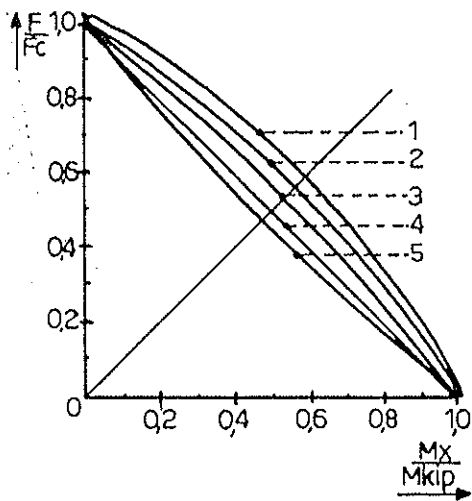


Fig. 2. Interaction curves for beams with rectangular cross section.

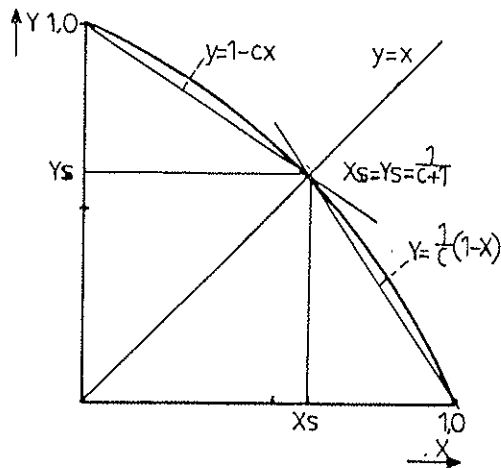


fig. 3. Approximation of the interaction curve by 2 straight lines.

parameters, then:

$$x_s = y_s = \frac{1}{1+c} = \frac{1.25 - 0.25 \cdot K_m + 2 \cdot K_m \cdot K_c}{2 + K_c} \text{ or: } c = \frac{2 + K_c}{1.25 - 0.25 \cdot K_m + 2 \cdot K_m \cdot K_c} - 1$$

and the interaction equations are for this value of c:

$$\frac{F}{F_c} + c \cdot \frac{M_x}{M_{lat}} \leq 1 \quad \text{if: } \frac{M_x}{M_{lat}} \leq \frac{F}{F_c} \tag{34}$$

$$c \cdot \frac{F}{F_c} + \frac{M_x}{M_{lat}} \leq 1 \quad \text{if: } \frac{M_x}{M_{lat}} \geq \frac{F}{F_c} \tag{35}$$

The value of F_t in eq.(30) has not much influence, so the lower bound is taken for torsionally weak beams wherefor $F_t \rightarrow F_{ey}$. Eq.(34) is, unsafe, in the code T.G.B. 1972, with:

$$K_{lat}/c = 2. \text{ So: } F/F_c + M_x/2 \cdot M_{ux} \leq 1 \text{ (art. 4.5.4).}$$

With: $c = 1$, and: $M_{lat} \approx F_c \cdot z/2$, where z is the lever arm of the moment ($M_x = z \cdot N_x$), is:

$$\frac{F}{2} + \frac{N_x \cdot z}{M_{lat}} \cdot \frac{F}{2} = \frac{F}{2} = N_x + \frac{F}{2}, \text{ giving the calculation based on the buckling of the compressed flange.}$$

This condition is fulfilled for torsional weak I- beams in pure bending. For rectangular beams this calculation is safe. However for short torsional weak I-beams and trusses lateral loaded on the compressed flange, this method is unsafe.

4 Loading of the stability bracing

4.1 General equations

The loading of the lateral support by the bracing can be determined by eq.(2'') and (3''), where the p changes sign and is equal to the loading of the bracing. At the place of the supporting bracing at height s , the deformation of the beam must be equal to the deformation of the bracing u_h . So:

$$u - u_0 + s \cdot (\varphi - \varphi_0) = u_h \quad (36)$$

Also the total load of the m supported beams: $m \cdot p$, has to be equal to the loading of the bracing. So:

$$u'''' - u_0'''' + s \cdot (\varphi'''' - \varphi_0''') = \frac{m \cdot p + W}{EI_h} = \frac{p_h}{EI_h} \quad (37)$$

where W is the loading by the wind and EI_h is the stiffness of the bracing.

Equations (2'') and (3'') become (with $s_q = 0$):

$$EI_y(u'''' - u_0''') + (M \cdot \varphi)'' + Fu'' + p = 0 \quad (38)$$

$$GI_v(\varphi'' - \varphi_0'') - M_x \cdot u'' + q \cdot e \cdot \varphi - p \cdot s = 0 \quad (39)$$

From eq.(37), eq.(38 and (39), the unknown loading p can be eliminated and two equations in u and φ remain. From the solution of these equations, p can be calculated. The solution of these two equations is analogous as for double bending as given in the appendix (see [6]). The lateral stiffness of the m supported beams is of lower order than the stiffness of the bracing, or: $m \cdot EI_y \ll EI_h$ and if, as before, the influence of φ_0 is neglected, then the loading of the bracing is:

$$P_V = \frac{\frac{m \cdot \pi^2 \cdot u_0}{L^2 \cdot s^2} \left[(G I_V - e \cdot M) \cdot \frac{F}{F_{eh}} + \frac{M^2}{F_{eh}} \right] + W \cdot \left(\frac{M \cdot (2 \cdot s - e) + G I_V - s^2 \cdot F}{s^2 \cdot F_{eh}} \right)}{\left(1 - \frac{F}{F_{eh}} \right) \cdot \left(1 + \frac{G I_V - e \cdot M}{F_{eh} \cdot s^2} \right) - \left(1 - \frac{M}{F_{eh} \cdot s} \right)^2} \quad (40)$$

with: $F_{eh} = \frac{\pi^2 \cdot E I_h}{m \cdot L^2}$.

4.2 Bracing and loading on the upper boundary of the lateral supported beams

For this case is: $F = 0$ and $e = s = h/2$ and eq.(40) becomes:

$$P_V = \frac{\pi^2 \cdot u_0 \cdot m \cdot M^2 / L^2 + W \cdot (M \cdot s + G I_{V0})}{G I_{V0} + M \cdot s - M^2 / F_{eh}} \quad (41)$$

For the loading of the bracing is:

$$P_V = \frac{\pi^4}{L^4} \cdot E I_h \cdot u_h \quad (42)$$

and elimination of $E I_h$ from eq.(41) and eq.(42) gives:

$$P_V = \frac{\pi^2 \cdot M^2 \cdot (u_h + u_0) \cdot m}{L^2 \cdot (G I_{V0} + M \cdot s)} + W \quad (43)$$

If the influence of φ_0 was not neglected eq.(43) would have been:

$$P_V = \frac{\pi^2 \cdot M^2 \cdot (u_h + u_0) \cdot m}{L^2 \cdot (G I_{V0} + M \cdot s)} + \frac{\pi^2}{L^2} \cdot \varphi_0 \cdot m \cdot M + W \quad (44)$$

Equation (43) can be written:

$$P_V = \frac{m \cdot M}{L \cdot h} \cdot \frac{20 \cdot \frac{u_0 + u_V}{L}}{1 + \frac{2 \cdot G I_{V0}}{M \cdot h}} + W \quad (45)$$

It is safe to take $M = M_{ux}$ in the denominator, giving a general equation for p_V . For rectangular beams is the term:

$$\frac{2 \cdot G I_V}{M_{ux} \cdot h} = \frac{\bar{E}}{16} \cdot \frac{0.9 \cdot h \cdot b^3 \cdot 12}{3 \cdot h \cdot f_b \cdot b \cdot h^2} \approx 75 \cdot \frac{b^2}{h^2}$$

For common beams is: $u_0/L < \sim 1/400$ and a bracing is useally stiffer than: $u_h/L < 1/600$, and p_V is for a beam with $h = 10 \cdot b$ (without wind):

$$P_V \approx \frac{m \cdot M}{21 \cdot L \cdot h}, \text{ and the total force is: } P_V = \frac{2}{\pi} \cdot p_V \cdot L = 0.03 \cdot \frac{m \cdot M}{h}$$

This is equivalent to the value of the T.G.B.: $0,03 \cdot m \cdot F_{\max}$ of braced bars.

For a rigid bracing is $u_v = 0$ and is $P_v \approx 0,02 m \cdot M/h$, as also is given in the T.G.B.

4.3 Bracing at the center or in the tension zone of lateral supported beams

The same approach as for unbraced beams can be followed for braced beams [8] and the loading of each beam is by:

$$p = p_v/m - W/m$$

leading to a similar equation as eq.(11') for the second order moment. The beam has to satisfy the failure conditions leading to a similar equation as eq.(15').

The same simplifications for braced beams can be given as is done in chap. 3 for unbraced beams (see [8]) leading to comparable equations. If the bracing is in the upper part of the compression zone of the beam ($2s - e \geq -\sqrt{Gl_{v0}/F_{eh}}$) the equations of 3.1 apply and the interaction equation is the same as eq.(19).

In general the system may become unstable if the bracing is at the tension zone and the loading is on the compression side or in the centre (for instance for pure bending is $e = 0$) so when $2s - e$ is negative or: $2s - e \leq -\sqrt{Gl_{v0}/F_{eh}}$ (≈ 0). This instability can only be avoided by sufficient torsional stiffness of the beams thus:

Stability is provided if: $s \geq e/2$ (bracing at the compression side of the beam) or when: $Gl_{v0} \geq (1/0.75^2) \cdot M_{u,lat} \cdot (e - 2 \cdot s) = 1.75 \cdot M_{u,lat} \cdot (e - 2 \cdot s)$ where $s < e/2$, (bracing at the tension side, loading at the compression side) and M_{ux} is positive and s and e are positive when pointing from the centre to the direction of the compression side.

Because of this last requirement $h/b < \sim 4$ is necessary to have no reduced bending strength for rectangular beams with bracing at the lower tension edge of the beam.

If this requirement is not fulfilled the following design rules apply:

$$M_{lat} = \frac{M_{ux}}{1 + \sqrt{\frac{u_0 M_{ux}^2}{M_{uy} Gl_{v0}} \cdot \left(1 + \frac{M_{ux}}{M_{c0}}\right)}} \quad \text{if } M_{ux} \leq M_{c0} \quad (46)$$

$$M_{lat} = \frac{M_{c0}}{1 + \sqrt{\frac{u_0 M_{ux}^2}{M_{uy} Gl_{v0}} \cdot \left(1 + \frac{M_{c0}}{M_{ux}}\right) \cdot \frac{M_{c0}^2}{M_{ux}^2}}} \quad \text{if } M_{ux} \geq M_{c0} \quad (47)$$

$$\text{with: } M_{c0} = \frac{Gl_{v0}}{e - 2z} ; \quad e - 2z \geq \sqrt{Gl_{v0}/F_{eh}}$$

With the notations given before:

$$k_m = M_{c0} / (M_{u,lat} (1 + 0.56 \cdot \sqrt{\eta E / (8f_m)}))$$

$$k_{ins} = M_{lat} / M_{u,lat}$$

eq.(46) and (47) become:

$$k_{ins} = \frac{1 + 0.56\sqrt{\eta E/(8f_m)}}{1 + \frac{1}{\sqrt{k_m}} \left(1 + \frac{1}{k_m}\right) \sqrt{\eta \lambda_y r_x' / (e - 2z)}} \quad \text{for } k_m \geq 1 \quad (46')$$

$$k_{ins} = \frac{1 + 0.56\sqrt{\eta E/(8f_m)}}{\frac{1}{k_m} + \sqrt{k_m} \left(1 + k_m\right) \sqrt{\eta \lambda_y r_x' / (e - 2z)}} \quad \text{for } k_m \leq 1 \quad (47')$$

Literature

- [1] Kuipers, J.; Buckling strength of plywood; Ploos v. Amstel H.; Report 4-78-2 TC 35; Report 4-75-1 TC 34; H.V.I.- documentation nr. 10 and nr. 14.
- [2] Chen and Atsuta, Theory of beam-columns vol. 2, chapt. 3.
- [3] Hlalach and Cziesielski, Berichte aus der Bauforschung, h. 47.
- [4] Larsen, Beregning af Troekonstruktioner, Kobenhavn, 1967.
- [5] Larsen and Theilgaard, ASCE-Journ. vol. 105, nr. ST 7, July 1979.
- [6] Brüninghoff, dissertation, Karlsruhe 1972.
- [7] van der Put, Kip van volle wand constructies en dunwandige profielen, Report 4-81-11 KB 20, pg. 52, Stevinlaboratory.
- [8] van der Put, Algemene stabiliteitsberekening voor constructie-elementen van hout, Report 4-86-12 KB 21 stevinlaboratory.

Appendix 1

Galerkin resolution of the differential equations.

The differential equations (2''') and (3'''): $\bar{L}_2(u, \varphi) = 0$ and $\bar{L}_3(u, \varphi) = 0$ are solved for the first expanded of the Fourier sinus series:

$$u = \bar{u} \cdot \sin(\pi \cdot z/L); \quad u_0 = \bar{u}_0 \cdot \sin(\pi \cdot z/L); \quad \varphi = \bar{\varphi} \cdot \sin(\pi \cdot z/L); \quad \varphi_0 = \bar{\varphi}_0 \cdot \sin(\pi \cdot z/L);$$

$$p = \bar{p} \cdot \sin(\pi \cdot z/L); \quad M_y = \bar{M}_y \cdot \sin(\pi \cdot z/L), \quad \text{where } p = d^2(M_y)/dy^2.$$

For the loading in the main direction M_x , q , two known expanded terms are regarded in order to see the accuracy of the description by the first expanded term for special loadings. The second expanded term with $\sin(2 \cdot \pi \cdot z/L)$, has no influence in this case.

$$M_x = M_1 \cdot \sin(\pi \cdot z/L) + M_3 \cdot \sin(3 \cdot \pi \cdot z/L); \quad q = q_1 \cdot \sin(\pi \cdot z/L) + q_3 \cdot \sin(3 \cdot \pi \cdot z/L).$$

In the Galerkin equations: $\int_0^L \bar{L}_2(u, \varphi) \cdot f_1(z) \cdot dz = 0$ and: $\int_0^L \bar{L}_3(u, \varphi) \cdot f_1(z) \cdot dz = 0$, is:

$$f_1(z) = f_1(z) = \sin(\pi \cdot z/L)$$

and these equations become:

$$\int_0^L \left[E I_y \cdot \frac{\pi^4}{L^4} \cdot (\bar{u} - \bar{u}_0) \cdot \sin^2(\pi \cdot z/L) - F \cdot \bar{u} \cdot \frac{\pi^2}{L^2} \cdot \sin^2(\pi \cdot z/L) - \bar{\varphi} \cdot \frac{\pi^2}{L^2} \cdot \sin^2(\pi \cdot z/L) \cdot \left\{ M_1 \cdot \sin\left(\frac{\pi \cdot z}{L}\right) + M_3 \cdot \sin\left(3 \cdot \frac{\pi \cdot z}{L}\right) \right\} + 2 \cdot \frac{\pi^2}{L^2} \cdot \bar{\varphi} \cdot \cos(\pi \cdot z/L) \cdot \sin(\pi \cdot z/L) \cdot \left\{ M_1 \cdot \cos\left(\frac{\pi \cdot z}{L}\right) + 3 \cdot M_3 \cdot \cos\left(3 \cdot \frac{\pi \cdot z}{L}\right) \right\} + \bar{\varphi} \cdot \frac{\pi^2}{L^2} \cdot \sin^2(\pi \cdot z/L) \cdot \left\{ M_1 \cdot \sin\left(\frac{\pi \cdot z}{L}\right) + 9 \cdot M_3 \cdot \sin\left(3 \cdot \frac{\pi \cdot z}{L}\right) \right\} - M_y \cdot \frac{\pi^2}{L^2} \cdot \sin^2(\pi \cdot z/L) \right] \cdot dz = 0$$

$$\int_0^L \left[- G I_m \cdot (\bar{\varphi} - \bar{\varphi}_0) \cdot \frac{\pi^2}{L^2} \cdot \sin^2(\pi \cdot z/L) + \bar{u} \cdot \frac{\pi^2}{L^2} \cdot \sin^2(\pi \cdot z/L) \cdot \left\{ M_1 \cdot \sin\left(\frac{\pi \cdot z}{L}\right) + M_3 \cdot \sin\left(3 \cdot \frac{\pi \cdot z}{L}\right) \right\} + e_m \cdot \bar{\varphi} \cdot \sin^2(\pi \cdot z/L) \cdot \left\{ q_1 \cdot \sin\left(\frac{\pi \cdot z}{L}\right) + q_3 \cdot \sin\left(3 \cdot \frac{\pi \cdot z}{L}\right) \right\} + \bar{p} \cdot s_m \cdot \sin^2(\pi \cdot z/L) \right] \cdot dz = 0$$

In these equations are:

$$\frac{\pi}{L} \cdot \int_0^L \sin^2(\pi \cdot z/L) \cdot dz = \int_0^L \sin^2(\pi \cdot z/L) \cdot d(\pi \cdot z/L) = \int_0^\pi \sin^2(\alpha) \cdot d\alpha = \frac{\pi}{2}$$

$$\int_0^\pi \sin^3(\alpha) \cdot d\alpha = \frac{4}{3}; \quad \int_0^\pi \sin^2(\alpha) \cdot \sin(3\alpha) \cdot d\alpha = -\frac{4}{15}; \quad \int_0^\pi \sin(\alpha) \cdot \cos^2(\alpha) \cdot d\alpha = \frac{2}{3}$$

$$\int_0^\pi \sin(\alpha) \cdot \cos(\alpha) \cdot \cos(3\alpha) \cdot d\alpha = -\frac{2}{5}. \quad \text{So the equations become:}$$

$$E I_y \cdot \frac{\pi^4}{L^4} \cdot (\bar{u} - \bar{u}_0) \cdot \frac{\pi}{2} - F \cdot \bar{u} \cdot \frac{\pi^2}{L^2} \cdot \frac{\pi}{2} - \bar{\varphi} \cdot \frac{\pi^2}{L^2} \cdot M_1 \cdot \frac{4}{3} + \bar{\varphi} \cdot \frac{\pi^2}{L^2} \cdot M_3 \cdot \frac{4}{15} + 2 \cdot \frac{\pi^2}{L^2} \cdot \bar{\varphi} \cdot M_1 \cdot \frac{2}{3} +$$

$$- 2 \cdot \frac{\pi^2}{L^2} \cdot \bar{\varphi} \cdot 3 \cdot M_3 \cdot \frac{2}{5} - \bar{\varphi} \cdot \frac{\pi^2}{L^2} \cdot M_1 \cdot \frac{4}{3} + 9 \cdot M_3 \cdot \bar{\varphi} \cdot \frac{\pi^2}{L^2} \cdot \frac{4}{15} - \bar{M}_y \cdot \frac{\pi^2}{L^2} \cdot \frac{\pi}{2} = 0$$

and:

$$- Gl_m \cdot (\bar{\varphi} - \bar{\varphi}_0) \cdot \frac{\pi^2}{L^2} \cdot \frac{\pi}{2} + \bar{u} \cdot \frac{\pi^2}{L^2} \cdot M_1 \cdot \frac{4}{3} - \bar{u} \cdot M_3 \cdot \frac{\pi^2}{L^2} \cdot \frac{4}{15} + e_m \cdot \bar{\varphi} \cdot q_1 \cdot \frac{4}{3} - e_m \cdot \bar{\varphi} \cdot q_3 \cdot \frac{4}{15} + \bar{p} \cdot s_m \cdot \frac{\pi}{2} = 0$$

or:

$$El_y \cdot \frac{\pi^2}{L^2} \cdot (\bar{u} - \bar{u}_0) - F \cdot \bar{u} - \bar{\varphi} \cdot \frac{8}{3 \cdot \pi} \cdot M_1 + \bar{\varphi} \cdot \frac{8}{15 \cdot \pi} \cdot M_3 - \bar{M}_y = 0$$

and:

$$- Gl_m \cdot (\bar{\varphi} - \bar{\varphi}_0) + \frac{8}{3 \cdot \pi} \cdot M_1 \cdot \bar{u} - \frac{8}{15 \cdot \pi} \cdot M_3 \cdot \bar{u} + e_m \cdot \bar{\varphi} \cdot q_1 \cdot \frac{L^2}{\pi^2} \cdot \frac{8}{3 \cdot \pi} - e_m \cdot \bar{\varphi} \cdot q_3 \cdot \frac{L^2}{\pi^2} \cdot \frac{8}{15 \cdot \pi} + \bar{p} \cdot \frac{L^2}{\pi^2} \cdot s_m = 0$$

With: $q = \frac{8}{3\pi} \cdot \bar{q}_1 \cdot \left(1 - \frac{\bar{q}_3}{5 \cdot \bar{q}_1}\right)$; $M_x = \frac{8}{3\pi} \cdot M_1 \cdot \left(1 - \frac{M_3}{5 \cdot M_1}\right)$; $F_{ey} = \frac{\pi^2}{L^2} \cdot El_y$; $e'_m = e_m \cdot \frac{q \cdot L^2}{\pi^2 \cdot M_x}$ and:

$$s'_m = s_m \cdot \frac{\bar{p} \cdot L^2 / \pi^2}{\bar{M}_y} \text{ are these equations:}$$

$$F_{ey} \cdot (\bar{u} - \bar{u}_0) - F \cdot \bar{u} - \bar{\varphi} \cdot M_x - \bar{M}_y = 0$$

$$Gl_m \cdot (\bar{\varphi} - \bar{\varphi}_0) - M_x \cdot \bar{u} - e'_m \cdot \bar{\varphi} \cdot M_x - s'_m \cdot \bar{M}_y = 0$$

From these equations are \bar{u} and $\bar{\varphi}$ solvable. So is:

$$\bar{u} = \frac{\bar{M}_y \cdot (Gl_m - e'_m \cdot M_x + s'_m \cdot M_x) + M_x \cdot Gl_m \cdot \bar{\varphi}_0 + F_{ey} \cdot \bar{u}_0 \cdot (Gl_m - e'_m \cdot M_x)}{(F_{ey} - F) \cdot (Gl_m - e'_m \cdot M_x) - M_x^2}$$

The total moment $M_{y,F}$ (with M_y and M_x as first order part) follows from:

$$M_{y,F} = - El_y \cdot (u - u_0)'' \rightarrow \bar{M}_{y,F} = \frac{\pi^2}{L^2} \cdot El_y \cdot (\bar{u} - \bar{u}_0) = F_{ey} \cdot (\bar{u} - \bar{u}_0) \rightarrow$$

$$M_{y,F} = \frac{M_y \cdot (Gl_m + (s'_m - e'_m) \cdot M_x) + Gl_m \cdot M_x \cdot \bar{\varphi}_0 + M_x^2 \cdot u_0 + F \cdot u_0 \cdot (Gl_m - e'_m \cdot M_x)}{(F_{ey} - F) \cdot (Gl_m - e'_m \cdot M_x) - M_x^2} \cdot F_{ey}$$

Appendix 2: Approximations of M_c

In general the Euler moment of lateral buckling is:

$$M_{c0} = \sqrt{F_{ey} \cdot GI_{m0}} \cdot \left(\sqrt{(e_{m0}/2)^2 \cdot (F_{ey}/GI_{m0}) + 1} - \sqrt{(e_{m0}/2)^2 \cdot (F_{ey}/GI_{m0})} \right) =$$

$$= \frac{F_{ey} \cdot h}{2 \left(1 - \frac{EI_y}{EI_x}\right)} \cdot \left(\sqrt{\frac{e^2}{h^2} + \frac{4GI_v(1 - EI_y/(EI_x))}{h^2 F_{ey}}} - \frac{e}{h} \right)$$

or:

$$\sigma_{c0} = \frac{\sigma_{Eu} \cdot h/(2r_x)}{1 - I_y/I_x} \cdot \left(\sqrt{\frac{e^2}{h^2} + \left(\frac{4GI_t}{h^2 F_{ey}} + \frac{4C_w}{h^2 I_y} \right) \cdot \left(1 - \frac{I_y}{I_x}\right)} - \frac{e}{h} \right) \quad (1)$$

Only high beams need to be controlled for lateral buckling.

For high beams (e.g. $I_y < I_x/4$) eq.(1) can be simplified to:

$$\sigma_{c0} = \sigma_{Eu} \cdot \frac{h}{2r_x} \cdot \left(\sqrt{\left(\frac{e}{h}\right)^2 + \left(\frac{4GI_t}{h^2 F_{ey}} + \frac{4C_w}{h^2 I_y} \right)} - \frac{e}{h} \right) \quad (2)$$

For I-profiles and for trusses I_t has to be neglected and also for short beams the warping rigidity dominates and eq.(2) becomes:

$$\sigma_{c0} = \sigma_{Eu} \cdot \frac{h}{2r_x} \cdot \left(\sqrt{\left(\frac{e}{h}\right)^2 + \left(\frac{4C_w}{h^2 I_y} \right)} - \frac{e}{h} \right) \quad (3)$$

or for I-beams and trusses:

$$\sigma_{c0} = \sigma_{Eu} \cdot \left(\sqrt{\left(\frac{e}{h}\right)^2 + 1} - \frac{e}{h} \right) \quad (4)$$

For pure bending ($e = 0$) this becomes:

$$\sigma_{c0} = \sigma_{Eu} \quad (5)$$

and for a loading at the upper edge ($e = h/2$) is:

$$\sigma_{c0} = 0,62 \cdot \sigma_{Eu} \quad (6)$$

This predicted low value of lateral buckling is verified by a computer calculation of a short truss with a small lateral loading to simulate an initial displacement.

For long beams the torsional rigidity may dominate and eq.(2) becomes:

$$\sigma_{c0} = \sigma_{Eu} \cdot \frac{h}{2r_x} \cdot \left(\sqrt{\left(\frac{e}{h}\right)^2 + \left(\frac{4GI_t}{h^2 F_{ey}} \right)} - \frac{e}{h} \right) \quad (7)$$

or for pure bending ($e = 0$):

$$\sigma_{c0} = \sigma_{Eu} \cdot \frac{h}{2r_x} \cdot \sqrt{\frac{4GI_t}{h^2 F_{ey}}} = \frac{\pi EI_y}{LW_x} \cdot \sqrt{GI_t/(EI_y)} \quad (8)$$

or for beams with a rectangular cross section ($E = 16G$):

$$\sigma_{c0} = \frac{\pi b^2}{Lh} \cdot \sqrt{GE} = \frac{\pi Eb^2}{4Lh} \quad (9)$$

In general eq.(1) is for beams with a rectangular cross section ($E/G = 16$):

$$\sigma_{c0} = \frac{\sigma_{Eu} \cdot 3}{1 - b^2/h^2} \cdot \left(\sqrt{\frac{e^2}{h^2} + \left(\frac{L^2}{h^2 \pi^2} + 0.3 \right)} \cdot \left(1 - \frac{b^2}{h^2} \right) - \frac{e}{h} \right) \quad (10)$$

Determining is a loading at the upper edge (compression side wherefore $e = h/2$). For high beams (e.g. $b < h/2$), loaded at the upper edge ($e = h/2$) eq.(10) becomes:

$$\sigma_{c0} = 3 \cdot \sigma_{Eu} \cdot \left(\sqrt{0,55 + L^2/(\pi^2 h^2)} - 0,5 \right) \quad (11)$$

For short high beams (with dominating warping rigidity: $GI_t \ll \pi^2 EC_w/L^2$ or: $L < h$ for beams with a rectangular cross section) in pure bending, $e = 0$, (e.g. the part between two lateral supports) eq.(10) becomes:

$$\sigma_{c0} = 3 \cdot \sigma_{Eu} \cdot \sqrt{0,3} = 1,64 \cdot \sigma_{Eu} \quad (12)$$

For compact beams torsional instability may be determining. When $EI_y = EI_x$ lateral buckling will not occur but uncoupled buckling and/or torsional buckling is possible. In the limit case M_c becomes for $EI_y \rightarrow EI_x$ (loading at the compression side or $e > 0$):

$$\begin{aligned} M_{c0} &= \sqrt{F_{ey} \cdot GI_{m0}} \cdot \left(\sqrt{(e_{m0}/2)^2 \cdot (F_{ey}/GI_{m0}) + 1} - \sqrt{(e_{m0}/2)^2 \cdot (F_{ey}/GI_{m0})} \right) = \\ &= \sqrt{F_{ey} \cdot GI_{m0}} \cdot (e_{m0}/2) \cdot \sqrt{F_{ey}/GI_{m0}} \cdot \left(\sqrt{1 + 4GI_{m0}/(F_{ey} e_{m0}^2)} - 1 \right) \approx \\ &\approx \sqrt{F_{ey} \cdot GI_{m0}} \cdot (e_{m0}/2) \cdot \sqrt{F_{ey}/GI_{m0}} \cdot \left(1 + 2GI_{m0}/(F_{ey} e_{m0}^2) - 1 \right) = GI_{m0}/e_{m0} = \\ &= GI_{v0}/e = (GI_t + \pi^2 C_w/L^2)/e \end{aligned} \quad (13)$$

When the torsional rigidity dominates is: $M_{c0} \approx GI_t/e$ (torsional buckling).

When the warping rigidity dominates is: $M_{c0} \approx \pi^2 C_w/(eL^2)$ (buckling of the upper flange). For I-beams and trusses loaded at the upper edge ($e = h/2$) this is:

$$M_{c0} = \frac{\pi^2 EI_y h^2/4}{L^2 \cdot h/2} = F_{ey} \cdot \frac{h}{2} \rightarrow N_{fl} = \frac{M_{c0}}{h} = \frac{F_{ey}}{2} = F_{ey,fl}$$

or the compression force in the upper flange by the Euler moment is equal to the

Euler buckling load of the upper flange. This is comparable with eq.(5) and smaller than the equivalent eq.(6).

For a beam with a square cross section the warping deformation is neglectable and also torsional buckling is not determining. The beam can only buckle in the loading direction.

For a cross beam (—|— with: $I_y = I_x$) with dominating warping rigidity and no rigid joints between the flanges is (counting only one flange):

$$\sigma_{co} = \frac{M_{co}}{bh^2/6} \approx \frac{\pi^2}{eL^2} \cdot 0,3 \cdot E \cdot \frac{hb^3}{12} \cdot \frac{h^2}{4} \cdot \frac{6}{bh^2} = \frac{\pi^2 Ehb^3}{L^2 12} \cdot \frac{0,9}{bh} = 0,9 \cdot \sigma_{Eu}$$

when $e = h/2$ (loading at the upper edge).

The same value is found for pure compression $\sigma_t = F_{tor}/A$:

$$\sigma_t = \frac{\pi^2}{L^2} \cdot \frac{EC_w}{I_x + I_y} \approx \frac{\pi^2}{L^2} \cdot \frac{Ehb^3/12}{bh^3/12} \cdot \frac{0,3 \cdot h^2/4}{bh} = \frac{\pi^2}{L^2} \cdot \frac{Ehb^3/12}{bh} \cdot 0,9 = 0,9 \cdot \sigma_{Eu}$$

Thus for flange-less profiles at the compression side (⊥, |—|, ⊔) instability is due to buckling of the compressed flange-less web.

Appendix 3 Proposal for design rules for the Eurocode

5.1.6 Bending

The following conditions shall be satisfied:

$$\sigma_{m,d} \leq k_{inst} \cdot f_{m,d} \tag{5.1.6 a}$$

$\sigma_{m,d}$ follows from the mean moment of the middle half of the beam with length L (see figure 5.1.6) between the supports preventing rotation and lateral displacement.

$$\sigma_{m,d} = \frac{2}{L \cdot W_y} \cdot \int_{-L/4}^{+L/4} M dx \tag{5.1.6 b}$$

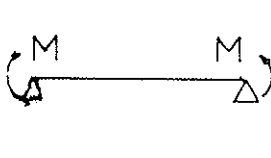
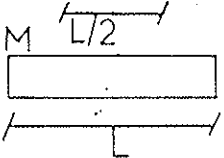
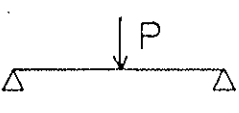
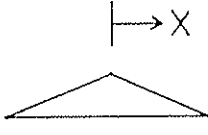
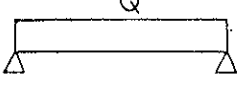
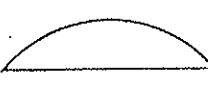
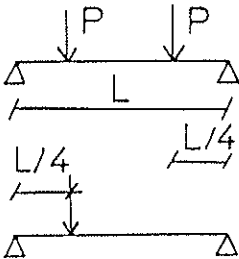
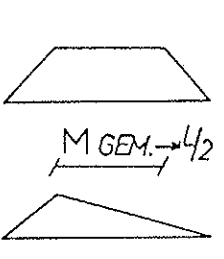
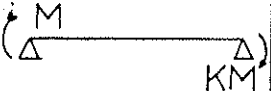
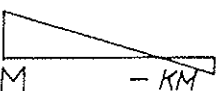
loading	bending moment	exact value M/ρ	$M/\rho = M_{mean}$ approx.
		$\frac{M}{1}$	$\frac{M}{1}$
		$\frac{PL/4}{1.35}$	$\frac{PL/4}{1.33}$
		$\frac{q \cdot L^2/8}{1.13}$	$\frac{q \cdot L^2/8}{1.09}$
		$\frac{PL/4}{1.04}$	$\frac{PL/4}{1}$
		$M(0.6+0.4 \cdot x)$	$\geq 0.4 \cdot M$

Figure 5.1.6. Examples of the mean moment over the middle half of the beam.

When the beam is loaded at the supports ($x = -\frac{L}{2}$ and $x = \frac{L}{2}$) by boundary moments M and αM (where $-1 \leq \alpha \leq 1$) is:

$$\sigma_{m,d} = \frac{M \cdot (0,6 + 0,4 \cdot \alpha)}{W_y} \geq \frac{0,4 \cdot M}{W_y} \quad (5.1.6 c)$$

The minimal value of $\sigma_{m,d}$ of $0,4 \cdot M$ applies also for combined lateral loading with boundary moments.

Cantilevers can safely be regarded as two times longer symmetrical loaded beams (having zero reactions at the ends).

k_{inst} is a factor (≤ 1) taking into account the reduced strength due to failure by lateral instability (lateral buckling and torsional buckling). k_{inst} shall be so determined that the design value of the total bending stress, taking into account the effect of initial curvature, eccentricities and the deformations developed, does not exceed $f_{m,d}$.

The strength reduction may be disregarded, i.e. $k_{inst} = 1$, if displacement and torsion are prevented at the supports and if

$$f_{m,k} / \sigma_{m,crit} \leq 0,56 \quad (5.1.6 d)$$

where $\sigma_{m,crit}$ is the critical bending stress calculated according to the classical theory of stability.

k_{inst} may also be put equal to 1 for a beam where lateral displacement of the compression side is prevented throughout its length and where rotation is prevented at the supports.

Under the assumption of an initial lateral deviation from straightness of less than $1/300$ k_{inst} may be determined from (5.1.6 e-f).

$$k_{inst} = \frac{k_m \cdot (1 + 0,56 \cdot \sqrt{\eta \cdot E_{0,k} / (8 \cdot f_{m,k})})}{k_m + \sqrt{0,5 \cdot k_{EZ} \cdot \eta \cdot \lambda_z \cdot f_{c,k} / f_{m,k}}} \quad \text{for } k_m \geq 1 \quad (5.1.6 e)$$

$$k_{inst} = \frac{k_m \cdot (1 + 0,56 \cdot \sqrt{\eta \cdot E_{0,k} / (8 \cdot f_{m,k})})}{1 + 0,5 \cdot (k_m + k_m^2) \cdot \sqrt{0,5 \cdot k_{EZ} \cdot \eta \cdot \lambda_z \cdot f_{c,k} / f_{m,k}}} \quad \text{for } k_m < 1 \quad (5.1.6 f)$$

In (5.1.6 e-f) is the loading in z-direction, being also the direction of the the weak axis and is:

$$\eta = \frac{i_z}{300 \cdot r_z} \quad (5.1.6 g)$$

where r_z is the core radius of the compression side, giving for solid timber:

$$\eta = \frac{b}{\sqrt{12}} \cdot \frac{6}{b} \cdot \frac{1}{300} = 0,006, \quad (5.1.6 h)$$

$$\lambda_z = \frac{l_{ef}}{i_z} \quad (5.1.6 \text{ i})$$

where l_{ef} is the buckling length and $i_z = \sqrt{I_z/A}$,

$$k_{Ez} = \frac{\sigma_{Ez}}{f_{c;0;rep}} = \frac{\pi^2 \cdot E_{0,k}}{\lambda_z^2 \cdot f_{c,k}} \quad (5.1.6 \text{ j})$$

$$k_m = \frac{\sigma_{m,crit}}{f_{m,k} \cdot (1 + 0,56 \cdot \sqrt{\eta \cdot E_{0,k} / (8 \cdot f_{m,k})})} \quad (5.1.6 \text{ k})$$

with

$$\sigma_{m,crit} = \frac{k_{Ez} \cdot h}{2 \cdot r_y} \cdot \frac{f_{c,k}}{1 - \frac{I_z}{I_y}} \cdot \left(\sqrt{\left(\frac{e}{h}\right)^2 + \left(1 - \frac{I_z}{I_y}\right) \cdot \left(\frac{4 \cdot l_{ef}^2 \cdot G_{mean} I_{tor}}{\pi^2 \cdot E_{0,mean} I_z \cdot h^2} + \frac{4 \cdot C_w}{h^2 \cdot I_z}\right)} - \frac{e}{h} \right) \quad (5.1.6 \text{ l})$$

where

$$C_w = \begin{cases} \text{a warping factor: } C_w = I_z h^2 / 4 & \text{for I-profiles and} \\ C_w = 0,3 \cdot I_z h^2 / 4 = h^3 \cdot b^3 / 160 & \text{for solid timber,} \end{cases}$$

e = eccentricity of the lateral loading, being the distance of the load with respect to the neutral axis if the beam is only laterally loaded. The sign of e is positive in the direction of the compression side or, $e = h/2$ for a symmetrical beam, only laterally loaded at the upper compression side,

$e = -h/2$ for only lateral loading at the tensional boundary and

$e = 0$ for lateral loading at the neutral axis of the beam or for loading by moments at the supports (no lateral loading).

For combined lateral loading with moments at the supports e has to be replaced by e' according to:

$$e' = \frac{e}{1 + \frac{\sigma_m}{\sigma_q}} \quad (5.1.6 \text{ m})$$

where σ_q is the design value of the bending stress by the mean moment of the middle half of the beam by only lateral loading (eq.(5.1.6 b) and σ_m is the design value of the bending moments at the supports (eq.(5.1.6. c).

When $I_z = I_y$, $\sigma_{m,crit}$ turns to the torsional value of:

$$\sigma_{m;cr} = \left(\frac{G_{mean} \cdot I_{tor}}{E_{0,mean} \cdot e \cdot W_y} + \frac{\pi^2 \cdot C_w}{l_{ef}^2 \cdot e \cdot W_y} \right) \cdot E_{0,k} \quad (5.1.6 \text{ n})$$

Simplifications of $\sigma_{m,crit}$ at the safe side are possible.

For solid beams (with $G_{mean}/E_{0,mean} = 1/16$) (5.1.6 l) becomes:

$$\sigma_{m,crit} = \frac{3 \cdot k_{EZ}}{1 - \frac{b^2}{h^2}} \cdot f_{c,k} \cdot \left[\sqrt{\left(\frac{e}{h}\right)^2 + \left(1 - \frac{b^2}{h^2}\right) \cdot \left(\frac{I_{ef}^2}{\pi^2 \cdot h^2} + 0,3\right)} - \frac{e}{h} \right] \quad (5.1.6 o)$$

For high solid beams (for instance if $b < h/2$) loaded by only bending ($e = 0$) this is safely:

$$= \frac{\pi \cdot b^2}{h \cdot I_{ef}} \cdot E_{0,k} \cdot \sqrt{\frac{1}{16} + \frac{\pi^2}{I_{ef}^2} \cdot 0,3 \cdot \frac{h^2}{16}} \quad (5.1.6 p)$$

For relatively long, high, solid beams loaded by bending alone ($e = 0$) this may safely be replaced by:

$$\sigma_{m,crit} = \frac{\pi \cdot b^2}{h \cdot I_{ef}} \cdot E_{0,k} \cdot \frac{1}{4} \quad (5.1.6 q)$$

For relatively short, high, solid beams loaded by bending alone ($e = 0$) the warping rigidity dominates and may safely applied:

$$\sigma_{m,crit} = 1,64 \cdot k_{EZ} \cdot f_{c,k} \quad (5.1.6 r)$$

For relatively high, long, solid beams lateraly loaded at the upper compression side ($e = h/2$) is safely:

$$\sigma_{m,crit} = 3 \cdot k_{EZ} \cdot f_{c,k} \cdot \left(\sqrt{0,55 + \frac{I_{ef}^2}{\pi^2 \cdot h^2}} - 0,5 \right) \quad (5.1.6 s)$$

For trusses and thin-webbed profiles with a dominating warping rigidity the torsional rigidity I_{tor} in (5.1.6 l) should be neglected and is:

$$\sigma_{m;cr} = \frac{k_{EZ} \cdot h}{2 \cdot r_y} \cdot \frac{f_{c;0;rep}}{1 - \frac{I_z}{I_y}} \cdot \left(\sqrt{\left(\frac{e}{h}\right)^2 + \left(1 - \frac{I_z}{I_y}\right) \cdot \left(\frac{4 \cdot C_w}{h^2 \cdot I_z}\right)} - \frac{e}{h} \right) \quad (5.1.6 t)$$

For high profiles with with flanges in the compression zone, whereby these flanges mainly determine the rigidity I_z (for instance I - and T - profiles and trusses) this is:

$$\sigma_{m,crit} = k_{EZ} \cdot f_{c,k} \cdot \left(\sqrt{\frac{e^2}{2} + 1} - \frac{e}{h} \right) \quad (5.1.6 u)$$

For thin high profiles with a low warping rigidity (when I_z of the compressed zone, being the web, is much smaller dan I_z of the total beam, for instance for \perp , \perp - or \perp - profiles, torsional instability may become determining and the calculation can be based on the torsional or warping rigidity of this web and is for the lateral loading at the compression side and dominating warping rigidity:

$$\sigma_{m,crit} = 0,9 \cdot k'_{EZ} \cdot f_{c,k} \quad (5.1.6 v)$$

where k'_{EZ} is the value of k_{EZ} when only the compressed web of the profile is counted for the rigidity.

For dominating torsional rigidity of the web the equation for long solid beams can be applied.

With respect to torsional buckling by compression alone is also:

$$\sigma_{c;0;d} < 0,9 \cdot k'_{EZ} \cdot f_{c;0;d} \quad (5.1.6 \text{ w})$$

and k_{EZ} has to be replaced by $0,9 \cdot k'_{EZ}$ in the expressions for columns of 5.1.10.

5.1.10 Columns

The bending stresses due to initial curvature and induced deflection shall be taken into account, in addition to those due to any lateral load.

The theory of linear elasticity may be used to calculate the resultant bending moment.

For the initial curvature a sinusoidal form may be assumed corresponding to a maximum eccentricity of the axial force of:

$$u_0 = \eta r \lambda \quad (5.1.10 \text{ a})$$

where r is the core radius.

For solid timber η shall as a minimum be taken as:

$$\eta = 0.006 \quad (5.1.10 \text{ b})$$

(corresponding for a rectangular cross-section to an initial eccentricity of about 1/300 of the length), and for glued laminated timber:

$$\eta = 0.004 \quad (5.1.10 \text{ c})$$

The stresses should satisfy the following conditions:

$$\frac{\sigma_{c,0,d}}{k_c \cdot f_{c,0,d}} + \frac{\sigma_{m,d}}{k_{inst} \cdot f_{m,d}} \cdot k_{mc} \leq 1 \quad \text{for} \quad \frac{\sigma_{c,0,d}}{k_c \cdot f_{c,0,d}} \geq \frac{\sigma_{m,d}}{k_{inst} \cdot f_{m,d}} \quad (5.1.10 \text{ d})$$

$$\frac{\sigma_{c,0,d}}{k_c \cdot f_{c,0,d}} \cdot k_{mc} + \frac{\sigma_{m,d}}{k_{inst} \cdot f_{m,d}} \leq 1 \quad \text{for} \quad \frac{\sigma_{c,0,d}}{k_c \cdot f_{c,0,d}} \leq \frac{\sigma_{m,d}}{k_{inst} \cdot f_{m,d}} \quad (5.1.10 \text{ e})$$

where:

$$k_{mc} = \frac{2 + k_c/k_{EZ}}{1,25 - 0,25 \cdot k_{inst} + 2 \cdot k_{inst} \cdot k_c/k_{EZ}} - 1, \quad (5.1.10 \text{ f})$$

$$k_c = 0,5 \cdot (1 + 20\eta) \cdot \left(\xi - \sqrt{\xi^2 - \frac{4 \cdot k_{EZ}}{1 + 20 \cdot \eta}} \right) \quad (5.1.10 \text{ g})$$

with:

$$\xi = 1 + \left(1 + \eta \cdot \lambda_z \cdot (1 + 20 \cdot \eta) \cdot \frac{f_{c,0,k}}{f_{m,k}} \right) \cdot \frac{k_{Ez}}{1 + 20 \cdot \eta} \quad (5.1.10 \text{ h})$$

If $\lambda_z < \lambda_y$ the equations of 5.2.6 apply for instability in the z-direction (direction of the loading) only.

5.2.6 Bracing

Adequate bracing shall be provided to avoid lateral instability of individual members and the collapse of the whole structure due to external loading such as wind.

The stresses due to initial curvature and induced deflection shall be taken into account.

The theory of linear elasticity may be used.

The initial deviations from straightness at midspan shall as a minimum be taken as 1/450 for glued laminated beams and as 1/300 for other structures.

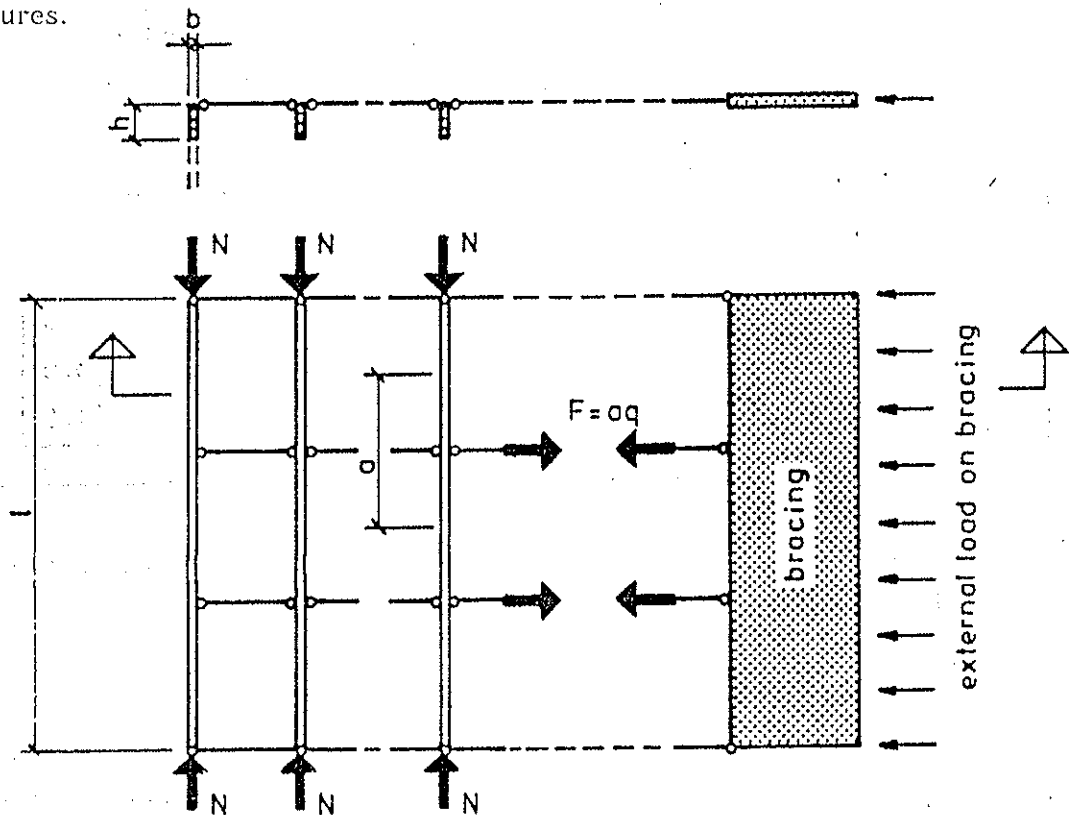


figure 5.2.6 a. Bracing system

With n equal members (e.g. beams or chords in a truss) of rectangular cross-section, the bracing should in addition to external loads (e.g. wind) be designed for a uniform load q per unit length:

$$q_{br,d} = \frac{n \cdot N_{c,d}}{l \cdot k_{br,c} \cdot k_{br,m}}$$

where

$$k_{br,m} = \frac{9 \cdot \pi}{32} \cdot \left(1 + 1.5 \pi \cdot \left(1 - 0.63 \frac{b}{h} \right) \cdot \left(\frac{b}{h} \right)^2 \cdot \frac{E_{o,k} \cdot G_{mean}}{f_{m,k} \cdot E_{o,mean}} \right),$$

for beams with rectangular cross sections, and:

$$k_{br,m} = 1 \quad \text{for compression gords of trusses.}$$

$$k_{br,c} = \frac{l}{8 \cdot (k_n \cdot k_l \cdot u_o + u_{br})}$$

$N_{c,d}$ is the design value or the axial force in the member.

Where the member is a beam with a rectangular cross section with a maximum moment M_d and depth h , $N_{c,d}$ should be taken as $N_{c,d} = 1.5 \cdot M_d / h$.

Where the member is a truss $N_{c,d}$ is the maximum compressive force.

$$k_l = \sqrt{\frac{15}{l}} \leq 1, \quad (\text{where } l \text{ is the span in m}).$$

$$k_n = 0.5 \left(1 + \frac{1}{n} \right)$$

u_o is the initial deviation from straightness at midspan

u_{br} is the deflection of the bracing caused by the sum of q and the external loads calculated with

$$E = E_{o,k} \cdot f_{m,d} / f_{m,d}$$

By the calculation of u_{br} the effect of slip in the joints should be taken into account.

Stability of the braced beams

When the bracing is connected to the members at the compression side or at the neutral axis of the lateral supported members the stresses of these members should satisfy the following condition:

$$\frac{\sigma_{c,o,d}}{k_c \cdot f_{c,o,d}} + \frac{\sigma_{m,d}}{k_{mom} \cdot f_{c,o,d}} \leq 1$$

where

$$k_c = 0.5 \cdot (1 + 20\eta) \cdot \left(\xi - \sqrt{\xi^2 - \frac{4 \cdot k_{EY}}{1 + 20 \cdot \eta}} \right) \leq 1$$

$$\xi = 1 + \left(1 + \eta \cdot \lambda_y \cdot (1 + 20 \cdot \eta) \cdot \frac{f_{c,o,k}}{f_{m,k}} \right) \cdot \frac{k_{EY}}{1 + 20 \cdot \eta}$$

$$k_{\text{mom}} = 1 - \frac{k_c}{k_{E_y}} \cdot \frac{\sigma_{c,o,d}}{f_{c,o,d}}$$

When the bracing is connected to the tension side of the lateral supported members k_{inst} is:

$$k_{\text{inst}} = \frac{1 + 0.56 \sqrt{\eta E_{0,k} / (8 f_{m,k})}}{1 + \frac{1}{\sqrt{k_m}} \left(1 + \frac{1}{k_m}\right) \sqrt{\eta \lambda_{z,y} r_y / (e - 2z)}} \quad \text{for } k_m \geq 1$$

$$k_{\text{inst}} = \frac{1 + 0.56 \sqrt{\eta E_{0,k} / (8 f_{m,k})}}{\frac{1}{k_m} + \sqrt{k_m} \left(1 + k_m\right) \sqrt{\eta \lambda_{z,y} r_y / (e - 2z)}} \quad \text{for } k_m < 1$$

with k_m according to 5.1.6,

e the excentricity of the lateral loading according to 5.1.6,

z the height of the connection of the bracing with the same sign convention as for e.

INTERNATIONAL COUNCIL FOR BUILDING RESEARCH STUDIES AND DOCUMENTATION
WORKING COMMISSION W18A - TIMBER STRUCTURES

A BRIEF DESCRIPTION OF FORMULA OF BEAM-COLUMNS IN CHINA CODE

by

S Y Huang
Chongqing Institute of Architecture and Engineering
Department of Civil Engineering
Shapinba, Chongqing, China

MEETING TWENTY - THREE

LISBON

PORTUGAL

SEPTEMBER 1990

A BRIEF DESCRIPTION ON FORMULA OF BEAM-COLUMNS IN CHINA CODE

S.Y. Huang

Chongqing Institute of Architecture and Engineering
Dept of Civil Engineering, Shapinba, Chongqing, CHINA

ABSTRACT

In this paper a formula of beam-columns in China Code for Timber Structure Design, GBJ5-88, is introduced as well as its theoretical analysis and test results. Considering non-linear property of material and second order effect of loaded members, a simple unified formula is presented used for calculation of eccentrically loaded columns, beam-columns and combined loading members.

INTRODUCTION

For calculation of timber beam-columns an empirical method, fiber-stress formula and advanced fiber-stress formula had been performed sequentially in previous code. Their assumptions are of ideal elasticity of timber and linear superposition for member's stresses.

In this paper the non-linear property of timber has been considered and also the second order effects on loaded members have been taken into account in the formula in the new code.

As early as in 1963 the preliminary theoretical analysis on this topic had been done. In the period of 1966-1968 the tests on axially loaded columns, eccentrically loaded columns and beam-columns were carried out. The test specimens were made of Yunnan Pine (*Pinus yunnanensis* Franch.) with knots as well as with free knots, and their slenderness ratios were 25-100, relative eccentricities rate from 0-5. However, later, only a part of research results was accepted at the meeting on modifying timber code in 1968 due to the fact that for short members the theoretical results were not good agreed with tests.

During the period of 1971-1973 we paid a high regard to the research on structural timber

columns. The specimens were made of Sichuan Fir (*Abies fargesii* Franch.) with section of 100x100 and slenderness ratios from 36 to 125. However, due to no sufficient research on short members no convincing observations were made at the conference on modifying timber code in 1973.

Subsequently, during the period of 1973-1980 in addition to checking the theoretical analysis for short members, the complementary tests on them were carried out and the test informations of short columns obtained in 1960 and 1967 had been referred to as well, we had found that the test values of short columns were remarkable lower than those corresponding straight line formula.

Together with the research on reliability the tests on columns loaded axially were carried out again in 1984. The specimens of structural timber columns were made of Sichuan Fir with section of 100x100 and slenderness ratios from 25 to 125. At the same time, similar tests on some wood species such as Mumahuang (*Casuarina equisetifolia*), Longyuannan (*Eucalyptus exserta*) and Poplar (*Populus bolleana*) were carried out in Guangdong, Xinjiang and other provinces of China with the unified plan and arrangements by the Working Group Modifying Code for Timber Structure Design. Then the equivalent modulus of elasticity, E_k , and the buckling coefficients of axially loaded timber columns have been determined.

On the bases of a large amount of tests specimens the relevant parameters of the theoretical formula in this paper could be determined. During the period of 1984-1985 this proposed formula in this paper was checked in contrast with formula in previous code according to different eccentricity, slenderness and species by using a large amount of computations, and it was also verified by tests results. At the meeting in 1985, the plenary session of the Working Group Modifying Timber Code approved

that the proposed formula of timber beam-columns was so available as to be accepted into the timber code which would be published in 1988.

By the way, it should be mentioned that it is difficult to take into account both the second order effects on loaded members and the non-linear property of material by means of pure theoretical analysis method, but easy by means of electrical computer method. However, the results of computation by computer are a large amount of datum but for code it needs a simple formula. In this paper a practicable engineering method can be used, that is, the formula can be derived from assumptions by using simplified theoretical analysis method and the relevant parameters of the formula would be determined by using test method.

the assumption of plan deformation of cross-section and the relationship of stress-strain shown in Figure 2.

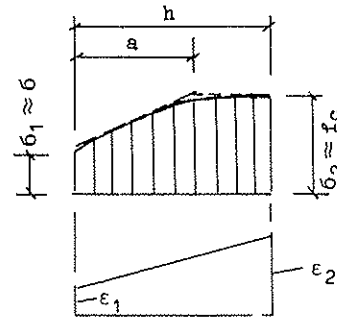


Figure 3

ASSUMPTIONS AND SIMPLIFIED ANALYSIS

There is a typical member, as shown in Figure 1, with a hinge at each end of the member, a longitudinal force is N, acting on the each end with eccentricity, e_0 , and a lateral force 2P, acting on the middle of length.

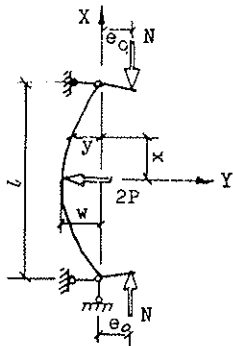


Figure 1

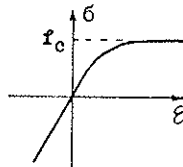


Figure 2

Impossibility of buckling for eccentrical loaded columns within the elasticity limit of material has been pointed out from some papers and it has been confirmed by theoretical analysis and tests. It has been shown in tests that when loading just up to failure, the graph of stress distribution appears to be sharp at the convex side of cross-section but uniform smooth at the opposite side. Considering this fact, the real graph of stress distribution may be approximately simplified.

It is in assumption that at the concave side of member there is a plastic zone of cross-section in which the stresses are uniform and equal to strength f_c , and modulus of elasticity is equal to zero, simultaneously, at the convex side of member there is a sharply slanted zone in which the stresses are varied approximately as sloped straight line and the slightly varied modulus of elasticity can be simplified to be equivalent single one E_k , which is a function of failure stress and will be determined by tests on columns.

The section of the member is rectangular with width b, and depth h. The non-linear property of timber is shown in Figure 2.

Let us suppose, as loading just up to failure load, the fiber strain ϵ_1 , at the convex side and ϵ_2 at the concave side of the member can be measured. Then the graph of stress distribution in the section of member can be drawn as shown in Figure-3, according to

From Figure 3, the following equations can be established in accordance with static equilibrium condition:

Longitudinal force

$$N = b h f_c - \frac{1}{2} b a (f_c + \bar{\sigma}) \quad (1)$$

Internal moment

$$M_1 = \frac{1}{2} b a (f_c + \bar{\sigma}) (h/2 - a/3) / \eta \quad (2)$$

 External moment

$$M_e = M + \Delta M \quad (3)$$

Where initial moment
 $M = N e_0 + P (l / 2 - x)$
 additional moment
 $\Delta M = - N y / \eta$

From Equation (1) we can get

$$\sigma = \frac{b h f_c - N}{0.5 b a} - f_c \quad (4)$$

Where σ is the fiber stress at the convex side of member. It is positive sign in tension but negative in compression. In Equation (3) M is the initial moment without taking into account the second order effect, so it may be called as actual moment at failure which can be obtained by tests. However, both internal and additional moments are theoretical moment calculated according to assumption. It is considered that the theoretical moments perhaps could not completely be equal to the actual moment due to no perfect theoretical assumptions. Therefore an adapting parameter η of theoretical model should be introduced into the above equations. η would be determined by tests.

Then, put the theoretical moment equal to the actual moment

$$M_1 - \Delta M = M$$

that is,

$$\left[(b h f_c - N) \left(\frac{h}{2} - \frac{a}{3} \right) + N y \right] / \eta = N e_0 + P (l / 2 - x)$$

$$(b h f_c - N)(h/2 - a/3) = N (\eta e_0 - y) + \eta P (l / 2 - x) \quad (5)$$

From Equation (5), we get

$$a = t + \eta p x + q y \quad (6)$$

$$p = \frac{3P}{b h f_c - N} ; \quad q = \frac{3N}{b h f_c - N} \quad (7)$$

$$t = 1.5h - \eta q e_0 - 0.5 \eta p l$$

At failure, the curvature of flexural axis of member at a point with a distance x , from origin of coordinate is

$$\frac{1}{\rho} = \frac{\sigma + f_c}{E_k a} = \frac{b h f_c - N}{0.5 b E_k a^2}$$

that is

$$\frac{d^2 y}{dx^2} = \frac{\delta}{(t + \eta p x + q y)^2} \quad (8)$$

where

$$\delta = \frac{b h f_c - N}{0.5 b E_k} \quad (9)$$

Solving the differential equation (8) we can get

$$N = \frac{\pi^2 E_k I}{l^2} (1 - K)^2 (1 - K_0) \quad (10)$$

Where $I = \frac{b h^3}{12}$ moment of inertia

$$K = \frac{2 \eta (M + N e_0)}{(b h f_c - N) h} \quad (11)$$

$$K_0 = \frac{2 \eta N e_0}{(b h f_c - N) h} \quad (12)$$

When $M = 0$ in Equation (11), that is, $P=0$ in Figure 1, then it may be called eccentrically loaded columns.

For this case from Equation (10) we can get

$$N = \frac{\pi^2 E_k I}{l^2} (1 - K_0)^3 \quad (10-a)$$

When $e_0=0$ in Figure 1 and Equations (11) and (12), then the member will be loaded with axial and lateral loads and it may be called beam-columns. For this case from Equation (10) we can get

$$N = \frac{\pi^2 E_k I}{l^2} (1 - K)^2 \quad (10-b)$$

From Equations (10-a) and (10-b) we are aware that the eccentrically loaded columns are different from beam-columns, in capacity the former is lower than the latter under a same moment.

In addition, the deflection at the middle of the length of member could also be got (disregard the negative sign):

$$w = \frac{1}{6} (1 - k) (b h f_c - N) h / N \quad (13)$$

STRENGTH OF SHORT MEMBERS

It has been shown that the strength of short members without column effect is related to different test condition, it is

described as follows :

A. Theoretical Strength of Material

Let us suppose that the stress distribution in the cross-section accords with the assumption of simplified elasticity-plasticity property of timber, as shown in Figure 4, and that when the plastic deformation is fully developed, both compressed and tense stress at the outmost fiber of cross-section may be increased up to f_c and f_t respectively. Then the acceptable moments may be obtained as

$$\frac{M}{Wf_m} = \left(1 - \frac{N}{Af_c} \right) \left[1 + \left(\frac{3f_c}{f_m} - 1 \right) \frac{N}{Af_c} \right] \quad (14)$$

$$A = b h ; \quad W = \frac{bh^2}{6} \quad (15)$$

$$f_m = f_c \left(\frac{3f_t}{f_c} - 1 \right) / \left(\frac{f_t}{f_c} + 1 \right) \quad (16)$$

Where f_c --- compression strength parallel to the grain
 f_t --- tension strength parallel to the grain
 f_m --- bending strength

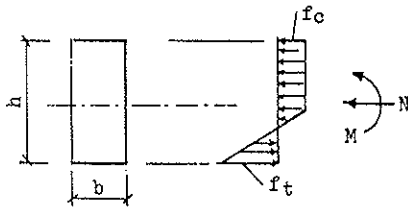


Figure 4

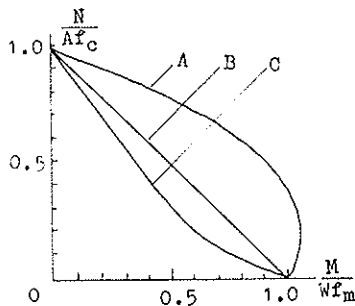


Figure 5

The relationship between $\frac{N}{Af_c}$ and $\frac{M}{Wf_m}$ for Sichuan Fir has been drawn as curve A in Figure 5.

The curve A would characterize the theoretical acceptable moment which has been obtained

based on the relation of stress-strain of material, considering deeply developed plastic deformation, at the most utilization of compression and tension strength of timber. Hence it is a ideal case which might difficultly be realized in practice. Its possibility perhaps appears only when a large deflection at the middle of length of longer column occurs suddenly caused by instability of column.

B. Strength of Beam-Columns

The research and tests on the strength of beam-columns without column effect had already been carried out in Soviet Union as early as in 1940-1950. It has been confirmed that the Equation (17) shown as a sloped line B, in Figure 5 should be approximately applicable for short members without column effect.

$$\frac{M}{Wf_m} = 1 - \frac{N}{Af_c} \quad (17)$$

This formula is widely used in almost all existing codes for practice in this field.

C. Strength of Eccentrically loaded Columns

However, for short members loaded eccentrically shown in Figure 6, the test results are lower than both A and B. We had performed the tests of short members in 1960, 1967 and 1977. It had been found that the failure occurred always at the concave side of members caused by the folds of timber fibers, and at the convex side of members there were no vestige of damage, either the fiber strain shortened or the fiber strain slightly extended is so small, far from the strain corresponding to tension strength. Therefore the bending effort of members corresponding to tension strength always could not be utilized.

Based on the statistic test datum, the following equation (18) drawn as curve C in Figure 5, approximately would be used :

$$\frac{Ne_0}{Wf_m} = 1 - \frac{N}{Af_c} + \left(\frac{N}{Af_c} \right)^{1/2} - \left(\frac{N}{Af_c} \right)^{1/3} \quad (18)$$

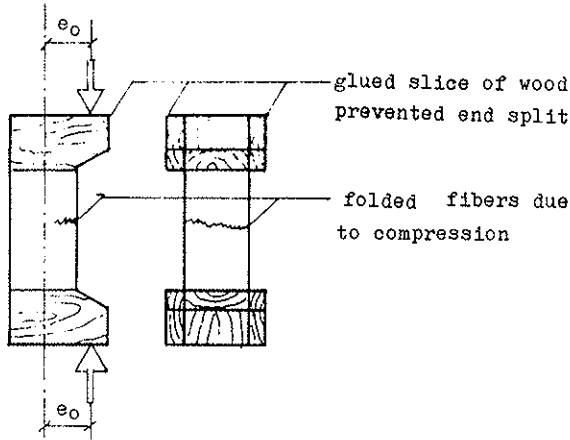


Figure 6

As a result of the above, the strength criterion of members without column effect would be suggested by means of the principle of neither unsafeness nor conservation. For all members the following conditions should be satisfied:

1. In the case of combined axial and lateral loading, the initial moment of short members should not exceed the moment calculated from Equation (17);
2. In the case of eccentric loading, the end moment of short members should not exceed the moment calculated from Equation (18);
3. In the case of taking into account the second order effect, the maximum moment at the middle of length of members should not exceed the moment calculated from Equation (14).

DETERMINATION OF THE ADAPTING PARAMETER

Introduce the following expression into Equation (10)

$$\frac{\pi^2 E_k I}{l^2} = \varphi A f_c$$

It then becomes

$$\frac{N}{A f_c} = \varphi (1 - K)^2 (1 - K_0) \quad (19)$$

Where φ is buckling coefficients of axially loaded columns

When $e_0 = 0$ in Figure 1, it is of beam-columns, and Equation (19) becomes

$$\frac{N}{A f_c} = \varphi (1 - K)^2 \quad (20)$$

When $P = 0$ in Figure 1, it is of eccentrically loaded columns, and Equation (19) becomes

$$\frac{N}{A f_c} = \varphi (1 - K_0)^3 \quad (21)$$

If $\lambda \rightarrow 0$, the above eqs. (20) and (21) should in practice coincide with their strength criterion obtained from tests of short members described above. This is the principle made to determine the adapting parameter of theoretical analysis model.

Further, when $e_0 = 0$ then $K_0 = 0$ and when $\lambda \rightarrow 0$, then $\varphi = 1$. From Eqs. (20) and (11) we can get

$$M = (1 - \sqrt{\frac{N}{A f_c}}) (1 - \frac{N}{A f_c}) b h^2 f_c / (2 \eta) \quad (22)$$

Put Eq. (22) equal to Eq. (17), then we get

$$\eta = 3 f_c / f_m (1 - \sqrt{\frac{N}{A f_c}}) \quad (23)$$

Substitute Eq. (23) into Eqs. (11) and (12) they become

$$K = (M + N e_0) / [w f_m (1 + \sqrt{\frac{N}{A f_c}})] \quad (24)$$

$$K_0 = N e_0 / [w f_m (1 + \sqrt{\frac{N}{A f_c}})] \quad (25)$$

DETERMINATION OF THE EQUIVALENT MODULUS OF ELASTICITY

When $P = 0$ and $e_0 = 0$ in Figure 1, it is of axially loaded columns. From Equations (24) and (25) $K = K_0 = 0$ then Equation (10) becomes

$$N = \frac{\pi^2 E_k I}{l^2} \quad (26)$$

Based on the test data of axially loaded columns and using the analysis method of equivalent elasticity modulus, we can find the relationship between equivalent elasticity modulus E_k , and buckling stress σ_k

as shown in Figure 7. Consequently, we can get the equivalent modulus of elasticity and buckling coefficients of axially loaded columns. Please refer to [1] and [2].

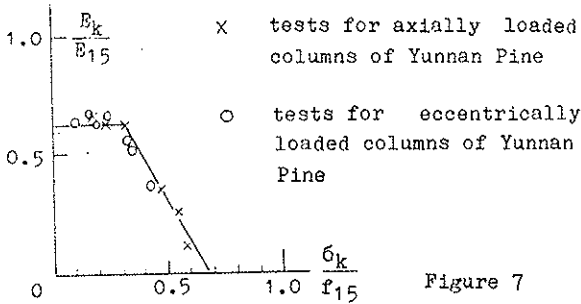


Figure 7

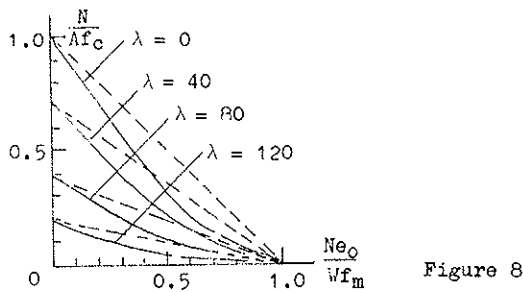


Figure 8

RESULTS AND CONCLUSIONS

Finally, the unified simple formula has already been presented, which is applicable to the eccentrically loaded columns, beam-columns and other columns with eccentric loads and lateral loads.

From Equations (19), (24) and (25) it can be obtained

$$\frac{N}{\varphi \varphi_m A f_c} = 1 \quad (27)$$

$$\varphi_m = \left[1 - \frac{M + Ne_0}{W f_m (1 + \sqrt{\frac{N}{A f_c}})} \right]^2 \left[1 - \frac{Ne_0}{W f_m (1 + \sqrt{\frac{N}{A f_c}})} \right] \quad (28)$$

- Where φ — buckling coefficient of axially loaded columns
- φ_m — reduced coefficient taking into account the effect of combination of eccentric and lateral loads
- M — moment produced by lateral loads
- Ne_0 — moment produced by longitudinal loads N , with eccentricity e_0 , at the ends of columns

And also, Equation (28) can be rewritten as

$$\varphi_m = [1 - k]^2 [1 - kK]$$

$$k = \frac{Ne_0}{M + Ne_0}$$

Where k is the ratio of only eccentric moment to total moment.

If $k = 0$, then Equation (28) becomes

$$\varphi_m = \left[1 - \frac{M}{W f_m (1 + \sqrt{\frac{N}{A f_c}})} \right]^2 \quad (29)$$

It is of beam-columns. When $\lambda \rightarrow 0$ Equations (27) and (29) result in

$$\frac{M}{W f_m} = (1 - \sqrt{\frac{N}{A f_c}}) (1 + \sqrt{\frac{N}{A f_c}}) = 1 - \frac{N}{A f_c}$$

This equation is exactly as the same as Equation (17).

If $k = 1$, then Equation (28) becomes

$$\varphi_m = \left[1 - \frac{Ne_0}{W f_m (1 + \sqrt{\frac{N}{A f_c}})} \right]^3 \quad (30)$$

It is of eccentrically loaded columns. When $\lambda \rightarrow 0$ then Equations (27) and (30) result in

$$\frac{Ne_0}{W f_m} = 1 - \left(\frac{N}{A f_c}\right)^{5/6} + \left(\frac{N}{A f_c}\right)^{1/2} - \left(\frac{N}{A f_c}\right)^{1/3} \quad (31)$$

This equation has substantially a good agreement with Equation (18).

If $k = 0$ and $M = 0$, then Equations (28) and (27) become

$$\frac{N}{\varphi A f_c} = 1 \quad (32)$$

This equation just coincides to the formula of axially loaded columns.

It is recognized that the unified simple formula is available for every extreme case and also it has been verified by tests.

According to Equations (27) and (30) the calculated results of the eccentrically loaded columns made of Sichuan Fir would be drawn in Figure 8, in which the broken line corresponds to empirical formula.

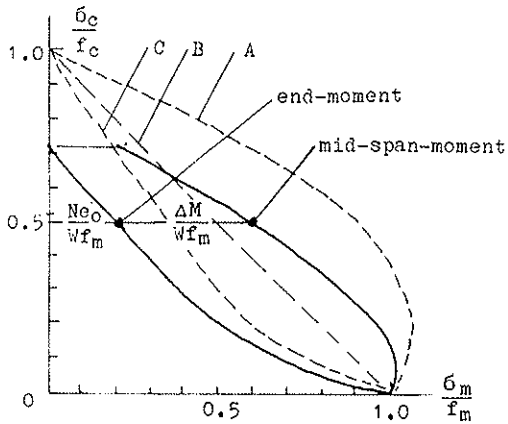


Figure 9

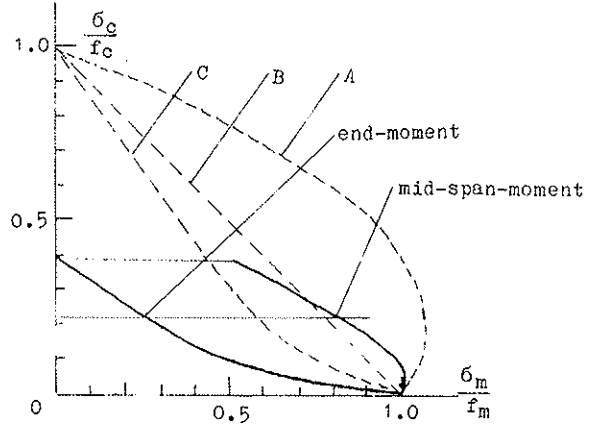


Figure 10

REFERENCES

In order to check the maximum moment at failure at the middle of length of columns the equation (13) for deflection can be used.

Additional moment $\Delta M = Nw = (1-K)(bh f_c - N)h / 6$ that is

$$\frac{\Delta M}{Wf_m} = \frac{f_c}{f_m} \left[1 - \frac{N}{Af_c} - \frac{Ne_0}{Wf_m} \left(1 - \sqrt{\frac{N}{Af_c}} \right) \right] \quad (33)$$

In other hand, the end moment of eccentrically loaded columns can, from Equations (27) and (30), be calculated as following

$$\frac{Ne_0}{Wf_m} = \left(1 - \sqrt{\frac{N}{\varphi Af_c}} \right) \left(1 + \sqrt{\frac{N}{Af_c}} \right) \quad (34)$$

The results of the end-moment and mid-moment of the eccentrically loaded columns of Sichuan Fir have been obtained from Equations (33) and (34), and drawn into Figure 9, 10, 11, for $\lambda = 40, 80, 120$, respectively.

It is visible that the mid-moments are enclosed within the curve A of the theoretical strength of material.

[1] Working Group Modifying the Code for Timber Structure Design, "Tests on the axially loaded columns with knots of Yunnan Pine and Sichuan Fir", YEJIN JIANZHU No. 7, 1975.

[2] S.Y. Huang, P.M. Yu, J.Y. Hong, "Buckling and reliability checking of timber columns", CIB-W18A/22-2-1, East Berlin, 1989.

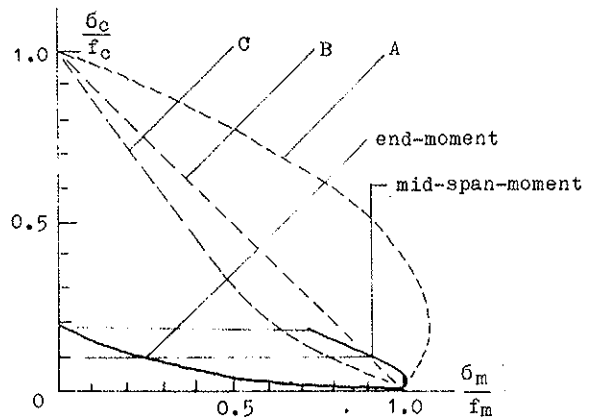


Figure 11

**INTERNATIONAL COUNCIL FOR BUILDING RESEARCH STUDIES AND DOCUMENTATION
WORKING COMMISSION W18A - TIMBER STRUCTURES**

**SEISMIC BEHAVIOR OF BRACED FRAMES
IN TIMBER CONSTRUCTION**

by

M Yasumara
Building Research Institute
Ministry of Construction
Japan

MEETING TWENTY - THREE

LISBON

PORTUGAL

SEPTEMBER 1990

SEISMIC BEHAVIOR OF BRACED FRAMES IN TIMBER CONSTRUCTION

MOTOI YASUMURA*

1. INTRODUCTION

Trussed frames with the diagonal braces are the most simple and efficient structural element to resist against the lateral forces such as the wind load and the earthquake load. This structure is widely used in glued-laminated timber construction as well as in conventional wooden construction. As the failure of the braced frames generally depends on the buckling of the braces or the failure of the end joints, it shows smaller ductility and deformability than the framed structures in case of the earthquake. In timber structure, wooden members show generally brittle failures, so it is necessary to secure the ductile property in mechanical joints. In this study, the braced frames of the glued-laminated timber having different types of end joints were subjected to the reversed cyclic lateral loads, and the mechanical properties of the frames were investigated.

Load-displacement hysteresis loops were modeled with the bi-linear slip model with reference to the experimental results, and the time-history earthquake response analysis was carried out to investigate the influence of the yield design load level on the response spectrum.

2. DESCRIPTION OF SPECIMEN

Seven braced frames of glued-laminated timber were subjected to the reversed cyclic lateral loads. Specimens were designed in consideration of an one-story building of 7.5 meters in height and the seismic design load of 50kN was assumed. The height and the length of the specimen was respectively 7.5 and 3.6 meters,

*Senior Research Officer, Dr.Agr.,Dpt. of Structural Engineering, Building Research Institute, Ministry of Construction, Tsukuba, Japan

and the cross section of the columns were 15-by 30 centimeters. Species of the glued-laminated timber was Ezomatsu (*P.jezoensis* Carr.) and Todomatsu (*A. sachalinensis* Fr.Schm.), and the thickness of the laminae was two centimeters.

In braced frames the end joints show sometimes brittle failure due to the stress perpendicular to the grain caused by the rotation of the braces at the end joint. In order to avoid this effect, six specimens had the steel pin joints at the end of the braces as shown in Fig.1. To compare the effects of the pin joints, one specimen had steel side plates without pin joints as shown in Fig.2. Two types of specimens having the joints with the steel side plates and the inserted steel plate were tested. The ratio of the thickness of the braced members to the diameter of a bolt was four, eight and twelve. The thickness of braces, the diameter of bolts and the number of bolts varied according to the joint types as shown in Table 1. The details of joints are shown in Figs.3 and 4.

3. TEST METHOD

Fig.5 shows the outline of the test apparatus. The specimen was set on the reaction floor and the reversed cyclic lateral loads as shown in Fig.6 were applied at the top of the specimen. The vertical and horizontal displacements of the specimen and the strain of the members were measured with the electronic transducers and the strain gages.

4. EXPERIMENTAL RESULTS

4.1 DESCRIPTION OF FAILURE

All the specimens failed with the destruction of the end joints of the braced members due to the shear failure or fracture of wood. In some specimens partial failure of wood occurred along the bolt line after yielding, and it spread with the increase of the load. In other specimens, the end joints failed suddenly with the shear failure or fracture of wood at the joints. In any case the joints failed finally in tension. Although steel pin joints were applied, the rotation of plates was observed in compression

braces.

4.2 HYSTERESIS LOOPS

Load-displacement curves of each specimen are shown in Fig.7. They show the non-linear hysteresis loops with slips due to the embedding of a bolt into wood. Initial slips due to the clearance of bolt holes of one millimeter was observed in some specimen. The residual displacement increased as the displacement increased. The unloading stiffness was approximately twice to third times as large as the initial stiffness. The degrading after the yielding of a bolt was observed in some specimens in which the thickness-to-bolt-diameter-ratio was eight and twelve, but the yield point was not clear. This indicates that the braced frames are basically non-ductile even though the ductility of the joints by securing the large thickness-to-bolt-diameter-ratio gives slightly higher ductile properties in structure.

4.3 EQUIVALENT VISCOUS DAMPING

The equivalent viscous damping was obtained from the hysteresis curves of each specimen, and the calculated values are shown in Fig.8, where the equivalent viscous damping is obtained from the ratio of the absorbed energy to the external work performed in each loop.

The equivalent viscous damping of each specimen showed very similar values and was approximately 15% when the horizontal displacement was less than $1/200$ of the specimen height, and it decreased to approximately 10% when the horizontal displacement was approximately $1/100$ of the specimen height.

4.4 STRENGTH AND DUCTILITY

Fig.9 shows the skeleton curves of the load-displacement relationships in each specimen, and Table 2 summarizes the experimental results. In Table 2 the maximum loads are compared with the calculated yield load. Here, the yield load was calculated from the yield theory of the bolted joints[1][2], and the embedding strength of 2.79kN/cm^2 for glulam and the yield point of 23.5kN/cm^2 for steel were assumed.

The maximum load of the specimen having the thickness-to-bolt-

diameter-ratio of eight and twelve was 1.25 to 1.82 times (1.44 times in average) as large as the calculated yield load, while that in the specimen having the thickness-to-bolt-diameter-ratio of four was equal to or smaller than the calculated yield load. Table 2 describes the ductility factor obtained from the ratio of the maximum displacement to the yield displacement. In order to exclude the effects of the initial slips, the initial slips were subtracted from the maximum displacement and the yield displacement. The ductility factor of the specimen having the steel pin joints and the thickness-to-bolt-diameter-ratio of eight and twelve was 1.64 to 2.25 (1.93 in average), while that of the specimen of the thickness-to-bolt-diameter-ratio of four was 1.0. The ductility factor of the specimen without steel pin joints was 1.32 and showed smaller value than the specimen having the steel pin joint. These facts lead the following design implications in braced frame structures;

- (1) Thin braces in comparison with the diameter of a bolt should be avoided, and the thickness-to-bolt-diameter-ratio of braced members should be equal or superior to eight.
- (2) Stress perpendicular to the grain due to the rotation of a brace at the end joint should be avoided by means of a steel pin joint or other equivalent methods.

The ductility factor of the braced frames which agree with the above items should be 2.0 in average or 1.5 considering the variation. The ductility factor of other types of braced frames should be 1.0.

5. TIME-HISTORY EARTHQUAKE RESPONSE ANALYSIS

5.1 ANALYTICAL PROCEDURE

Time-history earthquake response analysis was performed on a braced frame. Single-degree-of-freedom lumped mass model was used, and the load-displacement relationship was modeled with the bi-linear slip model as shown in Fig.11. This model includes;

- (1) loading on the primary curve before yielding
- (2) loading on the post yielding primary curve

- (3) unloading from peak on the primary curve
- (4) reloading with soft spring
- (5) loading with hard spring toward previous peak
- (6) unloading from inner peak
- (7) reloading toward peak without pinching effect

The spring constant on the post yielding primary curve was assumed to be a half times as large as that before the yield as shown in Fig.10, and the damping was assumed to be 2%. This value seems to be small for timber construction, however damping of 2% was taken because the forced vibration test on the full-scale building with braced frames[3] showed the damping of 1 to 3%, and the hysteresis model used in this analysis included the hysteretical damping before the yielding.

Input earthquake ground motions were based on the records of N-S component of the 1940 El Centro, E-W component of the 1952 Taft and E-W component of the 1968 Hachinohe. Here, the 1940 El Centro N-S component was generated as a kind of standard accelerogram in this analysis, and the 1952 Taft E-W component and the 1968 Hachinohe E-W component were generated as the accelerogram which gives higher response to the building having the short natural period and long natural period respectively. These accelerograms were linearly scaled to have the maximum acceleration of 400cm/sec² and 300cm/sec² in El Centro(NS) and Taft(EW), and 300cm/sec² and 225cm/sec² in Hachinohe(EW), respectively.

5.2 ANALYTICAL RESULTS

Figs.12 and 13 show the input earthquake ground motion of the 1968 Hachinohe E-W component and non-linear time-history earthquake response respectively. Fig.14 shows the example of the force-displacement response at the natural period of 0.8 second and mg/Qy values of 2.0 and 2.5. Ductility factor response spectrums obtained from the non-linear time-history earthquake response analysis are shown in Figs.15 to 18, and the average value of the ductility factor response of three accelerograms is shown in Fig.19.

In order to submit the effect of spectrum shaping, the accelerogram was linearly scaled at every natural period so that the maximum linear acceleration response became 1g. Fig.20 shows

the amplification factor in linear response with $h=0.02$, and Figs.21 to 23 show the ductility factor response spectrum. Here, "Au" is the maximum acceleration of the normalized ground motion input at that period which gives the linear acceleration response of 1g., and "Ay" is the maximum acceleration of the ground motion which gives the yield force in linear response.

It is possible to obtain the "q" value information from Fig.19 if the soil profile is determined. For the building whose natural period is relatively short Fig.19 gives the direct information to determine the "q" value of braced frames. For example Fig.19 shows that if the yield load of the structure is greater than a half of the weight of the building, the ductility factor response will be smaller than 1.7 in El Centro(NS) 400gal and the equivalent earthquake. Although Figs.21 to 23 tend to give more conservative ductility factor response than Fig.19 they show the similar information to Fig.19 when the natural period of the building is shorter than 1.6 second.

6. CONCLUSIONS

Summarizing the results of this study, the following conclusions are lead.

- (1) All the specimens failed with the destruction of the end joints of the braced members due to the shear failure or fracture of wood. In any case the joints failed finally in tension. Although steel pin joints were applied, the rotation of plates was observed in compression braces.
- (2) Load-displacement curves showed the non-linear hysteresis loops with slips due to the embedding of a bolt into wood. The unloading stiffness was approximately twice to third times as large as the initial stiffness. The degrading after the yielding of a bolt was observed in some specimens, but the yield point was not clear. This indicates that the braced frames are not basically ductile structure .
- (3) The equivalent viscous damping of each specimen showed very similar values and was approximately 15% when the horizontal displacement was less than $1/200$ of the specimen height, and it

decreased to approximately 10% when the horizontal displacement was approximately 1/100 of the specimen height.

(4) The maximum load of the specimen having the thickness-to-bolt-diameter-ratio of eight and twelve was 1.25 to 1.82 times (1.44 times in average) as large as the calculated yield load, while that in the specimen having the thickness-to-bolt-diameter-ratio of four was equal to or smaller than the calculated yield load.

(5) The ductility factor of the specimen having the steel pin joints and the thickness-to-bolt-diameter-ratio of eight and twelve was 1.64 to 2.25 (1.93 in average), while that of the specimen of the thickness-to-bolt-diameter-ratio of four was 1.0. The ductility factor of the specimen without steel pin joints was 1.32 and showed smaller value than the specimen having the steel pin joint.

(6) When the braced frames are designed the thickness-to-bolt-diameter-ratio of braced members should be equal or superior to eight and the stress perpendicular to the grain due to the rotation of a brace at the end joint should be avoided by means of a steel pin joint or other equivalent methods.

(7) The ductility factor of the braced frames which agree with the above items should be 2.0 in average or 1.5 considering the variation. The ductility factor of other types of braced frames should be 1.0.

(8) It is possible to obtain the "q" value information from Fig.19 if the soil profile is determined. Although Figs.21 to 23 tend to give more conservative ductility factor response than Fig.19 they show the similar information to Fig.19 when the natural period of the building is shorter than 1.6 second.

7. LITERATURE

[1] LARSEN, H.J., "THE YIELD LOAD OF BOLTED AND NAILED JOINTS", IUFRO-5, Congress September-October 1973.

[2] YASUMURA, M., "ULTIMATE PROPERTIES OF BOLTED JOINTS IN GLUED-LAMINATED TIMBER", CIB-W18A, Meeting 20, September 1987.

[3] "Report 1989: DEVELOPMENT OF THE ADVANCED TIMBER CONSTRUCTION SYSTEMS-STRUCTURAL DIVISION", BRI, March, 1990.

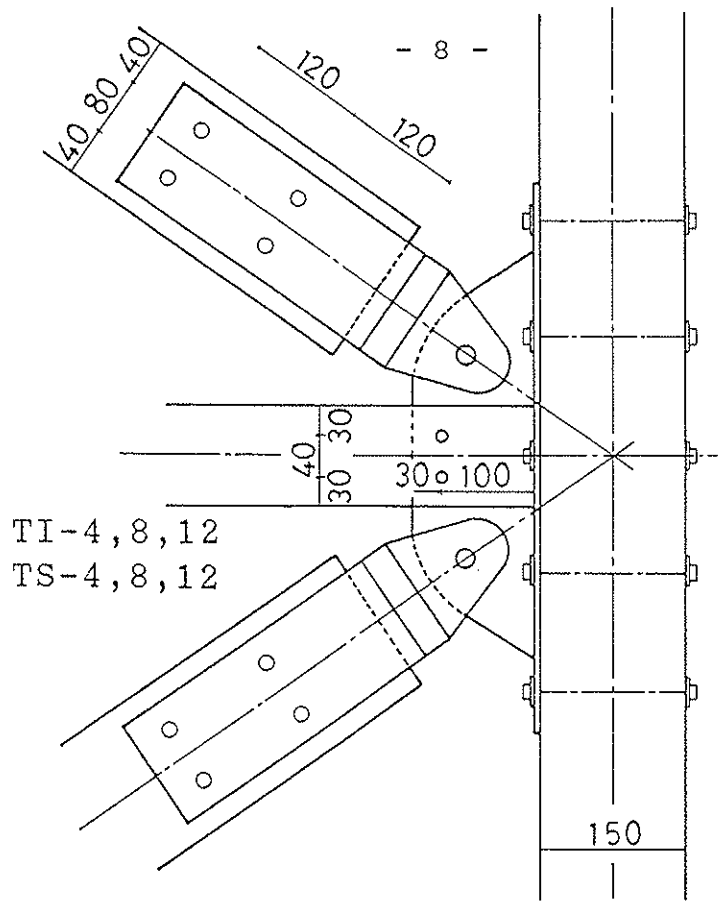


Fig.1 Joint with a steel pin joint

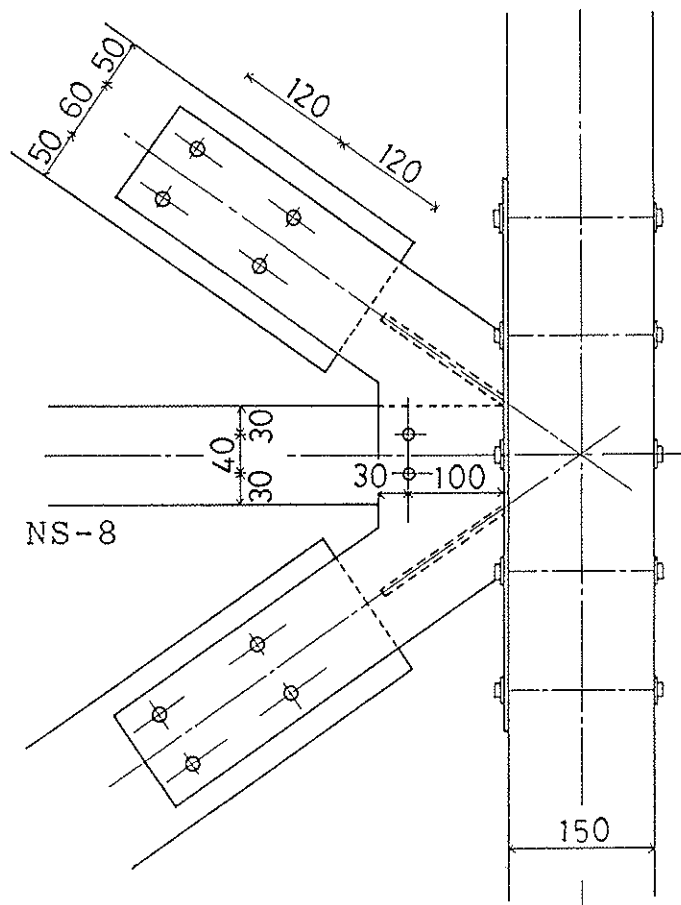
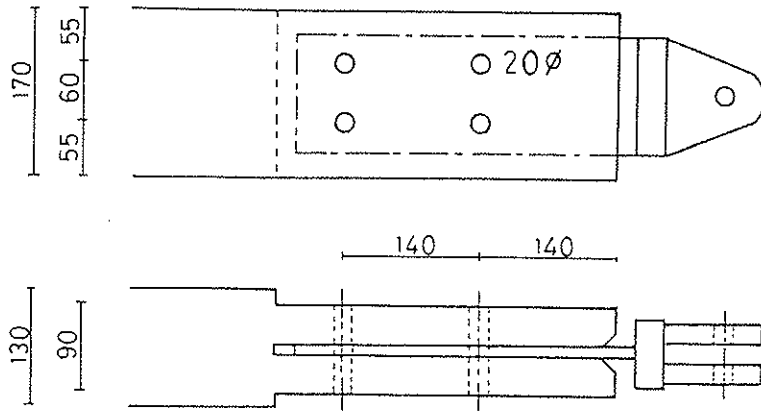
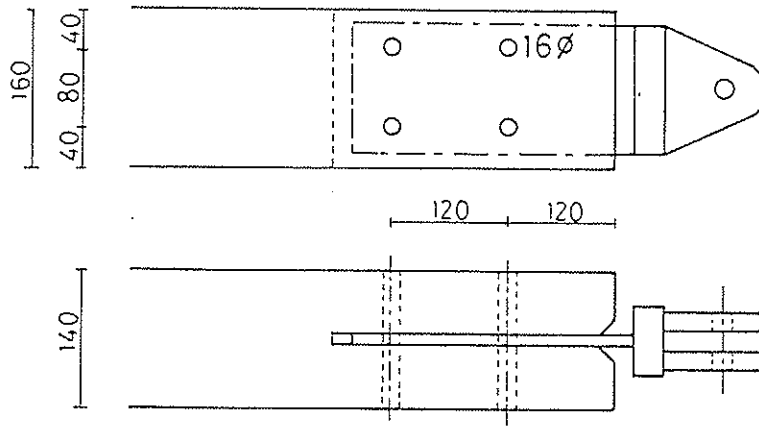


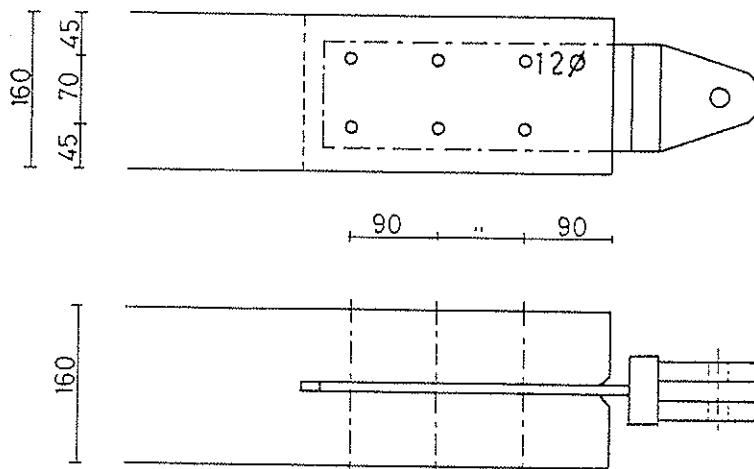
Fig.2 Joint without steel pin joints



TI-4

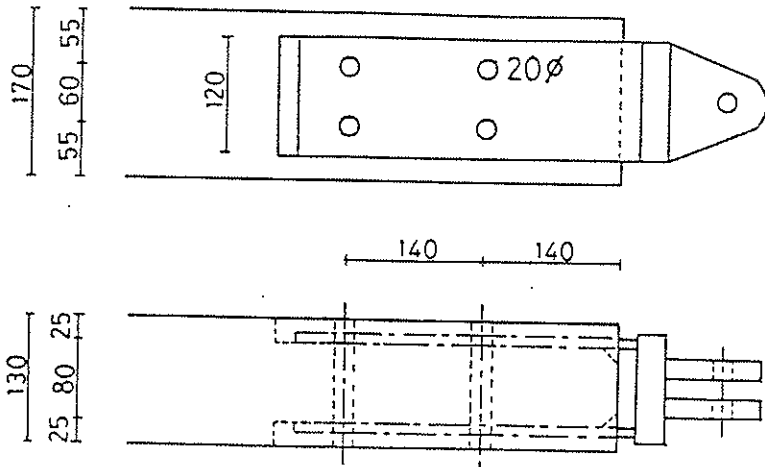


TI-8

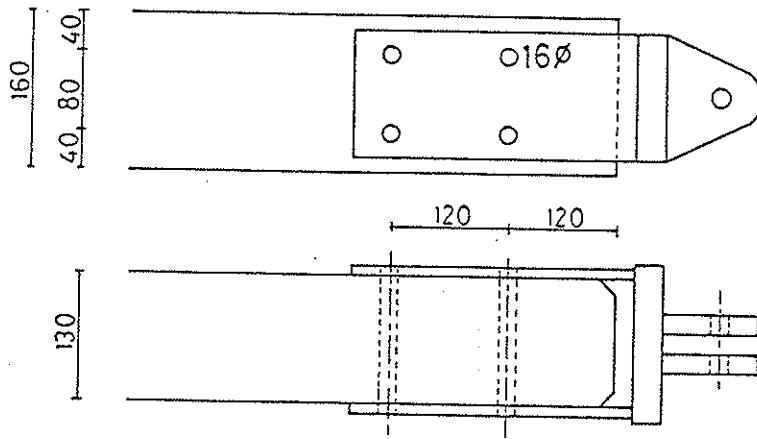


TI-12

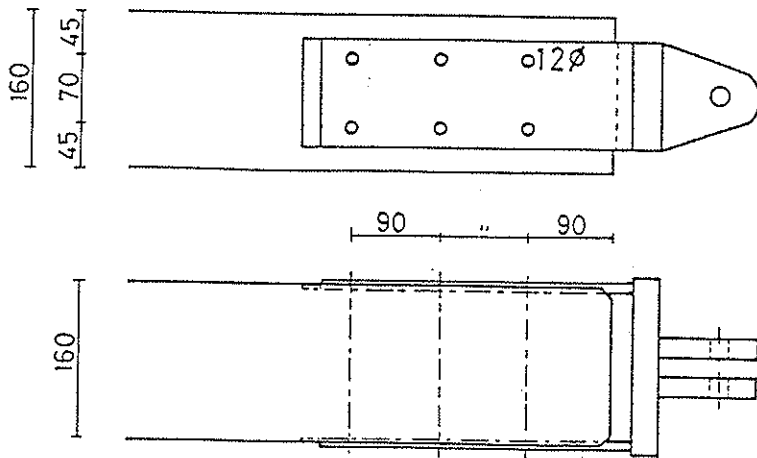
Fig.3 Detail of joints with inserted steel plate



TS-4



TS-8



TS-12

Fig.4 Detail of joint with steel side plates

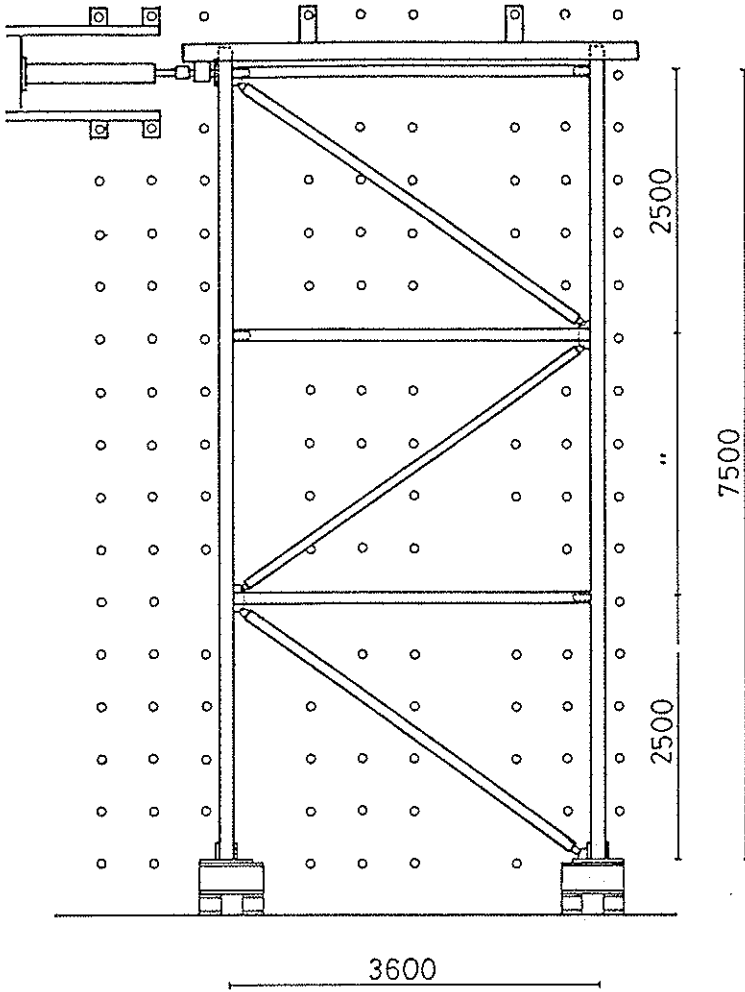


Fig.5 Outline of specimen and test apparatus

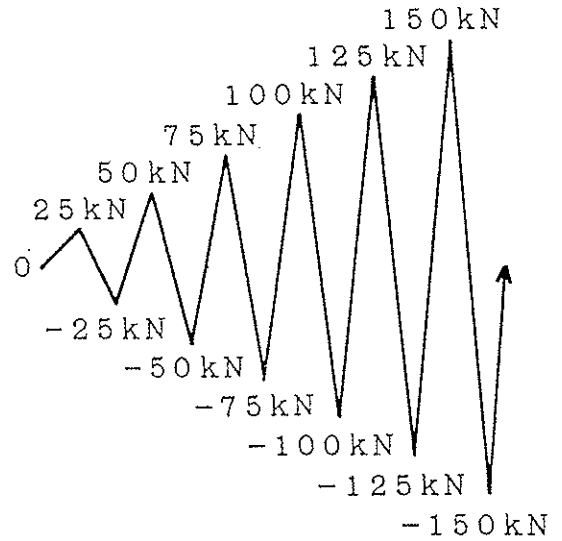


Fig.6 Loading history

Table 1. Outline of specimens

SPECIMEN	JOINT TYPE	L/d*	BOLT DIAMETER (mm)	Number of Bolts	THICKNESS of BRACE (mm)
TI- 4	Inserted	4.0	20	4	130 (90)**
TI- 8	steel	8.1	16	4	140
TI-12	plate	12.5	12	6	160
TS- 4	Steel	4.0	20	4	130 (80)**
TS- 8	side	8.1	16	4	130
TS-12	plates	12.5	12	6	150
TN-8	Without pin joint	8.1	16	4	130

* Thickness to bolt diameter ratio.
 ** Thickness of brace at the joint.

DUCTILITY FACTOR RESPONSE

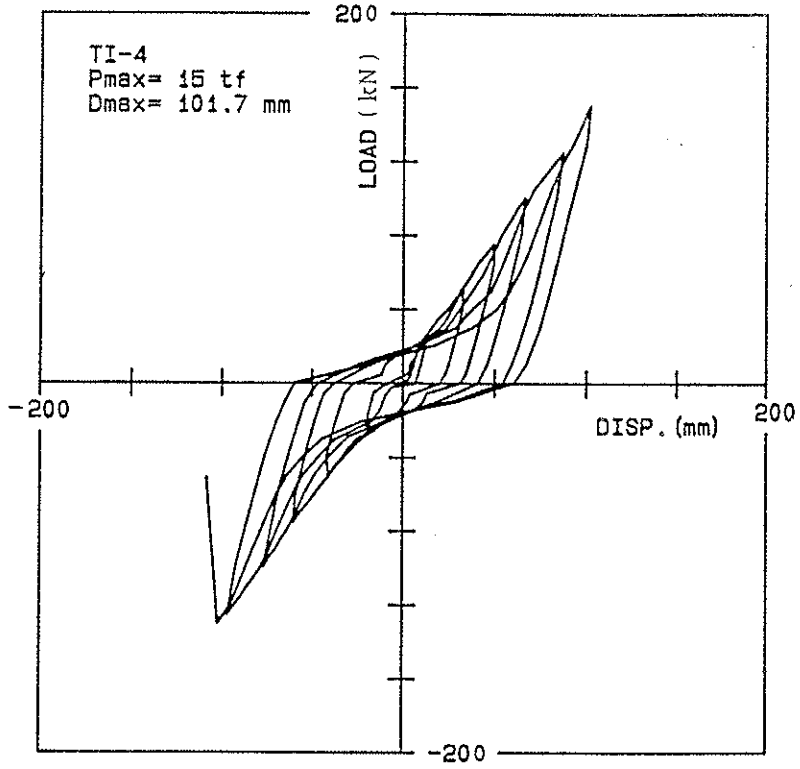


Fig.7(a) Load-displacenment relationship

DUCTILITY FACTOR RESPONSE

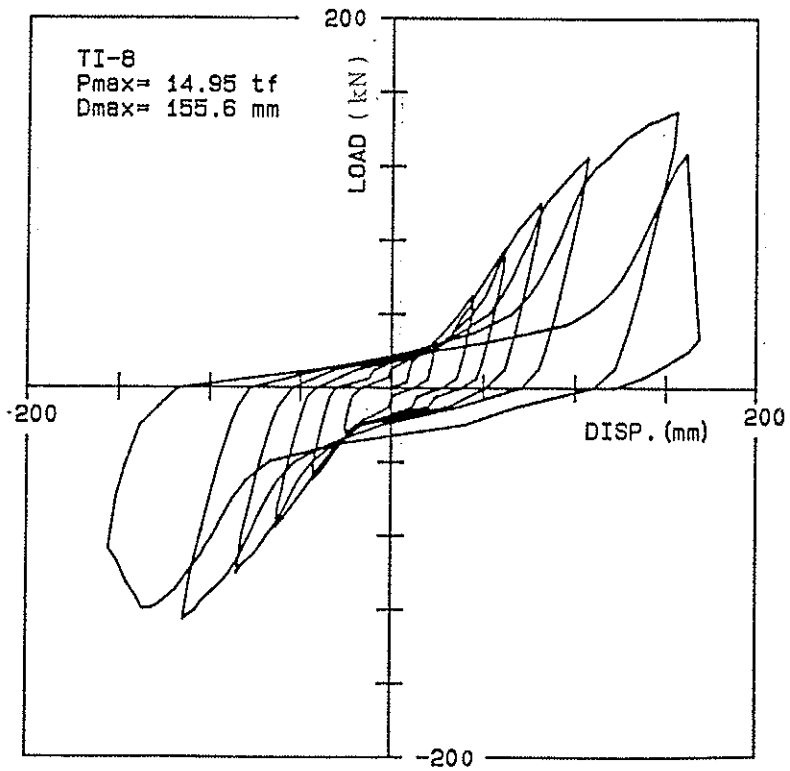


Fig.7(b) Load-displacenment relationship

DUCTILITY FACTOR RESPONSE

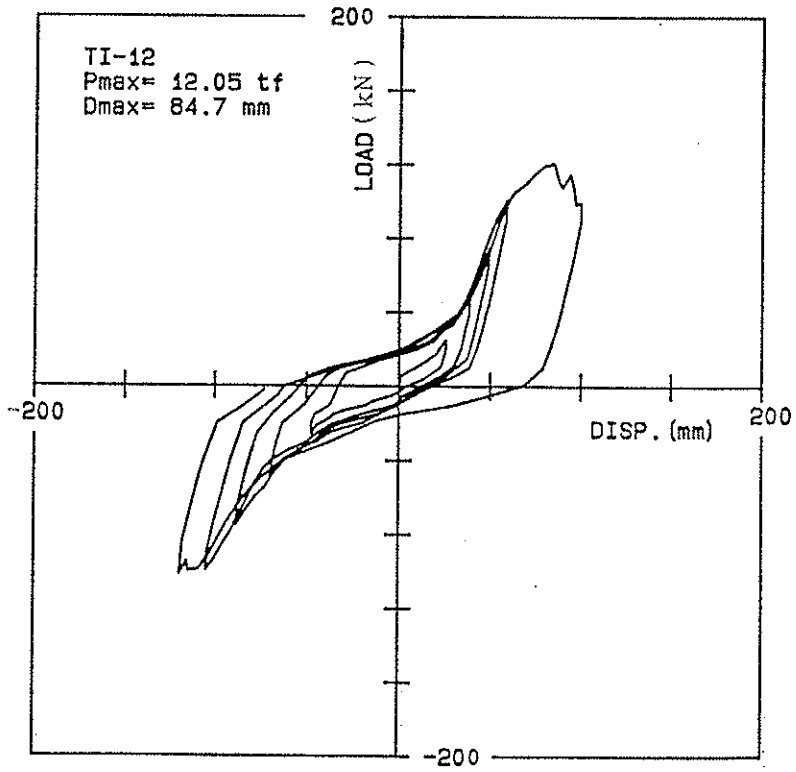


Fig.7(c) Load-displacement relationship

DUCTILITY FACTOR RESPONSE

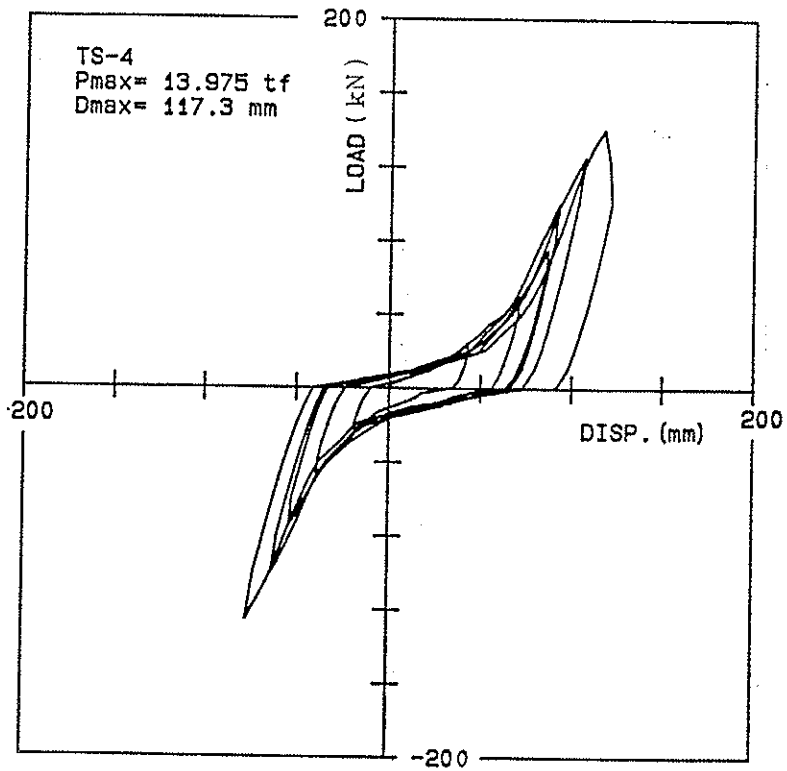


Fig.7(d) Load-displacement relationship

DUCTILITY FACTOR RESPONSE

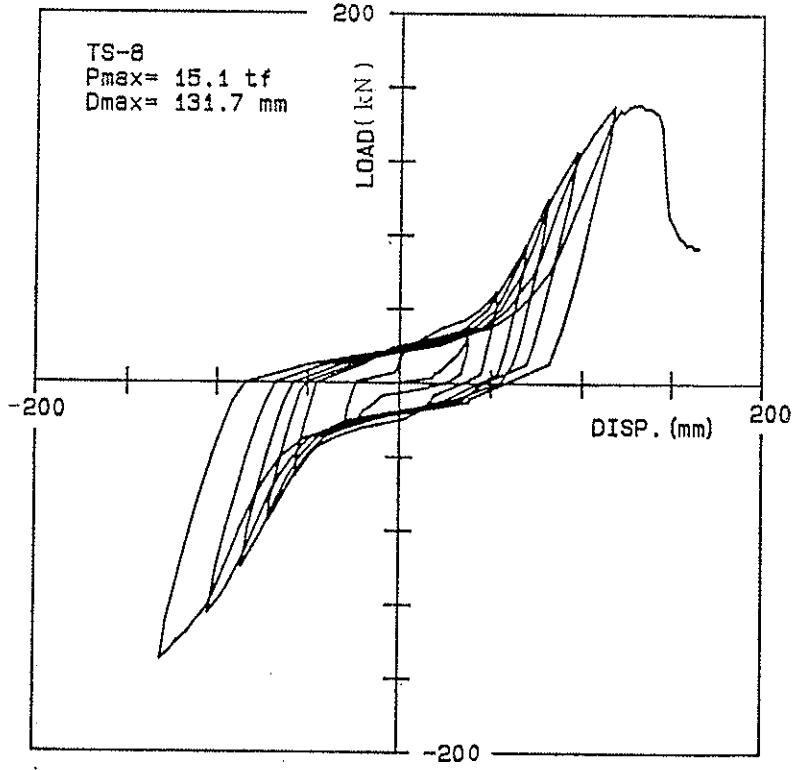


Fig.7(e) Load-displacenment relationship

DUCTILITY FACTOR RESPONSE

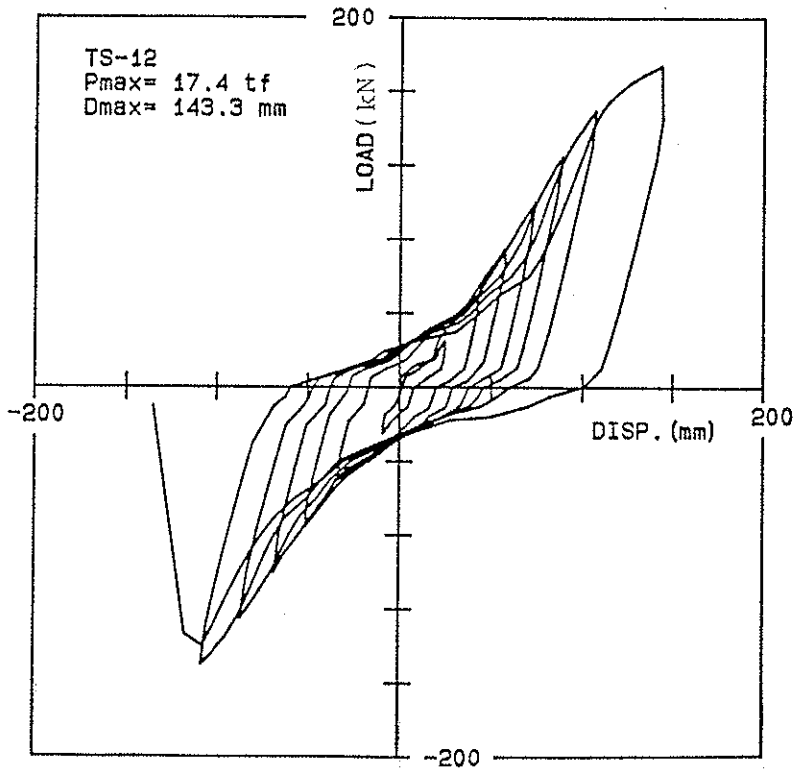


Fig.7(f) Load-displacenment relationship

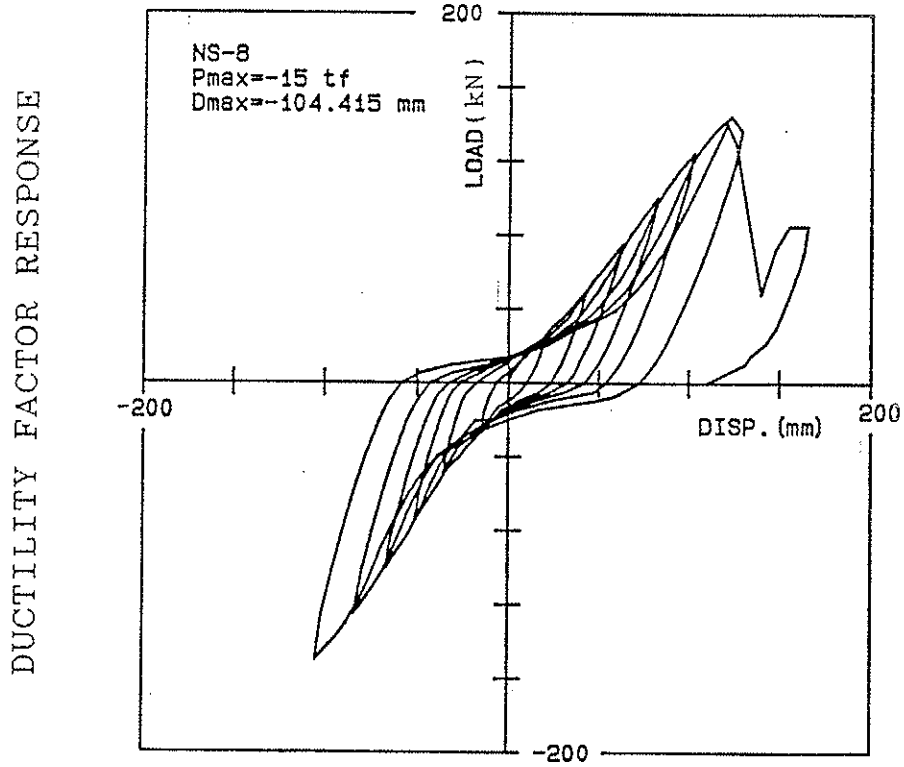


Fig.7(g) Load-displacement relationship

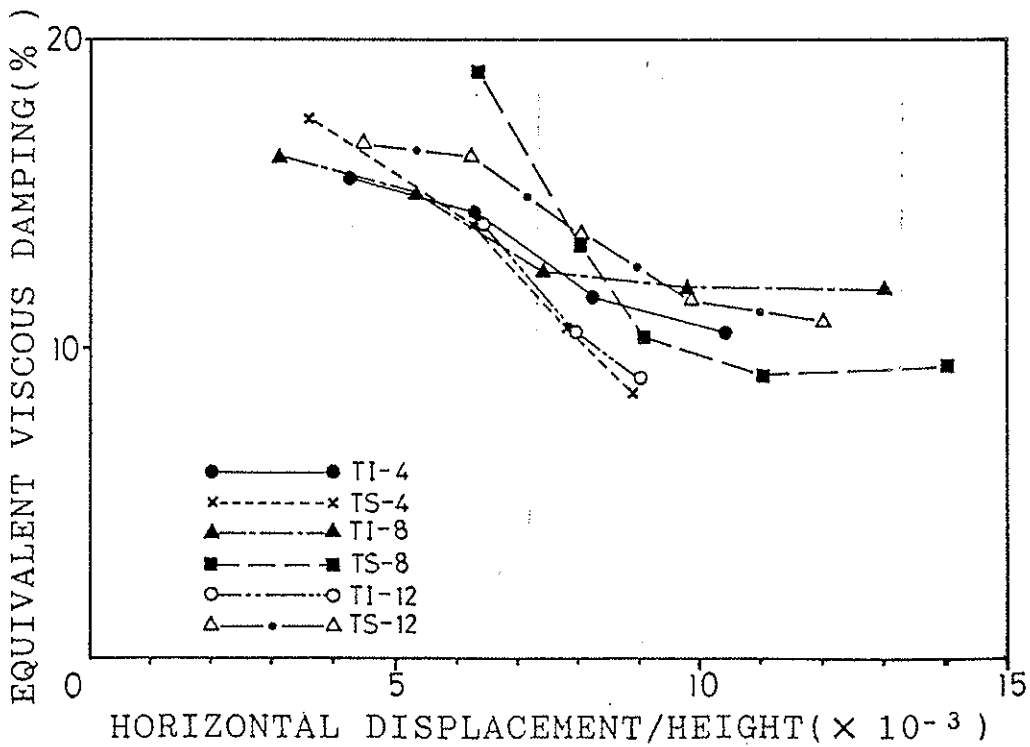


Fig.8 Equivalent viscous damping of each specimen

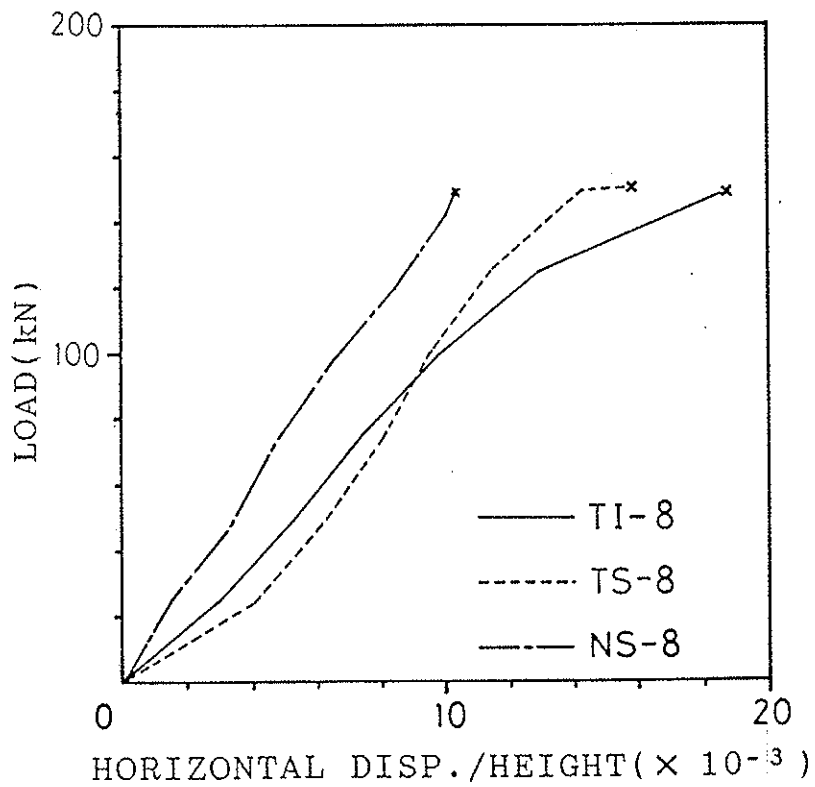
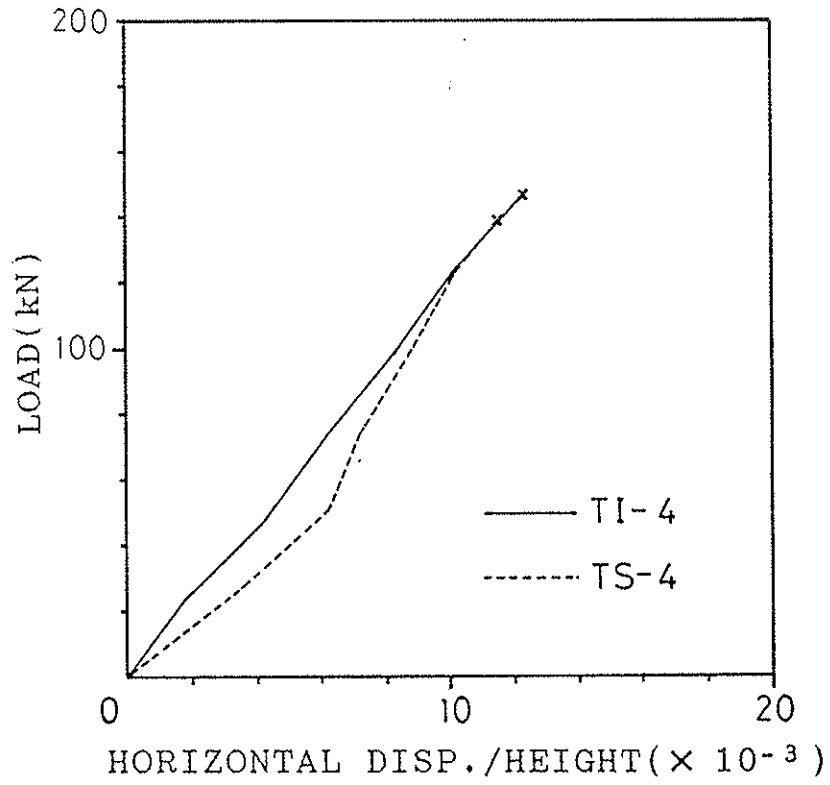


Fig.9(b) Skeleton of load-displacement curves in Specimens TI-8,TS-8 and NS-8

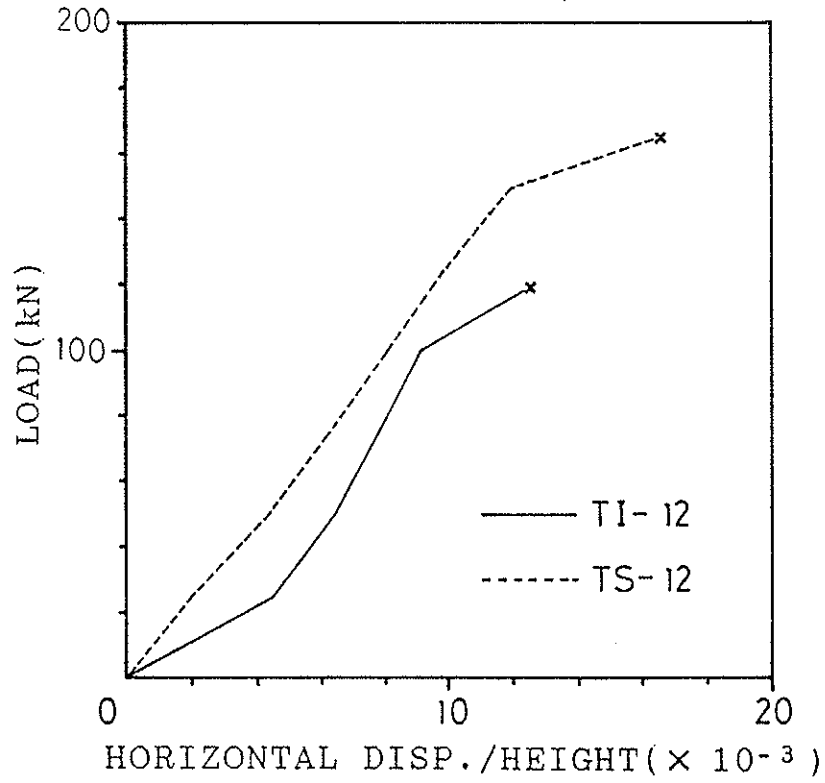


Fig.9(c) Skeleton of load-displacement curves in Specimens TI-12 and TS-12

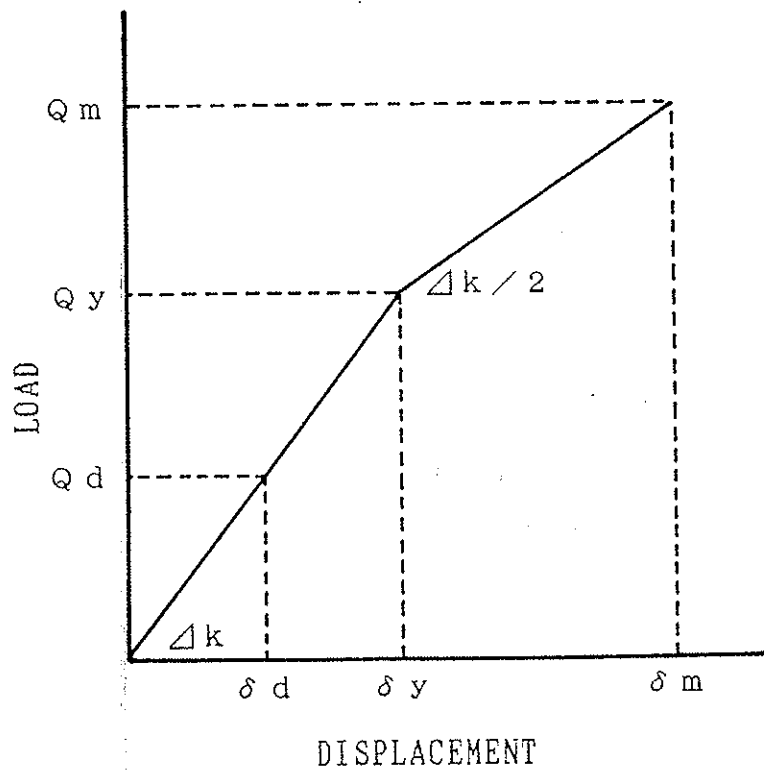


Fig.10 Modeling of the primary curves in braced frames

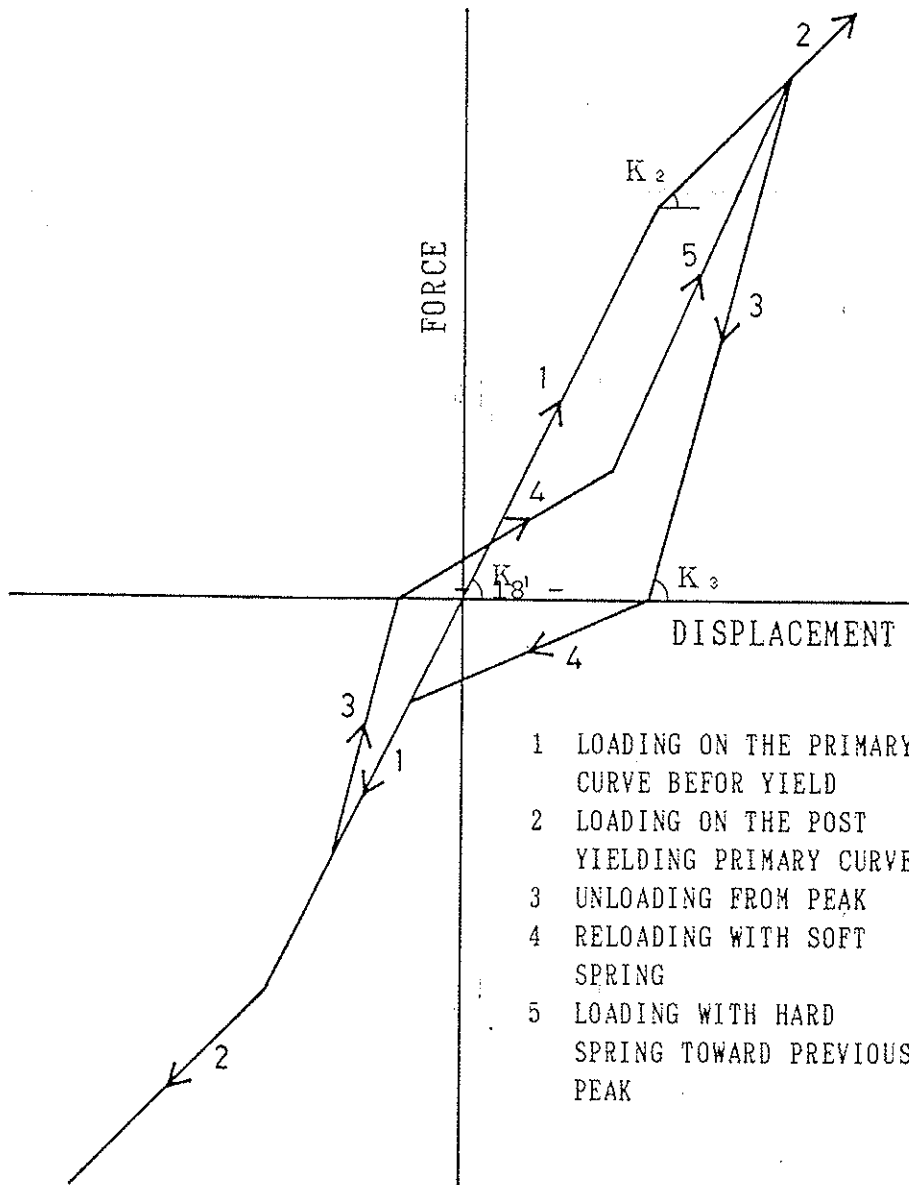


Fig.11 Hysteresis model for braced frames

HACHINOHE (EW) 300gal

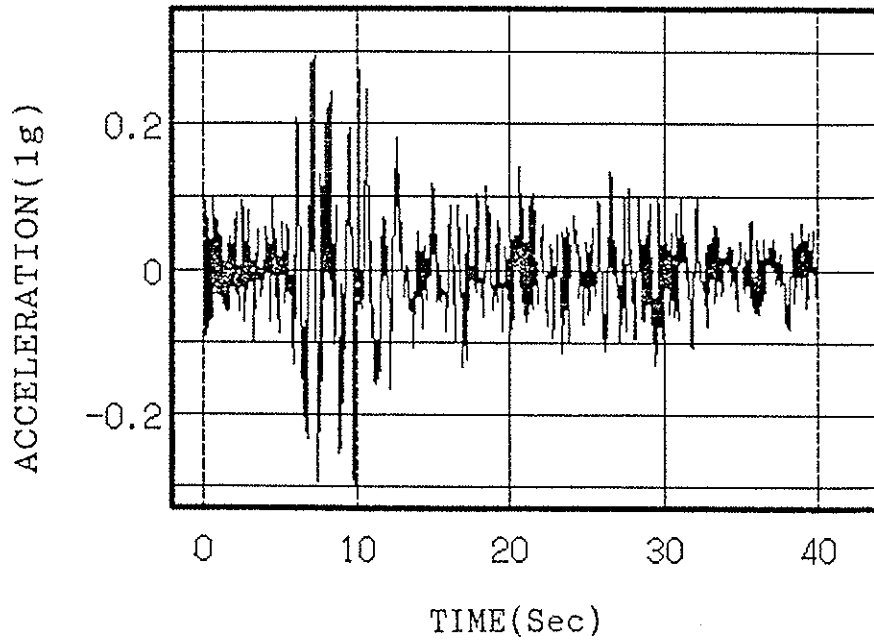


Fig.12 HACHINOHE(EW) accelerogram

HCH(EW) 300gal T=0.8sec. Mg/Qy=2.5

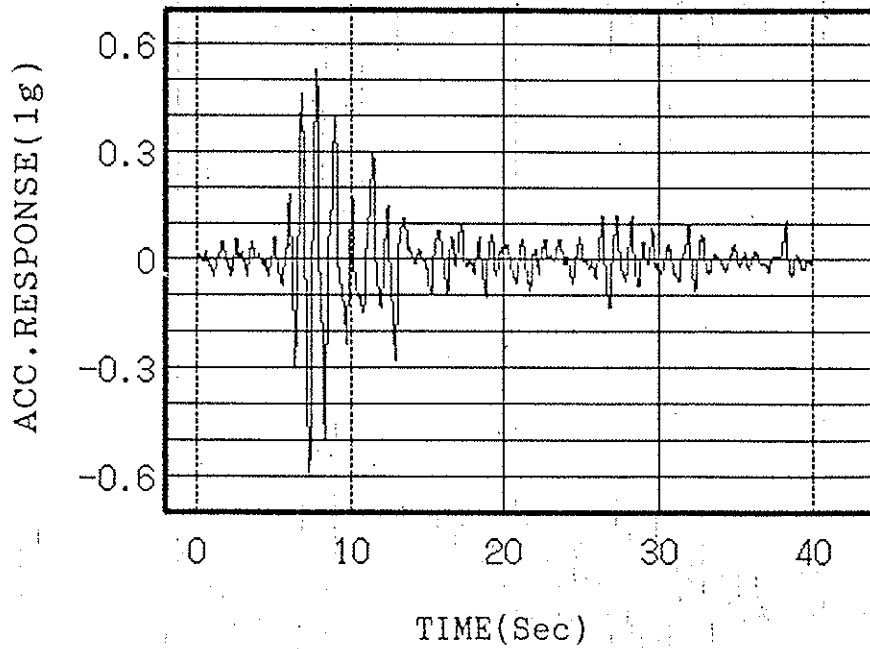


Fig.13 Acceleration response by non-linear model

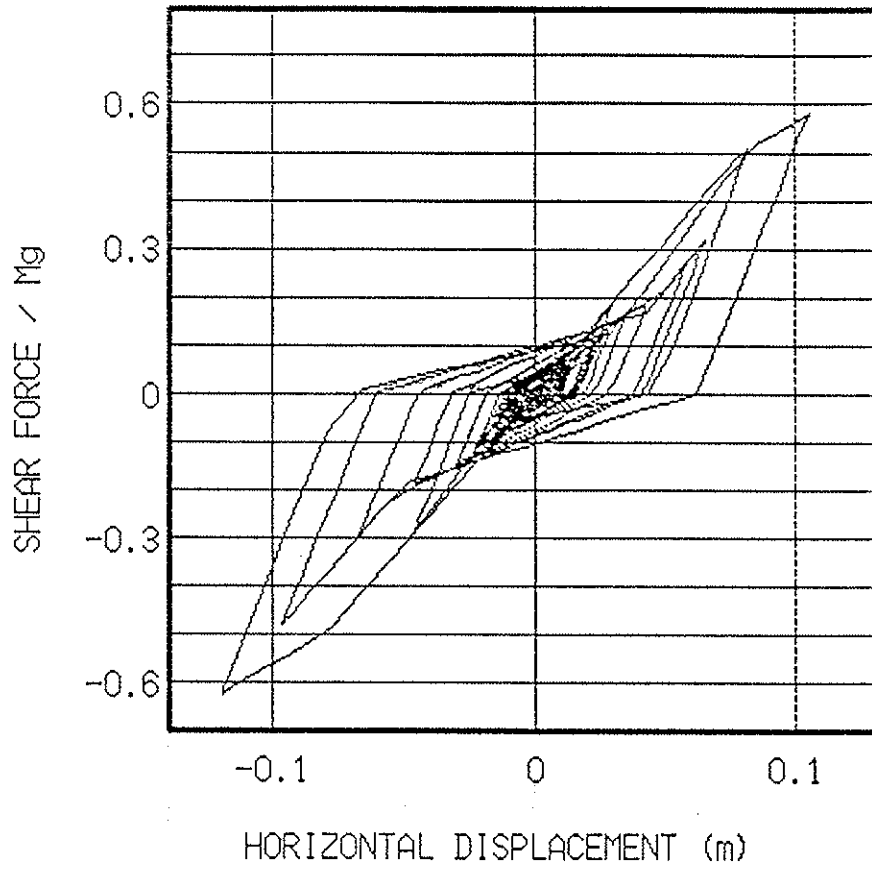
Table 2 Experimental results

SPECIMEN	YIELD. LOAD* (kN)	DISP. Dy (x10 ⁻³)	MAX. LOAD (kN)	DISP. Dm (x10 ⁻³)	INITIAL SLIP Do(x10 ⁻³)	$\frac{Dm-Do}{Dy-Do}$
TI-4	147	-	147 (1.0)**	12.3	0.2	-
TI-8	101	10.0	147 (1.46)	18.8	0.6	1.94
TI-12	94	8.9	118 (1.25)	12.5	3.3	1.64
TS-4	147	-	137 (0.93)	11.5	3.4	-
TS-8	111	9.0	148 (1.33)	16.0	3.4	2.25
TS-12	94	9.2	171 (1.82)	16.6	1.0	1.90
NS-8	111	7.8	147 (1.32)	10.3	0	1.32

* Calculated from the yield theory of bolted joints with $F_c=2.79\text{kN/cm}^2$ and $F_y=23.5\text{kN/cm}^2$

** Ratio of the maximum load to the yield load.

HCH(EW) 300gal $\bar{21}$ $T=0.8\text{sec.}$ $Mg/0y=2.0$



HCH(EW) 300gal $T=0.8\text{sec.}$ $Mg/0y=2.5$

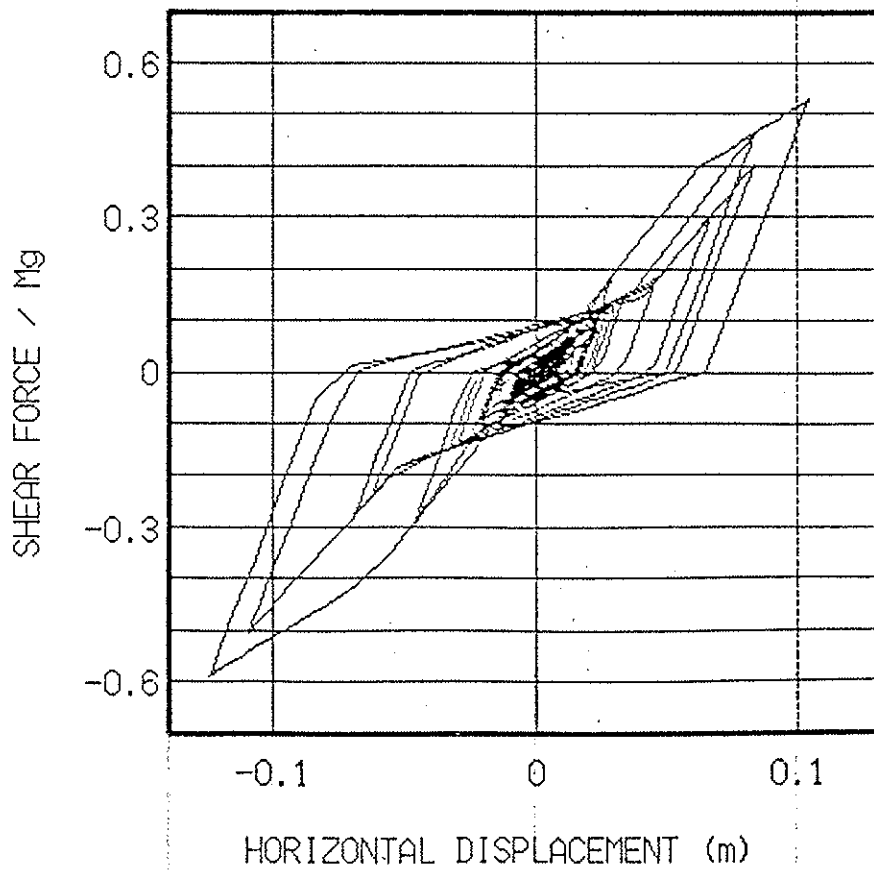


Fig.14 Example of the force-displacement response

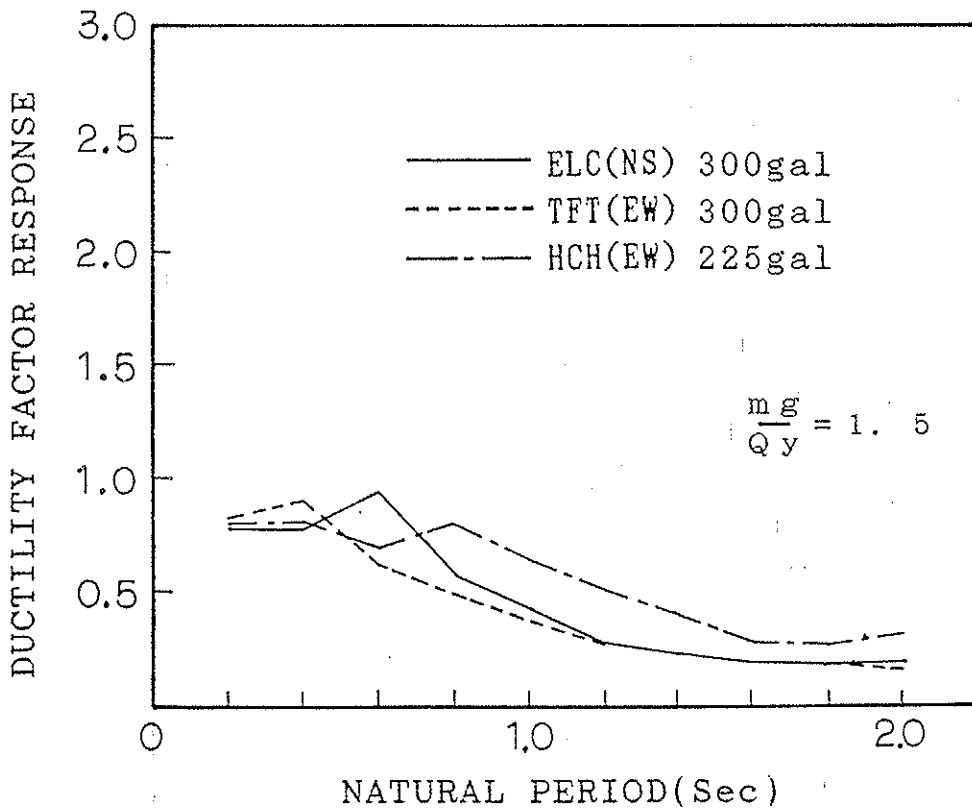
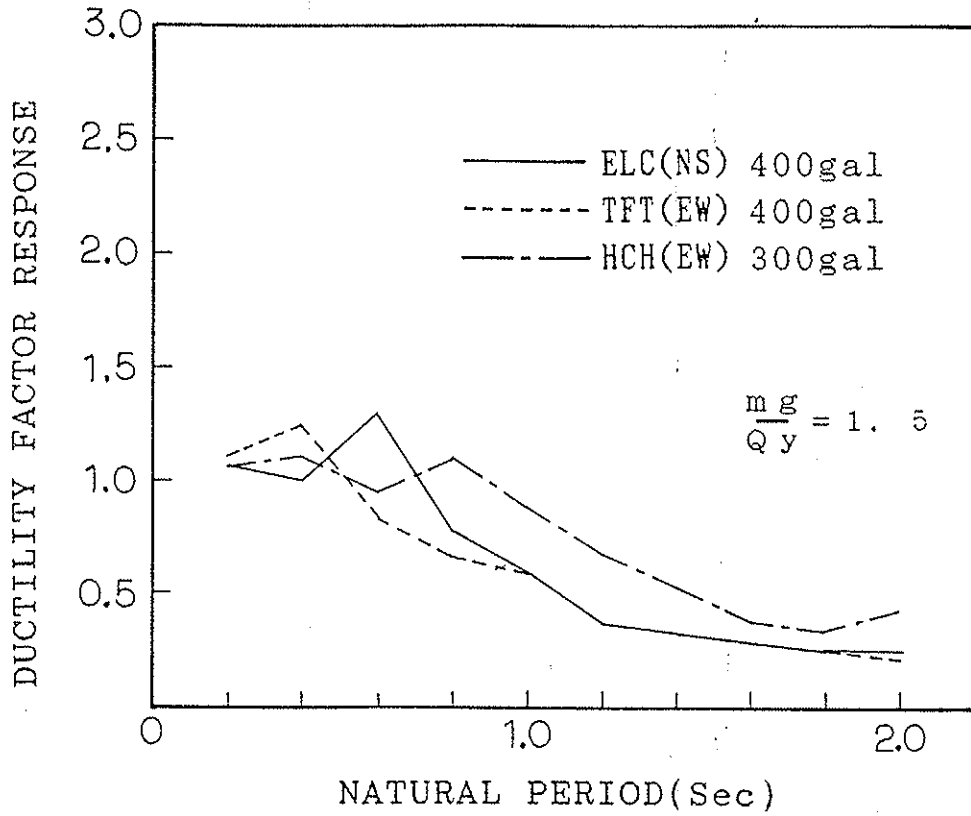


Fig.15 Ductility factor response spectrum in $mg/Qy=1.5$

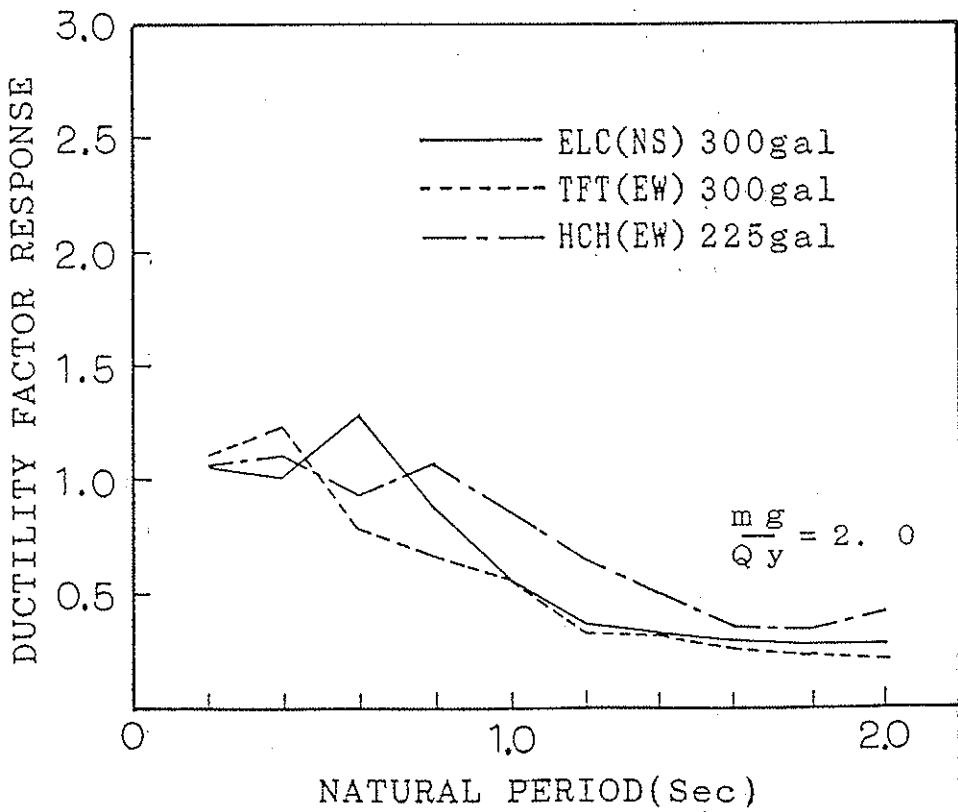
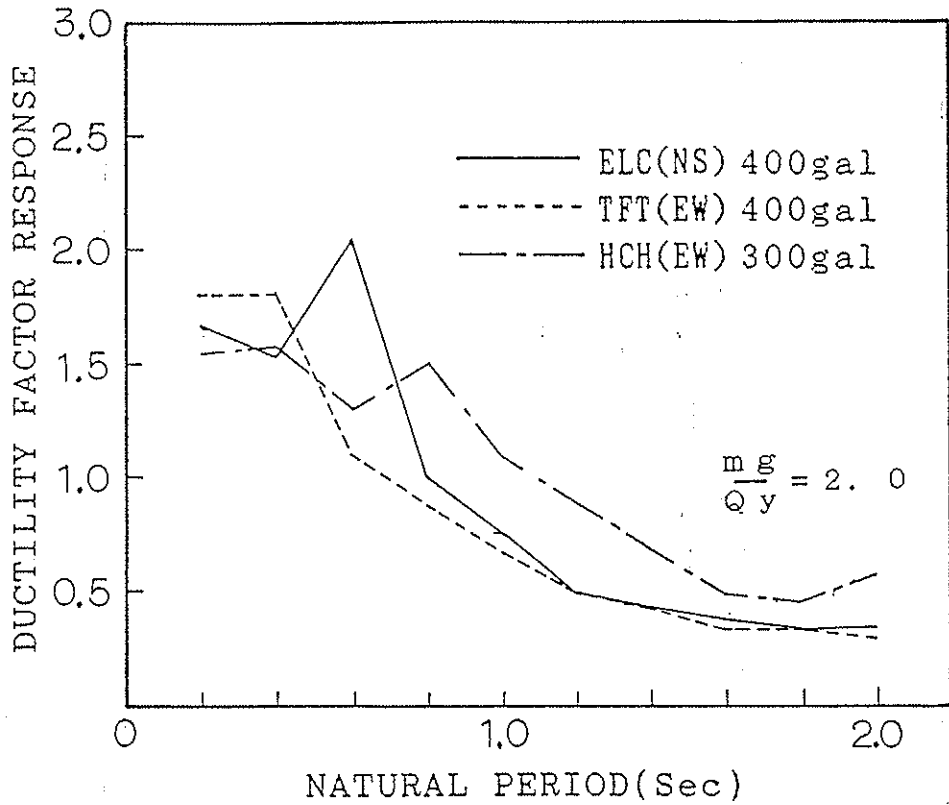


Fig.16 Ductility factor response spectrum in $mg/Qy=2.0$

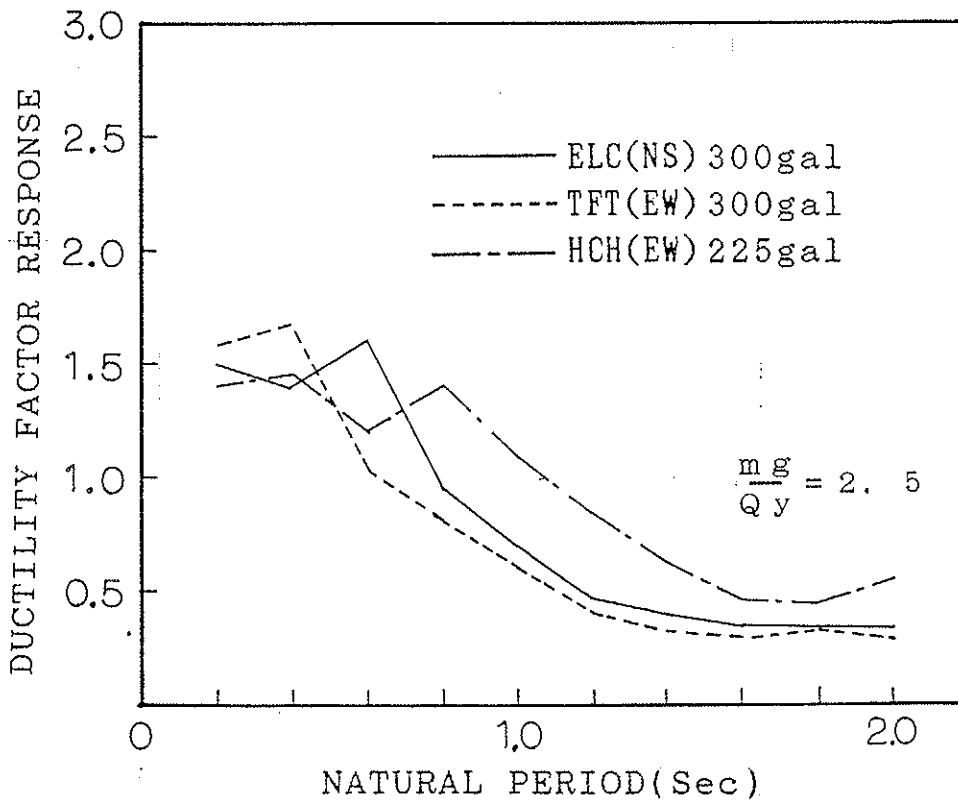
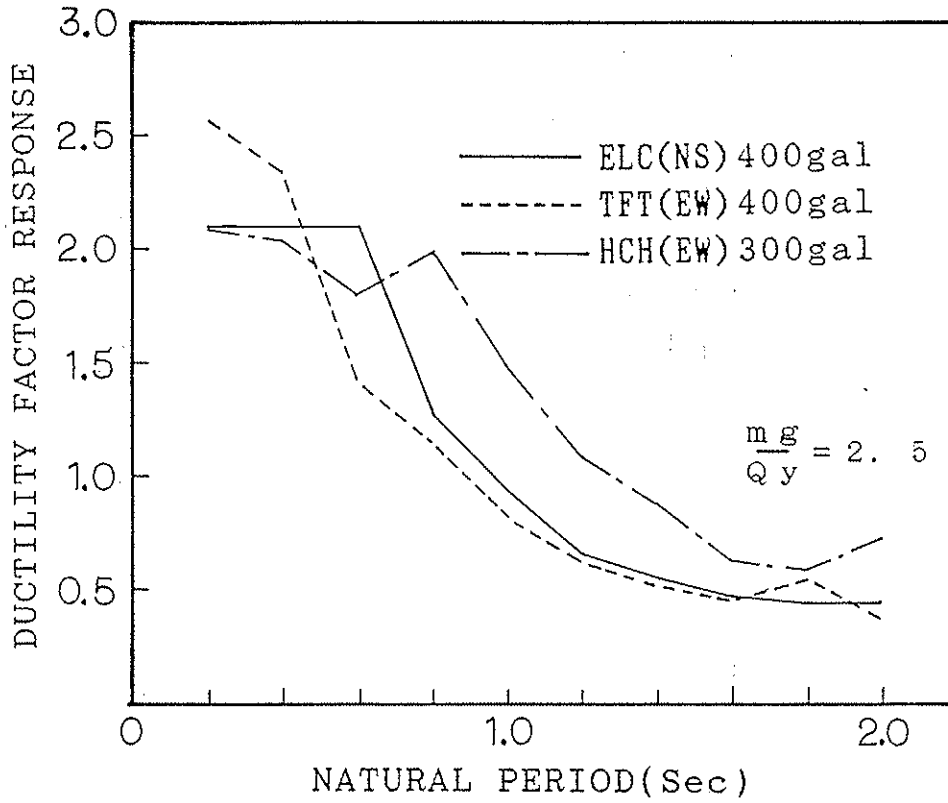


Fig.17 Ductility factor response spectrum in $mg/Qy=2.5$

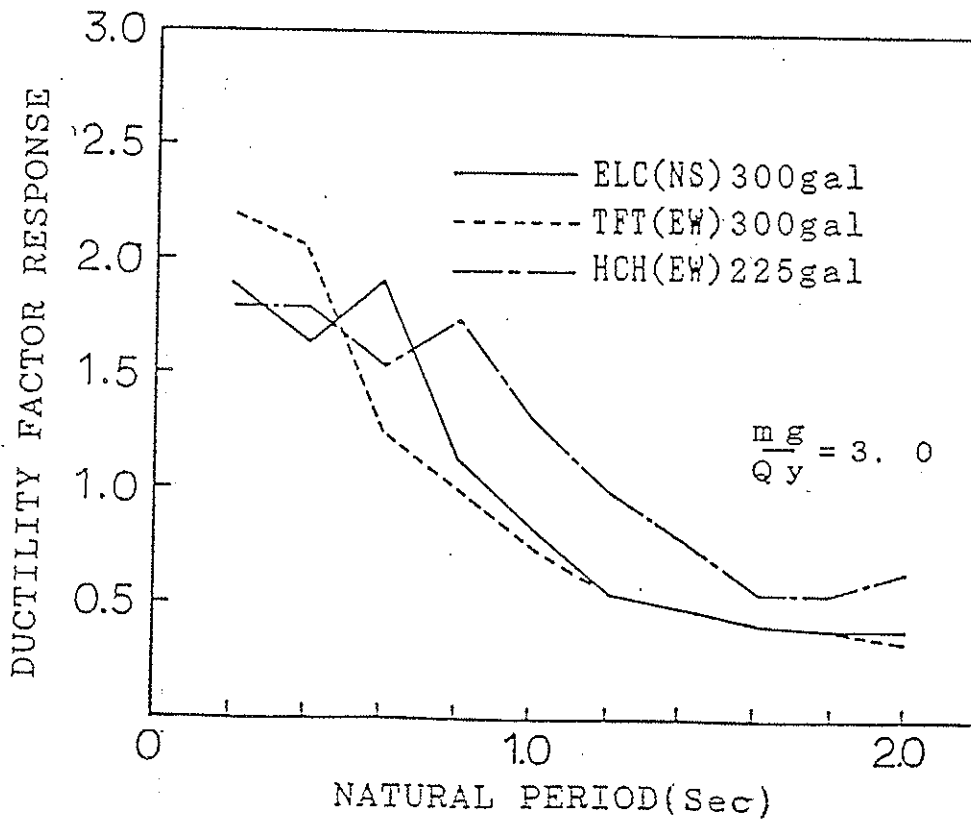
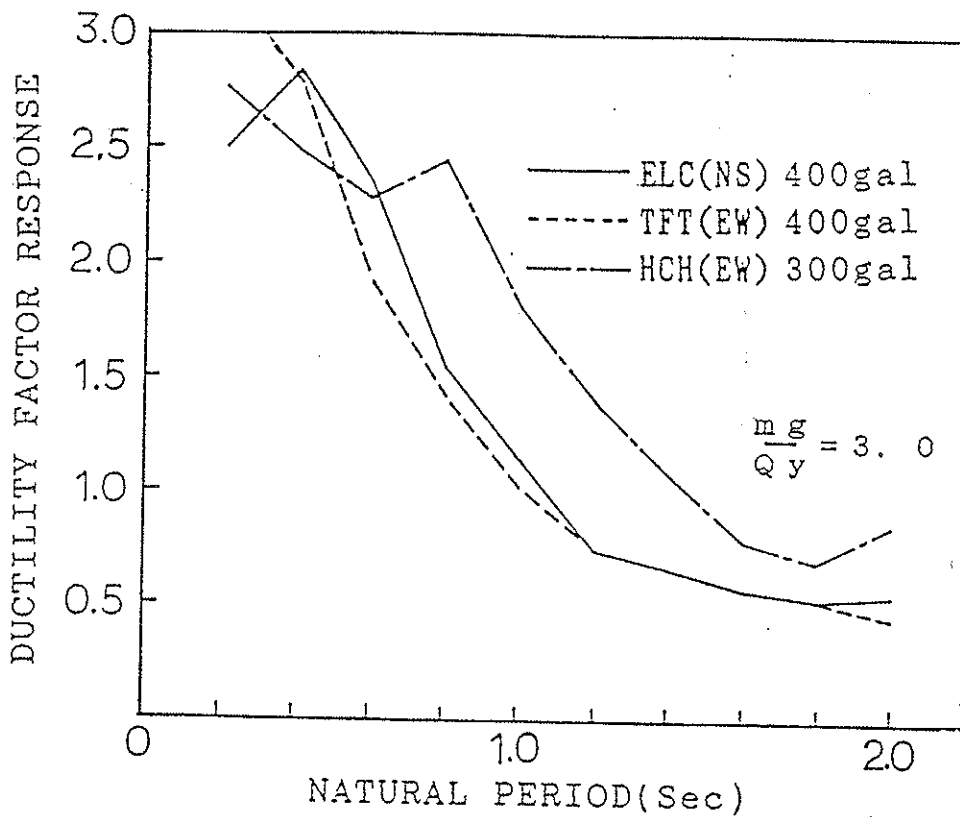


Fig.18 Ductility factor response spectrum in $\frac{m g}{Q_y} = 3.0$

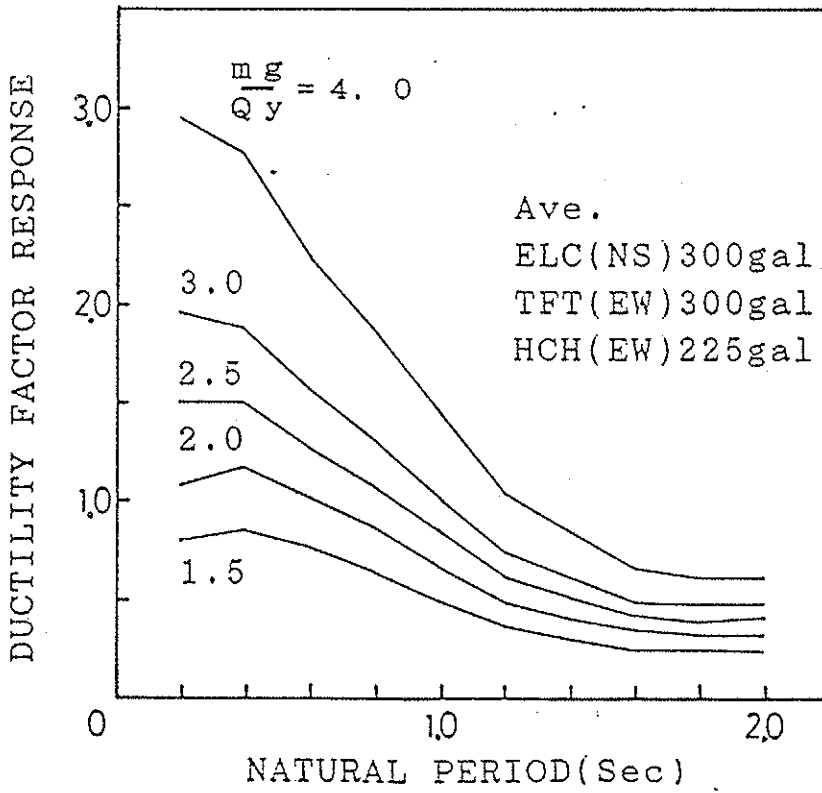
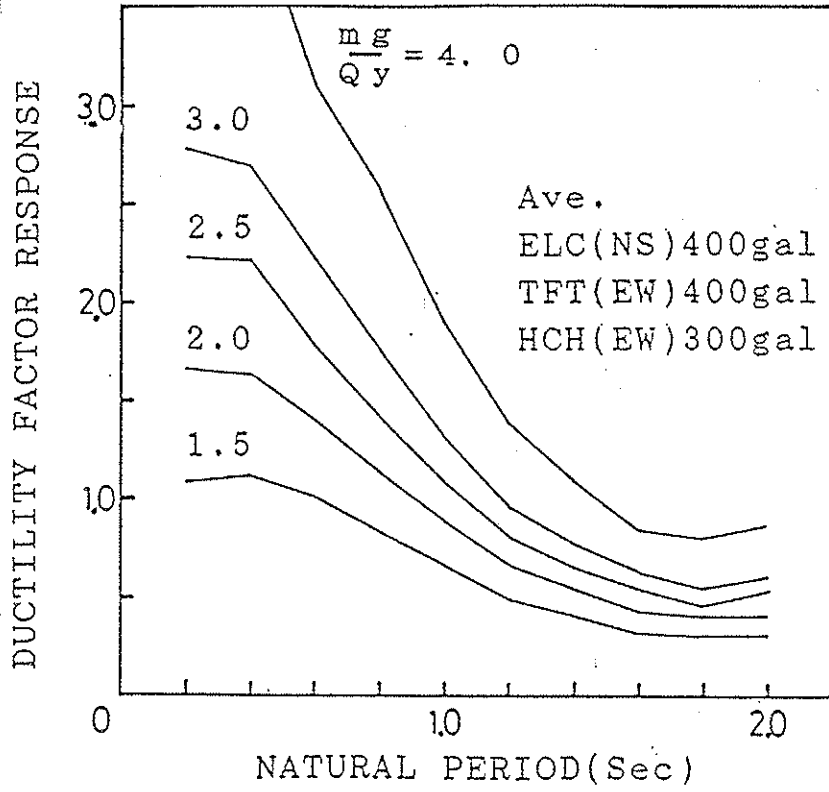


Fig.19 Ductility factor response spectrum in average values of three accelerograms

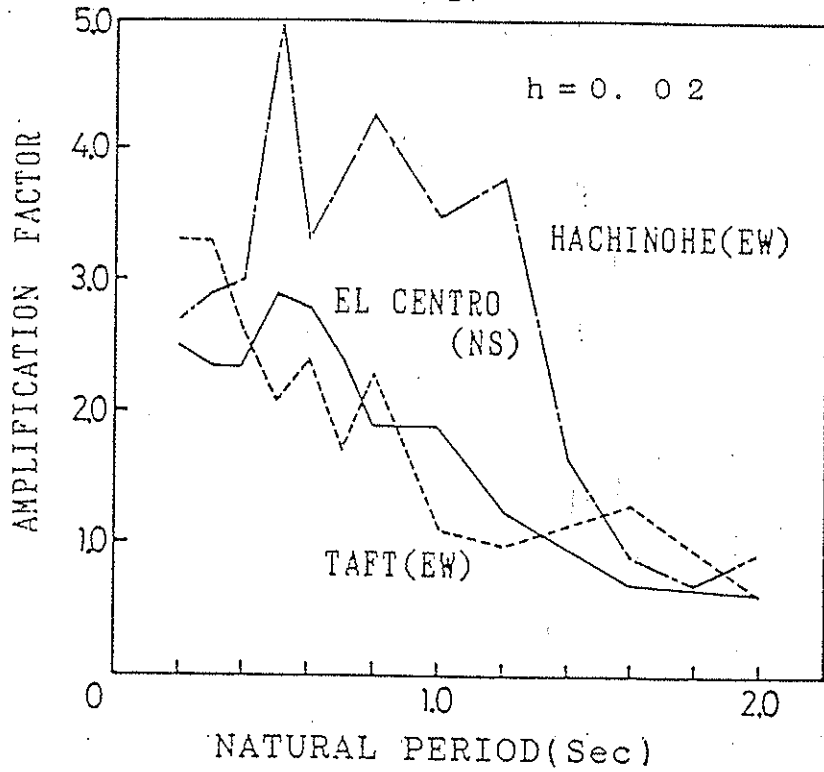


Fig.20 Amplification factor response spectrum

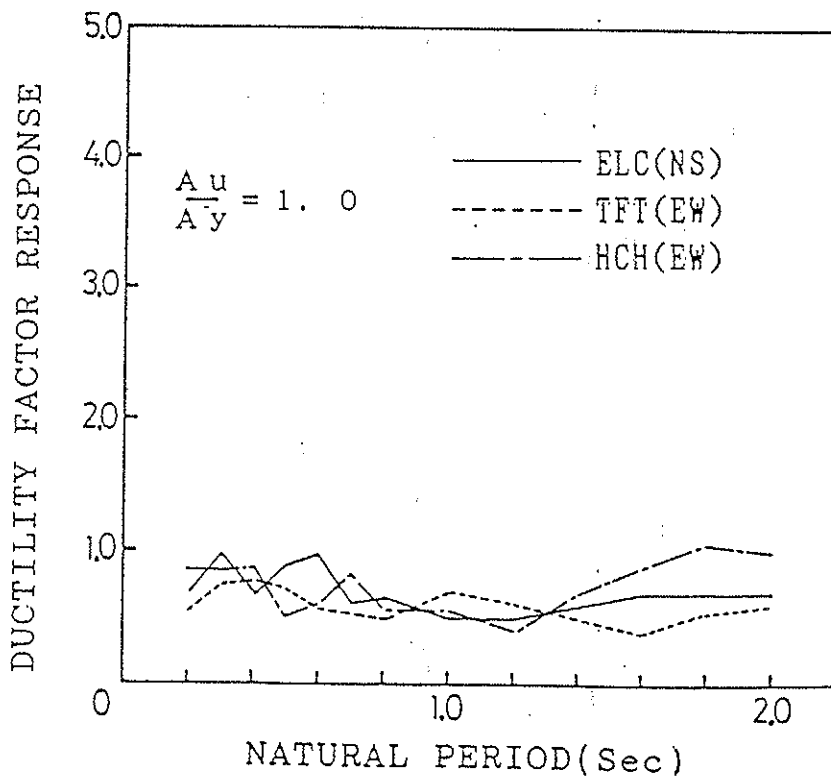


Fig.21 Ductility factor response spectrum
in $A_u/A_y = 1.0$

A_u : Maximum ground motion acceleration which gives maximum acceleration of $1g$ in linear response

A_y : Maximum ground motion acceleration which gives yield force in linear response

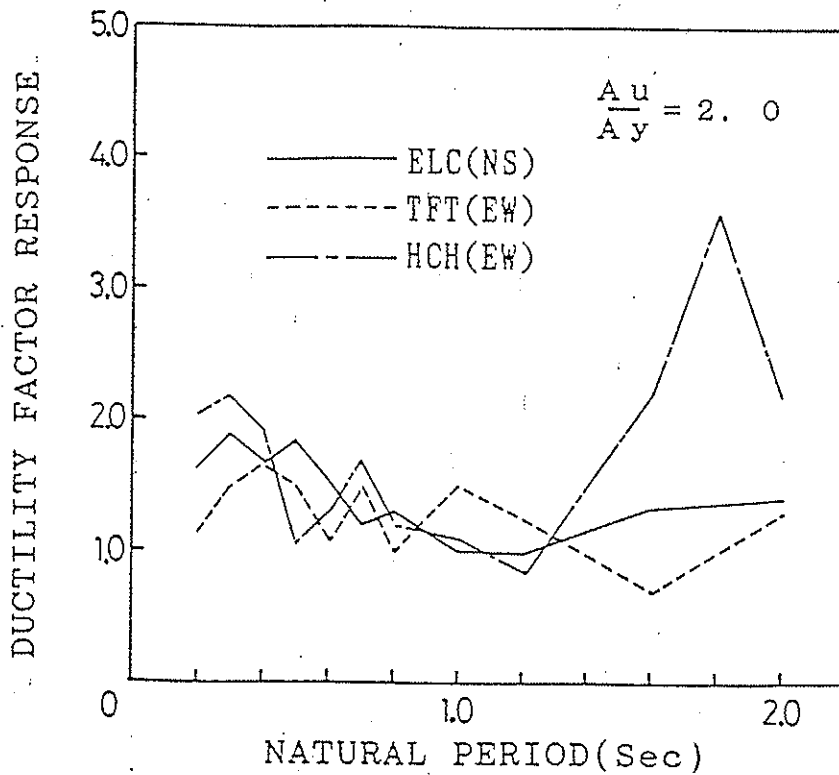
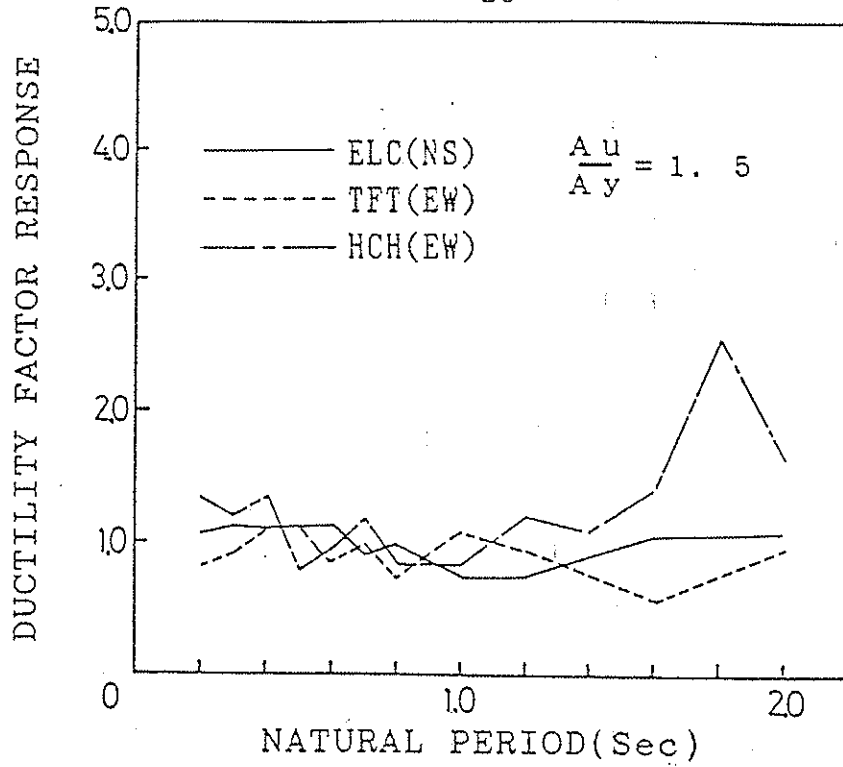


Fig.22 Ductility factor response spectrum
in $A_u/A_y=1.5$ and 2.0

A_u :Maximum ground motion acceleration which gives maximum acceleration of $1g$ in linear response

A_y :Maximum ground motion acceleration which gives yield force in linear response

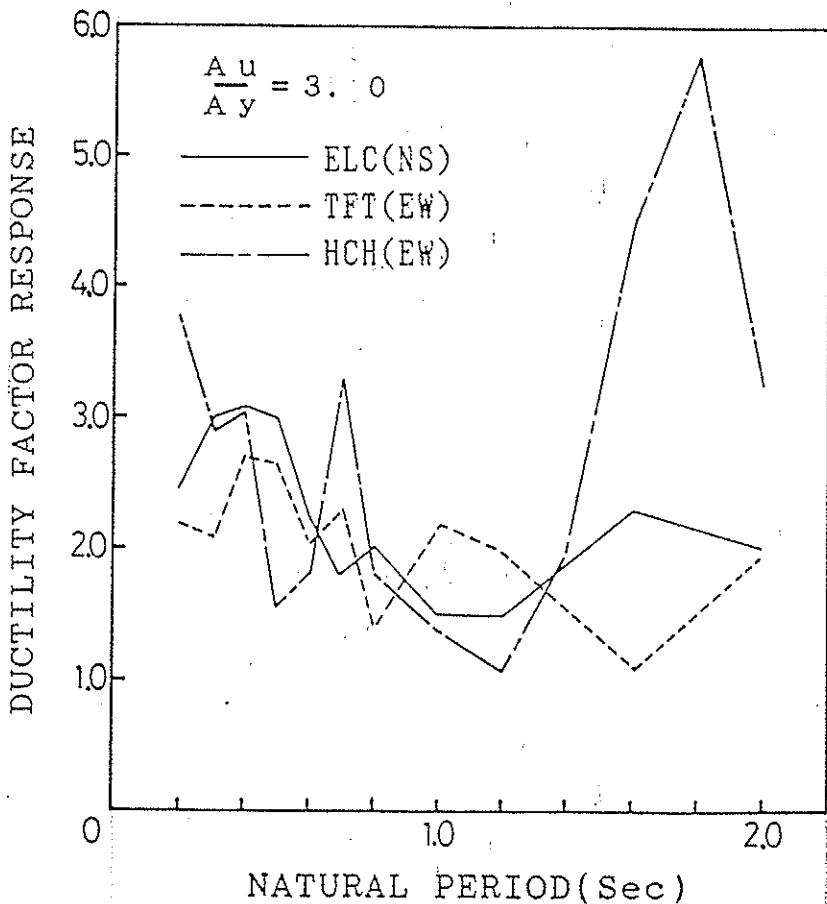
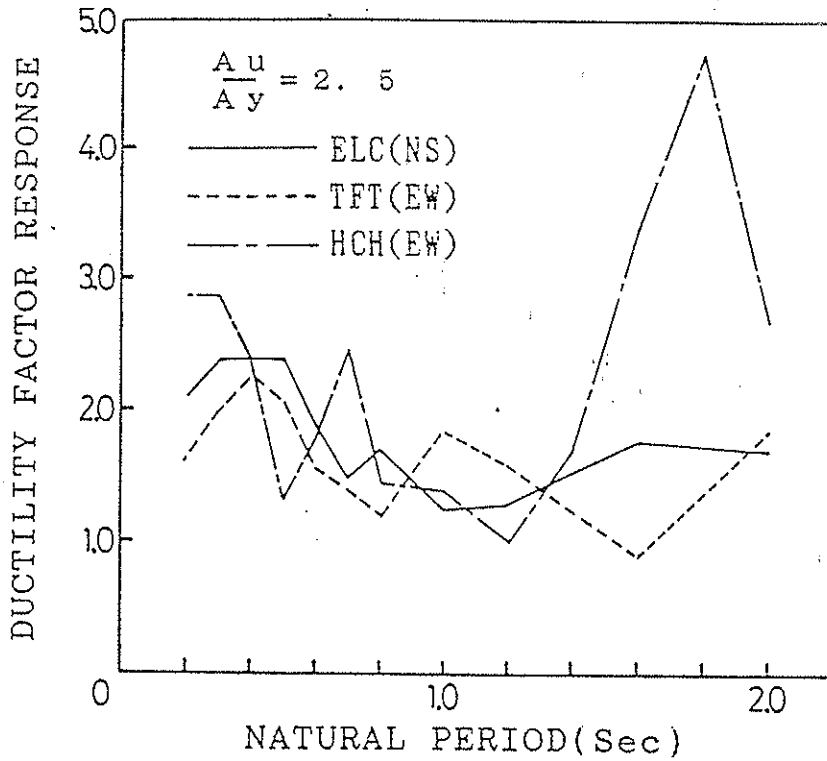


Fig.23 Ductility factor response spectrum in $A_u/A_y=2.5$ and 3.0

A_u : Maximum ground motion acceleration which gives maximum acceleration of $1g$ in linear response

A_y : Maximum ground motion acceleration which gives yield force in linear response

A N N E X

Criteria for Semi-ductile Trussed Frames with Diagonal Braces

I . Semi-ductile frames : $q = 2.0$ to 2.5

It is expected that the frame should fail with the failure of the end joints of braced members which have sufficient ductility.

- a) The ratio of the thickness of wooden members to the diameter of a bolt should not be less than EIGHT. If the thickness-to-bolt-diameter-ratio of a joint except for the end joints of a brace is less than EIGHT, the bearing force at the joint should be less than TWO-THIRDS of the yield load when the bearing force of the end joints of a brace reaches the yield load. In any case the thickness-to-bolt-diameter-ratio should not be less than FOUR.
- b) The joints connecting the wooden members should have enough spacing between bolts and spacing between the rows of bolts to have sufficient ductility.
- c) There should be no brittle failure at the joint due to the stress perpendicular to the grain of wood.
- d) There should be no failure of wooden members due to the buckling, bending and tension. The stress in wooden members should be less than TWO-THIRDS of the strength of wood when the bearing force of the end joints of a brace reaches the yield load.
- e) Steel members should not brake.

II . Non-ductile frames : $q=1.5$

It is expected that the wooden members do not fail before the yield of joints.

- a) The joints should have sufficient strength and should not fail under the yield load with the shear or the stress perpendicular to the grain.
- b) Wooden members should not fail before the yield of joint by buckling, bending and tension.
- c) Steel members should not brake before the yield of joint.

III . Others : $q=1.0$

INTERNATIONAL COUNCIL FOR BUILDING RESEARCH STUDIES AND DOCUMENTATION
WORKING COMMISSION W18A - TIMBER STRUCTURES

ON A BETTER EVALUATION OF THE SEISMIC BEHAVIOR FACTOR
OF LOW-DISSIPATIVE TIMBER STRUCTURES

by

A Ceccotti
A Vignoli
University of Florence
Italy

MEETING TWENTY - THREE

LISBON

PORTUGAL

SEPTEMBER 1990

ON A BETTER EVALUATION OF THE SEISMIC BEHAVIOUR FACTOR OF LOW-
DISSIPATIVE TIMBER STRUCTURES

by

A. Ceccotti & A. Vignoli
University of Florence
Italy

Summary

Some results concerning the seismic verification of low-dissipation timber structures designed according to Eurocode 8 assuming a behaviour factor $q=2$ are given in this paper.

The semirigid connection design was performed considering the suggestions given by the Authors in a previous paper.

The numerical simulation was carried out using a time domain non linear dynamic analysis .

1. Introduction

Three kinds of timber structures are considered in the draft version of Eurocode 8 [1]:

- non-dissipative
- low-dissipative
- medium-dissipative.

But due to the lack of knowledge the value of the behaviour factor reducing design inertia forces (" q ") was fixed uniformly equal to 1 for each kind of structure.

Afterwards a number of important research papers have been published and an international Workshop on this subject has been held too [2].

Ceccotti e Larsen have suggested [3] to give to q the following values:

- non-dissipative, $q=1$
- low-dissipative, $q=2$
- medium-dissipative, $q=2.5$

In a recent work [4] the Authors have given quantitative indications which can unable to obtain values of q higher than 1. In particular they defined three parameters essential for the structural behaviour of base hinged portals:

$$k = M_{yj} / M_{ub}$$
$$f = M_{uj} / M_{ub}$$
$$d_j = \Phi_{uj} / \Phi_{yj}$$

where

M_{yj} is the yielding joint moment
 M_{ub} is the ultimate beam moment
 M_{uj} is the ultimate joint moment
 d_j is the joint ductility
 Φ_{yj} is the yielding joint rotation
 Φ_{uj} is the ultimate joint rotation

The Authors suggested that it is possible to obtain a better seismic behaviour if the following conditions are fulfilled (Fig.1):

$$0.6 < k < 0.8$$

$$0.8 < f < 0.9$$

$$d_j > 6$$

In the present paper a first verification of such indications is performed.

2. Materials and methods - Dimensioning

Three glued laminated timber base hinged portals (A, B, C) of very different span and height so as to have a wider range of

the examined span/height ratio, have been designed.

They have been dimensioned according to the EC8 rules for high seismicity zones (peak ground acceleration 0.35 g) following the response spectrum method and using the static analysis. This has been able since the structure is similar to an elementary oscillator. The maximum value of the normalized spectral value was assumed as response coefficient due to the fact that each portal has its period less than 0.6 seconds.

The considered values of the various parameters are the following:

- self-weight plus dead load = 6 KN/m
- characteristic snow load = 6 KN/m
- characteristic wind load = 3 KN/m
- factors for snow load $\psi_0 = 0.7$ $\psi_2 = 0.3$
- characteristic bending strength of timber: 25 MPa
- static modulus of elasticity (mean): 10000 MPa
- modification factor for increasing stiffness for instantaneous actions: 1.2
- q = 2
- $\alpha = 0.35$

The following load combinations have been considered:

- fundamental combinations
 - 1.35 dead + 1.5 snow ($k_{mod} = 0.80$, $\gamma_m = 1.25$)
 - 1.35 dead + 1.5 snow + 1.5 snow ($k_{mod} = 0.90$, $\gamma_m = 1.25$)
 - accidental combinations (earthquake)
 - dead + E + ψ_2 snow ($k_{mod} = 1.20$, $\gamma_m = 1.00$)
- as suggested by Eurocode EC5 and EC8.

The joints compliance and the moment redistribution [5,6] have been considered for the verification of the sections.

In Figg. 2,3 and 4 the assumed dimensions for portal beams and columns and the chosen characteristics for angle semi-rigid connections are given following the suggestions given in [4].

We underline particularly that the beam resistance is higher than the one of the joints and that their ductility is equal to 6.

3. Calculations

The numerical simulation have been performed using a non-linear analysis as considered in EC8.

The used calculation programme was DRAIN-2D. For the semi-rigid connections an hysteretical behaviour with pinching as described in [7] has been considered.

Eight different accelerograms were applied to the base of the frames: four registered accelerograms and four simulated ones.

For the C portal we have considered also the contemporaneous presence of a vertical earthquake having the same characteristics of the horizontal one but with an intensity of 0.7 times .

For timber a linear-elastic behaviour until the rupture has been considered.

The damping coefficient for internal viscosity of the material and friction between the structural elements has been assumed equal to 5%

4. Results and observations

The so obtained results are given in Figg. 2,3 and 4 as ultimate acceleration producing collapse.

For all portals the collapse acceleration is always higher than the one required by EC 8.

From the Fig. 4 we can see that in the big span portal C design for static loads is more important than the seismic one.

5. Conclusions

From this research it seems possible to state that designing low dissipation semi-rigid connection portal frame timber structures following EC 5 and EC 8 rules but assuming $q = 2$ and using simple dimensioning rules for semi-rigid joints, it is possible to obtain structures whose resistance easily fullfills the Code strength requirements for seismic zones.

6. References

- [1] AA.VV., 1989: Eurocode 8, common unified rules for structures in seismic regions, Report EUR 8850 for the Commission of the European Communities, DGIII, Bruxelles, Belgium.
- [2] AA.VV., 1989: Proceedings of Workshop on Structural Behaviour of Timber Constructions in Seismic Zones, Firenze, Italy.
- [3] A.Ceccotti & H.J.Larsen, 1989: Background document for Chapter 5 of Eurocode 8, part 1, may 1988, "Specific Rules for Timber structures", Report 8076 for the Commission of the European Communities, DGIII, Bruxelles, Belgium.
- [4] A.Ceccotti & A. Vignoli, 1990: Engineered Timber Structures. An Evaluation of Their Seismic Behaviour, Proceedings of 1990 International Timber Engineering Conference, Tokio, Japan.
- [5] A.J.M.Leijten, 1987: Standard short duration tests on locally reinforced moment joints with dowels and bolts, Delft University of Technology, reports 26-33-34-35-36, Delft, The Netherlands.
- [6] G.Di Gangi, 1990: Studio del comportamento sismico di portali di legno lamellare: simulazioni numeriche e messa a punto del metodo di prova pseudo-dinamica, tesi di laurea, Department of Civil Engineering, University of Florence, Italy.
- [7] A.Ceccotti & A.Vignoli, 1989: A hysteretic behavioural model for semi-rigid joints, European Earthquake Engineering n.3/89, Bologna, Italy.

Acknowledgments

We gratefully acknowledge the help of our former student Giuseppe di Gangi who performed the actual calculations.
This research was granted by Italian Ministry of Education.

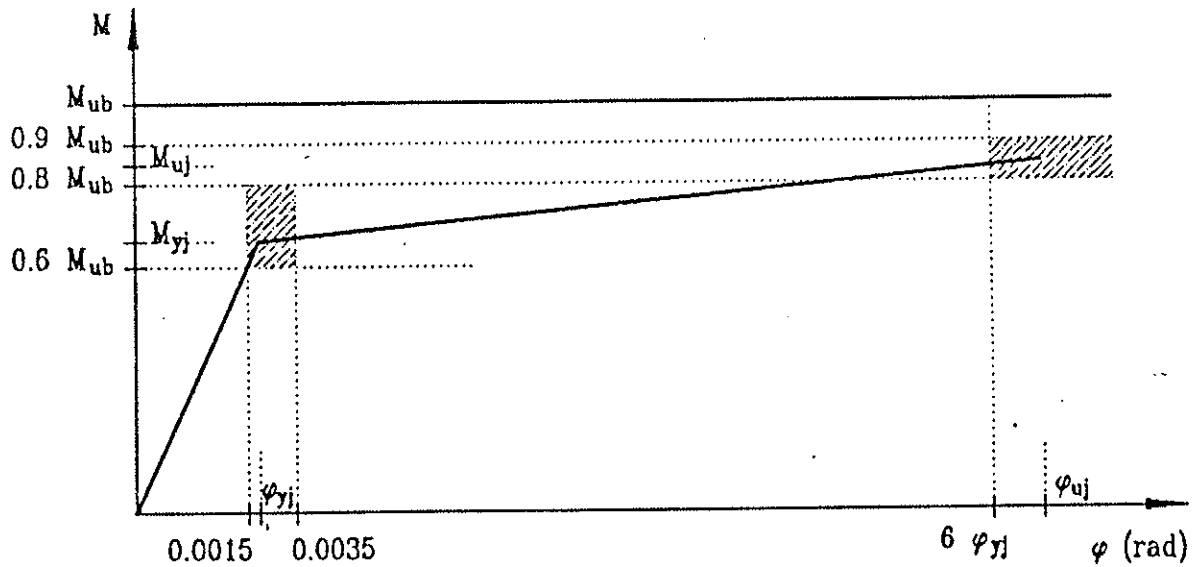


Fig. 1 - Example of numerical guidelines for a well calibrated design in seismic zones [4].

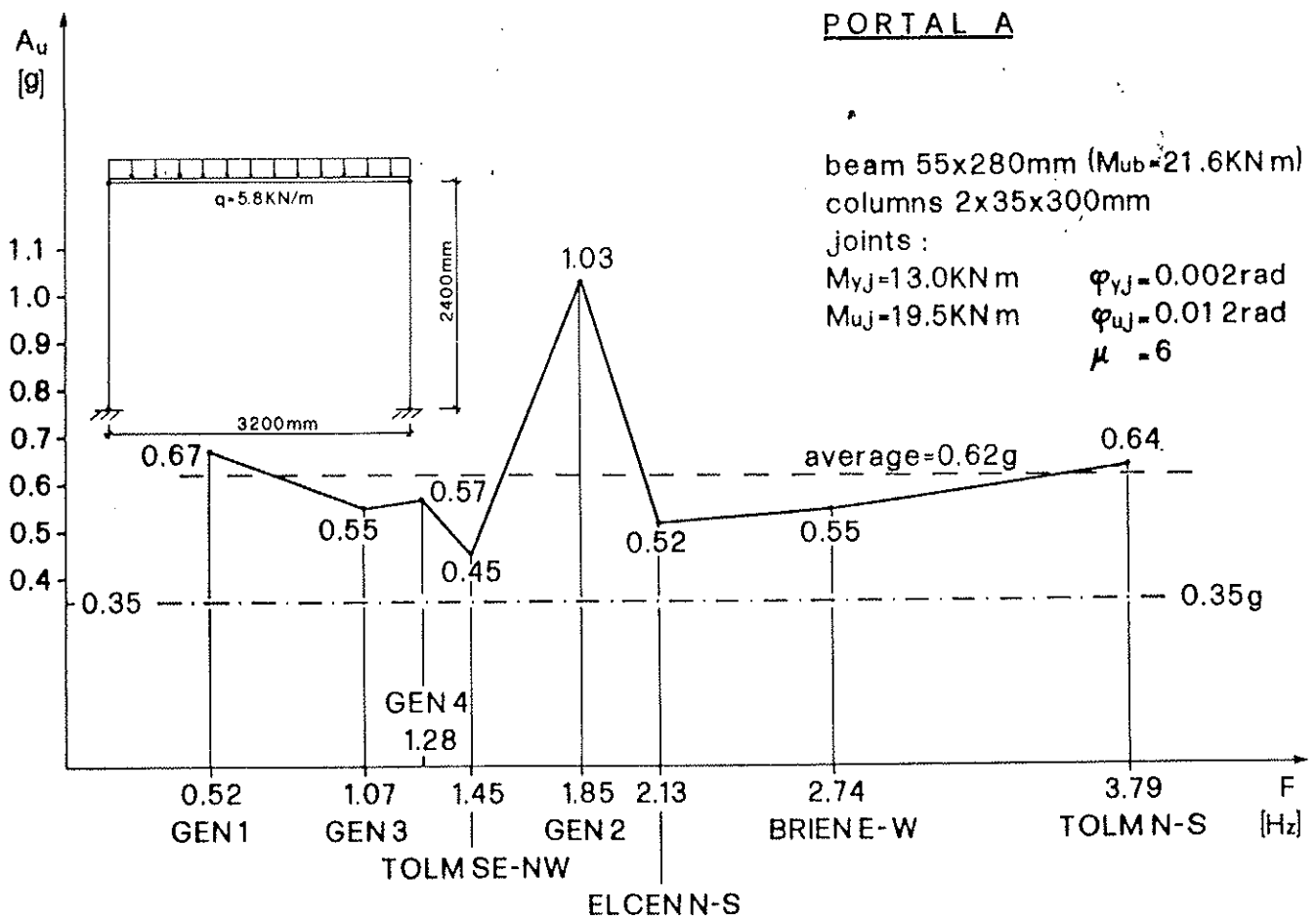


Fig. 2

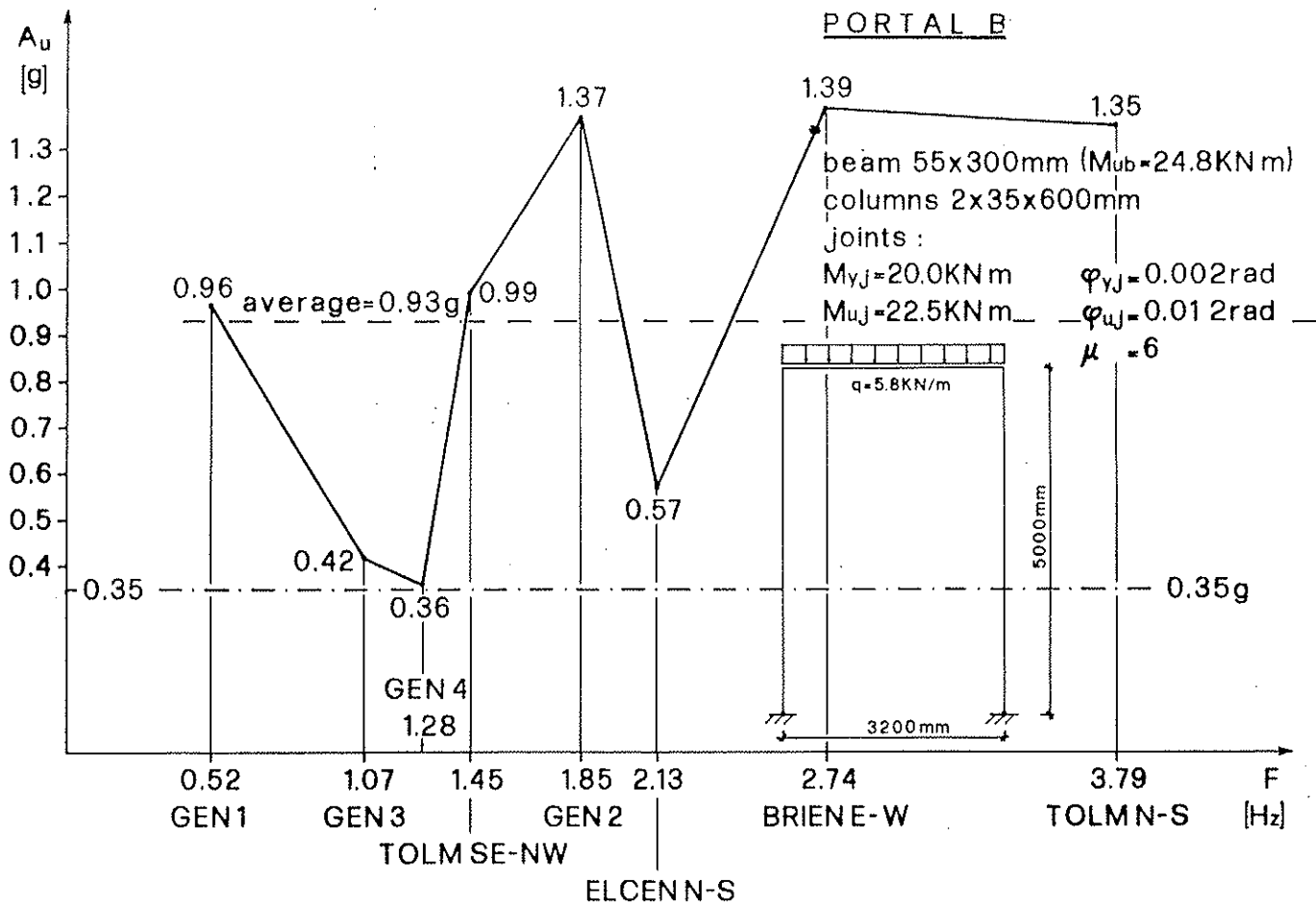


Fig. 3

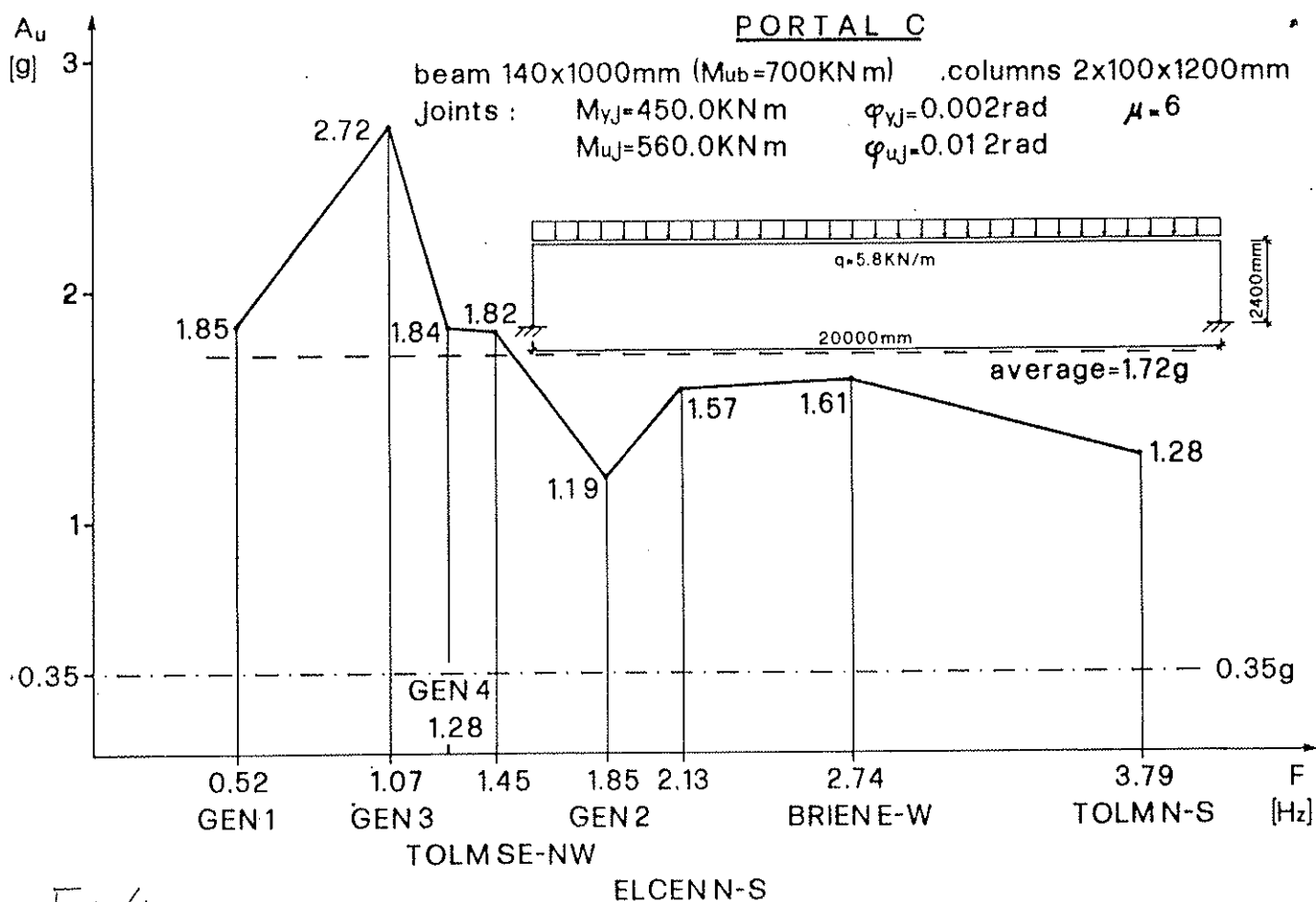


Fig. 4

INTERNATIONAL COUNCIL FOR BUILDING RESEARCH STUDIES AND DOCUMENTATION

WORKING COMMISSION W18A - TIMBER STRUCTURES

DISPROPORTIONATE COLLAPSE OF TIMBER STRUCTURES

by

C J Mettem

J P Marcroft

Timber Research and Development Association

United Kingdom

MEETING TWENTY - THREE

LISBON

PORTUGAL

SEPTEMBER 1990

Abstract

Regulations and Codes of Practice are placing increasing emphasis on structures being planned and designed so that they are not unreasonably susceptible to the effects of accidents. The UK Building Regulations contain one such requirement entitled 'disproportionate collapse' which is applicable to two building categories. Only one of these is of relevance to UK timber building manufacturers, and it covers 'single storey public buildings having a clear span exceeding nine metres.'

This paper describes, with reference to a specific form of roof construction, the differing ways in which the 'disproportionate collapse' requirement has been interpreted. It gives the authors' preferred interpretation and outlines a procedure which designers can follow to satisfy the preferred interpretation of the requirement. The specific form of roof construction considered covers non-load-sharing parallel primary frameworks supported at wallplate level, and supporting single-span secondary construction.

1.0 Regulations

Regulations and Codes of Practice are placing increasing emphasis on structures being planned and designed so that they are not unreasonably susceptible to the effects of accidents. The current UK Building Regulations contain a requirement entitled "Disproportionate Collapse", shown in Table 1, which is applicable to two categories of building.

Requirement	Limits on application
Disproportionate collapse A3. The building shall be so constructed that in the event of an accident the structure will not be damaged to an extent disproportionate to the cause of the damage.	This requirement applies only to-- (a) a building having five or more storeys (each basement level being counted as one storey); and *(b) a public building the structure of which incorporates a clear span exceeding nine metres between supports.

Table 1. A3 requirement 'Disproportionate Collapse' for The Building Regulations, 1985, England and Wales (* a revision presently being proposed restricts category (b) further to single-storey or the top storey of buildings.)

Mechanical resistance and stability The construction works must be designed and built in such a way that the loadings that are liable to act on it during its construction and use will not lead to any of the following: (a) collapse of the whole or part of the work; (b) major deformations to an inadmissible degree; (c) damage to other parts of the works or to fittings or installed equipment as a result of major deformation of the load-bearing construction; (d) damage by an event to an extent disproportionate to the original cause.
--

Table 2. Essential Requirement 1 of the Construction Products Directive

Furthermore the Construction Products Directive, which at some stage in the 1990's will supersede the National Building Regulations of the European Community member states, contains in its essential requirements a specific reference to disproportionate collapse. Essential requirement no. 1 entitled 'Mechanical resistance and stability' is given in Table 2 and it can be seen that its part (d) contains in essence the same requirement as that of the UK Building Regulations. No limitation is placed on the building categories to which it is applicable.

As already mentioned, the 'disproportionate collapse' requirement in the UK is only applicable to two building categories. However for the timber industry this effectively reduces to one category as the first category 'buildings containing more than five storeys' is precluded by fire constraints from using timber as the main structural material. The second category 'public single-storey buildings containing a clear span exceeding nine metres' is, however, a building category for which the use of timber is being actively promoted and the research work at TRADA has concentrated on this area. This paper is even more specific, discussing the topic in relation to the economically important hybrid structures where the parallel non-load-sharing primary members are supported at wallplate level (usually on masonry walls) and provide support to single-span secondary construction.

2.0 Interpretation of the Requirements of the Regulations

There is some confusion amongst practitioners as to how to implement the 'disproportionate collapse' requirement of the UK Building Regulations in respect of public single-storey buildings having a clear span exceeding nine metres and it has been interpreted in a number of different ways. However before considering the differences in the interpretations their common ground will be discussed.

The four most commonly-cited accidental events are gas explosion, vehicle impact, tree impact and sabotage. The only magnitude for accidental loading accepted by the Regulatory Bodies in the UK is 34 kN/m². This is because while it is widely accepted that this magnitude of accidental loading is only appropriate for storeys towards the base of a multi-storey building there is an absence of data regarding the magnitude of accidental loadings appertaining to single-storey buildings. As designing single-storey buildings to resist 34 kN/m² is not a realistic option, the approach adopted assumes local failure at appropriate locations within the structure.

Another area of common ground is in respect of the stability of the areas of building to either side of the damaged zone. It is generally agreed that no area of building should be isolated from the building's bracing system by an accidental event. This is discussed further in section 3.0.

The area where the 'disproportionate collapse' requirement is interpreted in differing ways relates to the permissible extent of damage. There are two prevalent views in the United Kingdom and these are best illustrated by use of an example. Consider a roof structure comprising a series of parallel non-load-sharing primary frameworks supported on masonry walls:

Interpretation 1. In the event of the removal of a section of one support wall from under a single primary framework the secondary construction is expected, with an overstress, to transfer the loads of the failed primary framework to the adjacent intact primary frameworks. No part of the roof construction falls to the ground.

Interpretation 2. In the event of the removal of a section of one support wall from under a single primary framework, the failed primary framework and the secondary construction which it was previously supporting are allowed to fall to the ground provided that the area of damage does not extend beyond the primary frameworks on either side of the failed primary framework.

As one would expect, the two interpretations have significantly different effects on the roof's design. The implications of each interpretation are considered in turn below.

Implications of Interpretation 1.

1. Single-span secondary construction, even with strengthened end connections, almost invariably cannot support the loads of the failed primary frame. Interpretation 1 leads the designer towards specifying double-span secondary construction.
2. The requirement to design double-span secondary construction to resist the loads of a failed primary frame at an overstress results in an increase in section size for the secondary construction over that required by normal design for all except the lightest of roof claddings.
3. For double-span secondary construction the failed primary frame tends to 'peel away' from the secondary construction at locations close to the point of failure (removed wall for example). Again only the secondary construction end connections associated with lightweight roof claddings, where there is a wind uplift criterion, tend to have sufficient withdrawal capacity to resist this. Hence interpretation 1 can require significant strengthening of the secondary construction end connections.
4. The primary frames adjacent to the failed primary frame are required to support additional loads from the failed primary frame at an overstress. However usually no increase in section size over that required by normal design considerations is necessary.
5. The design of the roof and side bracing are not affected.

Implications of Interpretation 2.

1. Single-span or double-span secondary construction can be used with no implication on section size in either case.
2. No changes need to be made to the secondary construction end connections.
3. There is no implication for the section size of the primary frames.

4. For certain types of secondary construction, depending on the magnitude of the wind (or other applicable horizontal) loading on the bracing system, there may be a requirement to strengthen the roof and/or side bracing.

Conclusion from comparison. The authors are of the opinion that in the UK the incidence of reported events of accidental loadings on single-storey structures incorporating a clear span exceeding nine metres has not been such as to justify the application of the more rigorous interpretation 1. Hence interpretation 2 represents a more appropriate course of action. A procedure for ensuring that the requirements of interpretation 2 are met is presented after a brief discussion on the placement of bracing systems for parallel-framed structures.

3.0 Placement of Bracing Systems in Parallel-framed Structures

The view has already been stated that the planning and design of the bracing system to a building should be such that no part of the building is isolated from the bracing system by the damaged zone resulting from an accidental event.

For parallel-framed structures the worst scenario is a single braced bay in the middle of the building. This is because should an accidental event cause failure of one of the primary frames forming part of the roof bracing, then even assuming that the remaining primary frames are not dragged down by the failed primary frame, the two parts of the building still standing only have the cladding to rely upon for their stability against wind and other forms of horizontal load.

It is hence desirable that even parallel-framed structures comprising a small number of primary frames should have a minimum of two braced bays and that these are normally best located in the end bays of the building. Many organisations, of course, already follow this practice.

Many parallel-framed structures rely on diaphragms extending the full length of the building to brace the structure against lateral forces. Clearly these types of structure can readily ensure that the parts of the building on either side of the damaged zone retain adequate stability.

4.0 Outline of Procedure to Ensure Avoidance of Disproportionate Collapse for Certain Types of Parallel-framed Structures

4.1 Scope

This procedure is only applicable to roof structures where parallel non-load-sharing primary frames are supported at wallplate level and provide support to single-span secondary members.

The procedure is aimed at satisfying the already-described interpretation 2 of the 'disproportionate collapse' requirement.

4.2 Basis of Procedure

The following discussion makes reference to the four-bay building shown in Figures 1a-1d. To establish the basis for the procedure let us consider how loads acting on primary frame III are redistributed following the failure of primary frame III.

1. The loads acting on primary frame III are transferred to the adjoining secondary members by the connection between the secondary members and primary frame III.
2. The secondary members acting in the three-pin tie system shown in Figure 1d transfer the loads to the secondary member-primary frame connections at primary frames II and IV.
3. The secondary member-primary frame connections at frames II and IV transfer these loads into primary frames II and IV.
4. Primary frames II and IV act as chord members to the roof bracings at each end of the building which transfer the loads to the side bracings.
5. The loads from primary frame III are transferred to the foundations by the side bracings.

For single-span secondary members it is known that the failed primary frame III will almost invariably fall to the ground. If the failure occurs in steps 1-3 of the above load path the collapse is considered to be in due proportion to the cause. On the other hand if the failure occurs in steps 4-5 then the entire building may collapse and the collapse would be considered disproportionate. As in reality the tensile capacity of the secondary members is always greater than that of its end connections, whether the collapse is disproportionate depends on whether the secondary member end connections can resist sufficiently large tensile forces to cause failure of the roof or side bracing. Hence the basis of the procedure to make certain that collapse is not disproportionate is to ensure that the roof and side bracing can resist the most onerous horizontal load diagram that can be developed by the secondary member-primary frame connections in the failed bays.

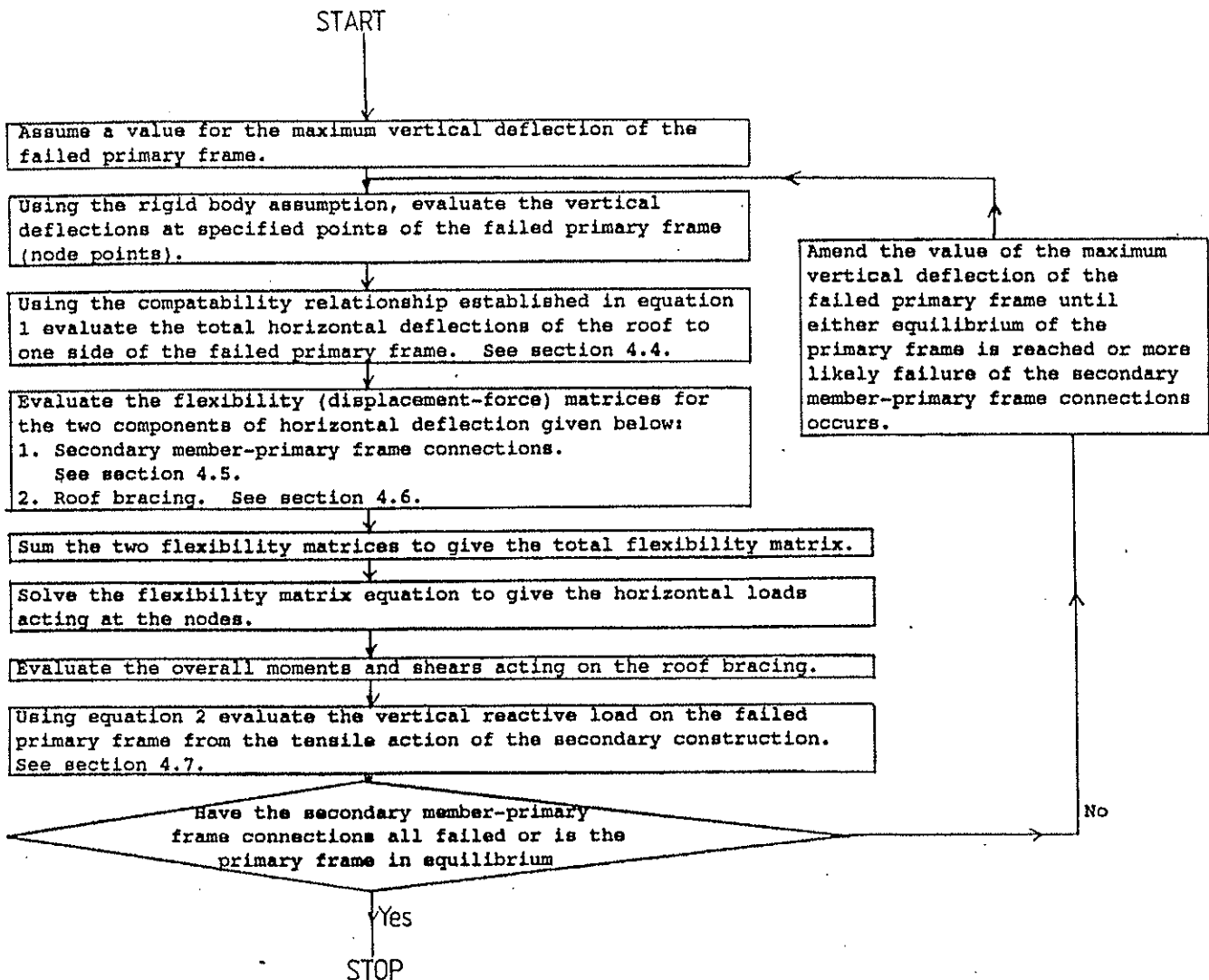
4.3 Summary of Method

In deciding how to analyse the effects of the failed primary frame two factors become apparent.

1. Loads. Prior to the accident the dead and imposed loading on primary frame III is in equilibrium with the reactive loads provided by the support walls. After the accident, although the dead and imposed loading on the now-failed primary frame III remains unchanged, the reactive loads provided by the secondary construction almost invariably cannot attain sufficient magnitude to put the primary frame in equilibrium and the primary frame collapses to the ground. Consequently the external force system acting on primary frame III is not fully known and the conventional route of knowing the external forces together with the stiffness (force-displacement) matrix for the member to determine the deformations and then internal forces cannot readily be used.

2. Deflection. Although there are no fixed values of vertical deflection for the failed primary frame, for any point of the failed primary frame the range of vertical deflections through which it passes during its collapse to the ground is known. More importantly a satisfactory assumption can be made about the relationship between the vertical deflections at different points in the failed beam. This assumption is simply that the primary frame falls as a rigid body and is valid because when the loads on the secondary member-primary frame connections are close to their ultimate values the overall downward movements of the primary frame far exceed any differential movements (due to flexural behaviour of the primary frame) within the primary frame.

This assumption enables the roof's behaviour to be approximated using the outline procedure given in Figure 2.



4.4 Geometric Compatibility of Deformations

At any secondary member location along the failed primary frame a relationship can be established between the vertical downward movement of the failed primary frame and the total horizontal movement in the roof to one side of the failed primary frame using equation 1.

4.5 Flexibility Matrix for Secondary Member-Primary Frame Connections

Typical load-slip curves for a nailed and bolted end connection are shown by the dashed lines in figures 3a and 3b. However the terms in the flexibility matrix reflect the modelling of the load-slip curves by the two solid straight lines of figure 3a and 3b. The load-slip behaviour of all the secondary member end connections along a primary frame have assumed mean densities for the secondary member and primary frame.

In an analysis of any given failure mode for a primary frame the analysis has been continued past the point at which the first secondary member-primary frame connection fails and in many cases it has been found that the most onerous loads are exerted on the roof bracing when a number of secondary member-primary frame connections have failed.

4.6 Flexibility Matrix for the Roof Bracing

The Uncertainties Involved in Determining the Deflected Shapes of Roof Bracings. For any given form of roof bracing there are a great many uncertainties involved in determining its deflected shape under a given load diagram. Four of the more significant uncertainties are listed below:

1. Even for the simplest of connections there are uncertainties regarding load-slip characteristics. For many bracing connections the total movement is made up of a number of smaller components each of which is subject to some uncertainty.
2. It is uncertain how much of the primary frame contributes structurally to the axial rigidity of the chord members of the wind girder? For example for a wind girder connected to the top chords of trusses how much does the remainder of the truss enhance the axial rigidity of its top chord?
3. Under wind loading the gable posts transfer loads to the node points of a wind girder. On the other hand following failure of a primary frame it is likely that the secondary members will cause flexural deformations between the node points.
4. Plate action of the roof cladding reduces the deflections of the bracing, but this is difficult to quantify.

The Approach Taken in Modelling the Roof Bracing. It is doubtful whether some of the aforementioned uncertainties could be resolved with even the most sophisticated of analyses. In view of this the approach taken is as follows:

1. Approximate the roof bracing to a massive horizontal beam of flexural rigidity (Young's modulus* $Moment of Inertia$), EI .

2. Assign 'best estimate', upper bound and lower bound values to EI, such that the actual deformed shape of the roof bracing under a given load diagram falls at all points along its length between the deformed shapes appertaining to the lower bound and upper bound values of EI as shown in Figure 4.
3. It is known that following the failure of a primary frame, a series of point loads will be applied to the roof bracing at the secondary member locations. Considering a point load from a single secondary member, as shown in Figure 5, equations 3a-3c extracted from (1) can be used to determine the component of deflection from any given secondary member at all the remaining secondary member locations along the primary frame. The roof bracing flexibility matrix can be determined on this basis.

4.7 Relationship between Reactive Forces in Three-pin Tie System of Failed Bay

The effective vertical reaction from any given line of secondary members on the failed primary frame can be evaluated using equation 2 once the horizontal reactions on the nearest intact primary frames from the same line of secondary members have been determined.

4.8 Application of the Procedure

Before the iterative procedure of the flow chart in section 4.3 can be embarked upon, the analyst must resolve the following:

1. Upper bound, lower bound and 'best estimate' values of the roof bracing's flexural rigidity.
2. Decision regarding the failure modes. In the case cited in this paper, it was considered that only two failure modes needed to be analysed:

Failure Mode 1. Removal of one support wall (maximizing the overall shears acting on the roof bracing).

Failure Mode 2. Localized but absolute failure at midspan of a primary frame (maximizing the overall moments acting on the roof bracing).

Thus the procedures of the flow chart in section 4.3 have to be followed six times to cover the permutations of primary frame failure mode and roof bracing flexural rigidity. From these analyses, it is possible to produce envelopes of the horizontal loads, overall shear forces and overall bending moments acting on the roof bracing.

The analyst is now in a position to check the bracing design produced for normal design considerations against the requirements for accidental load considerations. The checks for accidental load cases will invoke considerably different load factors and material modification factors, dependent upon the exact nature of the Code of Practice being followed.

5.0 Simplification of Procedure

5.1 Method of Simplification

Although the procedure outlined in section 4.0 only involves basic structural mechanics, it is felt to be too time-consuming to be suggested as a routine to be followed by most design engineers. It is considered that it might be more acceptable if it were recommended that designers take account of the loads due to a failed primary frame by applying simple horizontal loads, taken from diagrams. The procedure would be similar to designing against wind loads.

5.2 Derivation of Horizontal Load Diagrams for Roof Bracing

To derive the horizontal load diagrams described in section 5.3, the procedure of section 4.0 was applied with the following range of parameters:

1. Various primary frame spans between 9 and 24 m.
2. The two failure modes described in section 4.8.
3. A range of nailed and bolted secondary member-primary frame connections.
4. Using the 'best estimate', upper bound and lower bound flexural rigidities for the roof bracing below:
 - Upper bound . . . EI value equivalent to a midspan deflection of $0.0002 \times$ Primary frame span under a horizontal load of 4 kN/m.
 - Best estimate . . . EI value equivalent to a midspan deflection of $0.001 \times$ Primary frame span under a horizontal load of 2 kN/m.
 - Lower bound . . . EI value equivalent to a midspan deflection of $0.005 \times$ Primary frame span under a horizontal load of 0.5 kN/m.

The effects of varying the flexural rigidity of the roof bracing for all of the primary frame spans and secondary member-primary frame connections investigated followed the trends given in figures 6a and 6b for failure modes 1 and 2 respectively. The greater horizontal loads on the roof bracing in the direction of the failed primary frame (secondary construction in tension) occurred for the stiffer roof bracing systems. However horizontal loads on the roof bracing in the opposite direction to the failed primary frame (secondary construction in compression) could occur over part of the roof bracing system, for less-stiff roof bracings. These could reverse the sign of the overall moment acting at some points on the roof bracing. The magnitude of these particular moments increased with decreasing roof bracing flexural rigidity.

5.3 Horizontal Load Diagrams to be Applied to Roof Bracing for Accidental Events

To cater for the effects of a failed primary frame, it is recommended that the following two load cases are applied to the roof bracing with an important proviso concerning the overall shear force.

H_p = Mean ultimate load capacity
of secondary member-primary
frame connection

Load Case 1. A uniform horizontal load acting in a direction towards the failed primary frame, of intensity (units- force/length) h_1 where

$$h_1 = \frac{0.7 \times H_p}{\text{Secondary member spacing}}$$

Load Case 2. A uniform horizontal load acting in a direction away from the failed primary frame, of intensity (units- force/length) h_2 where

$$h_2 = \frac{0.45 \times H_p}{\text{Secondary member spacing}}$$

For both load cases 1 and 2, the overall shear force acting on the roof bracing between the quarter-span points is to be taken as the overall shear forces acting at the quarter-span points.

As has already been mentioned, the checks on the bracing system for these two load cases will be carried out using considerably different load factors and material modification factors, from those applied under normal design conditions, dependent upon the exact nature of the Code of Practice being followed.

6.0 Summary

In order to ensure the avoidance of disproportionate collapse for parallel-framed structures, two tasks should be brought to the attention of the designer:

1. In the event that accidental loading causes local failure in a primary frame, he should be required to ensure that the adjacent primary frames are not dragged down by the failed primary frame.
2. His attention should be drawn to the necessity to ensure that the undamaged areas on either side of the damaged zone retain sufficient stability to be able to withstand appropriate wind and other horizontal loads.

Both steps require that bracing is placed in a minimum of two bays, and that normally the bracing is best placed in the two end bays of the building. Step 1 could be satisfied for roof structures incorporating parallel primary frames supported at wallplate level and supporting single-span secondary members using the procedure given in section 5.3.

References

1. Kleinlogel, A. and Lorsch, H.G., Beam formulas. Crosby Lockwood & Son Ltd. 1953.

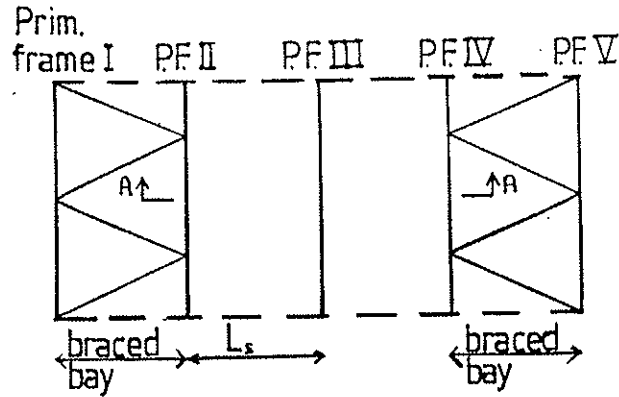


Figure 1a - Plan of four-bay building prior to accident

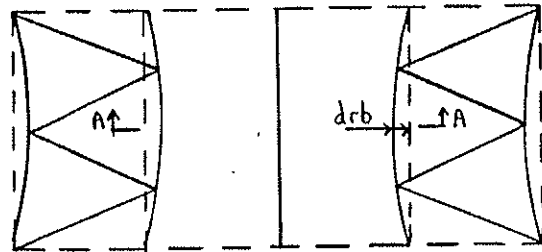


Figure 1b - Plan of roof after failure of primary frame III

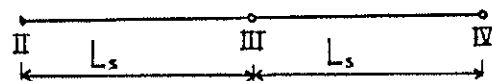


Figure 1c - Elevation A-A prior to accident



Figure 1d - Elevation A-A after accident

Geometric Compatibility

$$(L_s - drb)^2 + (dV)^2 = (L_s + s)^2$$

$$(dV)^2 = 2L_s(drb + s) + s^2 - (drb)^2$$

As $L_s \gg s$ and $L_s \gg drb$

and if $dh = s + drb$

$$dh = \frac{(dV)^2}{2L_s} \dots \dots \dots \text{EQUATION 1}$$

Note - s = slip in secondary member - prim. frame connections of one secondary member

Relationship between reactive forces

By resolving vertically and taking moments about the central pin,

$$W = \frac{2H_l(dV)}{L_s - drb} \dots \dots \dots \text{EQUATION 2}$$

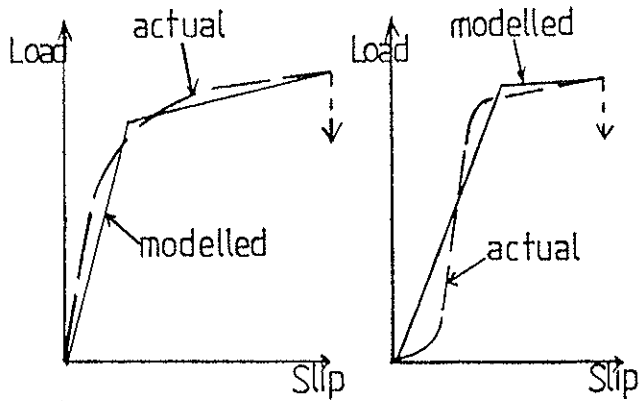


Fig. 3a - Typical Nailed Connection

Fig. 3b - Typical Bolted Connection

Figure 3 - Modelling of load-slip behaviour of secondary member-primary frame connections

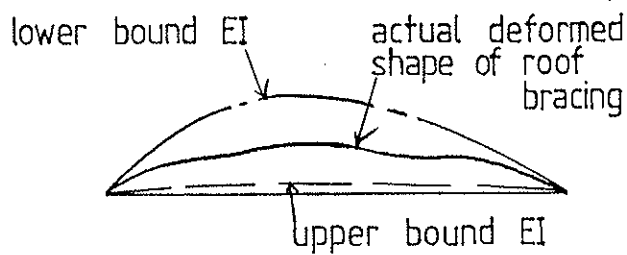


Figure 4

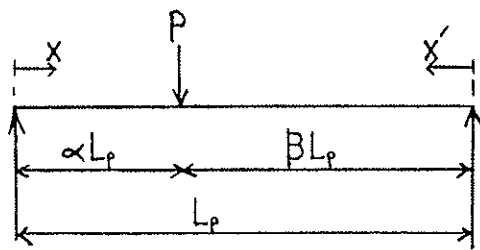


Figure 5

EQUATIONS 3a - 3c below:

$$\text{Deflection to l.h.s. of point load at } x \text{ from l.h.s. support} = \frac{P L_p^3 B}{6EI} \left[(1 - \beta^2) \left(\frac{x}{L_p} \right) - \left(\frac{x}{L_p} \right)^3 \right]$$

$$\text{Deflection under point load} = \frac{P L_p^3 \alpha^2 \beta^2}{3EI}$$

$$\text{Deflection to r.h.s. of point load at } x' \text{ from r.h.s. support} = \frac{P L_p^3 \alpha}{6EI} \left[(1 - \alpha^2) \frac{x'}{L_p} - \left(\frac{x'}{L_p} \right)^3 \right]$$

Key to figures 6a & 6b

- upper bound roof bracing flexural rigidity
- - - - - best estimate of roof bracing flexural rigidity
- · — · — lower bound roof bracing flexural rigidity

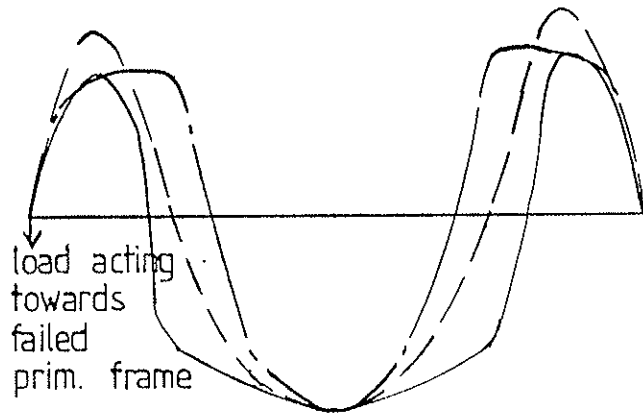


Figure 6b - Absolute but localised of primary frame at midspan

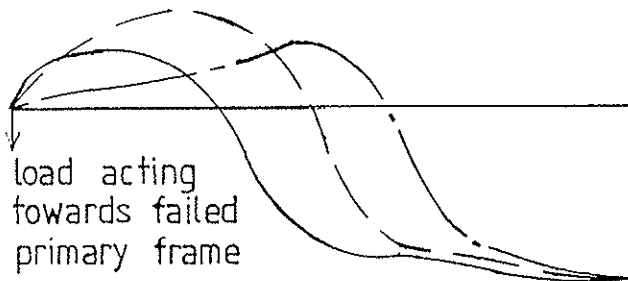


Figure 6a - Failure of primary frame by removal of one support wall

Figure 6 - Effect of differing roof bracing flexural rigidities on the horizontal load diagrams acting on the roof bracing when the most heavily secondary member-primary frame connection is just below its ultimate load

INTERNATIONAL COUNCIL FOR BUILDING RESEARCH STUDIES AND DOCUMENTATION

WORKING COMMISSION W18A - TIMBER STRUCTURES

PERFORMANCE OF TIMBER FRAME STRUCTURES DURING

THE LOMA PRIETA CALIFORNIA EARTHQUAKE

by

M R O'Halloran

E G Elias

American Plywood Association

United States of America

MEETING TWENTY - THREE

LISBON

PORTUGAL

SEPTEMBER 1990

PERFORMANCE OF TIMBER FRAME STRUCTURES DURING
THE LOMA PRIETA, CALIFORNIA EARTHQUAKE
17 OCTOBER 1989

by M. R. O'Halloran, E. G. Elias⁽¹⁾

CIB STRUCTURAL TIMBER DESIGN CODE

The CIB Timber Code (5) provides for the development of design procedures for timber components and special structures. Section 7.4 is intended to provide specific provisions for the development of bracing requirements. Currently, the draft code does not contain references to either standard methods of test, sampling, or analysis of test data reporting wall bracing or diaphragm action.

OBJECTIVE

The purpose of this paper is to present a review of the structural performance of timber frame buildings following the 1989 Loma Prieta earthquake. Results of this inspection reinforces the need for standardization in design of timber frame structures to resist seismic loading.

BACKGROUND

The behavior of timber structures in seismic zones has been the topic of several previous CIB papers on structural stability. The design of small wood-framed houses to resist seismic loading was first discussed by Hansen in 1984 (7). Hansen described the role of walls and partitions in withstanding the effects of seismic activity and the appropriateness of timber frame construction for this application. The approach to analyzing the response of timber frame components to seismic activity has been varied.

Theoretical evaluations of connections and plane timber structures comprised of rigid and semi-rigid joints has been investigated by Ceccotti and Vignoli (2, 3, 4). In 1986, Yasamura described tests on racking resistance of wood-framed walls with openings (13). Experimental test results on non-symmetric panel constructions were examined with a mathematical model. The model accounted for a non-linear load-slip relationship for the nailed joints.

⁽¹⁾ This paper includes information provided in APA Report T89-28 by W. A. Baker, D. H. Brown, and J. R. Tissell as a result of their inspection trip.

Meanwhile in the United States, Tissell was evaluating the performance of plywood shear walls and diaphragms with varying sized openings (9, 11). A plane-frame structural analysis program was employed to analyze the glue-nail constructions. Engineering theory utilizing design values for lateral fastener loads and plywood shear capacities was used to mathematically compute allowable load values for seismic design. And finally, in 1986, Hiroshima described non-destructive vibrational tests run on two-story timber frame buildings (8).

The CEN technical committee TC-124 Timber Structures is currently drafting a test method whose objective is to establish design values for the racking properties of wood-based panels (9). The test method described is similar to the United States ASTM E72 *Standard Methods of Conducting Strength Tests of Panels for Building Construction* (1). ASTM E72 is the primary test method used in the United States to evaluate shear-resisting building components under lateral racking loads. The American Plywood Association has used this method for close to 40 years to evaluate structural panel sheathing. Tissell has recently reported test results utilizing ASTM E72 supporting design information on unblocked shear walls, stapled shear walls, sheathing over metal framing, double-sided walls, plywood over gypsum sheathing and the effects of stud spacings and width (12). Over 494 tests are summarized in this 1990 report. Results of the ASTM E72 tests have formed the basis for allowable shears for structural panels provided in the United States Uniform Building Code (UBC) as well as other U.S. model codes. The UBC is used in the Western United States, including Loma Prieta, California. Structural panel walls and decks constructed in accordance with code provisions based on ASTM E72 tests performed very well during this earthquake.

INSPECTION REPORT

In the late afternoon of October 17, 1989 a strong earthquake was felt throughout the San Francisco/Oakland Bay area (population: 5.9 million). The earthquake, subsequently known as the Loma Prieta Earthquake, registered 7.1 on the Richter scale. Much publicity was given to the collapse of a section of the double-decked Nimitz freeway in Oakland where the majority of fatalities occurred, and to the Marina district in San Francisco where a number of outdated residential buildings were destroyed, either by the earthquake or by the ensuing fire resulting from broken gas lines.

Other areas reporting heavy damage were Santa Cruz County, location of the earthquake's epicenter, and the town of Los Gatos, near the Santa Cruz Mountains. Farther north on the San Francisco peninsula, several homes in the Los Altos Hills area received heavy damage.

Despite the magnitude of the quake, the loss to human life and property was minimal compared to earthquakes worldwide in the past twenty years. Table 1 presents a record of recent major earthquakes and their associated death tolls. Timber frame construction designed to resist seismic activity accounted in part for the minimal damage and loss of life in the San Francisco Bay area.

Table 1. Major International Earthquakes (6)

Year	Location	Magnitude	Loss of Life
1990	Iran	7.3	40,000 (est)
1989	Loma Prieta, CA, USA	7.1	63
1988	Armenia	6.9	25,000
1985	Mexico City	8.1	10,000
1978	Iran	7.7	25,000
1976	Tangshon, China	8.2	800,000
1976	Guatemala	7.5	23,000
1971	Sylmar, San Fernando Valley, CA, USA	6.4	<10
1970	Peru	7.7	66,800
1971	Anchorage, AK, USA	8.4	<10

On October 23, a team of three engineers from the Technical Services Division of the American Plywood Association (APA) traveled to the San Francisco Bay area to observe the effects of the earthquake on wood construction. The primary objective was to determine if deficiencies may exist in U.S. building codes published subsequent to the Sylmar quake in the San Fernando Valley of California in 1971. The Sylmar earthquake resulted in several building code changes designed to strengthen buildings against severe lateral forces.

The team discovered in short order that damage was quite widely scattered. Vast areas between the highly publicized damage zones appeared to have little or no structural damage from the earthquake. Team investigations, therefore, concentrated in the local areas of damage mentioned above.

Conventional Wood-Framed Buildings

The epicenter of the earthquake was located in the Santa Cruz Mountains near the Loma Prieta school. The quake opened up several ground fissures of considerable length. The fissures necessitated pavement repairs in several places where they crossed the road. In this area, primarily populated with wood-frame residences, the extremes of no apparent structural damage whatsoever to complete destruction were observed. Even in areas where damage was high, many wood-frame "success stories" were encountered. The house pictured in Figure 1 appeared to sustain no structural damage other than the collapse of the masonry chimney. The house was two stories with a sloping lot and wood-framed daylight basement to the rear and

was sided with plywood panels which acted as bracing. It was located approximately 100 feet (30 m) from a ground fissure, and undoubtedly was shaken rather severely. In fact, it was located about 600 feet (183 m) from a house that was completely destroyed in the earthquake (house shown in Figure 5).

Dennis J. McCreary, staff engineer with the International Conference of Building Officials, promulgators of the Uniform Building Code (UBC), visited Santa Cruz County shortly following the earthquake. He observed, "It appeared that where there were failures in wood-frame buildings, they were due to inadequate connections, or lack of structural continuity in design."

Cripple Walls

"Cripple" or "pony" walls appeared to have been the source of failure in a number of damaged homes. Cripple walls are typically stud walls which spring from the foundation to the first floor framing. They are often used on stepped foundations in buildings built on sloping sites and are usually short, but can be as much as full story height. When cripple walls have a stud height exceeding 14 inches (360 mm), the Uniform Building Code requires that they be considered first-story walls for the purpose of determining the bracing required. The code also requires that cripple walls exceeding 14 inches (360 mm) shall be framed with studs not less in size than that of the studding above and, when they exceed 4 feet (1200 mm) in height, cripple walls shall be framed of studs having the size required for an additional story. These requirements clearly indicate that such walls are required to provide resistance to lateral forces, and are not merely skirting.

Several instances were observed where houses had been moved laterally off their foundations. In every case of this type which was observed, the cripple walls were laying flat on their sides as shown in Figure 2. Although these walls were typically sheathed or sided with plywood panels, nailing was typically much sparser than required by the code. Thus, the panels themselves could not provide sufficient lateral resistance to prevent racking of the cripple walls. No instance was observed where a cripple wall collapsed which was nailed in accordance with code requirements.

Homes Constructed Prior to 1970

In an older section of Los Gatos, many houses were observed that had slipped laterally off their foundations. The age of these houses would indicate that they were board sheathed and the foundations appeared to be unreinforced masonry. Due to the age of the houses, and that they were obviously constructed before modern building codes, no detailed inspections were made by the team.

In the same area, the house shown in Figure 3 was seen. Even though it has a double garage in the ground floor, it appeared undamaged. This house appeared to be built under recent building codes.

Major Framing Connections

Two of the badly damaged houses that were examined showed very little connection between the major floor framing members and the foundation. While both of these houses had stepped foundations, each had one side where the floor framing bore directly upon the sill plate which was well bolted to the concrete foundation.

In the rectangular house where the nominal 2-inch (38 mm) floor joists were on the sill plate, there was no evidence of fasteners between the joists and the plate. The Uniform Building Code requires three 8-penny nails per joist for this connection. The perimeter band joist was nailed to each joist; however, the band joist was fastened to the sill plate with toe nails approximately 4 feet on center.

The second house was octagonal in shape, and the floor was framed with nominal 4-inch-wide (89 mm) beams (see Figure 4). A careful examination of the sill plate showed at the most only one toe nail connecting the floor joists to the sill plate.

Again, the floor framing members were nailed to the perimeter band joist and, in this case, the perimeter band joist was anchored to the foundation using hold-down anchors with lag screws into the band joist. The earthquake movement was such that the lag screws failed in withdrawal from the band joist.

Construction in the Marina District

The portion of San Francisco known as the Marina district is an area where the rubble from the 1906 earthquake was dumped and then subsequently filled with sand dredged from the bay. During the 1989 earthquake the fine sand liquified and, in many cases, flowed up through cracks in the road or sidewalk. In other instances, the sidewalks were badly distorted by pressure from the sand.

The typical building in this area is a four-story apartment consisting of three floors above ground floor garages. Around the most badly damaged buildings, inspection was by observations possible from outside the police barricades.

The large number of garage door openings on the ground floor of these buildings resulted in only a very small length of exterior wall for racking resistance. These walls were typically concealed by masonry veneer; however, in many instances, the masonry had fallen away exposing the sheathing. The sheathing was typically horizontal boards and in the one building where the sheathing had fallen off with the masonry, there was cut-in 2 x 4 diagonal bracing. The few interior partitions that were visible in the garages were sheathed with gypsum wallboard.

While several of these apartment buildings did collapse, many more showed evidence only of distortion at the first floor. Figure 5 shows one of these buildings. House movers were already at work placing shoring to prevent further collapse, and steel beams so that the buildings could be jacked up and the ground floor restored.

One small, approximately 2-1/2-story apartment building shown in Figure 6 was entirely sheathed with plywood. On this particular building the exterior damage was superficial, with a small 2-foot-high brick veneer wall falling away from the building. Investigation showed no ties between the brick and the building. Upward ground movement was sufficient to completely jam the garage door, so the owner found it necessary to saw off the bottom of the door to open it after the quake. The concrete garage floor was totally destroyed and will have to be replaced, but the building above showed no evidence of damage.

At another location, a contractor was adding plywood sheathing to the interior of a garage to add lateral resistance to a relatively undamaged apartment building. The contractor pointed out that there were no anchor bolts from the sill plate to the foundation, so his first step was to drill in anchor bolts. He then added blocking between the studs and was applying 3/8" plywood horizontally to the walls.

One large apartment complex in the Marina district was destroyed by fire initiated when natural gas lines were broken due to the earthquake. This can also be related to lateral load resistance of buildings. According to Franklin Lew, Manager of Seismic Safety Program for the city and county of San Francisco, "Wood-frame buildings designed to provide lateral resistance are less likely to sway and drift in an earthquake. This limits breakage of electrical, gas and water lines within the building, thus reducing the chance for catastrophic fires."

Masonry Chimneys

The chimney damage shown in Figure 1 was common to many houses whether or not they were further damaged. The chimneys typically were not reinforced and were not tied sufficiently to the structure. Chimney failures were seen in many of the areas observed. Some residences constructed in the last 15 or 20 years have utilized insulated steel chimney flues enclosed by decorative plywood siding. A number of these were observed, and none were collapsed except for one which incorporated stone veneer.

Industrial Buildings

During the 1971 Sylmar, California earthquake there were numerous failures due to masonry and concrete walls pulling away from roof systems. The failures were initiated by weak connections between the walls and the roof framing. The Uniform Building Code was subsequently improved to correct this situation by requiring a positive tie between the walls and roof framing.

A small industrial building in Campbell, about 20 miles (33 km) from the epicenter, had minor damage of this type. A 4x12 timber ledger was bolted to the masonry wall.

The plywood sheathing of the panelized roof was the only tie to the wall capable of resisting outward (tension) forces acting on the wall. The nails holding the plywood to the top of the ledger held, but the ledger split along the bolt lines. The splits in the ledger were apparently caused by cross-grain bending. As mentioned above, this detail is no longer permitted by the Uniform Building Code. In spite of the damage, the plywood roof diaphragm functioned satisfactorily, preventing damage to the masonry walls.

Masonry Buildings

Masonry buildings typically perform poorly in earthquakes, particularly those that are unreinforced. Without reinforcement, masonry buildings fail in a brittle fashion. In the town of Los Gatos, about 15 miles (20 km) from the epicenter, an entire block of one- and two-story masonry stores had been severely damaged and will undoubtedly be demolished.

Unlike wood construction, which is light in weight, masonry is heavy. Its greater weight leads to greater lateral forces to resist than wood construction.

SUMMARY AND CONCLUSIONS

A team of engineers from the American Plywood Association visited the San Francisco Bay area shortly following the Loma Prieta earthquake of October 17, 1989. Damage from the earthquake occurred in scattered locations within the region. Within these locations, the heaviest damage appeared to be to buildings with unreinforced masonry walls. All observed wood-framed buildings which were damaged were either built before the 1973 Uniform Building Code introduced updated earthquake regulations, or incorporated critical construction features but with inadequate connections, or other features which were not nailed or stapled in accordance with minimum code requirements.

It is the conclusion of the APA team of observers that framed construction built to meet current provisions of the Uniform Building Code performed very well. No code deficiencies for this type of construction were observed. However, greater attention must be paid to design and installation of connections and fastenings, and to structural continuity, especially in small buildings which may not be engineered.



Figure 1. Two-story house with wood-framed daylight basement located about 100 feet from ground fissure in Santa Cruz Mountains. No apparent structural damage except collapsed masonry chimney.

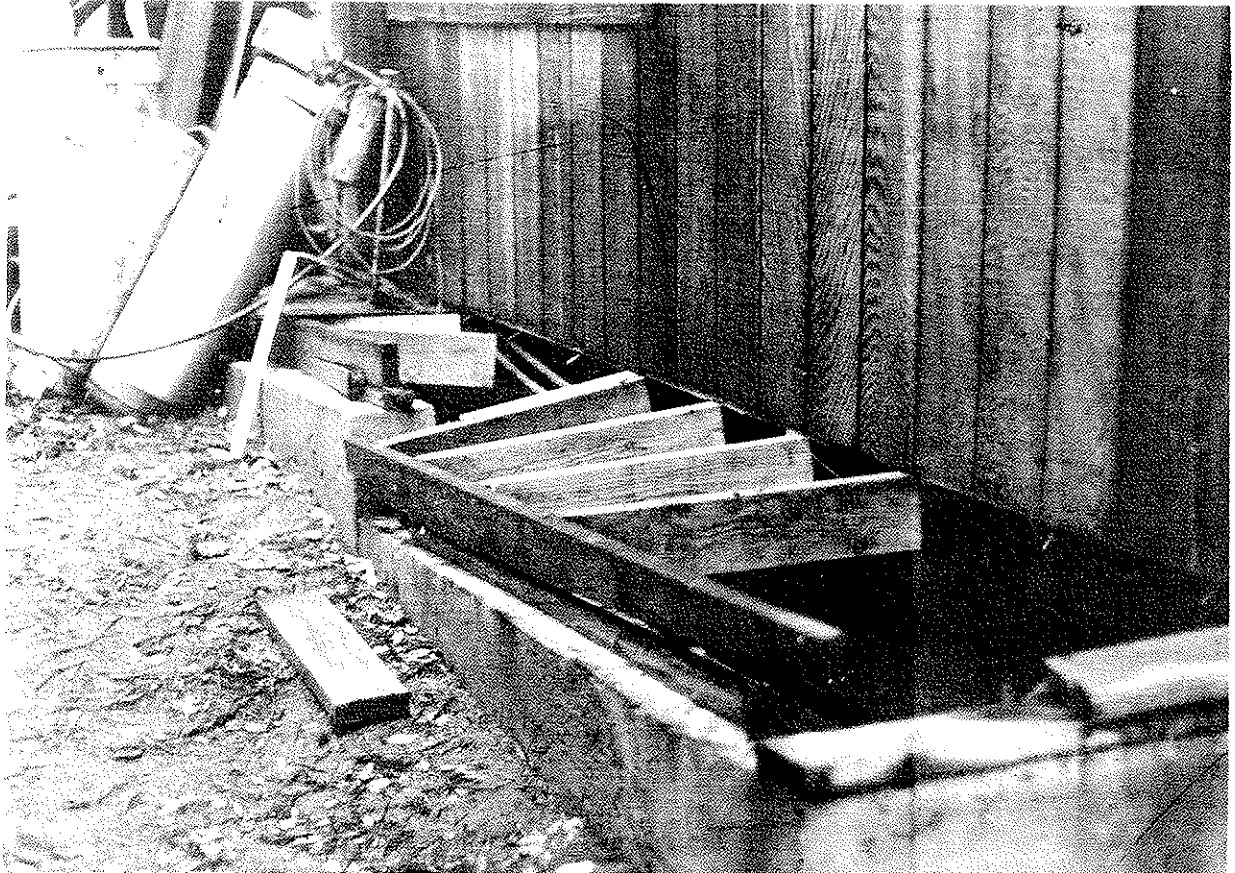


Figure 2. Collapsed cripple wall on house in Santa Cruz Mountains. Plywood sheathing on all cripple walls was inadequately fastened, allowing house to shift off foundation which split the sill plate along the bolt line.

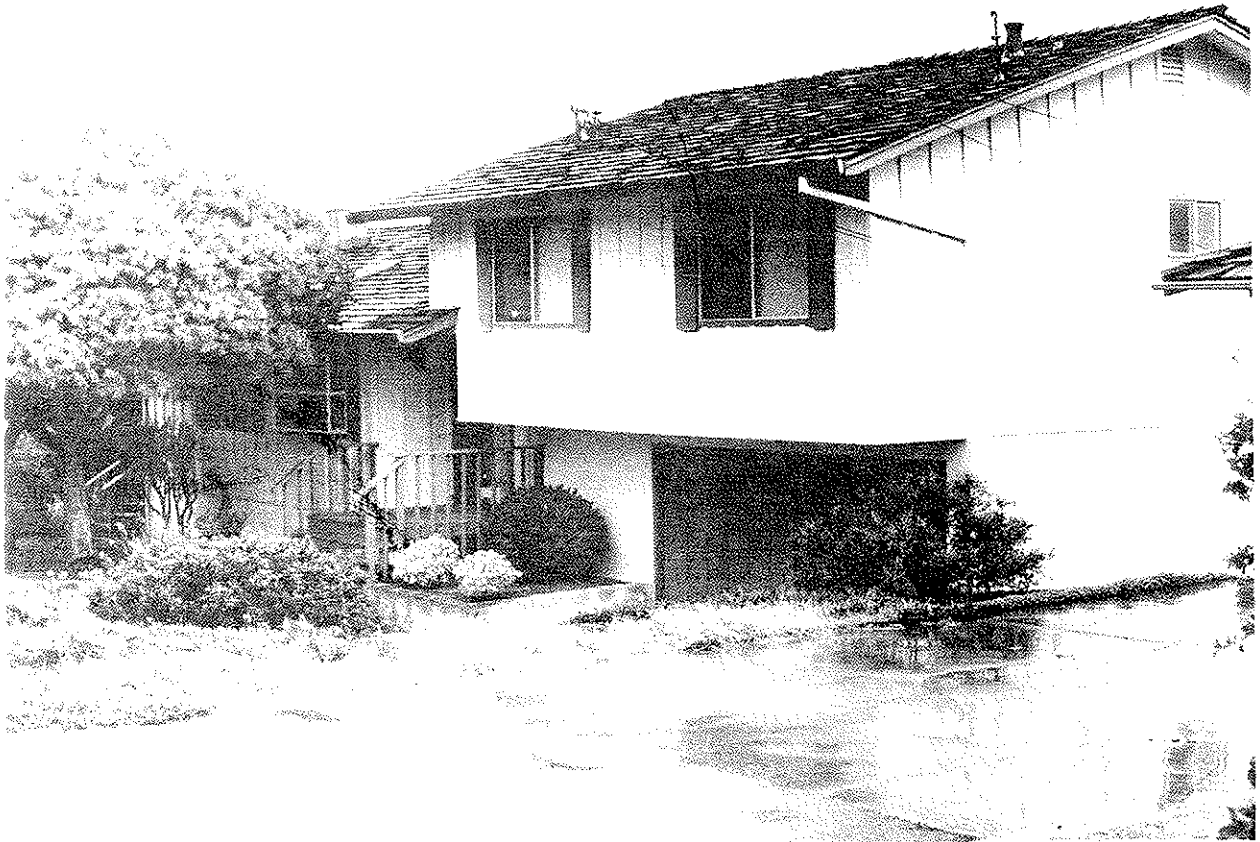


Figure 3. Undamaged split level house located in area of Los Gatos where many older one-story houses slipped laterally off their foundations.

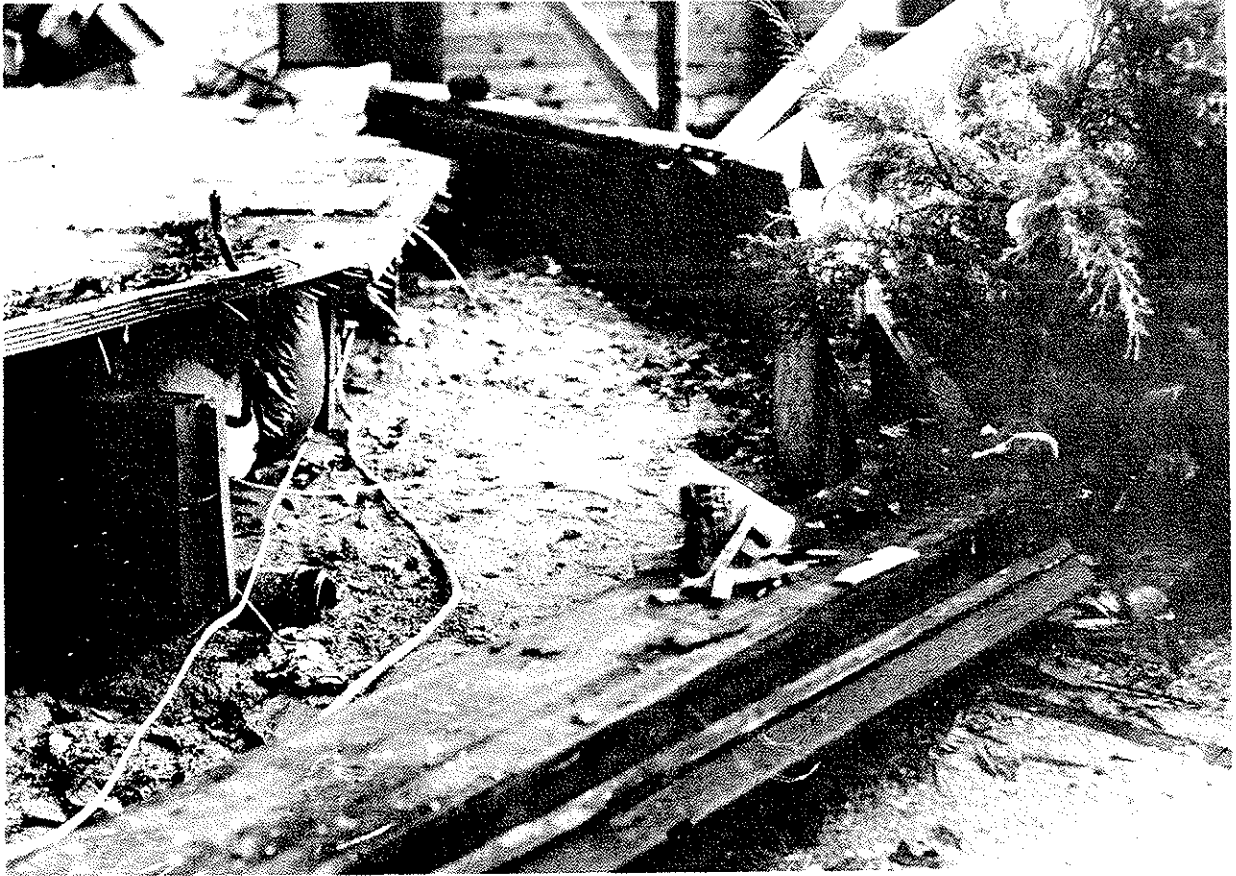


Figure 4. Completely destroyed house in Santa Cruz County. The lag screws connecting the band joist to the anchors failed in withdrawal. Other than a single toe nail, no fasteners were found tying the floor joists to the well anchored sill.

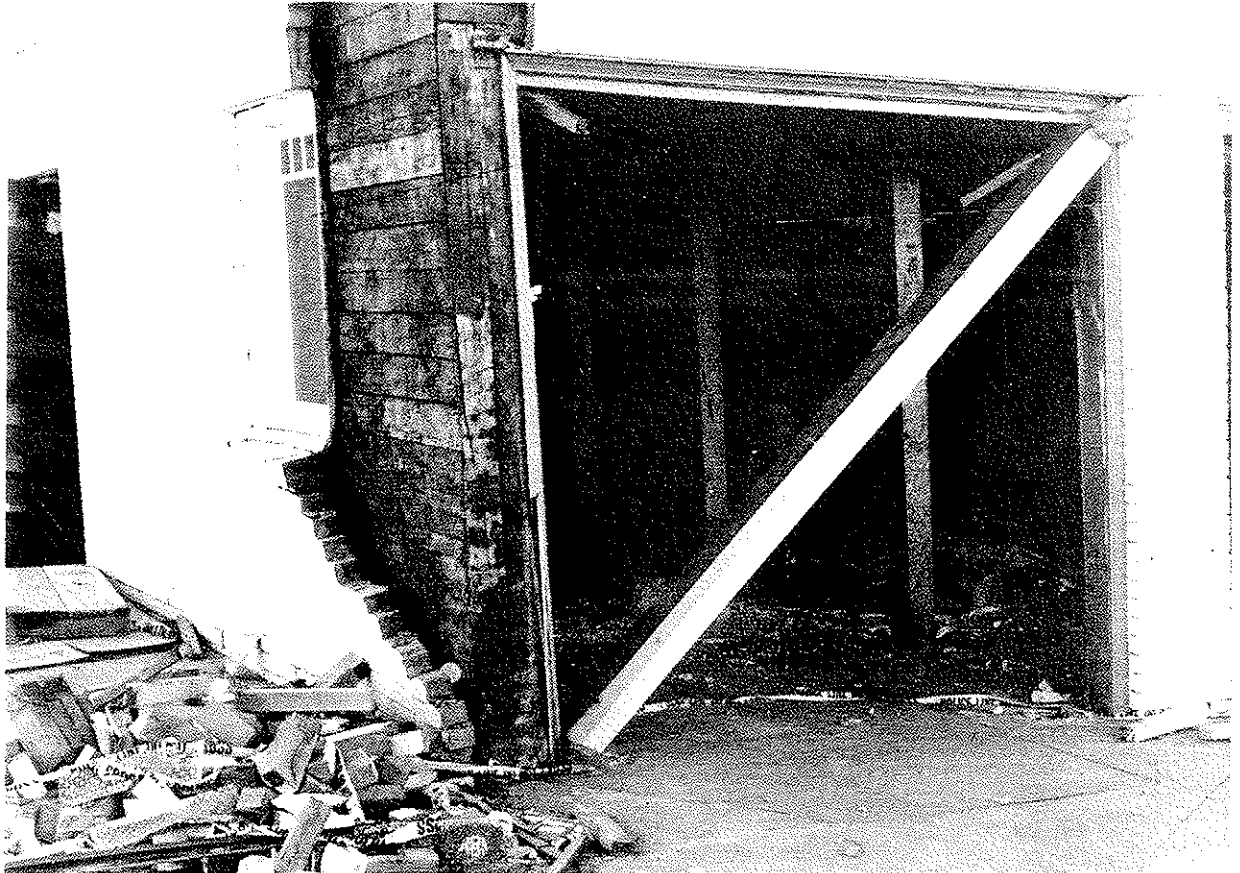


Figure 5. Corner apartment building in the Marina district. The masonry veneer was anchored to the sheathing by nails embedded in the mortar. House movers have shored the garage level in preparation for restoring the building.



Figure 6. Plywood sheathed and sided apartment building near the building shown in Figure 5. Except for the badly damaged concrete garage floor, this building had minor damage.

LITERATURE CITED

1. American Society for Testing and Materials. 1980. Standard Methods of Conducting Strength Tests of Panels for Building Construction. ASTM Designation E72-80.
2. Ceccotti, A. and A. Vignolli. 1987. Connections Deformability in Timber Structures; a Theoretical Evaluation of it's Influence on Seismic Effects. CIB-W18A/19-51-1.
3. Ceccotti, A. and A. Vignolli. 1988. Behavior Factor of Timber Structures in Seismic Zones. CIB-W18A/20-15-1.
4. Ceccotti, A. and A. Vignolli. 1989. Behavior Factor of Timber Structures in Seismic Zones (Part Two). CIB-W18A/21-15-5.
5. Council for Building Research. Studies and Documentation. 1983. Structural Timber Design Code. CIB Publication 66.
6. DePineres, O. G. 1987. A Safer Earthquake Design Approach. Civil Engineering. American Society of Civil Engineers. May, 1987. Page 52. New York, NY.
7. Hansen, K. F. 1985. Seismic Design of Small Wood Framed Houses. CIB-W18A/17-15-2.
8. Hiroshima, Y. 1987. Non-Destructive Vibration Tests on Existing Wooden Dwellings. CIB-Q18A/19-15-5.
9. pr EN TC 124.106. 1990. Timber Structures - Timber Frame Walls: Racking Strength and Stiffness of Structural Wall Testing.
10. Tissell, J. R. and J. R. Elliott. 1981. Plywood Diaphragms. Research Report 138. American Plywood Association. Tacoma, Wa.
11. Tissell, J.R. and J. D. Rose. 1988. Plywood End Shear Walls in Mobile Homes. Research Report 151. American Plywood Association. Tacoma, Wa.
12. Tissell, J. R. 1990. Structural Panel Shear Walls. Research Report 154. American Plywood Association. Tacoma, Wa.
13. Yasamura, M. 1987. Racking Resistance of Wooden Frame Walls with Various Openings. CIB-Q18A/19-15-3.

INTERNATIONAL COUNCIL FOR BUILDING RESEARCH STUDIES AND DOCUMENTATION

WORKING COMMISSION W18A - TIMBER STRUCTURES

DETERMINATION OF THE FRACTURE ENERGIE OF WOOD FOR TENSION

PERPENDICULAR TO THE GRAIN

by

W Rug

M Badstube

German Academy of Architecture and Building

German Democratic Republic

and

W Schöne

Research Institute of BAUFA

German Democratic Republic

MEETING TWENTY - THREE

LISBON

PORTUGAL

SEPTEMBER 1990

C o n t e n t s

1. Introduction
2. Test procedure
 - 2.1. Objectives
 - 2.2. Test arrangement and test material
 - 2.3. Test procedure
 - 2.3.1. Preparation of the test specimens
 - 2.3.2. Execution of the testing
 - 2.4. Evaluation
3. Test results and conclusions
4. Literature (references)

Annexes:

- Annex 1 - Tables of all test results
- Annex 2 - One force-deformation diagram (series A, test-no 1)
- Annex 3 - Photographic representation of the crack development by means of an example and representation of the fracture surface (series A)
- Annex 4 - Measurement photographs as to location and width of the annual rings (series A, test-no 1...3)
- Annex 5 - Test experiments as to the problems of sound emission

1. Introduction

The fracture energy of timber being exposed to tension acting across the grain is a parameter which is required for the calculation of the shear stress of girders with notchings at the supports (see the reference /1/).

Since hitherto only a few test results and findings concerning the fracture energy have been available, in 1989 the CIB W 18 A working commission has agreed to perform further tests and experiments with the participation of interested institutions.

2. Test procedure

2.1. Objectives

The objectives of the tests are the investigation into the crack development parallel to the grain and the determination of the corresponding fracture energy with a view to enabling a drawing of conclusions therefrom to the behaviour in practice of notched beams or connections (joints/fasteners) being exposed to stresses and strains acting perpendicularly to the grain.

Considering the dependence of the results and findings on the test method being adopted, a standardized (i.e. uniform) method has been taken as the basis for all tests /6/.

The tests and investigations performed in the GDR referred to a determination of the influence of the timber moisture on the fracture energy of mechanically sorted high-strength timber, of the influence of a visual grade-related sorting on the fracture energy with an equal degree of timber moisture and of the fracture energy of glued laminated timber as compared with that of structural timber.

2.2. Test arrangement and test material

The test arrangement of the test material used is being shown by Table 1 (see page 4). The test arrangement demonstrating in detail the example of testing a timber square with a glue-inserted middle piece of glued laminated timber is being illustrated by the Figures 1, 2 and 3 (see the pages 5, 6 and 7, respectively).

2.3. Test procedure

2.3.1. Preparation of the test specimens

- Storage of the glued test specimens in the climatic test cabinet until reaching the equilibrium moisture rate ω .
Variant: A with $\omega = 12 \%$;
 B with $\omega = 18 \%$;
 C with $\omega = 24 \%$;
 D to F with $\omega = 12 \%$.
- After having reached the equilibrium moisture rate ω , the weighing of the total sample is being carried out.
- Immediately prior to beginning the test, the slot in the middle piece is being provided.
- Measurement and recording of all geometrical parameters of the test specimens.

2.3.2. Execution of the testing

Testing machine: "TIRATEST 2300"-type universal testing machine,
 manufactured by the machine tool builders' trust Werkzeugmaschinenkombinat "Fritz Heckert" of Karl-Marx-Stadt (Chemnitz), factory at Rauenstein

Testing speed: 0.6 mm per minute

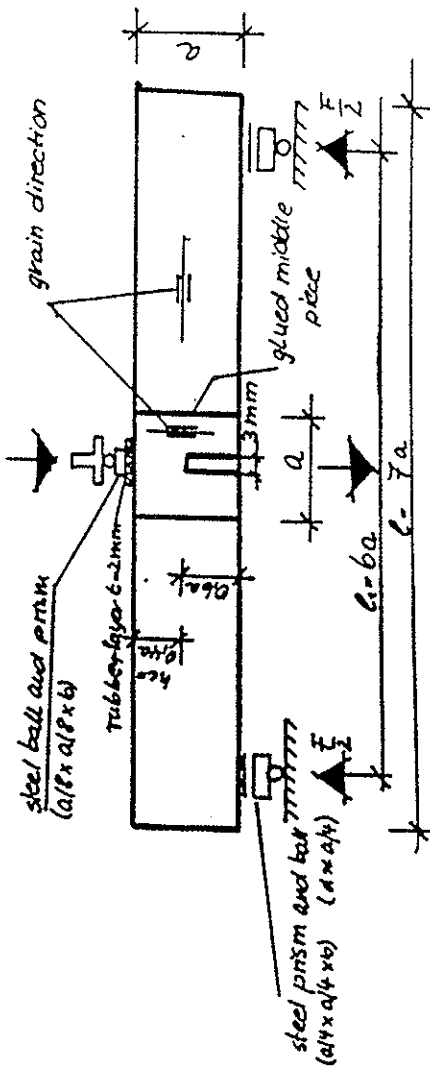
Load application: constant until the complete failure of the test specimen concerned

(to be continued on page 8)

./..

Table 1: Test procedure for tests to determine the fracture energy

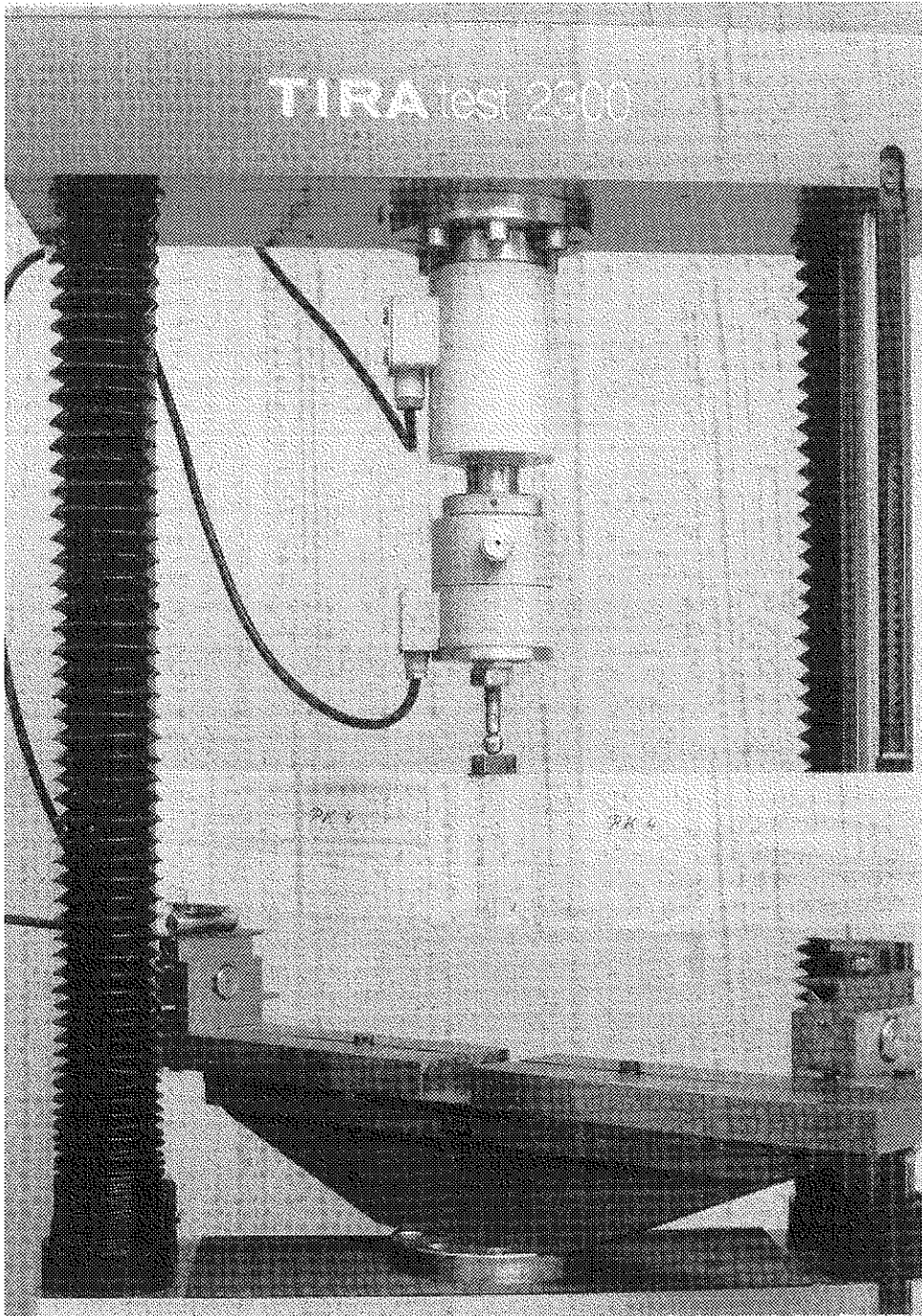
solid wood glued lami-
 b = 45 mm nated timber
 a = 90 mm b = 45 mm
 he = 36 mm a = 128 mm
 l = 630 mm he = 51,2 mm
 l = 540 mm l = 896 mm
 l = 768 mm
 Layer thickness T = 32 mm
 (= 4 Layers)
 slotted area being free from knots



Test series	according to	8 r a d	according to Eurocode 5	species	Number of tests	moisture content
						C _J
A	GDR-Code /2/	C 7		red pine	12	12
	Em = 12000 N/mm ²					
B	GDR-Code /2/	C 7		red pine	12	18
	Em = 12000 N/mm ²					
C	GDR-Code /2/	C 7		red pine	12	24
	Em = 1200 N/mm ²					
D	FRG-Code /3/	C 5		red pine	12	12
E	FRG-Code /3/	C 3		red pine	12	12
F	GDR-Code /4/			white wood	12	12

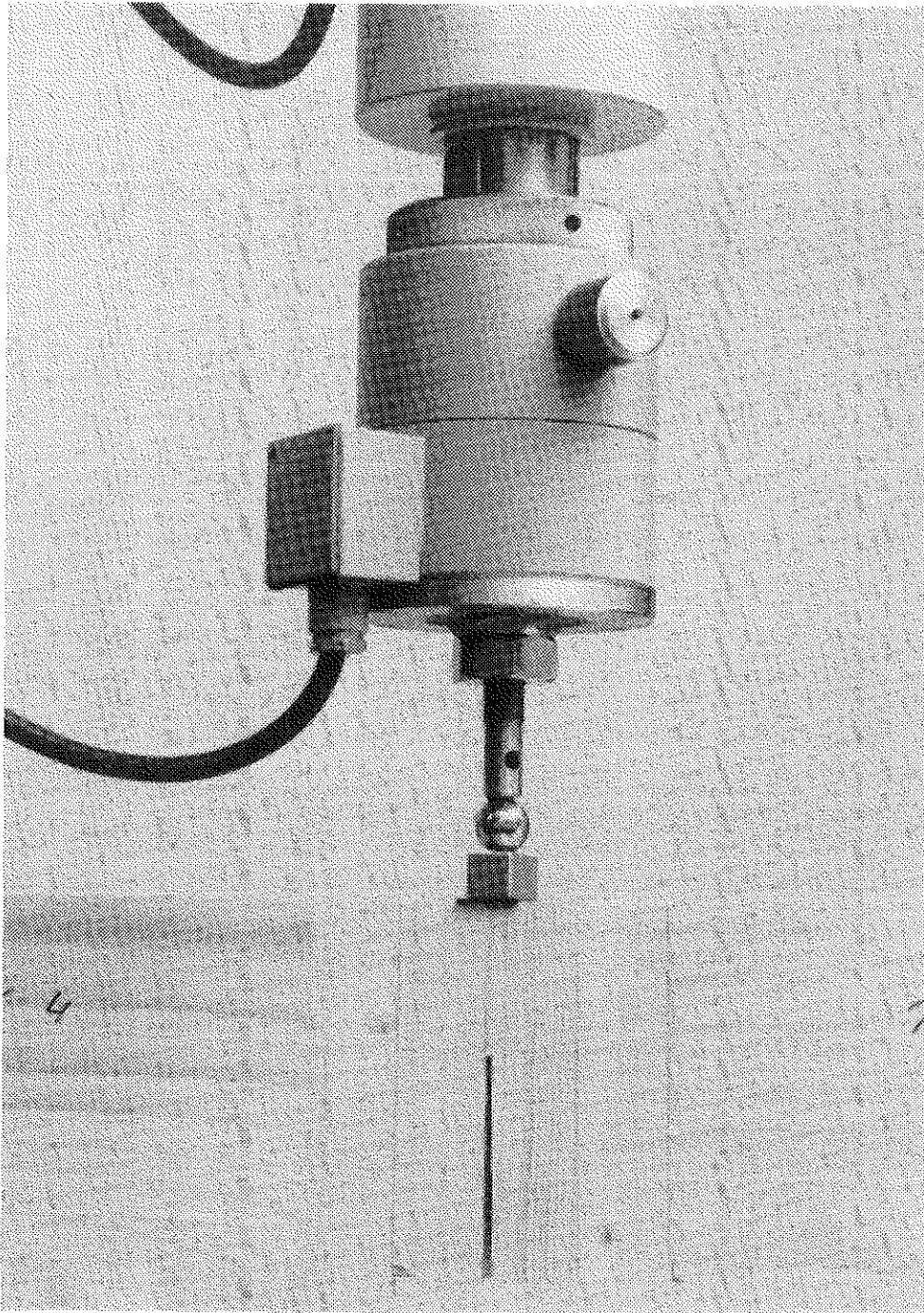
Gesamtübersicht am Beispiel der Prüfung einer Holzkantel mit eingeleimtem BSH-Stück.

Total view with the example of testing a timber square with a glue-inserted piece of glued laminated timber.



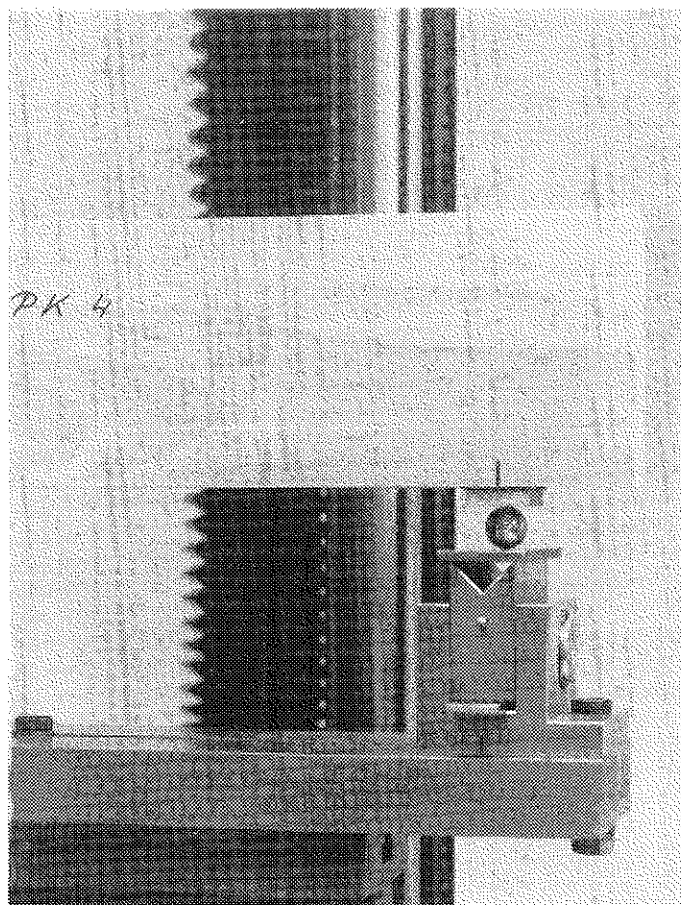
Prüfkörper Variante F
Variant F test specimen

Punkt der Lasteintragung über Kraftmeßwandler, Stahlkugel
($d=a/8$), Stahlprisma ($a/8 \times a/8 \times b$) und Gummilage ($t \sim 2\text{mm}$);
Point of load application by means of force transmitter,
steel ball ($d=a/8$), steel prism ($a/8 \times a/8 \times b$) and rubber
layer ($t \sim 2\text{mm}$);



Prüfkörper Variante F
Variant F test specimen

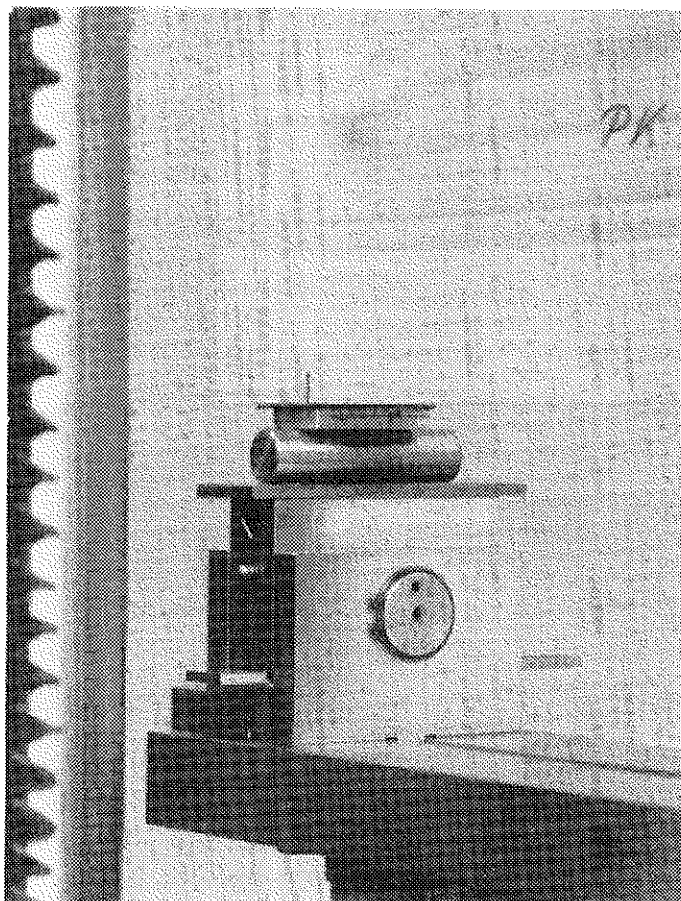
Ansicht des rechten Auflagers/View of the right-hand support



Prüfkörper
Gummilage ($t \sim 2\text{mm}$)
Stahlprisma ($a/4 \times 5\text{mm} \times b$)
Stahlkugel ($d \sim a/4$)

Test specimen
rubber layer ($t \sim 2\text{mm}$)
steel prism ($a/4 \times 5\text{mm} \times b$)
steel ball ($d \sim a/4$)

Ansicht des linken Auflagers/View of the left-hand support



Prüfkörper
Gummilage ($t \sim 2\text{mm}$)
Stahlprisma ($a/4 \times 5\text{mm} \times b$)
Stahlzylinder ($d \sim a/4 \times b$)

Test specimen
rubber layer ($t \sim 2\text{mm}$)
steel prism ($a/4 \times 5\text{mm} \times b$)
steel cylinder ($d \sim a/4 \times b$)

(Continuation from page 3 as to item 2.3.2.)

- Measurement data:
- . Recording (plotting) of a load-deformation diagram
 - . Immediately after the fracture, the timber moisture of the middle piece is being determined (weighing and drying tests according to DIN 52 183 /5/ or according to ISO 3130, respectively) and determination of the apparent specific gravity of the middle piece.

2.4. Evaluation

The evaluation was being effected by analogy with the reference /6/.

The characteristic values (parameters) determined and evaluated were as follows:

- b - width of the test specimen (mm);
- h_e - timber height (depth) within the slotted area (mm);
- F_{max} - maximum force (N);
- m - weight immediately prior to the testing (g);
- u_o - deformation at the moment of the complete failure of the sample (mm);
- ω_{real} - really determined timber moisture (%);
- ρ - apparent specific gravity (kg/m^3);
- W - measured work (Nmm);
- G - fracture energy (Nmm/mm^2).

The statistical interpretation includes the determination of

- x_{mean} - mean value of one series of measurements;
- s - standard deviation;
- v - variation coefficient.

In addition, measurement photographs of all test specimens (middle pieces) were being provided from which all data as to the location and width of the annual rings may be inferred.

One force-deformation diagram for each test specimen has been plotted. The point x_1 is marking the beginning of the visible cracking.

The acoustic attendant phenomena of the crack development have been investigated into by means of a sound emission instrument at two additional test specimens. With a view to providing an initial orientation, two of the diagrams are including a lotting (recording) of the sound occurrences (expressed in mV) over the deformation u .

In order to safeguard the results and findings, further tests and investigations will be required.

3. Test results and conclusions

A summary of the results and findings of all tests and determination is being provided in the report /7/.

The conclusions are as follows (see table 2 and figure 4):

a) influence of moisture content (timber with high density)

- a small decrease of fracture energy related to mean value up to moisture content of 18 %
- a more continually effect of moisture content of fracture energy related to the 5 % - fractil

b) influence of sorting

- no difference between visual sorted timber (grouped in grade II according to DIN 4074) and machine sorted timber.
The reason is the accidental high density of visual sorted timber.
- the fracture energy of visual sorted timber (grouped in grade III according to DIN 4074) differ essential (approximately 15 % related to mean value and 25 % related to 5 % fractil)

c) fracture energy of glue

- glue has the lowest value fracture energy (approximately 30 % related to the mean value and 40 % related to the 5 % fractil)

Table 2: Summary of the results of all Test series

series	density $w[\text{kg/m}^3]$	fracture energy $G[\text{Nmm/mm}^2]$	compared to	
			series A	series D
A	509...547...573 $v = 4,5 \%$	$\bar{x} = 0,350$	100	
		$v = 9,40 \%$	-	-
		$G_{5\%} = 0,296$	100	
B	539...574...616 $v = 4,4 \%$	$\bar{x} = 0,326$	93,0	-
		$v = 10,40 \%$	-	-
		$G_{5\%} = 0,256$	91,2	-
C	438...478...548 $v = 9,5 \%$	$\bar{x} = 0,328$	93,7	-
		$v = 13,30 \%$	-	-
		$G_{5\%} = 0,256$	86,5	-
D	491...515...536 $v = 3,2 \%$	$\bar{x} = 0,358$	102	100
		$v = 12,80 \%$	-	-
		$G_{5\%} = 0,282$	95,3	100
E	412...453...521 $v = 8,7 \%$	$\bar{x} = 0,307$	87,7	85,60
		$v = 17,80 \%$	-	-
		$G_{5\%} = 0,217$	73,31	76,95
F	545...580...607 $v = 4,5 \%$	$\bar{x} = 0,255$	72,85	71,12
		$v = 17,40 \%$	-	-
		$G_{5\%} = 0,182$	61,42	64,47

Fracture energy $\left[\frac{Nmm}{mm^2} \right]$
G

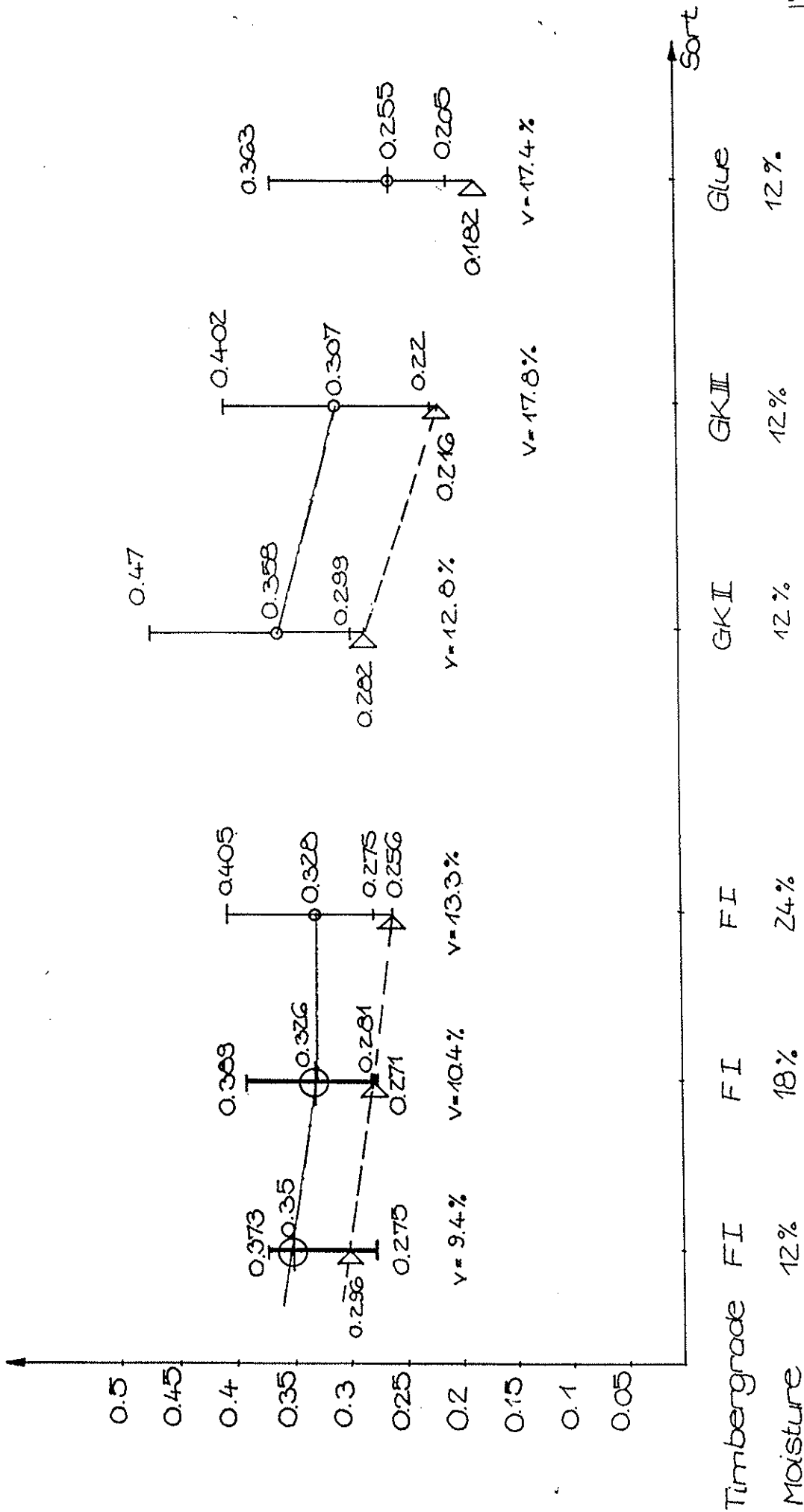


Figure 4: Fracture Energy of all tests

4. Literature (references)

- /1/ Per Johan Gustafsson and Hans Jörgen Larsen:
DESIGN OF END-NOTCHED BEAMS; CIB Paper
W 18 A / 22-10-1, Berlin, GDR; September 1989
- /2/ TGL 33 135/03 - E 89: Holzbau; Tragwerke; Berechnung
nach Grenzzuständen
(Timber construction; Loadbearing structures; Limit
states design)
- /3/ DIN 4074, Teil 1. Sortierung von Nadelholz nach der
Tragfähigkeit; Nadelschnittholz. - September 1989
(DIN..., Part 1. Sorting of softwood by the load-
bearing capacity; Mill run softwood.)
- /4/ TGL 33 136/01: Holzbau; Bauteile aus Brettschichten,
geklebt. Technische Bedingungen. - Januar 1987
(TGL...: Timber construction; Structural components
made of glued laminated timber. Technical conditions.
January 1987)
- /5/ DIN 52 183: Prüfung von Holz; Bestimmung des Feuchte-
gehaltes. - November 1977
(DIN...: Testing of timber; Determination of the
moisture content)
- /6/ Determination of the Fracture Energy of Wood for Ten-
sion Perpendicular to the Grain
CIB - W 18 A Group, Draft Standard, November 1989
- /7/ Rug, W.; Badstube, M.; Schöne, W.:
Determination of the Fracture Energy of Wood for Ten-
sion Perpendicular to the Grain
Report, Berlin/Leipzig 1990

A N N E X 1

Tables of all test results

Tabellarische Zusammenstellung der Einzelergebnisse
"Bruchenergie von Holz bei Zug rechtwinklig zur Faser"
(Tabular compilation of test results)

Variante A: NSH F 1, $\omega = 12\%$
=====
(series A)

PK-Nr.	b (mm)	h _e (mm)	F _{max} (N)	m (g)	μ _o (mm)	ω _{redl} (%)	S (kg/m ³)	W (Nmm)	G ($\frac{Nmm}{mm^2}$)
1	44,0	35,8	175	1126,0	8,6	12,2	509	434,00	0,306
2	44,0	36,0	169	1210,0	10,7	12,2	538	489,79	0,349
3	44,0	36,3	206	1173,0	10,7	12,4	526	534,03	0,373
4	44,0	36,3	201	1210,0	10,4	12,5	568	501,83	0,353
5	44,0	36,1	182	1198,0	10,6	12,4	550	486,15	0,345
6	44,0	36,0	210	1169,0	9,6	12,4	570	516,32	0,361
7	43,9	36,0	188	1189,0	10,7	12,7	516	547,26	0,386
8	43,8	36,0	214	1162,0	9,5	13,0	573	525,84	0,368
9	44,0	36,4	230	1118,0	10,5	12,4	516	569,31	0,391
10	43,7	36,0	209	1283,0	10,6	12,6	562	493,43	0,356
11	43,8	36,1	216	1207,0	7,9	12,6	560	388,78	0,275
12	44,0	36,0	190	1071,0	9,5	12,8	572	475,79	0,332

x_{mean} 199
s 18,4
v 9,2

9,9 12,5 547 0,350
0,9 0,24 24,4 0,033
9,4 1,9 4,5 9,4

x_{5%} = 0,2957

Tabellarische Zusammenstellung der Einzelergebnisse
"Bruchenergie von Holz bei Zug rechtwinklig zur Faser"

(Tabular compilation of test results)

Variante B: NSH F I, $\omega = 18 \%$

(series B)

PK-Nr.	b (mm)	h _s (mm)	F _{max} (N)	m (g)	μ ₀ (mm)	ω _{redL} (%)	g (kg/m ³)	W (Nmm)	G ($\frac{Nmm}{mm^2}$)
1	44,6	36,1	164	1390,8	10,0	16,8	539	476,35	0,338
2	44,8	35,7	163	1272,7	9,2	17,8	581	413,91	0,295
3	44,8	36,1	196	1221,1	11,2	17,2	548	488,04	0,343
4	44,7	35,7	149	1331,8	9,6	16,6	548	514,01	0,361
5	44,6	36,2	159	1255,1	10,3	16,8	547	456,19	0,322
6	44,7	36,0	182	1310,1	11,1	16,8	590	555,66	0,389
7	44,7	35,7	150	1205,1	5,7	17,7	576	399,49	0,271
8	44,8	36,3	139	1391,0	9,9	17,8	616	458,01	0,324
9	45,0	35,9	123	1402,4	9,8	17,8	612	373,73	0,273
10	44,6	36,4	125	1366,2	11,3	17,8	561	471,17	0,337
11	44,5	35,9	161	1212,9	11,8	17,3	585	470,82	0,339
12	44,8	36,2	160	1235,1	11,3	17,6	581	449,40	0,319
x _{mean}			156		10,1	17,3	574		0,326
s			21,0		1,6	0,48	25,5		0,034
v			13,5		16,0	2,7	4,4		10,4

x_{5%}=0,2700

**Tabellarische Zusammenstellung der Einzelergebnisse
"Bruchenergie von Holz bei Zug rechtwinklig zur Faser"**

(Tabular compilation of test results)

Verfahren C1 MSH F I, ω = 24 %

(series C)

PK-Nr.	b (mm)	h _e (mm)	F _{max} (N)	m (g)	μ_0 (mm)	ω_{real} (%)	S (kg/m ³)	W (Nmm)	G ($\frac{\text{Nmm}}{\text{mm}^2}$)
1	44,7	35,9	204	1284,0	9,6	23,0	548	432,88	0,307
2	44,9	36,0	225	1316,0	12,0	24,1	482	563,64	0,397
3	44,8	35,9	202	1320,0	11,7	23,2	482	512,12	0,365
4	45,0	36,0	180	1277,0	8,9	23,3	438	428,61	0,299
5	44,9	36,1	193	1242,0	11,2	23,6	494	500,08	0,351
6	45,0	36,1	157	1359,0	9,3	23,1	466	410,55	0,291
7	45,0	36,0	156	1462,0	9,2	23,4	499	401,03	0,288
8	45,0	36,1	162	1454,0	10,4	23,2	486	423,92	0,306
9	44,8	35,8	196	1411,0	10,6	22,8	464	426,16	0,311
10	45,0	36,2	156	1405,0	11,9	24,1	463	485,59	0,348
11	45,0	36,2	192	1437,0	8,8	23,2	452	385,77	0,275
12	45,0	36,1	156	1260,0	12,2	23,5	464	582,89	0,405

\bar{x}_{mean}

182	10,5	23,4	478	0,328
23,6	1,3	0,49	45,5	0,044
12,9	12,3	2,1	9,5	13,3

$x_{5\%} = 0,256$

Tabellarische Zusammenstellung der Einzelergebnisse
"Bruchenergie von Holz bei Zug rechtwinklig zur Faser"

(Tabular compilation of test results)

Variante D: NSH GK II, $\omega = 12\%$

(series D)

PK-Nr.	b (mm)	h _e (mm)	P _{max} (N)	m (g)	v ₀ (mm)	ω_{real} (%)	g (kg/m ³)	W (Nmm)	G ($\frac{Nmm}{m^2}$)
1	44,7	36,0	214	1138	10,7	12,1	520	444,36	0,313
2	44,5	36,2	224	1117	10,3	12,2	508	519,96	0,358
3	44,4	36,2	219	1230	11,2	12,4	491	495,46	0,350
4	44,9	35,7	219	1326	12,5	12,4	536	672,84	0,470
5	44,5	36,2	225	1294	10,2	12,3	513	502,39	0,352
6	44,4	36,0	225	1075	9,4	12,2	497	428,82	0,299
7	44,5	36,0	215	1140	10,7	12,0	507	461,65	0,325
8	44,5	36,8	218	1154	11,0	12,4	521	488,11	0,336
9	44,6	35,6	232	1083	11,2	12,3	508	498,33	0,351
10	44,7	35,8	223	1128	11,4	12,5	516	489,23	0,345
11	44,7	35,8	243	1125	11,8	11,8	552	592,06	0,411
12	44,5	36,0	221	1113	11,7	12,4	514	546,91	0,381

\bar{x}_{mean}

224

11,0

515

0,358

s

9,2

0,8

16,3

0,046

v

4,1

7,5

3,2

12,8

$x_{5\%} = 0,2824$

Tabellarische Zusammenstellung der Einzelergebnisse
"Bruchenergie von Holz bei Zug rechtwinklig zur Faser"

(Tabular compilation of test results)

Variante E: NSH GK III, $\omega = 12\%$

(series E)

PK-Nr.	b (mm)	h _e (mm)	F _{max} (N)	m (g)	u ₀ (mm)	ω real (%)	β (kJ/m ³)	W (Nmm)	G $\left(\frac{\text{Nmm}}{\text{mm}^2}\right)$
1	44,4	35,8	222	1268	9,2	13,2	430	486,78	0,342
2	45,0	35,8	204	1033	9,6	14,2	516	449,89	0,309
3	44,3	35,8	210	1246	7,0	13,6	412	368,83	0,260
4	44,9	36,0	194	1105	8,5	13,5	465	360,85	0,252
5	44,7	36,0	194	1290	8,3	13,9	521	384,72	0,272
6	44,4	36,0	224	968	10,4	13,6	431	520,94	0,357
7	44,4	35,7	184	1268	6,9	11,6	501	303,63	0,222
8	44,8	35,9	162	1158	9,8	12,2	416	419,37	0,295
9	44,4	35,7	210	1186	7,1	12,8	442	385,56	0,269
10	44,8	35,9	180	1182	11,3	12,9	426	487,69	0,344
11	44,5	35,8	192	1138	11,1	12,6	458	519,75	0,365
12	44,4	35,9	214	1070	11,4	12,5	418	581,91	0,402
\bar{x} mean			199		9,2	13,0	453		0,307
s			18,3		1,7	0,74	39,4		0,054
v			9,2		18,1	5,7	8,7		17,8

$x_{5\%} = 0,2168$

Tabellarische Zusammenstellung der Einzelergebnisse
"Bruchenergie von Holz bei Zug rechtwinklig zur Faser"
 (Tabular compilation of test results)

Variante P: **BSH - Sorte 3,** $n = 12$ %
 (series P)

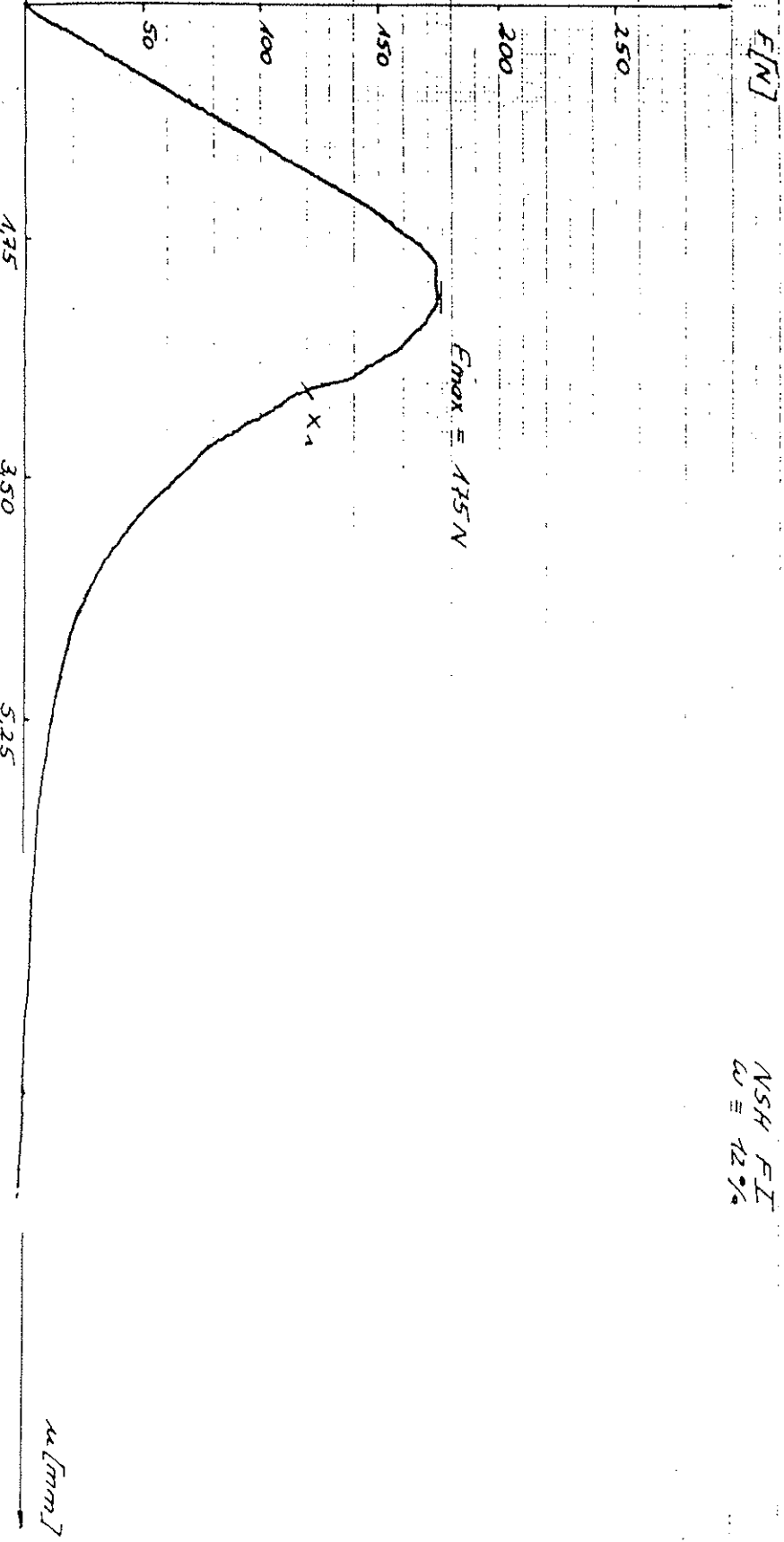
Pr-Nr.	b (mm)	h ₀ (mm)	F _{max} (N)	m (g)	h ₀ (mm)	ω _{rech} (%)	ρ (kg/m ³)	W (J/mm)	Q ($\frac{Nm}{mm^2}$)
1	45,0	51,3	241	2271	8,2	10,5	584	539,63	0,273
2	45,0	51,5	223	2361	7,4	10,5	557	501,76	0,253
3	45,2	51,3	254	2294	14,2	10,9	550	680,89	0,363
4	45,2	51,5	209	2057	6,7	10,2	596	434,49	0,216
5	45,2	51,5	240	2254	6,0	10,7	594	420,63	0,209
6	45,3	51,3	285	2243	6,8	9,7	603	474,60	0,236
7	45,3	51,7	258	2237	6,2	10,1	559	413,21	0,205
8	45,0	51,4	235	2604	7,5	10,8	606	607,04	0,304
9	45,0	51,6	231	2102	6,1	10,7	607	465,45	0,236
10	45,1	51,4	251	2511	6,8	10,8	545	464,73	0,236
11	45,0	51,3	257	2154	6,5	10,2	604	508,90	0,267
12	45,0	51,4	252	2396	7,4	10,4	565	514,50	0,259
Anzahl									
250									
s									
21,6									
v									
8,6									
29,2									
6,1									
4,5									
17,4									

$s_{5\%} = 0,1818$

A N N E X 2

Force-deformation diagram (series A, test-no 1)

Variante A

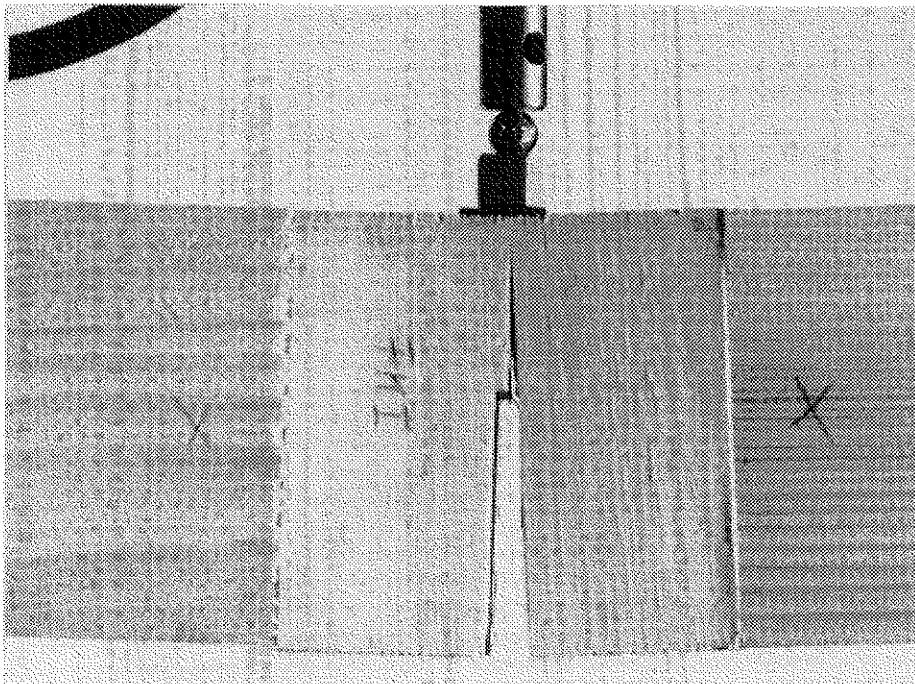
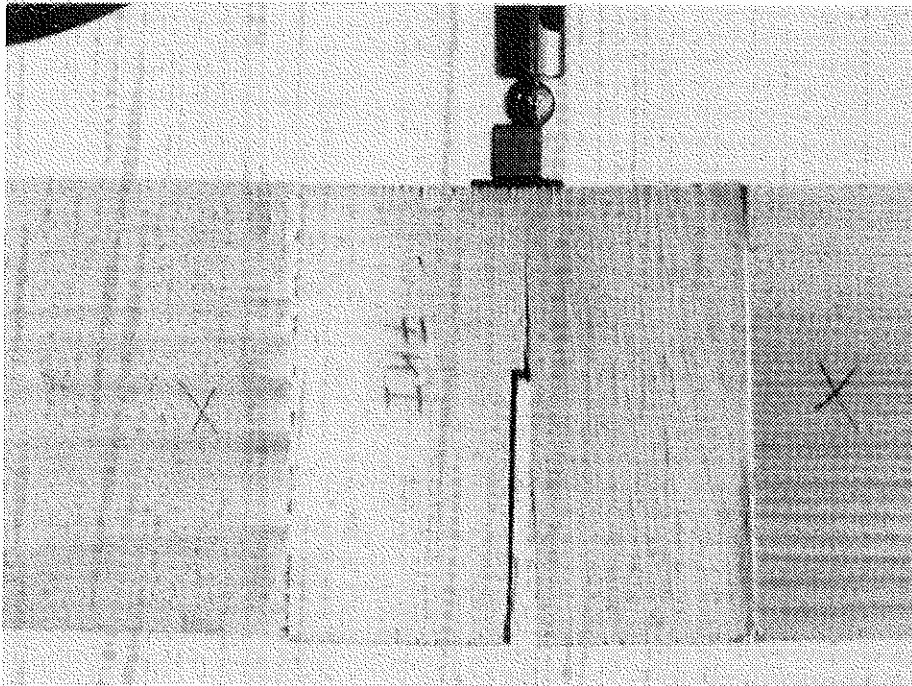
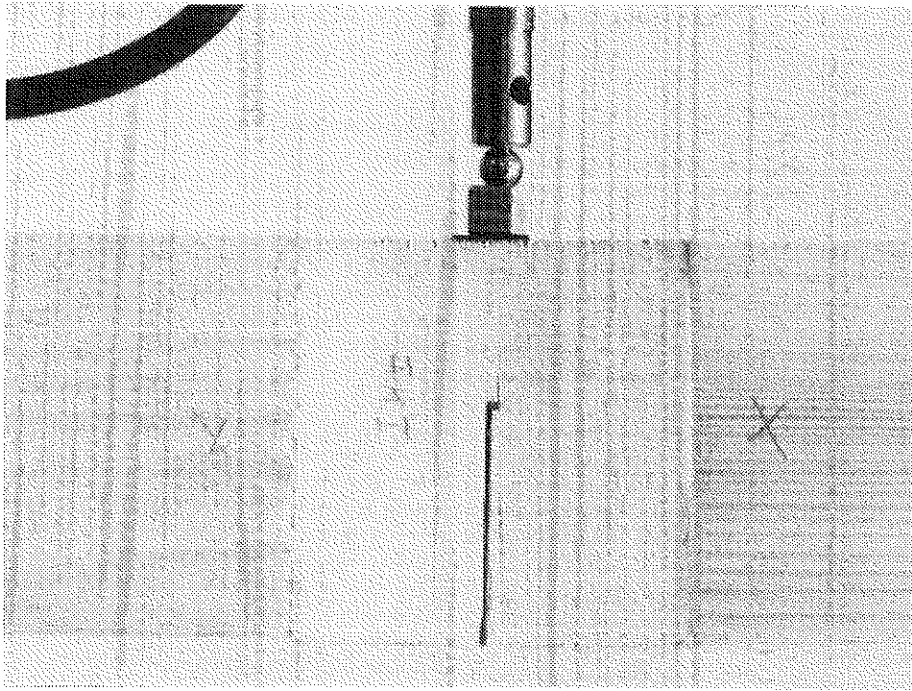


PRÜFERBER NR. 1

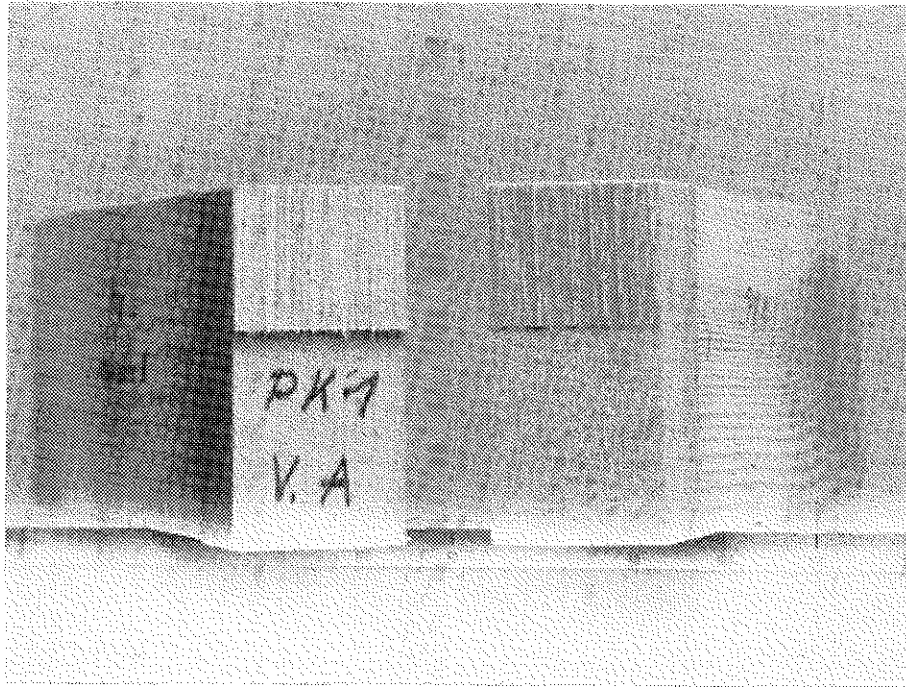
NSH FI
 $\omega = 12\%$

A N N E X 3

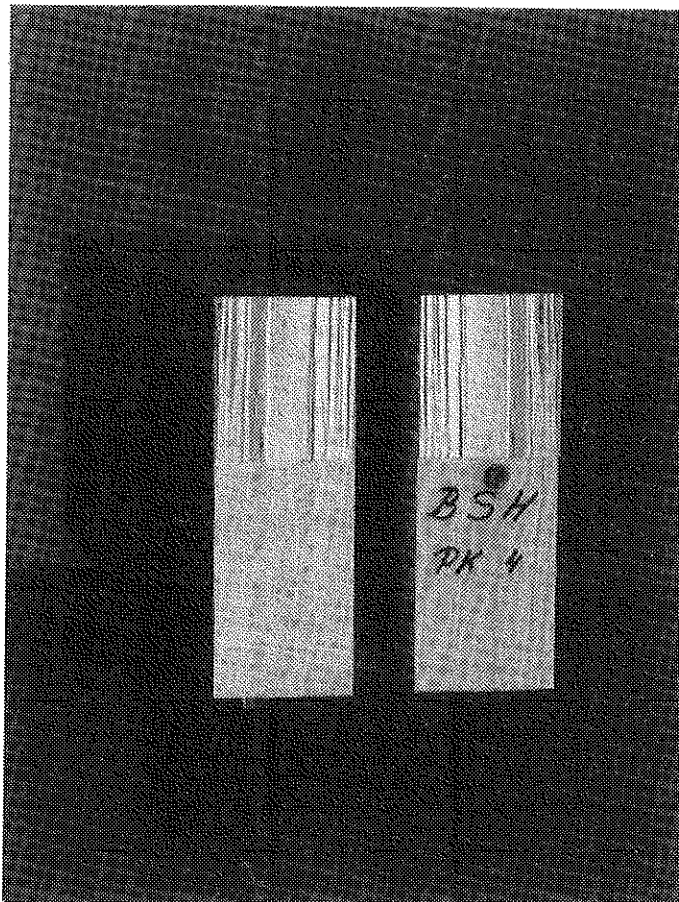
Photographic representation of the crack development
by means of an example and representation of the
fracture surface (series A)



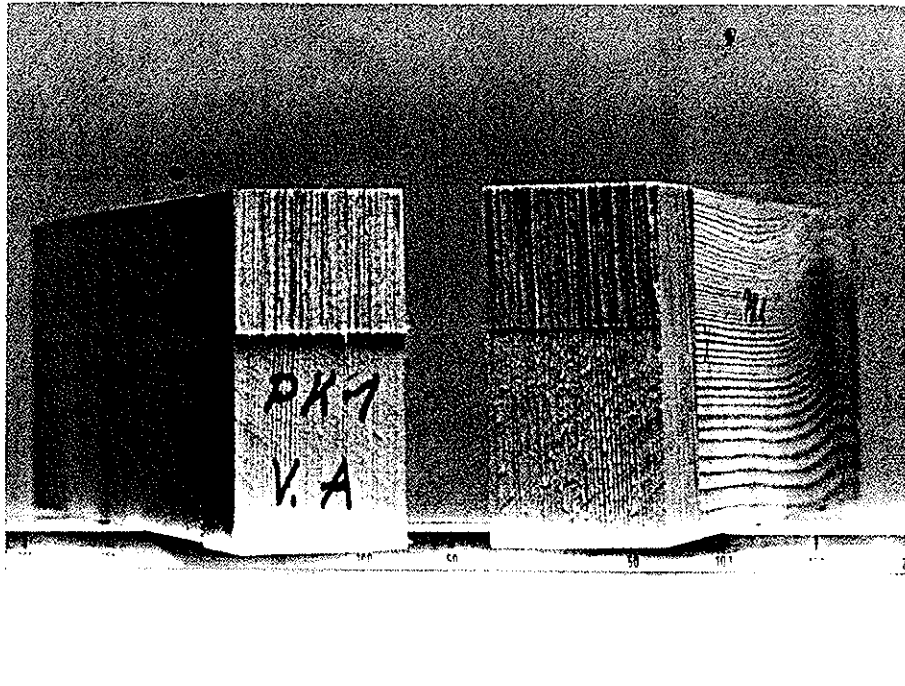
Darstellung der
Rißentwicklung
am Prüfkörper
der Variante A
(NSH F I, $\omega = 12\%$)



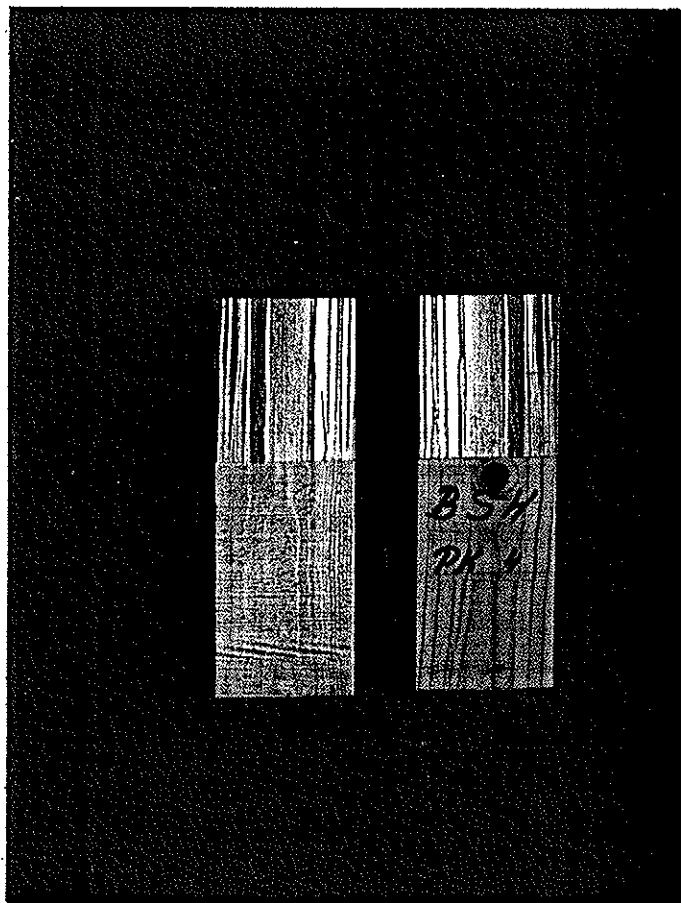
Darstellung der Bruchfläche am Prüfkörper 1 der Variante A (NSH F I, $\omega = 12\%$)



Darstellung der Bruchfläche am Prüfkörper 4 der Variante F (BSH - Sorte 3, $\omega = 12\%$)
Bruch neben der Leimfuge



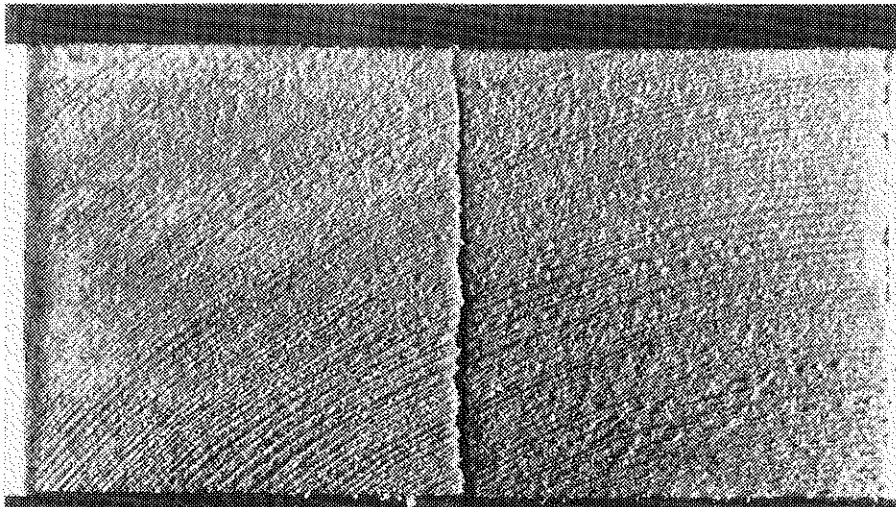
Darstellung der Bruchfläche am Prüfkörper 1 der Variante A (NSH F I, $\omega = 12\%$)



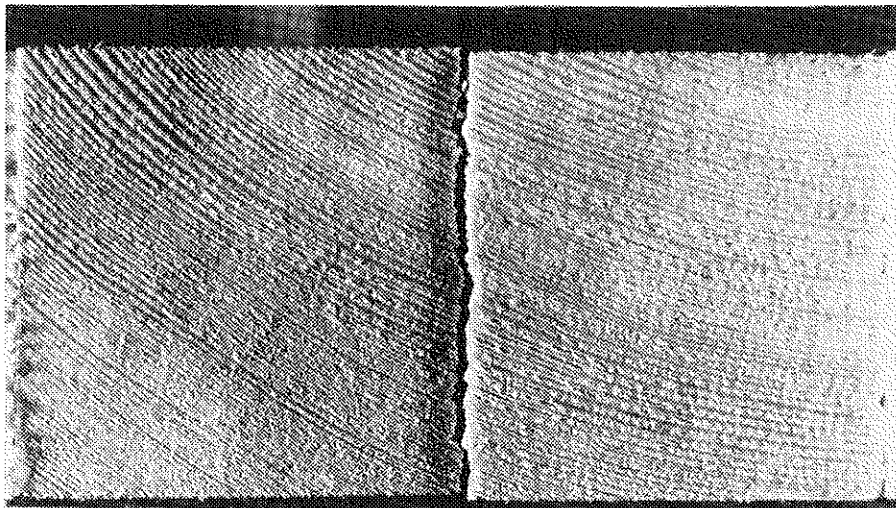
Darstellung der Bruchfläche am Prüfkörper 4 der Variante F (B3H - Sorte 3, $\omega = 12\%$)
Bruch neben der Leimfuge

A N N E X 4

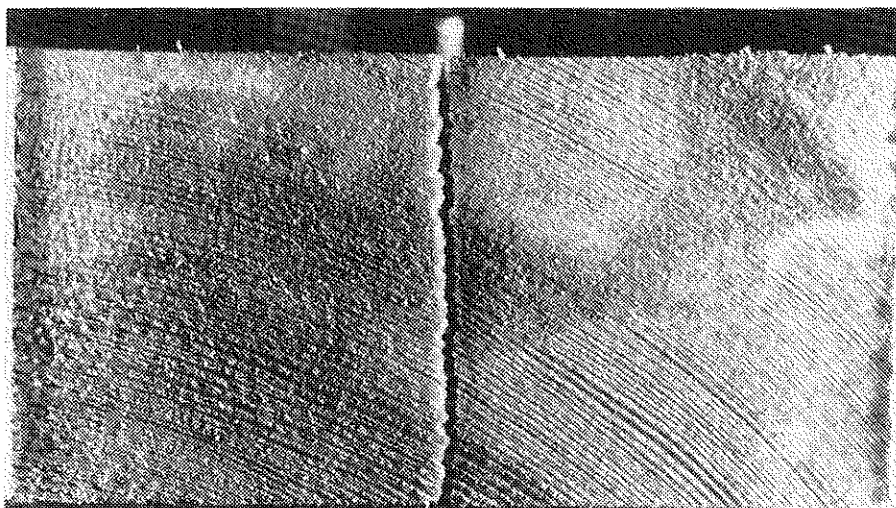
Measurement photographs as to location and width of
the annual rings (series A, test-no 1...3)



F I, 12 %, PK 1



F I, 12 %, PK 2



F I, 12 %, PK 3

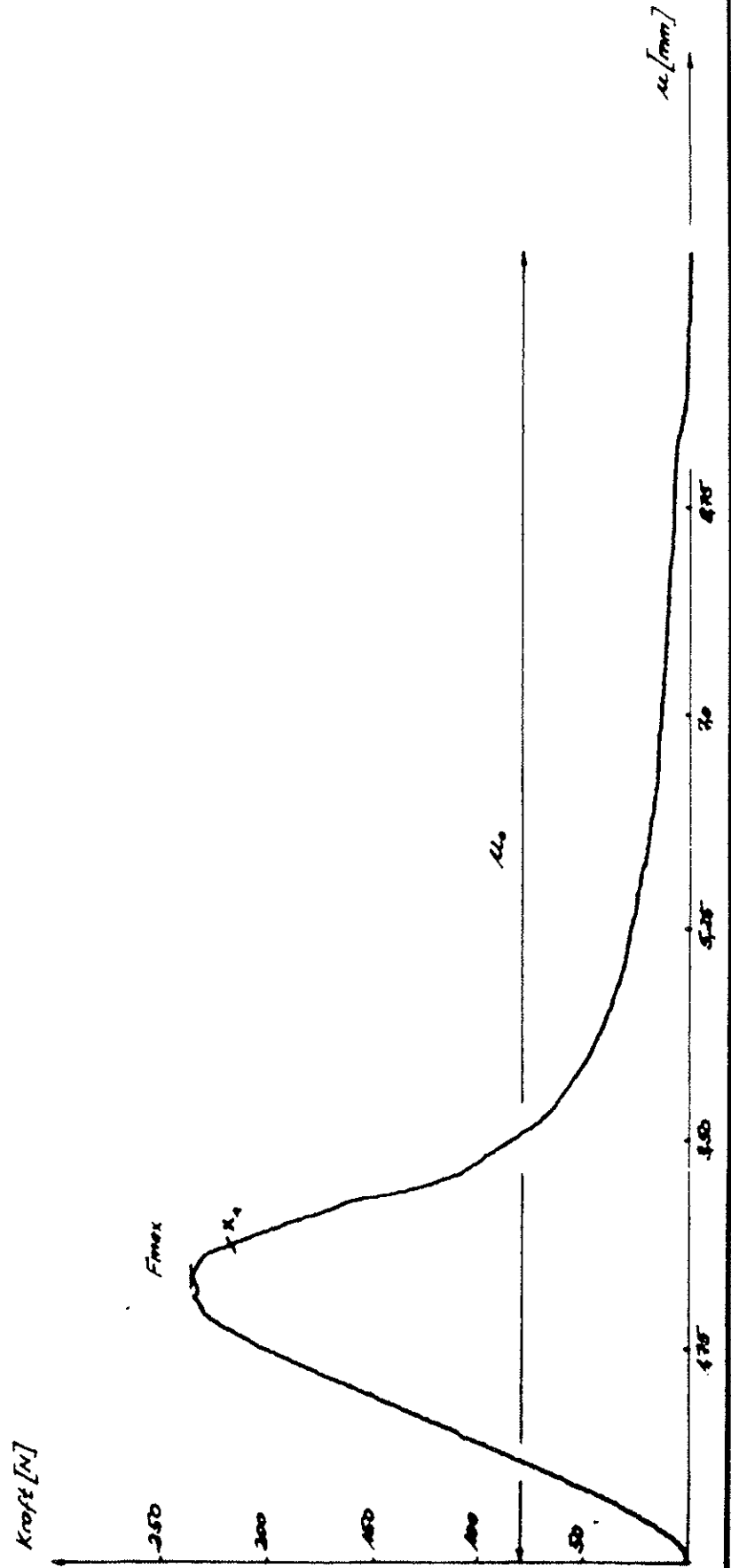
A N N E X 5

Test experiments as to the problems of sound emission

PK-NR. 5E1

TESTVERSUCH (KOLLMOLE)

Kraft-Verlängerungs-Diagramm



PK-NR SE 1

TESTVERSUCH (Montage)

AUFZEICHNUNG EINES

SCHALLEMISSIONS-DIAGRAMMS

Ausgangspunkt
der Schall-
emission
[mK] 100

1200

1800

2400

3000

3600

100

1000

INTERNATIONAL COUNCIL FOR BUILDING RESEARCH STUDIES AND DOCUMENTATION

WORKING COMMISSION W18A - TIMBER STRUCTURES

THE FRACTURE ENERGY OF WOOD IN TENSION PERPENDICULAR TO THE GRAIN

RESULTS FROM A JOINT TESTING PROJECT

by

H J Larsen

Danish Building Research Institute

Denmark

and

Division of Structural Mechanics

Lund Institute of Technology

Sweden

P J Gustafsson

Division of Structural Mechanics

Lund Institute of Technology

Sweden

MEETING TWENTY - THREE

LISBON

PORTUGAL

SEPTEMBER 1990

INTRODUCTION

There are several problems in the design of timber structures that can only be dealt with correctly by applying fracture mechanics methods. As examples may be mentioned end-notched beams and failure by splitting in joints with load perpendicular to the grain. It is, however, only recently that practical design methods have been based on fracture mechanics, instead empirical methods have been used by which fracture problems have been regarded as fictitious shear problems. There are a number of reasons for this. The resulting expressions have been too complicated for practical use, and there has been insufficient knowledge on the material parameters.

In [Gustafsson, 1988a] a simple method for the design of end-notched beams was proposed, and CIB W18A has agreed to introduce the method in a future version of CIB Timber Design Code. It will also be introduced in a redraft of [Eurocode 5, 1987] for timber structures. The method is described in [Larsen and Gustafsson, 1989] together with a proposal for a test method for determining the basic material parameter in the method; the fracture energy in tension perpendicular to the grain.

At a CIB W18A meeting in September 1989 it was agreed to set up a joint project in which a number of CIB W18A members would determine the fracture energy for a variety of timber species and grades with the following purposes:

- to evaluate the test method, and
- to determine the fracture energy and its variation with density, moisture content, growth ring pattern, etc.

This report summarizes the hitherto findings of the project. The following institutes have contributed to the project:

- Akademia Rolnicza, Katedra Mechaniki i Techniki Ciepnej, Poznan, Poland
- Bauakademie der DDR, Abteilung Ingenieurholzkonstruktionen, DDR
- Danish Building Research Institute, Denmark
- Forest Products Laboratory, Madison, USA
- Lund University of Technology, Division of Structural Mechanics, Sweden
- Lund University of Technology, Division of Building Materials, Sweden
- Luleå University of Technology, Division of Structural Engineering and Mechanics, Sweden
- Royal Technical University, Department of Lightweight Structures, Sweden
- South Bank Polytechnic, London, England
- Technical University of Denmark, Department of Structural Engineering, Denmark
- Technical Research Centre of Finland, Laboratory of Structural Engineering, Finland

TEST METHOD

The test method is described in Annex B.

The principle of the method is shown in Fig. 1–2. The fracture energy is determined as the total external work necessary for complete failure of the beam divided by the tested area ($h_c b$)

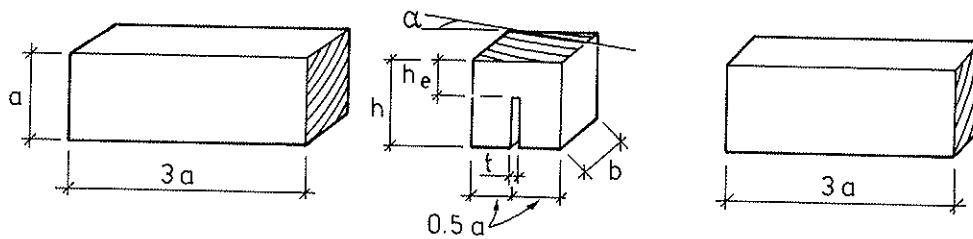


Fig. 1

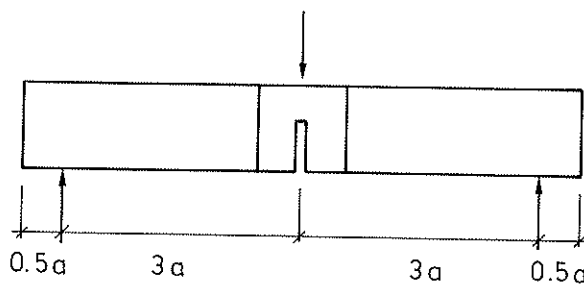


Fig. 2

The reason for the choice of this method is that it is cheap and simple and the material parameters can be determined directly from quantities measured in the test, i.e. without having to make assumptions about other material properties such as modulus of elasticity, which is necessary for the widely used compact tension specimen.

The tested volume should be free of knots. This leads to safe values, knots increase the fracture energy often quite considerably.

RESULTS

The results from the individual test series etc are given in Annex A1–A11. When nothing special is noted it is assumed that the purpose of the test is as stated in the introduction, i.e. to evaluate the test method and get information on the fracture energy for different species and grades.

In all cases the persons responsible for the testing are mentioned. When available, reference is also made to separate reports published by the participating institutes containing details on the preparation of the specimens and their treatment, loading and measuring equipment etc.

The results and conclusions of the individual lists are also given in the annexes with one exception: the dependence of fracture energy on density is discussed in the following section.

FRACTURE ENERGY VERSUS DENSITY

In the following the relation between fracture energy $G_{I,C}$ and density $\rho_{\omega,\omega}$ is analyzed for the test results reported in Annex A1–A4, A6–A8, A10 and A11.

The data from Luleå (Annex A5) are not included because the preparation and storing of the specimens deviated from the standard. The same applies to data from Lund reported in Annex 9, where the depth of the test specimens was only 20 mm (standard 80 mm).

The data are identified by the number of the annex in which they are reported. For data 2 (Denmark) the measured energy values are corrected to the standard size by the correction factors found in the table of results.

The results for Nordic redwood (data 1–4 and 8) is shown in Fig. 3, where the regression line is shown for the individual populations. Each covers only a small interval of densities and there is no general trend. The correlation coefficient is low, the numerical values being about 0.4 with 0.12 and 0.6 as extremes.

Taken as one population, however, there is a clear trend, see Fig. 4. The correlation coefficient is 0.78, a satisfactory high value. In Fig. 5 the data for wood from Poland, DDR and U.K. are added together with the Stockholm results for spruce. It is seen that the regression line is unchanged. In Fig. 6 further results from USA are added. The regression line differs from that of European softwood alone, especially for high densities. The correlation coefficient is 0.74.

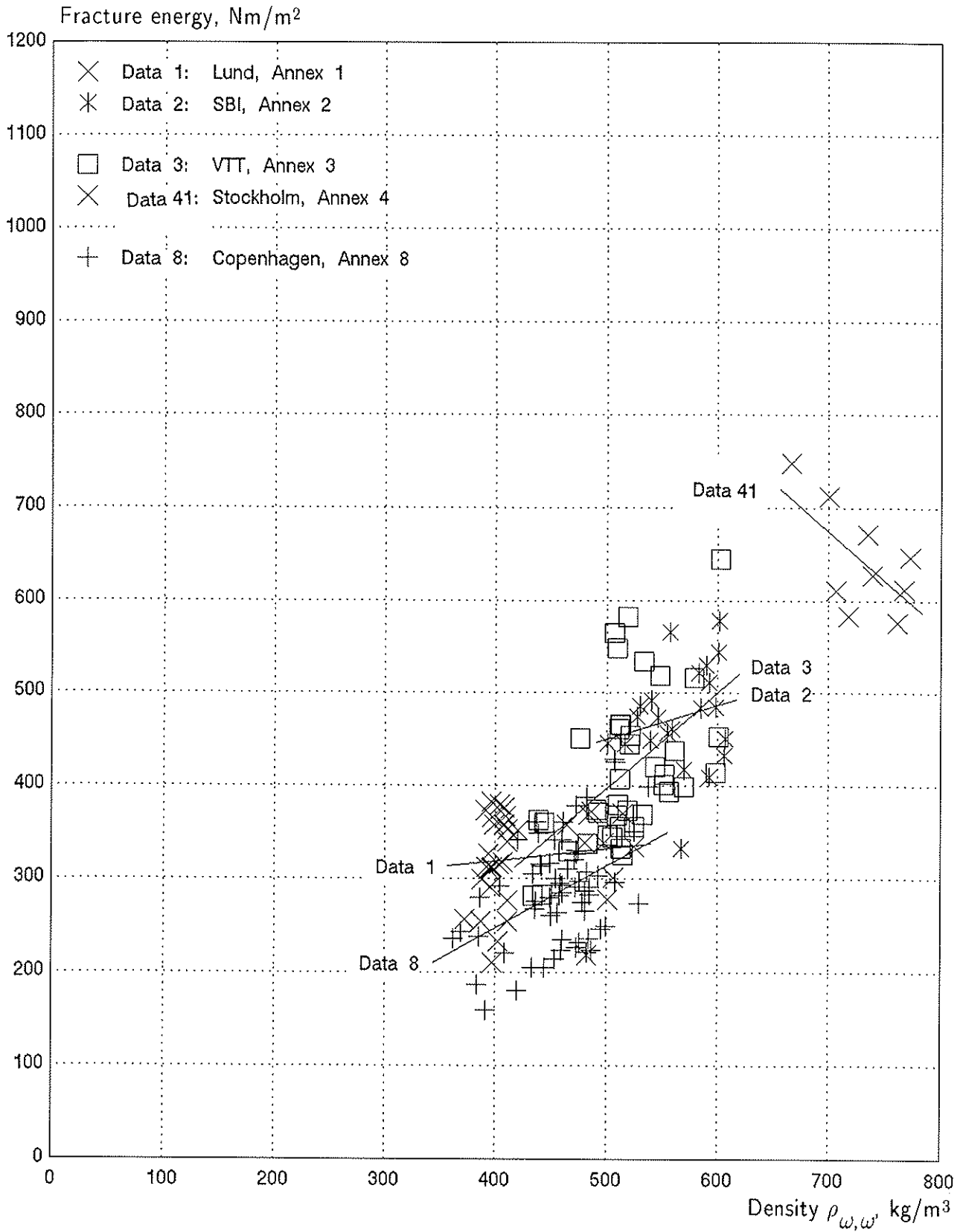


Fig. 3 Fracture energy versus density for Nordic redwood

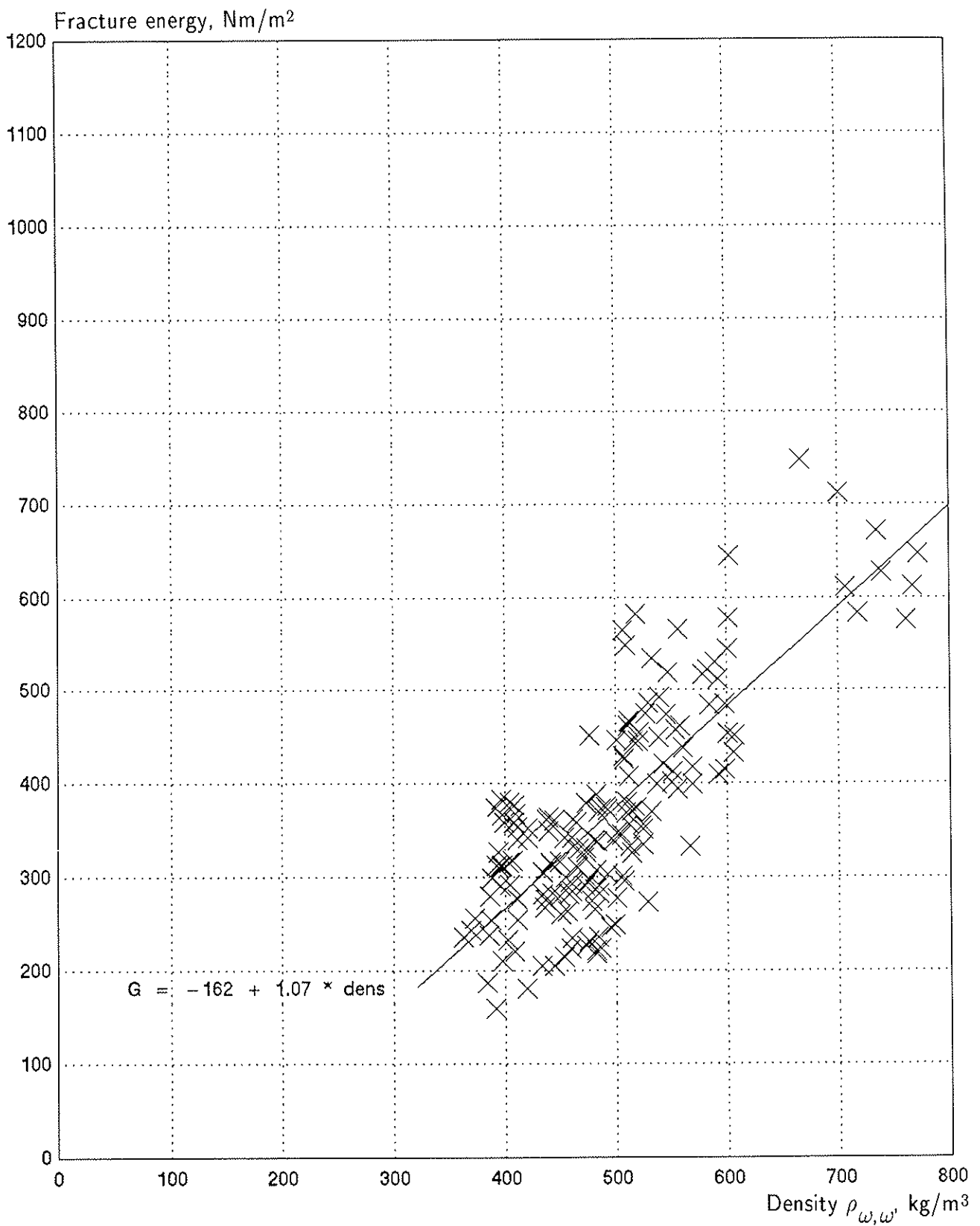


Fig. 4 Fracture energy versus density for Nordic redwood. The data are the same as shown in Fig. 3 but they are regarded as one population

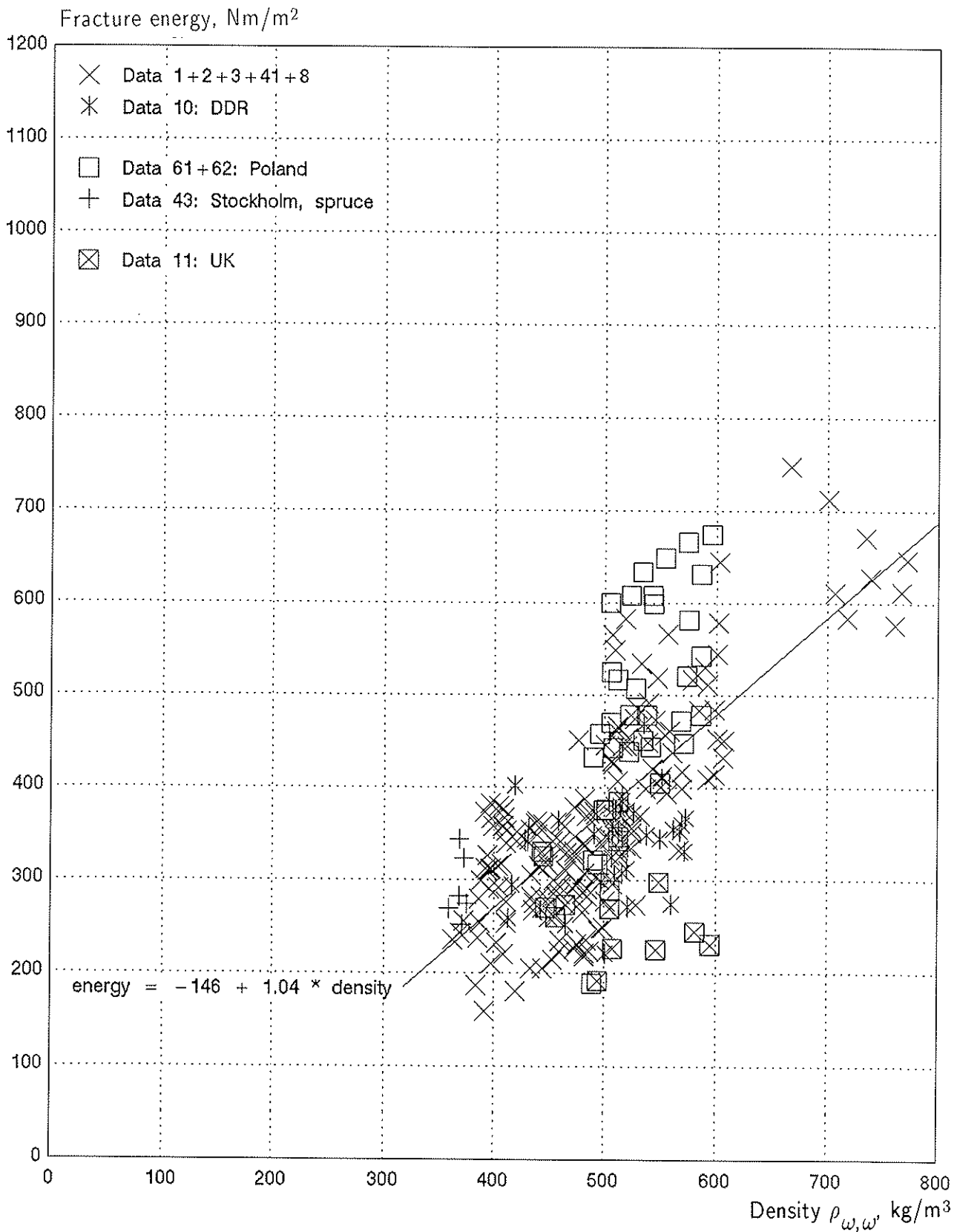


Fig. 5 Fracture energy versus density for European softwoods regarded as one population

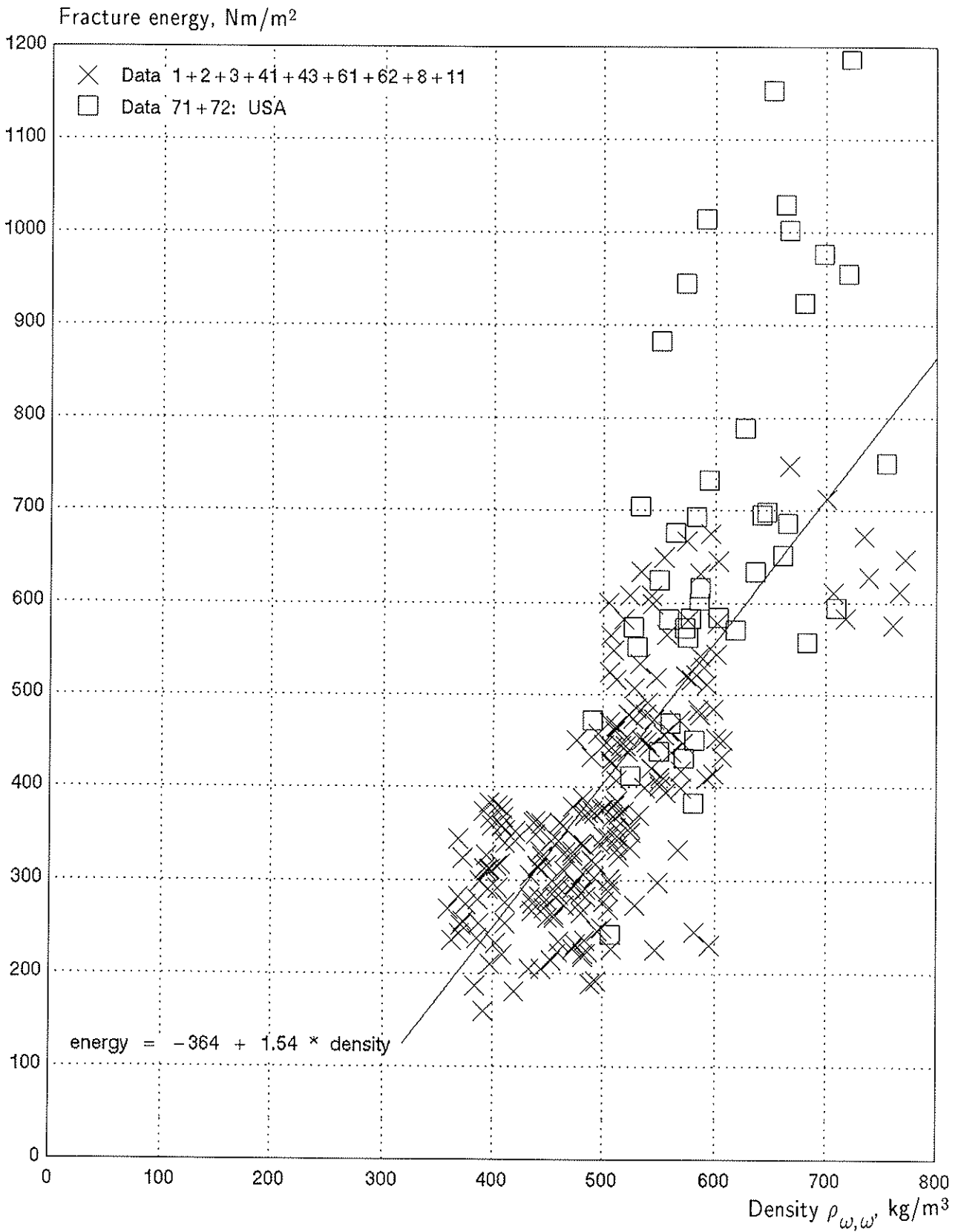


Fig. 6 Fracture energy versus density for all test results regarded as one population

CONCLUSIONS

The test method is simple and with modern testing machines it is easy to get stable load deflection curves.

The fracture energy increases linearly with the density. On single regression line can be used for all the reported species. For individual species or groups of species slightly more precise relationships can be obtained.

No influence of the growth ring orientation has been found.

There is not enough data to indicate whether the fracture energy is dependent on the moisture content.

There is a marked depth effect. Doubling the depth from 40 mm to 80 mm and from 80 mm to 160 mm increases the test values by about 20 percent. The length of the specimens has only a minor effect, if any.

NOTATION

a	sidelength of the tested volume
b	width of tested volume
$G_{I,C}$	fracture energy in mode I; in Nm/m ²
h_c	depth of tested area
ω	moisture content; in percent
$\rho_{\omega,\omega}$	density determined from mass and volume at moisture content ω , in kg/m ³
α	between the direction of the stress and the growth rings

REFERENCES

- 1) CIB Structural Timber Design Code. CIB Publication 66, 1983
- 2) Daerga, Per Anders et al.: Fracture Energy of Pine Determined in Three—point Bending. Div. of Struct. Eng. Luleå University of Technology, Sweden, 1990
- 3) Eurocode 5; Common Unified Rules for Timber Structures. Commission of the European Communities, Report EUR 9887. 1987

- 4) Gustafsson, Per Johan: A Study of Strength of Notched Beams. CIB W18A Paper 21—10—1, Parksville, Canada, 1988a.
- 5) Gustafsson, Per Johan and Enquist, Bertil: Träbalks Hållfasthet vid Rätvinklig Urtagning. Lund Institute of Technology, Div. of Struct. Mech., Report TVSM—7042, 1988b.
- 6) Kretschmann, David E.: Results from the Trial of CEN Draft Standard to Determine Fracture Energy. Forest Products Laboratory, Madison, USA, 1990.
- 7) Larsen, Hans Jorgen and Gustafsson, Per Johan: Design of End—notched Beams. CIB W18A Paper 22—10—1, Berlin, DDR, 1989
- 8) Fäldt, Gitte, Ranta—Maunus, Alpo and Rundt, Mats: Determination of the Fracture Energy of Wood for Tension Perpendicular to the Grain, Technical Research Centre of Finland, Lab. of Struct. Eng., Espoo, Finland, 1990
- 9) Rug, Wolfgang and Badstube, Manfred: Determination of the Fracture Energy of Wood for Tension Perpendicular to the Grain. CIB W18A Paper 23— —, Lisbon, Portugal.

ANNEX A1

Lund Institute of Technology, Division of Structural Mechanics (1988–89), Sweden

Contact person

Bertil Enquist

References

Series 1: [Gustafsson and Enquist, 1988b]

Supplementary purposes

To investigate the influence of

- the load applications (one line load in the centre versus two line loads)
- the depth of the saw cut on the stability of the test ($h_c=0.5 h$ versus $h_c=0.4 h$)
- the influence of the length of the tested volume (a)

Wood

Swedish Redwood, *Pinus Silvestris*

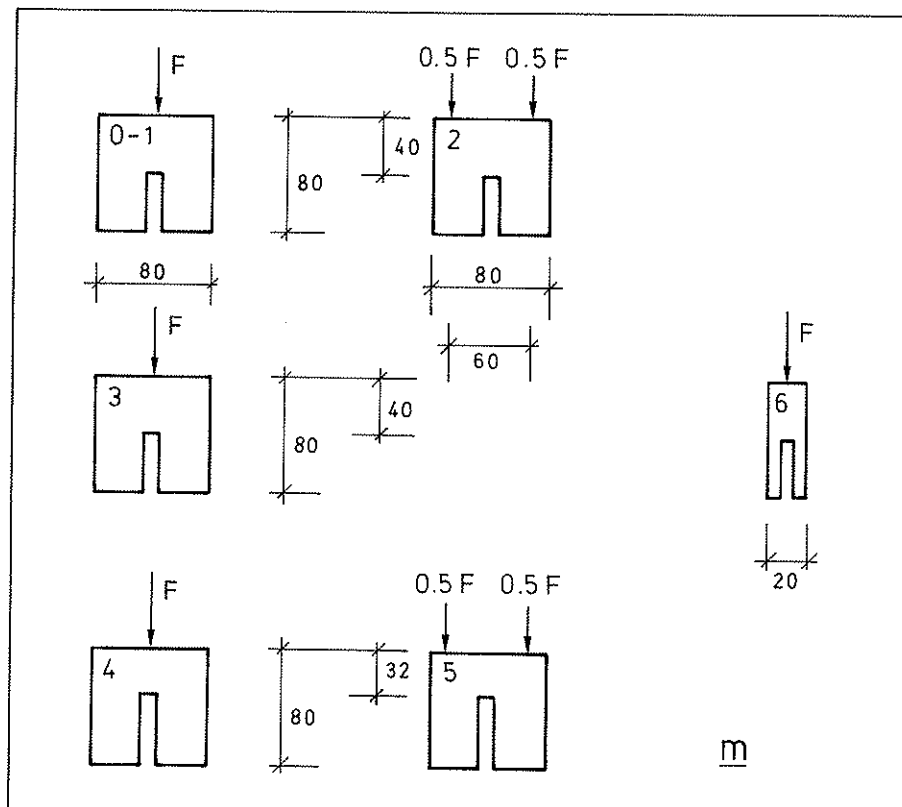
The 14 specimens in series 0 were from 7 different plank

All specimens in series 1–2 were from one plank

All specimens in series 3–6 were from another plank

Geometry and loading

The series number is denoted in the figure. The width were in all cases about 45 mm.



Results

Test values are mean values with coefficient of variation in (percent)

Series	0	1	2	3	4	5	6	
No. of spec.	14	6	6	6	6	6	6	
– unstable	3	5	4	0	0	0	1	
α		<	about 45°				>	
ω	%	14.9(2)	13.1(1)	13.0(1)	14.3(1)	13.2(2)	14.5(1)	14.8(3)
$\rho_{\omega,\omega}$	kg/m ³	462(12)	487(1)	488(1)	394(2)	404(2)	402(1)	405(3)
$G_{I,C}$	Nm/m ²	300(18)	335(10)	353(10)	312(12)	346(8)	341(11)	293(26)

Conclusions

- There is no difference between the results with one or two line loads. Therefore the simplest – one line load – is prescribed in the draft standard.
- The stability of the test is better with an effective depth of 0.4h (depth of saw cut 0.6h) than with 0.5h. Therefore an effective depth of 0.4 is prescribed in the draft standard.

ANNEX A2

Danish Building Research Institute, Denmark and
Lund Institute of Technology, Division of Structural Mechanics, Sweden

Contact person

Hans Jorgen Larsen and Bertil Enquist

References

Supplementary purposes

To investigate the influence of the size of the specimens

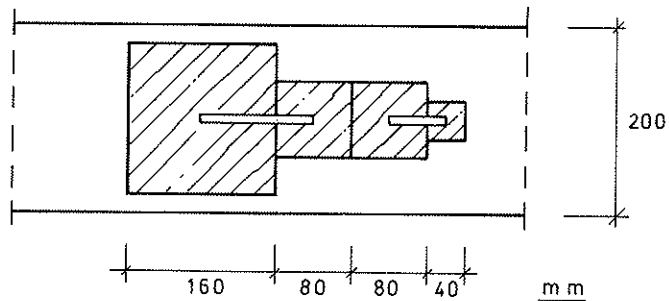
Deviations from draft standard

In series 1 the length and depth were doubled (160x160 mm). In series 3 they were halved (40x40 mm)

Wood

Redwood, *Pinus Silvestris*

The test specimens were each cut as shown from one plank about 45 mm thick (planed)



Results

Test values are mean values with coefficient of variation in (percent)

Series	1	2	3
No. of spec.	6	12	6
– unstable	1	0	0
a mm	160	80	40
ω %	14.3(1)	14.0(2)	14.0(2)
$\rho_{\omega,\omega}$ kg/m ³	584(4.5)	566(5.5)	548(5.5)
$G_{I,C}$ Nm/m ²	551(19) ¹	483(11)	413(6)
$G_{I,C}/G_{I,C,80}$ ³	1.20(6.41)	1	0.87(7.73)

- ¹ 589(12) when two with pitch are disregarded, one of which was also unstable and thus already disregarded
- ² One with a knot in the tested area and having $G_{I,C}$ in excess of 1000 Nm/m² is disregarded
- ³ Ratio of matched specimens with series 2 as reference

Conclusions

There is a statistically significant (99.9 level) size effect, a higher fracture energy is found for larger specimens (depths) corresponding to about 15–20% for every time the side length is doubled.

ANNEX A3

VTT Technical Research Centre of Finland, Laboratory of Structural Engineering, Finland

Contact person

Alpo Ranta–Maunus

References

[Fäldt, Ranta–Maunus and Rundt, 1990]

Deviations from draft standard

The specimens for series B and C were stored at a relative humidity (RH) of 80 percent (against 65 percent). The specimens for series C were on purpose stored at 45 percent RH the last 2 days before testing.

Wood

Pinus Silvestris. The width was about 40 mm.

Results

Mean values and coefficient of variation in (percent)

Series		A	B	C
No. of spec.		20	10	10
ω	%	10.8(2)	12.3(2)	11.4(2)
$\rho_{\omega,\omega}$	kg/m ³	517(9)	518(8)	521(8)
$G_{I,C}$	Nm/m ²	408(23)	415(15)	436(19)

Conclusions

The effect of differences in moisture content is not statistically significant.

ANNEX A4

Royal Technical University, Stockholm, Department of Lightweight Structures, Division of Structural and Timber Engineering, Sweden

Contact person

Ulf Arne Girhammar and Staffan Hultgren

References

Series 41 and 42: Redwood *Pinus Sylvestris*

Series 43: Spruce

Wood

The width was about 40 mm.

Deviations from standard

The length of the tested volume in series 42 was only 40 mm (against 80 mm).

Test results

The values are mean with coefficient of variation in (percent)

Series		41	42	43
a = b	mm	80	40	80
No. of spec.		10	9	8
– unstable		3	0	2
ω	%	13.1(2)	13.5(4)	–
$\rho_{\omega,\omega}$	kg/m ³	480(4)	750(5) ¹⁾	369(1)
α		15 ⁰ –70 ⁰	25 ⁰ –45 ⁰	45 ⁰ –60 ⁰
$G_{I,C}$	Nm/m ²	408(23)	415(15)	291(12)

- 1) If the results for series 42 are corrected to 80 mm by a factor of 1/0.87 (see Annex A2) and to a density of 418 (see Fig. 5) a fracture energy of 394 Nm/m² is found.

ANNEX A5

Luleå University of Technology, Division of Structural Engineering and Division of Structural Mechanics, Sweden

Contact person

P.A. Daerga, B.E. Nielsen and A. Olsson. Division of Structural Engineering
A. Vallgren. Division of Structural Mechanics

References

[Daerga et al., 1990]

Wood

Redwood. *Pinus Silvestris* from northern Sweden. Although the average growth ring width was very small — only about 0.8 mm — the density was relatively low. The width of the specimens were about 44 mm.

Deviations from standard

The specimens were stored at 25 percent relative humidity (against 65 percent). The saw cut was made when the beams were manufactured, i.e. about a month before testing. The rubber layers recommended in the standard were omitted.

Results

Mean values with coefficient of variation in (percent)

No. of spec.		6 (all stable)
--------------	--	----------------

ω	%	7.7(10)
$\rho_{\omega,\omega}$	kg/m ³	445(3)
α		about 90°
$G_{I,C}$	Nm/m	201(8)

Conclusions

The last method is simple to use and with a servo-hydraulic closed-loop testing machine it is not a problem to obtain stable and reliable results.

ANNEX A6

Akademia Rolnicza, Katedra Mechaniki i Techniki Ciepłej, Poznań, Poland

Contact person

Ryszard Ganowicz and Piotr Olejniczek

ReferencesSupplementary purpose

To determine the influence of the growth ring orientation on the fracture energy.

Wood

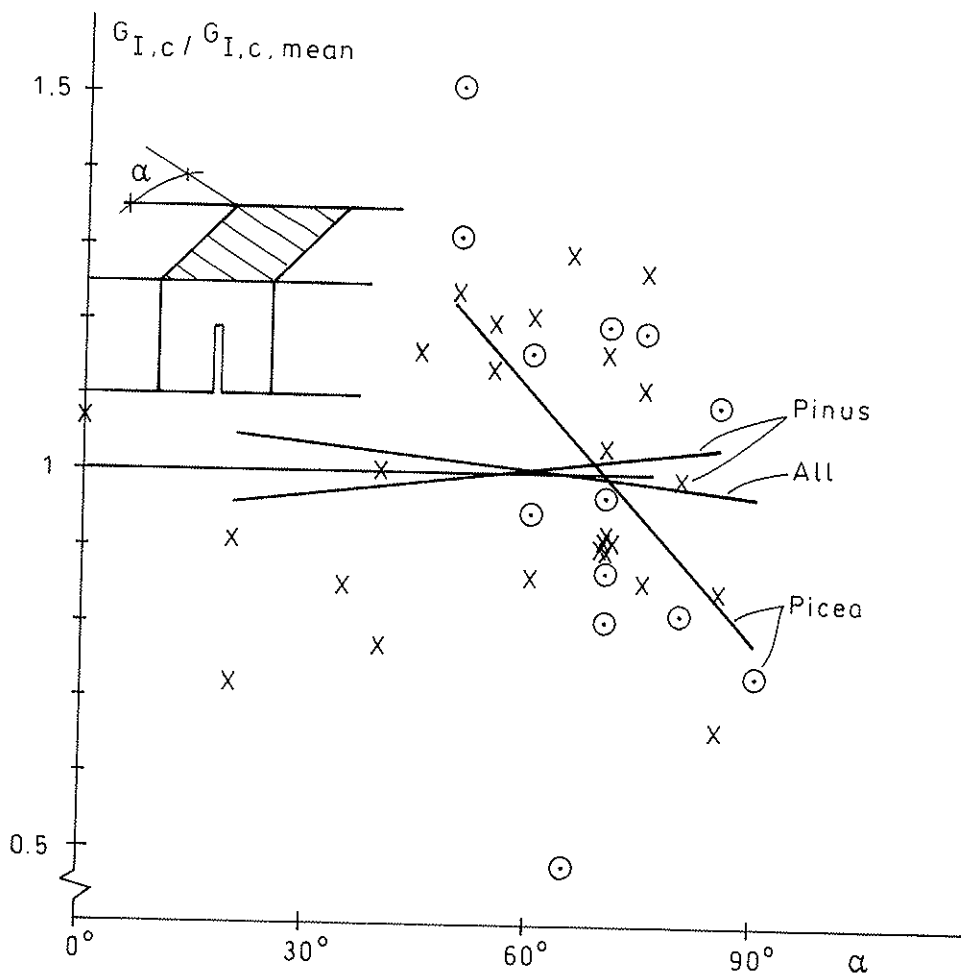
Whitewood, Picea Abies and Redwood, Pinus Sylvestris. The width of the specimens were about 45 mm

Test results

Mean values with coefficient of variation in (percent)

	Picea Abies			Pinus sylvestris		
	un— stable	semi stable	stable	un— stable	semi stable	stable
No. of spec.	13	18	13	12	7	24
ω %	Not reported, standard climate used					
$\rho_{\omega,\omega}$ kg/m ³	499(1)	497(2)	502(2)	561(5)	538(6)	549(5)
$G_{I,C}$ Nm/m ²	365(14)	348(22)	346(27)	494(11)	527(12)	524(18)

In the following figure the relative fracture energies (i.e. the individual test results relative to the species mean) are plotted against the angle α .



Conclusions

- The fracture energy for the unstable or semistable cases are not significantly lower than for stable cases. Only the results from the stable cases are, however, taken into consideration.
- For *Picea abies*, the fracture energy decreases with increasing α (i.e. the lowest values are found for tension in the radial direction. The same trend is found if all test results are taken together. The correlations are however weak/very weak (correlation coefficient about -0.50 and -0.10 respectively). For *Pinus Sylvestris* there is an opposite trend (very weak, correlation coefficient about 0.10 ,

ANNEX A7

Forest Products Laboratory, Madison, USA

Contact person

David E. Kretschmann

References

[Kretschmann, 1990]

Supplementary purpose

To determine whether there is a size effect.

To present information on Mode I fracture relationships and to compare the test results with other.

Mode I results.

Deviations from the draft standard

The dimensioning deviated from the draft standard (80x56 mm and 40x28 mm instead of 80x80 mm, see table below.

WoodSouthern yellow pine (*Pinus Echinata*) and *Pinus Taedar*. The widths are given in the table below.Results

Mean value and

		Series 1		Series 2	
		rejected ¹	accepted	rejected ¹	accepted
a	mm		56		28
b	mm		35		20
h	mm		80		40
No. of spec.		9(7) ¹	13	10(1) ¹	29
ω	%		11.9(9)		11.8(10)
$\rho_{0,\omega}^2$			550(12)		540(10)
$\rho_{\omega,\omega}^2$			615(12)		603(10)
α			~0°		~30°
$G_{I,C}$		553(41)	706(45)	651(16)	671(23)

¹ and ²: see next page

- 1 The total number of rejects are given together (in paranthesis) with the number rejected due to unstable load–deflection curve. Other reasons for rejection were: checks before testing, distorted specimens or presence of pith.
- 2 Dry weight, volume at testing.

Conclusions

- The mean value for the smaller specimens are on average 5 percent larger than the bigger. Due to the large coefficient of variation and because also other variables are different, this difference is not significant.
- In [Kretschmann, 1990] it is stated: "The method proved to be simple to use giving results which indicate a slight size effect. It seemed, however, that a lot of material is required to conduct this test as compared to compact tension test specimen. I was also surprised that no comments were made in the standard requiring the placing of a sharp crack in the notch root. The comparison of these results with K_{Ic} values determined from compact tension specimens indicate that the area under the curve method for determining fracture toughness over estimates the value for K_{Ic} ".

ANNEX A8

Technical University of Denmark, Department of Structural Engineering

The testing has been done at Lund Institute of Technology, Division of Structural Mechanics (Bertil Enquist)

Contact person

Hilmer Riberholt and Ralph Jensen

ReferencesWood

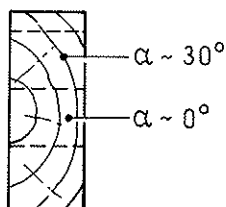
Nordic whitewood (Picea Abies)

Results

Test values are mean values with coefficient of variation in (percent)

No. of spec.		41	21	62
ω	%			
α^1		~ 0	$\sim 30^\circ$	
$\rho_{\omega,\omega}$	kg/m ³	455(8)	465(8)	458(8)
$G_{I,C}$	Nm/m ²	287(23)	286(15)	286(20)

- ¹ All specimens were cut from planks with a year ring pattern as shown either at middepth (α about 0°) or at quarter depth (α about 30°)

Conclusions

The difference in growth ring orientation has no influence in the results.

ANNEX A9

Lund Institute of Technology, Division of Building Material, Sweden

Contact persons

Lars Boström and Bo Johansson

ReferencesDeviations from the draft standard

The sidelengths of the tested volume were 20x20x20 mm.

Wood

Redwood. Pinus Sylvestris.

Results

No. of spec.		5
ω	%	~12
$\rho_{\omega,\omega}$	kg/m ³	460
$G_{I,C}$	Nm/m ²	250 (coefficient of variation: 10%)

Conclusions

The fracture energy is significantly lower than for the results reported in Annex A1–2. This can be explained by the small specimen size.

ANNEX A10

German Academy of Architecture and Building, Berlin and Research institute of BAUFA, Leipzig

Contact persons

Wolfgang Rug and Manfred Badstube, Berlin
Werner Schöne, Leipzig

References

[Rug, Wolfgang and Badstube, Manfred, 1990]

Supplementary purposes

- To determine the influence of the moisture content
- To determine the influence of different visual grades
- To determine the fracture energy of the glue lines in glued laminated timber.

Deviations from the draft standard

The depth is 90 mm for ordinary wood and 128 mm for glued laminated timber (corresponding to 4 lamellas).

Wood

3 different grades of solid redwood (red pine) were tested. Grade I was mechanically graded (mean $E=12000$ MPa). Grade II and III were visually graded. The glued laminated timber was made from whitewood.

Results

Test results are mean values with coefficient of variation in (percent)

Series	A	B	C	D	E	F
No. of spec.	12	12	12	12	12	12
– unstable	3	5	4	0	0	0
Timber grade	I	I	I	II	III	Whitewood
h mm	90	90	90	90	90	128
ω %	12.5(2)	17.3(3)	23.4(2)	12.2(2)	13.0(6)	10.4(6)
$\rho_{\omega,\omega}$ kg/m ³	547(5)	574(4)	478(10)	515(3)	453(9)	580(26)
$G_{I,C}$ Nm/m ²	350(9)	326(10)	328(13)	358(13)	307(18)	255(17)
$G_{I,C}(\rho=547)^{1)}$	350	305	396	388	402	235

- 1) $G_{I,C}$ referred to a density of 547 kg/m³ i.e. the density of the reference series A. By the calculations the relation found in Fig. 5 is used.

Conclusions

- There is no significant influence of the moisture content. If only series A and B are compared there is a significantly decrease of the fracture energy with increasing moisture content, but this trend is contradicted by the results of series C.
- There is no influence of grade apart from the one reflected in the density.
- The fracture energy of the glulam glueline is significantly lower – only about 2/3 – than for solid timber with a corresponding density.

ANNEX A11

South Bank Polytechnic, Mechanical Engineering, Design and Manufacture, UK.

Contact person

David G. Hunt, South Bank Polytechnic and Merab M. Rukhadze, Georgien Technical University, Tbilis, USSR

Wood

Redwood. Pinus Silvestris. The width was about 40 mm.

Deviations from standard

The depth of the specimens was only 40 mm (against 80 mm)

Test results

The values are mean values with coefficient of variation in (percent)

No. of spec.		12
ω	%	10
$\rho_{\omega,\omega}$	kg/m ³	503(11)
$G_{I,C}$	Nm/m ²	263(16)

D R A F T S T A N D A R D

DETERMINATION OF THE
FRACTURE ENERGY
OF WOOD
FOR TENSION PERPENDICULAR TO THE GRAINNovember/September
1989 1990

Foreword

In the design of timber structure knowledge of the fracture energy is needed, e.g. for the design of end notched beams and joints with load acting perpendicular to the grain.

The fracture energy depends on the test method. It is thus necessary to have a standardized method to make results from different laboratories comparable.

The method described in this standard is based on a proposal from Per Johan Gustafsson*, who found that the fracture energy thus determined could be used directly in the design of end notched beams.

* Per Johan Gustafsson and Hans Jørgen Larsen: DESIGN OF ENDNOTCHED BEAMS, CIB paper W18A/22-10-1, Berlin DDR, September 1989

1 SCOPE

This standard specifies a method for determining the fracture energy of wood in tension perpendicular to the grain (mode I).

2 REFERENCES

ISO 3130 Wood - Determination of moisture content for physical and mechanical tests

3 SYMBOLS

a	sidelength of the tested volume, see figure 1; in mm
b	width of tested volume and area, see figure 1, in mm
$G_{I,c}$	fracture energy in mode I; in N/mm
g	gravity acceleration; $9,81 \text{ m/s}^2$
h_c	depth of tested area, see figure 1; in mm
m	mass of the test specimen; in kg
m_ω	mass of tested volume at moisture content ω ; in kg
u	deflection; in mm
u_0	deflection at failure; in mm
W	work done by midpoint force; in Nmm
ω	moisture content; in %
ρ_ω	density determined from mass and volume at moisture content ω ; in kg/m^3

4 TESTING

4.1 Principle

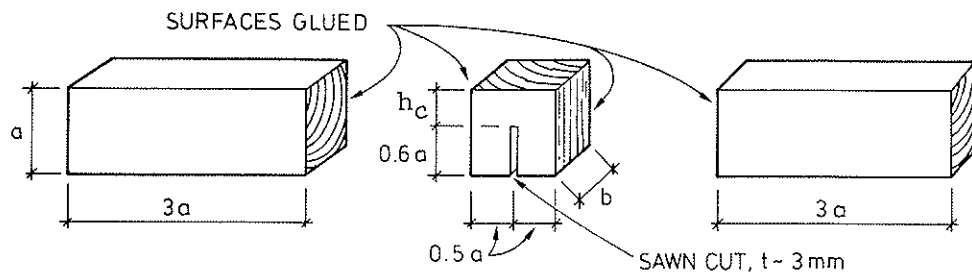


Figure 1 The test specimen is composed of three pieces of wood glued together to form a beam with cross-section $(a \cdot b)$ and a length of about $7a$.

The tested volume is a right prism $a \cdot a \cdot b$ with one face perpendicular to the grain and with a saw cut parallel to two of the faces parallel to the grain, see figure 1.

The tested area is $h_c \cdot b$, with $h_c = 0.4a$.

The tested specimen is a beam with cross section $a \cdot b$ and length $7a$, produced by gluing $3a$ long wood beams to the two planes parallel to the saw cut, see figure 1 and 2.

Note: An example on a jig for producing the specimen is shown in Annex A.

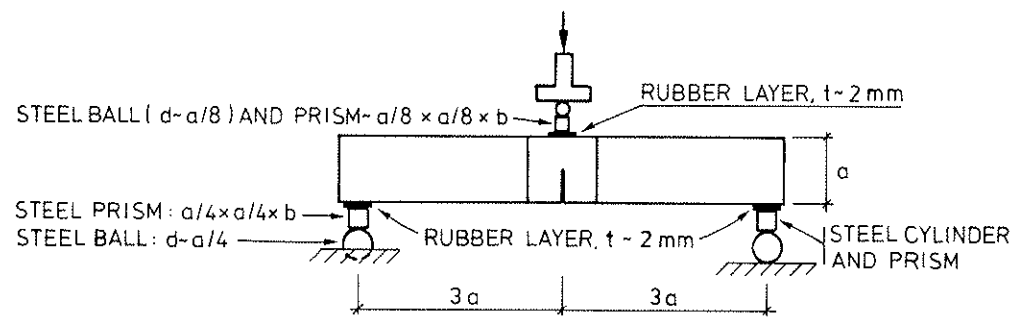


Figure 2 The beam is loaded in three-point bending

The beam is simply supported - in one end on a steel prism resting on a steel ball, in the other end on a steel prism resting on a steel cylinder - and is loaded at midpoint through a steel ball and prism. Between the wood beam and the steel prisms are placed a 2 mm rubber layer.

The beam is loaded until failure in about 3 minutes with a constant rate of movement of the cross head of the machine.

The fracture energy is calculated as the work done by the midpoint force and the dead weight divided by the tested area (the area above the saw cut).

6.2 Apparatus

A testing machine able to load with a constant rate of movement of the cross head.

Equipment to measure the mid span load of the beam with an accuracy of $\pm 1\%$ of the maximum load applied.

Equipment to measure the cross head movement or the mid span deflection with an accuracy of $\pm 1\%$.

Equipment to support and load the beam as shown in figure 2.

6.3 Test specimen

The wood to be tested should be conditioned in a climate of $(20 \pm 2)^\circ\text{C}$ and $(65 \pm 5)\%$ RH until equilibrium.

After conditioning the test volume is shaped.

Its mass m_w is determined to the nearest 0.1 g. Its sidelengths are measured to the nearest 0.1 mm.

The two timber beams $a \cdot b \cdot 3a$ are glued to the tested volume.

Note: There are many suitable glues e.g. resorcinol or PVA

After curing the test specimen is again stored in a climate of $(20 \pm 2)^\circ\text{C}$ and $(65 \pm 5)\%$ RH until equilibrium and kept in this climate until testing.

Immediately before testing the 3 mm wide saw cut is made, and the mass of the test specimen determined.

6.4 Test Procedure

Place the beam on the support and load in the mid span with a constant rate of movement of the cross-head of the test machine, so that collapse is obtained in about $\frac{a}{80}$ (3±1) minutes, with a in mm.

Determine the complete load deflection diagram by measuring continuously corresponding values of load and deflection.

Note: Deflection may be measured as the movement of the point of load application relative to the supports, or as the movement of the cross-head. In the latter case, the machine must expose only elastic deformations so that no energy consuming irrecoverable plastic deformation occurs in the machine or in the load and support equipment.

Note: For the test results to be valid it is required that the load deflection response is stable. The response is unstable if at some instant during the test, the load decreases momentarily. An unstable response may be due to too low a stiffness of the testing machine or the load and support equipment.

Measure the depth, h_c , of the tested area (above the saw cut).

After the testing the moisture content is determined in accordance with ISO 3130 (weigh - dry - weigh), by taking a reasonable part of the material of the tested volume.

6.5 Results

Calculate the density of the tested volume as
$$= m_0 / (a \cdot a \cdot b)$$

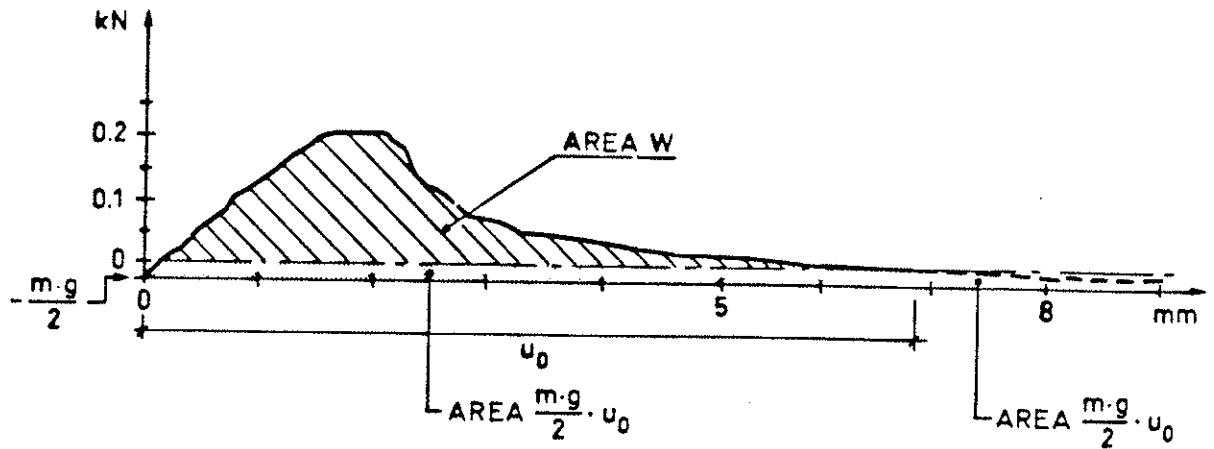


Fig. 3 From the complete and stable load deflection curve the external work is calculated as $W + mgu_0$

Calculate the fracture energy as

$$G_{I,c} = (W + mgu_0)/(h_c b)$$

where

- W is the work done by the midpoint force
- m is the mass of the beam
- g is the gravity acceleration
- u_0 is the deflection at failure

Note: W is obtained as the area under the load deflection curve, see figure 3.

Note: The work from the mass of the beam before u_0 is $mgu_0/2$, and it is assumed that the failure energy after u_0 is of the same magnitude.

7 REPORT

The report should at least contain

- Botanical identification of the tested wood
- Density of the tested volume
- The growth ring width and pattern, especially in the tested area above the saw cut

Note: This can conveniently be done by taking a Xerox copy

- Geometry of the tested volume of the area, see Annex 2
- Moisture content at testing
- Time to failure
- Special features of the load deflection curves, e.g. whether it is stable or not
- Fracture energy
- Load carrying capacity (maximum load)

INTERNATIONAL COUNCIL FOR BUILDING RESEARCH STUDIES AND DOCUMENTATION
WORKING COMMISSION W18A - TIMBER STRUCTURES

APPLICATION OF FRACTURE MECHANICS TO TIMBER STRUCTURES

by

A Ranta-Maunus
Technical Research Centre of Finland (VTT)
Laboratory of Structural Engineering
Finland

MEETING TWENTY - THREE

LISBON

PORTUGAL

SEPTEMBER 1990

APPLICATION OF FRACTURE MECHANICS TO TIMBER STRUCTURES

Summary of the state-of-the-art report
prepared by RILEM TC 110

by

Alpo Ranta-Maunus

Technical Research Centre of Finland (VTT)

Laboratory of Structural Engineering

Kemistintie 3, SF-02150 Espoo, FINLAND

CONTENTS	page
PREFACE	1
5 DESIGN BY FRACTURE MECHANICS	1
5.1 Existing design codes	1
5.11 Notched beams	2
5.12 Lap joints, butt joints in laminations	4
5.2 Standard proposals	5
5.3 Other potential applications	6
5.31 New strength theories	7
5.32 Acceptance limits for cracks in service	8
5.33 Shear failure	9
5.34 Stress peak areas	10
5.4 Unlikely applications	12
6 RECOMMENDATIONS	13
6.1 Standardization of test methods	13
6.2 Development of design methods	13
6.3 Research needs	14
REFERENCES	14

Prepared for CIB W18A meeting in Lisbon, September 1990.

PREFACE

RILEM TC 110-TFM has prepared a state-of-the-art report on the application of fracture mechanics to timber structures. The report is divided into chapters written by the authors as follows:

- | | |
|---------------------------------|---------------|
| 1. Introduction | by Gustafsson |
| 2. Fracture mechanics models | Valentin |
| 3. Fracture properties of wood | Boström |
| 4. Fracture analysis | Gustafsson |
| 5. Design by fracture mechanics | Ranta-Maunus |
| 6. Recommendations | Ranta-Maunus |

This paper involves two last chapters of the present version of the report (including the numbering system). RILEM TC 110-TFM has now completed its work and the final report will be published during the early part of 1991.

5 DESIGN BY FRACTURE MECHANICS

5.1 Existing design codes

The existing design codes for timber structures do not usually include fracture mechanics in any form. The most direct use of fracture mechanics appears in the Australian Timber Engineering Code (AS 1720-1975). The application is made in a hidden form: design equations show only conventional terms like normal stress, shear stress and shear strength, as will be shown later.

The shear design of dimension lumber contained in the recently released Canadian Engineering Design in Wood code (CAN-086.1-M89) was developed using an indirect application of fracture mechanics (Foschi et al, 1989). In the calibration of the design procedure, two possible modes of longitudinal shear failure in lumber were considered - one of which is based on linear elastic fracture mechanics concepts. For the first mode, shear failure is assumed to occur in the clear wood.

This failure mode treats the ASTM D143 offset block strength as a random variable and includes the effect of the volume of material under stress on the ultimate shear strength. For the second mode, shear failure is assumed to be the result of rapid propagation of an end split. Previous editions of the Canadian Design Codes were based solely on ASTM D143 shear test results and the assumption that every piece of lumber contained the most severe check, shakes or splits possible. Consequently, the previous approach resulted in very conservative shear design stresses. In the new code, the shear capacity of end-split lumber is a function of two random variables: the mode II stress intensity factor, and the crack length for the size and species of lumber under consideration. Critical mode II stress-intensity factors were obtained from bending tests on single end-notched beams for several wood species, while the size and frequency of crack lengths were collected from an in-grade lumber testing program where lumber had been conditioned to approximately 15 % moisture content.

5.11 Notched beams

For the design of the strength of notched beams, the criterion is given in eqn (3.2.6) of AS 1720-1975 in the form

$$0.3\sigma + \tau \leq C_3 f_v \quad (1)$$

where $\sigma = 6M/bh_n^2$, the nominal bending stress,
 $\tau = 1.5V/bh_n$, the nominal shear stress at net section,
 f_v = the permissible shear strength, and
 C_3 = is given in the table.

In order to demonstrate the size effect produced by eqn. (1), we rewrite in the case of large notches ($h_o > 0.1h$ in Fig.1) in the form

$$0.3\sigma + \tau \leq c h^{-1/n} f_v \quad (2)$$

where $c = 2.2$ to 3 ,

$n = 2$ to 4 , are given coefficients depending on the angle of the notch, and
 $h =$ is the height of beam [mm]

For small notches ($h_o < 0.1h$), the design equation is of the type

$$0.3\sigma + \tau \leq c h_o^{-1/n} f_v \quad (3)$$

with c and n different from eqn. (2).

It should be noticed that formula (1) combines the effect of shear and bending stresses in a simple way and uses the value of shear strength as a substitute for the mixed mode fracture toughness. The size effect provided by the term $h^{-1/n}$ is in good agreement with many theoretical approaches and experimental results.

Some modifications have been proposed to the Australian design code which would lead to the following equation

$$\sigma + 4\tau \leq g f_v \quad (4)$$

with g values given in Table 1.

A plot of eqn (4) is shown in Figure 2.

Table 1. Coefficient g for eqn. (4). Dimensions in [mm].

Notch angle slope l_o/h_o (Fig. 1)	g	
	$h_o \geq 0.1 h$	$h_o < 0.1 h$
0	$9.0 h^{-0.45}$	$3.2 h_o^{-0.45}$
2	$9.0 h^{-0.33}$	$4.2 h_o^{-0.33}$
4	$9.0 h^{-0.24}$	$5.2 h_o^{-0.24}$

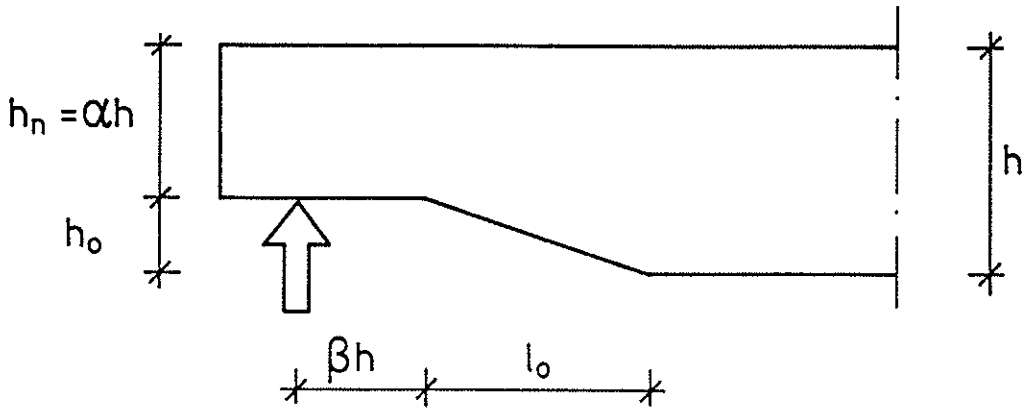


Fig. 1. The notch geometry.

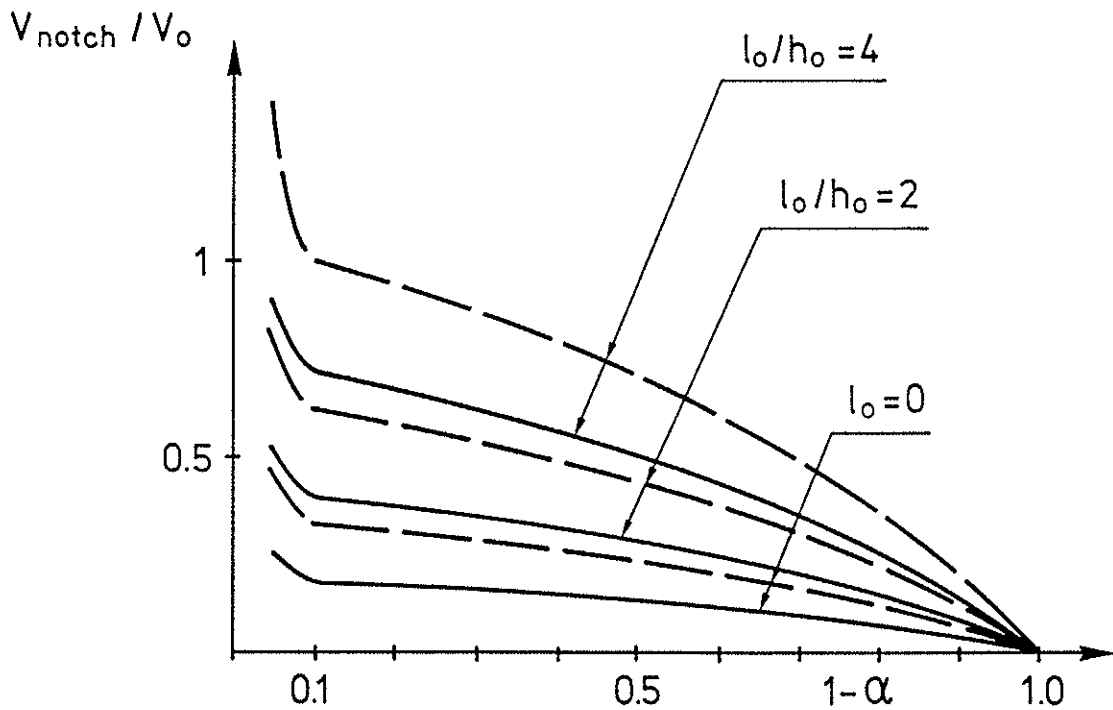


Fig. 2. The relative strength of a notched beam in comparison to the shear strength of an unnotched beam with height $h_n = \alpha h$. The scale is adjusted so that the strength of a beam with $h = 200$ mm, $l_0/h_0 = 4$ and $h_0 = 0.1h$ is 1. $\beta = 1$ and $h = 200$ mm (---) or $h = 800$ mm (—). New Australian formulation as in eqn (4).

5.12 Lap joints, butt joints in laminations

In AS 1720-1975 equations are given for glued lap joints (4.10.3) and butt joints of glulam laminations (7.4.2.1).

These are based on stress intensity factors induced by the notches (Fig. 3). The equations are not quoted here, but they result in a size effect for the load carrying capacity of the type $t^{-0.5}$, where t is the thickness of a single member or lamination.

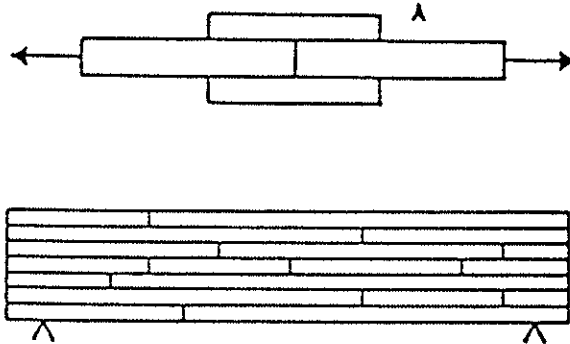


Fig. 3. Lap joint and butt joint.

5.2 Standard proposals

A design standard for notched beams has been proposed for CIB-W18A by Larsen and Gustafsson (1989). It is based on the fracture energy concept, and the paper involves a testing method for the determination of the material value, fracture energy $G_{C,k}$. The design condition is

$$\tau_d < \frac{1}{k_m} \frac{1.5 [E_{O,k} G_{C,k} / h]^{0.5}}{[0.6\alpha(1-\alpha)E_{O,k} / G_k]^{0.5} + (\beta + l_z/h)[6(1/\alpha - \alpha^2)]^{1.5}} \quad (6)$$

where $E_{O,k}$ is the characteristic value of the modulus of elasticity parallel to the grain

G_k is the characteristic value of the shear modulus

$G_{C,k}$ is the characteristic value of the fracture energy for splitting along the grain

l_z is the length of the failure region

$\tau_d = 1.5 V/bh_n$ is the nominal shear stress for effective cross-section

k_m is the partial coefficient for material properties

Eqn (6) is illustrated in Figure 4. The advantage of the method lies in its simplicity: one equation gives a reasonable result for various notch sizes and locations. Also critical arguments can also be directed at the simplicity: the method assumes that the fracture energy is independent of the fracture mode (I vs. II), which is a rough approximation. Another oversimplification is that the present version of the method does not take into account the effect of tapering of the notch (notch angle), which is traditionally assumed to be important. Methods based on notch singularity result in a significant dependence on notch geometry (see Fig. 2).

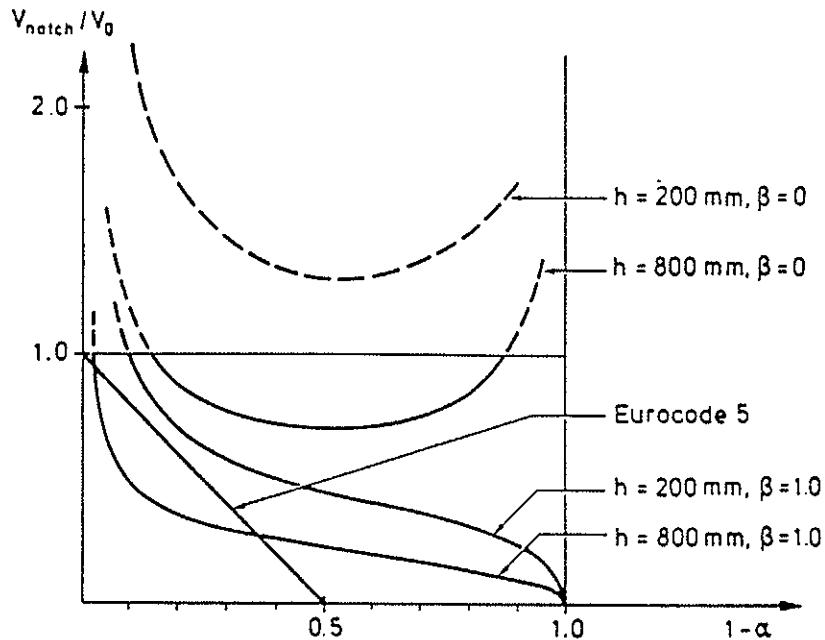


Fig. 4. The ratio between the strength of a notched beam and the shear strength of an unnotched beam of height $h_n = \alpha h$ in accordance with eqn (6) (from Larsen & Gustafsson, 1989).

5.3 Other Potential applications

Besides the design of notched beams, several areas can be indicated in which fracture mechanics may have a role when developing new design methods. As far as the the design code text is concerned, it is likely that new terms like fracture

toughness, will be avoided as long as possible, and the design equations written with conventional terms.

The topics listed below consist of some well-defined areas as well as areas in which the research is not yet in progress.

5.31 New strength theories

In general, timber used in constructions and clear wood are considered quite different materials. This is justified because there is a major difference in tension and bending failure modes when stress is mainly acting in the grain direction. The failures in timber are usually result from disturbances in grain direction often caused by knots.

The splitting mode fracture behaviour, as caused by shear force and tension perpendicular to the grain, is different: clear wood is as weak as, or weaker than, timber with the same density, knots or the slope of grain not having a detrimental effect on the shear strength (Larsen & Riberholt, 1973). This is the basic reason why a fracture criterion based on the behaviour of clear wood can be safely used for the analysis of timber structures in cases where the fracture is caused by splitting. The knots in timber can stop the growth of cracks and raise the load carrying capacity, which complicates the validation of theoretical results, but does not make them unreliable when the reason for a large deviation in results is recognized. As a conclusion fracture mechanics is a potential tool when developing new strength theories for splitting.

A general fracture criterion for the splitting mode could be developed. It should be probabilistic in nature. If based on concepts requiring the existence of initial cracks, an important issue would be the statistical distribution of the initial crack sizes. Combined with a detailed stress analysis taking into account the moisture-induced state of stress, the application of the fracture criterion could reveal new design

criterion for shear and perpendicular-to-grain stresses, including the volume effect.

Probabilistic fracture mechanics has been applied in some other fields of technology, such as in the aircraft industry and in safety analyses of nuclear power plant components. Recently fracture mechanics has been applied also in timber engineering, as a part of probabilistic design system (Foschi et al, 1989).

The load duration effect has been regarded as a crack propagation problem, as has been mentioned earlier in this report. Consequently, fracture mechanics has the potential to be applied in duration of load studies. When doing this the complex state of stresses induced by moisture variation should be taken into account (Ranta-Maunus, 1990).

In special cases like blades of wind mills, a fatigue analysis of wooden structures is needed. When fatigue is regarded as crack propagation, fracture mechanics is a natural method to be applied.

5.32 Acceptance limits for observed cracks in service

The most obvious and direct application of fracture mechanics, the stress intensity factor calculation, can be made in connection with existing visible cracks in a ready-built construction as a part of the decision-making process on whether the structure has the required load-carrying capacity or not. This situation is administratively different from the design phase, in which the cracks do not yet exist; they are something to be avoided.

New tools for judgement, simple graphs for instance, can be developed based on fracture mechanics for cases when large cracks are present. However, this is not a simple task because of

- difficulties in measurement of crack depth and shape

- mixed mode fracture of a finite length crack combined with a varying stress perpendicular to the grain caused by moisture variation.

5.33 Shear failure

It has been often argued that it is difficult to obtain shear failure of a glulam beam in laboratory tests, if the material is not considerably checked. Consequently, it has been claimed that shear failure need not be considered unless there is a sawn notch or drying checks in the beam. If this is true for timber in general, we have to conclude that a pre-existing crack or notch is the cause of shear failure, and the criterion for shear capacity should be converted in to a criterion for acceptable discontinuities. This would be a typical fracture mechanics problem.

The problem of beams with side cracks is not widely discussed in literature. A study concerning symmetrical side cracks concludes that a crack depth of 15 % of the width of the beam (on both sides of the beam) gives the same shear capacity at the capacity given by the characteristic shear strength (Murphy, 1980). Further studies should be made on the effect of side cracks. When performing these, the effect of drying stresses should be considered.

The problem of a beam with a single end crack has been analyzed by a probabilistic method (Foschi, Folz, Yao, 1989). As a part of comprehensive work, both shear failure of defect free wood, and the growth of existing end cracks are included as failure modes in the reliability analysis. The term inherent crack length is introduced to indicate the size of crack below which the conventional shear strength criterion gives lower shear capacity than the fracture mechanics criterion. The results are given in the form of a reliability index β for the total of both failure modes, and the contribution of pre-existing cracks is not separated. The main recommendation based on

this analysis is that the shear design condition of beams should include a volume effect of the form

$$\tau \leq f_v \left(\frac{L_o H_o}{LH} \right)^{0.5} \quad (7)$$

where τ is shear stress, f_v shear strength involving appropriate code coefficients, and L and H refer to the length and height of the beam.

It is interesting to notice that different approaches of separate problems, shear failure of a beam in eqn. (7) and failure of a notched beam in eqn. (2) result in quite similar size effect.

A complication with shear failure is that in structures shear stress is usually followed by simultaneous stress perpendicular to the grain. Whether it is tensile or compressive has a great influence on the load-carrying capacity. This also makes it difficult to test the shear strength of materials.

5.34 Stress peak areas

Traditionally the stress concentrations around holes and notches have been calculated by the use of the theory of elasticity. However, the peak value of stress is related to the radius of curvature, and with small values of radius the peak stress values do not directly indicate the potential for failure (Stieda, 1966). In principle, the application of fracture mechanics is natural in cases where a high stress peak occurring in a small volume is the cause of fracture. The stress peak can be the result of structural discontinuity, and be influenced by a steep moisture gradient.

Two different approaches can be applied when no structural discontinuity is present: one assuming a crack in a high-stress area, another dealing with fracture theories which need no initial crack. When assuming a crack, a probabilistic ap-

proach is appropriate, or a concept of a design crack can be introduced. The design crack concept means that, based on experience, a certain size of crack will be assumed in any location in the structure, and the onset of crack growth is analyzed by LEFM. This kind of design method is applied in the aircraft and nuclear industries.

In addition to the other applications mentioned in this chapter, a list of potential applications in which a high-stress area, but not necessarily a stress singularity, is the cause of fracture, is given as follows:

Holes in beams. Various shapes of holes are made in glulam beams. Sharp corners are usually avoided, but drying checks can be present around the hole. The failure mode is a combination of modes I and II (Fig. 5a).

Hangings. Hangings causing tension perpendicular to the grain in primary beams may cause the splitting of the beam. When hanging is made by nailing, the initial cracks are induced. Failure mode is quite pure mode I.

Cambered beams. In curved beams of varying height, a locally varying state of stress is caused, tension perpendicular to grain being an important component (Fig. 5c). Together with a drying crack and residual stresses due to moisture changes the mode I fracture or a combination of modes I and II is possible. The problem has been discussed by Leicester (1974). A theoretical and experimental work concerning checked wood loaded by tension perpendicular to the grain is given by Schniewind and Lyon (1973).

Mechanical joints. Splitting of wood is one of the fracture modes of mechanical joints. The application of fracture mechanics is illustrated by Sobue and Komatsu (1989). Also the splitting of wood during drying under a constraint caused by the mechanical joint can be analyzed by fracture mechanics.

Nail driving. Design codes have rules to indicate when nails can be used without predrilled holes. These rules could be evaluated by the use of fracture mechanics as shown by Sobue and Komatsu (1989) (Fig. 5d).

Drying checks. The splitting and checking during drying could be analyzed by fracture mechanics, probably by the use of a fracture criterion which works without the assumption of an initial crack.

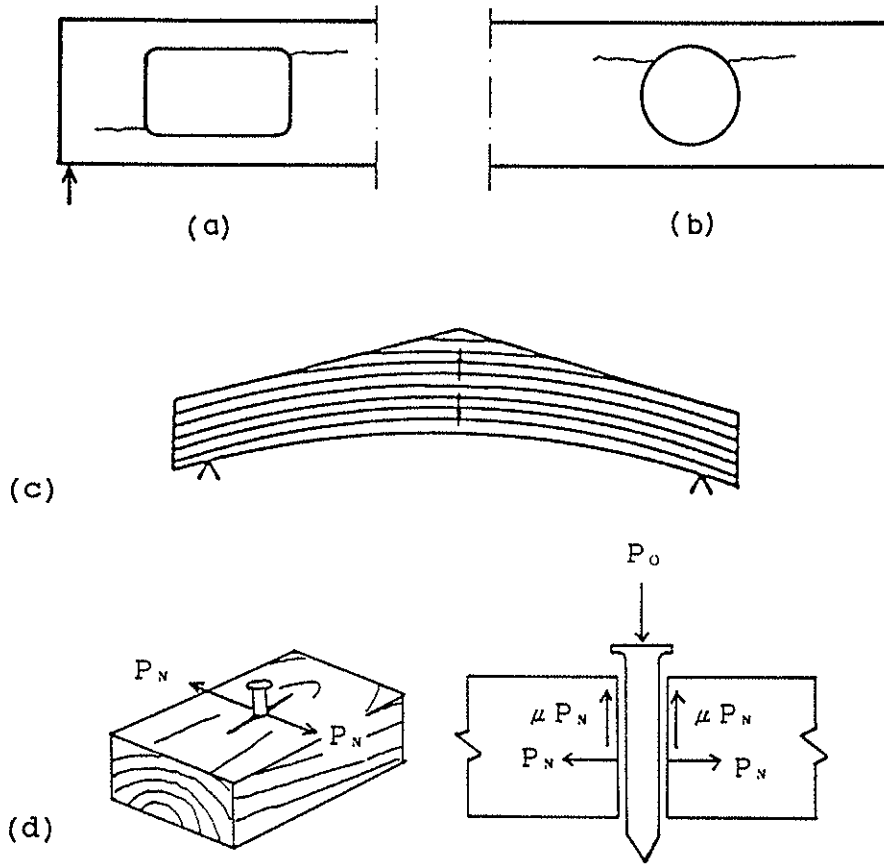


Fig. 5. Illustration of some applications of fracture mechanics.

5.4 Unlikely applications

Fracture mechanics, as defined in this report, is not a general tool which could replace earlier design methods. In order to emphasize this, a short description will be given of cases where the application of fracture mechanics may be possible, but is not seen as effective or practical.

The bending strength of timber, being influenced by numerous factors, would be very difficult to handle by fracture mechanics, and it is not seen how design practices could be improved by this means. This takes note of the idea that knots are very different from sharp cracks and not easily analyzed by fracture mechanics. Moreover, tension and compression in the grain direction are in the same category as bending. This is true even if the effect of knot size has been predicted fairly well with equations based on LEFM (Pearson, 1974).

6 RECOMMENDATIONS

RILEM TC 110-TFM recommends a new technical committee to be formed to work in the area specified in paragraphs 6.1 and 6.2. Furthermore, some recommendations concerning research related to the application of fracture mechanics to timber are outlined in paragraph 6.3. Because the area of possible applications of fracture mechanics is wide as has been indicated in earlier chapters, but the number of researchers working in the area is small, only the areas of highest priority are pointed out in this chapter.

6.1 Standardization of test methods

There is a need for standardized test methods for determining the fracture properties of wood and for testing full size members when verifying theoretical results. The development of test standards for the three basic fracture modes as well as mixed modes would make it possible to compare the results obtained in different laboratories and ensure an internationally compatible database for supporting code development.

6.2 Development of design methods

Internationally acceptable methods for predicting the shear

capacity of timber structures need to be developed. These methods should include the design of notched and unnotched beams. The methods should consider the effects of the following: member size, placement of loads, varying moisture content and duration of load. The benefits of the new design methods would be a more realistic assessment of the load carrying capacity of timber members under shear stresses.

6.3 Research needs

There are several areas in which more research is needed before applications in design become available. The following areas are emphasized here:

- a new general strength criterion for combined shear and tension perpendicular-to-grain should be derived for wood members, with emphasis to glued laminated timber structures. The method could be based on probabilistic fracture mechanics. The lack of data on initial crack size and shape distributions, however, is one of the key issues to overcome in taking this approach. The effect of residual stresses due to moisture variations should also be taken into account. International co-operation in research would be necessary to achieve this goal.

- more research is needed for development of fracture criteria for situations with stress gradients such as mechanical joints, notches or drying stresses.

REFERENCES

- Foschi R.O., Folz B.R. & Yao F.Z., 1989, Reliability-based design of wood structures. Structural Research Series, Report 34. Dept of Civil Engineering, University Of British Columbia, Vancouver, Canada. 282 p.
- Larsen H J & Gustafsson P J, 1989, Design of endnotched beams. CIB-W18A meeting 22 in Berlin, paper 28. p. 729 - 742.

- Larsen H.J. & Riberholt H., 1973, Forsog med uklassificeret konstruktionstræ. Technical University of Denmark, Rapport Nr R 31, 28 p.
- Leicester R.H., 1974, Fracture strength of wood. First Australian Conference on Engineering Materials. 14 p.
- Leicester R.H., 1974, Applications on linear fracture mechanics in the design of timber structures. Cont. Australian Fracture Group p. 157 - 164.
- Leicester R.H. & Poynter W.G., 1980, On the design strength of notched beams. IUFRO Wood Engineering Group. Oxford April 1980. Paper 2/13. 9 p.
- Murphy J.F., 1980, Strength of wood beams with side cracks. IUFRO Timber Engineering Group Meeting, Oxford.
- Pearson R.G., 1974, Application of fracture mechanics to the study of the tensile strength of structural lumber. Holz-forschung 28(1), p. 11 - 19.
- Ranta-Maunus A., 1990, Creep in timber structures: analysis of the effect of varying humidity. IUFRO 5.02 Meeting. Saint John, New Brunswick, Canada.
- Schniewind A.P. & Lyon D.E., 1973, A fracture mechanics approach to the tensile strength perpendicular to grain of dimension lumber. Wood Science and Technology 7, 45 - 59.
- Sobue N. & Komatsu K., 1989, Crack propagation along rows of bolts, cracks of nail plate jointed members. RILEM TC-110 TFM meeting 18 - 19 October 1989. Tsukuba, Japan.
- Stieda C.K.A., 1966, Stress concentrations around holes and notches and their effect on the strength of wood beams. Journal of Materials, Vol 1, No.3, p.560 - 582.
- Walsh P.F., Leicester R.H. & Ryan A., 1973, The strength of glued lap joints in timber. Forest Products Journal Vol 23, No.5, p.30 - 33.

